ACTA CHIMICA

ACADEMIAE SCIENTIARUM HUNGARICAE

TOMUS 62 FASCICULUS 1

AKADÉMIAI KIADÓ, BUDAPEST

1969

ACTA CHIM. ACAD. SCI. HUNG.

ACTA CHIMICA

A MAGYAR TUDOMÁNYOS AKADÉMIA KÉMIAI TUDOMÁNYOK OSZTÁLYÁNAK IDEGEN NYELVŰ KÖZLEMÉNYEI

Az Acta Chimica német, angol, francia és orosz nyelven közöl értekezéseket a kémiai tudományok köréből.

Az Acta Chimica változó terjedelmű füzetekben jelenik meg, egy-egy kötet négy füzetből áll. Évente átlag négy kötet jelenik meg.

A közlésre szánt kéziratok a szerkesztőség címére (Budapest 112/91 Műegyetem) küldendők.

Ugyanerre a címre küldendő minden szerkesztőségi levelezés. A szerkesztőség kéziratokat nem ad vissza.

Az Acta Chimica előfizetési ára kötetenként belföldre 120 Ft, külföldre 165 Ft. Megrendelhető a belföld számára az „Akadémiai Kiadó"-nál (Budapest V., Alkotmány utca 21. Bankszámla 05-915-111-46), a külföld számára pedig a „Kultúra" Könyv- és Hírlap Külkereskedelmi Vállalatnál (Budapest I., Fő utca 32. Bankszámla: 43-790-057-181) vagy annak külföldi képviseleteinél és bizományosainál.

Die Acta Chimica veröffentlichen Abhandlungen aus dem Bereiche der chemischen Wissenschaften in deutscher, englischer, französischer und russischer Sprache.

Die Acta Chimica erscheinen in Heften wechselnden Umfanges. Vier Hefte bilden einen Band. Jährlich erscheinen 4 Bände.

Die zur Veröffentlichung bestimmten Manuskripte sind an folgende Adresse zu senden:

Acta Chimica
Budapest 112/91 Műegyetem

An die gleiche Anschrift ist auch jede für die Redaktion bestimmte Korrespondenz zu richten.

Abonnementspreis pro Band: 165 Forint. Bestellbar bei dem Buch- und Zeitungs-Außenhandels-Unternehmen »*Kultúra*« (Budapest I., Fő utca 32. Bankkonto No. 43-790-057-181) oder bei seinen Auslandsvertretungen und Kommissionären.

ACTA CHIMICA

ACADEMIAE SCIENTIARUM HUNGARICAE

TOMUS 62

AKADÉMIAI KIADÓ, BUDAPEST

1969

ACTA CHIM. ACAD. SCI. HUNG.

ACTA CHIMICA

TOMUS 62

Fasciculus 1: 1969
Fasciculus 2: 1969
Fasciculus 3: 1969
Fasciculus 4: 1969

INDEX

Acta Chimica Academiae Scientiarum Hungaricae, Tomus 62 (1), pp. 1—6 (1969)

THE USE OF COMPLEXING AGENTS IN ION EXCHANGE CHROMATOGRAPHY, II

SEPARATION OF COBALT(II) AND NICKEL(II) IONS ON CATION EXCHANGE COLUMN USING AMMONIACAL AMMONIUM ACETATE SOLUTION AS ELUENT

J. INCZÉDY, P. KLATSMÁNYI-GÁBOR and L. ERDEY

(Institute for General and Analytical Chemistry, Technical University, Budapest)

Received November 4, 1968

A method has been developed for the chromatographic separation of cobalt(II) and nickel(II) ions in unusual order, using ammoniacal ammonium acetate as eluent. The method was planned by calculation of proper distribution coefficients using complex stability constants, acid dissociation constants and ion exchange constants taken from the literature. The experimental data were compared to the calculated ones, and an adequate agreement was found.

In the previous paper [1] the separation of nickel(II) and cobalt(II) ions on cation exchange column using oxalate ions as complex forming agents has been reported. It was shown, that the nickel(II) ions — forming more stable complexes with oxalate ions, than cobalt(II) ions — could be eluted first before cobalt(II) ions, and using the most suitable composition of the eluent, efficient and rapid separation could be attained.

Now an attempt has been made to develop a separation procedure, in which the order of appearance of the separated ions is reversed in the effluent, *i.e.* cobalt(II) ions appear before nickel ions.

To select the suitable complexant a number of complexing agents were examined and acetate ion was found to form a more stable complex with cobalt(II) ions than with nickel(II) ions. However, the stabilities of these complexes are low. Therefore it was expedient to act according to the following points of view: (1) to use acetate ions in fairly high concentration, (2) to look for a second complexing agent, the complex of which is more stable with nickel(II) ions than with cobalt(II) ions, but the complexes formed are absorbed on the cation exchange resin similarly or more strongly than the free aquo-complexed metal ions.

A complexant of this sort is ammonia, forming positively charged ammine complexes with both metal ions.

On the basis of the stability data it seemed possible that the formation of the nickel-acetate complexes is suppressed by ammonia to a greater extent, than that of the cobalt complexes. It was expected that a medium ammonia

concentration the opposite influences result in a pregnant differentiating effect.

On the basis of the above considerations the volume distribution coefficients of nickel(II) and cobalt(II) ions were calculated in the case when 1 *M* ammonium acetate solutions, containing varying amounts of free ammonia — having different pH — were used as eluents.

It must be stressed that the adsorption strength of the free metal ions and of the ammine complexes of different coordination number are not the same. According to investigations [2] the species having proper geometrical symmetry are bound more strongly to the resin than the species having unpaired ammonia groups as ligands. In the case of the complexes of cobalt(II) ions only one, *i.e.* the four coordinated complex is adsorbed with particular selectivity. However, among the nickel(II)-ammine complexes the four and six coordinated species excel in adsorption with increasing adsorption strength.

Thus, in the calculations the different adsorption strengths were to be taken into consideration.

The overall distribution coefficient D of cobalt(II) ions on cation exchange resin in the presence of ammonium acetate at different pH of the solution can be expressed by the following equation:

$$D_{Co} = \frac{(Co^{2+}) + \sum' (Co[NH_3]_i^{2+}) + (Co[NH_3]_4^{2+}) + (Co - OH^+) + (Co - ac)}{C_{Co}} \quad (1)$$

In the nominator the concentration terms of the species, being adsorbed to different extent in the resin phase are presented (all in round brackets). i denotes the coordination numbers from 1 to 6 except 4. The denominator is the total analytical concentration of the metal ion in the aqueous phase.

Since the tendency of cobalt(II) ions (and also of nickel(II) ions) to form hydroxo complexes is much smaller than to form ammine complexes, the concentrations of hydroxo complexes can be neglected.

Introducing the individual partition coefficients of the adsorbable species

$$d_o = \frac{(Co^{2+})}{[Co_2^+]}; \quad d_i = \frac{(Co[NH_3]_i)}{[Co[NH_3]_i]} \quad \text{etc.}$$

and the complex product formulas

$$[Co(NH_3)_i] = [Co]\,[NH_3]^i\,\beta_i;$$

$$[Co - ac_i] = [Co]\,[ac]^i\,\gamma_i$$

equation (1) can be transformed. With square brackets concentrations in the aqueous phase are expressed. β_i and γ_i denote the complex products of the complexes containing i ligands. At the transformation of equation (1) it was assumed — as first approximation — that the partition coefficients of the free metal ion and of all the species other than the four coordinated ones are the same, and the partition coefficient of the monovalent acetate complex ions is half of the former ones. The uncertainty of the value of the last named term has a very little influence on the value of the overall distribution coefficient.

Inserting the proper equations into equation (1) and taking into consideration, that

$$C_{Co} = [Co] + [Co]\,[NH_3]\,\beta_1 + \\ + [Co]\,[NH_3]^2\,\beta_2 + \ldots + [Co]\,[ac]\,\gamma_1 + [Co]\,[ac]^2\,\gamma_2$$

one obtains after dividing both the nominator and denominator with [Co],

$$D_{Co} = \frac{d_o(1 + [NH_3]\,\beta_1 + [NH_3]^2\,\beta_2 + \ldots.) + d_4[NH_3]^4\,\beta_4 + \frac{d_o}{2}\,[ac]\gamma_1}{1 + [NH_3]\,\beta_1 + [NH_3]^2\,\beta_2 + \ldots + [ac]\,\gamma_1 + [ac]^2\,\gamma_2} \qquad (2)$$

The equation deduced for the calculation of the distribution coefficient of nickel(II) ions is not quite the same, since the different adsorption strengths of the four and also six coordinated complexes must be taken into consideration:

$$D_{Ni} = \frac{d_o(1 + \sum^{i=1,2,3,5} [NH_3]^i\beta_i) + d_4[NH_3]^4\,\beta_4 + d_6[NH_3]^6\,\beta_6 + \frac{d_o}{2}\,[ac]\,\gamma_1}{1 + \sum_{i=1}^{i=6} [NH_3]^i\,\beta_i + \sum_{i=1}^{i=2} [ac]^i\gamma_i} \qquad (3)$$

The values of the complex products were taken from the literature. The complex products of the cobalt complexes: $\log \beta_1 = 2.05$; $\log \beta_2 = 3.62$; $\log \beta_3 = 4.61$; $\log \beta_4 = 5.31$; $\log \beta_5 = 5.43$; $\log \beta_6 = 4.75$ [3]; $\log \gamma_1 = 1.1$; $\log \gamma_2 = 1.5$ [4]. Those of the nickel complexes: $\log \beta_1 = 2.75$; $\log \beta_2 = 4.95$; $\log \beta_3 = 6.64$; $\log \beta_4 = 7.79$; $\log \beta_5 = 8.50$; $\log \beta_6 = 8.49$ [3]; $\log \gamma_1 = 0.7$; $\log \gamma_2 = 1.25$ [5].

The free ammonia concentration was calculated by the use of the acid dissociation constant of the ammonium ion ($\log k = -9.45$, corrected to ionic strength of 1) at different pH values. The individual distribution coefficients were calculated according to the following equation [1], [6]:

$$\log d = \log K^* + 2 \cdot \log Q - 2 \cdot \log [NH_4^+] \qquad (4)$$

Q denotes the volume capacity of the resin; $[NH_4]$ was just unity, and the K^x concentration constant values were estimated on the basis of separate investigations [2].

$$K^x_{Co-NH_4} = 3.5 \quad ; \quad K^x_{(CoNH_3)_4-NH_4} = 10.7$$
$$K^x_{Ni-NH_4} = 3.5 \quad ;$$
$$K^x_{Ni(NH_3)_4-NH_4} = 11.1; \quad K^x_{Ni(NH_3)_6-NH_4} = 13.4$$

The calculated partition coefficients in the case of cobalt(II) ions were: $d_0 = 12.6$; $d_4 = 38.5$; and in the case of nickel(II) ions: $d_0 = 12.6$; $d_4 = 40$; $d_6 = 48$.

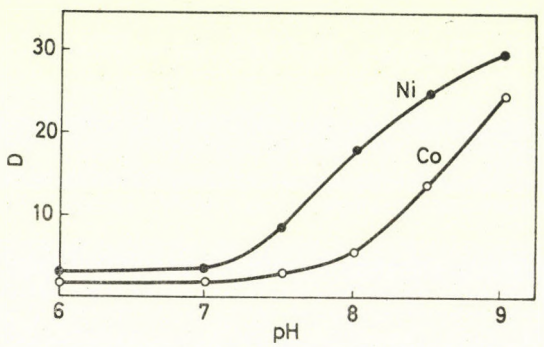

Fig. 1. Distribution coefficients of cobalt(II) and nickel(II) ions from 1 M ammonium acetate solutions calculated using Eqs. (2) and (3) as function of the pH

From the distribution coefficients of cobalt(II) and nickel(II) ions calculated at different pH values using equation (2) and (3) graphs were constructed as can be seen in Fig. 1. For the selection of the best pH value in the separation of the two metal ions, the $(D_{Ni} + a)/(D_{Co} + a)$ ratios were also calculated at different pH values [1]. a denotes the void fraction of ion exchange column ($\sim$0.4).

According to the obtained data, the best separation was expected if a 1 M ammonium acetate solution of pH ca 8.1 was used as eluent.

On the basis of preliminary calculations experiments were carried out on ion exchange column for the elution of trace amounts of nickel(II) and cobalt(II) ions, using 1 M ammonium acetate solution of different pH as eluent. In the elution experiments the effluent was collected automatically in fractions and analysed. From the obtained data chromatograms were constructed, the peak eluent volume (V_{max}) determined and the volume distribution coefficients, the peak eluent volume ratios calculated. For the

calculation of distribution coefficients equation (5) was used.

$$D = \frac{V_{max}}{X} - a \tag{5}$$

X denotes the column volume in ml.

The obtained data are summarised in Table I. As can be seen, the highest

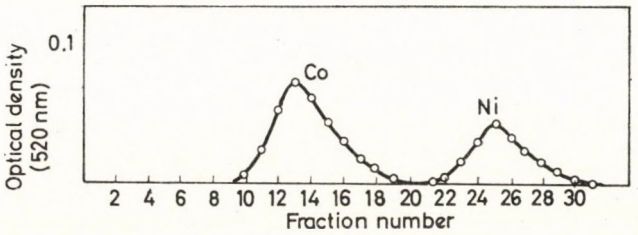

Fig. 2. Chromatographic separation of cobalt(II) and nickel(II) ions using 1 *M* ammonium acetate solution of pH 8.4 as eluent. Ion exchange column: Amberlite CG—120 Type I; 7×80 mm; Flow rate: 0.4 ml/min. Volume of fractions: 2 ml

Table I

Elution of cobalt(II) and nickel(II) ions with 1 M ammonium acetate solution of different pH
(Ion exchange column: 7×80 mm; Amberlite CG—120, Type I)

pH of eluent	$V_{max, Co}$ ml found	$V_{max, Ni}$ ml found	$\frac{V_{max, Ni}}{V_{max, Co}}$	D_{Co} found	D_{Ni} found	Data taken from the graphs in Fig. 1.		
						D_{Co}	D_{Ni}	$\frac{D_{Ni}+a}{D_{Co}+a}$
7.1	13.7	17.6	1.28	4.04	5.3			
7.5	15.0	19.3	1.28	4.46	5.85	2.5	6.9	2.5
7.9	16.7	29.6	1.77	5.03	9.20			
8.1	23.2	39.4	1.70	7.15	12.4	4.6	18	3.7
8.4	26.2	50.5	1.93	8.1	16.0			
8.5	35.1	61.6	1.75	11.0	19.6	13.1	25.7	1.94
8.8	61.6	94.2	1.53	19.6	30.20			

ratio of the V_{max} values is about pH 8.4. The deviations between the calculated and experimentally found volume distribution coefficient values are not large. However the calculated distribution coefficients are somewhat lower in the case of cobalt(II), and somewhat larger in the case of nickel(II) ions, than those obtained by experiments. The deviations may be explained by the inaccuracy of the constants used.

The chromatogram obtained at the separation of cobalt(II) and nickel(II) ions in "reversed order" using an eluent of pH 8.4 is presented in Fig. 2

Experimental

Reagents. In all experiments A.G. chemicals were used. 1 *M* ammonium acetate solutions of different pH were prepared from 2 *M* ammonium acetate solution by adding the required amount of ammonia and diluting to the proper volume.

Ion exchange column. From Amberlite CG—120 Type I cation exchange resin column (7×80 mm) similar to that used in former experiments [1] was prepared, converted to NH_4-form with ammonium acetate solution and washed with deionized water.

Elution experiments. The elution experiments, the estimation of the metal ions in the collected effluent fractions, the construction of chromatograms (or elution graphs) were carried out as in the former experiments [1].

REFERENCES

1. INCZÉDY, J., KLATSMÁNYI-GÁBOR, P., ERDEY, L.: Acta Chim. Acad. Sci. Hung. **61** 261 (1969)
2. INCZÉDY, J.: Acta Chim. Acad. Sci. Hung. (in the Press)
3. BJERRUM, J.: Metal Ammine Formation in Aqueous Solution. Thesis, Copenhagen, 1941
4. SIDDHANTA, S. K., BANERJEE, S. N.: J. Ind. Chem. Soc. **35**, 343 (1958); C.A. **53**, 2919 (1959)
5. FRONAEUS, S.: Thesis, Lund 1948
6. RINGBOM, A.: Complexation in Analytical Chemistry. Wiley, New York, 1963

János INCZÉDY
Piroska KLATSMÁNYI-GÁBOR
László ERDEY
Budapest XI., Gellért tér 4.

Acta Chimica Academiae Scientiarum Hungaricae, Tomus 62 (1), pp. 7—17 (1969)

SOME TOPOLOGICAL FEATURES OF COVALENTLY BONDED MOLECULES, II

F. BILLES

(Department of Physical Chemistry, Polytechnical University of Budapest)

Received April 9, 1968

The informations necessary for recovering a structural matrix of the molecule are contained by the symmetry structural matrix. The algorithm of the above transformation can be performed with was described in the form of a computer program.

With the knowledge of the structural matrix the cycles and building sets of the molecule as well as the chains belonging to the building sets can be determined. The knowledge of the cycles and chains can be needed in the case of establishing connections between the internal coordinates of the molecule (*i.e.* establishing the redundancy conditions) as well as in the case of choosing the corresponding independent internal coordinates (*i.e.*, indirectly, determining the matrix **G**). Therefore, algorithms were worked out for simulating the cycles and chains by the aid of a computer.

Introduction

In the first part of this series of publication [1] the concepts of the structural matrix (**C**) and the symmetry structural matrix (**S**) have been introduced. Now we will present some of their properties and applications.

The atoms x_i of a covalently bonded molecule ($i = 1, 2, \ldots, n$ being the number of atoms in the molecule) form a certain set $\mathfrak{X}$ of points. The operator $\hat{\mathbf{\Gamma}}$ has the property of assigning the atoms to the neighbouring ones. Thus the molecule can be considered as a graph ($\mathcal{G}$) [2]. By the operator $\hat{\mathbf{\Gamma}}$ the valence lines u_j ($j = 1, 2, \ldots, m$ being the number of valence lines in the molecule) have been defined, which constitute a certain set $\mathfrak{U}$.

The structural matrix **C** is a special image of $\mathcal{G}$. Its rows and columns, respectively, are arranged according to the elements of $\mathfrak{U}$ and $\mathfrak{X}$, respectively. The elements C_{ji} of the matrix **C** may be 1 or 0 depending on whether the valence line u_j is connected or not to the atom x_i.

Every molecule has, according to its symmetry, symmetry elements. All the symmetry elements may be considered as girs or giroids, defining the identity as a monogir ($E \equiv C_1$), the plane of symmetry as a monogiroid ($\sigma = S_1$), while the centre of symmetry as a digiroid ($i = S_2$).

The elements $\begin{matrix}\mathfrak{X}_\alpha \subseteq \mathfrak{X} \\ \mathfrak{U}_\alpha \subseteq \mathfrak{U}\end{matrix}$ of a certain set $\begin{matrix}\mathfrak{X}_\alpha \\ \mathfrak{U}_\beta\end{matrix}$ of points, its representative

* Part I: BILLES, F.: Acta Chim. Acad. Sci. Hung. **51**, 295 (1967).

being $\begin{matrix}\mathfrak{X}_i \\ \mathfrak{U}_j\end{matrix}$, are said to be equivalent with respect to some symmetry element R of the molecule, in case they can be transformed into each other by the symmetry operations $\hat{R}_k$ connected to R (where $k = 1, 2, \ldots, O(\mathbf{R})$; $O(\mathbf{R})$ being the order of the cyclic subgroup belonging to the symmetry group $\mathfrak{R}$ of the molecule).

The quantity

$$\check{x}_\alpha = \frac{1}{O(R)} \sum_{r=1}^{O(R)} \hat{R}_r x_i \qquad (\alpha = 1,2, \ldots, w) \tag{1}$$

is called symmetry atom, w being the number of the equivalent atomic sets according to R. The quantity

$$\check{u}_\beta = \sum_{r=1}^{O(R)} \hat{R}_r u_j \quad (\beta = 1,2, \ldots, q) \tag{2}$$

is called symmetry valence line, q being the number of the equivalent valence line sets according to R. On the basis of Eqs. (1) and (2) we have

$$\check{\mathbf{x}} = \mathbf{W}\,\mathbf{x} \tag{3}$$

and

$$\check{\mathbf{u}} = \mathbf{Q}\,\mathbf{u} \tag{4}$$

Here $\check{\mathbf{x}}$ and $\check{\mathbf{u}}$ are, respectively, the column vectors formed by the symmetry atoms and symmetry valence lines, respectively, further $\mathbf{W}$ is an $n \times w$ transformation matrix and $\mathbf{Q}$ is an $m \times q$ one. $\mathbf{C}$ can formally be defined as

$$\mathbf{u} = \mathbf{C}\,\mathbf{x} \tag{5}$$

hence

$$\check{\mathbf{u}} = \mathbf{Q}\,\mathbf{C}\,\mathbf{x} = \mathbf{S}\,\check{\mathbf{x}} \tag{6}$$

The definitions (1) and (2) of the quantities $\check{x}_\alpha$ and $\check{u}_\beta$ are motivated by the fact that it is suitable to choose, in the matrix $\mathbf{S}$, the sum of the elements of the column vector belonging to the symmetry atom as the sum of the elements of the column vector belonging to the corresponding atoms. Namely, by these sums the index of the respective atom, *i.e.* the number of the valence lines belonging thereto, is given.

Some properties of the symmetry structural matrix

If the representative x_i of the set $\mathfrak{X}_\alpha$ of points coincides with the symmetry axis R then $O(\mathfrak{X}_\alpha) = 1$, in any other case $O(\mathfrak{X}_\alpha) = O(R)$.

If the representative u_j of the set $\mathfrak{U}_\beta$ of lines is considered as an opened domain and if u_j has only one point common with the symmetry axis R,

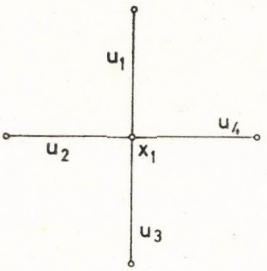

A type

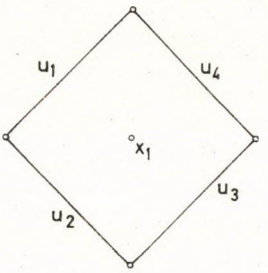

B type

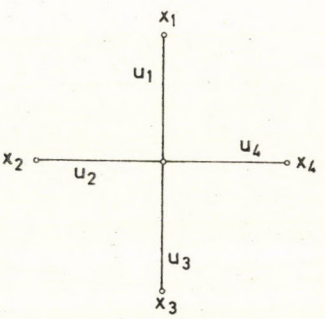

C_1 type

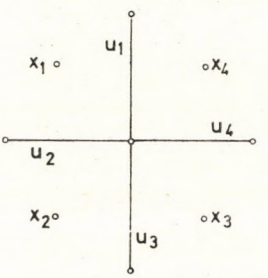

C_2 type

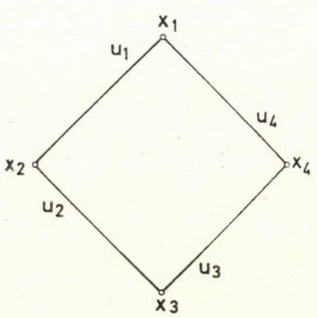

D_1 type

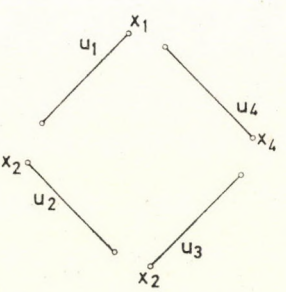

D_2 type

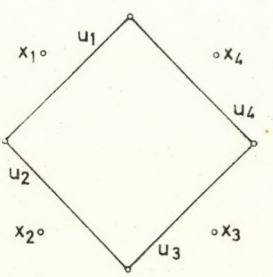

D_3 type

Fig. 1

then — since the valence lines do not intersect — $O(\mathfrak{U}_\beta) = 2$, while, if u coincides with the axis, $O(\mathfrak{U}_\beta) = 1$, and in any other case $O(\mathfrak{U}_\beta) = O(R)$.

Since by the symmetry operations $\hat{R}_k$ the surroundings of the individual atoms are also transformed, the indices of the individual atoms $\hat{R}_k x_i \in \mathfrak{X}_\alpha$ are identical. In view of the foregoing, the indices of these atoms related to the set $\mathfrak{U}_\beta$ of lines are also identical.

If $O(\mathfrak{X}_\alpha) = 1$ then x_i either constitutes the common boundary of the elements of $\mathfrak{U}_\beta$ (case A) or not (case B), see Fig. 1.

If $O(\mathfrak{X}_\alpha) = O(R)$ then two cases are possible:

(a) the elements of $\mathfrak{U}_\beta$ are radial with respect to the symmetry axis (type C) and either they are connected to the elements of $\mathfrak{X}_\alpha$ (type C_1) or do not touch them (type C_2),

(b) the elements of $\mathfrak{U}_\beta$ are axial with respect to the symmetry axis (type D) and either they connect all the elements of $\mathfrak{X}_\alpha$ (case D_1) or are connected to one (case D_2), or do not touch them (case D_3), see Fig. 1.

After performing the transformation $\mathbf{C} \rightarrow \mathbf{S}$ the following values for the elements S in the case of the different types are obtained:

type	A	B	C_1	C_2	D_1	D_2	D_3
$S_{\beta\alpha}$	$O(R)$	0	1	0	2	1	0

As we can realise on the basis of Fig. 1, the matrix elements $S_{\beta\alpha}$ are the indices of the representative x_i of the set $\mathfrak{X}_\alpha$ of points, related to the set $\mathfrak{U}_\beta$ of lines.

So, knowing the elements of S, the following can be stated with respect to the structural construction of the molecule [1]:

For the central construction the following sufficient (but not necessary) condition holds: S should contain only elements of value 1 and 0, there should be only one element of value $O(R)$, and S should be a 1×2 matrix.

The necessary condition of the central construction is that the sum of the elements of the column vector S_α of S should be $O(R)$, while the sum of the elements of all the other columns should be 1.

If the value of b elements of S is 2, then S contains at least b cycles, if $O(R) \neq 2$.

The transformation $\mathbf{S} \rightarrow \mathbf{C}$

The atoms of the molecule can be numbered in $n!$ different ways, whereas the valence lines can be numbered in $m!$ ones. Hence a given molecule may have different structural matrices of number $n!\,m!$, which can be transformed into each other by the respective structural matrices. In Fig. 2, the differently numbered forms of the same molecule can be seen. The following

relation obtains between the matrices $\mathbf{C}^a$ and $\mathbf{C}^b$:

$$\mathbf{C}^a = \mathbf{P}(3412)\ \mathbf{C}^b\,\mathbf{P}'(4132) \tag{7}$$

The circumstances are similar in the case of the matrices **S** belonging to the same R as well. Hence, in the case of a given molecule and a given symmetry element the number of the matrices **S** will be $w!\,q!$. In order to construct a matrix **S** as small as possible, it is suitable to choose a symmetry element such that $O(R)$ should be the possibly greatest.

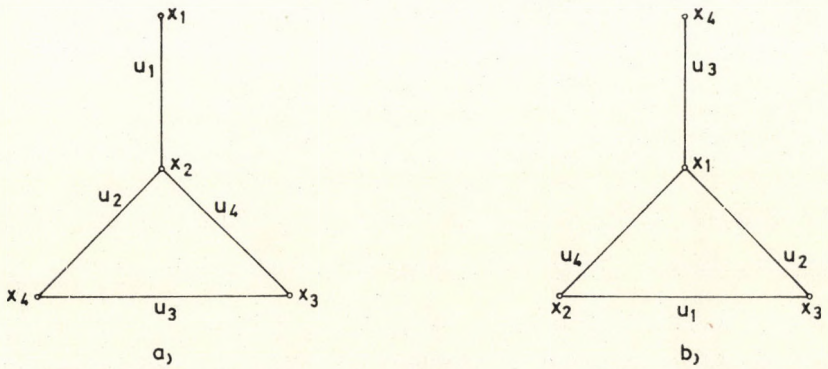

Fig. 2

With the knowledge of the quantities $O(R)$ as well as $O(\mathfrak{X}_\alpha)$ and $O(\mathfrak{U}_\beta)$ we have enough information for obtaining some matrix **C** of the molecule, if **S** is known. Therefore, in the case of using computers, **S** will be extended by the 0th column and row, respectively. The value of the 0,0 element is $O(R)$, the elements of the 0th row are the corresponding values of $O(\mathfrak{X}_\alpha)$ and those of the 0th column are the corresponding values of $O(\mathfrak{U}_\beta)$.

By the aid of the program given in this paper the algorithm of the transformation $\mathbf{S} \rightarrow \mathbf{C}$ is given, the sth element of $\mathfrak{X}_\alpha$ being numbered by $s + \sum_{r=1}^{\alpha-1} O(\mathfrak{X}_r)$ and the βth element of $\mathfrak{U}_t$ by $t + \sum_{r=1}^{\beta-1} O(\mathfrak{U}_r)$. Thus by the order of the symmetry atoms and lines in **S**, the order of the atoms and lines in **C** is unequivocally defined. That means that one of the possible matrices **C**, transformable into each other according to Eq. (7), has been unequivocally associated with **S**.

Hence

$$\check{\mathbf{u}} = \mathbf{Q}\,\mathbf{C}\,\hat{\mathbf{W}}^{-1}\,\check{\mathbf{x}}, \tag{8}$$

that is

$$\mathbf{S} = \mathbf{Q}\,\mathbf{C}\,\hat{\mathbf{W}}^{-1} \tag{9}$$

and

$$\mathbf{C} = \mathbf{Q}\ \mathbf{S}\,\hat{\mathbf{W}}^{-1} \tag{10}$$

Vector spaces defined on the skeleton of the molecules

The structural matrix has been obtained on the basis of the informations necessary for simulating the molecule structure with a computer (*i.e.* on the basis of the symmetry structural matrix). In order to obtain the relations between the inner coordinates of the molecule, *i.e.* the so-called redundancy conditions [3, 4, 5], the maximal chains [4] and cycles [5] of the molecule must be found. For working out the algorithms to determine these, we have to define some further quantities.

The skeleton $\mathfrak{V}$ of the molecule is the set of the atoms whose index is at least 2 [4]. The structural matrix $\mathbf{C}^{\vee}$ of the skeleton can be obtained from **C** while cancelling the columns where the sum of elements is 1, and cancelling from the matrix so obtained the rows for which the sum of the elements is 1. In a similar way the structural matrix $\mathbf{S}^{\vee}$ of the skeleton $\mathfrak{V}$ can be obtained from **S**.

In the following we will be concerned with quantities in connection with the skeleton of the molecule.

The valence lines u_j ($j = 1, 2, \ldots, \mu$, μ being the number of the rows of $\mathbf{C}^{\vee}$) and the atoms ($i = 1, 2, \ldots, \nu$, ν being the number of the columns of $\mathbf{C}^{\vee}$) of the skeleton should be numbered.

Let $\mathfrak{Y}$ be the set of all the subgraphs which can be defined on the skeleton. A binary vector space $\mathfrak{D}$ may be defined which is isomorphic to $\mathfrak{Y}$. Let us assign a vector e_j of dimension μ, its jth element being 1 whereas the others 0, to each valence line u_i of the skeleton.

Any subgraph $\mathfrak{Y}_k \leq \mathfrak{V}$ can be obtained as the sum (in the sense of set theory) of valence lines of number P (the atoms are considered as the zero dimensional cell of the parallelepiped of the subgraphs and should be disregarded). Let us number the subgraphs as well. Thus a subgraph $\mathfrak{Y}_k$ ($k = 1, 2, \ldots, P_k$) can be obtained as follows

$$\mathfrak{Y}_k = \bigcup_{j=1}^{P_k} u_j \tag{11}$$

The operation (11) can be performed by means of the image vectors e_j as well if introducing the logical (*i.e.* boolean) summation with respect to binary vectors. Thus some vector $d_k \in \mathfrak{D}$ of dimension μ can be written as

$$d_k = \sum_{j=1}^{P_k}{}' \,^{\text{Bool}}\, e_j \tag{12}$$

If we also introduce the logical multiplication between binary numbers, the binary vectors can be multiplied by some binary number ε_j ($\varepsilon_j = 0, 1$). By means of them the vectors d_k can be obtained as the linear combinations of

all the vectors e_j,

$$d_k = \sum_{j=1}^{\mu}{}^{\text{Bool}} \varepsilon_j \wedge e_j \tag{13}$$

By the expression (12) is shown that the transformation $\mathfrak{Y} \rightarrow \mathfrak{D}$ is consistent in operation. It can easily be seen that the vectors d_k constitute such a vector space of μ dimensions whose basis consists of the vectors e_j. Further, it is to be seen that $\mathfrak{D}$ is isomorphic to $\mathfrak{Y}$ since the transformation is consistent in operation and one to one correspondent:

$$\mathfrak{Y} \cong \mathfrak{D} \tag{14}$$

By means of the matrix $\mathbf{C}^{\vee}$ each vector d_k can be associated with a vector w_k:

$$w_k = \mathbf{C}^{\vee} d_k \tag{15}$$

With this relation the elements of **D** have been transformed into the vector space **W** of ν dimensions. This is not a one to one correspondence, the elements of w_k being non-negative integers. The components of the vectors w_k are the indices of the individual atoms, related to the subgraph $\mathfrak{Y}_k \in \mathfrak{Y}$. Let us denote the set of the image vectors w_k by $\mathfrak{W}^0$ ($\mathfrak{W}^0 \subset \mathfrak{W}$). $\mathfrak{D}$ and $\mathfrak{W}^0$ are isomorphic:

$$\mathfrak{D} \cong \mathfrak{W}^0 \tag{16}$$

Let us designate by $\mathfrak{Y}^1$ the set of those subgraphs $\mathfrak{Y}_k$ which can be simple paths (paths without branching that are connected and do not return to themselves); the image sets of $\mathfrak{Y}^1$ are $\mathfrak{D}^1$ and $\mathfrak{W}^1$. Let us denote by $\mathfrak{Y}^2$ the set of those subgraphs $\mathfrak{Y}_k$ which can be simple loops (cycles); the image sets of $\mathfrak{Y}^2$ are $\mathfrak{D}^2$ and $\mathfrak{W}^2$.

Determination of the cycles

A simple path can be each subgraph whose image vector w_k contains, besides elements of value 0 and 2, only two elements of value 1. However, not each of all such subgraphs is a simple path, namely, in case it is not connected, it may also contain simple loops (cycles). Thus first the cycles and then the simple paths must be found.

A cycle can be each subgraph whose image contains only elements of value 0 and 2. (These vectors w_k form the set $\mathfrak{W}^2(1)$.) Such a subgraph can consist of several disconnected cycles as well. The following algorithm serves for determining the cycles.

Let $w_1 \in \mathfrak{W}^2(1)$ be one of such vectors whose absolute value is the smallest among the elements of $\mathfrak{W}^2(1)$. To w_1 there corresponds surely a single cycle. After performing the operation

$$w_k - w_1 = w_k^1 \tag{17}$$

by means of every vector $w_k \in \mathfrak{W}^2(1)$, we obtain either vectors having only non-negative elements or vectors having negative elements, too. The original images of the latter do not contain the cycle $\mathfrak{Y}_1$. Let us denote the set of the vectors w_k belonging to these by $\mathfrak{W}^2(2)$. From the set $\mathfrak{W}^2(2)$ a vector of the least absolute value can again be chosen, which should be denoted by w_2. Then let us perform the subtractions of type (17) by means of the elements of the set $\mathfrak{W}^2(2)$. In case there are in the skeleton loops of number α, after the $(\alpha - 1)$th step there remains only a single vector $w_k \in \mathfrak{W}^2(\alpha)$, namely w_α. The images of the cycles become the vectors $w_1, w_2, \ldots, w_\alpha$.

Owing to the relation (16) the above algorithm can also be performed with the vectors $d_k \in \mathfrak{D}^2(1)$.

One obtains the measure of the connection between the cycles $\mathfrak{Y}_r, \mathfrak{Y}_s$ if the product of the corresponding vectors d_r and d_s, and w_r and w_s, respectively, are made.

For the valence lines:

$$\gamma_{rs}^d = e_r' \wedge d_s \,, \tag{18}$$

for the atoms:

$$\gamma_{rs}^w = w_r' w_s \tag{19}$$

If the two cycles have no common valence line then $\gamma_{rs}^d = 0$, if they have no common atom, i.e. the two cycles are not connected, then $\gamma_{rs}^w = 0$.

Determination of the simple paths and the building sets

The simple paths of the skeleton can be obtained with the following algorithm. The vectors $d_k \in \mathfrak{D}^1(1)$ which can be the images of simple paths are multiplied successively by the vectors $d_l \in \mathfrak{D}^2$:

$$\varrho_{kl} = d_k' \wedge d_l \tag{20}$$

If some vectors d_k have been successively multiplied by all the vectors d_l and if for each of the products thus obtained there holds

$$\varrho_{kl} < d_1' \wedge d_1 \, (l = 1, 2, \ldots, \alpha; d_1 \in \mathfrak{D}^2) \tag{21}$$

then $\mathfrak{Y}_k$ does not contain any cycle. Thereby we have chosen the elements of $\mathfrak{D}^1$.

Chains will be called such subgraphs which are connected and the indices of whose atoms, related to the subgraph, are not greater than 2; *i.e.* chains are called the original images of the set $\mathfrak{D}(1) = \mathfrak{D}^1 \cup \mathfrak{D}^2$.

A building set will be called such a set of independent chains (*i.e.* of chains having at the most common atoms) which covers the skeleton **V** completely and contains a minimum number of chains. This minimum number of chains we will call chain number (P) [5]. Some molecules may, of course, have several building sets, too.

The chain number and the building sets can be obtained according to the following algorithm.

(a) Let $\mathfrak{U}^2$ be empty: $\mathfrak{U}^2 = \mathbf{O}$. Thus the skeleton does not contain any cycle, *i.e.* it is a tree. The chain number P of this tree is

$$\varrho = 1 + \sum_{r=1}^{\nu} (q_r - 1), \tag{22}$$

where

$$q_r = \text{ent}\left(\frac{b_r^{\vee} + 1}{2}\right) \tag{23}$$

and $b_r^{\vee}$ is the index of the atom x_r, related to the skeleton.

Proof. Let the number of atoms be 2. Then the tree obviously contains only one path, and on the basis of Eq. (22) also $P = 1$. Let the number of atoms be $\nu - 1$ and let the chain number be $1 + \sum_{r=1}^{\nu-1} (q_r - 1)$. If soldering the νth atom to the skeleton by some valence line we have two possible cases:

When soldering to an atom x of the odd index $b_r^{\vee}$, one of the paths starting from x becomes a transit path and, since b was odd, $q_r^{\vee}$ does not change. On the other hand, $q_\nu = 1$, also because of this fact P does not change.

When soldering to an atom x_r of the even index $b^{\vee}$, the number of the paths starting from x_r increases by one (the value of q_r increases by one). Being $q_\nu = 1$, its value does not affect P, thus in this case also $P_\nu = P_{\nu-1} + 1$.

Thereby Eq. (22) has been proved.

(b) $U^2 \neq O$. In this case we could not give a closed relation like Eq. (22) for determining the chain number. To determine P the following algorithm can be used.

The vectors $d_k \in \mathfrak{D}^1 \cup \mathfrak{D}^2$ are considered as the different permutations with repetition of the numbers 0 and 1. Let us number them in the natural order of the permutations. Let us then form all the possible combinations without repetition of the vectors d_k thereby numbered. All the d_r vectors in the combination will now be successively multiplied by each vector $d_k \in \mathfrak{D}^1 \cup \mathfrak{D}^2$.

These multiplications are performed with all the combinations, in the natural order of the combinations, according to increasing class numbers. In the Pth class there will be at least one combination where no vector d_k can be found any more whose product with each vector d_r in the combination vanishes. This means that no chain d_k exists any more which is independent of the chains d_r in the combination. The chain number is given by P. The elements of the combinations taken P at a time, to which no independent chain has been found, are equivalent building sets.

Thus, by the algorithm not only the chain number but also the building sets are given.

In the case when only one building set and the chain number are needed, we can obtain them in a more simple way than above: by means of an algorithm similar to that used for finding the cycles.

Let $\mathfrak{D}(1) = \mathfrak{D}^1 \cup \mathfrak{D}^2$ be the set of the vectors that are sure to be chains. From among them let us choose that of the greatest absolute value. Let this be d_1. Now let us make the products

$$\zeta_{1,k} = d_1' \wedge d_k \tag{24}$$

with all the vectors $d_k \in \mathfrak{D}(1)$. Those d_k for which $\zeta_{1,k} = 0$ are independent of d_1. From the set $\mathfrak{D}(2)$ of the latter now let us seek one of the vectors of the greatest absolute value: d_2. Let us form the products

$$\zeta_{2,k} = d_1' \wedge d_k \quad \left(d_k \in \mathfrak{D}(2)\right) \tag{25}$$

etc., till we obtain the empty set: $\mathfrak{D}(P + 1)$. The set of the vectors $d_1, d_2, \ldots, d_P$ constitutes a building set.

The algorithms mentioned in the two latter sections render it possible to simulate the cycles and maximum chains with the aid of an electronic computer. The symmetry structural matrix contains all the informations necessary for these computations. A computer can be needed when determining the redundancy conditions [3, 4, 5], as well as the elements of WILSON's G matrix and those of F matrix belonging to the redundant coordinates, respectively.

Procedure for the transformation S → C

```
procedure SCTRANS (S, q, w, C);
comment the procedure SCTRANS transforms the randed symmetry structural matrix S[0:q,
      0:w] into the structural matrix C[1:m, 1:n], where m is the sum of elements of the
      zero-th column while n is that of the zero-th row of S;
value q, w; integer q, w; integer array S, C;
begin integer alpha, beta, a, b, k, l;
a: = 0;
for alpha: = 1 step 1 until q do
begin b: = 0;
for beta: = 1 step 1 until w do
begin
if S[alpha, 0] = 1 then
begin k: = a + 1;
if S[0, beta] = 1 then
begin l: = b + 1; C[k, l]: = S[alpha, beta]
end
else for l: = b + 1 step 1 until b + S[0, beta] do
C[k, l]: = S[alpha, beta];
goto ex
end S[alpha, 0] = 1
else for k: = a + 1 step 1 until a + S[alpha, 0] do
if S[0, beta] = 1 then
begin l: = b + 1;
C[k, l]: = S[alpha, beta] + S[0, 0]
end
else
begin for l: = b + 1 step 1 until b + S[0, beta] do
C[k, l]: = 0;
if S[alpha, beta] = 1 ∨ S[alpha, beta] = 2 then
C[k, k + b — a]: = 1;
if S[alpha, beta] = 2 then
begin
if k ≠ S[alpha, 0] + a then
C[k, k + b — a + 1]: = 1
else C[k, b + 1]: = 1
end
end S[alpha, 0] = S[0, 0];
ex:b: = 1
end beta;
a: = k
end alpha
end SCTRANS;
```

REFERENCES

1. BILLES, F.: Acta Chim. Acad. Sci. Hung. **51,** 295 (1967)
2. BERGE, G.: Théorie des graphes et ses applications. Dunod, Paris, 1963
3. BILLES, F.: Acta Chim. Acad. Sci. Hung. **45,** 285 (1965)
4. BILLES, F.: Acta Chim. Acad. Sci. Hung. **46,** 45 (1965)
5. BILLES, F.: Acta Chim. Acad. Sci. Hung. **49,** 97 (1966)

Ferenc BILLES; Budapest XI., Műegyetem rkp. 3.

Acta Chimica Academiae Scientiarum Hungaricae, Tomus 62 (1), pp. 19—26 (1969)

A QUANTITATIVE CHARACTERIZATION OF MIXING

K. SEITZ and R. TŐRÖS

(Research Institute for Technical Chemistry of the Hungarian Academy of Sciences Budapest)

Received April 10, 1968

For the quantitative characterization of the degree of mixing a descriptive scale was proposed which characterizes the completely mixed system, and the unmixed system, respectively with values (1, $+\infty$). The measure of the degree of mixing of any system is a positive integer which can be found with the help of a nomogram.

Introduction

As known, heat transfer processes, in the sectional heating of packed columns where the cooling medium is in motion and the packing is stationary, are described by differential equations proposed by ANZELIUS [1]. The description of the system consists in statements on the spatial heat-distribution of the heating (cooling) gas and of the granular (solid) packing, as a function of time.

The equations are

$$\frac{\partial T'}{\partial t} + v' \frac{\partial T'}{\partial x} = -b(T' - T) \quad \text{(I)}$$

$$\frac{\partial T}{\partial t} = a(T' - T) \quad \text{(II)}$$

where T = temperature of the medium to be heated (cooled)
T' = temperature of the heating (cooling) medium
a, b = constants that contain heat-transfer coefficients
x and t = coordinates, respectively, of space and time.

A less exact, but much more simple description of the system is possible if the entire heating medium and the entire medium to be heated are severally considered as homogeneous in respect to temperature. Then the transfer equations can be arrived at in the following way.

Let the specific heat of the solid packing be C, then the specific heat of a unit volume is γ, C. The overall volume of the packing is $L \cdot F(1 - \varepsilon)$,

where L = length of the apparatus and F = its cross section; ε = the proportion of voids. Heat content of the solid packing is $\gamma \cdot C \cdot L \cdot F(1-\varepsilon) \cdot T$.

The heat transferred on the surface of the packing can be expressed by the surface area and the heat transfer coefficient, further by the difference between the temperature of the packing and that of the gas. If the particles of the packing are spheres, the total surface is $v \cdot 4\, r^2\, \pi$, where v is the number of particles.

$v = \dfrac{3FL(1-\varepsilon)}{4r^3\pi}$. Thus the surface area is

$$\frac{3FL(1-\varepsilon)}{4r^3\pi} 4r^2\pi = \frac{3FL(1-\varepsilon)}{r}$$

The heat flow into (out of) the solid packing

$$j = \alpha \frac{3FL(1-\varepsilon)}{r}(T' - T)$$

Change in the heat content of the packing in unit time is

$$\gamma CL\, F(1-\varepsilon)\frac{dT}{dt} = \alpha \frac{3z}{v} FL(1-\varepsilon)(T' - T)$$

Here z describes the correction of Newton's heat transfer coefficient. In a simpler form the equation can be written as follows:

$$\frac{dT}{dt} = \frac{3\alpha z}{\gamma C v}(T' - T) \ldots\ldots\ldots\ldots\ldots \quad \text{(III)}$$

The equation valid for the gas phase is arrived at in a similar manner. The heat transferred by the gas is $\gamma' C' v'(T_0' - T')$, where T_0 is the temperature of the gas entering into the system. This heat alters the heat content both of the gas and the packing, so that

$$F_k \gamma' C' v'(T_0' - T') = V_g \gamma' C' \frac{dT}{dt} + z\alpha \frac{3FL(1-\varepsilon)}{v}(T' - T) \ldots\ldots \quad \text{(IV)}$$

where F_k = free cross section = εF

$$F_k v' = \varepsilon F \frac{v_0}{\varepsilon} = v_0 F$$

V_g = free volume = εFL

Considering the connexions in (IV), we have

$$v'\varepsilon FC'\gamma'(T'_o - T) = z\alpha \frac{3FL(1-\varepsilon)}{v}(T' - T) + C'\gamma' FL(1-\varepsilon)\frac{dT'}{dt'},$$

or

$$\frac{dT'}{dt} + \frac{3\alpha z}{vC'\gamma'}(T' - T) = \frac{v'\varepsilon}{L(1-\varepsilon)}(T'_o - T') \ldots . \qquad \text{(V)}$$

Equations (III) and (V) are analogues of equations (I) and (II).

In descriptions of mixing apparatus these two pairs of equations can be considered as two limiting cases: ANZELIUS' equations stand for the completely unmixed system, equations (III) and (V) for a system completely mixed and perfect homogeneity has been attained therein. A system when being mixed cannot be considered as completely mixed, only an aggregate of several completely mixed zones [2] perpendicular to the direction of flow. Reference to this fictitious construction is made thereby the data that can be measured at the exit port — temperature of the cooling, or heating, gas — are assigned to one of the $n = 1, 2$ divisions within the systems subdivided in theory in r zones. This number n is called the mixing unit number of a mixer.

In what follows we attempt to demonstrate the calculation, and then a nomogram for it will be proposed.

It is well known that the degree of mixing can be characterized through the mixing coefficient, respectively through the turbulent diffusion constant. We are well aware that the mixing unit number is not suitable for the expression of a general correlation [3].

It would be very gratifying if a relationship between the degree of mixing as viewed by us and probability calculus, respectively the entropy concept of information theory, could be established. However, such a connexion is but illusory because the interpretation of the entropy of mixing requires random motion of the single particles within a multitude, whereas a mixer deterministically affects the configuration of the particles of the packing. Thus neither a forced generalization nor a supposition of a stochastic scheme will here be resorted to in order to suggest any connexions.

Mathematical statement of the problem

For the description of a system composed of n completely mixed zones the calculation which gives equations (III) and (V) as a result is utilized. Let the heat balance equations for the i-th zone ($i = 1, 2, \ldots, n$) be considered. Equation (V)

$$\frac{dT_i}{dt} = \frac{3\alpha z}{\gamma C v}(T'_i - T_i) \qquad i=1, 2, \ldots, n \quad (1)$$

In equation (III) it must be noted that the free volume of the i-th zone is the n-th part of the total free volume, thus instead of $F \cdot L(1 - \varepsilon)$ we write $\frac{FL(1-\varepsilon)}{n}$, further, since heat transmitted refers to the surface area of the packing in the zone, instead of

$$\frac{3\alpha z F (1-\varepsilon) L}{v} \quad \text{we write} \quad \frac{1}{n} \frac{3\alpha F z L (1-\varepsilon)}{v}.$$

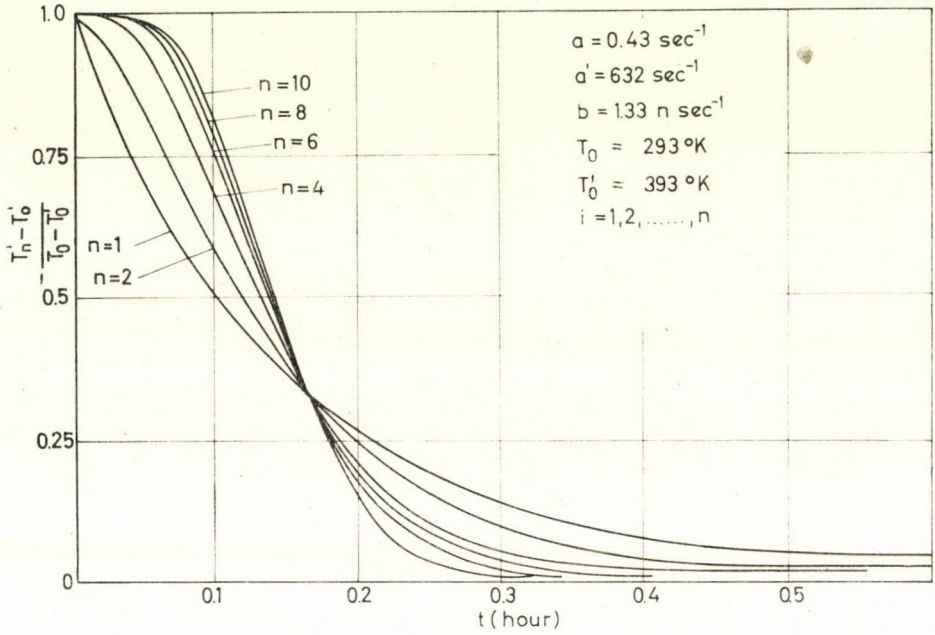

Fig. 1

Thus equation (V) reads

$$\frac{dT_i'}{dt} + \frac{3\alpha z}{\gamma' C' v}(T_i' - T_i) = \frac{nv'\varepsilon}{L(1-\varepsilon)}(T_{i-1}' - T_i') \qquad i=1,2\ldots,n \qquad (2)$$

Equations (1) and (2) give $2 \cdot n$ equations for the $T_1, T_2, \ldots, T_n$ and $T_1', T_2', \ldots$ $\ldots, T_n'$ unknown functions. The initial conditions attached to the system of equations are the following:

$$\begin{aligned} T_i(0) &= T_o \\ T_i'(0) &= T_{oi}' \end{aligned} \qquad (3)$$

T_{oi}' data are calculated from the residence time of the gas. In what follows, only the process of heating will be discussed since that of cooling s perfectly similar.

It will be expected that in the course of the process $T_i'(t) \to T_o'$, if $t \to \infty$, $T_i(t) \to T_o'$. With

$$\frac{3\alpha z}{\gamma C v} = a, \quad \frac{3\alpha z}{\gamma' C' v} \quad a', \quad \text{and} \quad \frac{nv'}{L} \cdot \frac{\varepsilon}{1-\varepsilon} = b,$$

the system of differential equations. when written in detail, will have the form

$$\begin{aligned}
\frac{dT^1}{dt} &= -aT_1 + 0 + \ldots + 0\, aT_1' + 0 + \ldots + 0 \\
\frac{dT_2}{dt} &= 0 - aT_2 + 0 + \ldots + 0 + aT_2' + 0 + \ldots + 0 \\
&\ldots\ldots \\
\frac{dT_n}{dt} &= 0 + 0 + \ldots - aT_n + 0 + \qquad \ldots + aT_n' \\
\frac{dT_1'}{dt} &= a' T_1 + 0 + \ldots + 0 - (a' + b) T_1' + \qquad \ldots + 0 \\
\frac{dT_2'}{dt} &= 0 + a'T_2 + \ldots + 0 + bT_1' - (a' + b)T_2' \quad \ldots + 0 \\
\frac{dT_n'}{dt} &= 0 + 0 + \ldots + a'T_n + 0 + \ldots + bT_{n-1}' - (a' + b)T_n'
\end{aligned} \tag{4}$$

and the matrix of the system is

$$\left[\begin{array}{l|l}
-a, 0, 0, \ldots\ldots, 0, & a, 0, 0, \ldots\ldots\ldots, 0 \\
0, -a, 0, \ldots\ldots, 0, & 0, a, 0, \ldots\ldots\ldots, 0 \\
\quad \ldots\ldots & \quad \ldots\ldots \\
\quad \ldots\ldots & \quad \ldots\ldots \\
\quad \ldots & \quad \ldots \\
0, 0, \ldots\ldots\ldots, -a, & 0, 0, \ldots\ldots\ldots\ldots, a \\
\hline
a', 0 \ldots\ldots\ldots, 0, & -(a' + b), 0, \ldots, 0 \\
0, a', \ldots\ldots\ldots, 0, & b, -(a' + b), \ldots, 0 \\
\quad \ldots & \quad \ldots \\
\quad \ldots\ldots & \quad \ldots\ldots \\
\quad \ldots\ldots & \quad \ldots\ldots \\
0, 0, \qquad\qquad a' & 0, 0, \ldots, b, -(a' + b)
\end{array}\right] \tag{5}$$

Solution of the system of equations

The solution of system (4) of equations consists in the determination of the eigenvalues of matrix (5), then in the applications of the Hermite polynomials.

Obviously, matrix **A** can be considered as the hypermatrix of four $\mathbf{A}_1$, $\mathbf{A}_2$, $\mathbf{A}_3$ and $\mathbf{A}_4$ matrices, each of n dimensions, thus

$$\mathbf{A} = \begin{bmatrix} \mathbf{A}_1, \mathbf{A}_2 \\ \mathbf{A}_3, \mathbf{A}_4 \end{bmatrix} \tag{6}$$

further

$$\begin{bmatrix} \mathbf{A}_1, \mathbf{A}_2 \\ \mathbf{A}_3, \mathbf{A}_4 \end{bmatrix} = \begin{bmatrix} \mathbf{E} & \mathbf{0} \\ \mathbf{A}_3\mathbf{A}_1^{-1}, & E \end{bmatrix} \cdot \begin{bmatrix} \mathbf{A}_1 & \mathbf{A}_2 \\ \mathbf{0}, \mathbf{A}_4 - \mathbf{A}_3\,\mathbf{A}_1^{-1}\,\mathbf{A}_2 \end{bmatrix} \tag{7}$$

$$\text{where } \mathbf{A}_1 = \begin{bmatrix} -(a+\lambda), 0, \ldots, 0 \\ 0, -(a+\lambda), \ldots, 0 \\ \ldots \\ \cdot\cdot \\ \cdot \\ 0, 0, \quad -(a+\lambda) \end{bmatrix} \quad \mathbf{A}_2 = \begin{bmatrix} a, 0, \ldots, 0 \\ 0, a, \ldots, 0 \\ \\ \\ \\ 0, 0, \ldots, a \end{bmatrix} \quad (8) - (8')$$

$$\mathbf{A}_3 = \begin{bmatrix} a', 0, \ldots, 0 \\ 0, a', \ldots, 0 \\ 0, 0, \ldots, a' \end{bmatrix} \quad \mathbf{A}_4 = \begin{bmatrix} -\lambda - (a'+b), 0, \ldots, 0 \\ b, -\lambda - (a'+b), \ldots, 0 \\ 0, 0, \quad , b, -\lambda - (a'+b) \end{bmatrix} \quad (9) - (9')$$

0, and **E** are, respectively, zero- and unit-matrices of n dimensions; λ is the eigenvalue parameter. (7) can be transformed further, since

$$\mathrm{Det}\begin{bmatrix} \mathbf{A}_1, \mathbf{A}_2 \\ \mathbf{A}_3, \mathbf{A}_4 \end{bmatrix} = \mathrm{Det}\begin{bmatrix} \mathbf{E} & \mathbf{0} \\ \mathbf{A}_3\mathbf{A}_1^{-1}, & \mathbf{E} \end{bmatrix} \cdot \mathrm{Det}\begin{bmatrix} \mathbf{A}_2 & \mathbf{A}_2 \\ \mathbf{0}, \mathbf{A}_4 - \mathbf{A}_3\mathbf{A}_1^{-1}\,\mathbf{A}_2 \end{bmatrix}, \tag{10}$$

consequently

$$\mathrm{Det}\begin{bmatrix} \mathbf{A}_1, \mathbf{A}_2 \\ \mathbf{A}_3, \mathbf{A}_4 \end{bmatrix} = \mathrm{Det}\left[\mathbf{A}_1\mathbf{A}_4 - \mathbf{A}_1\mathbf{A}_3\mathbf{A}_1^{-1}\mathbf{A}^2\right] \tag{11}$$

$$\mathbf{A}_1\mathbf{A}_4 = \begin{bmatrix} -(a+\lambda)(-a'-b-\lambda), 0, \ldots\ldots\ldots\ldots, 0 \\ -(a+\lambda)\,b, -(a+\lambda)(-a'-b-\lambda)\ \ 0, \ldots, 0 \\ \cdot\cdot \\ \ldots \\ 0, 0, \ldots, -(a+\lambda)\,b, -(a+\lambda)(-a'-b-\lambda) \end{bmatrix} \tag{12}$$

Since $\mathbf{A}_1$ and $\mathbf{A}_3$ are commutative

$$\mathbf{A}_1\mathbf{A}_3\mathbf{A}_1^{-1}\mathbf{A}_2 = \mathbf{A}_3\mathbf{A}_2 = \begin{bmatrix} aa', 0, \ldots, 0 \\ 0, aa', \ldots, 0 \\ 0, 0, \ldots, aa' \end{bmatrix} \tag{13}$$

and

$$\mathbf{A}_1\mathbf{A}_4 - \mathbf{A}_1\mathbf{A}_3\mathbf{A}_1^{-1}\mathbf{A}_2 = \begin{bmatrix} -(a+\lambda)(-a'-b-\lambda) - aa', 0, \ldots, 0 \\ -(a+\lambda)b, -(a+\lambda)(a'-b-\lambda) - aa', 0 \\ \cdot\cdot \\ \cdots\cdot \\ \cdots\cdots \\ 0, 0, -(a+\lambda)b, -(a+\lambda)(-a'-b-\lambda) - aa' \end{bmatrix} \tag{14}$$

$$\text{Det } [\mathbf{A}_1\mathbf{A}_4 - \mathbf{A}_1\mathbf{A}_3\mathbf{A}_1^{-1}\mathbf{A}_2] = [(a+\lambda)(a'+b+\lambda) - aa']^n \tag{15}$$

After rearrangement, the secular equation takes the form:

$$D(\lambda) = [\lambda^2 + (a + a' + b)\lambda + ab]^n \tag{16}$$

The equation has two real n-fold radicals, each is an eigenvalue of n-fold multiplicity of the problem. The eigenfunctions belonging to the eigenvalues λ_1 and λ_2 will not be determined; the solution will be written directly.

Any regular function $f(\mathbf{A})$ of matrix $\mathbf{A}$ can be produced as follows:

$$f(\mathbf{A}) = \sum_{k=1}^{2}{}' \sum_{j=1}^{n} [\alpha_{kj}(\mathbf{A} - \lambda_k \mathbf{E})^{j-1}] (\mathbf{A} - \lambda_{k+1}\mathbf{E})^n_{(k+2\to k)} \tag{17}$$

where $\mathbf{E}$ is a unit matrix of $2n$ dimensions and

$$\alpha_{kj} = \frac{1}{(j-1)!}\left[\frac{f(\lambda)}{(\lambda-\lambda_k)^n}\right]^{(j-1)}_{\substack{\lambda=\lambda_{k+1} \\ k=1,2,(k+2\to k) \\ j=1,2,\ldots,n}} \tag{18}$$

When now $f(\mathbf{A}) = e^{t\mathbf{A}}$, then, using the Leibniz rule

$$\alpha_{kj} = \frac{1}{(j-1)!} e^{\lambda_k t} \sum_{i=0}^{j-1} (-1)_j \binom{j-1}{i} n(n+1)\ldots(n+i-1)(\lambda_k - \lambda_{k+1})^{-(n+i)} t^{j-i-1}_{\substack{j=1,2\ldots,n \\ k=1,2,(k+2\to k)}} \tag{19}$$

In (19) we change index i to $j - i - l = s$, and, as abbreviations we introduce

$$C^{(1)}_{sjn} = (-1)^{j-1-s} \begin{pmatrix} j-1 \\ j-1-s \end{pmatrix} n(n+1)\ldots(n+j-s-2)\,(\lambda_1-\lambda_2)^{s+1-(n+j)}\,\frac{1}{(j-1)!}$$

$$C^{(2)}_{sjn} = (-1)^{s+1-(n+j)}\,C^{(1)}_{sjn} \tag{20}$$

$$0 \leqq s \leqq j-1 \qquad 1 \leqq j \leqq n.$$

then

$$\alpha_{kj} = e^{\lambda_k t} \sum_{s=o}^{j-1} C^{(k)}_{sjn}\, t^s, \quad (k = 1, 2)$$

The solution of equation

$$\frac{dT}{dt} = \mathbf{A}\,T \tag{21}$$

is

$$T = e^{\mathbf{A}t}\,T_0 \tag{22}$$

Using formulas (17)...(20) we get

$$e^{At} = \sum_{k=1}^{2} e^{\lambda_k t} \sum_{r=o}^{n-1} \left[\sum_{p=r+1}^{n} C^{(k)}_{rpn}\,(\mathbf{A} - \lambda_k \mathbf{E})^{p-1} \right] t^r\,(\mathbf{A} - \lambda_{k+1}\mathbf{E})^n \tag{23}$$

Thus for T the general solution is

$$T(t) = \sum_{k=1}^{2} e^{\lambda_k t} \sum_{r=o}^{n-1} \left[\sum_{p=r+1}^{n} C^{(k)}_{rpn}(\mathbf{A} - \lambda_k \mathbf{E})^{p-1} \right] t^r\,(\mathbf{A} - \lambda_{k+1}\mathbf{E})^n\,T_o \tag{24}$$

Owing to the many parameters, the illustration of the analytical solution is cumbersome, therefore we present for a typical set of data diagrams constructed with an analogue computer.

With the discussion of this calculation method we aimed at a comparison of geometrically similar mixing apparatus, and at their characterization by a scale of values defined by two standard ideal limiting cases.

We are indebted to Mr G. SASVÁRI for having drawn our attention to this problem, and for valuable suggestions, further to Mr J. GYÜRKI for having carried out the numerical calculations.

REFERENCES

1. ANZELIUS, A.: Z. angew. Math. Mech. **6**, 291 (1926)
2. GILLILAND, E. R.: Ind. Eng. Chem. **44**, 218 (1952)
3. BLICKLE, T.: Apparatus, Application, and Calculations of Fluidization (in Hungarian). Budapest, Akadémiai Kiadó, 1963

Károly SEITZ
Róbert TŐRÖS
Budapest XI., Budafoki út 47.

Acta Chimica Academiae Scientiarum Hungaricae, Tomus 62 (1), pp. 27—39 (1969)

KINETISCHE ANALYSE EINIGER FOLGEREAKTIONEN, V

AUTOKATALYTISCHE REAKTIONEN

T. KELEN, F. TÜDŐS* und Gy. GALAMBOS*

*(Forschungsinstitut für die Plastindustrie, Budapest und *Zentralforschungsinstitut für Chemie der Ungarischen Akademie der Wissenschaften, Budapest)*

Eingegangen am 19. September 1968

Es wurde die kinetische Analyse der autokatalytischen Reaktionssysteme $A \rightarrow E$, $A(+E) \rightarrow E(+E)$; $A + A \rightarrow E$, $A(+E) \rightarrow E(+E)$; $A + B \rightarrow E$, $A(+E) \rightarrow$ $\rightarrow E(+E)$ sowie die Behandlung der empirischen Differentialgleichung der Autokatalyse und die Prüfung der möglichen Ursachen der Ausbildung S-förmiger Konversionskurven durchgeführt. Es wurde festgestellt, daß der S-förmige Ablauf einer Endprodukt-Konversionskurve nur dann eine autokatalytische Reaktion anzeigt, wenn auch die Konversionskurve des Ausgangsstoffes S-förmig ist (Unterschied von den einfachen Folgereaktionen) und kein vom Endprodukt abweichendes Zwischenprodukt während der Reaktion sich anhäuft (Unterschied von den konkurrenten Folgereaktionen).

Der III. und IV. Teil unserer Mitteilung [1, 2] beschäftigte sich mit der kinetischen Behandlung der sog. konkurrenten Folgereaktionen. Das sind Prozesse, bei denen das im Primärschritt entstandene Zwischenprodukt (C) mit dem Stoff (A) weiterreagiert, aus welchem es entstanden ist. Sofern die Geschwindigkeit des zweiten Reaktionsschrittes größer ist als die des ersten, so ist der Prozeß durch das Zwischenprodukt quasi katalysiert. Dieser Reaktionstyp kann — vom Gesichtspunkt der Abnahme des Ausgangsstoffes — als autokatalytisch angesehen werden.

Als typische Fälle der autokatalytischen Reaktionen sind jedoch jene konkurrenten Folgereaktionen anzusehen, bei denen das im Primärschritt entstandene »Zwischenprodukt« (C) mit dem Endprodukt (E) identisch ist. Im Falle dieser Reaktionen repräsentiert der katalytische Effekt (hinsichtlich der Bildung des Endproduktes) wirklich »auto«-Katalyse: das Erscheinen des Endproduktes beschleunigt seine eigene Bildung.

In der vorliegenden Arbeit befassen wir uns mit der kinetischen Analyse der folgenden Systeme:

$$A \rightarrow E,\ A(+E) \rightarrow E(+E) \tag{1}$$

$$A + A \rightarrow E,\ A(+E) \rightarrow E(+E) \tag{2}$$

$$A + B \rightarrow E,\ A(+E) \rightarrow E(+E) \tag{3}$$

sowie mit der Behandlung der empirischen Differentialgleichung der Autokatalyse und mit der Prüfung der möglichen Ursachen der Ausbildung S-förmiger Konversionskurven (das Auftreten solcher Kurven wurde von vielen Autoren ausschließlich mit dem autokatalytischen Charakter des Prozesses interpretiert).

1. Das System A → E, A(→E) → E(+E)

Es seien die geschwindigkeitbestimmenden konsekutiven Schritte der untersuchten chemischen Reaktion die folgenden Prozesse erster und zweiter Ordnung:

$$A \rightarrow E + \ldots \tag{4}$$

$$A(+E) \rightarrow E(+E) + \ldots \tag{5}$$

Die zur Entstehung von je einem Mol des Endproduktes E laut (4) verbrauchte Menge des Stoffes A sei a_1 Mol, die bei der Reaktion von je einem Mol des Endproduktes E laut (5) verbrauchte Menge des Stoffes A sei a_2, ferner sei mit e die molare Menge des Endproduktes E bezeichnet, die laut (5) entstanden ist. Die jeweiligen Konzentrationen der verschiedenen Substanzen seien mit den entsprechenden großen Buchstaben (A, E) bezeichnet. Mit Hilfe dieser Bezeichnungen können die Änderungsgeschwindigkeiten der in den Reaktionen (4) und (5) teilnehmenden Substanzen wie folgt aufgeschrieben werden:

$$-\frac{dA}{dt} = a_1 k_1 A + a_2 k_2 AE \tag{6}$$

$$\frac{dE}{dt} = k_1 A + (e - 1) k_2 AE \tag{7}$$

Dieses Differentialgleichungssystem ist formell dem im Falle von konkurrenten Folgereaktionen $A \rightarrow C$, $A + C \rightarrow E$ abgeleiteten System ähnlich — s. [2], Zusammenhänge (4) und (5). Die Behandlung des Systems kann auf die gleiche Weise erfolgen — für das autokatalytische System s. ausführlich in [7].

2. Das System A + A → E, A(+E) → E(+E)

Es seien die geschwindigkeitbestimmenden konsekutiven Schritte der untersuchten chemischen Reaktion die folgenden Prozesse zweiter Ordnung:

$$A + A \rightarrow E + \ldots \tag{8}$$

$$A(+E) \rightarrow E(+E) + \ldots \tag{9}$$

Die Änderungsgeschwindigkeiten der an den Reaktionen teilnehmenden Stoffe können dann, durch Anwendung der in Punkt 1 angegebenen Bezeichnungen, folgend aufgeschrieben werden:

$$-\frac{dA}{dt} = a_1 k_1 A^2 + a_2 k_2 AE \tag{10}$$

$$\frac{dE}{dt} = k_1 A^2 + (e-1)\, k_2 AE \tag{11}$$

Dieses Differentialgleichungssystem ist formell dem im Falle von konkurrenten Folgereaktionen $A + A \rightarrow C$, $A + C \rightarrow E$ abgeleiteten System ähnlich — s. [1], Zusammenhänge (9) und (10). Die Behandlung des Systems kann auf gleiche Weise erfolgen — für das autokatalytische System s. ausführlich in [7].

3. Das System A + B → E, A(+E) → E(+E)

Es seien die geschwindigkeitbestimmenden konsekutiven Schritte der untersuchten chemischen Reaktionen die folgenden Prozesse zweiter Ordnung:

$$A + B \rightarrow E \tag{12}$$

$$A(+E) \rightarrow E(+E) + \ldots \tag{13}$$

Die zur Entstehung von je einem Mol des Endproduktes E laut (12) verbrauchte Menge des Stoffes B sei b Mol (die jeweilige Konzentration sei mit B, die Anfangskonzentration mit B_0 bezeichnet, die anderen Bezeichnungen stimmen mit den in Punkt 1 gebrauchten überein), dann können die Änderungsgeschwindigkeiten der in den Reaktionen teilnehmenden Substanzen wie folgt aufgeschrieben werden:

$$-\frac{dA}{dt} = a_1 k_1 AB + a_2 k_2 AE \tag{14}$$

$$-\frac{dB}{dt} = b k_1 AB \tag{15}$$

$$\frac{dE}{dt} = k_1 AB + (e-1)\, k_2 AE \tag{16}$$

Dieses Differentialgleichungssystem ist formell dem im Falle von konkurrenten Folgereaktionen $A + B \rightarrow C$, $A + C \rightarrow E$ abgeleiteten System ähnlich — s. [2], Zusammenhänge (36—38). Die Behandlung des Systems kann auf gleiche Weise erfolgen — für das autokatalytische System s. ausführlich in [7].

4. Die empirische Differentialgleichung der Autokatalyse

Zur Beschreibung kinetischer Kurven von zunehmendem Charakter wurde die empirische Differentialgleichung der Autokatalyse oft angewendet:

$$\frac{d\xi}{dt} = K\xi^{\mu}(1-\xi)^{\nu} \tag{17}$$

Hier bedeutet ξ die Konversion und K die Geschwindigkeitskonstante des Prozesses, μ und ν sind aber empirisch erhaltene Reaktionsordnungen. Diese Gleichung sagt kaum etwas über den Mechanismus des Prozesses aus; so zum Beispiel beschreibt sie auch viele verzweigte Kettenreaktionen gut [4], obwohl diese Prozesse nicht unter Autokatalyse ablaufen. Die Gleichung (17) gelangt auch für die »physikalische« Autokatalyse zur Anwendung; in diesen Fällen sind die »Reaktionsordnungen« μ und ν aus der Molekularität der Prozesse nicht abzuleiten, so können sie beliebige Werte aufweisen [5].

Die Bedingung der Anwendbarkeit der empirischen Gleichung (17) ist, daß die Konversion auch am Anfang des Prozesses nicht Null, d. h. die Bedingung für den Anfangswert der Konversion ($t = 0$)

$$\xi_0 \neq 0 \tag{18}$$

erfüllt sei. Widrigenfalls könnte der Prozeß nicht beginnen.

Die Zeitabhängigkeit der Konversion kann mit der unvollständigen Beta-Funktion — siehe zum Beispiel [3] — angegeben werden, welche nach Trennung der Variablen und nach Integrieren aus (17) zu gewinnen ist:

$$\Theta = K \cdot t = B_{\xi}[1-\mu, 1-\nu] - B_{\xi_0}[1-\mu, 1-\nu] \tag{19}$$

Wie einer der Verfasser (in Verbindung mit der Kinetik der Polymerisation von N-Vinylcarbazol in fester Phase) bereits gezeigt hat [5], kann die Lösung der Differentialgleichung (17) im Falle einiger spezieller Werte von μ und ν in sehr einfacher Form angegeben werden.

5. Die Form der autokatalytischen kinetischen Kurven

Es ist für alle behandelten autokatalytischen Reaktionssysteme charakteristisch, daß die Konzentration der am Prozeß teilnehmenden Stoffe sich in Abhängigkeit von der Zeit gemäß S-förmiger Kurven gestaltet. Die einzige Ausnahme ist der Stoff B des in Punkt 3 behandelten Systems, der nur am ersten Reaktionsschritt teilnimmt. Den anderen konsekutiven Reaktionssystemen gegenüber gibt es bei den autokatalytischen Reaktionen keinen

solchen Stoff (Zwischenprodukt), dessen Konzentration gemäß einer Maximumkurve zeitabhängig wäre; bei diesen Reaktionen ist nähmlich das Zwischenprodukt mit dem Endprodukt identisch. Im folgenden soll geprüft werden, wie der Wendepunkt der autokatalytischen Kurven von den Parametern der Reaktion abhängt.

Die Behandlung wurde für die folgenden Werte der stöchiometrischen Koeffizienten durchgeführt:

$$a_1 = 1,\ a_2 = 1,\ b = 1,\ e = 2 \tag{20}$$

a) *Das System* $A \rightarrow E,\ A + E \rightarrow 2E$

Die Abhängigkeit des Wendepunktes der kinetischen Kurven des in Punkt 1 behandelten Systems von den Parametern der Reaktion ist folgende:

$$\left(\frac{A}{A_o}\right)_{\text{infl.}} = \frac{1}{2}\left(1 + \frac{1}{\varkappa A_o}\right) \tag{21}$$

$$\left(\frac{E}{A_o}\right)_{\text{infl.}} = \frac{1}{2}\left(1 - \frac{1}{\varkappa A_o}\right) \tag{22}$$

Es kann festgestellt werden, daß die relativen Konzentrationen der Stoffe im Wendepunkt nicht nur vom Quotienten $\varkappa$ der Geschwindigkeitskonstanten, sondern auch von der Anfangskonzentration A_0 abhängen. Ein Wendepunkt tritt nur dann auf, wenn

$$A_o > \frac{1}{\varkappa} \tag{23}$$

ist. Die Wendepunkte der kinetischen Kurven beider an der Reaktion teilnehmenden Stoffe gehören zum gleichen Zeitwert.

b) *Das System* $A + A \rightarrow E,\ A + E \rightarrow 2E$

Die Abhängigkeit des Wendepunktes der kinetischen Kurven des in Punkt 2 behandelten Systems von den Parametern der Reaktion ist die folgende:

$$\left(\frac{A}{A_o}\right)_{\text{infl.}} = \frac{1}{2}\frac{\varkappa}{\varkappa - 1} \tag{24}$$

$$\left(\frac{E}{A_o}\right)_{\text{infl.}} = \frac{1}{2}\frac{\varkappa - 2}{\varkappa - 1} \tag{25}$$

In diesem Fall hängen die zu den Wendepunkten gehörenden relativen Konzentrationen nur vom Quotienten $\varkappa$ der Geschwindigkeitskonstanten ab. Die Wendepunkte der kinetischen Kurven beider Stoffe gehören zum gleichen Zeitwert.

c) *Das System* $A + B \rightarrow E$, $A + E \rightarrow 2E$

Die Abhängigkeit des Wendepunktes der kinetischen Kurven des in Punkt 3 behandelten Systems von den Parametern der Reaktion ist — wegen der Transzendenz der stöchiometrischen Zusammenhänge zwischen den Konzentrationen — in expliziter Form nicht anzugeben (die kinetische Kurve des Stoffes B besitzt keinen Wendepunkt):

$$\left(\frac{A}{A_0}\right)_{\text{infl.}} = \frac{1}{A_0} \cdot \frac{(B + \varkappa E)^2}{\varkappa(B+\varkappa E) - B} \tag{26}$$

$$\left(\frac{E}{A_0}\right)_{\text{infl.}} = 1 - \left(\frac{A}{A_0}\right)_{\text{infl.}} \tag{27}$$

Diese Ausdrücke können — mit Hilfe der stöchiometrischen Zusammenhänge — zum Beispiel graphisch ausgewertet werden. Die Wendepunkte der kinetischen Kurven beider Stoffe gehören zum gleichen Zeitwert.

d) *Das empirisch beschriebene autokatalytische System*

Wenn zur Beschreibung des autokatalytischen Prozesses die in Punkt 4 behandelte empirische Differentialgleichung angewendet wird, so kann zur Feststellung der »Reaktionsordnungen« μ und ν die folgende Relation benützt werden:

$$\xi_{\text{infl.}} = \frac{\mu}{\mu + \nu} \tag{28}$$

Der Wert von $\xi_{\text{infl.}}$ hängt nur von den »Reaktionsordnungen«, nicht aber von den Anfangsparametern und der Geschwindigkeitskonstante K ab. Im Falle der anderen autokatalytischen Systeme nähert sich der Wert der zum Wendepunkt der kinetischen Kurve des Endproduktes gehörenden Konversion 50% nur bei $\varkappa \rightarrow \infty$ an — siehe z. B. (22) und (25) —; in dem mit (28) beschriebenen Fall aber kann er 50% auch überschreiten. Zum Beispiel bei »Reaktionsordnungen« μ; $\nu = \frac{1}{2}; 1; \frac{3}{2}; 2$ ist der Wert wie folgt:

$$\frac{1}{5} \leqslant \xi_{\text{infl.}} \leqslant \frac{4}{5} \tag{29}$$

6. *S-förmige Konversionskurven*

Man stößt oft auf die Ansicht, daß die S-Form der Konversionskurve den autokatalytischen Ablauf des Prozesses eindeutig beweist. Tatsache ist demgegenüber, daß die S-Form nicht immer die Folge einer Autokatalyse ist, obwohl sie wirklich andeutet, daß die Entstehung oder Abnahme des betreffenden Stoffes während der Reaktion einigermaßen beschleunigt wird. Konversionskurven von beschleunigtem Charakter kommen nämlich in allen Folgereaktionssystemen vor.

Zur Illustration dieser Umstände sind in den Abbildungen 1—9 die Konversionskurven des Folgereaktionssystems $A \rightarrow C$, $C \rightarrow E$ ([6]; in den

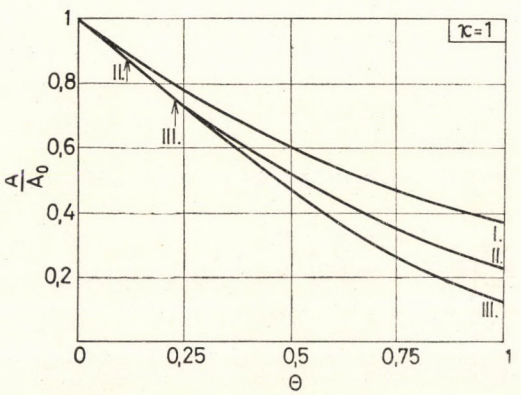

Abb. 1. Zeitabhängigkeit der relativen Konzentration des Ausgangsstoffes, für $\varkappa = 1$

Abbildungen: I), des konkurrenten Folgereaktionssystems $A \rightarrow C$, $A + C \rightarrow E$ ([2]; II) und der autokatalytischen Reaktion $A \rightarrow E$, $A + E \rightarrow 2E$ (III) dargestellt, bzw. sind in einer Tabelle die Daten über die Wendepunkte der Konversionskurven der erwähnten Systeme zusammengefaßt. Da die primären und sekundären Reaktionsschritte in den Systemen II und III von unterschiedlicher Molekularität sind und daher die Form der Konversionskurven nicht nur von den Geschwindigkeitskonstanten, sondern auch von der Anfangskonzentration des Ausgangsstoffes (A_0) abhängt, beziehen sich die vorgeführten Kurven bzw. Daten einheitlich auf den Wert $A_0 = 2$.

In Abb. 1—3 wurde die Zeitabhängigkeit der relativen Konzentrationen des Ausgangsstoffes dargestellt, für alle drei Systeme, im Falle von $\varkappa = 1$; 10; 100. Der Wendepunkt ist mit Pfeilen markiert.

Es kann festgestellt werden, daß bei der Kurve A/A_0—t im Falle des Systems I kein Wendepunkt vorliegt und ihr Ablauf von $\varkappa$ unabhängig ist. Im Falle des Systems II ist die Konversionskurve S-förmig und hängt die Lage des Wendepunktes vom $\varkappa$-Wert ab; der gesamte Kurvenablauf wird

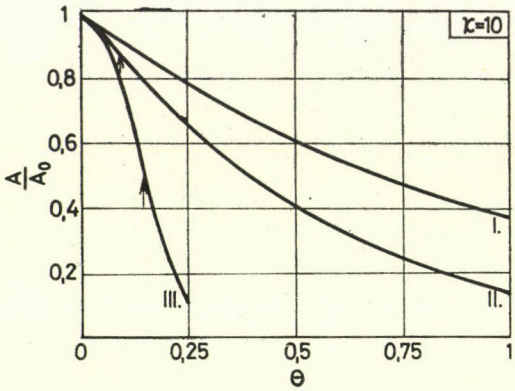

Abb. 2. Zeitabhängigkeit der relativen Konzentration des Ausgangsstoffes, für $\varkappa = 10$

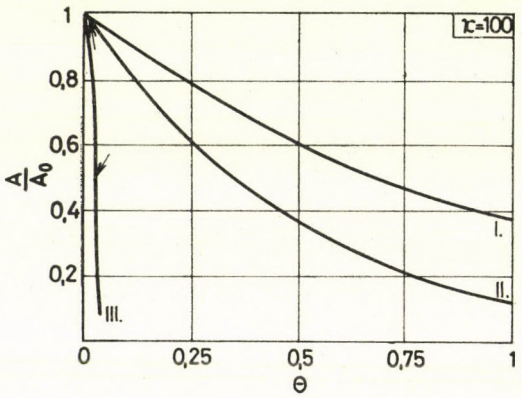

Abb. 3. Zeitabhängigkeit der relativen Konzentration des Ausgangsstoffes, für $\varkappa = 100$

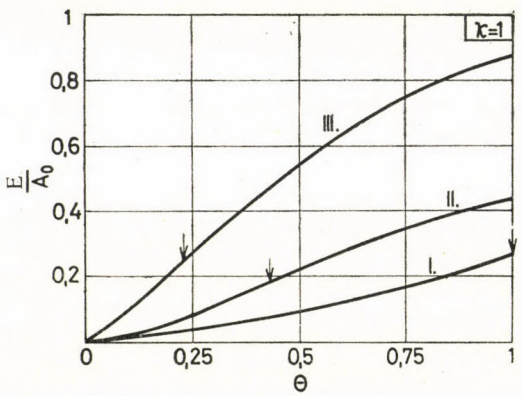

Abb. 4. Zeitabhängigkeit der relativen Konzentration des Endproduktes, für $\varkappa = 1$

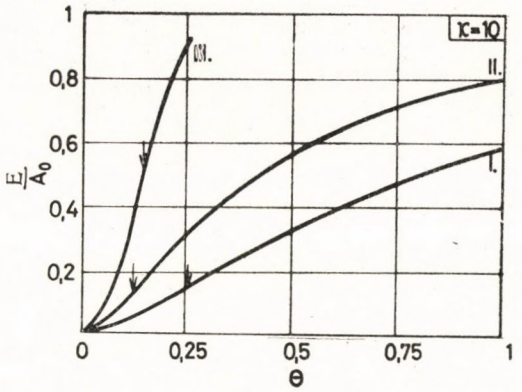

Abb. 5. Zeitabhängigkeit der relativen Konzentration des Endproduktes, für $\varkappa = 10$

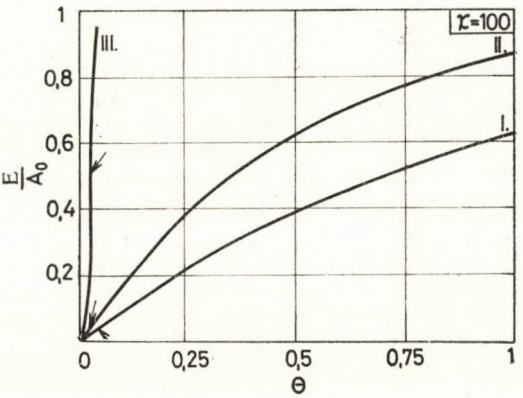

Abb. 6. Zeitabhängigkeit der relativen Konzentration des Endproduktes, für $\varkappa = 100$

aber durch $\varkappa$ nur wenig beeinflußt. Die S-förmigen Konversionskurven des Systems III weisen eine starke Abhängigkeit von $\varkappa$ auf.

In Abb. 4—6 wurde die Zeitabhängigkeit der relativen Konzentrationen des Endproduktes in den drei Systemen für die Werte von $\varkappa = 1$; 10; 100 dargestellt. Die Wendepunkte der Kurven sind mit Pfeilen markiert.

Es kann festgestellt werden, daß die $E/A_0 - \tilde{t}$ Kurven in allen drei Systemen S-Form haben. Der beschleunigte Charakter und die $\varkappa$-Abhängigkeit sind auch hier im Falle des Systems III am deutlichsten.

In Abb. 7—9 wurde die Endprodukt-Konversion E/A_0 (zwecks besserer Vergleichbarkeit) in Abhängigkeit von den dimensionslosen relativen Zeitwerten $t/t_{infl.}$ für den Fall von $\varkappa = 1$; 10; 100 dargestellt. Wegen der angewandten Zeittransformation gehören die Wendepunkte aller Kurven zum gleichen relativen Zeitwert ($t/t_{infl.} = 1$); dieser ist in den Abbildungen mit Pfeilen markiert.

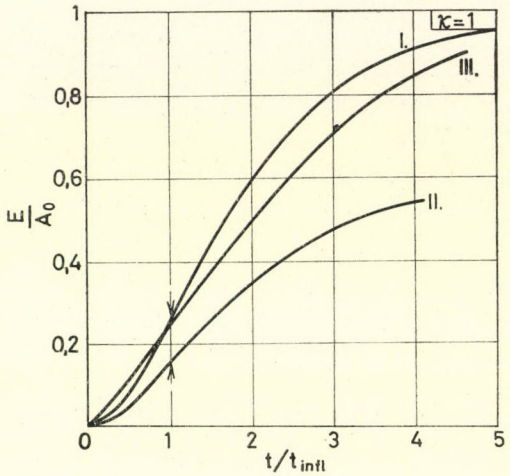

Abb. 7. Abhängigkeit der Endprodukt-Konversion von den relativen Zeitwerten, für $\varkappa = 1$

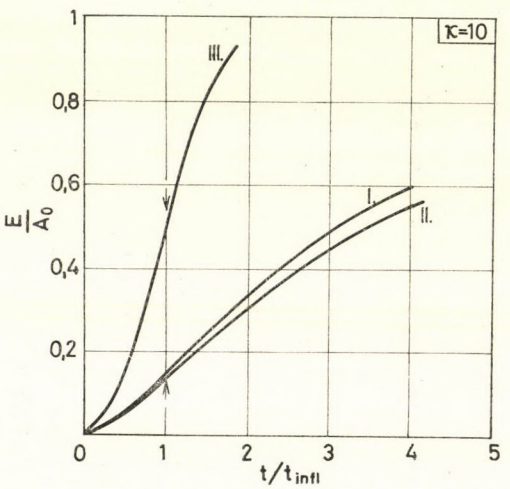

Abb. 8. Abhängigkeit der Endprodukt-Konversion von den relativen Zeitwerten, für $\varkappa = 10$

In dieser Darstellung zeigt das Folgereaktionssystem I im Falle von $\varkappa = 1$ überraschend eher einen ausdrücklichen »autokatalytischen« Charakter als das System III, obwohl letzteres wirklich eine autokatalytische Reaktion ist. Bei größeren $\varkappa$-Werten kommt freilich die beschleunigte Entstehung des Endproduktes im System III besser zum Ausdruck.

In der Tabelle I wurden die sich auf die Wendepunkte der Konversionskurven der drei Systeme beziehenden Daten für den Fall von $\varkappa = 1; 10; 100$ zusammengestellt. Die ersten fünf Reihen der Tabelle enthalten die Daten

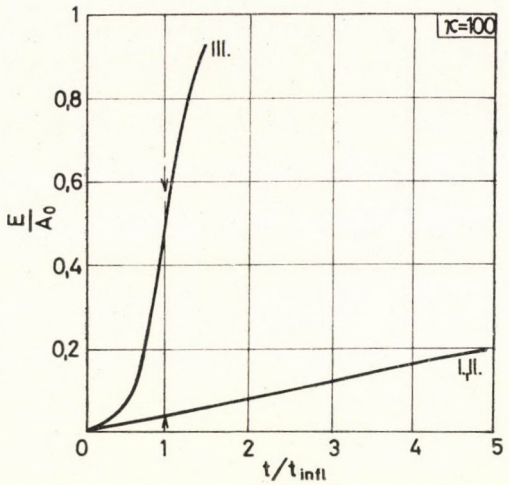

Abb. 9. Abhängigkeit der Endprodukt-Konversion von den relativen Zeitwerten, für $\varkappa = 100$

Tabelle I

	$A \rightarrow C$ $C \rightarrow E$			$A \rightarrow C$ $A + C \rightarrow 2E$			$A \rightarrow E$ $A + E \rightarrow 2E$		
	$\varkappa = 1$	$\varkappa = 10$	$\varkappa = 100$	$\varkappa = 1$	$\varkappa = 10$	$\varkappa = 100$	$\varkappa = 1$	$\varkappa = 10$	$\varkappa = 100$
E: Θ_{infl}	1,0000	0,2559	0,0465	0,3800	0,1239	0,0234	0,2310	0,1472	0,0264
$(A/A_0)_{infl}$	0,3679	0,7738	0,9543	0,6169	0,8183	0,9592	0,7500	0,5250	0,5025
$(C/A_0)_{infl}$	0,3679	0,0774	0,0095	0,2289	0,0448	0,0050	—	—	—
$(E/A_0)_{infl}$	0,2642	0,1488	0,0362	0,1543	0,1369	0,0359	0,2500	0,4750	0,4975
$(W/W_0)_{infl}$	0,3679	0,7738	0,9543	0,8993	1,5515	1,9184	1,1250	5,5125	50,5013
A: Θ_{infl}	—	—	—	0,1136	0,0888	0,0162	0,2310	0,1472	0,0264
$(A/A_0)_{infl}$	—	—	—	0,8823	0,8736	0,9728	0,7500	0,5250	0,5025
$(C/A_0)_{infl}$	—	—	—	0,0963	0,0406	0,0048	—	—	—
$(E/A_0)_{infl}$	—	—	—	0,0214	0,0858	0,0225	0,2500	0,4750	0,4975
$(W/W_0)_{infl}$	—	—	—	1,0522	1,5830	1,9067	1,1250	5,5125	50,5013

des Wendepunktes der Konversionskurve vom Ausgangsstoff, die anderen fünf Reihen jene des Endproduktes. Die Angaben $(W/W_0)_{infl.}$ sind die Werte der Abnahmegeschwindigkeit des Ausgangsstoffes im Wendepunkt, bezogen auf die Anfangsgeschwindigkeit.

Es kann festgestellt werden, daß die $(W/W_0)_{infl.}$-Werte der relativen Geschwindigkeit das Maß der Beschleunigung und dadurch den autokatalytischen Charakter der untersuchten Systeme gut widerspiegeln. (Auch im Wendepunkt der Endprodukt-Konversionskurve wurde die sich auf den Ausgangs-

stoff beziehende relative Geschwindigkeit angegeben, da die Anfangsgeschwindigkeit der Bildung des Endproduktes in den Systemen I und II gleich Null ist.) Der Wert der relativen Geschwindigkeit ist im System I bei allen $\varkappa$-Werten kleiner als 1, im System II zeigt er aber bei $\varkappa = 100$ eine etwa zweifache und im System III eine etwa fünfzigfache Erhöhung der Abnahmegeschwindigkeit des Stoffes A beim Wendepunkt, im Vergleich zur Anfangsgeschwindigkeit. Es sei hier bemerkt, daß die Wendepunkte der Kurven A/A_0 und E/A_0 im System II zu unterschiedlichen Zeitwerten, im System III (da das Zwischenprodukt hier mit dem Endprodukt identisch ist) zu gleichen Zeitwerten gehören: im letzteren System sind die beiden Kurven die gegenseitigen Spiegelbilder.

Demgemäß ist die Erhöhung auch der Zunahmegeschwindigkeit des Endproduktes E beim Wendepunkt (im Vergleich zur Anfangsgeschwindigkeit) im System III, bei $\varkappa = 100$, etwa fünfzigfach.

Die Feststellungen über die S-förmigen Konversionskurven können wie folgt zusammengefaßt werden:

a) Die Endprodukt-Konversionskurve ist in allen Folgereaktionssystemen S-förmig.

b) Die Konversionskurve des Ausgangsstoffes ist nur in konkurrenten Folgereaktionssystemen und in autokatalytischen Reaktionen S-förmig.

c) Auf Grund des in den Punkten a) und b) Gesagten kann festgestellt werden, daß die S-förmige Endprodukt-Konversionskurve nur dann eine autokatalytische Reaktion andeutet, wenn auch die Konversionskurve des Ausgangsstoffes S-förmig ist (Unterschied vom einfachen Folgereaktionssystem) und kein vom Endprodukt unterschiedliches Zwischenprodukt sich anhäuft (Unterschied vom konkurrenten Folgereaktionssystem).

d) Ein weiterer Unterschied von diesen Systemen besteht darin, daß das Maß der Umwandlung im Falle von Autokatalyse bei großen $\varkappa$-Werten im Wendepunkt 50% annähert, und diesen Wert im Falle von empirisch beschriebener (z. B. physikalischer) Autokatalyse sogar überschreitet.

e) Die die Beschleunigung der Reaktion anzeigende relative Geschwindigkeit $(W/W_0)_{infl.}$ (die experimentell einfacher und genauer zu bestimmen ist, als die Lage der Inflexion) kennzeichnet die kinetischen Kurven von beschleunigtem Charakter gut; manchmal ist es möglich, auf Grund der $(W/W_0)_{infl.}$-Werte die typische autokatalytische Reaktion vom konkurrenten Folgereaktionssystem zu unterscheiden.

LITERATUR

1. KELEN, T., TÜDŐS, F.: Kinetische Analyse einiger Folgereaktionen, III. Das konkurrente Folgereaktionssystem $A + A \rightarrow C$, $A + C \rightarrow E$. Acta Chimica Acad. Sci. Hung. **59** (3—4) 323—349 (1969)
2. KELEN, T.: Kinetische Analyse einiger Folgereaktionen, IV. Die konkurrenten Folgereaktionssysteme $A \rightarrow C$, $A + C \rightarrow E$ und $A + B \rightarrow C$, $A + C \rightarrow E$. Acta Chimica Acad. Sci. Hung. **60** (1—2) 87—96 (1969)

3. GRADSTEIN, I. S., RYSIK, I. M.: Tablizy Integralow, Sum, Rjadow i Proiswedjenij. Gos. Isd. Phys. Mat. Lit., Moskau, 1963
4. KONDRATEV, V. N.: Kinetika Chimitscheskich Gasowich Reakzij. Isd. Akad. Nauk UdSSR, Moskau, 1958
5. TÜDŐS, F., BOROS-GYEVI, E.: Kinetics of the Solid State Polymerization of N-Vinylcarbazole. Acta Chimica Acad. Sci. Hung. **56**, 67 (1968)
6. CHIEN, JEN-YUAN: J. Amer. Chem. Soc. **70**, 2256 (1948)
7. KELEN, T., TÜDŐS, F., GALAMBOS, G.: Kinetische Analyse einiger Folgereaktionen, V. Autokatalytische Reaktionen (ungarisch). Magyar Kémiai Folyóirat **6**, 260 (1969)

Tibor KELEN
Ferenc TÜDŐS
György GALAMBOS
Budapest II., Pusztaszeri út 57—69.

Acta Chimica Academiae Scientiarum Hungaricae, Tomus 62 (1), pp. 41—50 (1969)

X-RAY DIFFRACTION INVESTIGATION OF THE CRYSTAL AND MOLECULAR STRUCTURE OF 3-NITRO-PHENYLHYDRAZONE-ACETONE

Gy. MENCZEL

(Department for Experimental Physics, L. Eötvös University, Budapest)

Received September 27, 1968

The crystal structure determination of 3-nitro-phenylhydrazone-acetone was performed by X-ray diffraction methods. The crystals are monoclinic, the space group is C2/c. The structure was determined by two-dimensional and trial methods. The refinement was carried out by differential synthesis. Reliability index R = 0.169. The bond relations in the benzene ring are asymmetrical. The measured lengths of the carbon-nitrogen bonds are compared with data of similar compounds. The equation of the "best plane" through the benzene ring, that of the plane of the acetone and of the hydrazine were determined, and the angles between these planes were computed.

The phenylhydrazones play an important role in the organic preparative and analytical chemistry. The structure of the crystalline hydrazine was investigated by COLLIN and LIPSCOMB [1], that of the diformyl-hydrazine by TOMIIE, KOO and NITTA [2] and that of the diacetyl-hydrazine by SHINTANI [3]. FURBERG *et al.* published the structure of the arabinose-*p*-bromo-phenylhydrazone [4], and of the ribose-*p*-bromo-phenylhydrazone [5], both compounds are characterized by the presence of a heavy atom (bromine). No structural investigation on phenylhydrazones without a heavy atom has been reported. Some powder diffraction data are available in the paper of CLARK, KAYE and PARKS [6]. GERECS *et al.* [7], [8], [9], have prepared some phenylhydrazones of sugars, which are of chemical and structural interest.

Crystals of the 3-nitro-phenylhydrazone-acetone (abbreviated 3-NPHAc), $C_9N_3O_2H_{11}$

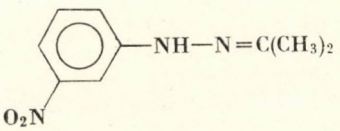

have been investigated by us by X-ray diffraction methods, in order to study the bond relations of the nitro-phenylhydrazones. The compound is interesting from the methodical point of view, too, because with 112 atoms in the unit cell (not counting hydrogens), it contains no atom heavier than oxygen.

Crystallographic data

The crystals were prepared by heating a mixture of acetone and *m*-nitrophenylhydrazone in aqueous alcohol [10]. (M.p. 126°C.) The crystals are red monoclinic plates elongated along the *b* axis. The face of the plates is the (100) plane. They have little mechanical strength and cannot be cut without losing their single crystal character.

The unit cell parameters measured on oscillation and Weissenberg photographs are the following:

$$a = 22.98 \pm 0.04 \text{ Å}, \qquad b = 3.900 \pm 0.015 \text{ Å},$$
$$c = 21.91 \pm 0.04 \text{ Å}, \qquad \beta = 100.2° \pm 0.2$$

Cell volume: 1934 $Å^3$ · F(000) = 816.

The density calculated with 8 molecules in the unit cell is $D_x = 1.323$ g cm^{-3}. The measured density was determined by flotation. As the crystals dissolved in organic liquids, an aqueous solution of $NaNO_3$ was used with some drops of isobutyl alcohol, in order to remove air bubbles from the surface of the crystals. The measured density is $D_m = 1.31 \pm 0.04$ g cm^{-3}.

Systematic absences:

Type of reflexions: hkl. Observed reflexions: $h + k = 2n$.

Type of reflexions: hol. Observed reflexions: $l = 2n$.

Two space groups are possible: Cc and C2/c. The statistical analysis of the intensity distribution with the method of Howells, Philips and Rogers [11] has shown the presence of a centre of symmetry, so the space group is C2/c.

Measurement of the intensities of the reflexions and the determination of the absolute scale of the intensities

Integrated and non-integrated Weissenberg photographs were made with unfiltered Cu radiation by the multiple film method: four layers around the *b* axis (0, 1, 2, 3), two layers around the *a* axis (0, 1) and one layer around the *c* axis (0). About 50% of the diffraction sphere was explored, 2100 reflexions were recorded, about 1000 of them were independent ones. The number of the independent reflexions with measurable intensity was 530. The quality of the spots with the Miller indices $k \geq 3$ was so bad that even a rough estimation of their intensities was impossible. The strong reflexions were measured with a Zeiss-Schnell photometer, the intensities of the weak reflexions were estimated visually by comparing them with the β spots of the strong reflexions. The measured relative intensities, I_m, were corrected by the Lorentz-polarization factor, Lp. The corrected intensity is: $I_{cor} = I_m$ Lp.

The intensities of the unobserved reflexions were taken half of the minimum measured value, then corrected by Lp factor and converted to common and absolute scale. The determination of the scale factors for the photographs of different k = const. layers and the determination of the absolute intensities (I_0) caused difficulties, as the specimens could not be cut to appropriate dimensions. The crystals used for the photographs around different axis had about the same dimensions: 1 mm in the *b* direction, 0.03 mm and 0.2 mm in the *a* and the *c* directions, respectively. The absorption correction was negligible on the k = const. layers, the maximum of μd being 0.2, but it was considerable on the h = const. layers which were used to convert the k = const. layer photographs to a common scale. As the calculation of the absorption correction was not possible we took advantage of the circumstance that the *b* parameter was short. The atoms were well resolved on the projection onto (010) and this projection showed the essential features of the structure.

The layers k = const. were first roughly converted to a common scale with the layers h = 0 and h = 1. After this, the absolute scale was determined by the three-dimensional Wilson method. This absolute scale was considered as a rough approximation, too, because the common scale of the intensities was uncertain. When the two-dimensional model for the projection onto (010) was found, the Wilson method was applied with the modification suggested by BUERGER [12]: the average of the theoretical intensity values were taken $F_c^2(hol)$ instead of Σf_j^2, for each $\sin^2 \theta$ interval. (F_c is the calculated structure factor.) When the three-dimensional model was found, a scale factor K(k) was determined separately for the layers k = 1 and k = 2, by means of the relation $\Sigma F_c^2 = K(k) \Sigma I_{cor}$. (At this computation the reflexions were not divided into groups.) After this the above procedure (Wilson method with F_c^2 instead of Σf_j^2) was repeated with three-dimensional data. The final value of the Debye factor is 3.25 $Å^{-2}$. So the intensities were corrected by the temperature factor: $\exp (6.50 \sin^2 \theta/\lambda^2)$.

Determination and refinement of the structure

As mentioned previously at first the projection onto (010) was determined. The symmetry of this projection is p2 and the identity periodes are halved both in the *a* and the *c* directions as the consequence of the C centering and the *c* glide plane respectively. There are centres of symmetry in a distance of a/4 and c/4, respectively from each other because in the projection the twofold symmetry axes give additional centres of symmetry.

The first two-dimensional model was found by means of a P(u, w) Patterson synthesis. The result of this computation was compared with the theoretical vector diagram of the molecule. The *b* axis being short we made the theoretical

vector diagram with the assumption that the image of the molecule was not significantly distorted on the projection. The theoretical vector diagram consisted of two parts: 1). The set of the intramolecular vectors, 2). the set of the vectors connecting the atomic centres of two molecules related by a centre of symmetry. The first part gave the orientation of the projection of molecule in the (010) plane, the second part determined the location of the centre of symmetry, that is the origin in the plane. As the three-dimensional computations showed later this was an apparent centre of symmetry and the origin has to be shifted by c/4 on the z axis.

182 intramolecular and 196 intermolecular vectors exist theoretically, but in consequence of many coincidences the identification of 10 strong peaks has been sufficient to give the result.

The refinement of the projection was carried out with two-dimensional Fourier synthesis. After the fifth synthesis the reliability index for the (hol) reflexions was $R = 0.22$. The Fourier and Patterson syntheses were computed with the program written by L. CSORDÁS for an URAL-2 computer [14].

The shortening on the projection of the approximately known bond lengths and the assumption that most part of the molecule was plane, determined roughly the *orientation of the molecule in three dimensions*. The position of this oriented molecule was then uncertain in the third direction. Two problems were to be solved: The localization of the molecule in the b direction, and the determination of the true origin on the (010) plane.

The following two independent methods gave the same result:

a) The origin was first arbitrarily fixed on the y axis. Then the molecule was *shifted as a rigid body step by step* in the b direction taken the length of a step $\Delta y = 0.04$. 224 reflexions with $k = 1$ were applied to this method. At each step F(hkl) and R computations were performed, for the chosen reflexions. At the best shift, the reliability index was first $R = 0.52$. This value was improved to 0.32 by shifting the origin by c/4 along the z axis.

b) The originally two-dimensional *method of* TAYLOR [15] was adopted to the one-dimensional problem.

The principle of the method — in one dimension — is that by shifting the molecule as a rigid body in the b direction the value of one chosen structure factor $F_c(hkl)$ changes as a cosine function of the shift Δy. The amplitude A(hkl) and the phase $\varphi(hkl)$ of this cosine function can be computed on the basis of the Fourier transform of the molecule. Those Δy values are to be found for which $|F_c(hkl)| = F_0(hkl)$. ($F_0(hkl)$ is the absolute value of the observed structure factor.) If $k = 1$, four solutions exist, among them two independent ones, the others can be obtained from these by adding 1/2 to the formers. Computing for two hkl-s, the common solution gives the wanted result. Owing to the possible errors we have chosen more reflexions. The Miller indices of these reflexions were not high, because the Miller indices

multiply the errors of the original model. For the chosen reflexions the condition $F_0(hkl) \leq A(hkl)/2$ was fulfilled, minimizing so the influence of the errors in the intensity measurement and the influence of the errors in the absolute scale. 15 reflexions with $k = 1$ were drawn into the computation. The necessity of the shift of the origin by c/4 was proved by the fact that without this for many reflexions $F_0(hkl) > A(hkl)$ was found. The position of the molecule in the *b* direction was the same as in method a).

The three-dimensional refinement was performed by four cycles of BOOTH's differential synthesis [16], and by six cycles of CRUICKSHANK's $\varrho_0 - \varrho_c$ synthesis [17]. After the last cycle the reliability index for all observed and unobserved reflexions was $R = 0.169$. For the computations the atomic scattering factors given in the International Tables for neutral atoms were used. Table I contains the final positional parameters with their estimated standard deviations (e.s.d.) computed by the method of CRUICKSHANK [18].

Table I

Positional parameters with their standard deviations in parentheses

	x	y	z
C (1)	0.4224 (3)	0.3441 (9)	0.3654 (4)
C (2)	0.4618 (4)	0.2667 (10)	0.3179 (4)
C (3)	0.4509 (5)	0.4946 (10)	0.4268 (4)
C (4)	0.2706 (3)	0.3187 (9)	0.3746 (3)
C (5)	0.2335 (4)	0.4343 (9)	0.4158 (4)
C (6)	0.1738 (3)	0.3827 (9)	0.4002 (3)
C (7)	0.1447 (4)	0.2362 (10)	0.3441 (3)
C (8)	0.1822 (4)	0.1272 (10)	0.3054 (4)
C (9)	0.2462 (4)	0.1550 (10)	0.3197 (4)
N (1)	0.3672 (3)	0.2934 (7)	0.3479 (3)
N (2)	0.3294 (3)	0.3691 (8)	0.3907 (3)
N (3)	0.1346 (3)	0.5205 (8)	0.4417 (3)
O (1)	0.1583 (3)	0.6700 (7)	0.4876 (3)
O (2)	0.0806 (2)	0.4733 (7)	0.4293 (2)

The values of the observed and calculated structure factors are available at the author.

Description of the structure

The projection onto (010) of two molecules related by a centre of symmetry is shown in Fig. 1. Table II contains the interatomic distances with their e.s.d. The bond angles are listed in Table III. Calculated by the method of DARLOW [19], all angles have approximately the same error; $\pm 0.6°$. The intramolecular distances and bond angles are shown also in Fig. 2.

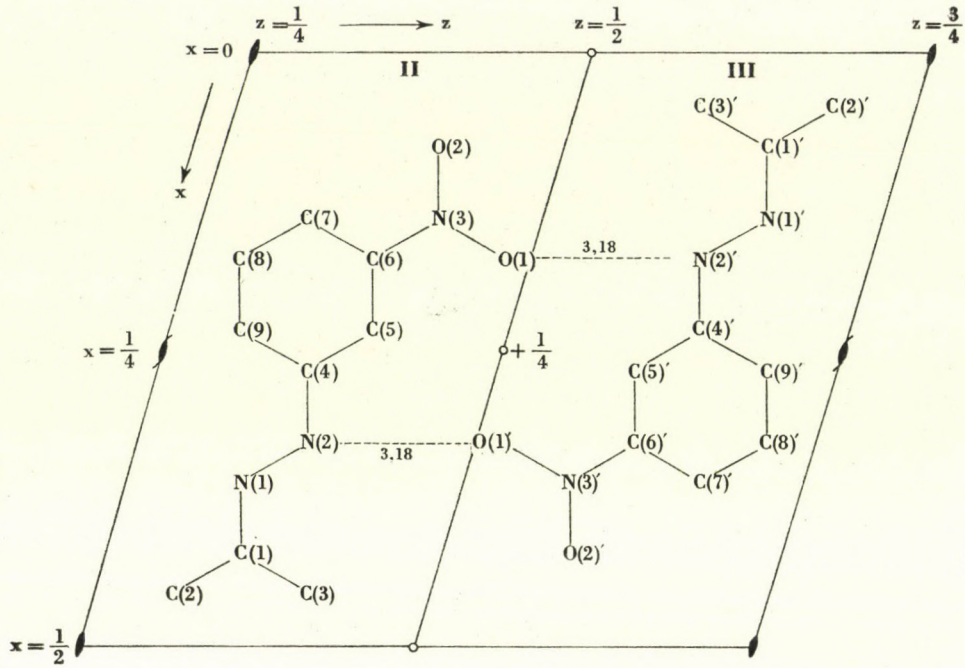

Fig. 1. The projection onto (010) of two molecules related by a centre of symmetry

Table II

Interatomic distances with their standard deviations

	Interatomic distances, Å	e.s.d. in 10^{-3} Å
C (1)—C (2)	1.526	9.6
C (1)—C (3)	1.509	10.2
C (1)—N (1)	1.273	8.6
N (1)—N (2)	1.417	7.4
N (2)—C (4)	1.351	8.1
C (4)—C (5)	1.419	9.0
C (5)—C (6)	1.369	9.0
C (6)—C (7)	1.413	8.8
C (7)—C (8)	1.377	9.6
C (8)—C (9)	1.453	10.2
C (9)—C (4)	1.390	9.4
C (6)—N (3)	1.489	8.3
N (3)—O (1)	1.237	7.5
N (3)—O (2)	1.206	7.4

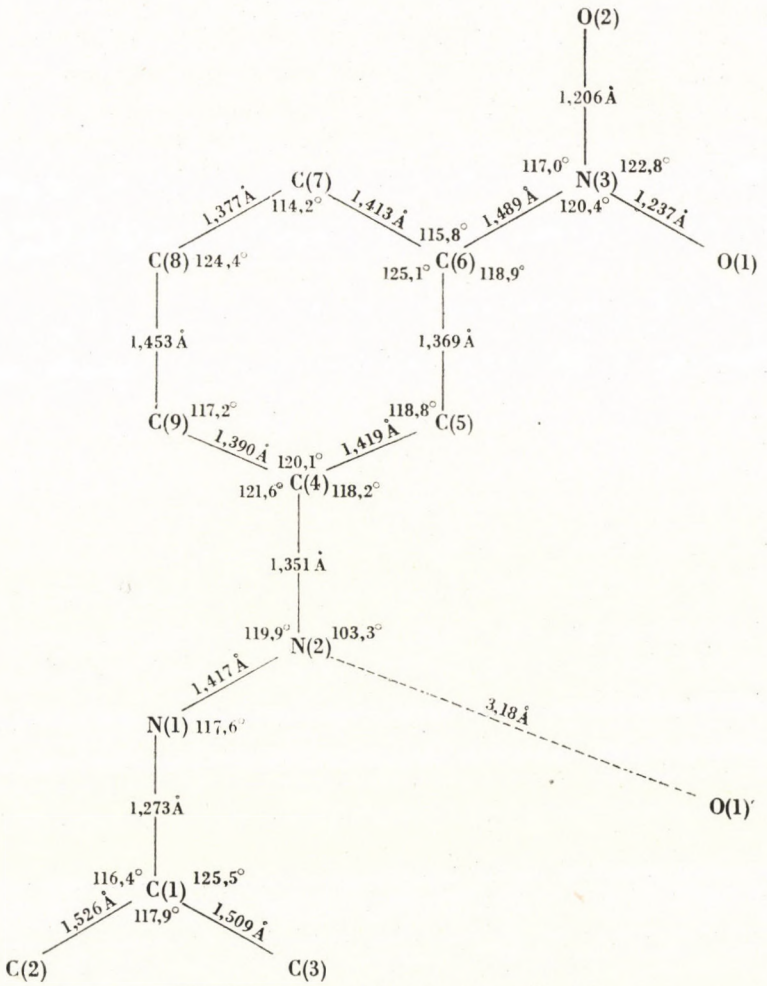

Fig. 2 Intramolecular distances and angles

Table III

Bond angles			
C (2)—C (1)—C (3)	117.9°	C (5)—C (6)—C (7)	125.1°
N (1)—C (1)—C (3)	125.5	C (6)—C (7)—C (8)	114.2
C (2)—C (1)—N (1)	116.4	C (7)—C (8)—C (9)	124.4
C (1)—N (1)—N (2)	117.6	C (8)—C (9)—C (4)	117.2
N (1)—N (2)—C (4)	119.9	C (5)—C (6)—N (3)	118.9
N (2)—C (4)—C (9)	121.6	C (7)—C (6)—N (3)	115.8
N (2)—C (4)—C (5)	118.2	C (6)—N (3)—O (1)	120.4
C (9)—C (4)—C (5)	120.1	C (6)—N (3)—O (2)	117.0
C (4)—C (5)—C (6)	118.8	O (1)—N (3)—O (2)	122.8

The bond relations in the benzene ring are asymmetrical, though the mean value of the bond lengths (1.402 Å) differs only slightly from that of those in benzene (1.393 Å) [20]. The bond angle at the carbon atom C (6) where the nitro group is attached is greater than 120° (125.1°). This is a general experience reported in the literature [21—26].

Three kinds of carbon-nitrogen bond exist in the molecule:

a) bond between an aromatic carbon and the nitrogen of the nitro group C (6)—N (3). Its length, 1.489 Å corresponds to the data reported for similar compounds [21—26];

b) bond between an aromatic carbon and the nitrogen of the hydrazine. Only a few data are published for this type of bond. In arabinose-*p*-bromophenylhydrazone [4] its length is 1.42 Å and in ribose-*p*-bromo-phenylhydrazone [5] 1.46 Å. The accuracy of this determinations estimated by the authors is very low, about 0.1 Å, as a consequence of the lack of the centre of symmetry and the small number of reflexions observed. The value 1.351 Å found in 3-NPHAc is near to the length of the bond in *p*-nitraniline (1.371 Å) measured between the aromatic carbon and the nitrogen of the amine group [22];

c) double bond between the nitrogen of the hydrazine and the carbon of the acetone C (1)—N (1). This bond is unusually short. In ribose-*p*-bromophenylhydrazone this bond length is 1.32 Å (with the accuracy quoted). No other data for phenylhydrazones have been reported, namely in arabinose-*p*-bromo-phenylhydrazone the sugar part appears with cyclic structure, therefore no bond of this type exists in it. The value 1.273 Å found in 3-NPHAc can be compared to the length of the C = N double bonds measured in dimethylglyoxime (1.27 Å) [27] and in acetoxyme (1.29 Å) [28].

Only one of the intermolecular distances was found to be shorter than 3.20 Å, the distance between N (2) and O (1)′: 3.18 Å. This was attributed to weak hydrogen bonding, later proved by IR measurements.

The equation of the "best plane" (denoted with P1) through the atoms of the benzene ring was determined by the method of SHOMAKER, WASER, MARSH and BERGMAN [29]. This plane is almost perpendicular to the (100) plane and is inclined by 26.3° to the (010) plane. The distances of the atoms from this plane are listed in Table V. The nitro group lies in this plane, only O (1) is slightly out of it. The equations of following planes are also determined: P2 is the plane through the atoms C (2) C (1) C (3), that is the acetone part of the molecule, P3 and P4 are the planes through the atoms C (1) N(1) N(2) and C (4) N (2) N (1) respectively, that is through the two parts of the hydrazine. The equations referred to the orthogonal axes x′, y, z′ where x′//x and z′//z*. The coordinates must be substituted in Å. The equations of the planes and the angles between the different planes are given in Table IV. The e.s.d. of these angles is $\pm 2°$. The acetone is rotated 8.0° and the planes P3 and P4 5.7° and 8.1°, respectively, from the aromatic plane. The planes P3 and P4

Table IV

Equations of the planes

P1	$0.0077\,x' + 0.8920\,y - 0.4450\,z' + 2.514 = 0$
P2	$-0.1000\,x' + 0.9209\,y - 0.3766\,z' + 2.552 = 0$
P3	$-0.0584\,x' + 0.9145\,y - 0.4020\,z' + 2.183 = 0$
P4	$-0.0476\,x' + 0.9344\,y - 0.3528\,z' + 1.967 = 0$

Angles between different planes

	P2	P3	P4	(010)	(100)
P1	8.0°	5.7°	8.1°	26.3°	85.2°
P2	—	2.0	3.4	—	—
P3	—	—	2.4	—	—

Table V

Deviations of atoms from plane P1

	Deviations in Å
C (1)	0.215
C (2)	0.393
C (3)	0.122
C (4)	0.006
C (5)	0.019
C (6)	−0.030
C (7)	0.014
C (8)	0.011
C (9)	−0.021
N (1)	0.199
N (2)	0.047
N (3)	0.026
O (1)	0.098
O (2)	−0.018

form an angle of 2.4°, while in arabinose-*p*-bromo-phenylhydrazone [4] this angle is 90° and in ribose-*p*-bromo-phenylhydrazone 15° [5].

The Lp factors, the structure factors, the differential synthesis, the bond lengths, the errors of the positional parameters, the equation of the P1 plane and the distances of the atoms from it, were computed by programs written by the author for an URAL-2 computer.

The author is very grateful to Prof. A. GERECS and his co-workers (Department for Chemical Technology, L. Eötvös University) for the preparation of the crystals, to L. CSORDÁS for his versatile help and very useful advices, to Prof. K. LEMPERT (Department for Organic Chemistry, Technical University) for recording the IR spectra, to Miss E. ZSOLDOS for her help in performing the calculations and drawings, and to the team of the University Computer Centre for their help in the computations.

REFERENCES

1. COLLIN, R. L., LIPSCOMB, W. N.: Acta Cryst. **4,** 10 (1951)
2. TOMIIE, Y., KOO, C. H., NITTA, I.: Acta Cryst. **11,** 774 (1958)
3. SHINTANI, R.: Acta Cryst. **13,** 609 (1960)
4. FURBERG, S., PETERSEN, C. S.: Acta Chim. Scand. **16,** 1539 (1962)
5. BJAMER, K., FURBERG, S., PETERSEN, C. S.: Acta Chim. Scand. **18,** 587 (1964)
6. CLARK, L. G., KAYE, W. I., PARKS, T. D.: Ind. Eng. Chem. **18,** 310 (1946)
7. GERECS, Á., SOMOGYI, L., KÓNYA, A., DUKOVECS, M.: Acta Chim. Acad. Sci. Hung. **30,** 95 (1962)
8. GERECS, Á., FÓTI, A., RUFF, F.: Acta Chim. Acad. Sci. Hung. **42,** 145 (1964)
9. FÓTI, A., RUFF, F., GERECS, Á.: Magy. Kém. Foly. **70,** 314 (1964)
10. FÓTI, A.: private communication
11. HOWELLS, E. R., PHILIPS, D. C., ROGERS, D.: Acta Cryst. **3,** 210 (1950)
12. BUERGER, M. J.: Crystal Structure Analysis. Wiley & Sons, New York, 1960
13. International Tables for X-Ray Crystallography, Vol. I. p. 384. Kynoch Press, Birmingham, 1952
14. CSORDÁS, L.: Acta Chim. Acad. Sci. Hung. **57,** 147 (1968)
15. TAYLOR, C. A.: Acta Cryst. **7,** 757 (1954)
16. BOOTH, A. D.: Fourier Technique in X-Ray Organic Structure Analysis. University Press. Cambridge, 1948
17. CRUICKSHANK, D. W. J.: Acta Cryst. **5,** 511 (1952)
18. CRUICKSHANK, D. W. J.: Acta Cryst. **2,** 154 (1949)
19. DARLOW, S. F.: Acta Cryst. **13,** 683 (1960)
20. COX, E. G., CRUICKSHANK, D. W. J., SMITH, J. A. S.: Proc. Roy. Soc. A. **247,** 1 (1958)
21. SAKORE, T. D., PANT, L. M.: Acta Cryst. **21,** 715 (1966)
22. SAKORE, T. D., TAVALE, S. S., PANT, L. M.: Acta Cryst. **22,** 720 (1967)
23. TRUEBLOOD, K. N., GOLDISH, E., DONOHUE, J.: Acta Cryst. **14,** 1009 (1961)
24. TROTTER, J.: Acta Cryst. **12,** 884 (1959)
25. TROTTER, J.: Acta Cryst. **12,** 605 (1959)
26. COPPENS, P.: Acta Cryst. **17,** 573 (1964)
27. MERRITT, L., LANTERMAN, E.: Acta Cryst. **5,** 811 (1952)
28. BIERLEIN, T. K., LINGAFELTER, E. C.: Acta Cryst. **4,** 450 (1951)
29. SHOMAKER, V., WASER, J., MARSH, R. E., BERGMAN, G.: Acta Cryst. **12,** 600 (1959)

György MENCZEL; Budapest VIII., Múzeum krt. 6—8.

Acta Chimica Academiae Scientiarum Hungaricae, Tomus 62 (1), pp. 51—63 (1969)

CALCULATION OF INFRARED BAND CONTOURS OF PLANAR ASYMMETRIC TOP MOLECULES, II

ON THE ACCURACY OF THE GENERAL RELATIONSHIPS

É. PAÁL and Gy. VARSÁNYI

(Institute of Physical Chemistry, Technical University, Budapest)

Received October 1, 1968

The accuracy of $\varkappa - \Delta\tilde{\nu}_{1/n}$ diagrams constructed according to the previous publication of the authors was investigated in case of pure A- and B-bands. The experimental fraction-value widths of A- and B-bands of fluorobenzene, chlorobenzene and thiophene were determined and compared with the values calculated from the diagrams. The maximum deviations are 4.5 cm^{-1} and 18.7%, respectively. The results obtained are discussed.

Introduction

In our previous publication [1] the calculation of infrared band contours of nine hypothetical planar asymmetric top molecules of different asymmetry parameters and rotational constants have been reported. Pure A-bands and B-bands have been calculated and the AB-hybrid bands, the transition moments of which enclose angles of 30°, 45° and 60° with the axis of the least moment of inertia, have been constructed. The half-, fifth- and tenth-value widths of individual bands have been determined. On the basis of the data obtained, $\varkappa - \Delta\tilde{\nu}_{1/n}$ (Figs 1, 2 and 3) as well as $B - \Delta\tilde{\nu}_{1/n}$ and $\varphi - \Delta\tilde{\nu}_{1/n}$ diagrams have been constructed. It was stated that the direction of the transition moment can be determined unambiguously on the basis of the fraction-value widths of the hybrid bands, if $\varkappa$ lies within the range -0.9 to -0.6 and the value of the medium rotational constant (B) is approximately 0.1500 cm^{-1}. If B is approximately 0.0500 cm^{-1}, such a determination is possible only in case of $\varkappa = -0.9$. If the value of B is smaller than 0.0500 cm^{-1}, the fraction-value widths give no information on the direction of the transition moment.

Comparison of calculated and real spectra

The accuracy of diagrams constructed on the basis of the fraction-value widths of pure A- and B-bands has been investigated within the domain of applicability by comparing the calculated fraction-value widths with the analogous values determined experimentally in case of some planar molecules.

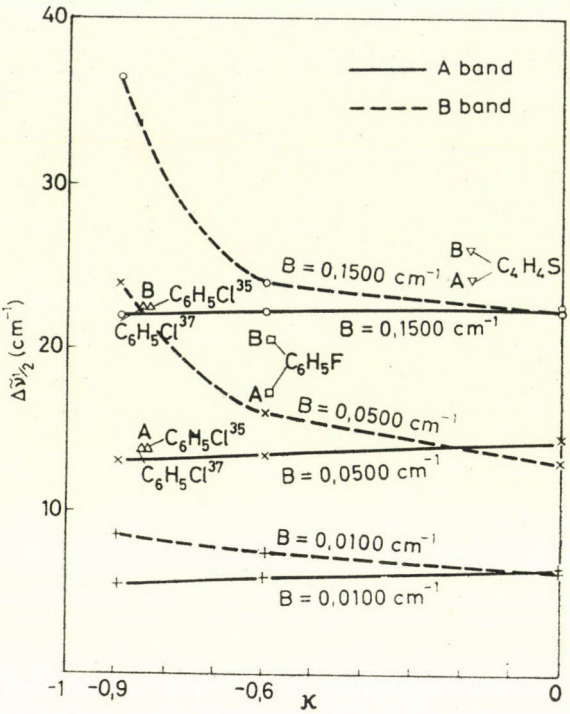

Fig. 1

1. Fluorobenzene (C_6H_5F)

The molecule of fluorobenzene has a C_{2v} type symmetry. Its 30 normal vibrations contain the following species: inplane vibrations: 11 A_1 + 10 B_2; out-of-plane vibrations: 3 A_2 + 6 B_1. Normal vibrations of species A_1, B_1 and B_2 are infrared active, whereas those of species A_2 are infrared inactive. ERLANDSSON [2] gives the asymmetry parameter and rotational constants of fluorobenzene to be as follows:

$$\varkappa = -0.58795 \pm 0.00001$$
$$A = 5664.35 \pm 0.15 \text{ Mc/s}$$
$$B = 2570.40 \pm 0.03 \text{ Mc/s}$$
$$C = 1767.91 \pm 0.03 \text{ Mc/s}$$

If the values of rotational constants are expressed in units of cm^{-1}, the following values are obtained:

$$A = 0.18881 \text{ cm}^{-1}$$
$$B = 0.08568 \text{ cm}^{-1}$$
$$C = 0.05893 \text{ cm}^{-1}$$

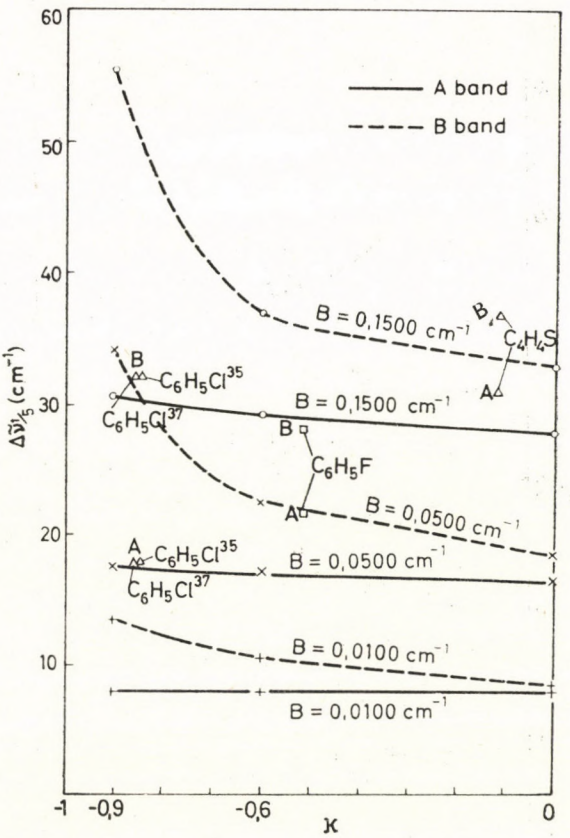

Fig. 2

The vibrations of fluorobenzene produce pure A-, B- and C-bands. Vapour spectra of fluorobenzene are depicted in Figs 4a and 4b.

The fact that in the immediate vicinity of the most intensive bands other bands can be found, made the evaluation more difficult. Thus, the determination of the background transmittance is rather inaccurate. The separation of the bands was carried out by evaluating, on the one hand, the less disturbed half of the band, and, on the other hand, by completing the bands overlapped obviously within the band system in question in order to obtain a background transmittance value suitable for calculations. The fraction-value widths obtained in case of bands of identical type were averaged. Data concerning A-bands are presented in Table I, whereas those of B-bands are tabulated in Table II. The fraction-value widths (half-, fifth- and tenth-value widths) were read from Figs 1, 2 and 3, then the deviations between calculated and obtained data were determined. Results are compiled in Table III. The letters

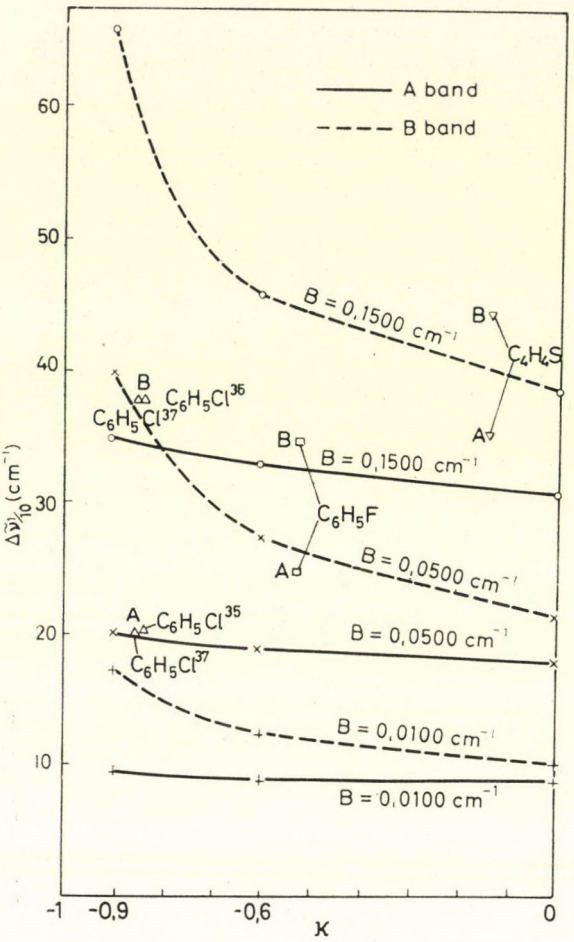

Fig. 3

in the Tables have the following meanings:

T_0 — background transmittance on the place of the maximum;
T_{max} — maximum transmittance;
T_a — background transmittance on the place of the fraction-value in question;
T — transmittance on the place of the fraction-value in question.

2. Chlorobenzene (C_6H_5Cl)

The symmetry and the species of normal vibrations of chlorobenzene are identical to those of fluorobenzene. Its asymmetry parameter and rotational constants have been determined by ERLANDSSON [3]; his results were

Table I

A-bands of fluorobenzene

Fraction--value	T_o (%)	T_{max} (%)	T_a (%)	T (%)	$\Delta\nu$(cm^{-1})
		1024 cm^{-1}			
1/2	78	67	78	72.3	12
1/5	78	67	78	76.7	18
1/10	78	67	79	77.8	22
		1158 cm^{-1}			
1/2	74	43	74	56.8	20
1/5	74	43	75	67.3	25
1/10	74	43	75	71.0	29
		517 cm^{-1}			
1/2	73	46	79	62.7	19
1/5	73	46	81	73.9	27
1/10	73	46	82	78.3	32

Table II

B-bands of fluorobenzene

Fraction-value	T_o (%)	T_{max} (%)	T_a (%)	T (%)	$\Delta\tilde{\nu}$ (cm^{-1})
		1068 cm^{-1}			
1/2	78	60.5	78	68.7	23
1/5	78	60.5	79	74.0	29
1/10	78	60.5	79	75.9	36
		403 cm^{-1}			
1/2	80	68	80	73.8	23
1/5	80	68	80	77.5	31
1/10	80	68	80	78.7	36

as follows:

$C_6H_5^{35}Cl$	$C_6H_5^{37}Cl$
$\varkappa = -0.8450$	$\varkappa = -0.8537$
A = 5666.7 Mc/s	A = 5666.7 Mc/s
B = 1576.9 Mc/s	B = 1532.0 Mc/s
C = 1233.3 Mc/s	C = 1206.3 Mc/s

or expressed in cm^{-1}:

A = 0.18889 cm^{-1}	A = 0.18889 cm^{-1}
B = 0.05189 cm^{-1}	B = 0.05106 cm^{-1}
C = 0.04111 cm^{-1}	C = 0.04021 cm^{-1}

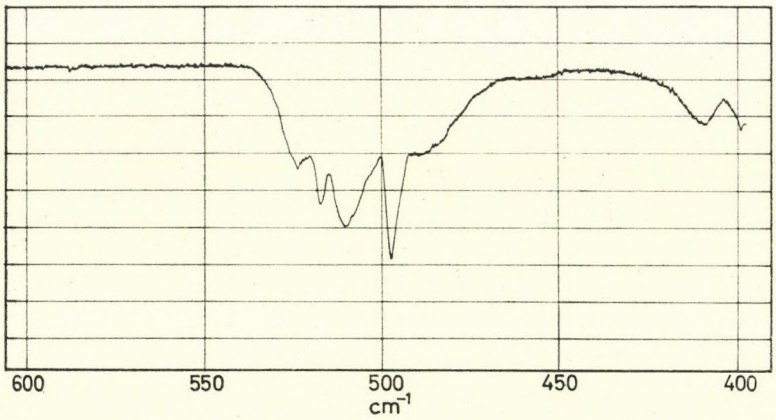

Fig. 4a

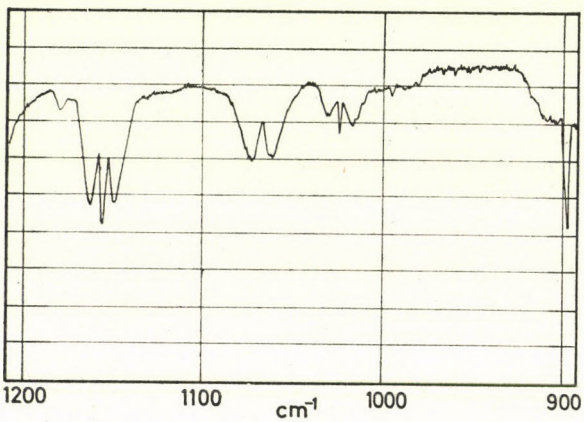

Fig. 4b

Table III

Comparison of calculated and real fraction-value widths of fluorobenzene

Fraction-value	$\Delta\tilde{\nu}_{real}$ (cm^{-1})	$\Delta\tilde{\nu}_{calc.}$ (cm^{-1})	Deviation	
			cm^{-1}	%
		A-band		
1/2	17	17.3	+0.3	+ 1.76
1/5	23.3	21.8	−1.5	− 6.43
1/10	27.7	24.8	−2.9	−10.47
		B-band		
1/2	23	20.5	−2.5	−10.87
1/5	30	28.3	−1.7	− 5.67
1/10	36	34.8	−1.2	− 3.33

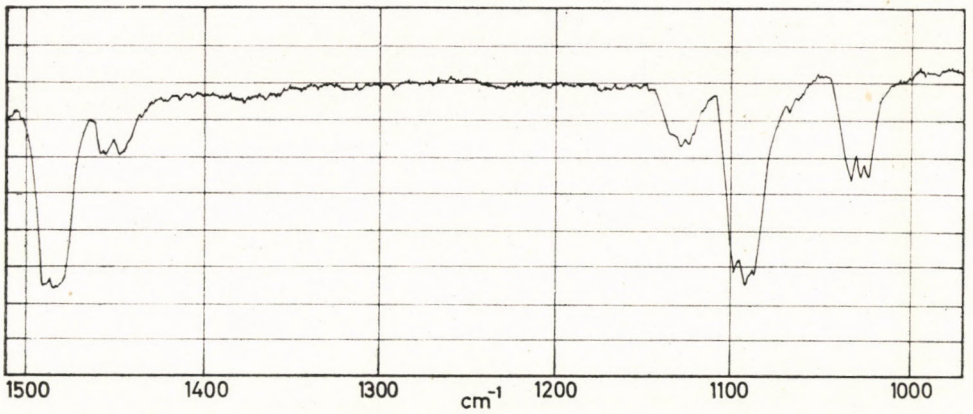

Fig. 5

The vapour spectrum of chlorobenzene is shown in Fig. 5. Bands that are relatively undisturbed were used for evaluation. Fraction-value widths concerning A-bands and B-bands obtained from the real spectrum are tabulated in Table IV and Table V, respectively. It had to be taken into consideration when fraction-value widths were determined, that chlorobenzene is an

Table IV

A-bands of chlorobenzene

Fraction-value	T_0 (%)	T_{max} (%)	T_a (%)	T (%)	$\Delta\tilde{\nu}$ (cm^{-1})
		1028 cm^{-1}			
1/2	78	53.8	77	63.9	18
1/5	78	53.8	77	71.5	21
1/10	78	53.8	77	75.6	24
		1093 cm^{-1}			
1/2	70	24.5	70	41.4	16
1/5	70	24.5	70	56.7	19
1/10	70	24.5	70	63.0	22

isotopic mixture of $C_6H_5{}^{35}Cl$ and $C_6H_5{}^{37}Cl$. The ratio of the two isotopic compound is the same as the isotopic ratio of natural chlorine, *i.e.* 75.4% of ^{35}Cl and 24.6% of ^{37}Cl. The fraction-value widths of chlorobenzene were calculated on the basis of Figs 1, 2 and 3, taking this isotopic ratio into consideration. Calculated and actual values are compared in Table VI.

Table V

B-band of chlorobenzene

Fraction-value	T_0 (%)	T_{max} (%)	T_a (%)	T (%)	$\Delta\tilde{\nu}$ (cm^{-1})
			1452 cm^{-1}		
1/2	75	61	75	67.6	23
1/5	75	61	75	72.0	35
1/10	75	61	75	73.5	38

Table VI

Comparison of calculated and real fraction-value widths of chlorobenzene

Fraction value	$\Delta\tilde{\nu}_{real}$ (cm^{-1})	$\Delta\tilde{\nu}_{calc}$ (cm^{-1})	Deviation	
			cm^{-1}	%
		A-band		
1/2	17	13.8	−3.2	−18.7
1/5	20	17.7	−2.3	−11.5
1/10	23	20.4	−2.6	−11.3
		B-band		
1/2	23	22.5	−0.5	−2.17
1/5	35	32.3	−2.7	−7.71
1/10	38	37.8	−0.2	−0.53

3. Thiophene (C_4H_4S)

Thiophene belongs to symmetry group C_{2v}, too. Its 21 normal vibrations can be divided into the following species: $8\,A_1 + 7\,B_2 + 3\,A_2 + 3\,B_1$. The molecule has the following asymmetry parameter and rotational constants according to BAK *et al.* [4]:

$$\varkappa = -0.09182$$
$$A = 0.268059\ cm^{-1}$$
$$B = 0.18064\ cm^{-1}$$
$$C = 0.107859\ cm^{-1}$$

Vapour spectra of thiophene are shown in Figs 6a, 6b and 6c. Fraction-value widths were determined as previously. The results of A-bands are listed

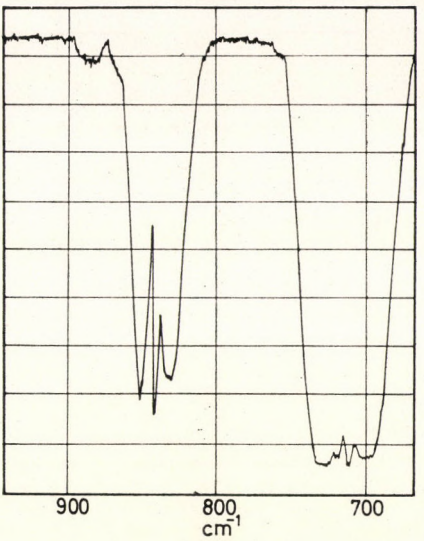

Fig. 6a

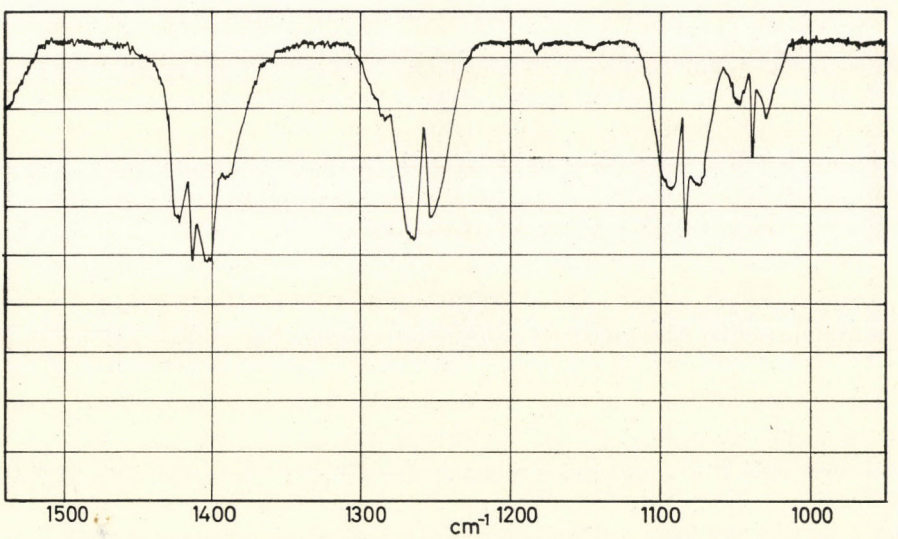

Fig. 6b

in Table VII and the results concerning B-bands are tabulated in Table VIII. Calculated and experimental values are compared in Table IX.

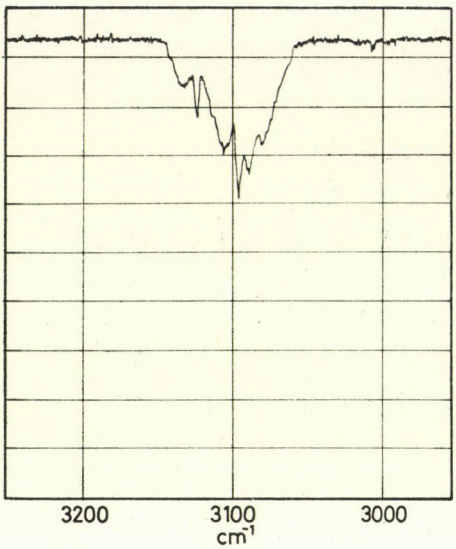

Fig. 6c

Evaluation

It can be seen from the above-mentioned data that in case of A-bands, the largest absolute deviation is 4.5 cm^{-1} (tenth-value width of thiophene), and the largest percentage of deviation is equal to 18.7% (half-value width of chlorobenzene), whereas in case of B-bands the largest absolute deviation is also 4.5 cm^{-1} (half-value width of thiophene) and the largest percentage of deviation is 15.00% (half-value width of thiophene), respectively. The calculated values are smaller than the real ones except for one case. The deviations may be explained by various reasons.

The experimental determination of spectral fraction-value widths cannot be exact, partly because of the disturbance of other bands in the vicinity (it is supported by the fact that different fraction-value widths were obtained in case of bands of identical type of the same molecule), and partly because of the inaccurate instrumental reading. The accuracy of reading is about 0.5 cm^{-1} in the 400—700 cm^{-1} spectral range and about 1 cm^{-1} in the 700—4000 cm^{-1} spectral range using a Zeiss UR-10 spectrometer under the conditions applied. In case of thiophene, the medium rotational constant of which is $B = 0.1806$, extrapolation may also cause errors to some extent.

The calculations of theoretical A-bands and B-bands were carried out on the basis of an approximation. The first approximation was introduced by calculating the terms graphically. The error is estimated to be less than 10% in this case. No considerable errors were caused by graphical approximation of terms in case of calculation of line positions; in most cases, this gives rise to small constant shifts (0.05—1.6 cm^{-1}). It influences the shape

Table VII

A-bands of thiophene

Fraction-value	T_o (%)	T_{max} (%)	T_a (%)	T (%)	$\Delta\tilde{\nu}$ (cm^{-1})
			840 cm^{-1}		
1/2	90	15	89	35.9	28
1/5	90	15	89	61.9	37
1/10	90	15	89	74.2	41
			1038 cm^{-1}		
1/2	93	70.5	91	79.2	23.5
1/5	93	70.5	91	86.1	34
1/10	93	70.5	92	89.5	40
			1083 cm^{-1}		
1/2	90	53	91	69.5	30
1/5	90	53	91	81.7	40
1/10	90	53	91	86.2	50
			1412 cm^{-1}		
1/2	74	49	78	63.5	29
1/5	74	49	78	71.8	32
1/10	74	49	78	74.9	37
			3126 cm^{-1}		
1/2	89	78	90	84.3	26
1/5	89	78	90	87.7	30
1/10	89	78	90	88.8	32

Table VIII

B-bands of thiophene

Fraction-value	T_o (%)	T_{max} (%)	T_a (%)	T (%)	$\Delta\tilde{\nu}$ (cm^{-1})
			873 cm^{-1}		
1/2	93	89	93	91.0	38
1/5	93	89	93	92.2	42
1/10	93	89	93	92.6	47
			1256 cm^{-1}		
1/2	89	56.5	90	71.7	30
1/5	89	56.5	90	82.2	41
1/10	89	56.5	90	86.0	48

Table IX

Comparison of real and calculated fraction-value widths of thiophene

Fraction value	$\Delta\tilde{\nu}_{real}$ (cm^{-1})	$\Delta\tilde{\nu}_{calc}$ (cm^{-1})	Deviation	
			cm^{-1}	%
A-band				
1/2	27.3	24.4	−2.9	−10.62
1/5	34.6	31.3	−3.3	− 9.55
1/10	40.0	35.5	−4.5	−11.25
B-band				
1/2	30*	25.5	−4.5	−15.00
1/5	41.5	37.3	−4.2	−10.12
1/10	47.5	44.7	−3.2	− 6.73

* The half-value width of the B-band is not a mean value. The intensity of the line at 873 cm^{-1} is so small that the determination of fraction-value width is very inaccurate. The noise and the inertia of the recording needle may cause considerable relative errors. This is suggested by the large deviation of the half-value width as compared with that of the band at 1256 cm^{-1}. The half-value width of the band at 1256 cm^{-1} was accepted as the half-value width of the B-band.

of the A-bands, and in case of $\varkappa = 0$, to a small extent, that of B-bands, too. It is assumed using the approximation mentioned that the lines of subbranch Q_q A pertaining to the same L values lie on the same place. Where the calculations carried out by using exact term values (which are available up to J = 40 [5]), these lines would be found in a more or less broad band, thus the very sharp maximum of Q is in fact somewhat broader than assumed. The situation is similar in case of subbranches R_r B II, R_p B II and Q_r B, if $\varkappa = 0$. In these cases the approximation assumed that the lines pertaining to the same J values are on the same place. Using a more accurate calculation, however, these lines lie also in a range of wave numbers, thus the actual B-band is somewhat broader than the calculated one.

The calculation of F intensity values can be carried out by reducing them to those of the symmetric top even in case of $\varkappa = 0$. If the shape of the calculated subbranches is compared with the course of line intensity calculated by WAIT and PINKHAM [6] using exact eigenvalues as the base, a very good agreement can be obtained.

The Boltzmann factor contains the term value, too. The maximum error of term values as high as 10% may cause large deviations only in cases of such large values of J and K, where the corresponding intensities amount only to a few hundredth per cents of the maximum intensities. In case of $\varkappa = 0$, however, the maximum error of the term values is smaller, but its value may be as high as 4—4.5% even with smaller values of J and K.

The intensity deviation corresponding to this can already be detected.

Another inaccuracy may originate from the fact that only transitions $\Delta K = 0, \pm 1$ and $\Delta L = 0, \pm 1$ have been taken into consideration among all possible transitions (except for subbranch R_p B I, where $\Delta L = 3$).

The deviations may be due, however, mainly to *the different values of the rotational constants in the ground and excited states* as well as to the fact that *the interconnections of vibration and rotation have been disregarded.* It is essential to take the latter facts into consideration in order to obtain more exact results.

*

The authors are thanking to Dr. S. HOLLY for recording the spectra and making them available for the authors.

REFERENCES

1. PAÁL, É., VARSÁNYI, GY.: Acta Chim. Acad. Sci. Hung. (in the press)
2. ERLANDSSON, G.: Arkiv för Fysik, **9**, 399 (1955)
3. ERLANDSSON, G.: Arkiv för Fysik, **8**, 341 (1954)
4. BAK, B., CHRISTENSEN, D., HANSEN-NYGAARD, L., RASTRUP-ANDERSEN, J.: J. Mol. Spectroscopy, **7**, 58 (1961)
5. ALLEN, H. C., JR., CROSS, P. C.: Molecular Vib-Rotors. J. Wiley, New York, 1963
6. WAIT, S. C., PINKHAM, C. A.: J. Mol. Spectroscopy, **19**, 34 (1966)

Éva PAÁL
György VARSÁNYI
} Budapest XI., Budafoki út 8.

Acta Chimica Academiae Scientiarum Hungaricae, Tomus 62 (1), pp. 65—74 (1969)

HETEROCYCLIC COMPOUNDS FROM SUGARS, I

PREPARATION OF 2-(POLYHYDROXYALKYL)-BENZOTHIAZOLINE DERIVATIVES

R. BOGNÁR, Z. KOLODYNSKA, L. SOMOGYI, Z. GYÖRGYDEÁK, L. SZILÁGYI and É. N. NEMES

(Institute of Organic Chemistry, L. Kossuth University, Debrecen; Antibiotics Research Group, Hungarian Academy of Sciences, Debrecen)

Received July 5, 1968

The condensation reactions of 2-aminothiophenol (**I**) and 2-amino-4-chlorothiophenol (**II**) with D-glucose and D-galactose have been studied. It has been established that 2-(pentahydroxypentyl)-benzothiazoline derivatives (**VII, VIII, XIII, XIV**) are formed which can be converted to O- and O,N-acetates (**XI, XII, XVII, XVIII** and **IX, X, XV, XVI**) by further acetylation. The syntheses of the 2-(pentaacetoxypentyl)-benzothiazolines have also been achieved using the acetates of *al*-sugars as the starting materials. The structures of the compounds have been confirmed by IR spectroscopic studies.

The reaction of *o*-aminothiophenols with carbonyl compounds has been the subject of numerous papers since 1880 when HOFMANN [1] reported the preparation of benzothiazole derivatives by condensing *o*-aminothiophenol (**I**) with aldehydes.

According to LANKELMA and SHARNOFF [2], and BOGERT and NAIMAN [3], the reaction takes place in several steps. First an anil is formed; this intermediate is then converted to a benzothiazoline derivative, which is easily oxidized into the corresponding benzothiazole.

In his well-known book "Characterisation of Organic Compounds", F. WILD [4] suggests that aromatic aldehydes and ketones be characterized by the product of their condensation with 4-chloro-2-aminothiophenol (**II**). According to this author, the condensation may result in the formation of benzothiazole or benzothiazoline derivatives, and the latter compounds are better suited for the characterization of higher aliphatic aldehydes. Benzothiazoles can be isolated in the case of aliphatic aldehydes and the majority of aromatic aldehydes, benzothiazoline derivatives being formed only with certain aromatic aldehydes. Still, all the examples given by the author for identification involve benzothiazoline derivatives. Therefore, this interesting method requires further detailed studies before it may find general application.

We studied the above reactions with monosaccharides, taking into account the fact that the C-2 atom of benzothiazolines formed by condensation with the carbonyl group of sugars will be asymmetric.

To our knowledge, no detailed study has been published on the condensation of *o*-aminothiophenol with sugars. SATTLER *et al.* [5] reported the

reaction of D-glucose, D-mannose, and D-arabinose with *o*-aminothiophenol in a short communication in 1951. The product of condensation was assumed to be a benzothiazoline derivative; it was sensitive to light, and unstable in aqueous solution. When exposed to air the solutions became cloudy, and crystalline bis-(2-amino-phenyl)disulphide precipitated, while sugar was detected in the solution. No thiol group could be detected by sodium nitroprusside, and attempts to oxidize the products to benzothiazole derivatives failed.

In order to elucidate the structures, properties, and reactions of the products, *o*-aminothiophenol and 2-amino-4-chlorothiophenol were condensed with D-glucose and D-galactose. The products were assumed to be benzothiazoline derivatives, therefore, for purposes of comparison, 2,2-dimethylbenzothiazoline (**III**) and its 5-chloro derivative (**IV**) have been prepared. These compounds have known structures, and, for structural reasons, they are not convertable into benzothiazoles by oxidation.

Comparing the IR spectrum of 2,2-dimethyl-benzothiazoline with those of the condensation products from simple sugars, we found that the pentahydroxypentyl derivatives obtained also had the characteristic IR bands of benzothiazoline.

Acetylation of the 2-(pentahydroxypentyl)-benzothiazolines (**VII**, **VIII**, **XIII**, **XIV**) yielded products of two kinds, depending on the experimental conditions. Acetylation with pyridine/acetic anhydride (24 hours at room temperature) yields a penta-O-acetyl derivative. Acetylation with acetic anhydride in the presence of sodium acetate or zinc chloride at elevated temperatures, or in the presence of perchloric acid without heating, results in the formation of a hexaacetyl derivative. Further acetylation of the pentaacetyl derivatives obtained with pyridine/acetic anhydride gives the hexaacetates in the case of both the gluco- and the galacto-benzothiazoline derivatives.

Similarly to the IR spectrum of 2,2-dimethyl-benzothiazoline, those of the pentaacetyl derivatives have an NH band at 3320—3360 cm^{-1}. The characteristic absorption due to the free NH group is not observed in the IR spectra of the hexaacetates, similarly to the case of 2,2-dimethyl-3-acetyl-benzothiazoline. The presence of an NH group capable of undergoing acetylation, as well as the formation of a tertiary amide (1670—1680 cm^{-1}) upon further acetylation, constitute evidence for the thiazoline structure.

The following experiments have been performed to obtain additional proof of the structure: *o*-aminothiophenol (**I**) and 4-chloro-2-aminothiophenol (**II**) were condensed with both *al*-pentaacetyl-D-glucose and *al*-pentaacetyl-D-galactose. Presumably due to the formation of diastereoisomeric compounds, in some cases only amorphous intermediates could be isolated when processing the products and further converting the compounds obtained from the *al*-sugar acetates. However, identical products have been obtained as a result of two

different routes, constituting evidence for the structures of the compounds under consideration. The *al*-galactose acetate gave the desired pentaacetates (**XVII, XVIII**) which were identical with the products obtained from **XIII** and **XIV** with pyridine/acetic anhydride, yielding the corresponding hexaacetate (**XV and XVI**) upon further acetylation.

Condensation of *al*-pentaacetyl-D-glucose with **I** and **II** yielded amorphous products of varying optical activities. From among the products synthesized by two different routes, *i.e.* from the free sugar and the aldehydo derivative, only the O,N-hexaacetates gave identical compounds (**IX** and **X**) upon further acetylation of the condensation product of the *al*-pentaacetyl-D-glucose with **I** and **II**.

These reactions can be regarded as proof of the structure of the non-acetylated condensation products, too.

The following equations summarize the above statements (*cf.* p. 68).

The physical constants of the compounds (*cf.* Experimental) are shown in the Tables. Depending on the method of preparation, some deviations are observed in the $[\alpha]_D$ values, and to a smaller extent in the m.p.-s, though the analyses were satisfactory in all cases. In some instances, the intermediates failed to crystallize. This is probably due to the formation of diastereoisomers in the condensation. Side reactions may also have taken place, the products could only be separated from the syrupy reaction mixture after further conversion into crystalline derivatives.

Work on the separation of the diastereoisomers and further study of the condensation reactions are in progress.

Experimental

The m.p.-s were determined in capillary tubes and are uncorrected. The IR spectra were obtained in KBr pellets with a Unicam SP 200 G apparatus or in carbon tetrachloride with a Zeiss UR-10 spectrometer.

2,2-Dimethylbenzothiazoline (III)

The best results were obtained using the method of KIPRIANOV [6]: a mixture of *o*-aminothiophenol and acetone was heated for 1 hr. at 100°C in a sealed tube.

2,2-Dimethyl-3-acetylbenzothiazoline (V)

(*a*) 1.4 g of 2,2-dimethylbenzothiazoline (**III**) in absolute benzene was refluxed with 5 ml of acetyl chloride for 90 min. The reaction mixture was then evaporated to dryness under reduced pressure, and the crystalline residue purified by recrystallization from *n*-heptane, or destillation under reduced pressure (b.p. 132—134°C at 2 torr to yield 1.32 g (55%), m.p. 49—50°C).

$C_{11}H_{13}NOS$ (207.3). Calcd. N 6.76; S 15.47; Ac 20.77. Found N 6.86; S 15.02; Ac 21.19%.

(*b*) The same product was obtained by heating III with approximately 5 parts of acetic anhydride for 1 hr. on a steam-bath, and pouring the reaction mixture into ice-water. After extraction with ether and drying, the solvent was evaporated and the residue crystallized from *n*-heptane.

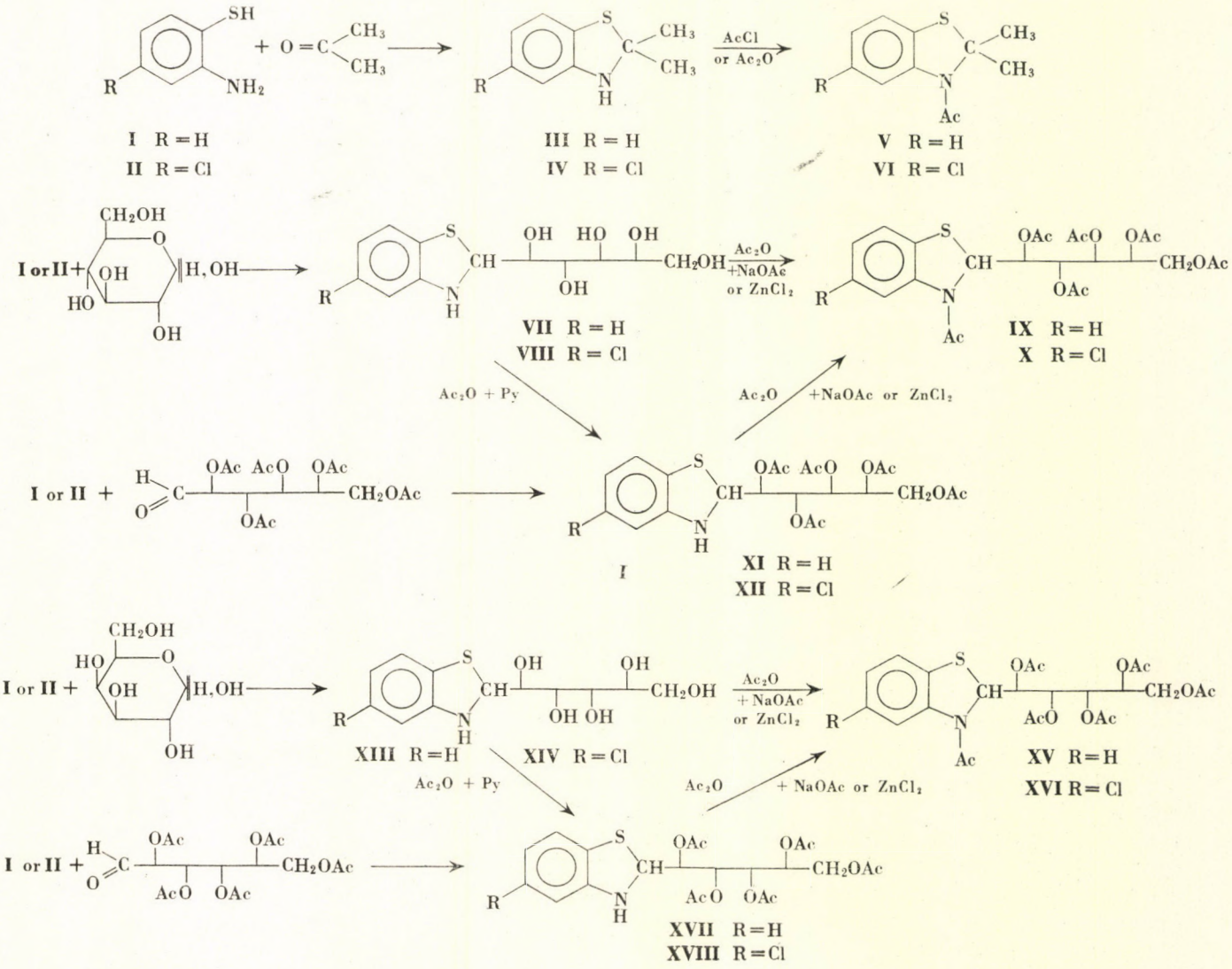
I R = H
II R = Cl
III R = H
IV R = Cl
V R = H
VI R = Cl
AcCl or Ac2O
I or II +
VII R = H
VIII R = Cl
IX R = H
X R = Cl
Ac2O + Py
Ac2O +NaOAc or ZnCl2
XI R = H
XII R = Cl
I
XIII R = H
XIV R = Cl
XV R = H
XVI R = Cl
XVII R = H
XVIII R = Cl
II

2,2-Dimethyl-5-chlorobenzothiazoline (IV)

This compound was prepared by the known procedure. Best results were obtained using the method of KIPRIANOV [6]: yield 66%, m.p. 37—38°C (lit. [3] yield 39%; m.p. 37—38°C).

2,2-Dimethyl-3-acetyl-5-chlorobenzothiazoline (VI)

Similarly to the preparation of **V** (*cf.* method (*a*) above), the acetylation was carried out with acetyl chloride. The crude product was recrystallized 3 times from *n*-heptane. Yield 58%, m.p. 56—57°C.

$C_{11}H_{12}ClNOS$ (241.7). Calcd. N 5.80; S 13.26; Ac 17.81. Found N 5.87; S 13.30; Ac 17.92%.

2-(D-Gluco-pentahydroxypentyl)benzothiazoline (VII)
2-(D-Gluco-pentahydroxypentyl)-5-chlorobenzothiazoline (VIII)
2-(D-Galacto-pentahydroxypentyl)benzothiazoline (XIII) and
2-(D-Galacto-pentahydroxypentyl)-5-chlorobenzothiazoline (XIV)

These compounds were prepared by the following methods:

(1*A*) A solution of 10 mmoles of 2-amino- or 2-amino-4-chlorothiophenol in 3 ml of pyridine was mixed with 10 mmoles of D-glucose or D-galactose. The mixture was heated on a steam-bath for 30 min. under nitrogen, then cooled and acidified with 10% HCl. The crystalline crude product separated on standing for 12 hrs. in a refrigerator. It was purified by recrystallization from a solvent (shown in the Table).

(1*B*) A solution of 10 mmoles of 2-amino- or 2-amino-4-chlorothiophenol in 10 ml of absolute methanol was mixed with 10 mmoles of the aldose and heated for 30 min. on a steam-bath. The reaction mixture was cooled, and after adding 10 ml of isopropanol it was allowed to stand in a refrigerator overnight. The crude product was recrystallized.

(1*C*) According to SATTLER and ZERBAN [5], 2-amino- or 2-amino-4-chlorothiophenol (10 mmoles) dissolved in 10 ml of glacial acetic acid was allowed to react with the aldose (10 mmoles) at room temperature for 3 days. The resulting mixture was processed as described in Section 1*B*.

The products were first dried in a vacuum desiccator over $CaCl_2$. The glucose derivatives were further dried at 70°C, and the galactose derivatives at 100°C, in a vacuum drying pistol over P_2O_5.

The characteristics of the above compounds are listed in Table I.

2-(D-Gluco-pentaacetoxypentyl)benzothiazoline (XI)
2-(D-Gluco-pentaacetoxypentyl)-5-chlorobenzothiazoline (XII)
2-(D-Galacto-pentaacetoxypentyl)benzothiazoline (XVII) and
2-(D-Galacto-pentaacetoxypentyl)-5-chlorobenzothiazoline (XVIII)

The above derivatives were prepared by two independent routes.

(2*A*) Acetylation of the acetyl-free products. 1 ml of the benzothiazoline derivative was let to stand with 4 ml of pyridine and 8 ml of acetic anhydride for 24 hrs. at room temperature. The product precipitating after the reaction mixture had been poured into ice-water, was separated, washed with water and, after clarification, crystallized from a solvent (see Table II).

(2*B*) Condensation of pentaacetyl-*al*-D-glucose or -D-galactose with *o*-aminothiophenol or 2-amino-4-chlorothiophenol.

(*2Ba*) **2-(D-Gluco-pentaacetoxypentyl)benzothiazoline (XI)**

0.6 g of *o*-aminothiophenol was dissolved in 5 ml of absolute methanol and 1.9 g of *al*-pentaacetyl-D-glucose was added. The mixture was heated on a steam-bath for 30 min. and the methanol evaporated under reduced pressure. Attempts to crystallize the residue failed.

Table I

Compound	Method of preparation	Yield (%)	M.p. (solvent)	$[\alpha]_D^{23}$ in pyridine (c)	Molecular formula and analysis
2-(D-Gluco-pentahydroxypentyl)-benzothiazoline (**VII**)	1*A* 1*B* 1*C**	12 77 52	166—7°C (*i*-PrOH)	−66.3° (0.33)	$C_{12}H_{17}NO_5S$ (287.3) Calcd. C 50.17; H 5.96; N 4.88; S 11.16 Found C 50.15; H 6.31; N 4.84; S 10.59%
2-(D-Gluco-pentahydroxypentyl)-5-chlorobenzothiazoline (**VIII**)	1*A* 1*B* 1*C*	69 86 74	132°C (*i*-PrOH)	−46.5° (0.47)	$C_{12}H_{16}ClNO_5S$ (312.8) Calcd. C 44.79; H 5.01; Cl 11.02; N 4.35; S 9.96 Found C 44.74; H 5.32; Cl 11.29; N 4.43; S 9.99%
2-(D-Galacto-pentahydroxypentyl)-benzothiazoline (**XIII**)	1*F* 1*B* 1*C*	63 19 74	191°C (MeOH or *i*-PrOH)	−50.95° (0.53)	$C_{12}H_{17}NO_5S$ (287.3) Calcd. C 50.17; H 5.96; N 4.88; S 11.16 Found C 50.81; H 6.21; N 4.88; S 11.44%
2-(D-Galacto-pentahydroxypentyl)-5-chlorobenzothiazoline (**XIV**)	1*A* 1*B* 1*C*	94 59 78	193—4°C (MeOH or *i*-PrOH)	−83.3° (0.50)	$C_{12}H_{16}ClNO_5S$ (321.8) Calcd. C 44.79; H 5.01; Cl 11.02; N 4.35; S 9.96 Found C 45.10; H 5.36; Cl 11.05; N 4.36; S 9.94%

* Lit. [5] m.p. 118—119.2°C; $[\alpha]_D^{20} = -15.6°$ ($c = 0.9$, water).

Table II

Compound	Method of preparation	M.p. (solvent)	$[\alpha]_D^{33}$ in pyridine (c)	Molecular formula and analysis
2-(D-Gluco-pentaacetoxypentyl)-benzothiazoline (**XI**)	2*A*, 2*B*	syrup		
2-(D-Gluco-pentaacetoxypentyl)-3-acetylbenzothiazoline (**IX**)	3*A*, 3*B*	132—133°C (MeOH)	+134° (0.48)	$C_{24}H_{29}NO_{11}S$ (539.6)
	3*Bc*	136—137°C (abs. EtOH)	+136° (1.0)	Calcd. C 53.43; H 5.42; N 2.60; S 5.94; Ac 47.88 Found C 53.80; H 5.86; N 2.76; S 5.79; Ac 47.82%
2-(D-Galacto-pentaacetoxypentyl)-benzothiazoline (**XVII**)	2*A*, 2*B*	143—144°C	− 4.75°	$C_{22}H_{27}NO_{10}S$ (497.5) Calcd. C 53.11; H 5.47; N 2.81; S 6.45; Ac 43.26 Found C 52.81; H 5.76; N 2.82; S 6.43; Ac 43.40%
2-(D-Galacto-pentaacetoxypentyl)-3-acetylbenzothiazoline (**XV**)	3*A*, 3*B*	131—132°C (EtOH)	−72.1° (0.43)	$C_{24}H_{29}NO_{11}S$ (539.6) Calcd. N 2.60; S 5.94; Ac 47.88 Found N 2.73; S 6.05; Ac 47.82%
2-(D-Gluco-pentaacetoxypentyl)-5-chlorobenzothiazoline (**XII**)	2*A*, 2*B*	Amorphous ($EtOH—H_2O$)	−33.1°	$C_{22}H_{26}ClNO_{10}S$ (531.96) Calcd. N 2.63; S 6.03; Ac 41.40 Found N 2.60; S 6.64; Ac 36.80%
2-(D-Gluco-pentaacetoxypentyl)-3-acetyl-5-chlorobenzothiazoline (**X**)	3*A*, 3*B*	Amorphous	+24.0°	$C_{24}H_{28}ClNO_{11}S$ (574.0) Calcd. N 2.44; S 5.59; Ac 45.00 Found N 2.51 S 5.54; Ac 45.82%
2-(D-Galacto-pentaacetoxypentyl)-5-chlorobenzothiazoline (**XVIII**)	2*A*	162°C (EtOH)	−93.9° (0.52)	$C_{22}H_{26}ClNO_{10}S$ (531.96) Calcd. C 49.67; H 4.93; N 2.63; S 6.03; Ac 41.40 Found C 49.70; H 4.97; N 2.40; S 6.05; Ac 40.83%
2-(D-Galacto-pentaacetoxypentyl)-3-acetyl-5-chlorobenzothiazoline (**XVI**)	3*A*, 3*B*	172—174°C (EtOH)	+43.7° (0.60)	$C_{24}H_{28}ClNO_{11}S$ (574.0) Calcd. N 2.44; S 5.59; Ac 45.00 Found N 2.45; S 5.50; Ac 44.76%

Table III

2-substituted benzothiazolines

IR spectroscopic data

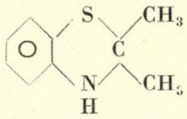	**(III)**	3320 (N—H); 1582; 755	(KBr)
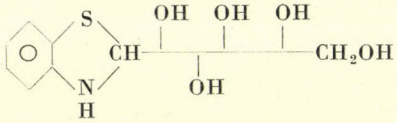	**(VII)**	3200—3430 (N—H, O—H); 1580; 735	(KBr)
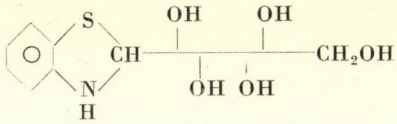	**(XIII)**	3150—3420 (N—H, O—H); 1580; 735	(KBr)
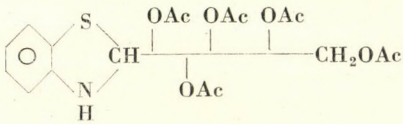	**(XI)**	3360, 3460 (N—H); 1750 (C=O ester); 1585; 785	(KBr)
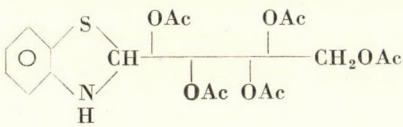	**(XVII)**	3320 (N—H); 1750 (C=O ester); 1585; 755	(KBr)
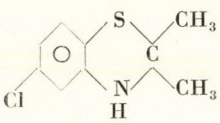	**(IV)**	3360 (N—H); 1580; 805	(KBr)
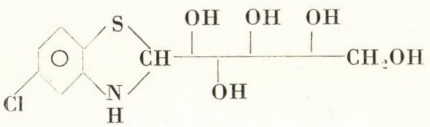	**(VIII)**	3200—3420 (N—H, O—H); 1580; 810	(KBr)
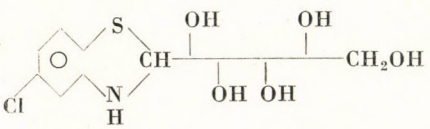	**(XIV)**	3240—3340 (N—H, O—H); 1580; 805 (doublet)	(KBr)
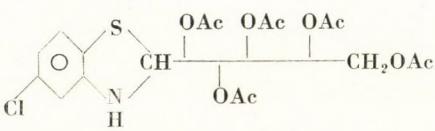	**(XII)**	3400—3500 (N—H); 1760 (C=O ester); 1585	(CCl_4)
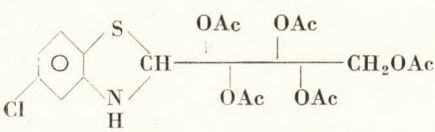	**(XVIII)**	3360 (N—H); 1750 (C=O ester); 1585; 805	(KBr)

(*2Bb*) 2-(D-Gluco-pentaacetoxypentyl)-5-chlorobenzothiazoline (XII)

0.8 g of 2-amino-4-chlorothiophenol was dissolved in 6 ml of glacial acetic acid and 1.95 g of *al*-pentaacetyl-D-glucose was added. After standing for 3 days, the mixture was poured into ice-water. The precipitated oily product soon solidified; it was separated, washed, and dissolved in ethanol. After clarification it was again precipitated by diluting the mixture with water. The IR spectrum of this substance indicated that it was identical with the product obtained in procedure (*2A*).

2-(D-Galacto-pentaacetoxypentyl)benzothiazoline (XVII) and 2-(D-Galacto-pentaacetoxypentyl)-5-chlorobenzothiazoline (XVIII)

These compounds were prepared by method (*2Bb*), reacting 2-aminothiophenol or 2-amino-4-chlorothiophenol with *al*-pentaacetyl-D-galactose. The crude product was purified by recrystallization from ethanol. On the basis of the IR spectra and mixed m.p. determination, these compounds were found to be identical with those prepared by procedure (*2A*).

Table III (contd.)

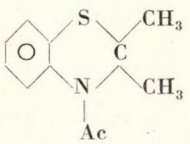	(V)	1670 (C=O amide); 1580; 750	(KBr)
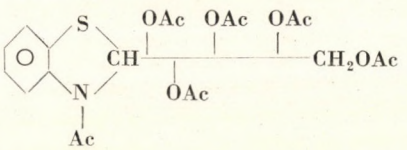	(IX)	1750 (C=O ester); 1670 (C=O amide); 1580; 770 (doublet)	(KBr)
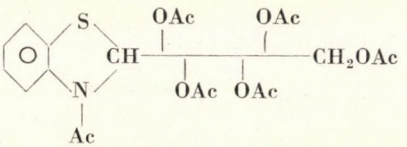	(XV)	1750 (C=O ester); 1670 (C=O amide); 1580; 750	(KBr)
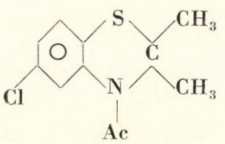	(VI)	1685 (C=O amide); 1575; 805 (doublet)	(KBr)
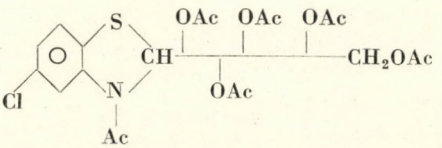	(X)	1760 (C=O ester); 1680 (C=O amide, shoulder); 1585	(CCl_4)
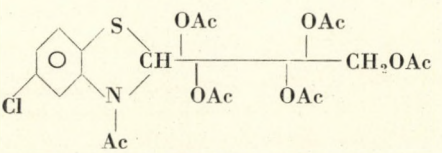	(XVI)	1750 (C=O ester); 1680 (C=O amide); 1575	(KBr)

2-(D-Gluco-pentaacetoxypentyl)-3-acetylbenzothiazoline (IX)
2-(D-Gluco-pentaacetoxypentyl)-3-acetyl-5-chlorobenzothiazoline (X)
2-(D-Galacto-pentaacetoxypentyl)-3-acetylbenzothiazoline (XV) and
2-(D-Galacto-pentaacetoxypentyl)-3-acetyl-5-chlorobenzothiazoline (XVI)

These compounds were prepared by the following methods:

(3*A*) Acetylation of the corresponding 2-(pentahydroxypentyl)-benzothiazolines.

(3*Aa*) A mixture of 1 g of the benzothiazoline derivative, 1 g of anhydrous sodium acetate, and 10 ml of acetic anhydride was heated on a steam-bath for 2 hrs. The mixture was then poured into ice-water, and the precipitated crude product recrystallized from a solvent (see Table II).

(3*Ab*) 1 g of the benzothiazoline derivative in 10 ml of acetic anhydride containing 1 g freshly heated $ZnCl_2$ was kept at 80°C for 30 min. The mixture was poured into ice-water and processed as described in (2*Aa*).

(3*Ba*) Acetylation of the 2-(pentahydroxypentyl)-benzothiazolines with pyridine acetic anhydride.

(3*Bb*) Acetylation with acetic anhydride/sodium acetate of the 2-(pentaacetoxypentyl)-benzothiazolines obtained by condensing 2-aminothiophenol with *al*-pentaacetyl-D-glucose and -galactose, using procedure (3*Aa*).

(3*Bc*) IX was prepared by the condensation of 2-aminothiophenol with *al*-pentaacetyl-D-glucose in glacial acetic acid, and subjecting the product to further acetylation. Procedure: 2.342 g (6 mmoles) of *al*-pentaacetyl-D-glucose in 8 ml of glacial acetic acid was mixed with 0.752 g (6 mmoles) of 2-aminothiophenol. The mixture was let to stand for 3 days under nitrogen at room temperature. 30 ml of acetic anhydride and 0.15 ml of 60% perchloric acid were then added. After 24 hrs., the mixture was poured on ice, and neutralized with solid $NaHCO_3$. The solution was extracted with chloroform, followed by washing with a $NaHCO_3$ solution and water. After drying over Na_2SO_4, it was concentrated to a syrup under reduced pressure. The residue was recrystallized from absolute ethanol along with a treatment by charcoal and fuller's earth. The crude product was 0.525 g (20.9%), m.p. 135°C. Recrystallization from ethanol gave 0.338 g, m.p. 136—137°C, $[\alpha]_D^{23} = +136°C$ ($c = 1$, pyridine). No m.p. depression was observed with the products obtained by procedures (3*A*) and (3*Ba*, *b*), and the IR spectra were identical.

Data of the above compounds are listed in Table II.

*

Thanks are due to the microanalytical laboratory of the Institute, headed by E. R.-DÁVID, for the analyses, and to Dr. S. SZABÓ for recording the IR spectra. Financial support of this research by the Hungarian Academy of Sciences is gratefully acknowledged.

REFERENCES

1. HOFMANN, A. W.: Ber. **13,** 1236 (1880).
2. LANKELMA, H. P., SHARNOFF, P. X.: J. Am. Chem. Soc. **53,** 2654 (1931)
3. BOGERT, M. T., NAIMAN, B.: J. Am. Chem. Soc. **57,** 1529 (1935)
4. WILD, F.: Characterisation of Organic Compounds. p. 129. Cambridge Univ. Press, 1962
5. SATTLER, L., ZERBAN, F. W., CLARK, G. L., CHIA-CHEN CHU: J. Am. Chem. Soc. **73,** 5908 (1951)
6 KIPRIANOV, A. I., PORTNIAGINA, V. A.: Zh. Obsch. Chim **25,** 2257 (1955)

Rezső BOGNÁR
Zofia KOLODYNSKA
László SOMOGYI
Zoltán GYÖRGYDEÁK
László SZILÁGYI
Éva NÁNÁSI-NEMES

Debrecen 10. Hungary.

Acta Chimica Academiae Scientiarum Hungaricae, Tomus 62 (1), pp. 75—85 (1969)

INVESTIGATION OF THE RHEOLOGICAL PROPERTIES OF GLUTEN, II

VISCO-ELASTIC PROPERTIES OF CHEMICALLY MODIFIED GLUTEN

R. LÁSZTITY

(Department of Food Chemistry, Technical University, Budapest)

Received August 8, 1968

Chemical modification of several groups in gluten protein and the study of the rheology of its derivatives thus obtained may furnish useful data for the elucidation of the correlations between the chemical structure of the gluten–protein complex and its rheological behaviour.

Among the possible chemical modifications the blocking of thiol groups with N-ethylmaleimide, desamidation, esterification of free carboxyls, conversion of amide into ester groups, and acylation of primary amino groups, seem chiefly to be of interest.

To record rheological properties, the measurement of the relaxation of stresses with a modified Neo-Laborograph instrument, and the measurement of the viscosity of gluten solutions are applied.

Blocking of thiol groups, and esterification of free carboxyl groups have no significant effect on the rheological properties of gluten. Interference with the amido groups, and acylation of primary amino groups cause radical changes in the rheological behaviour of gluten; hereby relaxation times are shortened, and a decrease in cohesivity is observed.

An important aim of studies in connexion with the rheology of gluten is the elucidation of the correlations between rheological properties and the chemical structure of gluten complex. A comprehensive review of this topic, including both from theoretical and practical points of view, has been published [1, 2].

It may be stated in general that besides the quality and quantity of the proteins present in the gluten complex, primarily covalent (disulphide) and non-covalent (hydrogen, hydrophobic) bonds that determine the structure of the protein complex can play a decisive role in the rheological properties of gluten. Accordingly, a study of the rheological behaviour of a chemically modified gluten may furnish useful data concerning the groups that participate in the formation of bonds, and concerning the importance of the several bonds, when considered from a rheological point of view.

Not much has been done in this field up to now. Studies of BARNAY *et al.* [3], of HOLME and BRIGGS [4], further that of BECKWITT *et al.* [5] might be regarded only preliminary steps.

In the course of our studies, the changes in rheological behaviour due to chemical modification of the most often occurring and most characteristic groups (amido, free carboxyl, primary amino, thiol) of gluten proteins have been studied.

Materials and methods

Substances studied were glutens separated from various wheat flours. These were, on the one hand, flours milled in the laboratory to an extraction rate of about 70 per cent, of the Bánkuti 1201 strain, from 1966 (samples 1 to 4), on the other hand, commercially available products, *viz.* flour BL 112,* from 1965 (samples 5 and 6) BL 80,** from 1966 (samples 7 and 8), and BL 112, from 1966 (samples 9 and 10). From the point of view of the baking industry, these were qualified third-, second-, and first-rate flours, and gave a correct representation of flours generally encountered in practice.

Gluten was separated according to the standard method [6] from the flours. The wet gluten product was dispersed in a 0.1 *N* solution of acetic acid, and centrifuged. The supernatant was adjusted with calcium hydroxide to pH 6, and the gluten which precipitated was collected by centrifuging. Purification of the product was carried out by repeated suspension in water and recovery by centrifuging. The final product contained less than 1 per cent of carbohydrates.

Study of the relaxation of gluten and of chemically modified gluten was carried out by means of an improved Neo-Laborograph formerly described [7, 8]. The viscosity of gluten solutions was measured in an Ostwald viscometer, at 25°C.

Chemical modification of gluten was as follows.

Preparation of a N-ethylmaleimide derivative of gluten

By intensive stirring, gluten (50 g) is suspended in acetic acid (0.05 *N*, 500 ml) cooled to 2°C and kept free from air by a stream of nitrogen. This gas displaces air also from the vessel wherein the suspension is stirred. By cooling with ice-water the rise of temperature during dispersion is prevented. According to the thiol content to be expected, the 20 times equivalent of N-ethylmaleimide (in the form of a 0.001 *N* solution) is added to the gluten suspension. Also this solution is made air-free with nitrogen and cooled to 2°C. About 10 to 30 ml of this imide solution is needed for each gram of gluten. This reaction mixture is kept during the reaction time (0.5 to 6 hours) between 2 and 6°C.

After the elapse of the reaction period, the solution is dialysed in cellophane tubes for 48 hours. The residue collected by centrifuging is freeze-dried.

In order to check the completeness of blocking, during the reaction samples were taken at various times from the reaction mixture and the amount of free thiol groups was determined amperometrically. How the blocking process progresses is shown by the time function curve in Fig. 1, according to which 4 to 5 hours are sufficient to obtain complete blocking.

For the rheological study of the gluten derivative, to the lyophylized product twice as much distilled water was added in a small size polythene sack which was then closed by welding, and kneaded by hand till its content formed a uniform homogeneous mass. This was used for relaxation measurements.

Preparation of desamidated gluten

Samples of gluten were desamidated, according to the method of HOLME and BRIGGS [4], with a warm 0.04 *N* hydrochloric acid. The progress of this reaction is shown in Fig. 2; complete desamidation requires about 7 to 8 hours. Control-samples were treated in the same way, with distilled water instead of with hydrochloric acid.

Penetrometric study of desamidated gluten

This was carried out according to AUERMAN [9] by means of a LABOR-type penetrometer. The gluten sample was compressed after kneading and removal of free water as directed.

* Wheat flour with max 1.12% ash content.
** Wheat flour with max 0.8% ash content.

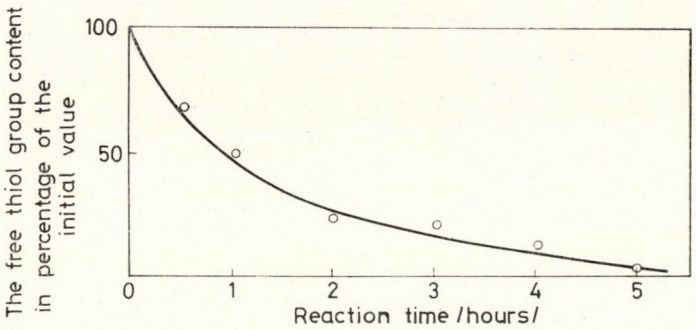

Fig. 1. Blocking, with N-ethylmaleimide, of the free thiol groups of the gluten in function of reaction time

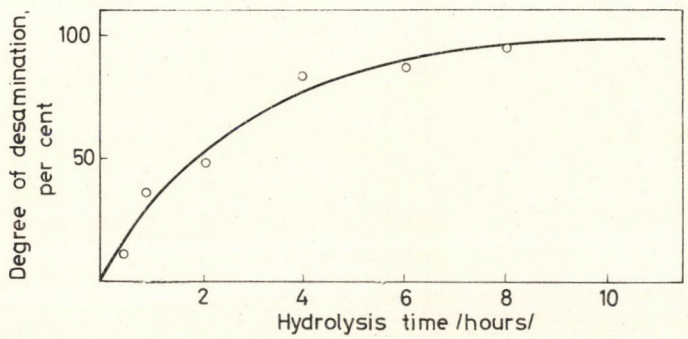

Fig. 2. Desamidation of gluten in function of time

Preparation of methylated and ethylated glutens

According to the method of BECKWITT *et al.* [5], gluten was subjected to methanolysis or ethanolysis. Dry ethanol, or methanol, and 1.2 *N* hydrochloric acid were used, at 30°C. Higher temperatures were not allowed because controls showed that then a considerable amount of dialysable products is formed, this points to some hydrolysis of proteins. Although complete methylation, or ethylation, could not be achieved in this way, but the fission of peptide bonds was avoided and therewith an indeterminable factor affecting rheological properties was excluded.

In order to check the progress of methylation, or ethylation CLARKE's alcoxyl method [10] was used. Besides this, the nitrogen of residual amide was determined by a method described earlier.

Preparation of acylated glutens

In order to prepare gluten that contains acylated primary amino groups, samples of gluten were suspended at 2°C, in a saturated solution of sodium acetate, then acetic acid anhydride was added in small portions. The required amount of anhydride was calculated on the basis of the free amino groups revealed by analysis according to the AACC method [11].

After acylation, the gluten derivative was purified by dialysis for 24 hours, and either used in experiments immediately, or lyophylized for storage, and rehydrated with distilled water prior to rheological measurements.

Results, and their evaluation

1. *The influence of N-ethylmaleimide blocking of free thiol groups of gluten on its rheological properties*

It is supposed that free thiol groups can affect the rheological properties of gluten in two ways. On the one hand, thiol groups may participate in the formation of hydrogen bonds and, on the other, they may affect the arrangement of disulphide bonds through a thiol-disulphide interaction and thus significantly influence their rheological behaviour. Blocking the free thiol groups both ways of interference would be excluded and this, according to the above assumption, should be reflected in the rheological behaviour. N-ethylmaleimide was used as a blocking reagent.

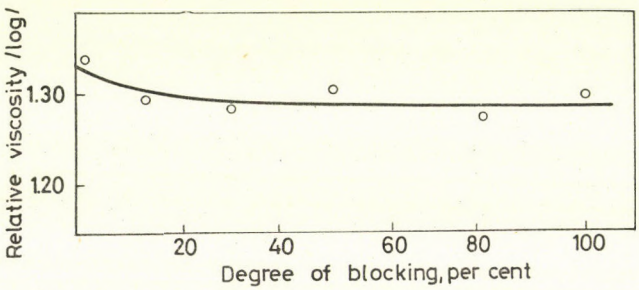

Fig. 3. Change of viscosity of solutions of the N-ethylmaleimide derivative of gluten as a function of the degree of blocking

Rheological features of N-ethylmaleimide derivatives of gluten are listed in Table I.

Data in Table I suggest that no significant change occurs in the viscoelastic behaviour of gluten, when its free thiol groups are blocked.

The viscosity of the gluten derivative suspended in 0.1 *N* acetic acid was also studied; results are collected in Fig. 3. The diagram indicates a small, but clearly observable decrease in the viscosity of gluten solutions blocked with N-ethylmaleimide, referred to controls.

These two series of experiments allow to draw the conclusion that free thiol groups have no significant effect on the rheological properties of glutens. The thiol-disulphide interaction in paste or dough, by several authors supposed to occur, does not play any practical role. It is probable that thiol groups participate in intra- or intermolecular bonding, however, no noticeable effect due to this is exerted upon rheological behaviour.

This refers also to eventual hydrogen bonds, as well as to supposed thiol–carbonyl interactions. Theoretically, in the latter case, due to an addition reaction, a thiol ester is formed.

Table I

Visco-elastic properties of the N-ethylmaleimide derivative of gluten

Sample No.	Blocking per cent	Relaxation time, sec.	L (g)
1	0	57	69
	57	64	75
	100	59	60
2	0	39	60
	57	41	65
	100	38	58
3	0	80	106
	57	89	125
	100	93	98
4	0	68	75
	57	75	80
	100	69	82
5	0	43	68
	57	39	59
	100	59	69
6	0	68	85
	57	70	80
	100	73	78
7	0	46	92
	57	50	97
	100	50	91
8	0	58	106
	57	54	120
	100	49	122
9	0	104	140
	57	121	130
	100	98	119
10	0	82	98
	57	78	96
	100	91	107

It seems probable that thiol groups are important on account of their biological functions but less so as structural factors.

As far as viscosity data are concerned, a small diminution may be due to re-arrangement of the molecules. Since treatment with N-ethylmaleimide means the creation of a hydrophobe state, the "re-arrangement" might be coupled to the formation of hydrophobe bonds. In this context it is well to mention that recent studies (AUER and DOTY [12], SAGE and FASHMAN [13], on synthetic polypeptides, *viz.* poly-leucine, and poly-phenylalanine) have shown species that possess an ordered structure even in 6 *M* guanidine hydrochloride, the formation of such structures being somehow bound to the presence of hydrophobe bondings. It might be supposed that in proteins, containing peptide chains of predominantly hydrophobe amino acids, the formation of parts with an ordered structure is possible. All in all, the free thiol groups do not play an important role in the rheology of gluten.

2. *The influence of desamidation on the rheological properties of gluten*

There is a great number of amidated carboxyl groups present in gluten proteins. In view of this number, high in comparison with other polar groups, the role of amido-groups in the formation of secondary bonds could be rather important. In the course of the present work the penetration indexes of glutens desamidated to various degrees were determined, further the viscosities of gluten solutions, in acetic acid, and in 8 *M* urea were measured. Results are listed in Tables II, III and IV.

Table II

Rheological properties of desamidated gluten

Sample No.	Difference in penetration (ΔP, %) in reference to controls					
	degree of desamidation					
	10	30	50	70	90	100
1	15	24	31	39	39	42
2	12	23	35	46	47	50
3	17	29	39	51	55	57
4	10	21	31	35	34	39
5	8	17	29	37	42	42
6	7	23	29	35	37	39
7	13	21	34	45	49	53
8	15	21	29	42	47	48
9	11	19	33	42	47	48
10	14	23	32	44	43	43

Table III

Characteristic viscosity of desamidated gluten solutions in acetic acid medium

Ser. No.	[η] dl/g degree of desamidation						Acetic acid concentration
	10	30	50	70	90	100	
1	0.425	0.445	0.462	0.480	0.505	0.510	0.05 *N*
	0.430	0.435	0.440	0.437	0.435	0.420	1.0 *N*
2	0.480	0.485	0.492	0.507	0.580	0.510	0.05 *N*
	0.475	0.480	0.481	0.475	0.470	0.469	1.0 *N*
3	0.460	0.475	0.490	0.502	0.500	0.499	0.05 *N*
	0.462	0.467	0.470	0.465	0.459	0.458	1.0 *N*
4	0.502	0.520	0.530	0.536	0.535	0.537	0.05 *N*
	0.490	0.501	0.506	0.508	0.506	0.501	1.0 *N*
5	0.397	0.412	0.431	0.432	0.430	0.429	0.05 *N*
	0.400	0.405	0.405	0.402	0.400	0.390	1.0 *N*

Table IV

Characteristic viscosity of the solutions of desamidated gluten in 8 M urea

Ser. No.	[η] dl/g degree of desamidation					
	10	30	50	70	90	100
1.	0.480	0.475	0.475	0.478	0.468	0.450
2.	0.550	0.552	0.545	0.547	0.530	0.527
3.	0.501	0.497	0.502	0.504	0.486	0.479
4.	0.560	0.550	0.552	0.540	0.531	0.535
5.	0.480	0.482	0.480	0.470	0.447	0.450

The data unequivocally suggest that, compared to controls, desamidated glutens are of softer consistence, *i.e.* their rheological properties are less good. The deviations in relative per cent penetrations increase by increasing the degree of desamidation, strongly first, later tending towards a limit value.

As far as solubilities are considered, desamidated gluten is more difficult to dissolve in strongly acid media (below pH 3) but is easily dissolved — in contrast to controls — by phosphate buffer of pH 8. Considering the substantial increase of free carboxyl groups and the acid character of the protein formed this fact seems to be understandable.

On the basis of results of viscosity measurements it can be stated, first, that desamidation primarily affects the viscosities of solutions in acetic acid.

According to data in Table III, this alteration involves the increase of characteristic viscosity, meaning that a change had occurred in the conformation of molecules which produces a more asymmetric structure. To explain this we may suggest that removal of amide groups involves elimination of secondary, *e.g.* hydrogen bonds in consequence of which a more loose structure will emerge. Presumably, due to the dissociation of carboxyl groups set free, within a molecule, between groups with identical charge, repulsive forces are operative. This supposition is supported by the experimental finding that increase of viscosity is substantially less in 1.0 *N* acetic acid at higher pH and lower dissociation, or that on these conditions sometimes no increase of viscosity is found at all. Probably on the one hand electrostatic repulsion is weaker, on the other hand new hydrogen bonds are formed between spatially favourably situated groups.

Similar conclusions can be drawn from viscosity data relating to glutens, and to desamidated glutens dissolved in 8 *M* urea. A comparison of viscosity data of solutions in 0.05 *N* acetic acid and in 8 *M* urea reveals that in reference to the acetic acid solution increase of viscosity of not desamidated controls is significantly higher than that of partially desamidated samples. The deviation can be explained on the basis that in amidated glutens there are substantially more hydrogen bonds present, and these are disrupted by the urea added and thus the conformations are altered.

At lower pH (1 *N* acetic acid) also desamidated gluten samples show viscosity data widely divergent from those of solutions with urea, sometimes these values are very nearly the same as those for the controls; and this finding supports the idea of new hydrogen bonds being formed, as mentioned in the discussion of data shown in Table III.

3. *Rheological behaviour of gluten samples esterified with methanol, or ethanol*

Esterification is one of the possibilities to transform the free carboxyl groups. The partial conversion of amide groups into esters is also feasible. In the course of our experiments the rheological properties of glutens esterified with methanol or ethanol, have been studied, together with the viscosity of the solutions prepared from the derivatives with 0.05 *N* acetic acid. Results are listed in Tables V, VI, VII and VIII.

Data from Table V as well as from Table VII show that by increasing the degree of esterification the rheological properties of gluten change for the worse relaxation time will be significantly shorter. During the first period, which corresponds to the esterification of the free carboxyl present, no essential change occurs; this suggests that the role of free carboxyls in the formation of secondary bonds is not significant.

Table V

Relaxation of gluten esterified with methanol

Ser. No.	Relaxation time, sec.						
	extent of methylation, mmole/g						
	0	0.30	0.50	1.0	1.5	2.0	3.0
1	82	79	60	54	48	45	46
2	45	44	36	30	28	25	26
3	73	70	60	52	45	40	41
4	55	56	51	41	35	32	34
5	69	65	54	48	40	36	30

Table VI

Viscosity of solutions of gluten esterified with methanol

Ser. No.	$[\eta]$ dl/g						
	level of methylation mmole/g						
	0	0.3	0.5	1.0	1.5	2.0	3.0
1	0.442	0.439	0.384	0.350	0.321	0.295	0.280
2	0.495	0.480	0.401	0.362	0.318	0.288	0.275
3	0.480	0.469	0.360	0.331	0.297	0.291	0.302
4	0.530	0.529	0.460	0.431	0.390	0.321	0.305
5	0.420	0.415	0.340	0.291	0.270	0.258	0.261

Table VII

Relaxation of gluten esterified with ethanol

Ser. No.	Relaxation time, sec.				
	level of ethylation mmole/g				
	0.0	0.5	1.0	1.5	2.0
1	83	75	50	42	40
2	45	43	28	24	25
3	73	69	44	38	36
4	55	50	32	29	26
5	69	61	46	31	29

Viscosity data unequivocally show that characteristic viscosity is very much reduced, this argues for more compact and less asymmetric molecules. The alteration consists perhaps therein that alkylated protein is highly hydrophobe, thus, in water, the degree of its hydratation will be lower.

Table VIII

Viscosity of solutions of glutens esterified with ethanol

Ser. No.	[η] dl/g				
	level of ethylation mmole/g				
	0.0	0.5	1.0	1.5	2.0
1	0.442	0.430	0.317	0.285	0.270
2	0.495	0.477	0.342	0.272	0.281
3	0.480	0.469	0.308	0.236	0.242
4	0.530	0.515	0.351	0.277	0.275
5	0.420	0.402	0.270	0.260	0.255

4. *Rheological properties of acylated samples of gluten*

In order to study the rheological properties of acylated gluten, the penetration figures of the hydrated gluten derivative were established, and the viscosities of their solutions in 0.1 *N* acetic acid were measured. Results are summarized in Tables IX and X.

Table IX

Penetration figures of acylated gluten

Ser. No.	Penetration, 0.1 mm			
	per cent of acylation			
	0	40	80	100
1	72	142	152	160
2	58	108	112	135
3	85	120	135	142
4	70	105	121	143
5	94	143	162	180
6	45	92	108	125
7	48	89	102	117
8	73	104	130	135

Data reveal that the rheological properties of acylated gluten are very much inferior to those of native gluten. The decrease of cohesivity suggests that primary amino groups play a substantial role in the formation of intermolecular non-covalent bonds.

Experimental results show that no major alteration in viscosity takes place; after an initial small decrease the viscosity values remain practically constant. Thus it can be concluded that no important change of molecular conformation occurs, or that primary amino groups participate principally in the formation of intermolecular bonds.

Table X

Characteristic viscosity of the solutions of acylated gluten

Ser. No.	[η] dl/g per cent of acylation			
	0	40	80	100
1	0.425	0.396	0.392	0.388
2	0.480	0.428	0.420	0.422
3	0.460	0.432	0.417	0.418
4	0.502	0.477	0.472	0.465
5	0.397	0.368	0.362	0.365
6	0.485	0.444	0.427	0.430
7	0.510	0.482	0.469	0.461
8	0.447	0.417	0.405	0.396

REFERENCES

1. LÁSZTITY, R : Kémiai Közlemények, **28,** 67 (1967)
2. LÁSZTITY, R: Die Nahrung **12,** 1 (1968)
3. BARNAY, J. E., POLLOCK, H. B., BOLZE, C. C.: Cereal Chem. **42,** 215 (1965)
4. HOLME, J., BRIGGS, D. R.: Cereal Chem **36,** 321 (1959)
5. BECKWITT, A. C., WALL, J. S., DIMLER, R. I.: Arch. Biochem Biophys 103 319 (1963)
6. Sütőipari Kutatóintézet (Bakery Research Institute) Laboratory Test Methods I., Budapest, 1963 (in Hungarian)
7. LÁSZTITY, R : Élelmiszervizsg. Közl. **6,** 170 (1960)
8. LÁSZTITY, R : Acta Chim. Acad. Sci. Hung. **53,** 169 (1967)
9. AUERMAN, L. JA.: Die Nahrung **6,** 545 (1962)
10. CLARKE, E. P.: J. of AOAC **15,** 136 (1932)
11. AACC (American Assoc. of Cereal Chemists) Cereal Laboratory Methods, St Paul's 1962
12. AUER, H. E., DOTY, P.: Biochemistry **5,** 1716 (1966)
13. SAGE, H. J., FASHMAN, G. B.: Biochemistry **5,** 286 (1966)

Radomir LÁSZTITY; Budapest XI., Műegyetem rkp. 3.

Acta Chimica Academiae Scientiarum Hungaricae, Tomus 62 (1), pp. 87—93 (1969)

THE SYNTHESIS OF N^{ε}-NIP-TETRA-DL-ALANYL-POLY-L-LYSINE

M. SZEKERKE** and R. WADE*

*(Institute of Organic Chemistry, L. Eötvös University, Budapest;** Chester Beatty Research Institute, Institute of Cancer Research, Royal Cancer Hospital, London S.W. 3.*)*

Received October 25, 1968

A branched chain polymer, considered a suitable model compound for immunological studies, has been designed using poly-L-lysine as backbone. To each ε-amino group of poly-L-lysine short alanine side chains, consisting of four units each, have been attached as carriers of the synthetic immunological determinant 4-hydroxy-3-iodo-5-nitrophenylacetic acid (NIP) coupled to each N-terminal alanine.

The stepwise synthesis of tetra-DL-alanine has been achieved by two different routes, using (*A*) the azide, and (*B*) the pentachlorophenyl active ester methods for the peptide couplings. Tetra-DL-alanine was transformed to the NIP-tetrapeptide pentachlorophenyl ester, a derivative suitable for coupling with the ε-amino groups of poly-L-lysine. The presumed structure of the poly-L-lysine derivative (**XVI**) has been confirmed by IR spectra, elemental analyses and also by the amino acid analyses of the hydrolyzed product.

Studies during the past 10 years have shown that synthetic polypeptides can serve as valuable model compounds for the immunochemist.

Multichain polyamino acids provide a highly suitable tool for elucidating the importance of the locus which the immunogenic sites occupy within the molecule. The term "multichain" polymers was introduced by SCHAEFGEN and FLORY [1] to denote branched polymers whose molecules are composed of linear polymeric chains attached to a polyfunctional core. Purely synthetic polyamino acids have been prepared by the use of polylysine and polyornithine, as multivalent initiators for the polymerization of N-carboxy-α-amino acid anhydrides [2, 3]. If each functional group of the initiator starts a polymeric chain, every multichain molecule will contain a number of peptide side chains equal to the number of the functional groups of the initiator. By the copolymerization of mixtures of different N-carboxy-α-amino acid anhydrides, polymers with a random sequence of α-amino acids are obtained.

From a serological study of multichain polymers SELA *et al.* [4] concluded that the antigenically important area cannot be hidden in the interior of a molecule.

In view of the precise architecture of molecules prepared by the stepwise synthetic techniques, it is to be expected, that investigation of polypeptides in which well-defined peptides prepared by stepwise synthesis are attached

* Present address: CIBA Laboratories Ltd., Horsham, Sussex.

to inert polymers or to macromolecular peptides, will open up new possibilities and permit an even more detailed immunological analysis.

The main purpose of this study was to develop a method by which the same peptide chain of known sequence may be attached to each ε-amino group of polylysine.

As a result of a discussion with Dr. N. A. MITCHISON,* a branched chain polymer has been designed, using poly-L-lysine as backbone. Short alanine side chains, consisting of four units each, would be attached to each ε-amino group of polylysine. Each side chain would carry, coupled to the N-terminal alanine, the synthetic immunological determinant 4-hydroxy-3-iodo-5-nitrophenylacetic acid (NIP), successfully applied in various experiments by MITCHISON *et al.* [5, 6]. DL-Alanine peptides have been favoured instead of L-alanine peptides because of their higher solubility in water.

The stepwise synthesis of tetra-DL-alanine has been achieved by two different routes.

Method A is summarized in Fig. 1.

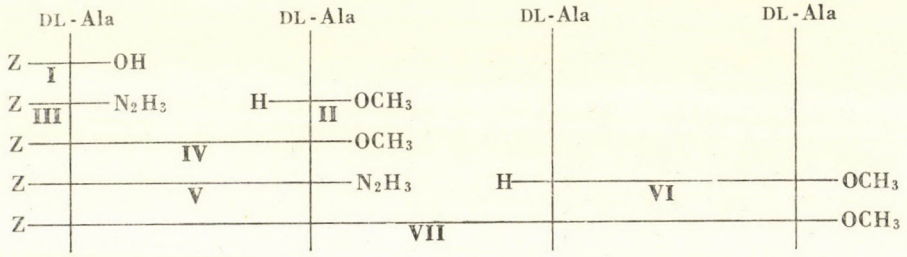

Fig. 1

Carbobenzyloxy-DL-alanine [7] (**I**) was converted to the corresponding hydrazide [8] (**III**) *via* the methyl ester [9] (**II**), and coupled with DL-alanine methyl ester (**II**) using the azide method. The resulting carbobenzyloxy-DL-alanyl-DL-alanine methyl ester (**IV**) was converted to the hydrazide (**V**), and coupled *via* the azide with the dipeptide ester **VI**, available from **IV** by hydrogenolysis, to yield the protected tetrapeptide (**VII**).

Method B is summarized in Fig. 2.

The protected tetrapeptide (**VII**) was prepared in this case by using pentachlorophenyl active esters for coupling. The advantages of this method for the synthesis of polypeptides with a known repeating sequence of amino acids have been outlined by KOVÁCS *et al.* [10, 11]. N-Carbobenzoxy-DL-alanine pentachlorophenyl ester (**VIII**) was prepared employing the method described by KOVÁCS *et al.* [11] for the preparation of the L-isomer. **VIII** was

* Division of Experimental Biology, The National Institute for Medical Research, Mill Hill, London.

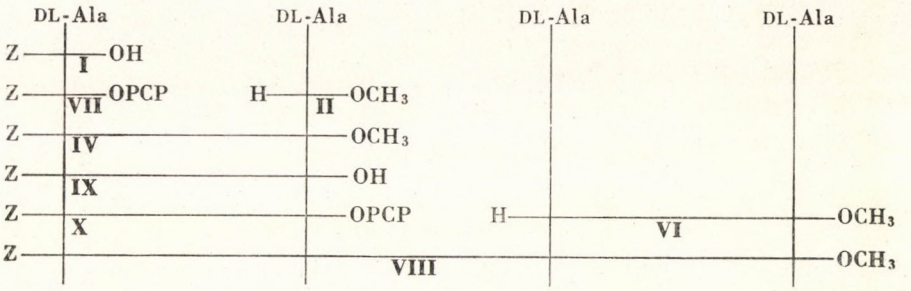

Fig. 2

coupled with DL-alanine methyl ester (**II**), to yield the dipeptide methyl ester (**IV**). The saponified product (**IX**) of **IV** gave, with pentachlorophenol and dicyclohexylcarbodiimide (DCC), N-carbobenzoxy-DL-alanyl-DL-alanine pentachlorophenyl ester (**X**). Coupling of the dipeptide active ester (**X**) with **VI** afforded the protected tetrapeptide (**VII**), identical with the product obtained by Method A.

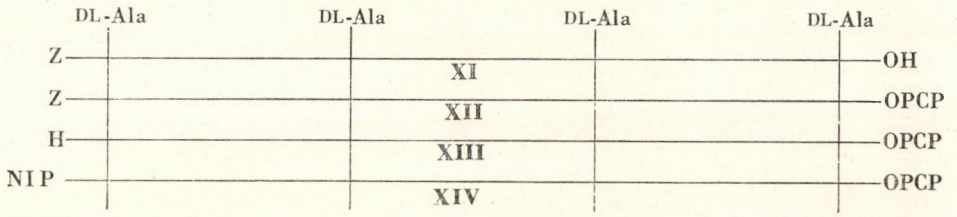

Fig. 3

To achieve coupling of the proposed side chain to the poly-L-lysine backbone, the pentachlorophenyl ester method was chosen. The synthesis of a suitable derivative for coupling the NIP-tetrapeptide pentachlorophenyl ester (**XIV**) is summarized in Fig. 3. The saponified product (**XI**) of the tetrapeptide (**VII**) was transformed to the corresponding pentachlorophenyl ester (**XII**). The tetrapeptide (**XIII**), obtained by hydrogenolysis from **XII**, was coupled with NIP azide (**XV**) [5] to yield **XIV**.

The final step of the synthesis, the coupling of **XIV** with the ε-amino groups of poly-L-lysine, was effected in dimethylformamide. The reaction proceeded at room temperature for 24 hours. After removal of the solvent under reduced pressure, the residue was diluted with water and dialyzed against 0.2 *M* $NaHCO_3$ for 4 days. The insoluble material formed was separated by centrifugation and lyophilized. The presumed structure (Fig. 4) (**XVI**) has been confirmed by IR spectra, elemental analyses and also by the amino acid analyses of the hydrolyzed product.

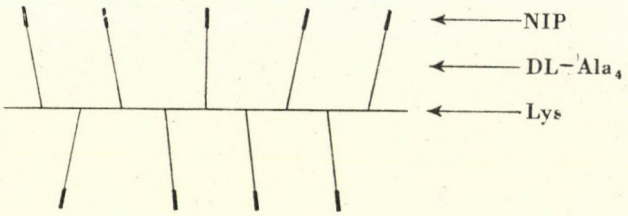

XVI

Fig. 4

Experimental

The microanalyses were carried out by Drs. G. WEILER and F. B. STRAUSS, Oxford, England. Amino acid analyses were carried out on the EEL automatic amino acid analyser. All m.p.'s are uncorrected and were taken on a Kofler apparatus. The infrared spectra were obtained in Nujol, using a Perkin-Elmer Infracord instrument. The compounds were checked for purity and the presence of possible contaminations or side products by thin-layer chromatography.

Reagent grade chemicals were used throughout. Amino acids and poly-L-lysine (Mol. wt. ~100,000) were obtained commercially.

N-Carbobenzoxy-DL-alanine (I)

The synthesis was achieved as described by OVERBY and INGERSOLL [7].

DL-Alanine methyl ester HCl (II)

The synthesis was achieved as described by ZAHN and SCHÜSSLER [9].

N-Carbobenzoxy-DL-alanine hydrazide (III)

The synthesis was carried out as described by ERLANGER and BRAND [8].

N-Carbobenzoxy-DL-alanine pentachlorophenyl ester (VIII)

This was synthesized in 75% yield according to the method of KOVÁCS *et al.* [11] described for the synthesis of the L-isomer; m.p. 159—160°C (from hot ethyl acetate–petroleum ether).

$C_{17}H_{22}NO_4Cl_5$. Calcd. C 43.25; H 2.5; N 2.98. Found C 43.4; H 2.7; N 3.1%.

N-Carbobenzoxy-DL-alanyl-DL-alanine methyl ester (IV)

Method A. To a suspension of **III** (10.35 g; 0.05 mole) in ice-cold water (250 ml) 5*N* hydrochloric acid (24 ml) and glacial acetic acid (60 ml) were added until a clear solution was obtained. Sodium nitrite (3.66 g; 0.053 mole) in cold water (15 ml) was rapidly added to the cold hydrazide solution. The azide separated as an oil and was extracted with cold ether (three 100-ml portions). The combined ether solution was washed with 3% aqueous $NaHCO_3$ (2×40 ml) and water (2×40 ml) and dried over Na_2SO_4. To the clear ether solution of the azide, an ether solution of DL-alanine methyl ester hydrochloride (8.08 g; 0.058 mole) and triethylamine (8.06 ml; 0.058 mole) was added. After stirring for 24 hrs at room temperature, the reaction mixture was extracted twice with 50-ml portions of 0.5 *N* HCl, water, 3% aqueous $NaHCO_3$ and water. After drying the ether layer with Na_2SO_4 and evaporation in vacuum,

a white solid was obtained, which was recrystallized from ethyl acetate–petroleum ether to give 9.25 g (60%) of **IV**, m.p. 115—116°C.

$C_{15}H_{20}N_2O_5$. Calcd. C 58.4; H 6.54; N 9.1. Found C 58.2; H 6.9; N 8.8%.

Method B. To a solution of the pentachlorophenyl ester **VIII** (4.7 g; 0.01 mole) in dry methylene chloride (50 ml) a mixture of DL-alanine methyl ester hydrochloride (1.6 g; 0.0115 mole) and triethylamine (1.6 ml; 0.0115 mole) in methylene chloride (10 ml) was added with stirring. 2-Hydroxy-pyridine [12] (0.15 g) was added to the above mixture and the stirring continued for 24 hrs at room temperature. The mixture was filtered from triethylamine hydrochloride, and the filtrate evaporated in vacuum. The residue was taken up in ethyl acetate (100 ml) and a further crop of triethylamine hydrochloride isolated. The filtrate was extracted three times with 30-ml portions of 1 *N* HCl, water, 5% $NaHCO_3$ solution and water. The ethyl acetate solution was dried over Na_2SO_4 and evaporated under reduced pressure. The residual oil was crystallized from ethyl acetate–petroleum ether. Two more recrystallizations from the same solvent mixture yielded 12.3 g (40%) of the chromatographically pure compound, m.p. 115—116°C (no depression with the product obtained by Method *A*).

$C_{15}H_{20}N_2O_5$. Calcd. C 58.4; H 6.5; N 9.1. Found C 57.9; H 6.4; N 9.5%.

N-Carbobenzoxy-DL-alanyl-DL-alanine hydrazide (V)

Hydrazine hydrate (0.65 ml; 95%) was added to a solution of **IV** (3.08 g; 0.01 mole) in dry ethanol (80 ml). The reaction mixture was kept for 24 hrs at room temperature. Crystallization started on the addition of ether. The mixture was allowed to stand in a refrigerator overnight. The crystals were collected and recrystallized from ethanol–ether to obtain 1.5 g (50%) of **V**, m.p. 157—158°C.

$C_{14}H_{20}N_4O_4$. Calcd. C 54.5; H 6.5; N 18.2. Found C 54.3; H 6.5; N 18.6%.

DL-Alanyl-DL-alanine methyl ester hydrochloride (VI)

The protected dipeptide **IV** was dissolved in dry methanol containing 1 eq. HCl and subjected to hydrogenolysis in a stream of hydrogen at room temperature in the presence of palladium-charcoal (5%). No CO_2 development was detectable after 2 hrs. The dipeptide methyl ester hydrochloride was isolated in 80% yield as an amorphous, hygroscopic solid, which could not be crystallized and was used for the next step without further purification.

N-Carbobenzoxy-DL-alanyl-DL-alanine (IX)

Saponification of the dipeptide **IV** was achieved in acetone with aqueous sodium hydroxide. The residue obtained from the normal procedure was crystallized from ether–petroleum ether to yield **IX** in 85% yield, m.p. 144—145°C.

$C_{14}H_{18}N_2O_5$. Calcd. C 51.2; H 6.2; N 9.5. Found C 51.2; H 6.3; N 9.8%.

N-Carbobenzoxy-DL-alanyl-DL-alanine pentachlorophenyl ester (X)

The dipeptide **IX** was converted into the active ester employing the method reported by PLESS and BOISSONNAS [13]. The product was recrystallized from ethyl acetate–petroleum ether; m.p. 180—181°C. Several recrystallizations were needed to remove traces of dicyclohexylurea. The final yield did not exceed 40%.

$C_{20}H_{17}N_2O_5Cl_5$. Calcd. C 44.3; H 3.2; N 5.2; Cl 32.7. Found C 44.5; H 4.3; N 4.8; Cl 32.95%.

N-Carbobenzoxy-DL-alanyl-DL-alanyl-DL-alanyl-DL-alanine methyl ester (VII)

Method A. The dipeptides **V** and **VI** were coupled by the azide method, as described previously for the preparation of **IV**. The residue obtained was crystallized from ethyl acetate–petroleum ether; m.p. 103—105°C; yield: 35%.

$C_{21}H_{30}N_4O_7$. Calcd. C 56.0; H 6.7; N 12.4. Found C 56.2; H 6.9; N 12.1%.

Method B. The dipeptides **X** and **VI** were coupled, as described previously for the preparation of **IV**. The oily residue obtained could be freed from by-products only by repeated recrystallizations. Yield: 25%. M.p. 103—105°C.

$C_{21}H_{30}N_4O_7$. Calcd. C 56.0; H 6.7; N 12.4. Found C 55.5; H 6.4; N 12.0%.

N-Carbobenzoxy-DL-alanyl-DL-alanyl-DL-alanyl-DL-alanine (XI)

Saponification of the tetrapeptide ester **VII** was achieved in acetone with aqueous sodium hydroxide. The demethylated derivative (**XI**) was obtained in a 45% yield. The compound was crystallized from ethyl acetate–petroleum ether, m.p. 94—96°C.

$C_{20}H_{28}N_4O_7$. Calcd. 55.03; H 6.47; N 13.85. Found C 55.35; H 6.3; N 13.4%.

N-Carbobenzoxy-DL-alanyl-DL-alanyl-DL-alanyl-DL-alanine pentachlorophenyl ester (XII)

XI was converted into the active ester (**XII**) adopting the method described by PLESS and BOISSONNAS [13]. The crude product was recrystallized several times from ethyl acetate–petroleum ether as traces of dicyclohexylurea were detectable by thin-layer chromatography and IR spectra. The yield of the purified product was only 25%; m.p. 138—140°C.

$C_{26}H_{27}O_7Cl_5$. Calcd. N 8.18; Cl 25.9. Found N 8.6; Cl 25.8%.

DL-Alanyl-DL-alanyl-DL-alanyl-DL-alanine pentachlorophenyl ester hydrochloride (XIII)

The protected tetrapeptide active ester was hydrogenated in dry methanol, containing 1 eq. HCl, in the presence of palladium on charcoal (5%), as described previously for the preparation of **VI**. The tetrapeptide active ester was isolated as the hydrochloride salt, yield 90%. The crude product was twice recrystallized from ethanol–ether; m.p. 145—146°C.

$C_{18}H_{22}N_4O_5Cl_6$. Calcd. N 9.55; Cl 36.34. Found N 9.95; Cl 36.05%.

NIP-DL-alanyl-DL-alanyl-DL-alanyl-DL-alanine pentachlorophenyl ester (XIV)

A solution of 0.58 g (0.001 mole) of the tetrapeptide hydrochloride (**XIII**) in 20 ml ethyl acetate was mixed with 0.14 ml of triethylamine to liberate the free base, then 0.42 g of NIP azide [5] (**XV**) (10% excess) in 25 ml acetone was added. The reaction mixture was stirred magnetically for 24 hrs at room temperature. The solvent was evaporated in vacuum, the residue diluted with chloroform and washed with 0.5 *N* HCl, water, 3% aqueous $NaHCO_3$, and water. The chloroform layer was dried over Na_2SO_4, and evaporated to dryness. The IR spectrum of the residue confirmed the expected structure. Only traces of NIP-derivative contamination were detectable by thin-layer chromatography. The crude product was recrystallized from ethyl acetate–petroleum ether; m.p. 155°C. Yield: 50%.

$C_{28}H_{25}O_9N_5ICl_5$. Calcd. N 7.97; Cl 20.15. Found N 7.76; Cl 19.02%.

N^{ε}-NIP-Tetra-DL-alanyl-poly-L-lysine (XVI)

A mixture of poly-L-lysine hydrobromide (0.23 g) (commercial origin) and triethylamine (0.28 ml) in dimethylformamide (10 ml) was added, with stirring, to a solution of **XIV** (0.88 g; 0.001 mole) in dry dimethylformamide (50 ml). 2-Hydroxypyridine (0.01 g) was also added, and the stirring continued for 24 hrs at room temperature. The solvent was evaporated in vacuum, the concentrated solution diluted with water and dialyzed against several changes of 0.2 *M* $NaHCO_3$ for 4 days. The insoluble precipitate formed was collected by centrifugation, washed with water and lyophilized. Yield: 420 mg (51%).

$C_{30}H_{36}N_7O_9$. Calcd. C 47.05; H 4.74; I 16.16. Found C 46.75; H 6.59; I 15.9; Na 1.38%.

The amino acid ratio after acid hydrolysis was: $Lys_{1.05}Ala_{3.85}$.

The IR spectra were consistent with the proposed structure (see Fig. 4).

We wish to thank Dr. N. A. MITCHISON for his helpful comments and suggestions, and Professor V. BRUCKNER and Professor A. B. FOSTER for their interest in this work.

This investigation received financial help from the World Health Organisation and was also supported by grants from the Medical Research Council, the British Empire Cancer Campaign for Research, and the National Cancer Institute, U.S. Public Health Service.

REFERENCES

1. SCHAEFGEN, J. R., FLORY, P. J.: J. Am. Chem. Soc. **70,** 2709 (1948)
2. SELA, M.: Bull. Res. Council Israel **4,** 109 (1954)
3. SELA, M., KATCHALSKI, E., GEHATIA, M.: J. Am. Chem. Soc. **78,** 746 (1956)
4. SELA, M., LUPU, N., YARON, A., BERGER, A.: Biochim. Biophys. Acta **62,** 594 (1962)
5. BROWNSTONE, H., MITCHISON, N. A., PITT-RIVERS, R.: Immunology **10,** 465 (1966)
6. BROWNSTONE, H., MITCHISON, N. A., PITT-RIVERS, R.: Immunology **10,** 481 (1966)
7. OVERBY, L. R., INGERSOLL, A. W.: J. Am. Chem. Soc. **82,** 2067 (1960)
8. ERLANGER, B. F., BRAND, E.: J. Am. Chem. Soc. **73,** 3508 (1951)
9. ZAHN, H., SCHÜSSLER, H.: Ann. **641,** 176 (1961)
10. KOVÁCS, J., KAPOOR, A.: J. Am. Chem. Soc. **87,** 118 (1965)
11. KOVÁCS, J., GIANNOTTI, R., KAPOOR, A.: J. Am. Chem. Soc. **88,** 2282 (1966)
12. BEYERMAN, H. C., VAN DEN BRINK, W. M.: Proc. Chem. Soc. **1963,** 266
13. PLESS, J., BOISSONNAS, R. A.: Helv. Chim. Acta **46,** 1609 (1963)

Mária SZEKERKE; Budapest VIII., Múzeum krt. 4/b.
Roy WADE; CIBA Laboratories Ltd., Horsham, Sussex, England

Acta Chimica Academiae Scientiarum Hungaricae, Tomus 62 (1), pp. 95—120 (1969)

PREPARATION AND INVESTIGATION OF LEWIS ACID COMPLEXES, V*

TITANIUM TETRACHLORIDE COMPLEXES OF ACETATES OF CYCLIC DI- AND TRIVALENT ALCOHOLS

Z. Csűrös,** Gy. Deák,** S. Holly,*** A. Török-Kalmár** and E. Zára-Kaczián****

*(Department of Organic Chemical Technology, Technical University, Budapest;** Central Chemical Research Institute of the Hungarian Academy of Sciences;*** Research Group for Organic Chemical Technology of the Hungarian Academy of Sciences, Budapest****)*

Received October 31, 1968

Complexes of cyclohexyl acetate, ethylene glycol diacetate, cyclopentane-*cis*-*trans*-1,2-diol diacetate, cyclohexane-*cis*- and *trans*-1,2-diol diacetate, *trans*-1,3-diol diacetate and α-and γ-cyclohexanetriol triacetate have been prepared with equimolar and excess quantities of titanium tetrachloride. On the basis of the compositions and infrared spectra of the complexes the probable structures are suggested. Linking of both oxygen atoms to the central metal atom of $TiCl_4$ is supposed in the 1 : 1 complex if the carbonyl oxygens of the ester groups are sufficiently near to each other. In other cases, such as those of cyclopentane-*trans*-1,2-diol diacetate or cyclohexane-1,3-diol diacetate, the combination of several substrate and $TiCl_4$ molecules result in the formation of a greater cycle. In triol triacetates, two carbonyl oxygens are connected to the titanium atom in the 1 : 1 complexes. The 1 : 2 complex has a different structure: two carbonyl oxygens of two substrate molecules are each connected to one molecule of $TiCl_4$, producing a cyclic structure. The residual ester groups are supposed to be attached to one molecule of titanium tetrachloride each.

Introduction

Reactions of esters with titanium tetrachloride were investigated first by Demarcay [1]. His model compounds were aliphatic and aromatic monocarboxylic esters (ethyl acetate, ethyl benzoate, ethyl butyrate, ethyl valerate, ethyl caproate, amyl acetate, methyl benzoate) and dicarboxylic esters (diethyl oxalate and diethyl succinate). According to his results, the compositions of the resulting complexes ($2\,TiCl_4 \cdot E$; $TiCl_4 \cdot E$; $TiCl_4 \cdot 2\,E$; or $TiCl_4 \cdot EE'$) depend on the conditions of the reaction (E = the ester component). Scagliarini and Tartarini [2] were the first to report complexes of dimethyl phthalate with titanium tetrachloride. Hertel and Demmer [3] prepared three different complexes of dimethyl fumarate, the molar ratios of $TiCl_4$ and the substrate being 2 : 1, 1 : 1 and 1 : 2. Thus the initial investigations proved the existence of two kinds of titanium tetrachloride complexes of esters of monocarboxylic acids having 1 : 1 and 2 : 1 molar ratio, while in the

* Part IV: Z. Csűrös, Gy. Deák, I. Gyurkovics, S. Holly, M. Haraszthy-Papp, A. Török-Kalmár and E. Zára-Kaczián: Periodica Polytechnica (Ch) **12**, 147 (1968).

case of dicarboxylic acids the 1 : 2 complex was also formed. These early investigations were of preparative character and no attempt was made to elucidate the process of complex formation. It is remarkable, that after the paper of HERTEL and DEMMER [3] no other communication dealt with this subject for twenty years. In 1952 OSIPOV published his first results of a physico-chemical investigation on the reaction of monocarboxylic esters with $TiCl_4$ [4]; this was followed by several other papers. In the course of these studies [5—15], in contrast to the initial experiments described above, the individual complexes were not isolated; the presence and compositions of the complexes were deduced from the measured physico-chemical data only. The method used was to prepare melts of the substrate and titanium tetrachloride in different ratios, and to determine the viscosity, density and conductivity of the melt. These data, even in the case of the first model compound, isoamyl acetate, when plotted as a function of the composition, showed that viscosity and its temperature dependence had definite maxima; the straight line representing the change of density had a break and the conductivity curve had a sharp minimum between two maxima, corresponding to 1 : 1 molar ratio of titanium tetrachloride and substrate. From these facts the formation of only one kind of isoamyl acetate complexes and steric hindrance of the formation of the 2 : 1 complex were concluded. In further work, in addition to the above methods, melting point diagrams were used [10] and other monocarboxylic esters were also investigated (Table I). In these studies the melting point diagrams always indicated formation of the 1 : 1 complex; however, on the basis of the heat of formation and other physico-chemical data, the existence of the 2 : 1 complex was also probable.

In the interpretation of the processes of complex formation, a new aspect was introduced by the investigations of RIVEST *et al.* [16—18], who used again the earlier method of isolating the complexes. In this work, complexes of esters of aliphatic dicarboxylic acids were prepared. Under the experimental conditions used, the formation of complexes with 1 : 1 or 1 : 2 ratio was established, depending on the structure of the substrate molecule. It was supposed, that in the complex of 1 : 1 ratio formed from esters of lower molecular weight, the carbonyl oxygen atoms of both ester groups participated in the formation of the complex, acting as electron pair donors, to give a cyclic structure (macrocycle) containing a hexacovalent titanium atom. In the complexes of 1 : 2 ratio, which are obtained from longer chain dicarboxylic esters, only one carbonyl group is attached to one molecule of titanium tetrachloride. This may indicate a pentacovalent titanium atom, too, but RIVEST *et al.* [17] suggested the presence of a hexacovalent titanium also in this case, supposing both oxygen atoms of the ester group to behave as electron pair donors. This was based on infrared spectra of solutions of the complexes in methylene chloride. In these spectra bands of the C—O—C stretching vibration, charac-

teristic of the ester group, were missing in the 1000—1200 cm^{-1} region. Complexes of esters with titanium tetrachloride prepared up to now are listed in Table I.

A more detailed investigation of the infrared spectra of complexes of esters with $TiCl_4$ and with other Lewis acids, was carried out by LAPPERT [19]. He showed beyond doubt that the linkage is established between the oxygen atom and the central metal atom of the Lewis acid in the course of complex formation. In agreement with theoretical considerations, this results in a decrease of the frequency of the C=O stretching vibration; the wavenumber of the $\nu_{as}C-\overset{\|}{C}-O$ stretching vibration will be higher, while the $\nu_{as}C-O-C$ band, appearing at lower wavenumber, shows a slight decrease. These examinations also gave information on the steric structures of the individual complexes.

According to views held today, the central metal atom in complexes of metal tetrahalide Lewis acids can complete its octet into decet or dodecet in the course of complex formation, while the original tetrahedral steric structure is converted into an octahedral one, having four halogen atoms and two donor atoms in its corners. There are two possible arrangements: *cis* and *trans*, having the two carbonyl oxygens at two neighbouring or at two opposite corners, respectively. LAPPERT [19] concluded the *cis* octahedral arrangement of some complexes from the splitting of the carbonyl band shifted to lower wavenumbers. In these complexes the carbonyl groups are coupled through the central metal atom, so vibrations of identical phase appear in the infrared spectra in the case of *cis* arrangement only.

Experiments and results

In the course of an investigation on the mechanism of the ring cleavage of 2,3,4-triacetyl-glucosan $\langle 1.5 \rangle \beta \langle 1.6 \rangle$ by titanium tetrachloride [36], the isolation and examination of the composition and structures of the products were required. This problem drew our attention to complexes of sugar esters with titanium tetrachloride.

In our first studies on this subject [37], only the compositions of the complexes prepared from model compounds with different molar ratios of the substrate and the Lewis acid were examined, as no suitable method was available for determining the structures of these complexes.

Apart from the actual problem, interest was attached to these investigations since no studies had been carried out previously on complexes of substrates having more than two complex-forming groups, *i.e.*, when they are polyfunctional in respect to electron pair donating. The model compounds used (levoglucosan-, glucose- and cellobiose esters) contained 3, 5 and 8 ester

Table I

Complexes of esters with titanium tetrachloride

Ester component (substrate)	Composition of the complex (substrate : $TiCl_4$) on the basis of			Isolated complex
	conductivity, density, and viscosity	heat of formation	melting point	
Diethyl oxalate				1 : 1 [16]
Diethyl malonate				1 : 1 [14]
Diethyl maleate				1 : 1 [14]
m-Cresyl acetate				1 : 1 [20]
Isoamyl acetate	1 : 1 [6]	1 : 1; 2 : 1 [12]	1 : 1 [10]	
Ethyl acetate	1 : 1 [5]	1 : 1 [7]	1 : 1 [10]	
Ethyl formate	2 : 1 [4]		1 : 1 [10]	
Butyl acetate	1 : 1; 2 : 1 [8]	1 : 1; 2 : 1 [7]	1 : 1 [10]	
Propyl acetate	1 : 1 [8]	1 : 1 [8]	1 : 1 [10]	
Methyl acetate			1 : 1 [10]	
Butyl formate	1 : 1; 2 : 1 [11]	1 : 1; 2 : 1 [12]	1 : 1 [10]	
Isobutyl formate			1 : 1 [10]	
Isoamyl formate	1 : 1; 2 : 1 [11]	1 : 1; 2 : 1 [12]	1 : 1 [10]	
Ethyl propionate			1 : 1 [10]	
Ethyl butyrate			1 : 1 [10]	
sec.-Octyl acetate		1 : 1; 2 : 1 [12]		
Ethyl stearate	1 : 1 [13]		1 : 1 [15]	
Ethyl valerate			1 : 1 [15]	
Ethyl caproate			1 : 1 [15]	
Ethyl *n*-heptoate			1 : 1 [15]	
Ethyl pelargonate			1 : 1 [15]	
Amyl acetate			1 : 1 [15]	
Hexyl acetate			1 : 1 [15]	
Octyl acetate			1 : 1 [15]	
Chloromethyl acetate	1 : 1; 2 : 1 [13]			
Diethyl succinate				1 : 1 [17]
Dimethyl phthalate				1 : 1 [2]
Diethyl fumarate				1 : 2; 1 : 1; 2: 1 [3]
Butyl chloroacetate			1 : 1 [10]	
Isobutyl chloroacetate			1 : 1 [10]	
Isoamyl chloroacetate			1 : 1 [10]	
Diethyl glutarate				1 : 1 [17]
Diethyl adipate				1 : 1; 1 : 2 [17]
Diethyl pimelate				1 : 2 [17]

Table I (continued)

Ester component (substrate)	Composition of the complex (substrate : $TiCl_4$) on the basis of			Isolated complex	
	conductivity, density, and viscosity	heat of formation	melting point		
Diethyl suberate				1 : 2	[17]
Diethyl azelate				1 : 2	[17]
Diethyl sebacate				1 : 2	[17]
Phenyl acetate				1 : 1	[21]
o-Tolyl acetate				1 : 1	[21]
m-Tolyl acetate				1 : 1	[21]
p-Tolyl acetate				1 : 1	[21]
Thymyl acetate				1 : 1	[21]

groups; surprisingly, the number of the bound molecules of $TiCl_4$ was lower than that of the functional groups: in the case of five functional groups (pentaacetylglucose) two, at eight functional groups (octaacetylcellobiose) three molecules of $TiCl_4$ were found as the highest possible number. The formation of the different complexes was explained by their special charge distribution.

RIVEST *et al.* [17] published their results about one year after our report. Their paper suggested the possibility that our model compounds could also have yielded such complexes in which the carbonyl oxygens of two ester groups were attached to one molecule of titanium tetrachloride. If in the case of levoglucosan-, glucose- and cellobiose acetates, considered as cyclic polyol acetates, the formation of such complexes can be verified, this may reveal the relation between the structure of the substrate and the number of Lewis acid molecules in the complex containing the highest number of $TiCl_4$. An influence of the steric structure of the model compound on the structure of the complex was also considered. To verify this latter assumption, dependence of the tendency to complex formation in esters of cyclic di- and polyols, and the composition of the complexes as a function of the relative steric positions of the ester groups were investigated first.

As Lewis acids and their complexes are very sensitive even to traces of water, the complexes were prepared under careful conditions in a "dry-box" or in an apparatus designed for this purpose (Fig. 1).

According to the general procedure, the calculated quantity of Lewis acid in chloroform solution was added, by drops, to a dry chloroform solution of the substrate, with continuous stirring. The precipitate, which separated spontaneously or on dilution with petroleum ether, was filtered off, washed with the solvent and dried.

The compositions of the complexes were determined by elemental analysis and by means of a previously developed method [38], by titrating the substance with pyridine in acetonitrile solution.

Determination of the compositions revealed the maximum number of Lewis acid molecules bound by the examined model compounds. However, no information was obtained regarding the structure and the validity of RIVEST's conception [17] for these cases.

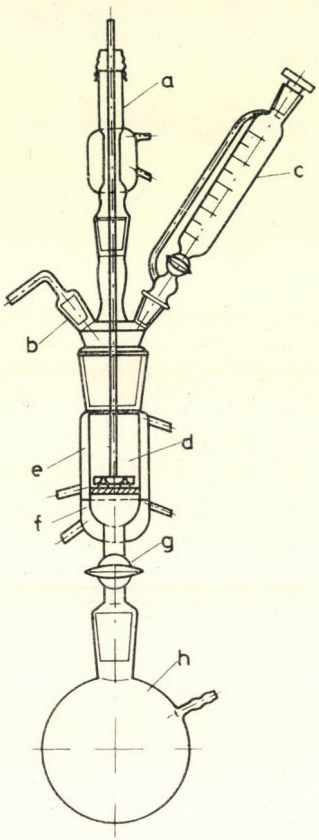

Fig. 1. Apparatus for the preparation of complexes of titanium tetrachloride

The purpose of our studies of the infrared spectra of these complexes was to throw light on the structural characteristics. On the basis of the above-mentioned examinations of LAPPERT [19] it was expected that the infrared spectra of the complexes of polyesters used as model compounds would help in elucidating the structures.

Since the complexes suffer decomposition in solution, we tried to obtain the spectra in KBr pellets or in paraffin oil mull. Owing to the low stability

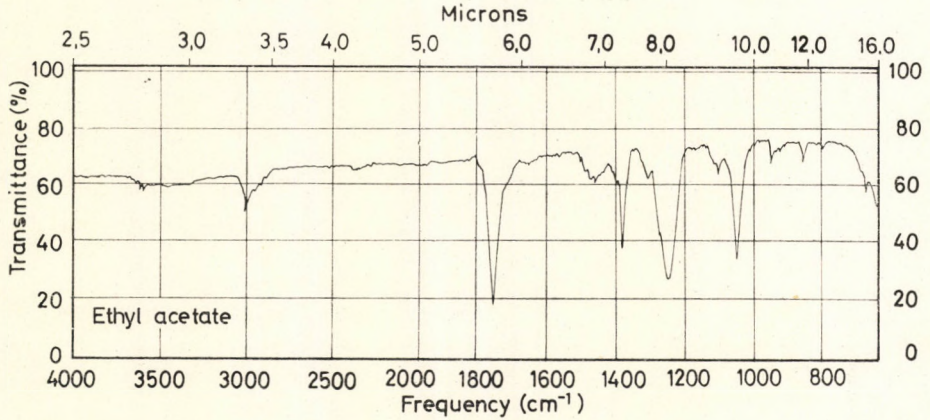

Fig. 2. Infrared spectrum of ethyl acetate (in KBr)

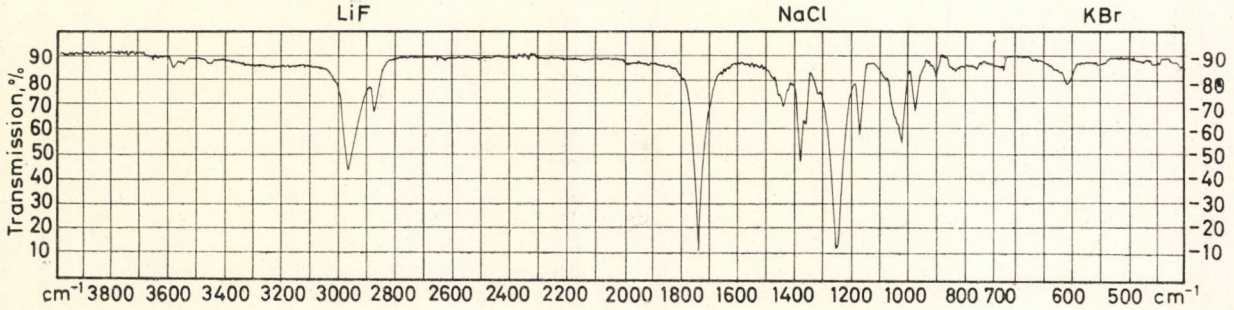

Fig. 3. Infrared spectrum of cyclopentyl acetate (in KBr)

of the substances, the samples were prepared in a dry-box. Preliminary experiments with KBr pellets soon indicated that this technique was unsuitable, as the complexes partly decomposed during recording the spectra, giving diffuse, unusable bands. Mulling in Nujol was found adequate, and this technique was used in the further work.

After establishing the experimental conditions and examination methods, complexes of the chosen model compounds were prepared; their composition and decomposition points were determined, and the infrared spectra recorded.

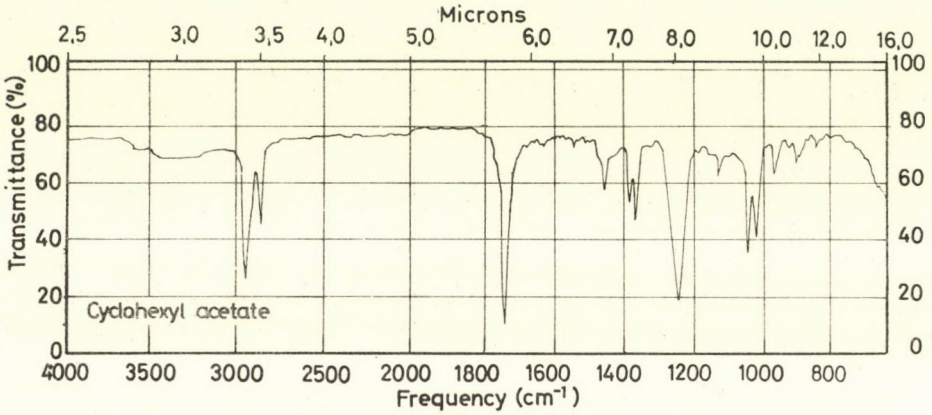

Fig. 4. Infrared spectrum of cyclohexyl acetate (in KBr)

The first model compounds were acetates of cyclohexane-1,2-*cis*- and *trans*-diols. It is known that in the *cis*-diol the hydroxyl groups are present in *a*, *e* or *e*, *a* positions, while in the *trans*-diol they have *e*, *e* or *a*, *a* positions. Conformation *e*, *e* is generally considered to be energetically more favoured. In the *a*, *e* and *e*, *e* conformations, the distance between the acetyl groups is the same. Thus in the case of 1,2-cyclohexanediol diacetates, the effect of the distance of the ester carbonyl oxygens on the complex formation and development of a macrocyclic structure could only be proved if the *trans*-diol diacetate reacted with $TiCl_4$ as the *a*, *a* conformer. Since this is not probable, the possible difference in the complex forming tendencies of acetoxy groups depending on the angle (60° or 180°) made by them, was studied on *cis*- and *trans*-cyclopentanediol diacetates having rigid, nearly planar steric structures.

First 1 : 1 complexes* of ethyl acetate, cyclopentyl acetate and cyclohexyl acetate were prepared to study the most characteristic changes in the infrared spectra produced by complex formation. These experiments were

* Further on, the complexes will be characterized by the ratio of substrate to Lewis acid component.

necessary, because the 1 : 1 complex of $TiCl_4$ and ethyl acetate was not investigated by LAPPERT [19]. The infrared spectra of the substances and their complexes (Figs 2—7) showed the following most characteristic changes: the $\nu C{=}O$ band of the substrate, found at 1750 cm^{-1} or near to it, disappears in the complex and a new, broader, very strong band appears at 1610—1615 cm^{-1}. At the same time, the bands of the $\nu_{as}C-\overset{\overset{\|}{O}}{\underset{\underset{O}{\|}}{C}}-C$ and $\nu_{as}C-O-\overset{\overset{\|}{O}}{\underset{\underset{}{\|}}{C}}$ stretching vibrations are missing at 1240 cm^{-1} and 1045 cm^{-1}, respectively. Instead

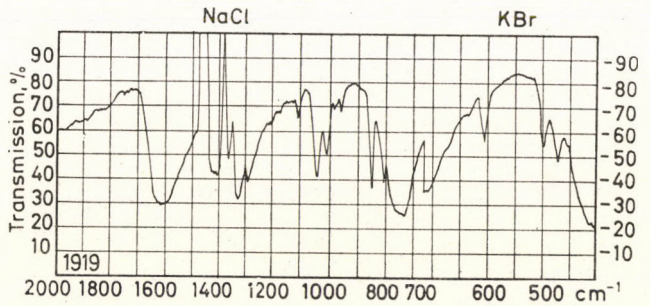

Fig. 5. Infrared spectrum of the 1 : 1 complex of ethyl acetate with $TiCl_4$ (in Nujol)

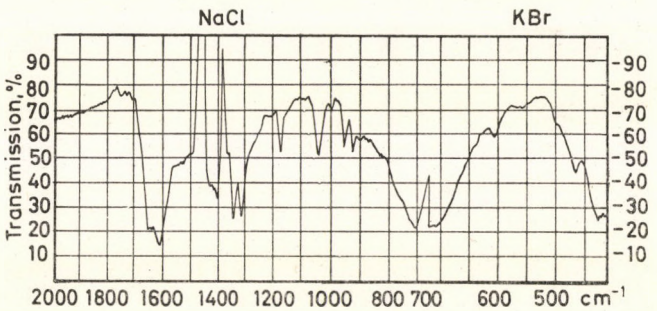

Fig. 6. Infrared spectrum of the 1 : 1 complex of cyclopentyl acetate with $TiCl_4$ (in Nujol)

of the former, a new band appears at 1310—1320 cm^{-1} (a dublet in cyclopentyl acetate), and the band at 1045 cm^{-1} is shifted by 5 cm^{-1} towards the lower wavenumbers. Further characteristics in the spectra of the complexes is a new, broad, strong band appearing in the region 705—730 cm^{-1}.

If the presence of pentacovalent titanium is supposed in the $TiCl_4$ complexes of the above esters, the appearance of the intense band between 730—705 cm^{-1} cannot be accounted for. Therefore, it is more probable, that both oxygen atoms of the ester group are connected to the titanium atom in the complex as suggested by RIVEST [17], producing hexacovalent titanium

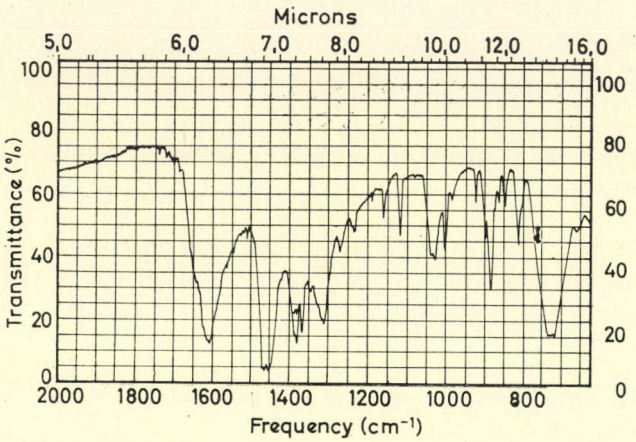

Fig. 7. Infrared spectrum of the 1 : 1 complex of cyclohexyl acetate with $TiCl_4$ (in Nujol)

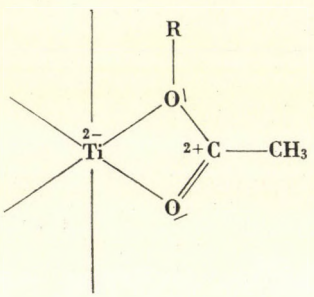

Fig. 8. Probable structure of complexes of monoesters with $TiCl_4$

(Fig. 8). This band between 730 and 705 cm^{-1} may arise from the out-of-plane deformation vibration of the charged "micro-cycle", while the $\nu C{=}O$ and $\nu_{as}C-C-O$ vibrations must be predominating, in the modes producing the
‖
bands at 1610 cm^{-1} and near 1300 cm^{-1}, respectively.

Ethylene glycol diacetate reacts with an excess of $TiCl_4$ to give both the 1 : 1 and 2 : 3 complexes. A comparison of the infrared spectra of the substrate (Fig. 9) and the complexes (Figs 10, 11) shows that, instead of the initial state, both complexes have a broad carbonyl band at 1635 cm^{-1}, and the shift of the C—C—O bands is similar to that observed in the cyclohexyl
‖
acetate complex.

In the 1 : 1 complex the original "free" carbonyl band is absent, indicating that one molecule of $TiCl_4$ is affixed to two carbonyl oxygens.

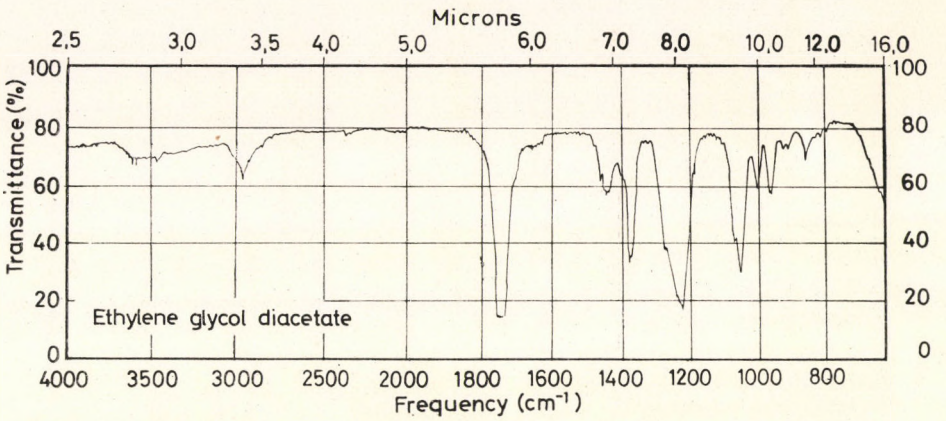

Fig. 9. Infrared spectrum of ethylene glycol diacetate (in KBr)

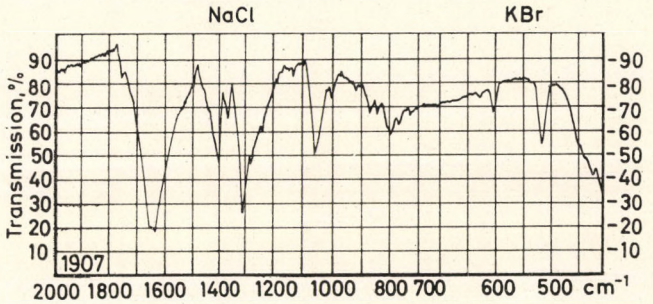

Fig. 10. Infrared spectrum of the 1 : 1 complex of ethylene glycol diacetate with $TiCl_4$ (in Nujol)

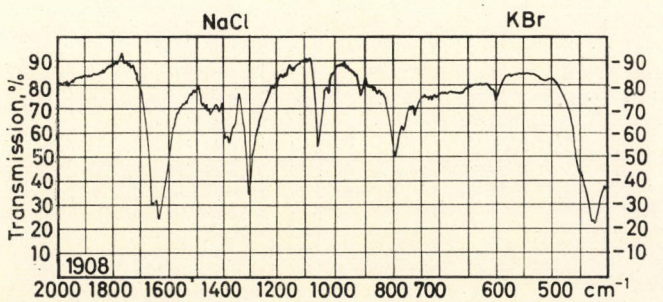

Fig. 11. Infrared spectrum of the 2 : 3 complex of ethylene glycol diacetate with $TiCl_4$ (in Nujol)

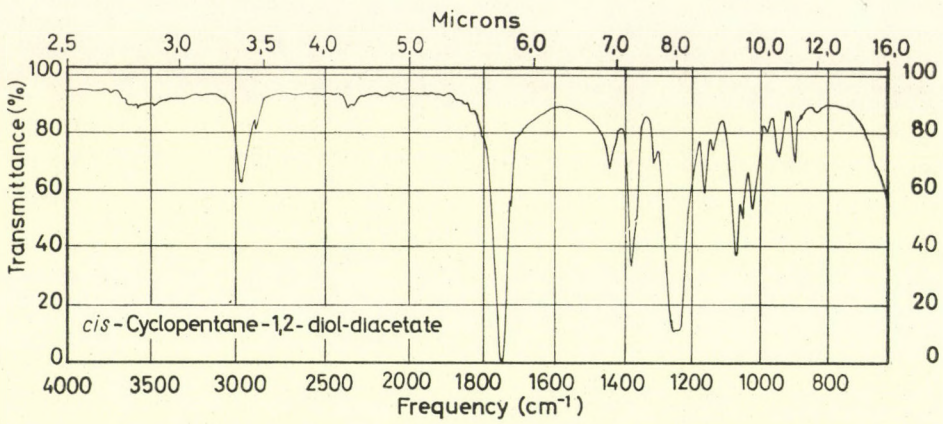

Fig. 12. Infrared spectrum of cyclopentane-*cis*-1,2-diol diacetate (in KBr)

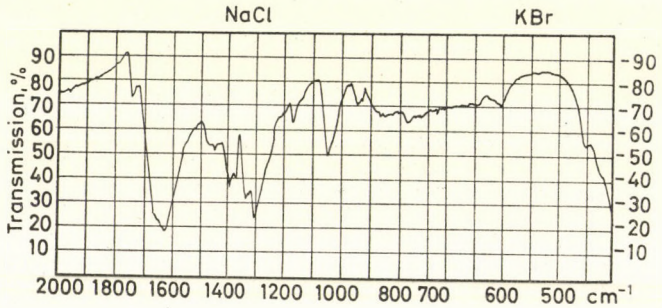

Fig. 13. Infrared spectrum of the 1 : 1 complex of cyclopentane-*cis*-1,2-diol diacetate with $TiCl_4$ (in Nujol)

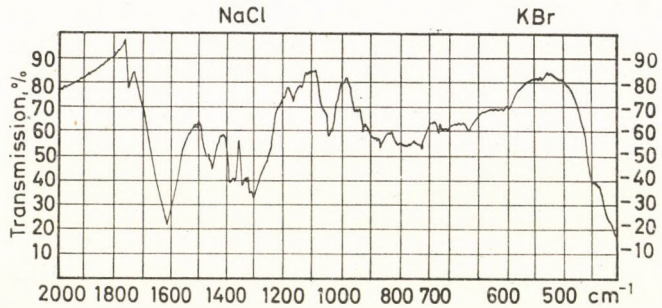

Fig. 14. Infrared spectrum of the 1 : 2 complex of cyclopentane-*cis*-1,2-diol diacetate with $TiCl_4$ (in Nujol

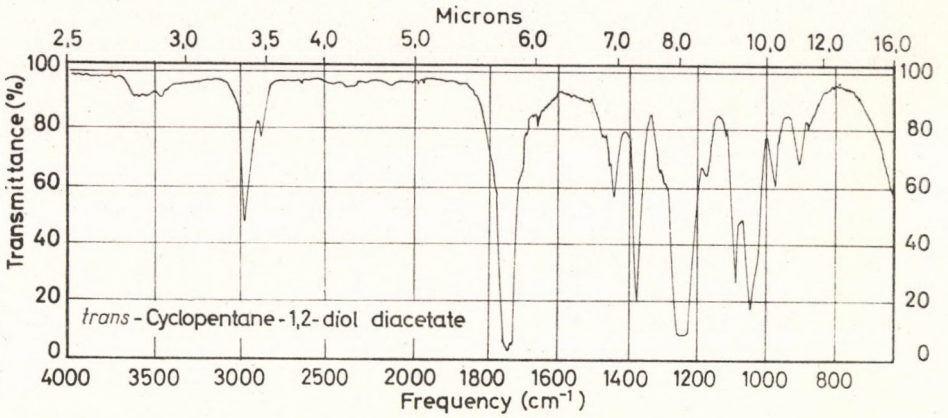

Fig. 15. Infrared spectrum of cyclopentane-*trans*-1,2-diol diacetate (in KBr)

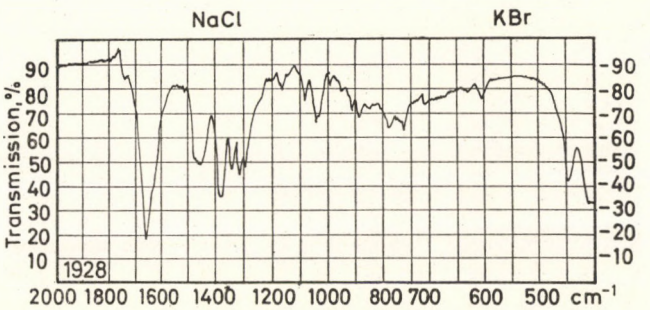

Fig. 16. Infrared spectrum of the 2 : 3 complex of cyclopentane-*trans*-1,2-diol diacetate with $TiCl_4$ (in Nujol)

The infrared spectra of the 1 : 1 and 1 : 2 complexes of cyclopentane-*cis*-1,2-diol diacetate (Figs 12—14) have a further characteristic feature. In the spectrum of the 1 : 2 complex, the shifted band of the carbonyl group in coordinate linkage has a shape similar to that of the carbonyl band in the cyclohexyl acetate complex (Fig. 7), while in the complex of 1 : 1 ratio (containing free carbonyl only as a contamination, as shown by its spectrum) the corresponding band is split, with a difference of 35 cm^{-1} between the two part-maxima. This splitting of the band indicates that the carbonyl oxygens of the two ester groups are situated on two neighbouring corners of a fictitious octahedron, *i.e.* the donor-acceptor relation is of *cis* character.

The *trans* isomer of cyclopentane-1,2-diol diacetate gives a 1 : 1 complex even if $TiCl_4$ is used in excess, thus differing from the case of the *cis* isomer. The spectrum (Figs 15, 16) reveals no splitting of the carbonyl band, *i.e.*, here the relation is of *trans* character.

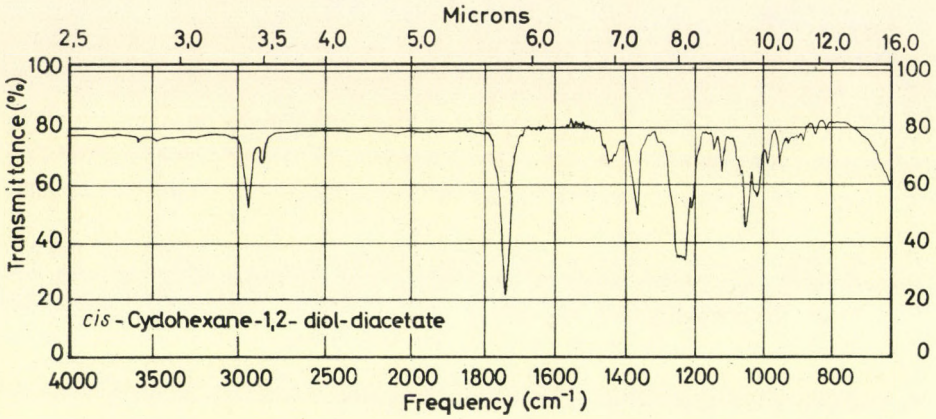

Fig. 17. Infrared spectrum of cyclohexane-*cis*-1,2-diol diacetate (in KBr)

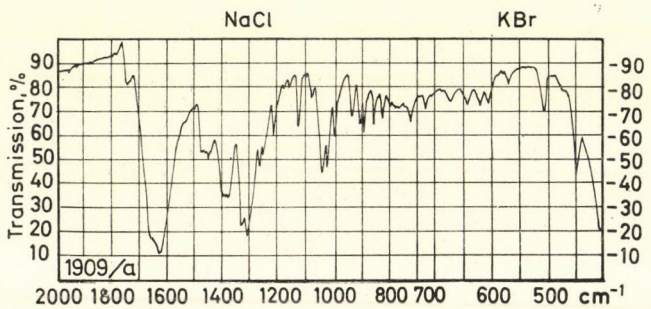

Fig. 18. Infrared spectrum of the 1 : 1 complex of cyclohexane-*cis*-1,2-diol diacetate with $TiCl_4$ (in Nujol)

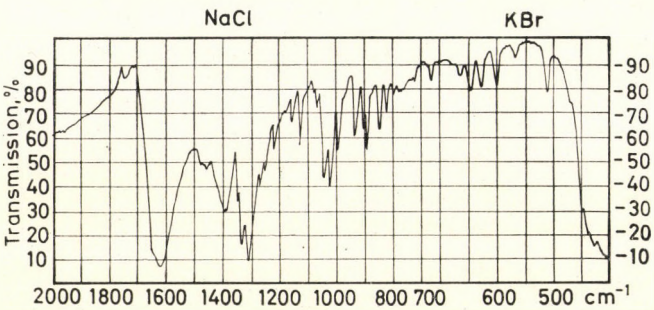

Fig. 19. Infrared spectrum of the 1 : 2 complex of cyclohexane-*cis*-1,2-diol diacetate with $TiCl_4$ (in Nujol)

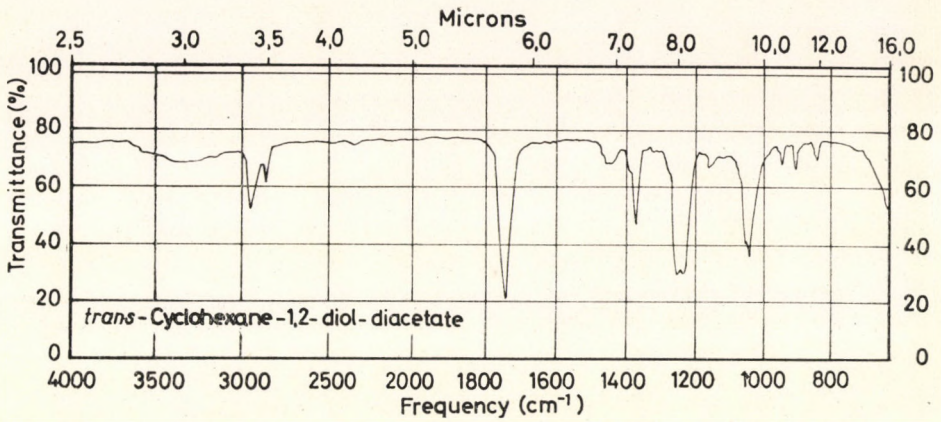

Fig. 20. Infrared spectrum of cyclohexane-*trans*-1,2-diol diacetate (in KBr)

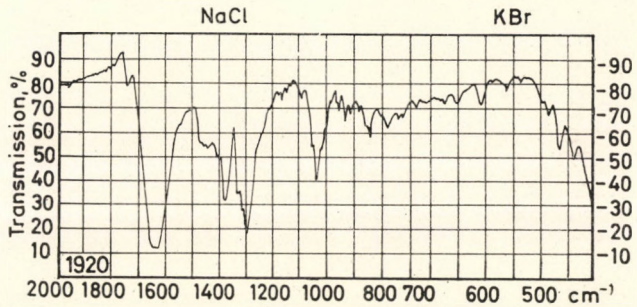

Fig. 21. Infrared spectrum of the 1 : 1 complex of cyclohexane-*trans*-1,2-diol diacetate with $TiCl_4$ (in Nujol)

Similarly to the corresponding cyclopentane derivative, cyclohexane-*cis*-1,2-diol diacetate yields a 1 : 2 complex with an excess of $TiCl_4$. According to the spectra (Figs 17—19), the 1 : 1 complex has *cis* structure in this case, too; the distance of the two part-maxima of the band assigned to the carbonyl in coordinate linkage is 40 cm^{-1}. In the spectrum of the 1 : 2 complex, the band of the carbonyl group is not significant enough, thus it is unsuitable for drawing conclusions regarding the structure.

In the case of cyclohexane-*trans*-1,3-diol diacetate (for the spectrum, see Fig. 20), the situation is similar to that of the *cis* isomer. In the infrared spectrum of the 1 : 1 complex (Fig. 21) the carbonyl band is shifted but not split, and it is considerably broader than the similar band of the 1 : 2 complex (Fig. 22).

The results obtained so far indicate that the two carbonyl groups are linked to the central metal atom of the Lewis acid in the 1 : 1 $TiCl_4$ complexes

of cyclopentane-*cis*-, and cyclohexane-*cis*- and -*trans*-1,2-diol diacetates. The structures may be represented as outlined in Fig. 23. If an excess of $TiCl_4$ is used, this cyclic structure suffers cleavage, and the *cis*-cyclopentane and -cyclohexane derivatives give rise to an energetically more favourable structure, in which each carbonyl group is connected to a Lewis acid molecule. However, in the infrared spectra of 1 : 1 complexes (Figs 14, 19, 22), the strong band at 705—735 cm^{-1}, which is present in the spectra of the mono-

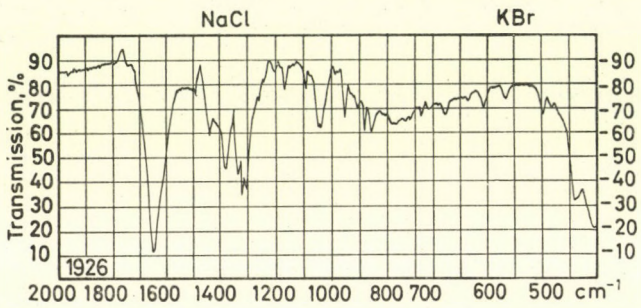

Fig. 22. Infrared spectrum of the 1 : 2 complex of cyclohexane-*trans*-1,2-diol diacetate with $TiCl_4$ (in Nujol)

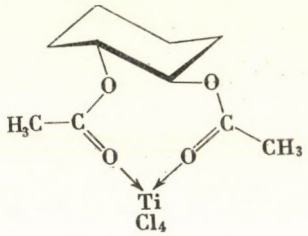

Fig. 23. Probable structure of the 1 : 1 complexes of $TiCl_4$

acetate complexes (Figs 5—7) is strikingly missing. In monoesters this band was due to native bonds connecting both oxygen atoms of the ester group to the titanium atom. In diol diacetates, favourable position of the ester groups makes possible another arrangement. It may be supposed, that in this case only the carbonyl oxygens are attached to the central metal atom, and the hexacovalent state of the latter is produced by the connection of $TiCl_4$ molecules, through chlorine atoms, since the molecules are fixed in space near to each other (Fig. 24). In the case of cyclopentane-*trans*-1,2-diol diacetate the situation is different. Because of the greater distance between the acetyl groups, formation of a macrocycle is unlikely. The infrared spectrum of the 1 : 1 complex of this compound is apparently in contrast with this, as no free carbonyl group is indicated. However, it is remarkable, that no band-

splitting, accompanying *cis* connections resulting in macrocycles, is observed in the spectrum. This suggests the presence of a complex formed by two molecules each of the substrate and $TiCl_4$, as shown in Fig. 25.

The above facts raised the problem of structure of the complexes formed from cyclohexane-1,3-diol diacetate containing rather distant acetyl groups.

We found that three kinds of complexes (2 : 1, 1 : 1 and 1 : 2) could be prepared from *trans*-1,3-diol diacetate (for the IR spectrum, see Fig. 26)

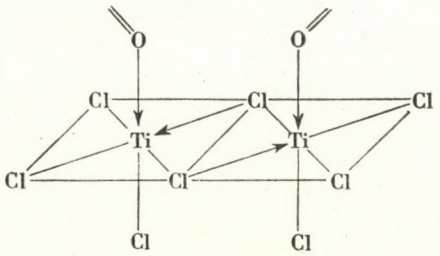

Fig. 24. Probable structure of the 1 : 2 complexes of 1,2-*cis*-diol diacetates with-$TiCl_4$

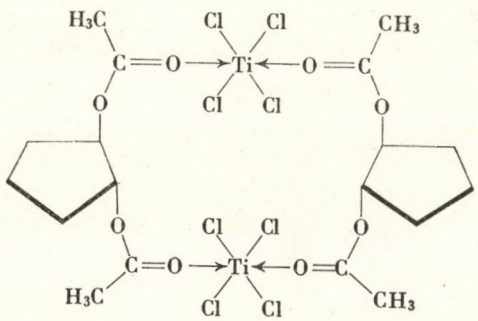

Fig. 25. Probable structure of the 1 : 1 complex of cyclopentane-*trans*-1,2-diol diacetate with $TiCl_4$

depending on the ratio of the components. In the 2 : 1 complex (Fig. 27), the original and shifted carbonyl bands appear together in the spectrum ("original" means here the carbonyl group not participating in a coordinate linkage). The band at 1240 cm^{-1}, assigned to the $\nu_{as}C-\underset{\|}{C}-O$ stretching vibration, is partly uncharged, partly shifted to 1305 cm^{-1}. In the case of the 1 : 1 complex, the spectrum (Fig. 28) shows coordinate bonds for both carbonyl groups, and no splitting of the carbonyl band is observed. The spectrum of the I : 2 complex differs from the former in the shape of the shifted carbonyl band which is narrower, and the band at 1310 cm^{-1} is accompanied by a new band at 1330 cm^{-1}. This new band was observed only as a shoulder in the spectrum of the 1 : 1 complex.

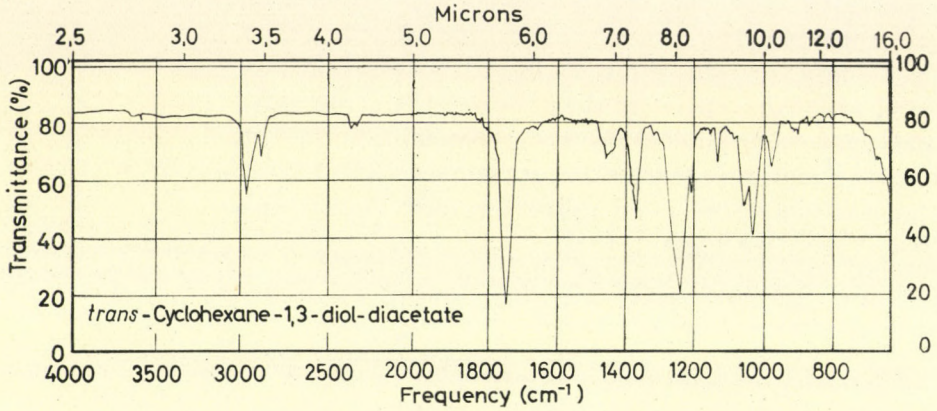

Fig. 26. Infrared spectrum of cyclohexane-*trans*-1,3-diol diacetate (in KBr)

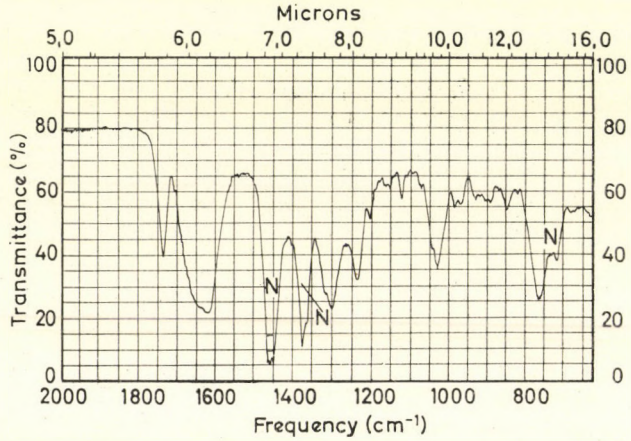

Fig. 27. Infrared spectrum of the 2 : 1 complex of cyclohexane-*trans*-1,3-diol diacetate with $TiCl_4$ (in Nujol)

These facts indicate that the structure of the 1 : 1 complex is similar to that shown in Fig. 25.

In our further work, the tendency to complex formation of trifunctional cyclohexane-1,2,3-triol triacetates was investigated. There are three stereoisomers of cyclohexanetriol: α-, β- and γ-triol. In the α-modification, the C-1, C-2, and the C-2, C-3 hydroxyl groups are in *trans* position to each other; in the γ-isomer they are in *cis* position. In the β-form the C-1 and C-2 hydroxyl groups are in *cis* position, while those at C-2 and C-3 are *trans*. We prepared the α- and γ-isomers and their complexes. In the spectrum of the 1 : 1 complex of the γ-isomer (for the spectrum, see Fig. 30) two new bands were observed

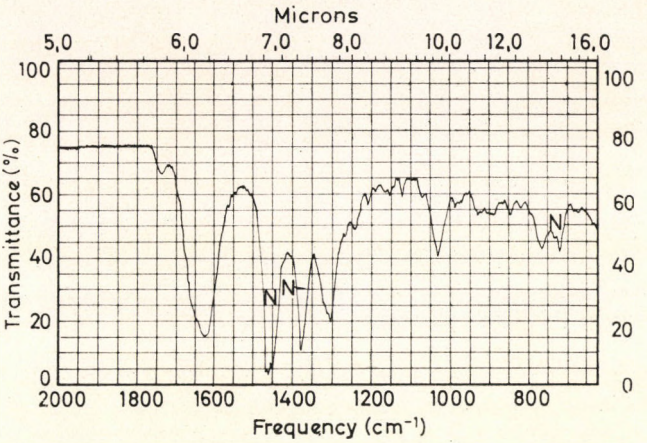

Fig. 28. Infrared spectrum of the 1 : 1 complex of cyclohexane-*trans*-1,3-diol diacetate with $TiCl_4$ (in Nujol)

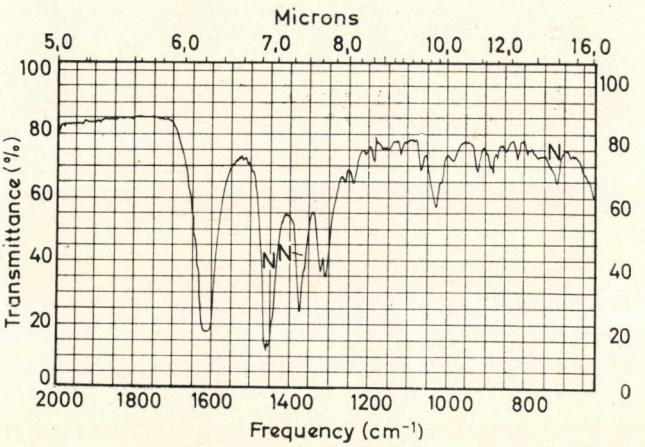

Fig. 29. Infrared spectrum of the 1 : 2 complex of cyclohexane-*trans*-1,3-diol diacetate with $TiCl_4$ (in Nujol)

at 1640 cm^{-1} and 1665 cm^{-1} (Fig. 31), in addition to the original carbonyl band at 1750 cm^{-1}. This indicates *cis* structure.

Using an excess of $TiCl_4$, the complex with 1 : 2 ratio was obtained. It has *trans* structure as shown by the presence of a single band at 1640 cm^{-1} having an inflexion (Fig. 32).

Thus an excess of $TiCl_4$ gives rise to a new structure instead of the attachment of another molecule of the Lewis acid to the free acetoxy group (Fig. 33). A complex with 1 : 3 ratio could not be prepared; the use of excess $TiCl_4$ resulted in the formation of the 1 : 2 complex only.

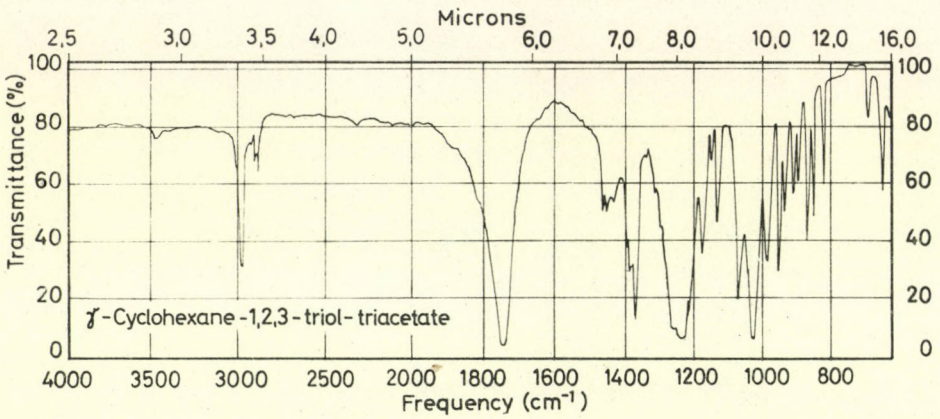

Fig. 30. Infrared spectrum of γ-cyclohexane-1,2,3-triol triacetate (in KBr)

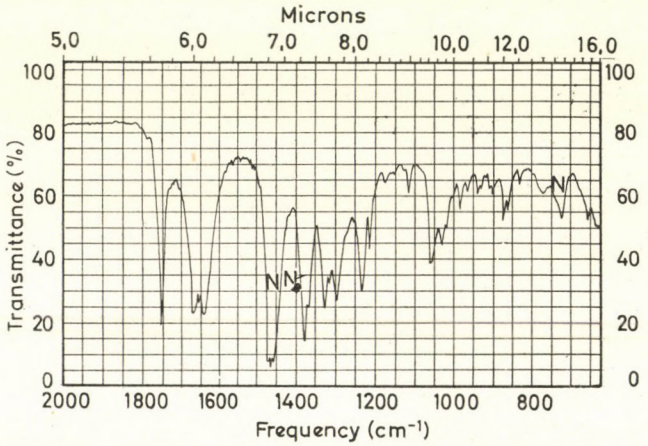

Fig. 31. Infrared spectrum of the 1 : 1 complex of γ-cyclohexane-1,2,3-triol triacetate with $TiCl_4$ (in Nujol)

An excess of $TiCl_4$ gave with the α-isomer (containing equatorial, axial and equatorial substituents, in this order) a 1 : 2 complex similar to that obtained from the γ-form (Figs 34, 35). No complex of 1 : 3 ratio could be prepared in this case, either.

The experiments made with cyclohexanediol and -triol acetates verified our assumption that the carbonyl oxygens of favourably situated neighbouring acetoxy groups may give rise to the formation of a macrocycle, in the same way as in the model compounds studied by RIVEST *et al.* [17]. It has also been shown that the formation of a macrocycle of *cis*-connection is independent of the steric positions of the substituents. This makes probable

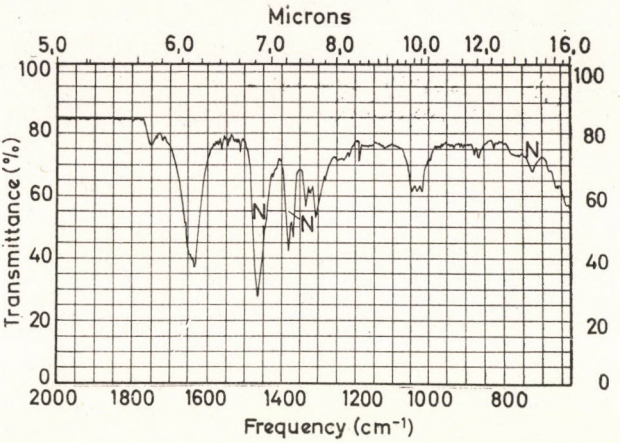

Fig. 32. Infrared spectrum of the 1 : 2 complex of γ-cyclohexane-1,2,3-triol triacetate with $TiCl_4$ (in Nujol)

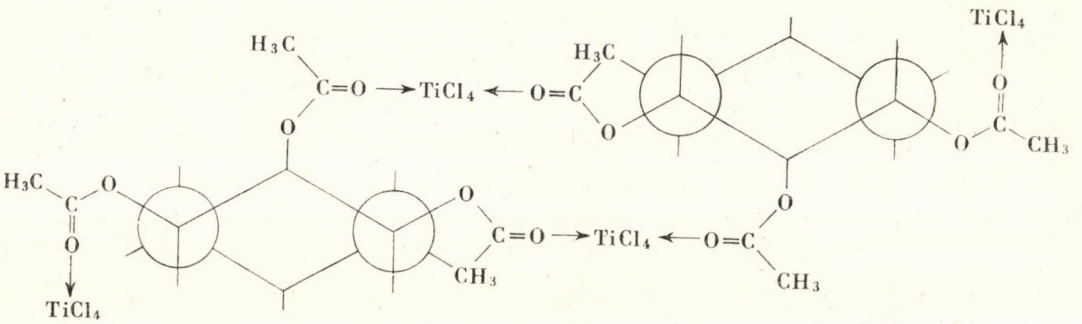

Fig. 33. Scheme of structure of the 1 : 2 complex of γ-cyclohexane-1,2,3-triol triacetate with $TiCl_4$

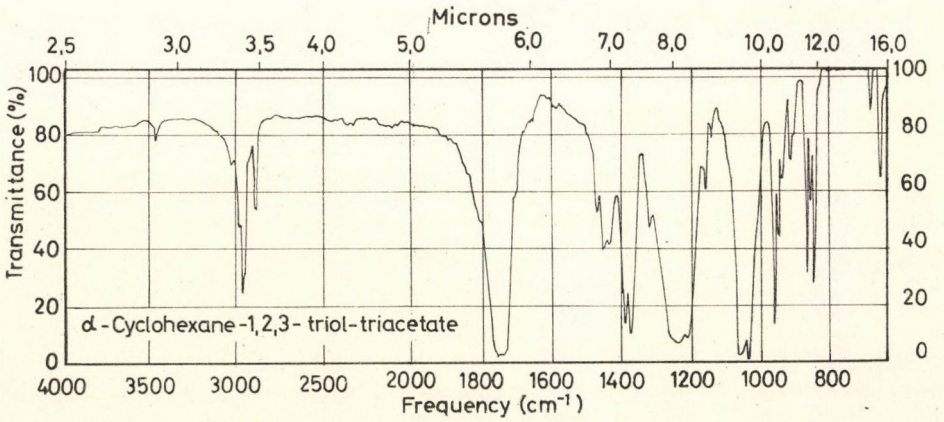

Fig. 34. Infrared spectrum of α-cyclohexane-1,2,3-triol triacetate (in KBr)

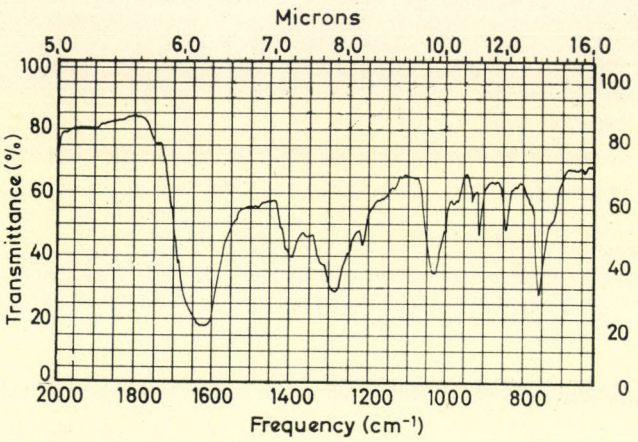

Fig. 35. Infrared spectrum of the 1 : 2 complex of α-cyclohexane-1,2,3-triol triacetate with $TiCl_4$ (in Nujol)

e, e conformation of the *trans* isomer in the course of complex formation. If the substrate and $TiCl_4$ are used in equimolar quantities and the carbonyl oxygen atoms are widely separated (cyclopentane-*trans*-1,2-diol diacetate, cyclohexane-1,3-diol and -1,4-diol diacetates), a greater cyclic structure is formed by means of intermolecular connections.

Our investigations also revealed that titanium tetrachloride, in contrast to an experimentally unsupported statement in the literature [22], is equally suitable for the formation of complexes with *cis* and *trans* structures, the process and the compositions of the complex being dependent on the structure of the substrate.

Experimental

1. *Materials*

Cyclohexyl acetate

The commercial product was purified by distillation.

Ethylene glycol diacetate

The commercial product was purified by distillation.

Cyclopentane-1,2-diol diacetates

The compounds were prepared from cyclopentene. The latter was prepared by the thermal cyclization of adipic acid with barium hydroxide [23], and reduction of the obtained ketone to cyclopentanol in the presence of Raney nickel at 70 atm. and 80°C [24], followed by dehydration of the resulting alcohol with 85% phosphoric acid [25].

(a) 1,2-cis-diol diacetate

Cyclopentene was oxidized to 1,2-*cis*-cyclopentane-diol with $KMnO_4$ in aqueous alcohol solution [26] and the product acetylated with acetic acid anhydride [27], then purified by distillation.

(b) 1,2-trans-diol diacetate

The oxidation of cyclopentene was carried out in formic acid solution with hydrogen peroxide [26].

Cyclohexane-1,2-diol diacetates

(a) 1,2-cis-diol diacetates

Cyclohexene was oxidized to the 1,2-*cis*-diol with H_2O_2 in absolute *t*-butanol solution in the presence of osmium tetraoxide at 0°C [28, 29], and then acetylated with acetic anhydride [27].

(b) 1,2-trans-diol diacetate

The oxidation of cyclohexene was carried out in anhydrous formic acid solution with hydrogen peroxide [30].

Cyclohexane-1,3-trans-diol diacetate

Phloroglucine (m.p. 213—216°C) was hydrogenated in alcoholic solution in the presence of Raney nickel catalyst in an autoclave at 105 atm. pressure at 125°C for 4 hrs. The product was purified by distillation in vacuum, to obtain cyclohexane-1,3-*trans*-diol diacetate in 27.8% yield (b.p. 147—156°C). For identification of the compound, its benzoate and urethan were prepared, which had the m.p.'s reported in the literature. The diol was then acetylated in the usual manner. The acetylated product was purified by distillation in vacuum.

Cyclohexane-1,4-diol diacetate

Hydroquinone was hydrogenated in alcoholic solution in the presence of Raney nickel catalyst at 110 atm. and 140°C for 2 hrs. The 1,4-diol was purified by distillation in vacuum and recrystallization, and then acetylated in the usual manner.

Cyclohexane-α-1,2,3-triol triacetate

Cyclohexene was allowed to react in the presence of absolute ethanol with bromine in carbon tetrachloride solution, at a temperature between —5°C and —1°C, to obtain 1,2-dibromocyclohexane [31]. This compound was heated in absolute methanol in the presence of sodium methoxide. First dehydrohalogenation of the compound took place, then the residual bromine atom was replaced by a methoxy group [32]. The resulting 3-methoxycyclohexene was converted into 3-methoxycyclohexene chlorohydrin by means of hypochlorous acid produced from a solution of monochlorourea [33] acidified with acetic acid. Alkaline dehydrohalogenation of 3-methoxycyclohexene chlorohydrin gave 3-methoxycyclohexene-α-oxide, which yielded α-dimethoxycyclohexanol on methanolysis [33]. Demethylation of the compound with aqueous hydrogen iodide and acetylation of the recrystallized triol with acetic anhydride in the presence of sodium acetate gave cyclohexane-α-1,2,3-triol triacetate in the purity reported in the literature, m.p. 128.5—130°C. (Lit. [34] m.p. 128—129°C.)

Cyclohexane-γ-1,2,3-triol triacetate [35]

Pyrogallol was hydrogenated in alcoholic solution in the presence of Raney nickel catalyst at 100 atm. and 150°C. Cyclohexane-*trans*-1,2-diol, appearing as by-product, was extracted with acetone from the raw product obtained by fractional distillation in vacuum; repeated recrystallizations from acetone gave the pure γ-1,2,3-triol in 17% yield.

The triol was acetylated with acetic anhydride in the usual way; the γ-triol triacetate purified by distillation in vacuum, had a refractive index identical with that given in the literature.

2. *Complexes with titanium tetrachloride*

(a) Preparation of the complexes in a dry-box

In these experiments the complexes were prepared in the apparatus shown in Fig. 36.

In the course of preparing the complex, the content of flask *A* was stirred using a magnetic stirrer. During the reaction and the filtration of the complex, dry nitrogen gas was passed through the apparatus; this was introduced through a side-tube of flask *A*. Flask *A*

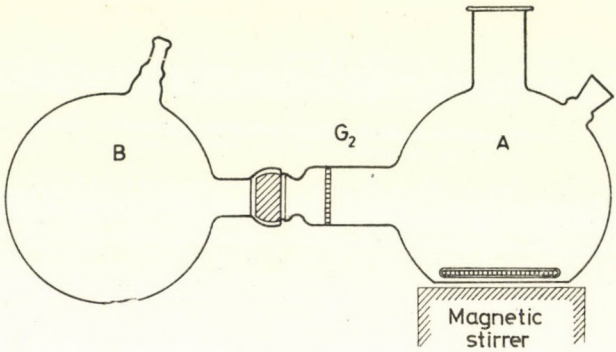

Fig. 36. Apparatus for the preparation of complexes of titanium tetrachloride

contained a hexane solution of the substrate in the case of preparation of the 2 : 1 complex, while a dry hexane solution of $TiCl_4$ was placed in it when preparating the 1 : 1 and 1 : 2 complexes. The solution of the other component was added, by drops and with continuous stirring, from a dropping funnel. In the preparation of the 1 : 1 complexes 10% (w/v) hexane solutions containing equimolar quantities of the substrate and $TiCl_4$ were mixed. When our purpose was the preparation of complexes with higher $TiCl_4$ content, double, or in the case of the triol acetates, triple molar quantities of Lewis acid were used. Repeated preparations of a given complex gave substances of slightly different m.p.'s, but the infrared spectra were identical. The spontaneously precipitating complex was stirred for 30—40 min., then the apparatus was turned into another position to allow filtration of the precipitate on a sintered glass filter sealed into the side tube, using slight suction. It was then washed with petroleum ether and dried over phosphorous pentoxide and paraffine shavings in a vacuum desiccator.

(b) Preparation of complexes in special apparatus

Using the apparatus shown in Fig. 1, heating or cooling could be applied in the course of the preparation of the complexes. The complex was prepared in reaction vessel *d*, equipped with a vibromixer *a*. Dry nitrogen gas was introduced into the apparatus through the pipe-end *b*. To prevent getting of the solution into the sintered filter sealed in the apparatus, the space between stop-cock *g* and the glass filter was filled with mercury before starting the work. In the cases when hot water was circulated in jacket *e*, cooling of the mercury was required;

this was performed by circulating cold water in jacket *f*; otherwise some mercury got into space *d* through the sintered filter. After completion of the complex formation, the mercury was allowed to flow into flask *h*, and the complex was filtered off under nitrogen pressure using a clean flask. Fresh solvent was added to the precipitate, which was stirred up and repeatedly filtered off, and finally dried in a stream of dry nitrogen until a powder-like substance was obtained. The apparatus was then opened in a dry-box, and the complex completely dried, as described above.

The operations connected with the analysis of the complexes and the preparation of paraffin mulls for recording the infrared spectra, were carried out in a dry-box in every case. The analyses of the complexes are given in Table II.

Table II

Composition of complexes with titanium tetrachloride

Substrate	Ratio of substrate and $TiCl_4$ in the complex	Cl %		Ti %		$TiCl_4$ %		Decomposition point, °C
		Calcd.	Found	Calcd.	Found	Calcd.	Found	
Cyclohexyl acetate	1 : 1	42.81	40.80	14.41	13.76	57.1	59.6	94— 97
Ethylene glycol diacetate	1 : 1	42.20	41.73	14.2	14.47			143—147
	2 : 3	49.48	49.25	16.70	18.37			146—149
cis-Cyclopentane-1,2-diol diacetate	1 : 1	37.70	38.25	12.00	12.27			143—144
	1 : 2	50.10	49.28	16.80	15.96			138—140
trans-Cyclopentane-1,2-diol diacetate	2 : 3	45.16	36.70	12.30	12.20	48.68	49.07	177—178
	1 : 2	38.90	47.54	16.50	15.71			153—154
trans-Cyclohexane-1,2-diol diacetate	1 : 1	36.40	36.29	12.30	12.24	48.68	48.02	125—135
	2 : 3	43.94	42.96			58.79	60.10	160—163
trans-Cyclohexane-1,3-diol diacetate	1 : 1	36.40	36.43	12.30	13.30			100—102
	1 : 2	48.90	47.65	16.50	16.22			135—137
α-Cyclohexane-1,2,3-triol triacetate	1 : 2	44.55	44.97	15.34	15.11			107—108
γ-Cyclohexane-1,2,3-triol triacetate	1 : 1	31.72	30.94	10.70	10.07	42.37	42.67	178—180
	1 : 2	44.55	43.48	15.34	16.37	59.53	58.10	168—173

The infrared spectra were recorded with Perkin-Elmer 237 and Zeiss UR 10 recording spectrophotometers.

REFERENCES

1. DEMARCAY, E.: Bull. soc. chim. France (2) **20,** 127 (1873)
2. SCAGLIARINI, G., TARTARINI, G.: Atti Accad. Lincei (6) **4,** 318 (1926)
3. HERTEL, E., DEMMER, A.: Ann. **499,** 134 (1932)
4. OSIPOV, O. A., KRAVCOV, E. E.: Zhur. Obshchei Khim **23,** 216 (1953); C.A. **46,** 12534c (1952)
5. LYSENKO, YU. A., OSIPOV, O. A.: Zhur. Obshchei Khim **24,** 53 (1954); C.A. **48,** 8104 (1954)
6. OSIPOV, O. A., SUCHKOV, V.: Zhur Obshchei Khim. **22,** 1132 (1952); C.A. **47,** 8010 (1953)

7. LYSENKO, YU. A., OSIPOV, O. A., FEODOS'EV, N. N.: Zhur. Fiz. Khim. **28,** 700 (1954); C.A. **49,** 5953 (1955)
8. OSIPOV, O. A., LYSENKO, YU. A., AKOPOV, E. K.: Zhur. Obshckei Khim. **25,** 249 (1955); C.A. **49,** 9368h (1955)
9. OSIPOV, O. A., SEMNEOV, A. D.: Zhur. Obshchei Khim. **25,** 2059 (1955); C.A. **50,** 3940b (1956)
10. LYSENKO, YU. A., OSIPOV, O. A., AKOPOV, E. K.: Zhur. Neorgan. Khim. 536 (1956); C.A. **50,** 13584 (1956)
11. LYSENKO, YU. A.: J. Zhur. Obshchei Khim. **26,** 3297 (1956) C.A. **52,** 15423 (1958)
12. OSIPOV, O. A., LYSENKO, YU. A.: Zhur. Neorgan. Khim. **5,** 1840 (1960); C.A. **56,** 6724 (1962)
13. LYSENKO, YU. A., OSIPOV, O. A.: Zhur. Neorgan Khim. **6,** 1656 (1961); C.A. **56,** 13771 (1962)
14. OSIPOV, O. A.: Zhur. Obshchei Khim. **32,** 1368 (1962); C.A. **59,** 12308 (1963)
15. LYSENKO, YU. A., OSIPOV, O. A., KRAVTSOV, E. E.: Zhur. Neorgan. Khim. **8,** 663 (1963); C.A. **58,** 13186g (1963)
16. AUBIN, R., RIVEST, R.: Can. J. Chem. **36,** 915 (1958)
17. RIVET, E., AUBIN, R., RIVEST, R.: Can. J. Chem. **39,** 2343 (1961)
18. JAIN, S. CH., RIVEST, R.: Can. J. Chem. **40,** 2234 (1962)
19. LAPPERT, M. F.: J. Chem. Soc. 1962, 542
20. Takeshi JOSHINO, Inchiro KIJIMA, Michio SUGIURA, Toru SHOJI: Yuki Gosei Kagaku Kyokai Shi **21,** 463 (1963); C.A. **59,** 7416g (1963).
21. GOEHRING, J., SUSZ, B. P.: Helv. Chim. Acta **49,** 486 (1966)
22. SUMAROKOVA, T., YARMUKHAMEDOVA, E.: J. Gen. Chem. USSR Eng. Trans. 1956, 3666
23. GILMAN, H.: Organic Syntheses Coll. Vol. I, 187 Wiley, New York, 1932
24. KASANSKI, B. A., TERENTJEWA, J. M., BULANOWA, T. F.: Synthesen organischer Verbindungen, I. 61. VEB Verlag Technik Berlin, 1959
25. BLATT, A. H.: Organic Syntheses, Coll, Vol. II, p. 152 Wiley, New York, 1950
26. OWEN, L. N., SMITH, P. N.: J. Chem. Soc. 1952, 4026
27. WIBERG, K. B., SAEGEBART, K. A.: J. Am. Chem. Soc. **79,** 6256 (1957)
28. MILAS, N. A., SUSMAN, S.: J. Am. Chem. Soc. **58,** 1302 (1936)
29. MILAS, N. A., SUSMAN, S.: J. Am. Chem. Soc. **59,** 2346 (1937)
30. HORNIG, E. C.: Organic Syntheses, Coll. Vol. III. p. 217. Wiley, New York, 1955
31. BLATT, A. H.: Organic Syntheses Coll. Vol. II. p. 171. Wiley, New York, 1943
32. GOGEK, C. j., MOIR, R. Y., MCRAE, J. A., PURVES, C. B.: Can. J. Chem. **29,** 938 (1951)
33. MCRAE, J. A., MOIR, R. Y., HAYNES, J. W., RIPLEY, L. G.: J. Org. Chem. **17,** 1621 (1952)
34. GORIN, P. A. J.: Can. J. Chem. **42,** 1748 (1964)
35. CHRISTIAN, W. R., GOGEK, C. J., PURVES, C. B.: Can. J. Chem. **29,** 911 (1951)
36. CSŰRÖS, Z., DEÁK, Gy., HARASZTHY-PAPP, M.: Acta Chim. Acad. Sci. Hung. **21,** 193 (1959)
37. CSŰRÖS, Z., DEÁK, GY., FENICHEL, L.: Acta Chim. Acad. Sci. Hung. **21,** 169 (1959)
38. CSŰRÖS, Z., DEÁK, Gy., FENICHEL, L., TÖRÖK-KALMÁR, A.: Periodica Polytechnica (Ch) **8,** 1 (1964)

Zoltán CSŰRÖS
Gyula DEÁK
Sándor HOLLY
Anna TÖRÖK-KALMÁR
Erzsébet ZÁRA-KACZIÁN

Budapest XI., Műegyetem rkp. 3.

Acta Chimica Academiae Scientiarum Hungaricae, Tomus 62 (1), pp. 121—123 (1969)

PREPARATION AND INVESTIGATION OF LEWIS ACID COMPLEXES, VI*

SYNTHESIS OF 2,3,4,6-TETRABENZOYL-β-D-GLUCOPYRANOSYL CHLORIDE

Z. CSŰRÖS, G. DEÁK and L. FENICHEL

(Department of Organic Chemical Technology, Polytechnical University, Budapest)

Received June 17, 1969

(Preliminary communication)

It is known [1] that one of the anomeric forms of peracylated halogen sugars is labile and under suitable conditions it is rapidly converted to the stable isomer. On the basis of experimental data, two rules have been established for acetyl derivatives [2] which permit to predict the configuration of the labile form from relative spatial position of individual groups in the Haworth projection formula. In the case of glucose, the labile form is the β-anomer.

The first method for the preparation of halogen sugars with labile configuration has been reported by SCHULBACH and GILBERT [3]. The procedure is based on the reaction of the acetobromo sugar of opposite configuration with fresh, active silver chloride in an inert solvent. The efficiency of the method depends on the activity of silver chloride, its drawback being poor reproducibility. Therefore, the observation by LEMIEUX and BRICE [4] is of practical importance, according to which, the reaction of pentaacetyl-β-D-glucose with titanium tetrachloride (a reactant first applied by PACSU [11] to the preparation of halogen sugars with stable configuration) yields β-acetochloroglucose under kinetic control. ZEMPLÉN *et al.* [5], and later KORYTNYK and MILLS [6] have developed a reproducible method of preparative value for the synthesis of β-acetochloroglucose, using aluminum chloride instead of titanium tetrachloride.

Unlike in the case of acetylated β-D-glucosylchloride derivatives, no data are found in the literature for the benzoyl derivative. NESS *et al.* [7] have prepared tetrabenzoyl-α-D-glucopyranosyl chloride from pentabenzoyl-β-D-glucose with titanium tetrachloride. By dissolving the pentabenzoate in chloroform containing 2.5 vol. % of titanium tetrachloride and processing the solution after 30 min, KORYTNYK and MILLS [6] have obtained

* Part V. CSŰRÖS, Z., DEÁK, GY., HOLLY, S., TÖRÖK-KALMÁR, A. and ZÁRA-KACZIÁN, E.: Acta Chim. Acad. Sci. Hung. **62**, 95 (1969).

a solid product with a chlorine content of 1% and with specific rotation of +14.2°. Thus, according to the above study, no replacement of the C_1 acetoxy group by chlorine is observed as opposed to the pentaacetate.

The outcome of the above experiment performed by KORYTNYK and MILLS [6] could not be understood on the basis of the structure of the compound and the reaction mechanism. Therefore, earlier studies by the present authors [8] have been extended to β-pentabenzoyl-D-glucose. If pentabenzoyl-β-D-glucose dissolved in chloroform (dried over calcium chloride) is reacted with an equimolar amount of titanium tetrachloride and, after 5 min, the solution is diluted with absolute petroleum ether, a yellow complex is precipitated (specific rotation in acetonitrile +42.7°). After decomposing the complex with water and chloroform, washing the chloroform phase until neutrality, and drying, evaporation in vacuum yields a syrup with a chlorine content of 5.6%, in good agreement with the calculated chlorine content of tetrabenzoylglucosyl chloride (5.78%). If, without isolation of the complex, the reaction is carried out with larger amounts and the syrup is crystallized twice from ether/petroleum ether, a crystalline solid is obtained (m.p. 109—111° C, specific rotation +45.7°) which, on the basis of its IR spectrum too, is identical with the expected 2,3,4,6-tetrabenzoyl-β-D-glucosyl chloride (Calcd. C 66.4; H 4.39; Cl 5.78. Found C 66.7; H 4.74; Cl 5.90%). The specific rotation value calculated from the molecular rotations of α- and β-pentabenzoylglucose [9] and α- and β-acetochloroglucose [3, 10] by means of the Hudson rule is +37.5°, in agreement with the experimental value for the substance prepared (within the error characteristic for similar calculations described in the literature).

Following the reaction by an IR-spectrophotometric technique described earlier, we found that in the present case, the 625 cm^{-1} C—Cl band is ill-defined and of low intensity, consequently, not suitable for rate studies. However, the 1110 cm^{-1} band which, in earlier studies on acetochloroglucoses, was only observed in the IR spectrum of the α-anomer, is easily recorded. This band appears after 15 min, indicating anomerization of the primarily formed β-chloro sugar benzoate. Similar results are obtained if the reaction is followed polarimetrically.

REFERENCES

1. HAYNES, L. J.: Adv. in Carbohydrate Chemistry, Vol. 10. p. 207. Academic Press, New York, 1955
2. LEMIEUX, R. U.: Adv. in Carbohydrate Chemistry. Vol. 9. p. 36. Academic Press, New York, 1954
3. SCHULBACH, H. H., GILBERT, R.: Ber. **63,** 2295 (1930)
4. LEMIEUX, R. U., BRICE, C.: Can. J. Chem. **30,** 295 (1952)
5. ZEMPLÉN, G., MESTER, L., ECKHART, E.: Acta Chim. Acad. Sci. Hung. **4,** 73 (1954)
6. KORYTNYK, W., MILLS, J. A.: J. Chem. Soc., **1959,** 636

7. NESS, R. K., FLETSCHER, H. G., HUDSON, C. S.: J. Am. Chem. Soc. **72,** 2200 (1950)
8. CSŰRÖS, Z., DEÁK, GY., FENICHEL, L., HOLLY, S., PÁLINKÁS, J.: Acta Chim. Acad, Sci. Hung. **56,** 325 (1968)
9. LEVENE, P. A., MEYER, G. M.: J. Biol. Chem. **76,** 513 (1928)
10. BRAUNS, D. J.: J. Am. Chem. Soc. **47,** 1280 (1925)
11. PACSU, E.: Ber. **61,** 1508 (1928)

Zoltán CSŰRÖS
Gyula DEÁK
László FENICHEL
Budapest XI., Műegyetem rkp. 3.

ACTA CHIMICA

ТОМ 62 — ВЫП 1

РЕЗЮМЕ

Применение комплексообразователей в ионообменной хроматографии, II

Разделение ионов кобальта (II) и никеля (II) на ионообменной колонке с помощью элюентаацетата аммония, содержащего аммоний

Й. ИНЦЕДИ, П. КЛАТШМАНИ-ГАБОР и Л. ЭРДЕИ

Был разработан метод разделения ионов кобальта(II) и никеля(II) в порядке, отличающемся от обычного. В качестве элюента использовался раствор ацетата аммония, содержащего аммоний.

Расчет наилучшего отношения распределения, необходимого для разделения, проводился на основе литературных данных для констант стабильности комплекса, диссоциации и ионного обмена. Результаты полученные экспериментальным путем, имеют хорошее совпадение с расчетными данными.

Некоторые топологические свойства молекул с ковалентными связями, II

Ф. БИЛЛЕШ

Структурная матрица симметрии содержит необходимые информации, чтобы из нее обратно получили один из структурных матриц молекулы. Описывается — в форме программы для электронной вычислительной машины — алгоритм позволяющий производить вышеописанную трансформацию.

При знании структурной матрицы можно поискать колец и составляющих множеств молекулы, а также цепи, относящиеся к отдельным составляющим множествам. Знание колец и цепей может стать необходимым при построении зависимостей между внутренними координатами — условий лишения — и при выборе годящихся независимых внутренних координат, т. е. косвенным путем, при расчете матрицы G. Поэтому выли разработаны алгорифмы годящиеся для симуляции колец и цепей электронными бычислительными машинами.

О количественной характеристике перемешивания

К. СЕЙТЦ и Р. ТЁРЁШ

Для количественного описания перемешивания вводилась наглядная мера, которая имеет значение, равное 1 для полностью смешанной системы и равное $+\infty$ для несмешанной системы. Величина степени смешения для любой системы является положительным целым числом. Определение этого числа возможно с помощью номограммы.

Кинетический анализ некоторых последовательных реакций, V

Автокаталитические реакции

Т. КЕЛЕН — Ф. ТЮДЁШ и Д. ГАЛАМБОШ

Проведен кинетический анализ автокаталитических систем $A \rightarrow E$, $A(+E) \rightarrow E(+E)$; $A + A \rightarrow E$, $A(+E) \rightarrow E(+E)$; $A + B \rightarrow E$, $A(+E) \rightarrow E(+E)$. Рассмотрено эмпирическое дифференциальное уравнение автокатализа в общем случае. Обсуждаются различные причины образования кривых конверсий формы S. Установлено, что S-форма кривой конверсии конечного продукта указывает на автокаталитический характер реакции только в том случае, если кривая конверсии исходного продукта также имеет форму S (отличие от последовательных реакций) и если не накапливается в течении реакции промежуточный продукт отличный от конечного продукта (отличие от последовательно-параллельных реакций).

Рентгено-диффракционное изучение кристаллического и молекулярного строения 3-нитрозо-фенилгидразон-ацетона, $C_9N_3O_2H$. H_{II}

ДЬ. МЕНЦЕЛЬ

Изучалось кристаллическое строение 3-нитро-фенилгидразон-ацетона с помощью рентгено-диффракционного метода. Кристаллы относятся к моноклинной системе, принадлежащей к пространственной группе C2/c. Строение определялось с помощью двухразмерного метода Паттерсона и, т. наз., „trial" метода. Уточнения производились синтезом дифференциала. Индекс надежности R = 0,169. Система связей бензольного кольца асимметрична. Измеренные величины связей углерод-азот сравнивались с данными для подобных соединений. Было установлено уравнение плоскости, «наиболее хорошо прилегающей» к бензольному кольцу, а также уравнения плоскости ацетона и двух частей плоскости гидразона. Были рассчитаны углы между этими плоскостями.

Расчет контуров ИК-полос для плоских молекул типа асимметрического ротатора, II

Изучение точности общей зависимости

Э. ПААЛ и Д. ВАРШАНИ

Изучалась точность диаграмм $\varkappa - \Delta\tilde{\nu}_{1/n}$, построенных описанным в предыдущем сообщении методом, в случае чистых полос A и B. Определялись ширины экспериментальных полос A и B при некоторых долях высот в случае фторбензола, хлорбензола и тиофена, и последние сравнивались с рассчитанными из диаграммы. Максимальное отклонение 4,5 $см^{-1}$ или 18,7%. Оцениваются полученные результаты.

Гетероциклические соединения из сахаров, I

Получение производных 2-(полигидрокси)алкил)-бензтиазолина

Р. БОГНАР, З. КОЛОДИНСКА, Л. ШОМОДЬИ, З. ДЬЁРДЬДЭАК, Л. СИЛАДИ и Е. НЕМЕШ

Изучалась реакция конденсации 2-амино-тиофенола (I) и 2-амино-4-хлортиофенола (II) с D-глюкозой и D-галактозой. Было установлено, что образуются производные 2-(пентагидрокси)пентил-бензтиазолина (VII, VIII, XIII, XIV), которые могут быть ацетилированы до O-ацетатов (XI, XII, XVII, XVIII) и O—N-ацетатов (IX, X, XV, XVI). Был осуществлен также синтез 2-(пентаацетокси) пентил-бензтиазолинов исходя из a1-сахарных ацетатов. Структура соединений подтверждалась спектроскопическими исследованиями.

Изучение реологических свойств клейковины, II

Вязкоэластические свойства химически модифицированных клейковин

Р. ЛАСТИТИ

Химическое модифицирование отдельных групп белков клейковины и изучение реологических свойств полученных производных клейковины служат ценным источником данных для определения зависимостей между химическим строением комплексов белков клейковины и их реологическими свойствами.

Среди возможных химических превращений являются, интересными в первую очередь, блокирование тиольных групп N-этилмалеинимидом, дезамидирование клейковины, этерификация свободных карбоксилов, превращение амидных групп в сложные эфиры и ацилирование первичных аминогрупп.

Для изучения реологических свойств может быть с успехом использовано измерение релаксации напряжения, с помощью модифицированного Неолабороrрафа, а также измерение вязкости растворов клейковины.

Блокирование тиольных групп, а также этирификация свободных карбонильных групп не оказывают значительного влияния на реологические свойства клейковины, в то время как превращение амидных групп, а также ацилирование первичных аминогрупп приводит к глубоким изменениям в реологических свойствах клейковины, а именно уменьшает время релаксации и ухудшает когезию.

Синтез N^{ε}-NIP-тетра-DL-аланил-поли-L-лизина

М. СЕКЕРКЕ и В. ВЭЙД

Проводился синтез разветвленного полимера со скелетом поли-L-лизина — модельного соединения для иммунологических исследований. К каждой ε-аминогруппе поли-L-лизинового скелета присоединяются короткие аланиновые боковые цепи, содержащие известное число аланиновых единиц, а к каждому N-терминалу аланина присоединяется 4-гидрокси-3-иодо-5-нитрофенил-уксусная кислота (NIP), как синтетический носитель иммунологического действия.

Синтез тетра-DL-аланина, представляющего боковую цепь, производился двумя путями с помощью использования а) соответствующих азидов и б) пентахлорфенильных активных сложных эфиров. Пентахлорфенильный эфир NIP-тетрапептида, получаемый из тетра-DL-аланина, оказался пригодным для образования связей между ε-аминогруппами поли-L-лизина и боковыми цепями. Структура полученного производного поли-L-лизина (XVI) доказывалась на основе ИК-спектров, данных элементарного анализа и результатов аминокислотного анализа продукта, полученного с помощью солянокислого гидролиза.

Получение и исследование комплексов кислот Дьюиса, V

Комплексы ацетатов циклических двух- и трех-основных спиртов с четыреххлористым титаном

З. ЧЮРЁШ, Д. ДЕАК, Ш. ХОЛЛИ, А. ТЁРЁК-КАЛМАР и Е. ЗАРА-КАЦИАН

Были изучены комплексы четыреххлористого титана, взятого в эквимолекулярных количествах или в избытке, с циклогексил-ацетатом, этиленгликоль-диацетатом, циклопентан-цис- и транс-1,2-диол-диацетатами, циклогексан-цис- и транс-1,2-диол-диацетатами, и транс-1,3-диол-диацетатом, а также с α- и γ-циклогексан-триол-триацетатом. На основе состава и ИК-спектров комплексов делались заключения о строении комплексов. Полагалось, что в случае соединений, в молекулах которых карбонильные атомы кислорода сложных эфирных групп находятся в достаточной близости друг к другу, в комплексе с составом 1:1 оба атома кислорода связаны с центральным атомом металла $TiCl_4$. В остальных случаях (циклопентан-транс-1,2-диол-диацетат, циклогексан-1,3-диол-диацетат) несколько молекул субстрата и молекула $TiCl_4$ образуют больший по размеру цикл. В случае триол-триацетатов в комплексе с составом 1:1 связаны с титаном два карбонильных кислорода. Структура же комплекса с составом 1:2 полностью отличается. Согласно нашим представлениям, присоединяются к одной молекуле $TiCl_4$, два карбонильных кислорода из двух молекул субстрата образуя циклическое соединение, а оставшиеся эфирные группы содержат в связанной форме по одной молекуле $TiCl_4$.

The AALC collection, including approx. 5500 punched cards gives the individual the advantages of modern data processing, without the need for expensive machines.

The advatages of cards!

The AALC collection of cards offers many advantages to its user. First, because only a card-file can be kept complete and up-to-date at any time. Book-form bibliographies are difficult to handle and are not apt for cross-indexing. Secondly with a card-file you do not have to make personal notes. If you wish to retain items of information from a book-bound bibliography, you cannot avoid noting them down (if you don't want to tear out the relevant pages!); with the AALC-file, however, you can indulge in the luxury of picking out the cards you are looking for.

The advantages of p u n c h e d cards!

By having the AALC collection on *punched* cards, you never have to replace cards in any particular order. Through the selection operation the cards you are looking for fall unerringly from the whole pack, irrespective of the place they occupy in the card-file. Using simple methods, you can collect all the cards that are particularly important for the topical field you are engaged in at a given time. A punched card file allows any questions to be combined according to the nature of your problem: it allows cross-indexing as well.

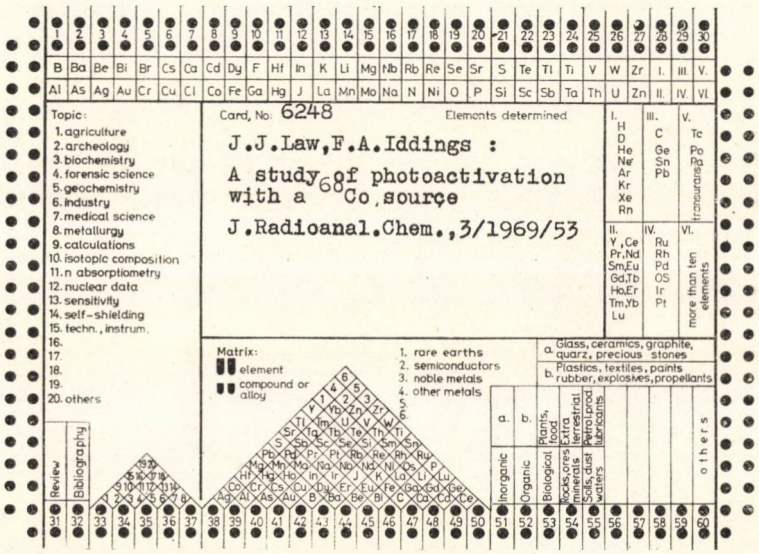

AALC—File
ACTIVATION
ANALYSIS
LITERATURE
CARDS
1935—1968

Unslotted:
US$ 0.05/card

Slotted:
US$ 0.06/card

IN PREPARATION

Ask for leaflets at the following address

AKADÉMIAI KIADÓ

Publicity Department, Budapest 502. P.O.B. 24

ACTIVATION ANALYSIS DOCUMENTATION CENTER

AKADÉMIAI KIADÓ

PUBLISHING HOUSE OF THE HUNGARIAN ACADEMY OF SCIENCES

The Acta Chimica publish papers on chemistry, in English, German, French and Russian.

The Acta Chimica appear in volumes consisting of four parts of varying size, 4 volumes being published a year.

Manuscripts should be addressed to

Acta Chimica
Budapest 112/91 Műegyetem

Correspondence with the editors should be sent to the same address.

The rate of subscription is 165 forints a volume. Orders may be placed with "*Kultúra*" Foreign Trade Company for Books and Newspapers (Budapest I., Fő utca 32. Account No. 43-790-057-181) or with representatives abroad.

Les Acta Chimica paraissent en français, allemand, anglais et russe et publient des mémoires du domaine des sciences chimiques.

Les Acta Chimica sont publiés sous forme de fascicules. Quatre fascicules seront réunis en un volume (4 volumes par an).

On est prié d'envoyer les manuscrits destinés à la rédaction à l'adresse suivante:

Acta Chimica
Budapest 112/91 Műegyetem

Toute correspondance doit être envoyée à cette même adresse.

Le prix de l'abonnement est de 165 forints par volume.

On peut s'abonner à l'Entreprise pour le Commerce Extérieur de Livres et Journaux «*Kultúra*» (Budapest I., Fő utca 32. Compte-courant No. 43-790-057-181) ou à l'étranger chez tous les représentants ou dépositaires.

«*Acta Chimica*» издают трактаты из области химической науки на русском, французском, английском и немецком языках.

«*Acta Chimica*» выходят отдельными выпусками разного объема. 4 выпуска составляют один том. 4 тома публикуются в год.

Предназначенные для публикации рукописи следует направлять по адресу:

Acta Chimica
Budapest 112/91 Műegyetem

По этому же адресу направлять всякую корреспонденцию для редакции.

Подписная цена «*Acta Chimica*» — 165 форинтов за том. Заказы принимает предприятие по внешней торговле книг и газет «*Kultúra*» (Budapest I., Fő utca 32. Текущий счет № 43-790-057-181) или его заграничные представительства и уполномоченные.

50,— Ft

Reviews of the Hungarian Academy of Sciences are obtainable at the following addresses:

ALBANIA

Ndermarja Shtetnore e Botimeve
Tirana

AUSTRALIA

A. Keesing
Box 4886, GPO
Sydney

AUSTRIA

Globus Buchvertrieb
Salzgries 16
Wien I

BELGIUM

Office International de Librairie
30, Avenue Marnix
Bruxelles 5
Du Monde Entier
5, Place St. Jean
Bruxelles

BULGARIA

Raznoiznos
1, Tzar Assen
Sofia

CANADA

Pannonia Books
2, Spadina Road
Toronto 4, Ont.

CHINA

Waiwen Shudian
Peking
P. O. B. 88

CZECHOSLOVAKIA

Artia
Ve Směčkách 30
Praha 2
Poštová novinová služba
Dovoz tisku
Vinohradská 46
Praha 2
Mad'arská Kultura
Václavské nám. 2
Praha I
Poštová novinová služba
Dovoz tlače
Leningradská 14
Bratislava

DENMARK

Ejnar Munksgaard
Nörregade 6
Copenhagen

FINLAND

Akateeminen Kirjakauppa
Keskuskatu 2
Helsinki

FRANCE

Office International de Documentation et Librairie
48, rue Gay Lussac
Paris 5

GERMAN DEMOCRATIC REPUBLIC

Deutscher Buch-Export und Import
Leninstraße 16
Leipzig 701
Zeitungsvertriebsamt
Fruchtstrasse 3—4
1004 Berlin

GERMAN FEDERAL REPUBLIC

Kunst und Wissen
Erich Bieber
Postfach 46
7 Stuttgart S.

GREAT BRITAIN

Collet's Holdings Ltd.
Dennington Estate
London Rd.
Wellingborough. Northants.
Robert Maxwell and Co. Ltd.
Waynflete Bldg. The Plain
Oxford

HOLLAND

Swetz & Zeitlinger
Keizersgracht 471—487
Amsterdam C.
Martinus Nijhof
Lange Voorhout 9
The Hague

INDIA

Current Technical Literature
Co. Private Ltd.
India House OPP
GPO Post Box 1374
Bombay I

ITALY

Santo Vanasia
Via M. Macchi 71
Milano
Libreria Commissionaria Sansoni
Via La Marmora 45
Firenze

JAPAN

Nauka Ltd.
92, Ikebukur O-Higashi 1-chome
Toshima-ku
Tokyo
Maruzen and Co. Ltd.
P. O. Box 605
Tokyo-Central
Far Eastern Booksellers
Kanda P. O. Box 72
Tokyo

KOREA

Chulpanmul
Phenjan

NORWAY

Johan Grundt Tanum
Karl Johansgatan 43
Oslo

POLAND

RUCH
ul. Wronia 23
Warszawa

ROUMANIA

Cartimex
Str. Aristide Briand 14—18
Bucureşti

SOVIET UNION

Mezhdunarodnaya Kniga
Moscow G—200

SWEDEN

Almquist & Wiksell
Gamla Brogatan 26
Stockholm

USA

Stechert Hafner Inc.
31, East 10th Street
New York, N. Y. 10003
Walter J. Johnson
111, Fifth Avenue
New York, N. Y. 10003

VIETNAM

Xunhasaba
19, Tran Quoc Toan
Hanoi

YUGOSLAVIA

Forum
Vojvode Mišića broj 1
Novi Sad
Jugoslovenska Knjiga
Terazije 27
Beograd

17. XI. 1969 Index: 26.007

ACTA CHIMICA

ACADEMIAE SCIENTIARUM HUNGARICAE

TOMUS 62 FASCICULUS 2

AKADÉMIAI KIADÓ, BUDAPEST

1969

ACTA CHIM. ACAD. SCI. HUNG.

ACTA CHIMICA

A MAGYAR TUDOMÁNYOS AKADÉMIA KÉMIAI TUDOMÁNYOK OSZTÁLYÁNAK IDEGEN NYELVŰ KÖZLEMÉNYEI

Az Acta Chimica német, angol, francia és orosz nyelven közöl értekezéseket a kémiai tudományok köréből.

Az Acta Chimica változó terjedelmű füzetekben jelenik meg, egy-egy kötet négy füzetből áll. Évente átlag négy kötet jelenik meg.

A közlésre szánt kéziratok a szerkesztőség címére (Budapest 112/91 Műegyetem) küldendők.

Ugyanerre a címre küldendő minden szerkesztőségi levelezés. A szerkesztőség kéziratokat nem ad vissza.

Az Acta Chimica előfizetési ára kötetenként belföldre 120 Ft, külföldre 165 Ft. Megrendelhető a belföld számára az „Akadémiai Kiadó"-nál (Budapest V., Alkotmány utca 21. Bankszámla 05-915-111-46), a külföld számára pedig a „Kultúra" Könyv- és Hírlap Külkereskedelmi Vállalatnál (Budapest I., Fő utca 32. Bankszámla: 43-790-057-181) vagy annak külföldi képviseleteinél és bizományosainál.

Die Acta Chimica veröffentlichen Abhandlungen aus dem Bereiche der chemischen Wissenschaften in deutscher, englischer, französischer und russischer Sprache.

Die Acta Chimica erscheinen in Heften wechselnden Umfanges. Vier Hefte bilden einen Band. Jährlich erscheinen 4 Bände.

Die zur Veröffentlichung bestimmten Manuskripte sind an folgende Adresse zu senden:

Acta Chimica
Budapest 112/91 Műegyetem

An die gleiche Anschrift ist auch jede für die Redaktion bestimmte Korrespondenz zu richten.

Abonnementspreis pro Band: 165 Forint. Bestellbar bei dem Buch- und Zeitungs-Außenhandels-Unternehmen »*Kultúra*« (Budapest I., Fő utca 32. Bankkonto Nr. 43-790-057-181) oder bei seinen Auslandsvertretungen und Kommissionären.

Acta Chimica Academiae Scientiarum Hungaricae, Tomus 62 (2), pp. 125—129 (1969)

BEITRÄGE ZUR CHEMIE DES SELENS UND DER SELENVERBINDUNGEN, XVI*

BESTIMMUNG VON SELENSPUREN IN REINSTTELLUR UND REINSTTELLURDIOXYD

S. ZSINDELY und L. BARCZA

(Forschungsinstitut für Nichteisenmetalle, Budapest und Institut für Anorganische und Analytische Chemie der L. Eötvös Universität, Budapest)

Eingegangen am 10. Februar 1968

Zur Bestimmung des Selengehaltes von Tellur wird die Reaktion von Se(IV) mit *o*-Phenylendiamin empfohlen. Im Falle von Reinsttellur ist eine vorherige Trennung überflüssig, es muß nur das Te(IV) beim gegebenen pH Wert (pH = 1—2) mit Citronensäure in Lösung gehalten werden. Das Reaktionsprodukt wird spektrophotometrisch bei 335 nm bestimmt. Die untere Grenze der Bestimmung liegt bei einem Se-Gehalt von $2 \cdot 10^{-4}$ %. Die Methode ist einfacher, zuverlässiger und schneller als die Bestimmung des Selens mit 3,3'-Diaminobenzidin.

Die sich stürmisch entwickelnde Fernmeldetechnik benötigt immer reinere Stoffe und so ist es verständlich, daß die Analytik der Spurenverunreinigungen von hochreinen Substanzen immer schwerere Probleme zu überwinden hat.

Bei der Untersuchung des Reinsttellurs stellt die Bestimmung des in sehr geringen Mengen vorhandenen Selens die größte Schwierigkeit dar. Es wird im allgemeinen die Reaktion von Se(IV) mit Diaminobenzidin vorgeschlagen: die mit der selenigen Säure gebildete Verbindung des Diaminobenzidins wird mit Toluol extrahiert und die Lichtabsorption der organischen Phase wird gemessen [1].

In der Reaktion der Se(IV) mit 3,3'-Diaminobenzidin bildet sich hauptsächlich 5-(3,4-Diaminophenyl)-2,1,3-Benzoselenadiazol. Ein Nachteil ist jedoch, daß das Produkt nur unter sorgfältig eingehaltenen Versuchsbedingungen entsteht, die Absorption nicht bei der empfohlenen Wellenlänge [1] ihr Maximum zeigt, und die Verbindung wegen den anwesenden freien Aminogruppen nur bei einem sorgfältig eingehaltenen pH-Wert extrahierbar ist. Sie verteilt sich zwischen der wäßrigen und der organischen Phase ziemlich ungünstig und der Verteilungskoeffizient hängt stark von der Ionstärke der wäßrigen Phase ab. Schließlich können die beiden *orto*-ständigen Aminogruppen mit seleniger Säure weiter reagieren, das so entstehende Diselen-Derivat besitzt völlig andere Eigenschaften als das Mono-Derivat [2].

Auf Grund dieser Tatsachen kann die obige Reaktion auch unter sorgfältig eingehaltenen Umständen nur für eine annähernde Bestimmung des Selengehaltes von Reinsttellur dienen.

* Mitteilung XV: Acta Chim. Acad Sci. Hung. **48**, 99—104 (1966).

Unseren Erfahrungen nach kann der Selengehalt des Reinsttellurs mit Hilfe von *o*-Phenylendiamin ohne die obigen Störungen direkt bestimmt werden. Der Vorteil des Verfahrens liegt in seiner Einfachheit, Selektivität und in seiner relativen Unempfindlichkeit gegen Änderungen der Versuchsbedingungen.

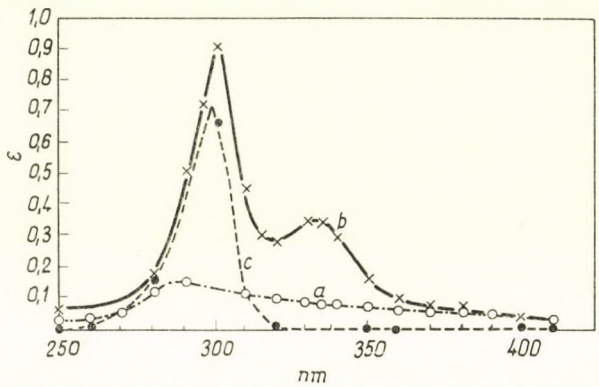

Abb. 1. Änderung der Extinktion als Funktion der Wellenlänge
a) = 0,500 g Tellur + 0,5 g NaOH + 5 g Citronensäure je 25 ml Lösung; *b)* = wie oben + 2,5 ml 1%ige *o*-Phenylendiamin-HCl-Lösung je 25 ml Lösung; *c)* = 0,5 g NaOH + 5 g Citronensäure + 2,5 ml 1%ige *o*-Phenylendiamin-HCl-Lösung je 25 ml Lösung

Die selenige Säure liefert mit *o*-Phenylendiamin eindeutig das sehr stabile 2,1,3-Benzoselenadiazol [3]:

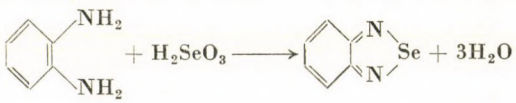

Die Extinktion der Verbindung zeigt bei 335 nm ein Maximum, welches für analytische Zwecke gebraucht werden kann.

In dieser Arbeit wird ein Verfahren beschrieben, welches die Bestimmung von Selenspuren in Reinsttellur bzw. Reinsttellurdioxyd bis zu einem Se-Gehalt von $2 \cdot 10^{-4}$ %, mit einem Relativfehler von ca. 5%, ohne vorherige Trennung ermöglicht.

Das Wesen des Verfahrens besteht darin, daß das Tellur in Salpetersäure aufgelöst, die sich ausscheidende tellurige Säure mit Citronensäure in einem Komplex übergeführt und nach Zugabe von *o*-Phenylendiamin in saurem Medium — zweckmäßig bei pH = 1—2 — die Extinktion der Verbindung bei 335 nm bestimmt wird. Eine Extraktion der Selenverbindung ist nicht nötig.

Unsere Untersuchungen zeigten, daß die Lösung bei 335 nm auch ohne Reagens eine nicht zu vernachlässigende Extinktion zeigt, die genau zweimal größer ist, als die bei 395 nm gemessene Extinktion, während die Selen-Verbindung des *o*-Phenylendiamins bei 395 nm nicht absorbiert (Abb. 1).

Um nicht gegen einer kein Reagens enthaltenden Lösung photometrieren zu müssen, scheint es daher einfacher zu sein, die Extinktion der das Reagens bereits enthaltenden Lösung sowohl bei 335 nm, als auch bei 395 nm zu bestimmen und den zweifachen Wert der letzteren vom Wert der ersteren abzuziehen. Nach unseren Untersuchungen ist die so verminderte Extinktion bei Reinsttellur immer dem Selengehalt der Probe proportional (Abb. 2)

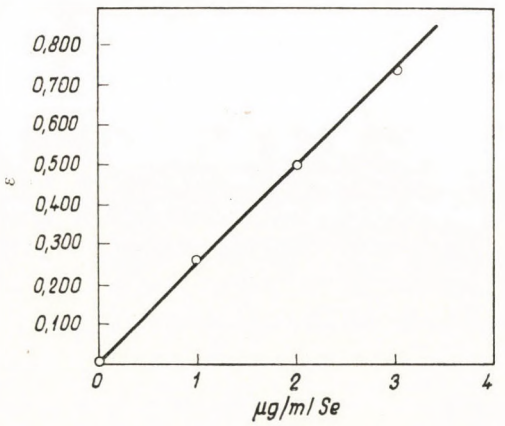

Abb. 2. Kalibrationskurve
$\varepsilon \times 4{,}0$ = Se μg/ml

Experimenteller Teil

Reagenzien:
Salpetersäure, 1 : 1 verdünnt, halogenfrei;
Natronlauge, fest, p. a.;
Citronensäure, p. a.;
20%ige Salzsäure;
1%ige *o*-Phenylendiammoniumchlorid-Lösung (einige Stunden lang verwendbar).

Selenstammlösung: Man löst genau gewogenes elementares Selen p.a. in halogenfreier Salpetersäure, dampft auf dem Wasserbad bis zur Trockene ein und verdünnt mit Wasser so, daß die Lösung 25 (μg Se) ml in Form von seleniger Säure enthalten soll.

Bestimmung in Reinsttellur: 0,5 g feinpulverisiertes Reinsttellur werden mit 35 ml Salpetersäure 1 : 1 in einem Becherglas übergossen. Die Probe löst sich beim Erhitzen auf. Man läßt die Lösung am Wasserbad bis zur Trockene eindampfen und gibt zum trockenen Rückstand ungefähr 0,5 g Natronlauge und 10 ml Wasser. Nach der vollständigen Auflösung der tellurigen Säure fügt man 5 g Citronensäure hinzu, gießt die Lösung in einen 25-ml-Meßkolben und spült das Becherglas zweimal mit je 3 ml Wasser nach. Der pH wird mit Salzsäure auf 1—2 eingestellt und zur Lösung werden 2,5 ml Reagenslösung zugegeben. Der Kolben wird mit Wasser bis zur Marke aufgefüllt, geschüttelt und nach einer Stunde wird die Extinktion in Quarzküvetten (1 cm) bei 335 nm sowie bei 395 nm gemeßen.

Bestimmung in Tellurdioxyd: Zu 0,5 g feinpulverisierten Tellurdioxyd werden in einem 100-ml-Becherglas etwa 0,6—0,7 g Natronlauge und 10 ml Wasser gegeben. Die Probe löst sich vollständig auf, dann fügt man 5 g Citronensäure hinzu und verfährt weiter wie bei der Bestimmung des Selengehaltes von Tellur.

Die Kalibrationskurve wird wie folgt aufgenommen: In mehreren 25-ml-Meßkolben werden je 5 g Citronensäure in 15 ml Wasser gelöst und aliquote Teile der Selenit-Stammlösung entsprechend 5,0—75,0 μg Se, werden in die Kolben pipettiert. Der pH wird mit Salzsäure auf 1—2 eingestellt. Man gibt in jeden Kolben 2,5 ml Reagenslösung und verfährt im weiteren wie oben.

Die Kalibrationskurve ist sehr einfach und gut reproduzierbar (Abb. 2) und muß nicht in jedem Fall neu aufgenommen werden: um den Selengehalt der Prüflösung in μg/ml erhalten zu können, kann der korrigierte Extinktionswert einfach mit 4,0 multipliziert werden.

Die Resultate sind in Tabellen zusammengefaßt. Aus diesen geht hervor,

Tabelle I

Prüfung der Empfindlichkeit der Methode nach vorheriger Zugabe von bekannten Selenmengen

Einwaage Tellur g	Zugabe Selen μg	Gefunden Selen μg	Selengehalt der Tellurprobe μg	Selengehalt nach Abzug des Se-Gehaltes des Tellurs μg	Differenz μg
0,500	25	71	45,5	25,5	0,5
0,500	40	84	45,5	38,5	—1,5
0,500	50	93,5	45,5	48,0	—2,0

Tabelle II

Selengehalt einiger Proben

Probe	Einwaage g	Gefunden Se μg	Gefunden Se 10^{-4} %	Mittelwert 10^{-4} %
Tellur I.	0,500	26,5	53	
	0,500	26,5	53	
	0,500	26,0	52	
	0,500	24,0	48	51
	0,200	10,5	53	
	0,300	16,0	53	
	0,700	34,0	49	
Tellur II.	0,500	41,0	82	81
	0,500	40,5	81	
Tellur III.	0,500	16,0	32	33
	0,500	17,5	35	
Tellurdioxyd	0,500	11,4	23	
	0,500	14,5	29	
	0,200	6,0	30	28
	0,200	5,7	29	
	0,200	6,0	30	

daß mit der Methode am günstigsten ein Se-Gehalt der Größenordnung von 10^{-3} % zu bestimmen ist. Da die sonstigen Verunreinigungen des Reinsttellurs bzw. Reinsttellurdioxyds höchstens in 10^{-3} % anwesend sind, braucht mit Störeffekten nicht gerechnet werden. Bei Tellurproben technischer Reinheit ist es aber zweckmäßig, ähnlich wie bei der Bestimmung des Selengehaltes von Schwefel, Schwefelverbindungen und sulfidischen Erzen, das Selen vom Tellur durch Destillation zu trennen [4].

LITERATUR

1. VEALE, C. R.: Analyst **85** 130 (1960).
2. BARCZA, L.: Microchim. Acta **1964** 967.
3. BARCZA, L.: Microchim. Acta **1964** 136.
4. BARCZA, L., ZSINDELY, S.: Z. anal. Chem. **199** 117 (1964).

Sándor ZSINDELY; Budapest XI., Fehérvári út 144.
Lajos BARCZA; Budapest VIII., Múzeum krt. 4.

Acta Chimica Academiae Scientiarum Hungaricae, Tomus 62 (2), pp. 131—140 (1969)

THE USE OF COMPLEX FORMING AGENTS IN ION EXCHANGE CHROMATOGRAPHY, III

ADSORPTION OF METAL AMMINE COMPLEXES ON CATION EXCHANGE RESIN

J. INCZÉDY

(Institute for General and Analytical Chemistry, Technical University, Budapest)

Received November 4, 1968

The adsorption of nickel(II), cobalt(II), copper(II), cadmium(II) and zinc(II) ions on cation exchange resin from ammonium chloride solutions containing various amounts of free ammonia was investigated. It was found that the tetrammine and in most cases the hexammine complex ions exhibit particular high adsorption strength. The approximate values of the ion exchange constants of the complex species were also calculated.

In connection with the planning of chromatographic separation of bivalent metal ions [1] the knowledge of data concerning the adsorption strengths of some metal ammine complexes was necessary.

In order to obtain quantitative data on the extent of adsorption of various ammine complexes static, batch experiments were carried out to determine the distribution coefficients of the bivalent complex forming metal ions: nickel(II), cobalt(II), zinc(II), cadmium(II) and copper(II) from ammonium chloride solution containing ammonia in varying concentrations.

To get more information on the form of the adsorbed nickel(II) complex species, cation exchange resin samples of known amount and capacity were loaded completely with nickel(II) ions or with nickel(II) complexes, using nickel(II) chloride solution without or with ammonia in different concentrations.

The saturated resin samples were separated quickly from the liquid phase by suction and analysed for nickel(II), ammonia and water. On the basis of the data obtained the number of moles of ammonia and water per adsorbed mole nickel(II) ions were calculated. It was found — in agreement with the results of STOKES and WALTON [2] — that the calculated average ligand number (bound ammonia per mole metal ion) belonging to the ammonia concentration of the liquids used was very close to that found experimentally in the resin phase. Thus, the compositions of the adsorbed complexes corresponded to those calculated on the basis of ligand concentration and complex product data in solution.

In the calculation of average ligand number at given ammonia concentration, the complex stability constants determined by BJERRUM [3] were used.

For the purpose of comparing the composition of the resin containing nickel(II) hexammine complex ion to that containing nickel(II)hexaquo complex, some data are given in Table I. The nickel(II) form resin took up

Table I

Results of the analysis of Ni-form and NH_4-form resin samples swollen in water and in cc. ammonia solution

Resin sample	Ni^{2+} or NH_4^+	NH_3	H_2O	NH_3	H_2O	column volume
	mequ.			mole per 1. equ. resin		ml
0.5 g air dry resin loaded with Ni^{2+} ions, swollen in water (green)	2.08	—	30.4	—	14.6	1.17
0.5 g air dry resin loaded with Ni-hexammine ions in presence of cc. NH_2, swollen in cc. NH_3-solution (violette)	2.08	6.4	21.0	3.1	10.0	1.04
0.5 g air dry NH_4-form resin, swollen in water	2.08	—	28.0	—	13.5	1.11
0.5 g air dry NH_4-form resin, swollen in cc. ammonia sol.	2.08	2.1	25.6	1.0	12.3	1.09

ammonia from the ammonia solution to form hexammine complex ions. The difference between the uptake of ammonia of the ammonium form and nickel(II) form resins of one equivalent has been found about 2 mole/equ. resin. The sum of the adsorbed water and ammonia molecules in the resin containing hexammine complex ions is less than the number of water molecules in the hydrated nickel(II) form resin. Significant contraction of the column volume of the nickel(II) form resin in cc. ammonia was observed. For comparison, the column volume data of 0.5 g air dry ammonium form resin sample was also determined in water and cc. ammonia and found as 1.11 and 1.09 ml respectively.

The distribution measurements were carried out with different metal ions under the same conditions. From the experimental volume distribution coefficients diagrams were constructed, as can be seen in Figs 1—5. Since it has been shown by preliminary experiments that the average composition of the adsorbed complexes corresponded to that in the solution at given ammonia concentration, the mole fractions Φ of the complex species having four and six ligands were calculated using the complex product data. The calculated mole fraction curves are also given in the diagrams. According to the

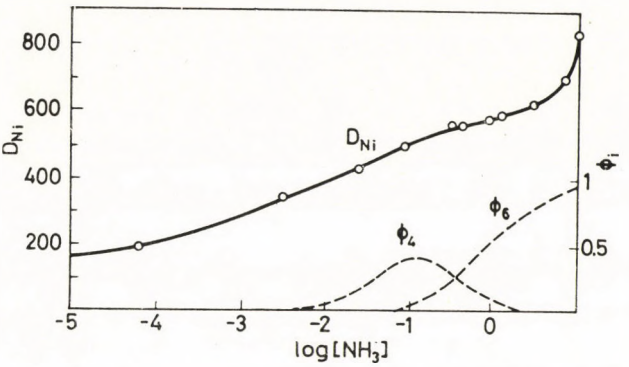

Fig. 1. Distribution coefficient D of nickel(II)ions on Dowex 50×8 cation exchange resin from 0.2 M NH_4Cl solution as a function of the logarithm of the free ammonia concentration (full line). With broken lines the calculated mole fractions (Φ) of the four- and six coordinated complex species are presented

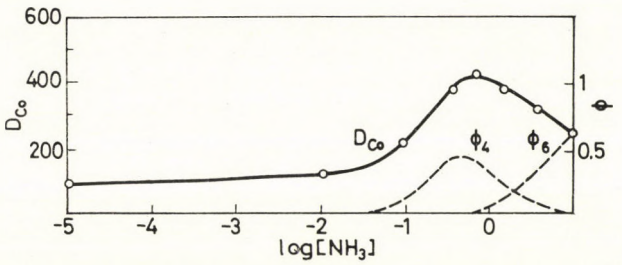

Fig. 2. Distribution coefficient (D) of cobalt(II) ions on cation exchange resin from 0.2 M NH_4Cl solution as a function of the logarithm of the ammonia concentration (full line). The mole fractions of the four and six coordinated species are presented with broken lines

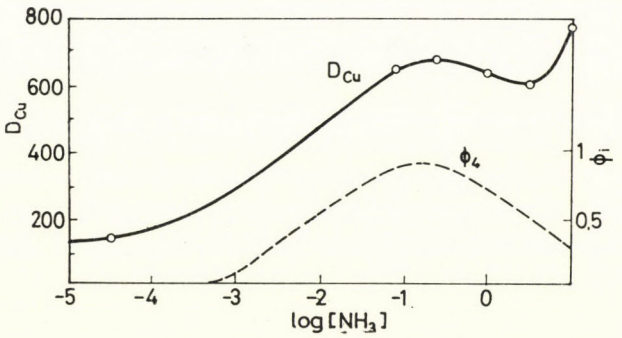

Fig. 3. Distribution coefficient (D) of copper(II) ions on Dowex 50×8 cation exchange resin from 0,2 M NH_4Cl solution as a function of the logarithm of the ammonia concentration (full line). With broken line the mole fraction (Φ) of the complex species is presented

obtained curves, it is clear that in the case of cobalt(II), copper(II), zinc(II), cadmium(II) and also of nickel(II) ions the tetrammine complexes exhibit much stronger adsorption, than the free, aquocomplexed metal ions. The maxima of the D curves coincide as first approximation with the maxima of the Φ_4 curves, but a shift or rather a hysteresis can be observed in all cases. It must be assumed that the equilibrium composition in the solution and in

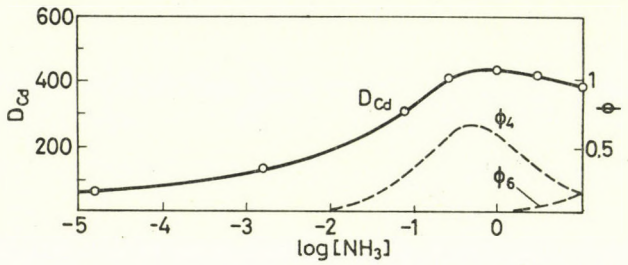

Fig. 4. Distribution coefficients (D) of cadmium(II) ions on Dowex 50×8 cation exchange resin from 0.2 M NH_4Cl solution as a function of the logarithm of the free ammonia concentration (full line). With broken lines the calculated mole fractions (Φ) of the complex species are presented

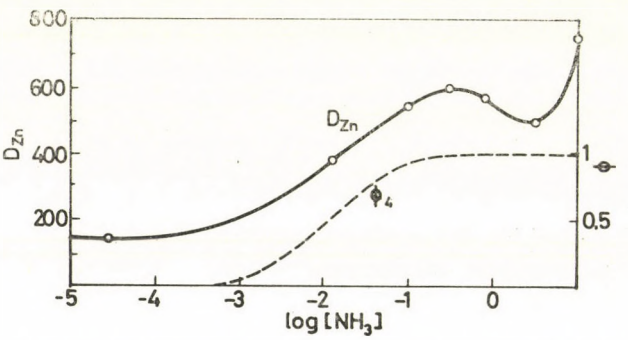

Fig. 5. Distribution coefficients (D) of zinc(II) ions on Dowex 50×8 cation exchange resin from 0.2 M NH_4Cl solution as a function of the logarithm of the free ammonia concentration (full line). With broken lines the calculated mole fractions of the complex species are presented

the resin phase is not quite the same. In the case of copper, zinc and nickel ions also the rapid increase of the distribution coefficients at high ammonia concentrations could be observed. This phenomenon can be attributed to the formation of hexammine complex. Thus the adsorption of octahedral hexammine complex ions on the ion exchange resin is extremely strong.

In the work of BJERRUM there are no data on the hexammine complex formation of copper(II) and zinc(II) ions in aqueous ammonia solutions, and therefore the curves of Φ_6 are omitted in Fig. 3 and 5, however, the formation of the six coordinated species in the resin phase also in these cases seemed to be very probable.

In order to obtain quantitative data for the extent of adsorption of the complex ions some approximate calculations were made. To obtain the ion exchange constants of the particular species, *i.e.* of the tetrammine and hexammine complexes, two methods of calculation were used.

In the first one it was assumed that all the species except the hexammine or tetrammine complexes are adsorbed on the resin to nearly the same extent. Considering the calculated composition of the metal complexes at given ammonia concentrations and the overall distribution coefficient measured, the partition coefficients of the individual species could be calculated.

The second method is based on the basic equation of the distribution coefficient

$$D = \frac{(\mathrm{M}) + (\mathrm{M(NH_3)}) + (\mathrm{M(NH_3)_2}) + \ldots + (\mathrm{M(NH_3)_6})}{C_M} \tag{1}$$

where M stands for the complex forming bivalent metal ion. The round brackets mean the concentrations in the resin phase. Considering the individual partition coefficients of the species

$$\frac{(\mathrm{M})}{[\mathrm{M}]} = d_o \qquad \frac{(\mathrm{M(NH_3)}_i)}{[\mathrm{M(NH_3)}_i]} = d_i$$

and the complex product expressions:

$$[\mathrm{M(NH_3)}_i] = [\mathrm{M}]\,[\mathrm{NH_3}]^i\,\beta_i$$

Eq. (1) can be transformed. Square brackets mean the concentrations in the liquid phase. d is the partition coefficient, and β the complex product.

Assuming that within a range of ligand concentration the formation of some complex species (*e.g.* hexammine) can be neglected, and the partition coefficients of the other ones except one (e.g. that of tetrammine) are equal, thus $d_0 = d_1 = d_2 = d_3 = d_5$ the following simplified equation can be written:

$$D = \frac{d_o\left(1 + \sum_{i=1}^{i=3}[\mathrm{NH_3}]^i\,\beta_i + [\mathrm{NH_3}]^5\,\beta_5)\right) + d_4\,[\mathrm{NH_3}]^4\,\beta_4}{1 + \sum_{i=1}^{i=5}[\mathrm{NH_3}]^i\,\beta_i} \tag{2}$$

or

$$D = \frac{d_o\alpha' + d_4[\mathrm{NH_3}]^4\,\beta_4}{\alpha}$$

The last equation can be linearised in the following logarithmic form:

$$\log\,(D\alpha - d_o\alpha') = \log\,(d_4\,\beta_4) + 4\log\,[\mathrm{NH_3}] \tag{3}$$

On the basis of experimental D data, and ligand concentration data the $\log (D\alpha - d\alpha')$ term has been calculated using constants taken from the literature and plotted against the logarithm of the ammonia concentration. From the intersect of the obtained line the value of d_4 was calculated. Such diagrams can be seen in Figs 6 and 7. From the obtained partition coefficient

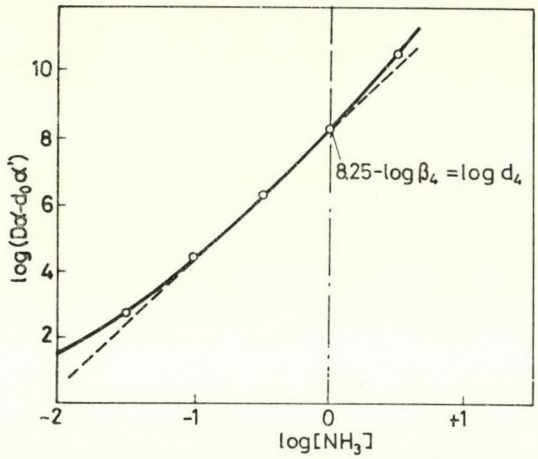

Fig. 6. Graphical evaluation of the partition coefficient of cobalt(II) tetrammine complex ion

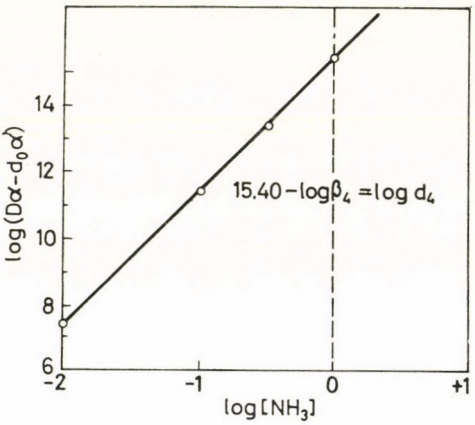

Fig. 7. Graphical evaluation of the partition coefficient of copper(II) tetrammine complex ion

values the approximate ion exchange constants of the species were calculated and tabulated in Table II. For the calculation of the constants the following equation was used:

$$K_i^x = d_i \left(\frac{[NH_4]}{(NH_4)} \right)^2 \tag{4}$$

Table II

Calculated volume ion exchange contants of some bivalent metal ions and metal ammine complex ions reffering to the ammonium ion

	d Partition coefficient in 0.2 M NH_4Cl sol.	K^z Volume ion exchange constant
Ni^{2+}	160	2.0
$Ni(NH_3)_4^{2+}$	900	11.1
$Ni(NH_3)_6^{2+}$	1050	13.4
Co^{2+}	95	1.2
$Co(NH_3)_4^{2+}$	870	10.7
Cu^{2+}	130	1.6
$Cu(NH_3)_4^{2+}$	700	8.7
Cd^{2+}	60	0.74
$Cd(NH_3)_4^{2+}$	636	7.8
$Cd(NH_3)_6^{2+}$	(1400)	(17)
Zn^{2+}	140	1.7
$Zn(NH_3)_6^{2+}$	610	7.5

The ammonium ion concentration in the liquid phase was 0.2 M in each experiment except one series, which was carried out with 1 M ammonium chloride solution. The concentration of ammonium ions in the resin phase was calculated by subtracting the adsorbed metal equivalents from the volume capacity of the resin.

In the case of the nickel(II) ions the distribution coefficient of the free, aquocomplexed metal ion was also measured in the presence of different amounts of ammonium nitrate and ammonium perchlorate concentration. The data obtained are presented in a logarithmic diagram in Fig. 8. On the basis of distribution measurements in solutions containing 0.2 and 1 M ammonium ion and 12 M of free ammonia, the partition coefficient of the hexammine species was also registrated in the same diagram. As can be seen the obtained lines having a slope nearly —2, slightly deviate from the ideal ones.

Experimental

Reagents. In all experiments reagent grade chemicals and deionized water were used. Metal salt stock solutions of 0.05 M concentration were prepared from cryst. $NiCl_2 \cdot 6\,H_2O$; $CoSO_4 \cdot 7\,H_2O$; $CuSO_4 \cdot 5\,H_2O$; $ZnSO_4 \cdot 7\,H_2O$; $Cd(NO_3)_2 \cdot 4\,H_2O$ resp. by weighing, dissolution, and dilution to the required volume. The concentrations of the solutions were controlled by chelatometric titrations.

Ammonia solution (a.g.) of 0.910 spec. gravity was used.

Ammonium chloride, ammonium nitrate solutions were prepared from the salts and standardized by titration. Ammonium perchlorate stock solution was prepared from perchloric acid solution by neutralization with ammonia to pH 5 and diluted to required volume.

Ion exchange resin. Dowex 50×8 resin of 50—100 mesh was treated with acid and alkali solutions according to prescription [4] and loaded with ammonium ions using 1 *M* ammonium chloride solution, washed out and dried in air, finally, stored in glass stoppered bottle. The capacity of the air-dried ammonium form resin, its volume in column was determined and found as follows: 0.5 g air-dry resin ~2.08 mequ ~1.11 ml

Instruments. For pH measurements Universal pH meter (Type OP 204, Radelkisz, Hungary); for polarographic measurements Polarograph PO 4 (Radiometer, Denmark) for photometric measurements Spekol (Zeiss, Jena, GDR) were used.

Determination of the ammonia, water and metal ion content of nickel(II)-form resin samples. 0.5 g of air-dry resin samples were weighed and transferred into glass ion exchange columns of small size. Nickel(II) chloride stock solution without ammonia, or containing

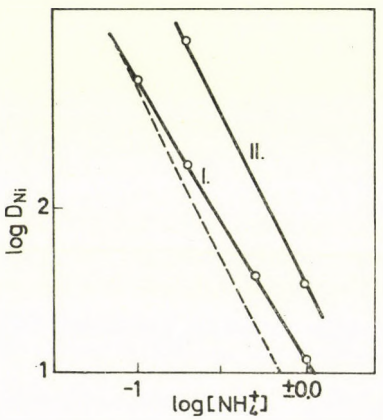

Fig. 8. Logarithmic diagram of the distribution coefficient of nickel(II) ions as a function of the ammonium salt concentration in the absence of free ammonia (I) and in presence of 12 *M* ammonia (II)

ammonia in known concentration, was poured on the resin column in high excess until complete saturation. The excess of nickel(II) ions or complexes was washed out from the resin samples with water or with ammonia solution of the same concentration as used before.

After short suction the resin samples were analysed for nickel(II), water and ammonia. The determination of nickel(II) ions was carried out by chelatometric titration using murexide as indicator in ammoniacal solution at pH 10 after complete elution of nickel ions from the resin sample with 2 *M* hydrochloric acid solution. The nickel(II) ion content of the resin samples in milliequivalents per gram resin was found to be always about the same, corresponding to the capacity of the resin determined by the usual salt splitting method [4]. The deviations were within the error of the determinations. For determining the ammonia content of the resin sample, it was added to 20 ml of 1 *M* standard hydrochloric acid solution and titrated with 1 *M* sodium hydroxide standard solution in the presence of methyl orange indicator. The ammonia content was calculated from the difference of the consumed volumes of standard solution. The water content of the resin samples was determined from ca 0.2 g portions of the samples by the Karl Fischer titration method using dead stop end point detection.

Determination of the column volume of the swollen resins of different forms. 0.5 g of air dry ammonium form resin was weighed and swollen in water, transferred to the required form and with the proper liquid poured in a calibrated glass cylinder of 5 mm diameter, containing glass filter disc at the bottom and a connection with rubber tube to a niveau device. After the resin was settled in the glass cylinder the liquid was sucked gently with hydrostatic pressure and the volume of the resin bed red off. By raising the niveau device the resin was washed back and the measurement repeated again. The measurements were carried out with NH_4-form, Ni-form resin samples using water and cc. ammonia as liquids.

Determination of the distribution coefficients of the metal ions, at different ammonia concentrations. 0.5 g of air-dry ammonium form resin sample were weighed into glass stoppered 200 ml flasks and 50 ml of the solution of different composition. The initial concentration of the metal ion was always $2 \cdot 10^{-3}$ *M*; that of the ammonium salt: 0.2 *M* (except one series); while the concentration of free ammonia was different.

The resin samples were shaken with solution periodically in the flasks and stored for 24 hours. In the case of the experiments carried out with cobalt(II) ions the time was reduced to 3 hours, and a more vigorous shaking was used to avoid the oxidation of the bivalent metal ions by air. After equilibration, known portions of the liquid phase were analysed for metal ion and ammonia. The latter was determined by pH measurement and also by acidimetric titration at higher concentrations. From the obtained data, the volume distribution coefficients of the metal ion were calculated, using also the capacity and column volume data of the resin sample (see above).

Determination of the distribution coefficient of nickel(II) ions at different ammonium ion concentrations. 0.5 g of air-dry resin samples in ammonium form were weighed in glass stoppered flasks and equilibrated as before with solution containing $2 \cdot 10^{-3}$ *M* nickel(II) ion and ammonium nitrate, chloride or perchlorate in different concentrations. After equilibration the concentration of nickel(II) ions was determined in a portion of the liquid phase. The volume distribution coefficients were then calculated.

Determination of nickel(II)-, cobalt(II)-, copper(II)-, zinc(II)- and cadmium(II) ions. For the determination of nickel(II) ions a photometric method using dimethylglyoxime (DMG) as reagent and bromine water as oxidant was used. The measurements were carried out at 530 nm [4]. The concentration of the cobalt(II) ions was determined also by photometric method based on the thiocyanate complex formation in acidic solutions using tin(II) chloride and ammonium thiocyanate solutions as reagents. The optical density of the solution containing 50 vol% acetone was measured at 625 nm [5]. Calibration graphs were prepared and used for the determination of the concentrations of metal ions from the optical density data.

Copper(II)-, zinc(II)- and cadmium(II)-ions were determined by polarographic method using ammoniacal ammonium chloride solution as supporting electrolyte. For the evaluation of the obtained polarograms calibration graphs were used.

Results and discussion

On the basis of the experimental results and calculated data the following conclusions can be drawn.

The metal ammine complex equilibria in the resin phase are almost the same as in solution, only a small shift between the complex formation in the two phases can be observed.

The complex species having a higher geometric symmetry, or rather having a closed structure, surrounded with ammonia molecules exhibit exceptionally strong adsorption. The phenomenon can be explained by assuming that the ions with closed ammonia spheres do not bind water molecules so strongly in the outer sphere, as the aquocomplex ions.

This assumption is supported also by the unusually large difference observed at the column volumes of the nickel(II)-form resin in water and in cc. ammonia.

Thus the size of the hexammine nickel(II) ion is almost the same as that of the hexaquo nickel(II) ion, however, the solvation ability of the latter is greater. Correspondingly, if the inner sphere of the complex ion is not completely filled with ammonia molecules, there are water molecules also present, the screening being not complete and further hydration is facilitated.

Except the case of cobalt(II) complexes, the highest adsorption strength exhibit the saturated six ligands containing complex species. One must assume that also in the case of copper(II) and zinc(II) ions there are also hexammine complexes bound to the resin.

The adsorption strengths of the four coordinated species are somewhat lower than those of the six coordinated ones, and the values of the ion exchange constants are very near to each other. However, a decrease in the K_4^x values from nickel(II) to zinc(II) can be observed (Table II).

According to theoretical considerations the four coordinated complexes of nickel(II), cobalt(II), copper(II) ions are planar, and those of the zinc(II) and cadmium(II) ions tetrahedral; however, in solutions the species cannot be assumed as rigid complex ions, and a similar symmetrical arrangement of all the complexes having four ammonia as ligands must be suggested.

It has to be remarked that the calculated K_4^x values in Table II, are only approximate, since the adsorption strength of all species except the four and six coordinated ones was assumed to be the same.

According to the experimental results summarized in Fig 8. one can state that the slope of the curve II corresponding to the theoretical case is very near to —2. However, in the case of the equilibrium between non-complexed nickel(II) and ammonium ions a deviation from the theoretical can be observed. The adsorption of the nickel(II) ions seems to be greater than that calculated if the concentration of the ammonium ions is high. For giving an explanation of this phenomenon it must be assumed, that appreciable complexation and also change of the position of equilibrium occurs in ammonium nitrate solutions, if the concentration is increasing, however, the pH is ca 5.

REFERENCES

1. Inczédy, J., Klatsmányi-Gábor, P., Erdey, L.: Acta Chim. Acad. Sci. Hung. **62,** 1 (1969).
2. Stokes, R. H., Walton, H. F.: J. Am. Chem. Soc. **76,** 3327 (1954)
3. Bjerrum, J.: Metal ammine formation in aqueous solution. Haase & Son, Copenhagen, 1941
4. Inczédy, J.: Analytical applications of ion exchangers. Pergamon Press, Oxford, 1966
5. Snell, F. D., Snell, C. T.: Colorimetric methods of analysis. Vol II. p. 346. Van Nostrand Co., New York, 1949
6. Snell, F. D., Snell, C. T.: Colorimetric methods of analysis. Vol IIA., p. 285. Van Nostrand Co., New York, 1959

János Inczédy; Budapest XI., Gellért tér 4.

Acta Chimica Academiae Scientiarum Hungaricae, Tomus 62 (2), pp. 141—149 (1969)

ION EXCHANGE MEMBRANES, XI

MEMBRANE POTENTIAL AND INTERNAL ACTIVITY

J. H. SIPOS, I. KÁLMÁN and J. MIKES

(Research Institute for the Plastics Industry)

Received February 2, 1968; in revised form September 2, 1968

The quantity of electrolyte in the membrane-phase of ion exchange membranes is composed of two parts: the fixed ions and their counter-ion partners form the unchanged ion quantity, and the co-ions diffusing from the external solution with the corresponding quantity of counter-ions represent the varying concentration term. Under the conditions of electrodialysis the motion-controlling potential comes from a driving and an inhibiting component where the driving components are both the external field strength and the diffusion potential, the inhibiting component is on the other hand the ion-exchange membrane potential determined by the ions of the membrane phase, with other words the internal activity of the membrane. These factors are correlated, though not linear.

Ion exchange membranes are generally not sufficiently described by the data published in the literature [1, 2] either in technological reports or in manufacturers' pamphlets. The data usually refer to optimum conditions [3] which are not valid for electrodialysis and thus their use is restricted to comparisons.

We have therefore attempted to construct a model [4] to describe the electrochemical phenomena by accounting for charge migration primarily by physical and physico-chemical methods to allow the study of the physical [5, 6, 7] and engineering [8, 9] parameters of the electrodialysis process.

The potential conditions on the anion exchange membrane during dialysis are shown by Fig. 1. The internal energy of the system is plotted on the vertical axis: this internal energy is determined by the ion activity of the solutions and of the membrane, respectively. The horizontal axis shows the position of the ion. The energy conditions are further influenced by the external field ($E = \operatorname{tg} \alpha$).

According to the theory of *p*-type conduction the ions are situated in the potential wells of the solvent and an energy equal to the height of the potential well is necessary to bring about their displacement. The external field distorts the shape of the potential well and from the aspect of ion displacement the direction of the field intensity is a preferred orientation.

If on the two sides of the membrane the solution activities are identical ($a_c = a_d$) then the membrane potential will be the same on both sides. If, however, there is a difference between the potentials of the diluting and con-

centrating solutions ($a_c \neq a_d$) then the potential well will have a distorted energy value, the potential well will appear for the co-ion in point "C" lower by a value of

$$U_N = \frac{R\,T\,e}{F\,z} \ln \frac{a_c}{a_d} \tag{1}$$

than the membrane potential. Fig. 1 is valid for the case $a_d < a_c$; if $a_d > a_c$ then U_N has to be accounted for with an opposite sign.

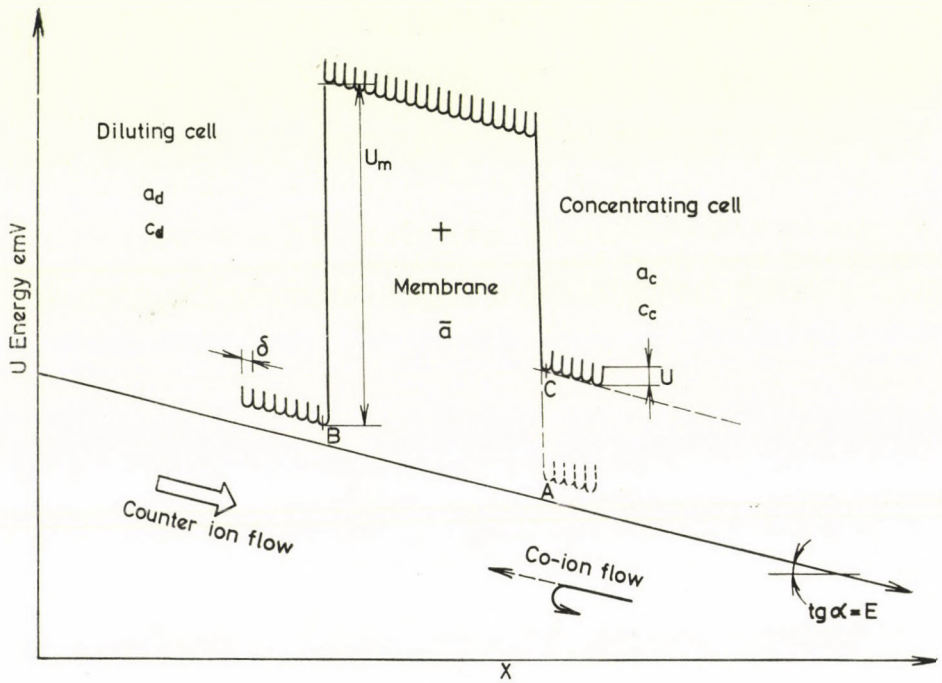

Fig. 1

We have left the polarization phenomena on the ion exchange membrane surface out of consideration, starting from the assumption that on the one hand these are concentrated to a thin interfacial layer, while on the other hand they are similar, though of opposite sign on the two sides of the membrane, provided the difference between the concentrations of the two solutions is not too great. (In practical operations no extreme conditions are applied.) Under these conditions the effect of the two interfacial layers will equalize each other during electrodialysis.

The same is true for cation exchange membrane, but obviously with opposite charges.

The rate of ion mobility in electrolyte solutions in the vicinity of the membrane may be formulated by the *p*-type conductance theory (2) for the counter-ion in point "*B*" which in the case of anion exchange membrane has a negative charge

$$\overline{V}_- = \frac{\delta}{2\tau_o^-} e^{-\frac{U}{kT}} \left(e^{\left(-\frac{U_m}{kT} + \frac{E\delta}{2kT}\right)} - e^{-\frac{E\delta}{2kT}} \right) \tag{2}$$

and for the positive co-ion point "*C*"

$$\overline{V}_+ = \frac{\delta}{2\tau_o^+} e^{-\frac{U}{kT}} \left(e^{\left(-\frac{U_m}{kT} + \frac{E\delta}{2kT} + \frac{U_n}{kT}\right)} - e^{-\frac{E\delta}{2kT}} \right) \tag{3}$$

The forces acting on the counter-ion are: the height "*U*" of the potential well which inhibits and the ion exchange membrane potential U_m which promoted together with the external field strength the mobility of the counter-ion. In the case of the co-ion U and U_m inhibit and E promotes ion migration, as reflected by the signs in the exponents.

The quotient of the potential well width, δ, and of the residence time of the ion in the well τ_o, that is the average velocity of the ions, is proportional to the absolute mobility of the ions:

$$\frac{\delta}{\tau_o} = \mu E. \tag{4}$$

Current efficiency

There are several correlations between electrodialysis and membrane parameters. The relationship between the permselectivity of the membranes bordering the cell and the current efficiency of the cell is given by Eq. (5).

$$\eta = t_a P_c + t_c P_a \tag{5}$$

In electrodialysis the current efficiency of the cell is equal to the quotient of the difference and sum of the charges transported by the positive and negative ions through the membrane in unit time

$$\eta = \left| \frac{i_+ - i_-}{i_+ + i_-} \right| = \left| \frac{1 - \frac{i_-}{i_+}}{1 + \frac{i_-}{i_+}} \right| \tag{6}$$

There is an unequivocal correlation between current intensity and ion velocities:

$$i_+ = z_+ e_+ n_+ V_+ \qquad (7)$$
$$i_- = z_- e_- n_- V_-$$

The number of mobile ions in unit volume (n) is directly proportional to the concentration, thus

$$i_+ = c_c V_+$$
$$i_- = c_d V_-$$

Substitution of these values into Eq. (6) leads to

$$\eta = \left| \frac{1 + \dfrac{c_d V_-}{c_c V_+}}{1 - \dfrac{c_d V_-}{c_c V_+}} \right| \qquad (9)$$

and substitution of the values of V_+ and V_- from Eqs (1), (2), and (3) into Eq. (9) leads after simplification to

$$\eta = \left| \frac{1 + \dfrac{c_d \mu_- \left(e^{\left(\frac{U_m}{kT} + \frac{E\delta}{2kT}\right)} - e^{-\frac{E\delta}{2kT}} \right)}{c_c \mu_+ \left(e^{\left(-\frac{U_m}{kT} + \frac{E\delta}{2kT} + \frac{U_n}{kT}\right)} - e^{-\frac{E\delta}{2kT}} \right)}}{1 - \dfrac{c_d \mu_- \left(e^{\left(\frac{U_m}{kT} + \frac{E\delta}{2kT}\right)} - e^{-\frac{E\delta}{2kT}} \right)}{c_c \mu_+ \left(e^{\left(-\frac{U_m}{kT} + \frac{E\delta}{2kT} + \frac{U_n}{kT}\right)} - e^{-\frac{E\delta}{2kT}} \right)}} \right| \qquad (10)$$

Substituting the value of U_N from Eq. (1) into Eq. (10) after rearrangement and simplification the following relationship is obtained for the value of current efficiency:

$$\eta = \left| 1 - \frac{2}{1 + \dfrac{\mu_- c_d}{\mu_+ c_c} e^{-\frac{U_m}{kT}} \left(1 + \dfrac{1 - \dfrac{a_c}{a_d}}{e^{\frac{U_m}{kT}} - 1} \right)} \right| \qquad (11)$$

Thus the current efficiency of ion exchange membrane electrodialysis depends on the ion exchange membrane potential, on the activities of the external solutions and on the mobility of the two ion types. Efficiency will increase with increasing membrane potential, but will either increase or decrease with changes in the ratio of external solution activity, that is will increase when the diluting solution ($a_d > a_c$), and decrease when the concentrating solution is the more concentrated ($a_c > a_d$). This is in agreement with the experimental results.

The ion exchange membrane potential is manifest only in its permselective effect, but cannot be measured directly.

For the description of the ion exchange membrane potential the Nernst equation may be used:

$$U_m = \frac{RTe}{Fz} \ln \frac{\bar{a}}{\frac{a_d + a_c}{2}}$$

where $\bar{a}$ refers to the inside of the membrane and is *per definitionem* the activity required for the description of the quantitative conditions.

After substituting the ion exchange membrane potential U_m to Eq. (11) the internal activity of the membrane $\bar{a}$ can be calculated:

$$\frac{\bar{a}}{\frac{a_c + a_d}{2}} = \frac{1}{2}\left(1 + \frac{\mu_+ c_c(1-\eta)}{\mu_- c_d(1+\eta)}\right) + \sqrt{\frac{1}{4}\left(1 + \frac{\mu_+ c_c(1-\eta)}{\mu_- c_d(1+\eta)}\right)^2 - \frac{a_c c_c \mu_+ (1-\eta)}{a_d c_d \mu_- (1+\eta)}} \tag{13}$$

Thus the internal activity of the membrane depends on the external solution activities, on the ion mobilities and the current efficiency of electrodialysis and can be determined from these data.*

Experimental results

The experiments were carried out with a nine-cell ion exchange membrane cell sequence (Fig. 2.).

Fig. 3 shows the correlations calculated from the data of potassium chloride electrodialysis. Current efficiency was measured during electrodialysis with various diluting and concentrating solutions. Internal activity was calculated from the correlations derived above and were plotted *vs.* the average of external activities. If the diluting and the concentrating solutions had the same activity, then internal activity *vs.* external one gave the middle

*Experiments concerning the average value nature of U_m are in progress.

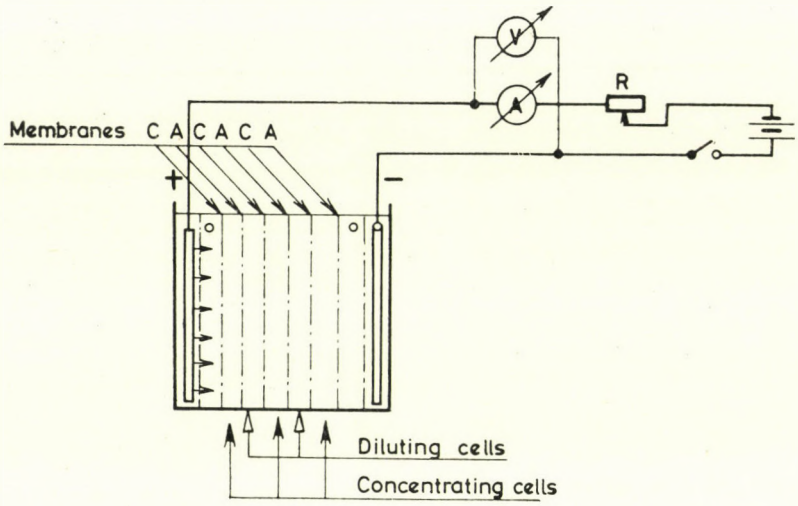

Fig. 2

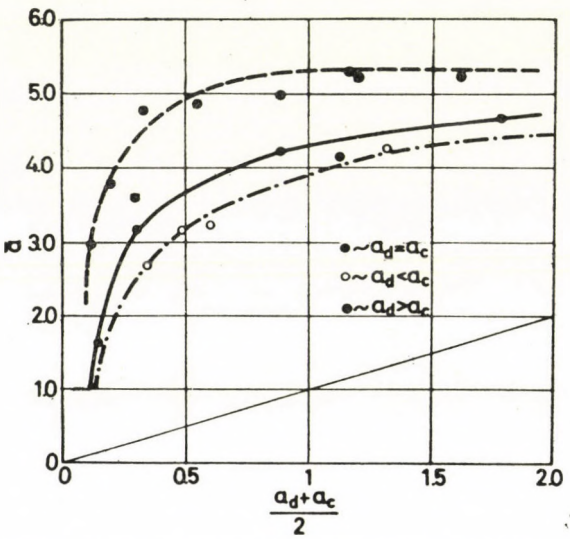

Fig. 3. Internal activity (*a*) *vs.* the activity of the external solution in case of KCl solution

curve (fully drawn). On the curve below it are the measuring points for the case when the concentration of the diluting solution is lower than that of the concentrating solution, while on the upper curve are the experimentally determined points for the case when the concentration of the diluting solution is higher than that of the concentrating solution.

It appears from the curves that with increasing external activities the internal activity will also increase, that it will approach a limit value characteristic of the membrane. For the investigated membranes in potassium chloride solutions this limit value is $\bar{a} = 5 \pm 0.4$. The points represent values calculated from the average concentration changes during a 2-hour electrodialysis process, therefore the middle curve has a somewhat lower position due to the

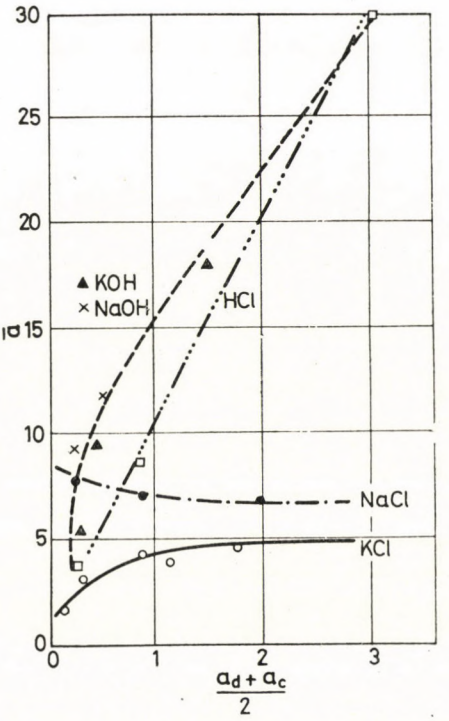

Fig. 4. Internal activity (a) *vs.* the activity of the external solution in case of various electrolytes

dilution of the diluting solution and the concentration of the concentrating solution in the course of the experiment compared to the initial $a_c = a_d$ condition.

Electrodialyses were performed with other electrolytes too, the results are summarized in Fig. 4.

In the case of salt solutions the curve approaches the above discussed limit value which changes with the ratio of ion mobilities. This latter phenomenon may be explained by the influence of the diffusion potentials, arising from the different mobilities of the ions, on the ion exchange membrane potential.

A different behaviour was observed in the range under investigation in the case of hydroxyl and hydrogen ions. With increasing external concentra-

tion the internal activity describes a monotonously rising curve which may be explained by the superimposition of several phenomena.

The first phenomenon to be mentioned in this respect is the very high mobilities of the H^+ and OH^- ions which because of their high transference number are manifest in the current efficiency. On the other hand, the selectivity of ion exchange membranes excludes these ions to a small degree, so that the internal ion composition of the membranes is significantly shifted in favour of the H^+ and OH^- ions, respectively.

Last but not least the fact should also be mentioned that the measuring results are based on the resultant permselectivity of cation exchange and anion exchange membrane pairs (complete electrodialysis cell).

Thus the resulting efficiency is the average of a very high permselectivity (*e.g.* sodium hydroxide on anion exchange membrane) and of a very low permselectivity (the same on cation exchange membrane).

Presumably, the acidic and alkaline cells cannot be considered a straightforward Donnan system.

Conclusions

Summing up the aforesaid it appears that the quantity of electrolyte in the membrane phase is composed of two parts: the fixed ions and their counter-ion partners form the unchanged ion quantity, and the co-ions diffusing from the external solution with the corresponding quantity of counter-ions represent the varying concentration term. The latter quantity depends on the external electrolyte concentration not only because of the diffusing electrolyte quantity, but under the conditions of electrodialysis also because of the change of the interfacial ion layer.

The concept of internal activity is necessary for the description of the membrane phase as a solution in which the motion of the ions can be evaluated from the known correlations.

The electrodialysing cell may be further approximated by a solution pair divided by a third electrolyte space with given ion concentration and bordered in first approximation by a mathematical plane. This internal space has Donnan nature in so far that one ion type is fixed (unable to leave its position) while it has freely moving counter-ions. This is accompanied by a complementary ion quantity depending on the external solution. Diffusion conditions are controlled by the ion layer on the interface (here again concentrated to a mathematic plane) through which the ions have to penetrate during their motion.

Thus the motion controlling potential comes from a driving and an inhibiting component where the driving components are both the external field strength and the diffusion potential, the inhibiting component is, on the

other hand, the ion exchange membrane potential. Though these factors are correlated, the correlation is not linear because of the effect of the internal fixed-ion quantity. It was attempted to bring into accord this physical picture with the relationship between the measurable conditions and the known solution laws.

Symbols

$\bar{a}$	internal activity of the ion exchange membrane
a_c	activity of the concentrating solution
a_d	activity of the diluting solution
c_c	concentration of the concentrating solution
c_d	concentration of the diluting solution
e	unit charge (4.8×10^{-10} e.u.)
E	external field strength (V)
F	Faraday number
i_+	current fraction transported by the positively charged ions
i_-	current fraction transported by the negatively charged ions
k	Boltzmann constant
n	number of mobile ions per unit volume
P_c	permselectivity of the cation exchange membrane
P_a	permselectivity of the anion exchange membrane
q	cross-section
R	universal gas constant
t_a	transport number of the anion
t_c	transport number of the cation
T	absolute temperature
U	activation energy (eV); height of the potential well
U_m	ion exchange membrane potential (eV)
U_N	concentration potential difference due to the different concentrations of the solutions on the two sides of the membrane (eV)
V_+	average velocity of cations
V_-	average velocity of anions
z	valency of the ions
δ	width of the potential well
τ_0	residence time in the potential well
μ_-	anion mobility
μ_+	cation mobility
η	current efficiency

REFERENCES

1. WEINER, S. A.: Ind. Engng. Chem. Proc. Res. Devl. **4**/4, 349 (1965)
2. RICKELS, R. N., FRIEDLANDER, H. Z.: Chem. Eng. **28**/3, 121 (1966)
3. SIPOS, J., MIKES, J.: Hungarian Chemical Congress, Debrecen, 1961
4. KÁLMÁN, I., SIPOS, J.: Ion Exchange Symposium, Balatonszéplak, 1963. Akadémiai Kiadó, Budapest, 1965 p. 57.
5. SIPOS, J., KÁLMÁN, I., MIKES, J. A.: Ion Exchange Symposium, Balatonszéplak, 1963. Akad. Kiadó, Budapest, 1965 p. 71.
6. MIKES, J. A., SIPOS, J., KÁLMÁN, I.: Hungarian Chemical Congress, Pécs, 1964
7. MIKES, J. A., SIPOS, J., KÁLMÁN, I.: IUPAC International Symposium on Macromolecular Chemistry, Prague, 1965. Preprint 384
8. KÁLMÁN, I., SIPOS, J., MIKES, J. A.: XXXVth International Congress of Industrial Chemistry Warsaw, 1964. Chimie et Industrie, 1964, Sept.
9. KÁLMÁN, I., SIPOS, J., MIKES, J. A.: Chem. Techn. **18**/7, 411 (1966)

Judit H. SIPOS
Iván KÁLMÁN
János MIKES
Budapest XIV., Hungária krt. 114.

Acta Chimica Academiae Scientiarum Hungaricae, Tomus 62 (2), pp. 151—156 (1969)

INVESTIGATIONS ON ION EXCHANGE EQUILIBRIA WITH RADIOACTIVE TRACER METHOD, XVI

DETERMINATION OF THE STABILITY CONSTANTS OF NEGATIVELY CHARGED ZINC CHLORIDE COMPLEXES WITH THE AID OF LIQUID ANION EXCHANGER

T. LENGYEL and J. TÖRKŐ

(Institute of Isotopes, Hungarian Academy of Sciences, Budapest)

Received July 1, 1968

Using liquid anion exchanger Amberlite LA-2, the formation constants of negatively charged chloro-complexes of zinc were determined. For the treatment of experimental data a new graphic method was developed. The constants $\lg K_3 = -0.30$ and $\lg K_4 = -0.07$ seem to be reliable though the comparison with literature data is rather difficult as the values published previously show a large scattering.

Introduction

Ion exchange technique has found wide-spread application in the study of complex formation between a charged central ion and a ligand of opposite charge. However, these investigations were directed first of all to cationic and neutral species, using cation exchangers.

In superficial appearance, the study of negatively charged complexes may be performed likewise with the aid of anion exchangers. Nevertheless, this procedure encounters serious difficulties which can be summarized as follows:

(a) Beside anionic complexes both the ligand and the anions present are bound in the resin (or organic) phase;

(b) Since no constant ionic strength can be set, the activity coefficients in the aqueous phase vary with the ligand concentration;

(c) When applying high ligand concentration in order to promote the formation of anionic complexes the so called "electrolyte invasion effect" may disturb distribution measurements, at least when resin-type exchanger is used;

(d) The activity coefficient in the exchanger cannot be considered constant, unless the concentration of the central ion is maintained extremely low and the ion exchanger is presaturated with the ligand.

These discrepancies may be eliminated if liquid anion exchangers presaturated with the corresponding ligand are used, the activity coefficient in the aqueous phase can be taken into account and radioactive tracer technique enabling the measurement of the central ion also in micro-concentrations is applied.

FRONAEUS [1] and MARCUS [2] were the first who attempted the calculation of stability constants based on distribution measurements, using ion exchange technique. Because of the difficulties raised by the resin-type exchanger, their treatment of experimental data is rather cumbersome and not relieved of inaccurate approximations.

ALLEN, and later on several authors [3—6] succeeded in using liquid anion exchangers for the investigation of complex species. This experimental technique has proved to be reliable but the calculation methods are still not definitively developed.

In this paper a graphic way of determining the stability constants of zinc-chlorocomplexes is presented, appearing to be simple and of considerable precision.

Theoretical

Let us take a divalent metal ion with a maximum coordination number $N = 4$ into consideration. The anionic complexes formed with a monodentate ligand will react with the ion exchanger presaturated with the corresponding ligand according to Eqs (1) and (2):

$$ {}_w[ML_3] + {}_o[RL] = {}_o[RML_3] + {}_w[L] \tag{1} $$

$$ {}_w[ML_4] + 2{}_o[RL] = {}_o[R_2ML_4] + 2{}_w[L] \tag{2} $$

The corresponding equilibrium constants for the exchange reactions may be written as

$$ K_{3ex} = \frac{{}_o[RML_3]\,{}_w[L]}{{}_w[ML_3]\,{}_o[RL]} \tag{3} $$

$$ K_{4ex} = \frac{{}_o[R_2ML_4]\,{}_w[L]^2}{{}_w[ML_4]\,{}_o[RL]^2} \tag{4} $$

In the region of ligand concentration where the existence of the cationic species $[M^{2+}]$ and $[ML^+]$ may be neglected, the distribution ratio referring to the partition of the central ion between the organic and aqueous phases can be defined as

$$ D = \frac{{}_o[RML] + {}_w[R_2ML_4]}{{}_w[ML_2] + {}_w[ML_3] + {}_w[ML_4]} \tag{5} $$

Introducing the notations

$$ K^*_{3ex} = K_{3ex}\,{}_o[RL] \tag{6} $$

and

$$ K^*_{4ex} = K_{4ex}\,{}_o[RL]^2 \tag{7} $$

and the corresponding complex formation constants

$$K_3 = \frac{{}_w[ML_3]}{{}_w[ML_2]\,{}_w[L]} \tag{8}$$

and

$$K_4 = \frac{{}_w[ML_4]}{{}_w[ML_3]\,{}_w[L]} \tag{9}$$

Eq. (5) can be rearranged to yield

$$\frac{1}{D} = \frac{1}{K^*_{3ex}K_3 + K^*_{4ex}K_3K_4} + \frac{{}_w[L]}{K^*_{3ex} + K^*_{4ex}K_4} + \frac{K_4\,{}_w[L]^2}{K^*_{3ex} + K^*_{4ex}K_4} \tag{10}$$

From Eq. (10) it is obvious that, in the region of ligand concentration at which the presence of species $[ML_4]$ may be neglected, a plot of 1/D *vs.* ligand activity $\{L\}$ (ligand concentration corrected with the activity coefficient) yields a straight line; the ratio of the slope s and intercept i of the linear section gives the value of K_3.

Consequently, at higher ligand activities where the presence of $[ML_4]$ is also to be taken into account, by plotting

$$\frac{\frac{1}{D} - i}{\{L\}} \text{ vs. } \{L\}$$

also a linear correlation is arrived at; the ratio of the slope s' and intercept i' of this straight line yields K_4.

Experimental

The static equilibrium measurements were carried out at 25 °C.

The determination of the distribution ratio was performed by radiometric assay of the zinc concentration in both phases. ^{65}Zn tracer of high specific activity enabled to keep the concentration of zinc at 5×10^{-6} *M*.

Amberlite LA-2 (molecular weight 374) diluted with toluene to 0.1 F concentration in the chloride form was used as liquid anion exchanger.

Chloride concentration was varied by using aliquots of 6 *M* sodium chloride solution. All the solutions were acidified to attain pH = 1.7 in the aqueous phase at equilibrium.

Results and discussion

The results of equilibrium measurements are summarized in Table I.

In the course of calculating ligand activities the activity coefficients were obtained from literature data [7].

Starting out from the experimental data Figs 1 and 2 were constructed, yielding the values $K_3 = 0.50$ and $K_4 = 0.86$. The formation constants are compared with literature data in Table II.

Table I

Distribution ratio as a function of ligand activity in the zinc chloride system

$[Zn] = 5 \times 10^{-8} M$ $[LA\text{-}2] = 0.1$ F pH ≈ 1.70

{Cl⁻}	1/D	{Cl⁻}	1/D
0.501	1.408	2.751	0.443
0.660	0.902	2.847	0.439
0.827	0.633	2.970	0.472
1.258	0.445	3.081	0.452
1.720	0.382	3.350	0.477
1.899	0.365	3.475	0.491
2.100	0.386	3.610	0.542
2.198	0.380	3.759	0.553
2.410	0.401	3.900	0.591
2.507	0.409	4.202	0.642
2.628	0.430	4.498	0.706

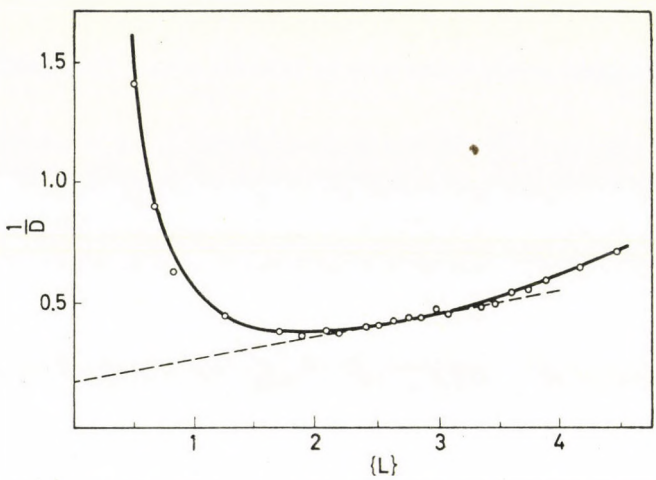

Fig. 1. 1/D as a function of ligand activity for the system zinc chloride $[Zn] = 5 \times 10^{-6} M$, $[LA\text{-}2] = 0.1$ F, pH ≈ 1.70

The considerable deviations may be due to the fact that measurements of weak complexes at high ionic strengths meet difficulties in ensuring reproducible experimental conditions.

It is to be mentioned, however, that most of the results quoted were originally obtained as overall formation constants, *i.e.* as β_l values and therefore the errors in determining stepwise formation constants were cumulated.

Anyhow, the lg K_3 value presented in this paper represents about the mean of the data published and the lg K_4 value is also in the same range when the data extremely deviating from the average are neglected.

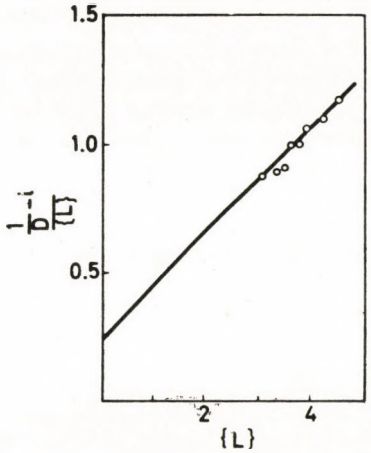

Fig. 2. $\frac{\frac{1}{D} - i}{\{L\}}$ as a function of ligand activity for the system zinc chloride

$[Zn] = 5 \times 10^{-6} M$, [LA-2] = 0.1 F, pH $\approx$ 1.70

Table II

Formation constants of species $[ZnCl_3]$ *and* $[ZnCl_4]$

lg K_3	lg K_4	Method of determination	Reference
—0.25	0.15	emf titration	[8]
—0.09	—	polarography	[9]
—0.68	0.37	cation exchange	[10]
—0.28	—0.13	anion exchange	[11]
—1.58	—0.12	liquid anion exchange	[12]
—0.65	—0.25	liquid anion exchange	[13]
—0.30	—0.07	liquid anion exchange	this work

*

The authors' thanks are due to Mr. Gy. Tóth for his valuable help in performing the measurements.

REFERENCES

1. Fronaeus, S.: Svensk. Kem. Tidskr. **61,** 1 (1953)
2. Marcus, Y., Coryell, C. D.: Bull. Res. Counc. Israel **A8,** 1 (1959)
3. Allen, K. A.: J. Phys. Chem. **60,** 943 (1956)
4. Allen, K. A.: J. Am. Chem. Soc. **80,** 4133 (1958)
5. Bryan, S. E., Good, M. L.: J. Inorg. Nucl. Chem. **21,** 339 (1961)
6. Allen, K. A., McDowell, W. J.: J. Phys. Chem. **67,** 1138 (1963)
7. Robinson, R. A., Stokes, R. H.: Electrolyte Solutions. Butterworth Sci. Publ., London, 1962

8. SHCHUKAREV, S. A., LILICH, L. S., LATYSHEVA, V. A.: Zhurn. Neorg. Khim. **1**, 225 (1956)
9. KIVALO, P., LUOTO, R.: Suomen Kem. **30B**, 163 (1957)
10. SHORT, E. L., MORRIS, D. F. C.: J. Inorg. Nucl. Chem. **18**, 192 (1961)
11. MARCUS, Y., MAYDAN, D.: J. Phys. Chem. **67**, 979 (1963)
12. SCIBONA, B., ORLANDINI, F., DANESI, P. R.: J. Inorg. Nucl. Chem. **28**, 1313 (1966)
13. DYRSSEN, D., DE JESUS TAVARES, M.: Proc. of the Internat. Conf. on Solvent Extraction Chemistry, p. 465. North-Holland Publ. Co., Amsterdam, 1967

Tamás LENGYEL
János TÖRKŐ
Budapest XII., Konkoly Thege M. út

Acta Chimica Academiae Scientiarum Hungaricae, Tomus 62 (2), pp. 157—162 (1969)

ANWENDUNG DES POTENTIOSTATS ZUR BESTIMMUNG DES MAXIMALEN KORROSIONSSTROMS VON GALVANISCHEN ELEMENTEN, I

J. DÉVAY, B. LENGYEL jun. und L. MÉSZÁROS

(Lehrstuhl für Physikalische Chemie, Chemisch-technische Universität, Veszprém; Elektrochemische Forschungsgruppe der Ungarischen Akademie der Wissenschaften)

Eingegangen am 5. Oktober 1968

Der maximale Korrosionsstrom von verschiedenen galvanischen Elementen wurde potentiostatisch gemessen und die Richtigkeit der Meßmethode durch vergleichende Messungen (Evans-Diagramm bzw. Messung der zeitlichen Änderung des Korrosionsstroms mit Strommesser) bestätigt. Es wurde festgestellt, daß der Potentiostat bei entsprechender Schaltung zur Messung des maximalen Korrosionsstroms geeignet ist. Der Vorteil des Verfahrens gegenüber den älteren Verfahren liegt darin, daß selbst bei galvanischen Elementen mit niedrigem innerem Widerstand der Wert des maximalen Korrosionsstroms und dessen zeitlicher Verlauf unmittelbar gemessen wird, und die aus der Extrapolierung stammenden Fehlermöglichkeiten ausgeschaltet werden.

Potentiostatische Verfahren wurden weitgehend in der Korrosionsforschung zur Untersuchung des Passivierungsmechanismus von Eisen [1—4], Stahl [5] und anderen Metallen [6—8] in verschiedenen Lösungen, zum Nachweis der Neigung nichtrostender Stähle zur interkristallinen Korrosion [9—10] und zur Untersuchung der Lochkorrosion [11—13], eingesetzt. Neben diesen Gebieten, wo potentiostatische Methoden ausgedehnt verwendet werden, wurden verschiedene Versuche unternommen, um das Anwendungsgebiet des Potentiostats auch auf andere Erscheinungen auszudehnen. So wurde u.a. der Widerstand gegenüber Spannungskorrosion bei Aluminium-Magnesium-Legierungen [14] und die Vorausbestimmung der Korrosionseigenschaften von Magnesium [15] untersucht. Auch die Wirkung verschiedener Inhibitoren [16] wurde potentiostatisch untersucht.

In der vorliegenden Arbeit wird über ein neues Anwendungsgebiet des Potentiostaten und zwar über seine Anwendung zur Messung des maximalen Korrosionsstroms von galvanischen Elementen (Modellen von Lokalelementen) berichtet.

Der maximale Korrosionsstrom wurde bis jetzt durch Konstruktion eines Evans-Diagramms aus den Polarisationskurven des Metallpaars, welches das galvanische Element bildet, bestimmt. Dieses Verfahren besteht im wesentlichen darin, die anodische Polarisationskurve des Anodenmetalls und die kathodische Polarisationskurve des Kathodenmetalls in einem gemeinsamen Diagramm darzustellen, wobei die Stromstärke als Abszisse, das Potential als Ordinate aufgetragen wird. Der maximale Korrosionsstrom ergibt sich als Schnittpunkt der graphisch extrapolierten anodischen und kathodischen

Polarisationskurven, da in diesem Punkt der Potentialunterschied zwischen der Kathode und der Anode verschwindet. Nach einem anderen bekannten Verfahren [17] wird die Kurzschlußstromstärke des Elements und ihre zeitliche Änderung gemessen. Bei der Anwendung der genannten Verfahren ergeben sich folgende Fehler bzw. Schwierigkeiten:

— Beim Evans-Diagramm wird die zeitliche Änderung der Korrosion nicht erfaßt; die Konstruktion des Diagramms ist zeitraubend und die graphische Extrapolierung führt zu relativ hohen Fehlermöglichkeiten.

— Beim Messen der Kurzschlußstromstärke wird nicht der maximale Korrosionsstrom erhalten, besonders dann, wenn der innere Widerstand des Meßinstrumentes im Vergleich zum inneren Widerstand des galvanischen Elementes nicht vernachlässigbar ist.

Durch Anwendung der potentiostatischen Meßmethode können diese Nachteile beseitigt werden. In der Meßanordnung mit drei Elektroden (Kathode, Anode und Bezugselektrode) wird die Prüfelektrode durch den Potentiostaten mit Hilfe eines elektromechanischen oder elektronischen Systems relativ zur Bezugselektrode auf einem gewünschten Potential gehalten und zwar so, daß der Unterschied der Ist-Spannung zwischen Bezugselektrode und Prüfelektrode und der eingestellten Soll-Spannung als Stellwert verwendet und dadurch die Klemmenspannung der Stromquelle bzw. die Stromstärke des Gleichstroms zwischen Kathode und Anode proportional zum Stellwert solange geändert wird, bis letzterer annähernd gleich Null ist. Der Potentiostat stabilisiert also den Potentialunterschied zwischen Bezugselektrode und Prüfelektrode bzw. hält ihn auf dem gewünschten Wert.

Wird nun als Bezugselektrode die Gegenelektrode, d. h. die Kathode bzw. Anode der Elektrolyse verwendet, so, je nach dem, ob die Anode oder die Kathode als Prüfelektrode an den Potentiostat bei Spannungssteuerung gleich Null wie ein Instrument, dessen innerer Widerstand gleich Null ist. In diesem Fall werden nämlich — unabhängig vom durchfließenden Strom — die beiden Elektroden des galvanischen Elements durch den Potentiostaten kurzgeschlossen, d. h. die Klemmenspannung des galvanischen Elements wird beim Wert Null gehalten. Dies ist aber eben die Grundbedingung für den Schnittpunkt im Evans-Diagramm.

Nach diesem Verfahren kann also der dem Evans-Diagramm entsprechende Korrosionsstrom, d. h. der maximale Korrosionsstrom des galvanischen Elements auf verhältnismäßig einfache Art unmittelbar gemessen und zugleich seine zeitliche Änderung verfolgt werden.

Es wurden Versuche mit galvanischen Elementen aus Zink-Eisen, Zink-Kupfer und Eisen-Kupfer durchgeführt. Die Elektroden, deren Oberfläche 10 cm^2 betrug und die mit Epoxydharz in Glasröhren befestigt waren, tauchten bei Zimmertemperatur in eine 5%ige KCl-Lösung. Vor den Messungen wurden die Elektroden mit Schleifpapier gereinigt, die Zn- und Fe-Elektroden in 0.1 *n*

HCl, die Cu-Elektroden in 0.1 *n* HNO_3 5 Minuten lang geätzt, anschließend mit dest. Wasser gespült und sofort verwendet. Die eine Elektrode wurde an den Prüfelektrodeneingang, die andere an den Gegenelektrodeneingang des Potentiostaten angeschlossen. Gegenelektrodeneingang und Bezugselektrodeneingang des Potentiostaten wurden kurzgeschlossen, d. h. die Gegenelektrode wurde als Bezugselektrode verwendet.

Vor Beginn der Arbeit wurde die am Potentiostaten eingestellte Nullspannung durch ein Gleichstromröhrenvoltmeter mit hohem Eingangswiderstand kontrolliert. Die zeitliche Veränderung des Korrosionsstroms wurde

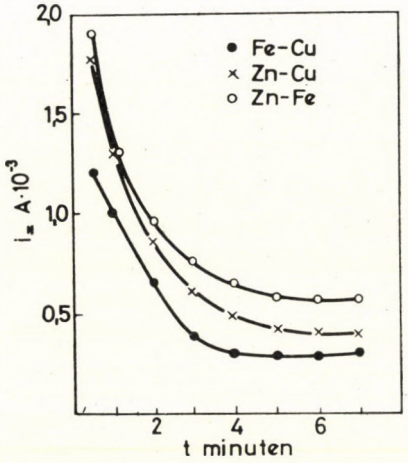

Abb. 1. Änderung des maximalen Korrosionsstroms als Funktion der Zeit bei den galvanischen Elementen Fe—Cu, Zn—Cu und Zn—Fe, potentiostatisch gemessen

mit einem Gleichstromregistrierinstrument registriert, welches mit dem Ausgangsstromkreis des Potentiostaten in Reihe geschaltet war.

Die Meßergebnisse der maximalen Korrosionsströme und ihrer zeitlichen Änderung bei den geprüften galvanischen Elementen sind in Abb. 1 dargestellt. Bei sämtlichen Elementen zeigt sich eine zeitliche Änderung des maximalen Korrosionsstroms.

Um die Richtigkeit des Verfahrens zu prüfen, wurden Vergleichsversuche durchgeführt, in dem die Elektroden des galvanischen Elements über Strommesser mit verschiedenen inneren Widerständen (10 Ω, 100 Ω, 1000 Ω) kurzgeschlossen und die Werte der Korrosionsströme gemessen wurden. Da aus Abb. 1 festgestellt werden konnte, daß der Korrosionsstrom nach 5 Minuten einen konstanten Wert erreicht, wurden sämtliche Ablesungen jeweils nach 5 Minuten durchgeführt. Die Meßergebnisse sind in Abb. 2 gezeigt. Der durch den Strommesser fließende Strom wurde als Abszisse, die über dem Widerstand des Strommessers auftretende Spannung als Ordinate dargestellt. Die

erhaltenen Meßpunkte wurden miteinander verbunden und auf den Widerstandswert Null extrapoliert, wodurch der maximale Korrosionsstrom erhalten wurde. Die Extrapolierung ist jedoch unsicher, da die Kurven nicht linear sind.

Der Wert des maximalen Korrosionsstroms bei den untersuchten galvanischen Elementen wurde auch mit Hilfe des Evans-Diagramms bestimmt. Dazu wurden die anodischen Polarisationskurven der Anoden und die katho-

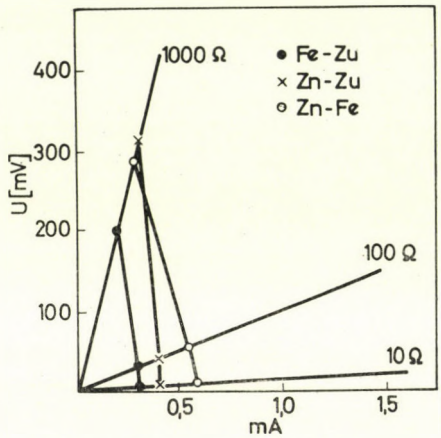

Abb. 2. Messung des maximalen Korrosionsstroms der galvanischen Elemente Fe—Cu, Zn—Cu, Zn—Fe bei Belastung mit verschiedenen Widerständen

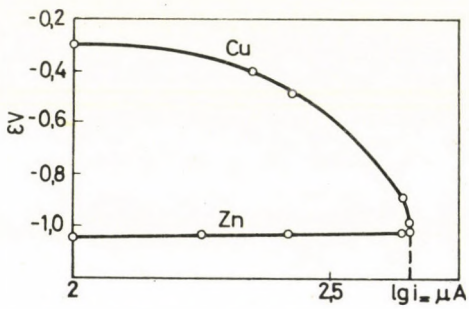

Abb. 3. Evans-Diagramm des galvanischen Elements Zn—Cu

dischen Polarisationskurven der Kathoden gegenüber einer 0.1 *n* Kalomelelektrode als Bezugselektrode aufgenommen und im Evans-Diagramm dargestellt. Der maximale Korrosionsstrom wurde durch den Schnittpunkt der extrapolierten Kurven angezeigt. Auch in diesen Versuchen wurden jeweils nach 5 Minuten Ablesungen durchgeführt. In Abb. 3—5 sind die gemessenen Werte der Elektrodenpotentiale als Funktion des Logarithmus der Stromstärke des polarisierenden Gleichstroms aufgetragen.

Tabelle I

Vergleich der mit verschiedenen Verfahren gemessenen Werte der maximalen Korrosionsströme

Meßverfahren	Korrosionsstrom Zn—Fe	(μA) in den Lokalelementen	
		Zn—Cu	Fe—Cu
Potentiostat	$5{,}6 \cdot 10^2$	$4{,}0 \cdot 10^2$	$2{,}8 \cdot 10^2$
Kurzgeschlossen über Widerstände	$5{,}8 \cdot 10^2$	$4{,}1 \cdot 10^2$	$3{,}1 \cdot 10^2$
Evans-Diagramm	$5{,}2 \cdot 10^2$	$4{,}5 \cdot 10^2$	$3{,}2 \cdot 10^2$

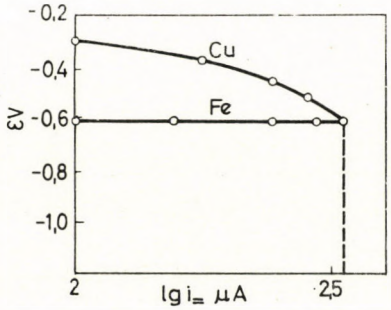

Abb. 4. Evans-Diagramm des galvanischen Elements Fe—Cu

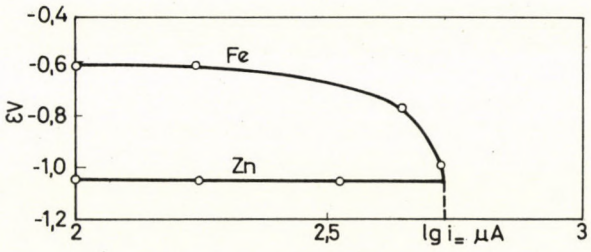

Abb. 5. Evans-Diagramm des galvanischen Elements Zn—Fe

Die nach drei verschiedenen Meßverfahren ermittelten Werte der maximalen Korrosionsströme in den untersuchten galvanischen Elementen sind in Tab. I zusammengefaßt.

Aus den Angaben ist ersichtlich, daß zwischen den mit dem potentiostatischen Verfahren erhaltenen Ergebnissen und den Ergebnissen der vergleichsweise angewandten Verfahren eine gute Übereinstimmung innerhalb des Meßfehlers vorhanden ist. Der Potentiostat kann also vorteilhaft und ohne die Fehlerquellen der früheren Meßverfahren zur unmittelbaren Messung der

maximalen Korrosionsströme in galvanischen Elementen und zur Bestimmung der zeitlichen Änderung dieser Ströme verwendet werden.

LITERATUR

1. VENU, K., BALAKRISHNAN, K., RAJAGOPOLAN, K. S.: Corr. Science **5,** 59 (1965)
2. NAGAYAMA, M., OKAMOTO, G.: Corr. Science **2,** 203 (1962)
3. FREIMAN, L. I., KOLOTYRKIN, YA. M.: Corr. Science **5,** 199 (1965)
4. KASHCHEEV, V. C., KABANOV, V. M., LAIKIS, B. I.: Corrosion **20,** 54 (1964)
5. BORTON, K. und SCHEIR, L. L.: Corr. Science **3,** 17 (1963)
6. SEASTROM, C. C.: Corrosion **20,** 179 (1964)
7. ARNOLD, K., VETTER, K. J.: Z. Elektrochem. **64,** 407 (1960)
8. POZDEEVA, A. A.: Corr. Science **6,** 149 (1966)
9. YOUNGER, R. N., BAKER, R. G., LITTLEWOOD, R.: Corr. Science **2,** 157 (1962)
10. CINMAN, A. I. und KUZUB, V. S.: Zh. fiz. himii **39,** 2020 (1965)
11. SCHWENK, W.: Corrosion **20,** 129 (1964)
12. ROZENFELD, I. L., DANILOV, I. S.: Saschchita metallow **1966,** No. 2, 134
13. GREENE, N. D., JUDD, G.: Corrosion **21,** 15 (1965)
14. BOOTH, F. F., TUCKER, G. E. G.: Corrosion **21,** 173 (1965)
15. CORIOU, H.: Bulletin d'Informations Scientifiques et Techniques du Commissariat à l'Energie Atomique No. 84 (1964)
16. ROZENFELD, I. L., PERSIANTSEVA, B. P., TERENTEV, P. B.: Corrosion **20,** 22 (1964)
17. AKIMOV, G. V.: Fémek korróziójának elmélete és vizsgálatának módszerei (ungarisch) (Theorie und Untersuchungsmethoden der Korrosion von Metallen), Nehézipari Könyv- és Folyóiratkiadó, Budapest, 1951

József DÉVAY
Béla LENGYEL jun.
Lajos MÉSZÁROS
Veszprém, Schönherz Z. u. 12. Ungarn

Acta Chimica Academiae Scientiarum Hungaricae, Tomus 62 (2), pp. 163—178 (1969)

SYNTHESIS OF NEW BENZO(a)QUINOLIZINE DERIVATIVES, I

P. Bite, E. Diszler, M. Fekete, Á. Villányi and M. Kürti

(Research Institute for Pharmaceutical Chemistry, Budapest)

Received March 18, 1968

For a more thorough study of the pharmacological properties of compounds containing the benzo(a)quinolizine skeleton, a number of oxime esters and acid amides, and several ether and amine derivatives have been synthesized, using the 2-oxy-imino and the 2-amino compounds as starting materials.

Among the derivatives of 1,2,3,4,6,7-hexahydro-11bH-benzo(a)quinolizine, several compounds have been shown to possess valuable pharmacological properties [1], but no mention has been made in the literature of the synthesis and study of a number of types of these compounds that also promise to be effective.

Earlier, one of the authors [2, 3] described a new and very simple method for the preparation of benzo(a)quinolizine derivatives (**I**). Owing to the yield shown in Table I, the preparation of several types of pharmacologically interesting derivatives has become feasible.

For the first type of compounds to be prepared, oxime esters (**IV**) were chosen, using mainly such acids for esterification which have been found to figure in pharmacologically active compounds. The oxime esters [4] prepared according to methods A, B, C, and D, respectively, are listed in Table IV. The new intermediary ketones (**II**) and oximes (**III**), not yet reported in the literature, are shown in Tables II, and III, respectively.

Reduction with lithium aluminium hydride of the oximes gave the corresponding 2-amino compounds, and from these the acid amides were prepared. The amides (**V**) synthesized according to various methods [5] are listed in Table V.

Some of our 2-amino-, and 2-hydroxyimino compounds were also made to react with 2,4-dinitrofluorobenzene and with phenylisocyanate, and some amines were treated with ethyl cyanoacetate, ethyl chloroformate, and ethylene bromohydrin.

The formation of oxime esters and of acid amides was followed, and the homogeneity of the products checked, by TLC using silica gel plates.

The results of the pharmacological study of these compounds will be published elsewhere.

Experimental

(All m.p.'s are uncorrected)

Thin-layer chromatography

Prior to use, the plates were coated with Silica Gel G, and dried at 120 °C for 10 min. Development was carried out in a solvent mixture of 39 ml of chloroform and 1 ml of methanol. For detection, a 0.5% solution of iodine in chloroform was used.

Preparation of the parent ketones

9,10-Dimethoxy- and 9,10-diethoxy-2-oxo-3-alkyl-1,2,3,4,6,7-hexahydro-11bH-benzo(a)-quinolizine were prepared according to [3], from 6,7-dimethoxy-3,4-dihydroisoquinoline hydrochloride containing 3.5 moles of water of crystallization, and 6,7-diethoxy-3,4-dihydro-isoquinoline hydrochloride, respectively.

Table I

Yields of the parent ketones

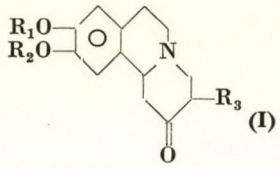

(I)

$R_1 = R_2$	R_3	M. p., °C	Yield %
CH_3	H	150—151	36—38
CH_3	CH_3	139—140	55—57
CH_3	C_2H_5	112—113	60—62
CH_3	n-C_4H_9	113—114	74—75
CH_3	i-C_4H_9	126—128	70—72
C_2H_5	C_2H_5	116—118	68—70
C_2H_5	i-C_4H_9	105—107	60—62

It is more advantageous to prepare 9,10-di-*n*-butoxy- and 9,10-dibenzyloxy-2-oxo-3-iso-butyl-1,2,3,4,6,7-hexahydro-11bH-benzo(a)quinolizine compounds by the alkylation, respectively by aralkylation of the corresponding 9,10-dihydroxy compounds.

2-Oxo-3-isobutyl-9,10-di-n-butoxy-1,2,3,4,6,7-hexahydro-11bH-benzo(a)quinolizine

A solution of 2-oxo-3-isobutyl-9,10-dihydroxy-1,2,3,4,6,7-hexahydro-11bH-benzo(a)-quinolizine (8.67 g; 0.03 mole) in acetone (200 ml) was mixed with *n*-butyl bromide (16.44 g; 0.12 mole) and anhydrous potassium carbonate (20 g), and the mixture was stirred and refluxed for 48 hrs. After cooling, the mixture was filtered, the solvent evaporated, and the residue recrystallized from acetone to yield 2.6 g of the product, m.p. 70—73 °C.

Preparation of oximes

General method. The ketone (0.1 mole) was dissolved in hot ethanol (100 ml) and hydroxylamine sulphate (0.052 mole) in water (60 ml) was added, then the solution was made alkaline by the addition of sodium hydroxide (0.11 mole) in water (5 ml). A precipitate formed immediately. The mixture was boiled for 5 min. on a water bath, allowed to cool, and let to stand in a refrigerator overnight. Filtration and washing with 80% ethanol gave the product in 98—100% yield.

Table II

New ketones

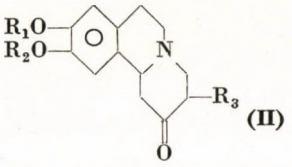

(II)

$R_1 = R_2$	R_3	M. p., °C (Base-HCl)	Empirical formula (Mol. weight)	Analysis of the base, %		
				C	H	N
C_2H_5	i-C_4H_9	105—107	$C_{21}H_{31}NO_3$	73.04*	8.98 *	4.06*
			345	72.86**	8.72**	4.26**
n-C_4H_9	i-C_4H_9	70— 73	$C_{25}H_{39}NO_3$	74.81	9.72	3.49
			401	74.77	10.02	3.48
Benzyl	i-C_4H_9	118—120	$C_{31}H_{35}NO_3$	79.31	7.46	2.98
		(207—209)	469	79.43	7.45	2.99
Benzoyl	i-C_4H_9	121—123	$C_{31}H_{31}NO_5$	74.86	6.23	2.81
		(214—216)	497	74.68	6.25	2.83

*Calcd. **Found.

Table III

New oximes

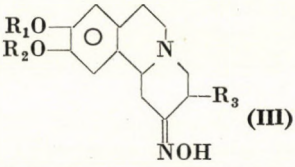

(III)

$R_1 = R_2$	R_3	M. p., °C (Base–HCl)	Empirical formula (Mol. weight)	Analysis of the base, %		
				C	H	N
C_2H_5	C_2H_5	138—140	$C_{19}H_{28}N_2O_3$	68.67	8.43	8.43
			332	69.13	8.64	8.64
C_2H_5	i-C_4H_9	162—164	$C_{21}H_{32}N_2O_3$	70.00	8.88	7.77
			360	69.83	9.03	7.76
n-C_4H_9	i-C_4H_9	179	$C_{25}H_{40}N_2O_3$	72.11	9.61	6.73
			416	72.31	9.31	6.67
Benzyl	i-C_4H_9	166—167	$C_{31}H_{36}N_2O_3$	76.86	7.43	5.79
			484	76.51	8.08	5.84
Benzoyl	i-C_4H_9	176—177	$C_{31}H_{32}N_2O_5$	72.65	6.25	5.46
			512	73.19	6.35	5.65

Table IV

New oxime esters

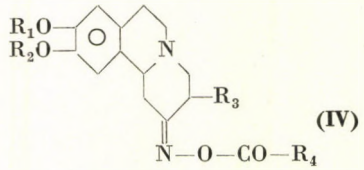

(IV)

$R_1 = R_2$	R_3	R_4	M. p., °C (Base—HCl)	Method	Empirical formula (Mol. weight)	Analysis of the base, %			
						C	H	N	Hal
CH_3	CH_3	C_2H_5	125	C)	$C_{19}H_{26}N_2O_4$ 346	65.89 65.58	7.51 7.69	8.09 8.11	
CH_3	CH_3	2′-nitro-3′,4′,5′-trimethoxyphenyl	166	C)	$C_{26}H_{31}N_3O_9$ 529	58.97 58.94	5.85 6.07	7.93 7.93	
CH_3	C_2H_5	CH_3	95— 96	A)	$C_{19}H_{26}N_2O_4$ 346	65.89 65.91	7.51 7.55	8.09 8.14	
CH_3	C_2H_5	benzyl	113	C)	$C_{25}H_{30}N_2O_4$ 422	71.09 71.23	7.10 7.31	6.63 6.32	
CH_3	C_2H_5	C_6H_5—CH=CH	138—140	A)	$C_{26}H_{30}N_2O_4$ 434	71.88 71.98	6.91 7.04	6.45 6.43	
CH_3	C_2H_5	3′,5′-dibromo-4′-methoxyphenyl	192—194 (175—176)	A)	$C_{25}H_{28}N_2O_5Br_2$ 596	50.33 50.44	4.69 4.70	4.69 4.67	26.8 26.64
CH_3	C_2H_5	3′,4′,5′-trimethoxyphenyl	164	A)	$C_{27}H_{34}N_2O_7$ 498	65.06 65.38	6.82 7.11	5.62 5.64	

CH_3	C_2H_5	pyridin-3'-yl	153	A)	$C_{23}H_{27}N_3O_4$ 409	67.61 67.61	6.82 7.05	10.24 10.28	
CH_3	n-C_4H_9	CH_3	104—105 (195—196)	A)	$C_{21}H_{30}N_2O_4$ 374	67.37 67.41	8.02 8.35	7.48 7.47	
CH_3	n-C_4H_9	C_2H_5	112—114	A)	$C_{22}H_{32}N_2O_4$ 388	68.04 68.16	8.22 8.63	7.21 7.16	
CH_3	n-C_4H_9	3',5'-dichloro-4'-methoxyphenyl	165—166 (178—179)	A)	$C_{27}H_{32}N_2O_5Cl_2$ 535	60.56 60.58	5.98 6.12	5.23 5.32	13.27 13.34
CH_3	n-C_4H_9	3',5'-dibromo-4'-methoxyphenyl	161—163 (183—184)	A)	$C_{27}H_{32}N_2O_5Br_2$ 624	51.92 52.11	5.12 5.22	4.49 4.40	25.64 25.95
CH_3	n-C_4H_9	3',4',5'-trimethoxyphenyl	154	A)	$C_{29}H_{38}N_2O_7$ 526	66.15 66.12	7.22 7.32	5.32 5.38	
CH_3	n-C_4H_9	pyridin-3'-yl	142	A)	$C_{25}H_{31}N_3O_4$ 437	68.65 68.70	7.09 7.46	9.62 9.63	
CH_3	i-C_4H_9	CH_3	99—100 (190—192)	A)	$C_{21}H_{30}N_2O_4$ 374	67.37 67.15	8.02 8.16	7.48 7.61	
CH_3	i-C_4H_9	C_2H_5	100—101	C)	$C_{22}H_{32}N_2O_4$ 388	68.04 67.87	8.22 8.32	7.21 7.29	
CH_3	i-C_4H_9	i-C_4H_9	77	C)	$C_{24}H_{36}N_2O_4$ 416	69.23 68.90	8.65 8.63	6.73 6.74	
CH_3	i-C_4H_9	benzyl	100—102	C)	$C_{27}H_{34}N_2O_4$ 450	72.00 72.14	7.55 7.70	6.22 6.18	
CH_3	i-C_4H_9	$C_6H_5CH=CH$	124—125	C)	$C_{28}H_{34}N_2O_4$ 462	72.72 72.71	7.35 7.57	6.06 6.07	
CH_3	i-C_4H_9	4'-fluorophenyl	132	C)	$C_{26}H_{31}N_2O_4F$ 454	68.72 68.70	6.82 7.17	6.16 6.14	4.18 4.02

Table IV continued

$R_1 = R_2$	R_3	R_4	M. p., °C (Base—HCl)	Method	Empirical formula (Mol. weight)	Analysis of the base, %			
						C	H	N	Hal
CH_3	i-C_4H_9	4′-nitrophenyl	159 (195—197)	B)	$C_{26}H_{31}N_3O_6$ 481	64.86 64.83	6.44 6.54	8.74 8.66	
CH_3	i-C_4H_9	3′-chloro-4′-methoxyphenyl	179	C)	$C_{27}H_{33}N_2O_5Cl$ 500.5	64.73 64.68	6.59 6.82	5.59 5.64	7.09 6.59
CH_3	i-C_4H_9	3′,5′-dichloro-4′-methoxyphenyl	161—162 (188—190)	A)	$C_{27}H_{32}N_2O_5Cl_2$ 535	60.56 60.52	5.98 6.05	5.23 5.20	13.27 13.24
CH_3	i-C_4H_9	3′,5′-dibromo-4′-methoxyphenyl	172—173	A)	$C_{27}H_{32}N_2O_5Br_2$ 624	51.92 51.97	5.12 5.36	4.49 4.49	25.6 24.92
CH_3	i-C_4H_9	3′,4′,5′-trimethoxyphenyl	173—174	A)	$C_{29}H_{38}N_2O_7$ 526	66.15 66.26	7.22 7.45	5.32 5.22	
CH_3	i-C_4H_9	pyridin-3′-yl	138—139	A)	$C_{25}H_{31}N_3O_4$ 437	68.65 68.79	7.09 7.20	9.62 9.82	
CH_3	i-C_4H_9	$ClCH_2$	214—216	D)	$C_{21}H_{29}N_2O_4Cl$ 408,5	61.68 61.82	7.09 8.22	6.85 6.80	8.69 8.69
C_2H_5	C_2H_5	CH_3	103—105 (180—185)	A)	$C_{21}H_{30}N_2O_4$ 374	67.37 67.43	8.02 8.16	7.48 7.72	
C_2H_5	C_2H_5	C_2H_5	105—106 (158—160)	B)	$C_{22}H_{32}N_2O_4$ 388	68.06 68.17	8.24 8.36	7.21 7.25	
C_2H_5	C_2H_5	3′,4′,5′-trimethoxyphenyl	161—162	A)	$C_{29}H_{38}N_2O_7$ 526	66.15 66.03	7.22 7.32	5.32 5.06	
C_2H_5	i-C_4H_9	CH_3	102—103	A)	$C_{23}H_{34}N_2O_4$ 402	68.65 68.30	8.46 8.68	6.96 6.29	
C_2H_5	i-C_4H_9	C_2H_5	112—113 (200—202)	A)	$C_{24}H_{36}N_2O_4$ 416	69.23 68.89	8.65 8.29	6.73 7.08	
C_2H_5	i-C_4H_9	3′,4′,5 -trimethoxyphenyl	175—176	A)	$C_{31}H_{42}N_2O_7$ 554	67.14 67.01	7.58 7.64	5.05 5.17	

Preparation of oxime esters

Method A. A solution of the oxime (0.03 mole) in abs. pyridine (90 ml) was cooled below 5 °C and a solution of the acid chloride (0.036 mole) in abs. pyridine (50 ml) was added dropwise, under stirring. The mixture was allowed to stand overnight at room temperature. It was then poured into ice-water, and the mixture extracted with benzene. The benzene was evaporated, and the residue crystallized from a mixture of ethyl acetate and ethanol. For analysis the product was recrystallized from acetone.

Method B. A suspension of the oxime (0.03 mole) and anhydrous sodium carbonate (0.08 mole) was prepared in dry benzene (50 ml). The mixture was stirred, and a solution of the acid chloride (0.033 mole) in dry benzene (60 ml) was added dropwise, while the temperature was maintained below 5 °C. The mixture was allowed to stand overnight, then it was poured into ice-water, and extracted, after brief standing, with benzene. The extract was worked up as described under Method A.

Method C. A solution of the acid chloride (0.033 mole) in abs. benzene (14 ml) was added by drops, below 5 °C, into a stirred suspension of the oxime (0.03 mole) and triethanolamine (0.036 mole) in abs. benzene (50 ml). The temperature of the mixture was maintained between 0 and 5 °C for 30 min., then the mixture was shaken at room temperature for 2 hrs, and allowed to stand overnight. The mixture was refluxed for 30 min. on a water bath and poured into ice-water. Further work-up was the same as described under Method A.

Method D. A solution of chloroacetyl chloride (0.03 mole) in dichloroethane (25 ml) was added dropwise during 1.5 hr. into a suspension of the oxime (0.03 mole), dichloroethane (50 ml), and triethylamine (0.0315 mole), kept between 0 and 5 °C. The mixture was stirred for 1 hr. at a temperature below 5 °C, then for 2 hrs at room temperature, poured into ice-water, and extracted with benzene. The residue obtained after evaporation of the benzene was crystallized from acetone.

2-(Phenylcarbamoyloxy-imino)-3-isobutyl-9,10-dimethoxy-1,2,3,4,6,7-hexahydro-11bH-benzo(a)quinolizine

To a suspension of the oxime (9.96 g; 0.03 mole) in abs. benzene (100 ml) there was added by drops, a solution of phenylisocyanate (5.36 g; 0.045 mole) in abs. benzene (12 ml). The stirred mixture was boiled for 4 hrs, and allowed to stand overnight at room temperature. The crystals that had separated were collected by filtration, and the benzene mother liquor was evaporated to dryness. The residue was crystallized from acetone to yield 2.48 g, m.p. 140—142 °C.

$C_{26}H_{33}O_4N_3$ (451). Calcd. C 69.17; H. 7.32; N 9.31. Found C 68.46; H 7.42; N 9.35%.

Synthesis of oxime ester quaternary salts
2-(Propionyloxy-imino)-3-isobutyl-N-methyl-9,10-dimethoxy-1,2,3,4,6,7-hexahydro-11bH-benzo(a)quinolizinium iodide

The oxime ester (11.64 g; 0.03 mole) dissolved in chloroform (50 ml) was mixed with methyl iodide (42.6 g; 0.3 mole) and the solution was allowed to stand at room temperature for 24 hrs. Petroleum ether was then added till slight turbidity appeared. An oily product separated, which became crystalline on scratching. The crude product (m. p. 136 °C) was recrystallized from acetone to obtain m.p. 180 °C. The yield was quantitative.

$C_{23}H_{35}O_4N_2I$ (530). Calcd. C 52.07; H 6.60; N 5.28; I 23.98. Found C 52.08; H 6.90; N 5.23; I 23.61%.

Synthesis of oxime ethers
2-(2′,4′-Dinitrophenyloxy-imino)-3-isobutyl-9,10-dimethoxy-1,2,3,4,6,7-hexahydro-11bH-benzo(a)quinolizine

A mixture of 2-hydroxyimino-3-isobutyl-9,10-dimethoxy-1,2,3,4,6,7-hexahydro-11bH-benzo(a)quinolizine (9.96 g; 0.03 mole), abs. benzene (200 ml), triethylamine (20.7 ml; 0.15 mole), and 2.4-dinitro-1-fluorobenzene (8.56 g; 0.046 mole) was boiled for 1 hr. It was then diluted with water, and the benzene phase was separated. This was washed with water and dried over K_2CO_3. The red amorphous substance obtained after evaporation of the solvent was crystallized from 80% ethanol; m. p. 167—168 °C.

$C_{25}H_{30}O_7N_4$ (498). Calcd. C 60.24; H 6.03; N 11.24. Found C 60.24; H 6.40; N 11.18%.

Acta Chim. Acad. Sci. Hung. 62, 1969

Table V

New acid amides

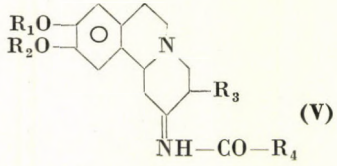

(V)

$R_1 = R_2$	R_3	R_4	M. p., °C (Base–HCl)	Method	Empirical formula (Mol. weight)	Analysis of the base, %			
						C	H	N	Hal
CH_3	CH_3	CH_3	226—227	B)	$C_{18}H_{26}N_2O_3$ 318	67.92 67.91	8.18 8.37	8.80 8.80	
CH_3	CH_3	C_2H_5	215—217	B)	$C_{19}H_{28}N_2O_3$ 332	68.67 68.81	8.43 8.82	8.43 8.43	
CH_3	CH_3	3′,5′-dichloro-4′-methoxyphenyl	236—238	A)	$C_{24}H_{28}N_2O_4Cl_2$ 479	60.12 60.17	5.84 6.04	5.84 5.84	14.86 14.07
CH_3	CH_3	2'-nitro-3′,4′,5′-trimethoxyphenyl	219—220	A)	$C_{26}H_{33}N_3O_8$ 515	60.58 60.60	6.40 6.58	8.15 8.12	
CH_3	C_2H_5	CH_3	221—222 (185—186)	A)	$C_{19}H_{28}N_2O_3$ 332	68.68 68.50	8.43 8.68	8.43 8.43	
CH_3	C_2H_5	C_2H_5	225—226 (238—241)	A)	$C_{20}H_{30}N_2O_3$ 346	69.36 70.00	8.67 8.82	8.09 8.10	
CH_3	C_2H_5	i-C_3H_7	247—248	A)	$C_{21}H_{32}N_2O_3$ 360	70.00 70.02	8.88 9.11	7.77 7.82	

CH_3	C_2H_5	4′-nitrophenyl	237—238 (218—220)	A)	$C_{24}H_{29}N_3O_5$ 439	65.60 65.61	6.60 6.78	9.56 9.57	
CH_3	C_2H_5	3′,5′-dichloro-4′-methoxyphenyl	231—232 (222—224)	A)	$C_{25}H_{30}N_2O_4Cl_2$ 493	60.85 60.81	6.08 6.34	5.68 5.36	14.40 14.77
CH_3	C_2H_5	3′,4′,5′-trimethoxyphenyl	117—118 (252—254)	A)	$C_{27}H_{36}N_2O_6$ 484	66.94 66.54	7.44 7.78	5.78 5.78	
CH_3	C_2H_5	2′-nitro-3′,4′,5′-trimethoxyphenyl	203—204	A)	$C_{27}H_{35}N_3O_8$ 529	61.24 61.39	6.61 6.68	7.93 8.01	
CH_3	C_2H_5	3′,5′-dimethoxy-4′-*n*-amyloxy-phenyl	190—191 (230—233)	A)	$C_{31}H_{44}N_2O_6$ 540	68.88 68.79	8.15 8.35	5.18 5.21	
CH_3	C_2H_5	pyridin-3′-yl	226—228 (178—180)	A)	$C_{23}H_{29}N_3O_3$ 395	69.87 69.70	7.34 7.50	10.65 10.49	
CH_3	n-C_4H_9	CH_3	210—212	A)	$C_{21}H_{32}N_2O_3$ 360	70.00 70.01	8.88 9.03	7.77 7.68	
CH_3	n-C_4H_9	C_2H_5	215—217 (238—240)	A)	$C_{22}H_{34}N_2O_3$ 374	70.58 70.50	9.09 9.28	7.49 7.48	
CH_3	n-C_4H_9	i-C_3H_7	223—224 (265—266)	A)	$C_{23}H_{36}N_2O_3$ 388	71.13 71.17	9.27 9.44	7.21 7.04	
CH_3	n-C_4H_9	Cl—CH_2	194—196	C)	$C_{21}H_{31}N_2O_3Cl$ 394,5	63.87 64.37	7.86 8.15	7.09 7.01	8.94 8.41
CH_3	n-C_4H_9	4′-nitrophenyl	206—208 (210—215)	A)	$C_{26}H_{33}N_3O_5$ 467	66.80 66.58	7.05 7.05	8.99 8.79	
CH_3	n-C_4H_9	3′,5′-dichloro-4′-methoxyphenyl	225—226 (218—220)	A)	$C_{27}H_{34}N_2O_4Cl_2$ 521	62.18 62.15	6.52 6.70	5.37 5.44	13.63 13.40
CH_3	n-C_4H_9	3′,5′-dibromo-4′-methoxyphenyl	222—224 (208—210)	A)	$C_{27}H_{34}N_2O_4Br_2$ 610	53.11 52.82	5.57 5.79	4.59 4.54	26.22 26.36

Table V continued

$R_1 = R_2$	R_3	R_4	M. p., °C (Base HCl)	Method	Empirical formula (Mol. weight)	Analysis of the base, %			
						C	H	N	Hal
CH_3	n-C_4H_9	3′,4′,5′-trimethoxyphenyl	230—232	A)	$C_{29}H_{40}N_2O_6$ 512	67.96 67.74	7.81 7.94	5.48 5.48	
CH_3	n-C_4H_9	3′,5′-dimethoxy-4′-n-amyloxy-phenyl	186—187 (231—233)	A)	$C_{33}H_{48}N_2O_6$ 568	69.71 69.57	8.45 8.54	4.92 5.03	
CH_3	n-C_4H_9	2′-nitro-3′,4′,5′-trimethoxyphenyl	217—218 (222—224)	A)	$C_{29}H_{39}N_3O_8$ 557	62.47 62.51	7.00 7.18	7.54 7.77	
CH_3	n-C_4H_9	pyridin-3′-yl	246—248 (188—190)	A)	$C_{25}H_{33}N_3O_3$ 423	70.92 70.94	7.80 7.80	9.92 9.79	
CH_3	n-C_4H_9	CH_3	204—205	B)	$C_{21}H_{32}N_2O_3$ 360	70.00 70.00	8.88 8.84	7.77 7.71	
CH_3	n-C_4H_9	C_2H_5	199—200 (250—253)	A)	$C_{22}H_{34}N_2O_3$ 374	70.58 70.67	9.09 9.08	7.49 7.49	
CH_3	n-C_4H_9	i-C_3H_7	227—228 (265—266)	A)	$C_{23}H_{36}N_2O_3$ 388	71.13 71.14	9.27 9.42	7.21 7.29	
CH_3	i-C_4H_9	i-C_4H_9	205—207	B)	$C_{24}H_{38}N_2O_3$ 402	71.64 71.72	9.45 9.61	6.96 7.10	
CH_3	i-C_4H_9	n-C_7H_{15}	184—185	A)	$C_{27}H_{44}N_2O_3$ 444	72.97 72.46	9.91 10.07	6.30 6.29	
CH_3	i-C_4H_9	Cl—CH_2	198—200	C)	$C_{21}H_{31}N_2O_3Cl$ 394,5	63.87 64.30	7.86 7.95	7.09 7.33	8.94 8.90
CH_3	i-C_4H_9	Cl—CH_2—CH_2	187—188 (270—272)	C)	$C_{22}H_{33}N_2O_3Cl$ 408,5	64.62 64.50	8.07 8.25	6.85 6.83	8.69 9.21

CH_3	i-C_4H_9	benzyl	200—202	A)	$C_{27}H_{36}N_2O_3$ 436	74.31 74.42	8.25 8.27	6.42 6.19	
CH_3	i-C_4H_9	C_6H_5—CH=CH	210	A)	$C_{28}H_{36}N_2O_3$ 448	75.00 75.18	8.03 8.64	6.25 6.28	
CH_3	i-C_4H_9	C_6H_5—O—CH_2	206—207	B)	$C_{27}H_{36}N_2O_4$ 452	71.68 70.97	7.96 7.73	6.19 6.56	
CH_3	i-C_4H_9	4′-chlorophenyl	199—201	B)	$C_{26}H_{33}N_2O_3Cl$ 456,5	68.12 67.76	7.23 7.56	6.12 6.19	7.77 7.82
CH_3	i-C_4H_9	4′-fluorophenyl	260—261	A)	$C_{26}H_{33}N_2O_3F$ 440	70.90 70.85	7.50 8.04	6.36 6.38	4.36 4.33
CH_3	i-C_4H_9	4′-nitrophenyl	223—224 (244—247)	A)	$C_{26}H_{33}N_3O_5$ 467	66.80 66.97	7.07 7.27	8.99 9.04	
CH_3	i-C_4H_9	3′-chloro-4′-methoxyphenyl	267—268	A)	$C_{27}H_{35}N_2O_4Cl$ 486,5	66.59 66.24	7.19 7.31	5.75 5.75	7.29 6.90
CH_3	i-C_4H_9	3′,5′-dichloro-4′-methoxyphenyl	243—245 (224—226)	A)	$C_{27}H_{34}N_2O_4Cl_2$ 521	62.18 62.12	6.52 6.56	5.37 5.79	13.63 13.87
CH_3	i-C_4H_9	3′,5′-dibromo-4′-methoxyphenyl	244—245 (210—212)	A)	$C_{27}H_{34}N_2O_4Br_2$ 610	53.11 52.97	5.57 5.49	4.59 4.58	26.22 26.69
CH_3	i-C_4H_9	3′,4′,5′-trimethoxyphenyl	240—241 (227—232)	A)	$C_{29}H_{40}N_2O_6$ 512	67.96 68.07	7.81 7.96	5.48 5.35	
CH_3	i-C_4H_9	3′,5′-dimethoxy-4′-*n*-amyloxy-phenyl	205—206 (223—226)	A)	$C_{33}H_{48}N_2O_6$ 568	69.71 69.71	8.45 8.62	4.92 4.91	
CH_3	i-C_4H_9	2′-nitro-3′,4′,5′-trimethoxyphenyl	210—211	A)	$C_{29}H_{39}N_3O_8$ 557	62.47 62.44	7.00 7.02	7.54 7.57	
CH_3	i-C_4H_9	1′-xenylpropyl	220—222	A)	$C_{35}H_{44}N_2O_3$ 540	77.77 77.70	8.14 8.50	5.18 5.03	

Table V continued

$R_1 = R_2$	R_3	R_4	M. p., °C (Base–HCl)	Method	Empirical formula (Mol. weight)	Analysis of the base, %			
						C	H	N	Hal
CH_3	i-C_4H_9	pyridin-3′-yl	253—254 (225—227)	A)	$C_{25}H_{33}N_3O_3$ 423	70.92 70.77	7.80 7.77	9.92 9.88	
CH_3	i-C_4H_9	xanthen-9′-yl	240—242	B)	$C_{33}H_{38}N_2O_4$ 526	75.28 74.92	7.22 7.38	5.32 5.28	
CH_3	i-C_4H_9	$(C_2H_5)_2$—N—CH_2	131—132 (192—194)	D)	$C_{25}H_{41}N_3O_3$ 431	69.83 69.43	9.51 9.59	9.74 9.75	
CH_3	i-C_4H_9	n-C_3H_7—NH—CH_2	141—143	D)	$C_{24}H_{39}N_3O_3$ 417	69.06 69.14	9.35 9.50	10.07 10.03	
CH_3	i-C_4H_9	i-C_3H_7—NH—CH_2	130—132	D)	$C_{24}H_{39}N_3O_3$ 417	69.06 69.10	9.35 9.46	10.07 10.02	
CH_3	i-C_4H_9	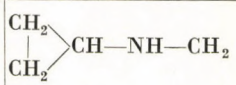	166—167	D)	$C_{24}H_{37}N_3O_3$ 415	69.39 69.26	8.91 8.95	10.12 10.08	
CH_3	i-C_4H_9	CH_2=CH—CH_2—NH—CH_2	132—133	D)	$C_{24}H_{37}N_3O_3$ 415	69.39 69.31	8.91 9.05	10.12 10.06	
CH_3 —	i-C_4H_9	piperidin-1′-ylmethyl	152—153	D)	$C_{26}H_{41}N_3O_3$ 443	70.42 70.41	9.25 9.68	9.47 9.30	

CH_3	i-C_4H_9	morpholin-4′-ylmethyl	164—165	D)	$C_{25}H_{39}N_3O_4$ 445	67.41 67.50	8.76 8.87	9.43 9.23	
C_2H_5	C_2H_5	CH_3	216—218	A)	$C_{21}H_{32}N_2O_3$ 360	70.00 70.01	8.88 8.86	7.77 7.70	
C_2H_5	C_2H_5	C_2H_5	216—217	A)	$C_{22}H_{34}N_2O_3$ 374	70.58 70.34	9.09 9.18	7.49 7.55	
C_2H_5	C_2H_5	3′,4′,5′-trimethoxyphenyl	213—215	A)	$C_{29}H_{30}N_2O_6$ 512	67.96 67.32	7.81 7.97	5.48 5.46	
C_2H_5	i-C_4H_9	CH_3	184—185	A)	$C_{23}H_{36}N_2O_3$ 388	71.13 71.18	9.28 9.47	7.21 7.35	
C_2H_5	i-C_4H_9	C_2H_5	201—202	A)	$C_{24}H_{38}N_2O_3$ 402	71.64 71.42	9.45 9.57	6.96 6.77	
C_2H_5	i-C_4H_9	3′,4′,5′-trimethoxyphenyl	223—224	B)	$C_{31}H_{44}N_2O_6$ 540	68.88 68.82	8.15 8.25	5.18 5.34	
n-C_4H_9	i-C_4H_9	CH_3	192—195	B)	$C_{27}H_{44}N_2O_3$ 444	72.97 72.99	9.90 10.46	6.31 6.33	
n-C_4H_9	i-C_4H_9	C_2H_5	214—215	B)	$C_{28}H_{46}N_2O_3$ 458	73.36 73.40	10.04 10.10	6.11 6.13	
n-C_4H_9	i-C_4H_9	3′,5′-dichloro-4′-methoxyphenyl	220—221	A)	$C_{33}H_{46}N_2O_4Cl_2$ 605	65.45 65.30	7.60 7.80	4.62 4.65	11.73 11.16

Synthesis of the 2-amino parent compounds

The suspension of the oxime (0.1 mole) in abs. tetrahydrofuran (164 ml) was added, during about 30 min., to a suspension of lithium aluminium hydride (8.3 g; 0.22 mole) in abs. tetrahydrofuran (250 ml), at 60 °C. The mixture was boiled for 1 hr., cooled, carefully diluted with water, filtered, and the material collected on the filter was washed with hot tetrahydrofuran. The solvent was evaporated, and the oily residue used without further purification for the synthesis of the amides. The hydrochlorides prepared with HCl in abs. ethanol were crystalline products.

Synthesis of the acid amides

Method A. To a suspension of the amine (0.03 mole) and sodium carbonate (0.13 mole) in abs. benzene (50 ml) there was added a solution of the acid chloride (0.033 mole) in benzene (30 ml) by drops, below 5 °C. After standing overnight, the mixture was boiled for 30 min., cooled, and filtered. The substance collected on the filter was purified by boiling in water, filtration, drying, and crystallization from a mixture of ethyl acetate and alcohol.

Method B. A stirred solution of the amine (0.03 mole) in abs. benzene (50 ml) and triethylamine (0.036 mole) was maintained at 5 °C, and a solution of the acid chloride (0.033 mole) in abs. benzene (20 ml) was added by drops. The mixture was allowed to stand between 0 and 5 °C for 30 min., and then at room temperature overnight. It was refluxed for 30 min. and poured into ice-water. The benzene layer was separated, washed, dried, and the solvent evaporated. The residue was crystallized from a mixture of ethyl acetate and ethanol.

Method C. A solution of chloroacetyl chloride (0.015 mole) in dichloroethane (25 ml) was added dropwise during about 1.5 hrs into a solution of the amine (0.03 mole) in dichloroethane (50 ml), maintained at a temperature below 5 °C. The mixture was then stirred for 1 hr. at +5 °C, for 2 hrs at room temperature, and poured into ice-water. The pH of the aqueous mixture was adjusted to 6—7 with a 10% solution of Na_2CO_3, and repeatedly extracted with chloroform. The combined extracts were dried with $CaCl_2$, filtered, and evaporated to dryness. The residue was crystallized from acetone.

Method D. The chloroacetylamino compound was prepared according to Method C then the appropriate amine was added in great excess, or as a solution in xylene, and this mixture was boiled for 2 to 4 hrs. After cooling, some ice was added and the mixture extracted repeatedly with benzene. The combined extract was washed with water, dried, and the solvent evaporated. The residue was recrystallized from ethyl acetate.

2-Formylamino-3-isobutyl-9,10-dimethoxy-1,2,3,4,6,7-hexahydro-11bH-benzo(a)quinolizine

Formic acid (98%; 2 ml) was added dropwise with cooling, to 2-amino-3-isobutyl-9,10-dimethoxy-1,2,3,4,6,7-hexahydro-11bH-benzo(a)quinolizine (5 g; 0.0157 mole), then the mixture was boiled for 3 hrs. The excess formic acid was distilled off under reduced pressure, and the residue dissolved in warm benzene. The addition of 10% Na_2CO_3 caused the separation of a solid that was collected by filtration and recrystallized from benzene to yield 2 g, m. p.198—200 °C.

$C_{20}H_{30}O_3N_2$ (346). Calcd. C 69.36; H 8.67; N. 8.09. Found C 69.24; H 8.80; N 8.06%.

2-(Cyanacetyl-amino)-3-isobutyl-9,10-dimethoxy-1,2,3,4,6,7-hexahydro-11bH-benzo(a) quinolizine

A solution of ethyl cyanoacetate (10.17 g; 0.09 mole) in abs. ethanol (10 ml) was added by drops to a solution of the amine (9.54 g; 0.03 mole) in abs. ethanol (10 ml), and the mixture was boiled for 8 hrs. For one night it was kept in a refrigerator, then the crystals which had separated were filtered off to obtain 2.9 g; m.p. 240—241 °C.

$C_{22}H_{31}O_3N_3$ (385). Calcd. C 68.66; H 8.24; N 10.97. Found C 68.57; H 8.05; N 10.90%.

2-(Carbethoxyamino)-3-isobutyl-9,10-dimethoxy-1,2,3,4,6,7-hexahydro-11bH-benzo(a)quinolizine

The amine (9.54 g; 0.03 mole) was dissolved in abs. ethanol (50 ml), and the solution was cooled below 5 °C. Ethyl chloroformate (4.34 g; 0.04 mole) was added dropwise to the stirred and cooled solution, while the reaction mixture was kept alkaline by the addition, as

necessary, of sodium ethoxide. After standing for 2 hrs at room temperature, the mixture was adjusted with 1*N* HCl to pH 7, then filtered and the filtrate evaporated. The residue was dissolved in benzene, the solution washed with water, dried, and the solvent evaporated. The residue was crystallized from acetone, and the crystals were washed with petroleum ether to obtain 2.5 g, m.p. 135—136 °C.

$C_{22}H_{34}O_4N_2$ (390). Calcd. C 67.69; H 8.71; N 7.17. Found C 67.50; H 8.88; N 7.15%.

2-(Phenylcarbamoylamino)-3-isobutyl-9,10-dimethoxy-1,2,3,4,6,7-hexahydro-11bH-benzo(a)quinolizine

A solution of phenylisocyanate (5.36 g; 0.045 mole) in benzene (30 ml) was added by drops to a solution of the amine (9.54 g; 0.03 mole) in benzene (100 ml). After boiling it for 4 hrs, the reaction mixture was allowed to stand overnight at room temperature. The crystals which had separated were collected by filtration and recrystallized from acetone to obtain 3.25 g, m.p. 197 °C.

$C_{26}H_{35}O_3N_3$ (437). Calcd. C 71.39; H 8.00; N 9.61. Found C 71.27; H 7.97; N 9.59%.

Quaternary salts of the amides
2-(3′,4′,5′-trimethoxybenzoylamino)-3-isobutyl-N-methyl-9,10-diethoxy-1,2,3,4,6,7-hexahydro-11bH-benzo(a)quinolizinium iodide

Methyl iodide (42.6 g; 0.3 mole) was added to a solution of the acid amide (16.2 g; 0.03 mole) in chloroform (50 ml), the mixture was let to stand for 24 hrs at room temperature. Petroleum ether was added till the appearance of slight turbidity. The crystals which separated the next day were filtered off. The crude product (m.p. 188°C) was recrystallized from acetone to obtain 9.4 g, m.p. 199°C.

$C_{32}H_{47}O_6N_2I$ (682). Calcd. C 56.30; H 6.89; N 4.10; I 18.62. Found C 56.03; H 7.28; N 4.03; I 18.90%.

Alkyl- and arylamino derivatives
2-(2′,4′-Dinitrophenylamino)-3-isobutyl-9,10-dimethoxy-1,2,3,4,6,7-hexahydro-11bH-benzo(a)quinolizine

A mixture of the amine (9.54 g; 0.03 mole), abs. benzene (200 ml), triethylamine (20.7 ml; 0.15 mole), and 2,4-dinitrofluorobenzene (8.56 g; 0.046 mole) was refluxed for 30 min. The reaction mixture was diluted with water and the two phases were separated. The benzene layer was washed with a little water, dried over K_2CO_3, and the solvent evaporated to leave a brown oil, which was purified as the hydrochloride to obtain the free base as crystals. Recrystallized from acetone, the product was 3.2 g, m.p. 154—155°C.

$C_{25}H_{32}O_6N_4$ (484) Calcd. C 61.98; H 6.61; N 11.57. Found C 61.67; H 7.03; N 11.35%.

2-(beta-hydroxyethylamino)-3-isobutyl-9,10-dimethoxy-1,2,3,4,6,7-hexahydro-11bH-benzo(a)quinolizine hydrobromide

A mixture of the amine (9.54 g; 0.03 mole), ethylene bromohydrin (6 g; 0.048 mole), and benzene (100 ml) was boiled for 30 min., and allowed to stand at room temperature overnight. The crystals were filtered off, and washed with benzene to give 1.6 g of the product, m.p. 245°C.

$C_{21}H_{35}O_3N_2Br$ (443) Calcd. C 56.88; H 7.90; N 6.32; Br 18.02. Found C 56.86; H 7.84; N 6.38; Br. 18.58%.

2-(1′,1′-Dicarbethoxyvinylamino)-3-isobutyl-9,10-dimethoxy-1,2,3,4,6,7-hexahydro-11bH-benzo(a)quinolizine

A mixture of the amine (9.54 g; 0.03 mole), diethyl ethoxymethylenemalonate (7.56 g; 0.035 mole) and abs. benzene (60 ml) was boiled for 1.5 hr., and allowed to stand at room tem-

perature overnight. The solvent was distilled off, and the residue crystallized from ethyl acetate, and recrystallized from acetone to give 2.52 g, m.p. 140—141 °C.

$C_{27}H_{40}O_6N_2$ (488). Calcd. C 66.39; H 8.19; N 5.73. Found C 66.24; H 8.26; N 5.85%.

*

Thanks are due to Dr. E. KASZTREINER for having made available a part of the acids needed for the preparation of acid chlorides. To Mrs. K. PÁLMAY and Mrs. Z. KUTNYÁNSZKY we are indebted for valuable technical assistance. To our Analytical Department (directed by Mr. A. MIZSEI) we express our thanks for the accurate accomplishment of a great number of microanalyses.

REFERENCES

1. PLETSCHER, A., BROSSI, A., GEY, K. F.: Intern. Rev. Neurobiol., **1962,** No. 4, 275—306
2. LÉNÁRD, K., BITE, P.: Acta Chim. Acad. Sci. Hung. **38,** 57 (1963)
3. LÉNÁRD, K., BITE, P.: Hung. Pat. 151 039 (1963)
4. BITE, P., DISZLER, E., FEKETE, M.: Hung. Pat. 154 338 (1968)
5. DISZLER, E., BITE, P., FEKETE, M., VILLÁNYI, A.: Hung. Pat. 154 952 (1969)

Pál BITE
Eszter DISZLER
Márton FEKETE
Ágnes VILLÁNYI
Marianne KÜRTI

Budapest IV., Újpest P. O. Box 82

Acta Chimica Academiae Scientiarum Hungaricae, Tomus 62 (2), pp. 179—189 (1969)

HETEROCYCLIC COMPOUNDS FROM SUGARS, II*

PREPARATION OF 2-POLYHYDROXYALKYLTHIAZOLE AND -BENZOTHIAZOLE DERIVATIVES

R. BOGNÁR, I. FARKAS, L. SZILÁGYI, M. MENYHÁRT, É. N. NEMES, and I. F. SZABÓ

(Institute of Organic Chemistry, L. Kossuth University, Debrecen)

Received July 5, 1968

New thioamide derivatives have been prepared by the addition of hydrogen sulphide to acetylated aldonitriles. The condensation of pentaacetyl-D-gluconic acid thioamide with chloroacetone, and that of pentaacetyl-D-galactonic acid thioamide with phenacyl bromide, give the corresponding substituted thiazole derivatives.

The condensation of acetylated aldonic acid chlorides with 2-aminothiophenol or 2-amino-4-chlorothiophenol results in the formation of 2-polyacetoxyalkylbenzothiazole or 2-polyacetoxyalkyl-5-chlorobenzothiazole derivatives. The polyacetoxy compounds can be saponified with sodium methoxide to 2-polyhydroxyalkylbenzothiazoles. Acetylated aldonic acid nitriles also condense with 2-aminothiophenol to give the corresponding 2-polyacetoxyalkyl-benzothiazoles in good yield.

The optical activity of the 2-polyhydroxyalkylbenzothiazoles and the steric position of the hydroxyl group at the carbon atom of the polyhydroxyalkyl chain attached to the benzothiazole ring, are connected by a relationship similar to the "benzimidazole rule".

In a previous paper [1] we reported a study of 2-polyhydroxyalkylbenzothiazolines formed in the reactions of 2-aminothiophenol or 2-amino-4-chlorothiophenol with simple sugars. In the present work we describe the synthesis of some 2-polyhydroxyalkylthiazole and -benzothiazole derivatives. Interest is attached to these studies because the compounds are closely related to the benzothiazoline derivatives from which they are expected to form when acted upon by oxidizing agents. In addition to this, compounds containing such ring systems are interesting from a pharmacological point of view, and because relatively little work has been done on the preparation such types of sugar derivatives.

The first successful extension of the HANTZSCH synthesis to carbohydrate derivatives was reported by BEYER and SCHULTZ [2]. These authors described the synthesis of pentaacetyl-D-gluconic acid thioamide and its cyclization with phenacyl bromide, resulting in the formation of 2-(D-glucopentaacetoxypentyl)-4-phenylthiazole. To our knowledge, no other aldonic acid thioamides have been reported, and no data about 2-polyhydroxyalkylbenzothiazoles were found in the literature.

We are reporting that the known thioamide synthesis [3] can also be applied to carbohydrates. In alcoholic solutions, ammonia catalysis effects the addition of hydrogen sulphide to acetylated aldonitriles, resulting in the forma-

*Part I: R. BOGNÁR *et al.* [1].

tion of thioamides in good yields. The structure of the thioamides is supported by their IR spectra. The results concerning thioamides are shown in Table I.

Table I

Acetylated aldonic acid thioamides

Compound	Yield %	m. p. $[\alpha]_D$ (in $CHCl_3$)	Characteristic IR bands (cm^{-1})
Pentaacetyl-D-gluconic acid thioamide [2]	67	154° +63° (c = 1.0)	3410, 3300, 3190, 1615, 1435
Tetraacetyl-D-xylonic acid thioamide (**I**)	88	138—139° +69° (c = 1.5)	3380, 3300, 3215, 1640, 1440
Pentaacetyl-D-galactonic acid thioamide (**II**)	67	139° +71° (c = 0.7)	3375, 3300, 3210, 1640, 1440
Pentaacetyl-D-glucosaminic acid thioamide (**III**)	63	154—155° +81° (c = 1.0)	3415, 3300, 3185, 1605, 1415

As expected, pentaacetyl-D-gluconic acid thioamide [2] and the galactonic acid analogue (**II**) reacts with chloroacetone and phenacyl bromide to give 2-(D-gluco-pentaacetoxypentyl)-4-methylthiazole (**IV**) and 2-(D-galacto-pentaacetoxypentyl)-4-phenylthiazole (**V**) respectively. Both compounds yield acetyl-free crystalline derivatives when saponified according to ZEMPLÉN.

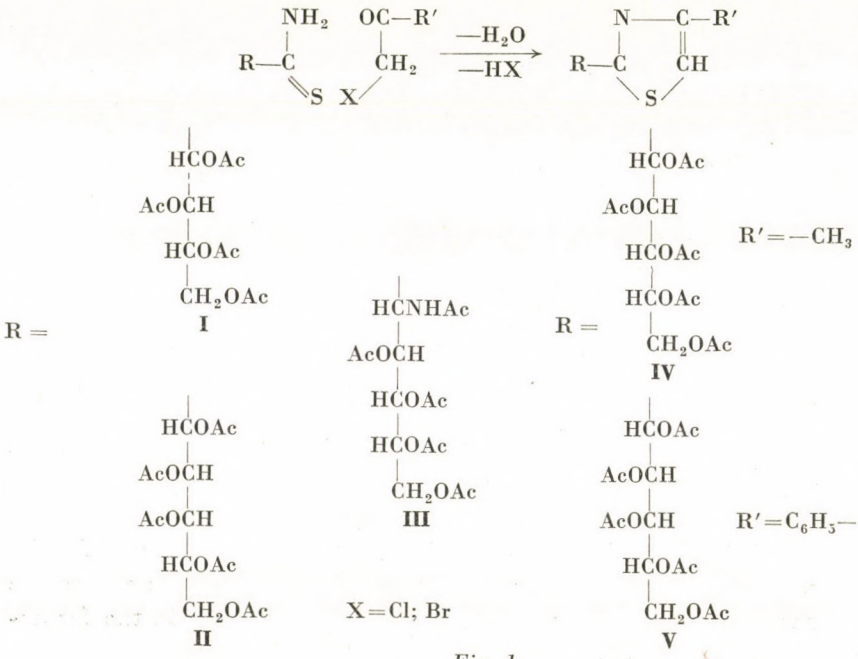

Fig. 1

The condensation of carboxylic acid derivatives with *o*-aminothiophenols is a general method of preparing derivatives of benzothiazoles [4]. The acetylated aldonic acid chlorides were found to react readily with both 2-aminothiophenol and 2-amino-4-chlorothiophenol in hot benzene in the presence of anhydrous pyridine. Using this method, we have prepared 2-substituted benzothiazole derivatives (**VI—X**) from tetraacetyl-D-arabonic acid chloride, pentaacetyl-D-gluconic acid chloride, and pentaacetyl-D-galactonic acid chloride. Tetraacetyl-D-galactaric acid dichloride, too, reacted according to expectation with *o*-aminothiophenol. It was possible to prepare 1,4-*bis*-(2'-benzothiazolyl)-D-galactotetraacetoxybutane (**XI**) and 1,4-*bis*-[2'-(5'-chlorobenzothiazolyl)]-D-galactotetraacetoxybutane (**XII**) by this method.

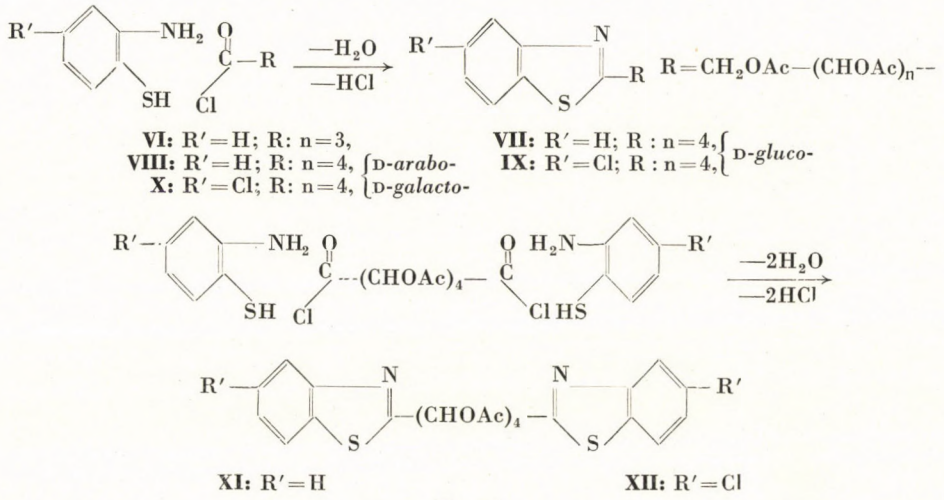

Fig. 2

KUHN and DRAWERT [5] have prepared different 2-substituted 2-thiazolines by reacting aliphatic nitriles with cysteamine. Similarly, the condensation of *o*-aminothiophenol with nitriles is expected to yield 2-substituted benzothiazole derivatives. Only a few examples are known [6, 7] where this reaction was used to prepare 2-substituted benzothiazoles. We found that acetylated aldonic acid nitriles readily reacted with *o*-aminothiophenol in hot alcohol with the formation of ammonia and 2-substituted benzothiazoles.

In some cases this procedure gave syrup-like acetates, which, however, could be deacetylated to yield crystalline 2-polyhydroxyalkylbenzothiazoles. The latter compounds, in turn, gave crystalline acetates when treated with acetic anhydride.

The 2-substituted benzothiazole derivatives prepared in two different ways proved to be identical in every respect. The benzothiazole structure is

also supported by IR spectroscopic data. The band at 1515—1545 cm^{-1} can be assigned to the skeletal vibration of the benzothiazole ring [8, 9]. The characteristic absorption of 1,2-disubstituted benzene derivatives around 750 cm^{-1} is also present in the spectra (*cf.* Table II). The 2-substituted benzothiazoles are characterized by the data given in Table II.

According to Table II, the optical activity of the 2-polyhydroxyalkylbenzothiazoles and the steric position of the hydroxyl group at the carbon atom of the polyhydroxyalkyl chain attached to the benzothiazole ring (*i.e.* C-2') are connected by a relationship similar to the "benzimidazole rule" [10].

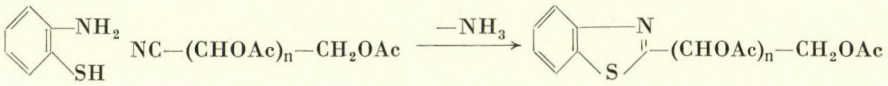

VI:		D-*arabo*-	**VII:**	D-*gluco*-
XIII:	n=3	L-*arabo*-	**VIII:** n=4	D-*galacto*-
XIV:		D-*xylo*-	**XVI:**	D-*manno*-
XV:		L-*xylo*-		

Fig. 3

Work on the relationship between 2-polyhydroxyalkylbenzothiazole and -benzothiazoline derivatives, mentioned in the introduction, is in progress. The oxidation of the benzothiazoline derivatives to the corresponding benzothiazoles is being studied.

Experimental

Tetraacetyl-D-xylonic acid thioamide (I)

10 g of tetraacetyl-D-xylonic acid nitrile was dissolved in 90 ml of ethanol at 50°C and hydrogen sulphide was introduced for 3 hrs, while the solution was maintained at 50°C in a water-bath. After saturation with H_2S about 1 hr, 0.2 ml of conc. ammonium hydroxide was added. The yellow solution was evaporated to dryness in vacuum and the residual syrup crystallized from 20 ml of ethanol, to obtain 8 g 88% of **I**, m.p. 138—139°C, $[\alpha]_D = +69°$ ($c = 1.51$, in $CHCl_3$).

$C_{13}H_{19}O_8NS$ (349.4). Calcd. N 4.01; S 9.17. Found N 3.96; S 9.14%.

Pentaacetyl-D-galactonic acid thioamide (II)

10 g of pentaacetyl-D-galactonic acid nitrile was dissolved in 200 ml of absolute ethanol at 50 °C and H_2S was bubbled through the solution for 1.5 hrs at this temperature. 2 ml of ethanol saturated with ammonia at 20 °C was then added and H_2S introduced for another 1.5 hrs. The solution was concentrated to 50 ml in vacuum. On dilution with water the thioamide crystallized. It was allowed to stand several hours in a refrigerator, and separated by filtration. Together with an additional crop from the mother liquor, 6.5 g (67%) of thioamide was obtained. After crystallization from alcohol the compound had m.p. 139°C, $[\alpha]_D = +71°$ ($c = 0.7$, in $CHCl_3$).

$C_{16}H_{23}O_{10}NS$ (421.5). Calcd. N 3.32; S 7.61. Found N 3.23; S 7.59%.

Recrystallization from ethyl acetate/petroleum ether yielded a different modification (m.p. 150 °C), which was identical with the above compound as shown by the optical activities ($[\alpha]_D = +71.6°$) and the IR spectra.

Table II

(a) 2-Polyacetoxyalkylbenzothiazoles

Compound	Method of prepa-ration*	Yield %	M. p., $[\alpha]_D$ (in $CHCl_3$)	Characteristic IR bands (cm^{-1})**
2-(D-*arabo*-tetraacetoxy-butyl)-, **(VI)**	A	25	75—76°; —3.8°	1515, 760
2-(D-*arabo*-tetraacetoxy-butyl)-, **(VI)**	B	90	76°; —3.2°	
2-(L-*arabo*-tetraacetoxy-butyl)-, **(XIII)**	B	75	75°; +3.5°	1515, 760 (identical with **VI**)
2-(D-*xylo*-tetraacetoxy-butyl)-, **(XIV)**	B	87	94°; +94.5°	1520—1510, 765
2-(L-*xylo*-tetraacetoxy-butyl)-, **(XV)**	B	92	91—92°; —94°	1520—1515, 765 (identical with **XIV**)
2-(D-*gluco*-pentaacetoxy-pentyl)-, **(VII)**	A	69	157—158°; +108°	1530, 1520, 745
2-(D-*gluco*-pentaacetoxy-pentyl)-, **(VII)**	B	74	158—159°; +110°	
2-(D-*galacto*-pentaacetoxy-pentyl)-, **(VIII)**	A	42	132—133°; +45.6°	1530, 1520, 768
2-(D-*galacto*-pentaacetoxy-pentyl)-, **(VIII)**	B	63	133—135°; +46.2°	
2-(D-*manno*-pentaacetoxy-pentyl)-, **(XVI)**	B	98	96—97°; +17.5°	1520, 760
2-(D-*gluco*-pentaacetoxy-pentyl)-5-chloro-, **(IX)**	A	70	113—114°; +107.4°	1545, 1515, 840
2-(D-*galacto*-pentaacetoxy-pentyl)-5-chloro-, **(X)**	A	64	149°; +40.2°	1545, 1517, 815

*A: from acid chloride. B: from nitrile.
**The IR spectra were recorded in KBr pellets.

(b) 2-Polyhydroxyalkylbenzothiazoles

Compound	Yield %	M. p.; $[\alpha]_D$ (in pyridine)
2-(D-*arabo*-tetrahydroxybutyl)-, **(VIa)**	80	207—208°; —133.5°
2-(L-*arabo*-tetrahydroxybutyl)-, **(XIIIa)**	80	206°; +134°
2-(D-*xylo*-tetrahydroxybutyl)-, **(XVIa)**	54	143—144°; + 82.8°
2-(L-*xylo*-tetrahydroxybutyl)-, **(XVa)**	85	144—145°; — 83.5°
2-(D-*gluco*-pentahydroxypentyl)-, **(VIIa)**	71	169—170°; + 74°
2-(D-*galacto*-pentahydroxypentyl)-, **(VIIIa)**	97	212—213°; + 41°
2-(D-*manno*-pentahydroxypentyl)-, **(XVIa)**	54	190—191°; — 60.6°
2-(D-*gluco*-pentahydroxypentyl)-5-chloro-, **(IXa)**	91	212—213°; + 79.5°
2-(D-*galacto*-pentahydroxypentyl)-5-chloro-, **(Xa)**	83	220—221°; +142°

Pentaacetyl-D-glucosaminic acid thioamide (III)

2.5 g of pentaacetyl-2-amino-2-deoxy-D-gluconic acid nitrile was dissolved in 25 ml of ethanol at 50° C. A vigorous stream of H_2S was passed through the solution for 1.5—2 hrs. while it was maintained at 40°C in a water-bath. In 10 min. after the stream of H_2S had been started, 0.2 ml of conc. ammonium hydroxide was added to the solution, which became orange-red when the reaction was completed. The thioamide precipitated on cooling, and was recrystallized from hot ethanol, to obtain 1.7 g (63%), m.p. 154—155° C, $[\alpha]_D = +81°$ ($c = 1.01$, in $CHCl_3$).

$C_{16}H_{24}O_9N_2S$ (420.4). Calcd. N 6.66; S 7.62. Found N 6.60; S 7.59%.

2-(D-gluco-pentaacetoxypentyl)-4-methylthiazole (IV)

4 g of pentaacetyl-D-gluconic acid thioamide in 4 ml of chloroacetone was heated for 15 min. at 75°C in a water-bath. The substance gradually dissolved and, after the reaction had gone to completion, a dark green solution was obtained, which was evaporated to dryness in vacuum. The residue was taken up in anhydrous ethanol and the solvent evaporated in vacuum, this procedure being repeated several times. After recrystallization, the product had m.p. 128°C. Yield: 1.18 g (27%); $[\alpha]_D = +96.2°$ ($c = 0.48$, in $CHCl_3$).

$C_{19}H_{25}O_{10}NS$ (459.5). Calcd. C 49.66; H 5.48; N 3.04; S 6.97. Found C 49.92; H 5.30; N 2.98; S 6.79%.

2-(D-gluco-pentahydroxypentyl)-4-methylthiazole (IVa)

1 g of **IV** was dissolved in 5 ml of warm absolute ethanol and 0.3 ml of 1 *N* sodium methoxide in methanol was added. The solution was allowed to stand in a refrigerator for 1 hr., then the crystalline product was filtered off and recrystallized from 5 ml of ethanol to yield 0.4 g (74%) of **IVa**, m.p. 160°C, $[\alpha]_D = +44.1°$ ($c = 0.6$, in pyridine).

$C_9H_{15}O_5SN$ (249.3). Calcd. C 43.36; H 6.07; N 5.61; S 12.86. Found C 43.52; H 5.84; N 5.55; S 12.73%.

2-(D-galacto-pentaacetoxypentyl)-4-phenylthiazole (V)

1 g of pentaacetyl-D-galactonic acid thioamide (**II**) was dissolved in 10 ml of anhydrous ethanol, 0.5 ml of absolute pyridine and 0.48 g of phenacyl bromide were added, and the solution was heated on a water-bath for 30 min. After cooling, the mixture was poured into ice-water, the precipitate filtrated off, washed with ice-water, and dried in a vacuum desiccator over P_2O_5. After three recrystallizations from aqueous ethanol, the yield was 0.28 g (23%); m.p. 120—121.5°C, $[\alpha]_D = +45.6°$ ($c = 0.4$, in $CHCl_3$).

$C_{24}H_{27}O_{10}NS$ (521.5). Calcd. N 2.68; S 6.13. Found N 2.64; S 6.07%.

2-(D-galacto-pentahydroxypentyl)-4-phenylthiazole (Va)

1 g of **V** suspended in 20 ml of anhydrous ethanol was mixed with a solution of 2 ml of 1 *N* sodium methoxide in absolute methanol. After rapid dissolution, abundant crystal formation was observed. The crystals were filtered off after standing for several hours and washed with methanol. Yield: 0.45 g (75%). Two recrystallizations from aqueous ethanol gave m.p. 217—219 °C, $[\alpha]_D = +132°$ ($c = 0.51$, in pyridine).

$C_{14}H_{17}O_5NS$ (311.3). Calcd. N 4.50; S 10.30. Found N 4.48; S 10.12%.

2-(D-arabo-tetraacetoxybutyl)-benzothiazole (VI)

(a) From acid chloride

A solution of 2.1 g of tetraacetyl-D-arabonic acid chloride and 0.74 g of *o*-aminothiophenol was prepared in 50 ml of absolute benzene, and 1.3 ml of absolute pyridine was added. The solution was refluxed on a water-bath for 1 hr., while N_2 was bubbled through it. After cooling, the solution was decanted from the precipitated pyridinium chloride, evaporated to dryness in vacuum and the residue recrystallized twice from petroleum ether, to yield 0.6 g (25%) of **VI**, m.p. 75—76°C, $[\alpha]_D = -3.8°$ ($c = 1.4$, in $CHCl_3$). The IR spectrum was identical

with that of the product obtained by procedure *(b)*. No mixed m.p. depression was observed with the products prepared according to procedures *(a)* and *(b)*.

(b) From nitrile

0.2 g of 2-(D-arabo-tetrahydroxybutyl)-benzothiazole (**VIa**) was subjected to acetylation in a mixture of 5 ml of absolute pyridine and 5 ml of acetic anhydride for 24 hrs at room temperature. Upon pouring on ice, a syrup was formed which was extracted with chloroform. The $CHCl_3$ solution was washed with a $NaHCO_3$ solution to remove the acid, then dried over anhydrous Na_2SO_4, and evaporated to dryness in vacuum. Absolute ethanol was distilled from the sryup several times in vacuum, soon resulting in crystallization, and yielding 0.3 g (90%) of **VI.** Recrystallized from petroleum ether, the substance had m.p. 76°C, $[\alpha]_D = -3.2°$ ($c = 1.8$, in $CHCl_3$). No melting point depression was observed with the product prepared by procedure *(a)*.

$C_{19}H_{21}O_8NS$ (423.4). Calcd. N 3.30; S 7.58. Found N 3.19; S 7.58%.

2-(D-arabo-tetrahydroxybutyl)-benzothiazole (VIa)

0.5 ml of *o*-aminothiophenol was added to 1 g of tetraacetyl-D-arabonic acid nitrile dissolved in 10 ml of absolute ethanol and the solution was refluxed for 4 hrs on a water-bath in a stream of nitrogen. The solvent was evaporated in vacuum and the residual yellow syrup directly deacetylated by dissolving it in 10 ml of absolute methanol and adding 2 ml of 1 *N* sodium methoxide in absolute methanol. After several hours of standing, the solution was neutralized with acetic acid, the precipitated substance filtered off, and washed with methanol. Yield: 0.65 g (80%). Recrystallization from cellosolve gave m.p. 207—208° C, $[\alpha]_D = -133.5°$ ($c = 0.3$, in pyridine).

$C_{11}H_{13}O_4NS$ (255.3). Calcd. N 5.48; S 12.55. Found N 5.18; S 12.50%.

2-(L-arabo-tetrahydroxybutyl)-benzothiazole (XIIIa)

1 g of tetraacetyl-L-arabonic acid nitrile was reacted with 0.5 ml of *o*-aminothiophenol. (For conditions and processing, see the preparation of **VIa**). The crude product obtained after deacetylation (0.65 g; 80%) was recrystallized from cellosolve; m.p. 206°C, $[\alpha]_D = +134°$ ($c = 0.33$, in pyridine). The IR spectrum was identical with that of **VIa.**

$C_{11}H_{13}O_4NS$ (255.3). Calcd. N 5.48; S 12.55. Found N 5.29; S 12.44%.

2-(L-arabo-tetraacetoxybutyl)-benzothiazole (XIII)

0.2 g of **XIIIa** was acetylated in a mixture of 5 ml pyridine and 5 ml acetic anhydride for 24 hrs at room temperature. The product was processed as described for **VI.** The crude product was recrystallized from petroleum ether, to yield 0.25 g (75%) of **XIII,** m.p. 75°C, $[\alpha]_D = +3.5°$ ($c = 1.44$, in $CHCl_3$). The IR spectrum was identical with that of **VI.**

2-(D-xylo-tetrahydroxybutyl)-benzothiazole (XIVa)

This compound was prepared from 1.2 g of tetraacetyl-D-xylonic acid nitrile and 0.6 ml of *o*-aminothiophenol as described for **VIa.** The crude product obtained on saponification with sodium methylate (0.44 g; 54%) was recrystallized from *n*-butanol; m.p. 143—144°C, $[\alpha]_D = +82.8°$ ($c = 0.28$, in pyridine).

$C_{11}H_{13}O_4NS$ (255.3). Calcd. N 5.48; S 12.55. Found N 5.30; S 12.40%.

2-(D-xylo-tetraacetoxybutyl)-benzothiazole (XIV)

0.2 g of **XVIa** was acetylated as described for **VI.** After recrystallization from petroleum ether, the product (0.29 g; 87%) had m.p. 94°C, $[\alpha]_D = +94.5°$ ($c = 0.35$, in $CHCl_3$).

$C_{19}H_{21}O_8NS$ (423.5). Calcd. N 3.30; S 7.58. Found N 3.28; S 7.42%.

2-(L-xylo-tetrahydroxybutyl)-benzothiazole (XVa)

1 g of tetraacetyl-L-xylonic acid nitrile was reacted with 0.5 ml of *o*-aminothiophenol. For conditions and processing, see the preparation of **VIa.** The crude product obtained after deacetylation (0.69 g; 85%) was recrystallized from *n*-butanol; m.p. 144—145°C, $[\alpha]_D = -83.5°$ ($c = 0.3$, in pyridine). The IR spectrum was identical with that of **XIVa.**

2-(L-xylo-tetraacetoxybutyl)-benzothiazole (XV)

0.25 g of **XVa** was acetylated with pyridine/acetic anhydride as described for **VIa.** The crude product (0.35 g; 92%) was recrystallized from petroleum ether; m.p. 91—92°C, $[\alpha]_D = -94°$ ($c = 0.2$, in $CHCl_3$). The IR spectrum was identical with that of **XIV.**

2-(D-gluco-pentaacetoxypentyl)-benzothiazole (VII)

(a) From acid chloride

6 g of pentaacetyl-D-gluconic acid chloride was dissolved in 60 ml of absolute ethanol and a mixture of 1.76 g of *o*-aminothiophenol, 1.4 ml of absolute pyridine, and 20 ml of absolute benzene was added dropwise, followed by refluxing on a water-bath for 1 hr. After cooling, the solution was decanted from the pyridinium chloride, and evaporated to dryness in vacuum. The residual syrup was recrystallized from hot ethanol. Two recrystallizations gave colorless needles (4.8 g; 69%), m.p. 157—158°C, $[\alpha]_D = +108°$ ($c = 0.69$, in $CHCl_3$). No m.p. depression was observed with the product prepared according to *(b)*.

$C_{22}H_{25}O_{10}NS$ (495.5). Calcd. N 2.82; S 6.47. Found N 2.85; S 6.44%.

(b) From nitrile

1 g of pentaacetyl-D-gluconic acid nitrile was dissolved in 10 ml of absolute ethanol 0.4 ml of *o*-aminothiophenol was added, and the solution was refluxed for 4 hrs on a water-bath in a stream of nitrogen. The crystals which separated on cooling (0.95 g; 74%) were filtered off and recrystallized twice from absolute ethanol, to obtain m.p. 158—159° C, $[\alpha]_D = +110°$ ($c = 0.57$, in $CHCl_3$). The IR spectrum was identical with that of the product prepared by method *(a)*, and no m.p. depression was observed with that product.

2-(D-gluco-pentahydroxypentyl)-benzothiazole (VIIa)

2 g of **VII** was suspended in 30 ml of absolute methanol and a solution of 2.5 ml of 1 *N* sodium methoxide in methanol was added. Fast dissolution was followed by abundant crystal formation. The crystals were filtered off after several hours' standing, and recrystallized from hot ethanol to obtain 0.82 g (71%) of **VIIa,** m.p. 169—170° C, $[\alpha]_D = +74°$ ($c = 0.5$, in pyridine).

$C_{12}H_{15}O_5NS$ (285.3). Calcd. N 4.91; S 11.23. Found N 4.80; S 11.21%.

2-(D-galacto-pentaacetoxypentyl)-benzothiazole (VIII)

(a) From acid chloride

2.5 g of pentaacetyl-D-galactonic acid chloride was dissolved in 25 ml of absolute benzene, and a mixture of 0.65 g of *o*-aminothiophenol, 10 ml of absolute benzene, and 0.5 ml of absolute pyridine was added dropwise, with stirring under nitrogen. The solution was refluxed for 1 hr. on a water-bath. After cooling, the benzene solution was decanted from the precipitated pyridinium salt and evaporated to dryness in vacuum. Repeated evaporation of ethanol from the syrup-like residue, resulted in crystallization of the latter. After two recrystallizations from 50% aqueous ethanol the product (1.23 g; 42%), had m.p. 132—133° C, $[\alpha]_D = +45.6°$ ($c = 1.12$, in $CHCl_3$).

$C_{22}H_{25}O_{10}NS$ (495.5). Calcd. N 2.82; S 6.47. Found N 2.79; S 6.29%.

(b) From nitrile

In this synthesis 1 g of pentaacetyl-D-galactonic acid nitrile was allowed to react with 0.4 ml of *o*-aminothiophenol, as described for **VII** (method *b)*. The crude product (0.8 g, 63%) was recrystallized from aqueous ethanol; m.p. 133—135 °C, $[\alpha]_D = +46.2°$ ($c = 0.76$, in $CHCl_3$).

On the basis of the IR spectrum and mixed m.p. determination, the product was identical with that of procedure *(a)*.

2-(D-galacto-pentahydroxypentyl)-benzothiazole (VIIIa)

1.05 g of **VIII** in 10 ml of absolute methanol was mixed with 1.2 ml of 0.5 *N* sodium methoxide in methanol. The solution was allowed to stand in a refrigerator overnight. The product was recrystallized from 80 ml of ethanol, and dried in a vacuum desiccator over P_2O_5 at 80° C to obtain 0.59 g (97%) of **VIIIa**, m.p. 212—213° C, $[\alpha]_D = +41°$ ($c = 0.48$, in pyridine).

$C_{12}H_{15}O_5NS$ (285.3). Calcd. N 4.91; S 11.23. Found N 4.73; S 11.32%.

2,2′-bis(pentaacetyl-D-galactonamido)-diphenyldisulphide

0.59 g of 2,2′-diaminodiphenyldisulphide was acylated with 2 g of pentaacetyl-D-galactonic acid chloride. For conditions and processing, see method *(a)* described for **VII.** Two recrystallizations from absolute ethanol gave 1.8 g (37%) of the product, m.p. 214—215° C, $[\alpha]_D = -73.7°$ ($c = 0.62$, in $CHCl_3$).

$C_{44}H_{52}O_{22}N_2S_2$ (1025.0). Calcd. N 2.73; S 6.25. Found N 2.70; S 6.15%.

Characteristic IR bands: 3350 (νNH), 1680 (νC=O, amide), 1580, 1515, and 760 cm^{-1}.

2-(D-manno-pentahydroxypentyl)-benzothiazole (XVIa)

1 g of pentaacetyl-D-mannonic acid nitrile was reacted with 0.4 ml of *o*-aminothiophenol as described for **VIa.** After saponification with sodium methoxide, the crude product (0.40 g; 54%) was recrystallized from *n*-butanol; m.p. 190—191 °C, $[\alpha]_D = -60.6°$ ($c = 0.31$, in pyridine).

$C_{12}H_{15}O_5NS$ (285.3). Calcd. N 4.90; S 11.24. Found N 4.76; S 11.05%.

2-(D-manno-pentaacetoxypentyl)-benzothiazole (XVI)

0.5 g of **XVIa** was acetylated as described for **VI** under *(b)*. The crude product (0.85 g; 98%) was recrystallized from petroleum ether; m.p. 96—97° C, $[\alpha]_D = +17.5°$ ($c = 0.7$, in $CHCl_3$).

$C_{22}H_{25}O_{10}NS$ (495.5). Calcd. N 2.83; S. 6.47. Found N 2.88; S 6.45%.

2-(D-gluco-pentaacetoxypentyl)-5-chlorobenzothiazole (IX)

2 g of pentaacetyl-D-gluconic acid chloride was allowed to react with 0.74 g of 2-amino-4-chlorothiophenol according to method *(a)* given for **VII.** Two recrystallizations from absolute ethanol gave 1.75 g (70%) of **IX,** m.p. 113—114 °C, $[\alpha]_D = +107.4°$ ($c = 0.81$, in $CHCl_3$).

$C_{22}H_{24}O_{10}NSCl$ (529.9). Calcd. N 2.64; S 6.05. Found N 2.62; S 6.08%.

2-(D-gluco-pentahydroxypentyl)-5-chlorobenzothiazole (IXa)

1 g of **IX** was suspended in 20 ml of hot absolute methanol, and 0.7 ml of 0.5 *N* sodium methoxide in absolute methanol was added. After dissolution, the deacetylated product rapidly crystallized. The next day it was filtered off, washed with absolute methanol, and recrystallized from hot 50% aqueous ethanol to obtain bright needles (0.55 g; 91%), m.p. 212—213° C, $\alpha]_D = +79.5°$ ($c = 0.26$, in pyridine).

l $C_{12}H_{14}O_5NSCl$ (319.8). Calcd. N 4.38; S 10.02. Found N 4.37; S 9.85%.

2-(D-galacto-pentaacetoxypentyl)-5-chlorobenzothiazole (X)

2 g of pentaacetyl-D-galactonic acid chloride was allowed to react with 0.74 g of 2-amino-4-chlorothiophenol as described for **IX.** The compound was recrystallized from absolute ethanol to yield 1.6 g (64%) of **X,** m.p. 149° C, $[\alpha]_D = +40.2°$ ($c = 0.52$, in $CHCl_3$).

$C_{22}H_{24}O_{10}NSCl$ (529.9). Calcd. N 2.64; S 6.05. Found N 2.66; S 6.02%.

2-(D-galacto-pentahydroxypentyl)-5-chlorobenzothiazole (Xa)

1 g of **X** in 25 ml of absolute methanol was saponified with 1 ml of 0.5 *N* sodium methoxide in absolute methanol according to the procedure described for **IXa.** The crystalline crude product was recrystallized from aqueous dimethyl formamide, to obtain 0.5 g (83%), m.p. 220—221° C $[\alpha]_D = +142°$ ($c = 0.7$, in pyridine).

$C_{12}H_{14}O_5NSCl$ (319.8). Calcd. N 4.38; S 10.02. Found N 4.45; S 9.87%.

1,4-bis-(2′-benzothiazolyl)-D-galacto-tetraacetoxybutane (XI)

3.65 g of tetraacetyl-D-galactaric acid dichloride was dissolved in 80 m lof hot absolute benzene, then 2.2 g of *o*-aminothiophenol in 20 ml of absolute benzene and 1.4 ml of absolute pyridine were added dropwise while stirring. The solution was warmed at 75° for 1 hr. in a water-bath. The solid residue, obtained on evaporating the solvent in vacuum, was dissolved in hot absolute pyridine, and absolute ethanol was added until a slight turbidity appeared. Further recrystallization from a mixture of pyridine and absolute ethanol gave a yield of 1.2 g (24%); m.p. 239—240° C (d.).

$C_{26}H_{24}O_8N_2S_2$ (556.6). Calcd. N 5.03; S 11.52. Found N 5.18; S 11.37%.

Characteristic IR bands: 1520 and 760 cm^{-1}.

1,4-bis-(2′-benzothiazolyl)-D-galacto-tetrahydroxybutane (XIa)

1.6 g of **XI** was suspended in 60 ml of absolute methanol, and 2 ml of 0.5 *N* sodium methoxide in absolute methanol was added. After refluxing for 30 min. on a water-bath, the suspension was shaken for 12 hrs. at room temperature. The filtered product was recrystallized from dimethyl formamide to obtain 0.5 g (45%) of **XIa,** m.p. 278—280° C (d.).

$C_{18}H_{16}O_4N_2S_2$ (388.5). Calcd. N 7.21; S 16.50. Found N 7.31; S 16.30%.

1,4-bis[2′-(5′-chlorobenzothiazolyl)]-D-galacto-tetraacetoxybutane (XII)

3.3 g of tetraacetyl-D-galactaric acid dichloride in 60 ml of hot absolute benzene was allowed to react with 2.54 g of 2-amino-4-chlorothiophenol as described for **XI.** The crude product was recrystallized twice from hot absolute pyridine to yield 2.6 g (52%) of **XII,** m.p. 285—286 °C (d.).

$C_{26}H_{22}O_8N_2S_2Cl_2$ (625.5). Calcd. N 4.48; S 10.24; Cl 11.30. Found N 4.60; S 10.17; Cl 11.26%.

Characteristic IR bands: 1545, 1515 and 805 cm^{-1}.

1,4-bis[2′-(5′-chlorobenzothiazolyl)]-D-galacto-tetrahydroxybutane (XIIa)

2 g of **XII** was saponified with 2.5 ml of 0.5 *N* sodium methoxide in absolute methanol, as described for **XIa.** Since the crude product was insoluble in common solvents as well as in hot glacial acetic acid, dioxan, pyridine, and dimethyl formamide, it was purified by extraction of the impurities with hot ethanol. Yield: 1.4 g (96%), m.p. 296—300° C (d.).

Attempts to prepare **XIIa** in pure state remained unsuccessful; however, upon acetylation with pyridine and acetic anhydride it was converted to **XII:**

1 g of **XIIa** was refluxed for 5 hrs in a mixture of 30 ml of absolute pyridine and 20 ml of acetic anhydride. The solid product was filtered off the next day, and washed with ethanol, to obtain 1.2 g (88%) of **XIIa,** m.p. 284—285° C (d.). No melting point depression was observed with **XII.**

*

Support of this work by the Hungarian Academy of Sciences is gratefully acknowledged. The authors are indebted to the microanalytical laboratory of the Institute (headed by Dr. É. R. DÁVID) for the analyses, and to Dr. S. SZABÓ and Z. DINYA for recording the IR spectra and assistance in their interpretation.

REFERENCES

1. Bognár, R., Kolodynska, Z., Somogyi, L., Györgydeák, Z., Szilágyi, L., N. Nemes, É.: Acta Chim. Acad. Sci. Hung. **62,** 65 (1969)
2. Beyer, H., Schultz, U.: Chem. Ber. **87,** 78 (1954)
3. Hurd, R. N., De La Mater, G.: Chem. Rev. **61,** 45 (1961)
4. Sprague, J. M., Land, A. H.: in Heterocyclic Compounds (Edited by R. C. Elderfield) Vol. **5,** p. 507. J. Wiley, New York, 1957
5. Kuhn, R., Drawert, F.: Ann. **590,** 55 (1954)
6. Hein, D. W., Alheim, R. J., Leavitt, J.: J. Am. Chem. Soc. **79,** 427 (1957)
7. Holan, G., Samuel, E. L., Ennis, B. C., Hinde, R. W.: J. Chem. Soc. **1967,** 20
8. Rao, C. N.: Chemical Applications of Infrared Spectroscopy, p. 325. Academic Press, New York, 1963
9. Katritzky, A. R., Ambler, A. P.: in Physical Methods in Heterocyclic Chemistry (Edited by A. R. Katritzky) p. 239. Academic Press, New York, 1963
10. Richtmyer, N. K., Hudson, C. S.: J. Am. Chem. Soc. **64,** 1612 (1942)
El-Khadem, H., El-Shafei, Z. M.: Tetrahedron Letters **1963,** 1887

Rezső Bognár
István Farkas
László Szilágyi
Márta Menyhárt
Éva N. Nemes
Ilona F. Szabó

Debrecen 10, Egyetem tér 1, Hungary

Acta Chimica Academiae Scientiarum Hungaricae, Tomus 62 (2), 191—212 pp. (1969)

IMPROVED SYNTHESES OF STEREOISOMERIC POLY-γ-GLUTAMIC ACIDS, I

SYNTHESES VIA POLYMETHYL ESTERS

M. KAJTÁR and V. BRUCKNER

(Institute for Organic Chemistry, L. Eötvös University, Budapest)

Received December 21, 1968

Syntheses of poly-γ-glutamic acid published earlier [4] have proved to be unsatisfactory for the practical preparation of this substance. Considering the possibilities of a better synthesis, the conclusion was drawn that the general scheme of the former syntheses could be adopted by substituting new methods for the earlier ones in every basic step of the synthesis. The new procedure for the preparation of poly-α-methyl-glutamate is based on the polyautoacylation reaction of the *p*-nitrophenyl and pentachlorophenyl ester salts of α,α'-dimethyl γ-glutamyl-glutamate (**X** and **XI**, respectively). An improved method was also elaborated for the synthesis of the four possible stereoisomers of the dipeptide active ester salts with a high grade of structural and optical purity. The poly-α-methyl-glutamates were obtained in fairly high yields (40—90%). Alkaline hydrolysis of the polyesters, followed by different methods of isolation, led to the stereoisomeric poly-γ-glutamic acids, namely, poly-γ-D-glutamic acid, poly-γ-L-glutamic acid, and the D—L and L—D mesoid poly-γ-glutamic acids in high yields (65—98%). The molecular weights of the different samples of both the polyesters (6—8000) and the polyacids (4—9000) were determined by two methods. The optical and structural purity of the polyacids were also studied. The observation that synthetic racemic poly-γ-glutamic acid (*i.e.* the equimolecular mixture of synthetic D- and L-poly-γ-glutamic acids) is practically insoluble in water may be regarded as a confirmation through synthesis of the earlier views relating to the structure of *subtilis* polypeptide. The mesoid polyacids, too, were found to be very scarcely soluble in water.

In the 1950's extensive research including degradative [1, 2] as well as synthetic [1, 3—6] investigations was made in this laboratory with the aim of elucidating the structure of bacterial polyglutamic acids [7]. In the course of this work, various types of polyglutamic acids, among them several stereoisomers of poly-γ-glutamic acid (**IV**) [4, 5]*, were synthesized. The comparison of the highly specific serological reaction of the different types of synthetic polyglutamic acids with that of the native substances led to unequivocal conclusions about the structure of the native polypeptides. These results were found to be in full agreement with those obtained by degradative studies, and so, the latter have also been confirmed by the synthesis [1, 4].

For further physico-chemical and serological studies, we needed a larger quantity of poly-γ-glutamic acid. Since the earlier methods did not seem satisfactory for the preparation of this substance on a larger scale, the development of a new synthesis more appropriate for this purpose became necessary.

*Poly-γ-L-glutamic acid was synthesized also by WALEY [8].

General considerations

As pointed out in our earlier investigations [3], the synthesis of poly-γ-glutamic acid cannot start from a simple derivative of glutamic acid with its amino or/and γ-carboxyl group suitably activated for a coupling reaction. Such a compound would undergo rather an intramolecular than an intermolecular reaction, *i.e.* instead of polymerizing, it would cyclize into a pyroglutamic acid derivative. Thus, for the synthesis of poly-γ-glutamic acid, one must take at least a γ-dipeptide derivative of glutamic acid into consideration as the starting material. On the basis of this reasoning, the earlier syntheses [4] were accomplished according to the general scheme summarized as follows.

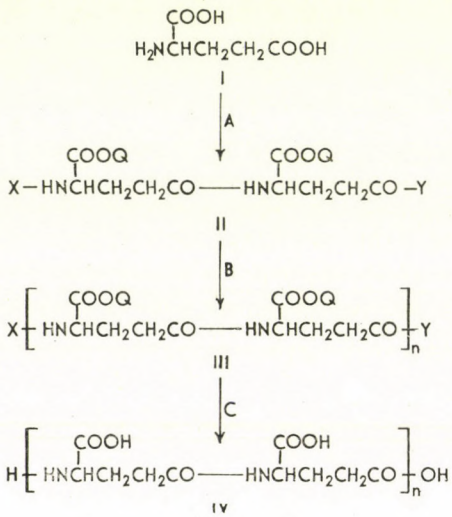

It seemed appropriate to adopt the same general scheme also in the new syntheses, provided that the insufficiencies in the single steps of the former synthesis would be eliminated, and more suitable methods would be substituted for the earlier ones. For this purpose, the following considerations were made.

(a) The dipeptide derivative **II** has to satisfy two main requirements to assure that the polymer **III** will not contain α-peptide bonds or any sort of chain branching. First, it must not contain any impurities of the corresponding α-isomer, and second, the aminolytic reactivity of its α- and γ-carboxyl groups (*i.e.* that of the appropriate derivatives of the carboxyl groups) should be widely different.

(b) The crucial step in the synthesis is reaction *B*, the conversion of the dipeptide derivative **II** into the poly-γ-glutamic acid derivative **III.** To obtain a polymeric product of high molecular weight, it is very important to avoid

side reactions. Thus, for performing this step, a perfectly unequivocal reaction must be chosen going as fast as possible and giving a high degree of conversion. In this respect the purity of the starting material (**II**) is also of utmost importance.

(c) In the last step of the synthesis, *i.e.* in the transformation of the poly-γ-glutamic acid derivative **III** into the free polyacid **IV** (step *C*) care must be taken that the peptide bonds already formed should not be damaged either by hydrolysis or by transpeptidation.

From the above considerations it is apparent that, though poly-γ-glutamic acid is built up of only one single amino acid, the general problems to be solved in its synthesis are similar to those emerging during the synthesis of polypeptides with known repeating sequence of amino acids [9, 10]. In both cases it is an oligopeptide (in our case a dipeptide) and not an amino acid derivative which is converted into a polypeptide. It may therefore be stated that the earlier syntheses of poly-γ-glutamic acid [4] are among the first examples for the solution of this synthetic problem (*cf.* [9]). In the last decade quite a lot of experience on the synthesis of "sequential polypeptides" has become available in the literature [9—14]. We could make good use of these results, too, in planning our new syntheses.

The first question to be settled was how to protect the α-carboxyl groups of the γ-glutamy -glutamic acid derivative **II.** It is well known that in the course of alkaline hydrolysis of peptides containing esterified α-aspartyl or α-glutamyl residues not only the hydrolysis of the ester groups, but also a partial isomerization of the α-linked residues into the corresponding ω-linked isomers take place [5]. Though the reverse isomerization of the ω-linked amino dicarboxylic acid residues into the α-isomers has not been observed with certainty as yet, the possibility of this reaction cannot be precluded. For this reason, we thought it advisable to look also for such ways of synthesis whose last step (reaction *C*) does not involve alkaline treatment. Therefore, in addition to new variations of the earlier syntheses [4] passing *via* polymethyl ester, we have also developed two other routes for the preparation of poly-γ-glutamic acid, namely *via* its polybenzyl and poly-*t*-butyl esters [16]. Accordingly, we synthesized three different types of the dipeptide derivative **II,** the α-carboxyl groups of which were protected by the three groups (Q) corresponding to the polyesters listed above.

Considering the possibilities [1, 4] for the transformation of the dipeptide derivatives **II** into the poly-γ-glutamic esters **III** (reaction *B*), we concluded that the most suitable method for this purpose would be the polyautoacylation reaction of an active ester of the dipeptide liberated from its salt by a tertiary base. Already in one of our earlier syntheses [4] we used α,α'-dimethyl γ-glutamyl-glutamate thiophenyl ester hydrobromide (**II**; Q = CH_3, Y = SC_6H_5, X = HBr.H) as the starting dipeptide derivative for the preparation of

poly-α-methyl-glutamate. In the present work, we chose the corresponding *p*-nitrophenyl and pentachlorophenyl ester salts as starting materials. The rate of aminolysis of a negatively substituted phenyl ester is at least three or four orders of magnitude higher than that of a methyl ester [17]. This difference in reactivity seemed to be sufficient to assure the selectivity required for the synthesis of a structurally pure γ-linked polypeptide. The application of the above two types of active esters as "polymerizing units" for the synthesis of sequential polypeptides was introduced and elaborated by DE TAR [10, 13] and by KOVÁCS [9, 12, 18] and their co-workers, respectively. In our case, the use of one or the other type of the active ester was in some instances limited by the esterifying groups on the α-carboxyls of the dipeptide derivative **II** (*cf.* [16]).

In recent years suitable new methods have been elaborated [19, 20] for the preparation of the α-esters of glutamic acid with a high grade of structural purity. This fact offered us a possibility to develop a new synthesis for the γ-glutamyl-glutamic acid derivatives as well (reaction *A*). Thus the preparation of these important starting compounds for the synthesis of poly-γ-glutamic acid in a form absolutely free from α-isomeric impurities (*cf.* [3, 4]) could be accomplished.

In the present paper we report a new synthesis of four stereoisomeric poly-γ-glutamic acids *via* their methyl esters. A preliminary paper on a part of this work has already been published [21]. Two other routes for the preparation of the polyacid through the corresponding polybenzyl and poly-*t*-butyl esters will be described later [16].

Synthesis of the dipeptide active ester salts

The preparation of the active ester salts of α,α'-dimethyl γ-glutamyl-glutamates of different configurations was accomplished in the following way.* The coupling of α-methyl N-carbobenzoxy-glutamate *p*-nitrophenyl ester (**V**) [20] with α-methyl glutamate (**VI**) [20] in dimethylformamide and in the presence of triethylamine resulted in the formation of α,α'-dimethyl N-carbobenzoxy-γ-glutamyl-glutamate (**VII**) in good yield. From the two antipodes of the glutamic acid derivatives **V** and **VI** all the four possible stereoisomers of **VII** were prepared. They are crystalline materials giving only single spots when chromatographed on thin layer. Their melting points are somewhat higher than those of the same substances prepared by the earlier method [3, 4]. The nitrophenyl and pentachlorophenyl esters **VIII** and **IX** were made from the dipeptide derivatives **VII** and the corresponding phenols with di-

*Abbreviations used in this paper conform to those recommended by the 5th European Peptide Symposium [22].

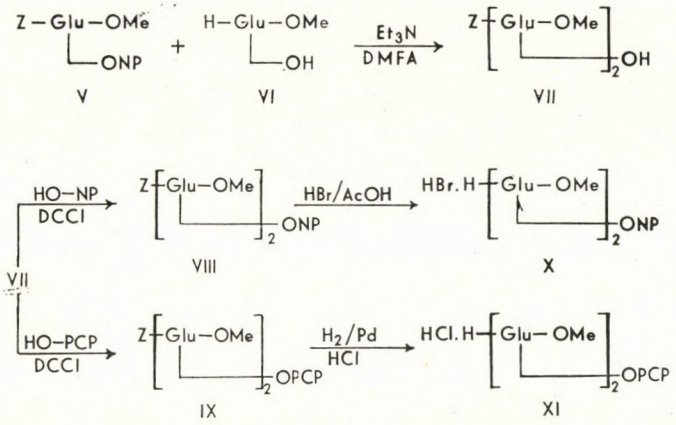

cyclohexylcarbodiimide as the condensing agent [23]. All stereoisomers of the protected dipeptide active esters **VIII** and **IX** crystallized well and were chromatographically pure. The carbobenzoxy group of the nitrophenyl ester **VIII** was removed by acidolysis with hydrogen bromide in glacial acetic acid [24]. The resulting nitrophenyl ester hydrobromides (**X**), the D—D and L—L isomers of which were prepared, were isolated as hygroscopic amorphous powders which could neither be crystallized nor analysed; they proved, however, to be homogeneous by thin-layer chromatography. The splitting of the N-protecting group of the dipeptide pentachlorophenyl ester **IX** was carried out by catalytic hydrogenation in the presence of slightly more than one mole of hydrogen chloride [9]. In contrast to the nitrophenyl ester hydrobromides (**X**), the pentachlorophenyl ester hydrochlorides of the four stereoisomeric α,α'-dimethyl γ-glutamyl-glutamates (**XI**) were chromatographically pure crystalline substances with sharp melting points; their elemental composition was found to be in good agreement with the calculated values.

Polymerization of the dipeptide active ester salts

The polymerization (or rather polyautoacylation) of the dipeptide active ester salts was performed in dimethylformamide or dimethyl sulfoxide solution (concentration 1—3 mmoles/ml) in the presence of 2—2.5 equivalents of triethylamine at room temperature or at 100° C. Under these conditions the following reaction takes place.

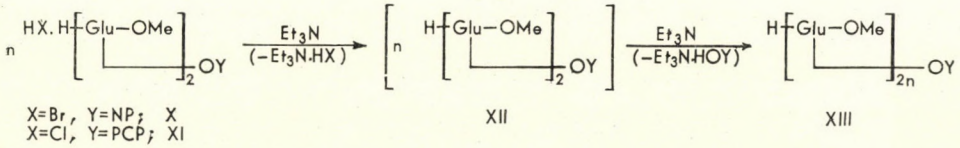

X=Br, Y=NP; X
X=Cl, Y=PCP; XI

XII

XIII

The best reaction parameters for the polymerization were determined in the case of both types of the starting dipeptide active ester salt. In selecting the convenient solvent, one must take into consideration that it has to dissolve readily both the dipeptide active ester salt and the polyester. The high solubility of the starting material is required to avoid the cyclization process competing with the polymerization in a dilute solution. The initial concentration should, therefore, be as high as possible. Early precipitation of the end product, on the other hand, would cause the polymerization reaction to break off and lead to polymers of low molecular weights. The solubility of the polymer is the other factor that determines the optimal concentration of the polymerizing reaction mixture. — For the polymerization of the nitrophenyl ester hydrobromides (**X**), warming in dimethylformamide solution proved to be the best method. On the other hand, the pentachlorophenyl ester hydrochlorides (**XI**) gave, under the same conditions, impure polymeric products. In the latter case, stirring the dimethyl sulfoxide solution of the dipeptide derivative (**XI**) at room temperature was found to be more advantageous (see Table I).

The progress of polymerization was followed semiquantitatively by spectroscopic measurements. In the IR spectrum of the dipeptide pentachlorophenyl ester hydrochloride (**XI**) in dimethyl sulfoxide two CO bands appeared: a more intense band at 1750 cm^{-1} due to the methyl ester groups, and a weaker one at 1780 cm^{-1} corresponding to the carbonyl group of the pentachlorophenyl ester. In a sample taken from the reaction mixture 5 minutes after the addition of the base, the intensity of the active ester band was only about 5—10% of the original value, and after 30 minutes no peak or shoulder appeared in the spectrum of the polymerization mixture at 1780 cm^{-1}. This experiment allowed us to conclude that in the first half an hour the polymerization reaction went almost to completion (at least in 98%).* In the case of the starting dipeptide derivatives **XI** of D—D or L—L configuration, however, the reaction mixture turned into an unstirrable gel only after 6—8 hours. This means that either the formation of the gel requires a longer time, or some chain growth has taken place even after 30 minutes. The mesoid (D—L and L—D) poly-α-methyl-glutamates are less soluble in dimethyl sulfoxide, and so they precipitate from the reaction mixture within one or two hours. This fact is possibly responsible for the somewhat lower molecular weights of these polyesters when compared with those built up from α-methyl glutamate residues of identical configuration (see Table I). The isolation of the polyesters was accomplished by diluting the reaction mixtures with ether and washing the precipitated substances with different solvents to eliminate by-products (see Experimental).

*The experimental error of the spectroscopic determination of the active ester group was about 2%.

The identification of the polyesters was made by elemental analysis. The number average molecular weights of the different preparations were calculated from the amino nitrogen contents determined by a modified VAN SLYKE method [25]. It may be noted that, according to the equation of the polymerization reaction (p. 195), the polyester should still contain one nitrophenyl or pentachlorophenyl ester group per molecule (**XIII**), and so, its molecular weight should also be determinable by the analysis of an element or functional group (chlorine or nitro group) characteristic of the active ester. However, our experiments showed that, though the polyester contains equal number of N-terminal and C-terminal groups, the molecular weights calculated from the active ester content (*e.g.* from the chlorine content of the polymer) were much higher than those obtained from the amino nitrogen values (*e.g.* 85,000 and 9,000 againts 6,400 and 5,600, respectively). This contradiction can probably be explained by the partial hydrolysis of the active ester group during the isolation and purification of the polyester.

Table I

Reaction conditions of the preparation and molecular weights of stereoisomeric poly-α-methyl-glutamates

No.	Starting dipeptide active ester salt		Solvent; temperature, °C	Yield, %	Amino-N, %	Number average molecular weight
	Structure	Configuration				
1	X	L—L	DMFA, 100°	44	0.19	7400
2			DMFA, 20°	39	0.56	2500
3			DMSO, 20°	23	1.86	750
4		D—D	DMFA, 100°	38	0.20	7000
5	XI	L—L	DMFA, 100°	80[a]	0.23	6100
6				27[b]	0.16	8800
7		D—D		90	0.22	6400
8		L—D	DMSO, 20°	80	0.25	5600
9		D—L		81	0.26	5400

a) dark coloured, impure product; b) washed with water.

The reaction conditions of the different polymerization experiments, together with the yields and molecular weights of the products are summarized in Table I. The analytical values of one representative poly-α-methyl-glutamate sample can be found in the Experimental. The data in Table I show that the pentachlorophenyl ester hydrochlorides of the stereoisomeric α,α'-dimethyl

γ-glutamyl-glutamates (**XI**) are — in respect of the yield — better starting materials for the practical synthesis of poly-α-methyl-glutamate, than the corresponding nitrophenyl ester hydrobromides (**X**).

Preparation of the free poly-γ-glutamic acids

In order to prepare poly-γ-glutamic acids, the polymethyl esters were hydrolyzed with 0.25*N* sodium hydroxide solution at 100° C for 45 minutes. The free polyacids were isolated from the hydrolyzate in different ways. The first method was the same as that used in the earlier syntheses [4]. The insoluble copper(II) salt of the polyacid was precipitated at pH 6; it was then dissolved in dilute hydrochloride acid, the solution demetallized by hydrogen sulfide, dialyzed against distilled water for several days, and finally freeze-dried. The other way for isolating the polyacid was the acidification of the hydrolyzate with ion exchange resin (Amberlite IR-120 in hydrogen cycle), and the subsequent freeze-drying of the solution without dialysis. The mesoid poly-γ-glutamic acids, being very poorly soluble in water, could be precipitated from the hydrolyzate also by simple acidification with hydrochloric acid. The yields of the isolation of the polyacids — depending on whether they had been dialyzed or not — varied between about 50 and nearly 100% of the theoretical (see Table II).

The poly-γ-glutamic acids are solid foams or amorphous white powders. All the samples contain some water which cannot be removed without damaging the polymer itself.

Four stereoisomers of poly-γ-glutamic acid were prepared through the new synthesis, namely poly-γ-D-glutamic acid, poly-γ-L-glutamic acid, and the D—L and L—D mesoid poly-γ-glutamic acids, *i.e.* poly-(γ-D-glutamyl-L-glutamic acid) and poly-(γ-L-glutamyl-D-glutamic acid). All of these substances had already been synthesized earlier [4, 5], but in considerably poorer yields.

Properties of the synthetic poly-γ-glutamic acids

(a) Solubility — In contrast to poly-γ-D-glutamic acid and poly-γ-L-glutamic acid, both readily soluble in water, their equimolecular mixture, *i.e.* the racemic poly-γ-glutamic acid is practically insoluble. Acidification of a solution of equimolecular quantities of sodium poly-γ-glutamate of D- and L-configuration results in the precipitation of the racemic polyacid. These findings are of some importance in connection with the solubility properties of *subtilis* polypeptide as well. It has been reported by THORNE and LEONARD [26] that the polyglutamic acid excreted by *Bac. subtilis* into the culture media contains various amounts of both D- and L-glutamic acid residues. The ques-

Table II

Reaction conditions of the preparation and molecular weights of stereoisomeric poly-γ-glutamic acids

No.	Confign.	Starting polyester[a]	Method of isolation	Yield,[g] %	Amino-N, %	Number average molecular weight	
						Calcd. from the amino-N	Calcd. from the ninhydrin reaction[h]
1	L	1	Cu-salt[b] D[c]	65	—	—	4100
2	L	2	resin[d] ND[e]	90	0.56	2500	2500
3	L	3	resin, ND	90	0.34	4100	3700
4	D	4	Cu-salt, D	68	0.37	3800	4100
5	L	5	Cu-salt, D	20	0.47	3000	5000
6	L	6	resin, ND	95	0.15	9300	9400
7	D	7	Cu-salt, ND	53	0.28	5000	4900
8	L—D mesoid	8	Cu-salt, ND	72	—	—	7100
9	L—D mesoid	8	resin, ND	98	—	—	5900
10	D—L mesoid	9	HCl[f] ND	60	—	—	6100
11	D—L mesoid	9	resin, ND	70	—	—	7100

a) The numbers refer to those of Table I; b) method *(a)* (see Experimental); c) dialyzed; d) method *(b)* (see Experimental); e) not dialyzed; f) method *(c)* (see Experimental); g) relating to the polyester; h) for details, see Table VIII.

tion, whether the glutamic acid residues of antipodal configuration are built into one single polypeptide molecule in various ratios, or the *subtilis* polypeptide is a mixture of different amounts of the two antipodal poly-γ-glutamic acids each built up entirely of either D- or L-glutamic acid residues, was solved by them on the basis of the following observations. Upon acidification of a solution of the sodium salt of *subtilis* polypeptide, a part of the free polyacid precipitated. Acid hydrolysis of this insoluble fraction led to inactive, *i.e.* racemic glutamic acid. The soluble fraction of the polypeptide, in turn, proved to be composed predominantly either of D- or L-glutamic acid, depending on which of the two stereoisomeric glutamic acid residues was present in a higher

amount in the original *subtilis* polypeptide. From this and other even more convincing evidences obtained from the results of experiments made with the isotope dilution technique, the authors have concluded that the *subtilis* polypeptide is a mixture of D- and L-poly-γ-glutamic acids. Our observations on the solubility of the synthetic racemic poly-γ-glutamic acid are in agreement with the facts outlined above, and so, they may be considered as a confirmation through synthesis of the earlier conclusions concerning the structure of *subtilis* polypeptide.

Similarly to the racemic poly-γ-glutamic acid, also the mesoid poly-γ-glutamic acids are very poorly soluble in water (their solubility is max. 1—2 mg/ml)*. It would be interesting to study the structural and associative forces responsible for this great difference in the solubility between the poly-γ-glutamic acids with asymmetric centres of uniform configuration on the one hand, and the racemic or the mesoid forms on the other, since there is no substantial difference in the molecular weights of the two types of polyacid. The polyglutamic acid isolated from the cultures of *Bac. megaterium* [27] contains D- and L-γ-glutamyl residues built in 1:1 ratio into the same peptide chain, thus being probably a mesoid poly-γ-glutamic acid. Unfortunately, no data on the solubility of this natural polypeptide in dilute acid can be found in the literature.

(b) Molecular weight — The number average molecular weights of the different samples of poly-γ-glutamic acids were determined by two methods.

(1) The amino nitrogen contents of the polyacids were determined by a modification of the VAN SLYKE method introduced by KAINZ *et al.* [25]. It was found that this modified procedure can also be used in the case of γ-glutamyl peptides [28], formerly inaccessible to analysis because of their stepwise degradation under the reaction conditions of the original VAN SLYKE method [29]. The molecular weights calculated from the amino nitrogen contents are presented in Table II.

(2) Another simple method for the determination of the free amino groups was based on the spectrophotometric measurements of the colour intensity of the ninhydrin reaction of polyglutamic acid solutions [30]. Solutions of known concentration of glutamic acid and of a series of γ-linked oligopeptides [31] were used for calibrating the method. It was found that the "colour yield" of the ninhydrin reaction in the case of the oligopeptides was, on an average, only 87% of that given by the glutamic acid solution of equal molar concentration. This discrepancy is probably to be attributed to the water content of the oligopeptides the exact amount of which could not be determined so far. As the polypeptides may contain about the same amount

*The insolubility of the mesoid poly-γ-glutamic acids was not observed in the course of our earlier work [4, 5], probably because of the low molecular weights of the products synthesized at that time.

of water (see below), the calculation of the molecular weights of the polyglutamic acids was based on the "colour yield" of the oligopeptides. The molecular weights determined by this method are also listed in Table II.

It can be seen that the molecular weight data obtained by the two methods are in fairly good agreement in some of the cases, while in others, there is a substantial difference between them. The situation is about the same when correlating the molecular weights of the polyacids with those of the corresponding polyesters. It cannot be told whether these discrepancies only arise from experimental error or they have some other origin as well. It should, however, be borne in mind that the accurate determination of the molecular weights with values between about 2000 and 10 000, is a rather difficult task. Our molecular weight data might therefore be considered only as approximate values. Experiments, with the aim of determining the molecular weights and the degrees of dispersity of the different polyglutamic acids more accuraetly, are in progress.*

As regards the relative molecular weights of the poly-γ-glutamic acids prepared by different ways, the method *via* the pentachlorophenyl ester seems to be superior to that *via* the nitrophenyl ester.

(c) Structural and optical purity — According to the elemental analysis, all samples of poly-γ-glutamic acid contain some water, but its exact amount has not been determined so far. The values for the water content calculated independently from the carbon, the hydrogen or the nitrogen content of the same sample do not agree with one another satisfactorily, and, what is even more surprising, the oxygen content which should be the most sensitive to water content, could not be determined accurately at all. All values obtained for the oxygen content of the free polyacids were unreasonably low. The cause of this very surprising fact is yet unknown. In consequence of these difficulties, the exact polypeptide content of our samples are not known. We can obtain the best agreement with the analytical figures by calculating with one mole of water per two glutamyl residues. This corresponds to about 6—7% of water in the polyacid.

The optical purity of poly-γ-L-glutamic acid was tested by total hydrolysis. A solution of the polyacid in 3*N* hydrochloric acid was heated at 100 °C for 3 hours. The optical rotatory dispersion of the hydrolyzate was measured between 588 and 280 nm, and compared with the ORD curves of two glutamic acid solutions of the same molar concentration, one of which had been treated

**Note added in proof.* Recent fractionation experiments made on a Sephadex G-50 column have shown that the undialyzed, high molecular weight samples of synthetic poly-γ-glutamic acid contain some sort of ninhydrin negative, low molecular weight substance, very probably of cyclopeptide nature, in a rather high quantity. According to this finding, the molecular weight data, higher than 5000, determined by amino-nitrogen analysis (either by the VAN SLYKE or the ninhydrin method) should be taken as, very probably, erroneous. Further investigations of this kind are in progress and will be published later.

under the conditions of the hydrolysis, and the other had not. The optical rotation of the hydrolyzate was found to amount to 94 $\pm 1\%$ of those of the two standard solutions. The latter solutions gave two identical dispersion curves showing that no racemization of the glutamic acid occurred during the acid hydrolysis. The glutamic acid content of the hydrolyzate (and, for comparison, also that of the standard solutions) was determined by the micro KJELDAHL method [32], and was found to be 94 $\pm 3\%$ of the value calculated from the weight of the polyglutamic acid (and from the glutamic acid content of the standards). This is in agreement with the estimated water content of the polymer. On the basis of these experiments, the conclusion can be drawn that — at least between the limits of the experimental error — our poly-γ-glutamic acid can be considered as optically pure. This means that no racemization took place in the course of the synthesis.

The specific rotation of the synthetic poly-γ-D-glutamic acid ($[\alpha]_D^{20}$ $+24.1°$) agrees quite well with the value ($[\alpha]_D^{20}$ $+23.5°$) described for the native *anthrax* polypeptide [4, 7]. Analysis of the optical rotatory dispersion of the poly-γ-glutamic acids and their esters together with the corresponding oligomers has already been published [33], and will be described in a more detailed form elsewhere. All results of these investigations seem to confirm the above conslusion that the polyglutamic acids synthesized by us are optically pure.

The structural homogeneity of the synthetic poly-γ-glutamic acids prepared by alkaline hydrolysis of the polymethyl ester has already been studied earlier [4], but, as a matter of fact, no absolutely conclusive results could be obtained thus far. The results of the total hydrolysis seem to be of interest in this respect, too. Though already the good agreement between the rotatory dispersion curve of the hydrolyzate and those of standard glutamic acid solutions can be taken as a proof for the completeness of the hydrolysis (since the optical rotations of the γ-oligopeptides of glutamic acid are either of opposite sign or, at least, of much less absolute value in this spectral range [33]), the hydrolyzate was also tested by thin-layer chromatography. No spots, however, beside that of glutamic acid, could be detected on the chromatogram. From the fact that the hydrolysis of the polyglutamic acid was complete under the very mild conditions used by us, we might also conclude that no (or at least very few) α-glutamyl linkages are to be encountered in the polyacid. The proneness of polyglutamic acid to hydrolyze readily under mild acidic conditions has been considered as a proof of the γ-linked structure also in the examination of the native polypeptide [34].

The results of our experiments on oligomeric model substances [31] showed, that, at least in those instances, apparently no significant transpeptidation occurred. The comparison of polyglutamic acids prepared from polyesters of different types seems also to confirm this conclusion [16]. However, the

question of $\gamma \rightarrow \alpha$ transpeptidation can by no means be regarded as settled, and requires further study. Such work is under way in our laboratory.

Experimental

The m.p.'s are uncorrected and were taken on a Tottoli apparatus. The optical rotations were measured on a visual polarimeter (Schmidt—Haensch) using a sodium lamp. Before microanalysis, the samples were dried in a vacuum desiccator over phosphorus pentoxide for 8—10 hrs at a temperature adjusted to the melting points of the single substances (50—100° C). Thin-layer chromatograms were made on silica gel (Kieselgel-G nach Stahl, Merck) using the following solvent mixtures:

a) *n*-butyl alcohol–pyridine–acetic acid–water (30 : 20 : 6 : 24),
b) *n*-butyl alcohol–acetic acid–water (4 : 1 : 1)
c) chloroform–methyl alcohol–acetic acid (75 : 20 : 5)
d) chloroform–hexane–acetic acid (8 : 1 : 2)

For the preparation of all the stereoisomers of the different compounds only one description is given. Any occasional differences in the work-up procedure are noted. The physical constants and analytical data of the single stereoisomers are summarized in Tables connected to the corresponding descriptions.

α-Methyl N-carbobenzoxy-D-glutamate dicyclohexylammonium salt

From 120 g of N-carbobenzoxy-D-glutamic acid anhydride — according to the method of KLIEGER and GIBIAN [20] — 98 g of α-methyl N-carbobenzoxy-D-glutamate dicyclohexylammonium salt was obtained. Yield : 44%; m.p. 178—180° C; $[\alpha]_D^{20}$ + 11.2° (*c* 2, methanol). The physical constants described [20] for the L-antipode are: m.p. 172—173° C; $[\alpha]_D^{20}$ —10.9° (*c* 1.02, methanol).

$C_{26}H_{40}N_2O_6$ (476.6). Calcd. C 65.52; H 8.46; N 5.88; OCH_3 6.52. Found C 65.57; H 8.44; N 5.53; OCH_3 6.59%.

α-Methyl N-carbobenzoxy-D-glutamate

The method of preparation differed slightly from that described for the L-isomer by KLIEGER and GIBIAN [20]. The above dicyclohexylammonium salt (80 g) was suspended in a mixture of ether (680 ml) and 1*N* H_2SO_4 (450 ml). The mixture was shaken for a few minutes until the crystals completely dissolved. After the separation of the phases, the ether solution was washed with three 100-ml portions of water, dried over anhydrous $MgSO_4$, and evaporated to dryness under reduced pressure. The remaining colourless oil soon crystallized. Yield: 48 g (97%); m.p. 68—69 °C. Recrystallization of a sample (8 g) from ethyl acetate (8 ml) and petroleum ether (8 ml) gave 4.8 g (60%) of the purified substance; m.p. 69—71° C; $[\alpha]_D^{20}$ +24.7° (*c* 1.0, methanol). The physical constants described [20] for the L-antipode are: m.p. 68—69° C (after recrystallization); $[\alpha]_D^{25}$ —25.9° (*c* 1.06, methanol).

$C_{14}H_{17}NO_6$ (295.3). Calcd. C 56.94; H 5.80; N 4.74. Found C 57.18; H 6.10; N 4.90%.

α-Methyl N-carbobenzoxy-D-glutamate *p*-nitrophenyl ester (V)

The method of preparation was the same as that described by KLIEGER and GIBIAN [20] for the L-antipode. From 32.5 g (0.11 mole) of α-methyl N-carbobenzoxy-D-glutamate 34 g (82%) of the nitrophenyl ester was obtained; m.p. 93—94° C; $[\alpha]_D^{20}$ +9.6° (*c* 1.2, acetic acid). The physical constants of the L-antipode [20] are: m.p. 91—92° C; $[\alpha]_D^{25}$ —9.9° (*c* 1, acetic acid).

$C_{20}H_{20}N_2O_8$ (416.4). Calcd. C 57.69; H 4.84; N 6.73; OCH_3 7.45. Found C 57.85; H. 5.12; N 6.68; OCH_3 7.62%.

α-Methyl D-glutamate (VI)

This substance was prepared according to the method of KLIEGER and GIBIAN [20]. Catalytic hydrogenation of 15 g (0.05 mole) of α-methyl N-carbobenzoxy-D-glutamate gave

6.9 g (85%) of the free semiester; m.p. 148—149° C; $[\alpha]_D^{20}$ —34.0° (*c* 3.8, water); R_F(a) 0.78, R_F(b) 0.79. The physical constants described [20] for the corresponding L-antipode are: m.p. 149—150° C; $[\alpha]_D^{25}$ +35.1° (*c* 2.01, water),

$C_6H_{11}NO_4$ (161.2). Calcd. C 44.71; H 6.88; N 8.69; OCH_3 19.26. Found C 44.83; H 6.75; N 8.54; OCH_3 19.03%.

α,α′-Dimethyl N-carbobenzoxy-γ-glutamyl-glutamate (VII)

α-Methyl glutamate (**VI**) (6.5 g; 40 mmoles) and triethylamine (5.5 ml; 40 mmoles) were added to a solution of α-methyl N-carbobenzoxy-glutamate *p*-nitrophenyl ester (**V**) (15.0 g; 36 mmoles) in dimethylformamide (100 ml). The suspension was stirred for 5 hrs at room temperature. By the end of this period α-methyl glutamate dissolved almost completely. The reaction mixture was allowed to stand overnight and then evaporated under reduced pressure. The oily residue was taken up in ethyl acetate (250 ml) and washed with 1*N* HCl (3×50 ml) and 10% NaCl solution (3×50 ml). The ethyl acetate solution, after being dried over anhydrous Na_2SO_4, was evaporated under reduced pressure. The oily residue — which sometimes crystallized — was dissolved in hot ethyl acetate (50 ml) to which petroleum ether (50 ml) was added. After standing overnight, the precipitated crystals were collected, washed with a cold mixture (50 ml) of ethyl acetate–petroleum ether (1 : 1), and dried. The yield was 13.4 g (85%).

Table III

Physical constants and elemental analyses of stereoisomers of **VII**

Confign.	M. p., °C		$[\alpha]_D^{20}$ (*c* 10, MeOH)		R_F (a)	Analysis			
		lit. [4]		lit. [4]		C%	H%	N%	OCH_3%
D—D	112—113°	109—110°	+28.0°	+28.3°	0.89	55.28	5.83	6.25	14.60
L—L	110—112°	109—110°	—28.1°	—28.3°	0.89	55.00	6.37	6.30	14.70
D—L	139—141°	—	— 3.7°	—	0.88	54.80	5.81	6.56	14.50
L—D	139—141°	136—137°	+ 3.5°	+ 4.3°	0.88	55.30	5.89	6.31	14.79
Calcd. for $C_{20}H_{26}N_2O_9$ (438.4)						54.79	5.98	6.39	14.16

α,α′-Dimethyl N-carbobenzoxy-γ-glutamyl-glutamate *p*-nitrophenyl ester (VIII)

To a solution of α,α′-dimethyl N-carbobenzoxy-γ-glutamyl-glutamate (**VII**) (13.1 g; 30 mmoles) and *p*-nitrophenol (3.7 g; 27 mmoles) in tetrahydrofurane (60 ml) dicyclohexylcarbodiimide (5.6 g; 27 mmoles), dissolved in a few ml of tetrahydrofurane, was added. The solution was stirred for 5 hrs at room temperature and then let to stand overnight. (Dicyclohexylurea began to separate in the first minutes of stirring.) After cooling for a short time, the dicyclohexylurea was filtered off (4.9 g; 80%), and the solution evaporated under reduced pressure. The resulting yellow oil was dissolved in chloroform (300 ml) and the solution washed with 5% K_2CO_3 solution (3×50 ml), 10% NaCl solution (3×50 ml), then with 0.5 *N* HCl (50 ml), and finally with water (50 ml). The chloroform solution was dried over anhydrous Na_2SO_4. After evaporation of the solvent under reduced pressure, there remained a crystalline mass which — in the case of the D—D and L—L stereoisomers — was dissolved in hot ethyl alcohol (120 ml), and the solution was allowed to cool slowly to room temperature. (The crude crystalline material could be dissolved in half of the amount of alcohol as given above, but at such a concentration the material would separate in too fine crystals to allow complete removal of the solvent. The poor ability to crystallize is responsible for the low yield of the purified substance.) After standing overnight, the crystals were separated, washed with alcohol (30 ml) and dried. The yield of the pure nitrophenyl ester (**VIII**) was 8.2 g (55%). The D—L isomer of the crude dipeptide nitrophenyl ester was crystallized from much less alcohol (15—20 ml). The yield of the pure substance was 9.5 g (63%).

Table IV

Physical constants and elemental analyses of stereoisomers of **VIII**

Confign.	M. p., °C	$[\alpha]_D^{20}$ (EtOH)	R_F (d)	Analysis			
				C%	H%	N%	O%
D—D	133—134°	+26.1° (*c* 4.5)	0.75	55.78	5.33	7.69	11.21
L—L	135—136°	—27.2° (*c* 3.8)	0.75	55.83	5.92	7.39	11.24
D—L	126—128°	— 9.0° (*c* 2.0)	0.75	55.45	5.73	7.40	11.75
Calcd. for $C_{26}H_{29}N_3O_{11}$ (559.5)				55.81	5.22	7.51	11.12

α,α′-Dimethyl γ-glutamyl-glutamate *p*-nitrophenyl ester hydrobromide (X)

The protected dipeptide nitrophenyl ester (**VIII**) (13.7 g; 24.5 mmoles) was dissolved in glacial acetic acid containing 28% of HBr (130 ml). The initial vigorous evolution of carbon dioxide ceased in 15—20 min. After standing for 40 min. at room temperature, the yellowish solution was poured into anhydrous ether (1.5 l). The precipitated hydrobromide was thoroughly rubbed with the solvent and then filtered off by suction as fast as possible. It was immediately placed into a vacuum desiccator and dried over cc. H_2SO_4 and KOH for a night. The dipeptide nitrophenyl ester hydrobromide was a very hygroscopic, amorphous, slightly yellow powder. The yield was 12 g (97%), R_F(c) 0.32. The substance could not be analyzed and was polymerized without further purification.

α,α′-Dimethyl N-carbobenzoxy-γ-glutamyl-glutamate pentachlorophenyl ester (IX)

Dicyclohexylcarbodiimide (2.7 g; 13 mmoles) in a few ml of dimethylformamide was added to a stirred solution of α,α′-dimethyl N-carbobenzoxy-γ-glutamyl-glutamate (**VII**) (6.6 g; 15 mmoles) and pentachlorophenol (3.5 g; 13 mmoles) in dimethylformamide (50 ml). The solution was stirred for 3 hrs at room temperature and then let to stand overnight. After being cooled for a few hours, the solution was filtered from the separated dicyclohexylurea crystals (2.6 g; 88%) and evaporated under reduced pressure (less than 1 mm). The oily residue was taken up in chloroform (150 ml) and extracted with three 30-ml portions of 5% K_2CO_3 solution, water (2×30 ml), 30 ml of 0.5*N* HCl, and finally with 30 ml of water. The chloroform solution was dried over anhydrous $MgSO_4$ and then evaporated *in vacuo*. The crude material was crystallized from ethyl acetate (100 ml) to give 6.2 g (70%) of the pure pentachlorophenyl ester (**IX**) in the case of the D—D and the L—L isomers; the mesoid type dipeptide active esters (D—L and L—D) were purified by crystallization from benzene (120 ml), to obtain 7.2 g (81%) of the pure substances.

Table V

Physical constants and elemental analyses of stereoisomers of **IX**

Confign.	M. p., °C	$[\alpha]_D^{20}$ ($CHCl_3$)	R_F (d)	Analysis				
				C%	H%	N%	O%	Cl%
D—D	161 —162.5°	—13.7° (*c* 1.5)	0.85	45.73	3.85	4.09		26.20
L—L	161.5—162.5°	+13.5° (*c* 1.6)	0.85	45.72	3.53	4.45	20.97	25.65
D—L	131 —135°	+ 6.2° (*c* 5.0)	0.88	45.96	4.03	4.04		25.90
L—D	134 —136°	— 6.5° (*c* 5.0)	0.88	45.25	3.91	4.10	20.60	25.90
Calcd. for $C_{26}H_{25}N_2O_9Cl_5$ (686.8)				45.47	3.67	4.08	20.97	25.81

α,α′-Dimethyl γ-glutamyl-glutamate pentachlorophenyl ester hydrochloride (XI)

A solution of the protected dipeptide pentachlorophenyl ester (**IX**) (6.9 g; 10 mmoles) in dimethylformamide (100 ml) was mixed with methanol (10 ml) containing hydrogen chloride (0.73 g; 20 mmoles), palladium(10%)-on-charcoal catalyst (1 g) was added, and the suspension was shaken in a stream of hydrogen until no more carbon dioxide could be detected in the departing gas (about 2—3 hrs). The catalyst was filtered off, and the solution evaporated to dryness under reduced pressure (less than 1 mm). The remaining crystalline substance was dissolved in hot dimethylformamide (25 ml), and the solution carefully diluted with ethyl acetate (50 ml). Crystallization of the dipeptide active ester salt began immediately. The slurry was allowed to stand at room temperature, then the crystals were filtered off, washed with ethyl acetate (25 ml) and dried on a steam bath. The white crystalline product weighed 5.1 g (89%).

Table VI

Physical constants and elemental analyses of stereoisomers of **XI**

Confign.	M. p., °C (decomp.)	$[\alpha]_D^{20}$ (*c* 5; DMFA)	R_F (c)	Analysis					
				C%	H%	N%	Cl%	Cl% (ionic)	OCH_3%
D—D	202—203°	+11.1°	0.39	37.28	3.54	4.92	35.92	6.05	10.80
L—L	204—205°	—11.4°	0.39	36.87	3.32	5.22	36.07	6.03	10.80
D—L	194—195°	—16.9°	0.42	36.69	3.50	4.60	35.77	6.09	10.70
L—D	195—197°	+16.5°	0.42	37.19	3.57	5.04	36.00	6.06	10.80
Calcd. for $C_{18}H_{20}N_2O_7Cl_6$ (589.1)				36.70	3.42	4.72	36.11	6.02	10.54

Stereoisomeric poly-α-methyl-glutamates (XIII)

Polymerization of the D-D and L-L stereoisomers of α,α′-dimethyl γ-glutamyl-glutamate *p*-nitrophenyl ester hydrobromide (X)

The dipeptide nitrophenyl ester hydrobromide (**X**) was dissolved in dimethylformamide or dimethyl sulfoxide. If the polymerization was effected with warming, the starting concentration of the solution was 3 mmoles/ml. For polymerization experiments carried out at room temperature, solutions of a concentration of only 1 mmole/ml could be used, since more concentrated solutions cannot be made at room temperature.

To the solution of the active ester salt (**X**) 2.2 equivalents of triethylamine were added; some triethylammonium bromide separated immediately. In the case of the polymerizations of the first type, the reaction mixture was warmed for 6—8 hrs on a boiling water bath. The solution turned gradually darker in colour and more and more viscous in consistence. In the polymerizations of the second type, the mixture was stirred at room temperature for 8—10 hrs and then let to stand for 2 days. No noticeable coloration of the solution was observed in these instances. After the polymerization had gone to completion, the reaction mixture was diluted with ten volumes of ether. The polyester and the triethylammonium bromide separated in the form of a viscous mass which was rubbed with several portions of ether to obtain a dry powder. For eliminating the triethylammonium bromide, the crude product was thoroughly triturated several times with acetone. The polyester was washed with ether and dried in a vacuum desiccator. The resulting poly-α-methyl-glutamate was obtained as a slightly coloured amorphous powder in 23—44% yield (see Table I, Nos 1—4).

Polymerization of the stereoisomers of α,α′-dimethyl γ-glutamyl-glutamate pentachlorophenyl ester hydrochloride (XI)

(a) To a solution of the dipeptide pentachlorophenyl ester hydrochloride (**XI**) in dimethylformamide (concentration 1 mmole/ml) 2.4 equivalents of triethylamine were added, and the solution was warmed on a steam bath for 8 hours. The solution, from which triethylammonium

chloride crystals had separated, turned gradually darker and became fairly viscous by the end of the reaction. The bulk of dimethylformamide was distilled off under reduced pressure, and the residue rubbed to a powder with a large amount of anhydrous ether. The product was suspended in hot chloroform and filtered off. This procedure was repeated several times for the elimination of triethylammonium chloride. The substance was finally washed with ether and dried. The resulting polyester was isolated as a brownish powder in a yield of 80% (see Table I, No. 5). This product proved to be impure, and the polyacid could be prepared from it only in very poor yield (*cf.* Table II, No. 5).

(b) The corresponding stereoisomer of the dipeptide pentachlorophenyl ester hydrochloride (**XI**) was dissolved in dimethyl sulfoxide. The concentration of the solution was 1 mmole/ml in the case of the D—D and L—L stereoisomers and 0.8 mmole/ml in the case of the D—L and L—D stereoisomers. After the addition of 2.2 equivalents of triethylamine, the solution was stirred at room temperature until it changed into an unstirrable gel. (This occurred in the course of the polymerization of the mesoid type active ester salts in about ½—1 hr., while the solutions of the D—D or L—L stereoisomers could be stirred for about 5—6 hrs.) The reaction mixture was let to stand for 1—2 days at room temperature, and then diluted with ether. The precipitated viscous mass was rubbed with several portions of ether until it turned into a powder. For eliminating the by-products (triethylammonium chloride, pentachlorophenol), the substance was washed several times with hot chloroform, then with acetone, and finally with ether. The mesoid poly-α-methyl-glutamates are practically insoluble in water, so they were washed with water instead of chloroform. (In a case when the poly-α-methyl-L-glutamate was washed with water, a very poor yield was obtained; *cf.* No. 6 in Table I.) The polyester was obtained in the form of amorphous white powders in yields of 80—90% (see Table I, Nos. 6—9). The elemental analysis of one representative sample of poly-α-methyl-glutamate (No. 7 in Table I) is presented below.

$(C_6H_9NO_3)_n$ (143.1)$_n$. Calcd. C 50.34; H 6.34; N 9.79; CH_3O 21.68. Found C 49.87; H 6.51; N 9.75; CH_3O 21.80; Cl 0.20%.

Observation of the progress of polymerization by IR spectroscopy

Samples of 0.1 ml were withdrawn from the dimethyl sulfoxide solution (concentration 1 mmole/ml) of the dipeptide pentachlorophenyl ester hydrochloride (**XI**) before, and 5 and 30 min. after the addition of the triethylamine. The samples were diluted to 1.0 ml with dimethyl sulfoxide, and the IR spectra of these solutions were recorded immediately between 1700 and 1900 cm^{-1}.

Stereoisomeric poly-γ-glutamic acids (IV)

Hydrolysis of the polyesters

The polyester was suspended in 1.5 equivalents of 0.25*N* NaOH, and the mixture was warmed for 45 min. on a steam bath. (The polyester dissolved within 5—10 min.) The hydrolyzate was then cooled and worked up by one of the following methods.

Isolation of the polyacids

(a) The hydrolyzate of the D—D or L—L polyester was neutralized with 6*N* HCl to pH 6. A saturated solution of copper sulfate was then added until no more precipitate was formed. The copper salt isolated by centrifugation was washed several times with water, acetone, and ether. The weight of the dried substance was about equal to that of the polyester hydrolyzed. The copper salt was then dissolved in 0.1*N* HCl (the quantity being about 20% more than calculated stoichiometrically), and hydrogen sulfide was bubbled through the solution. The precipitated copper sulfide was centrifuged and washed with several portions of 0.1*N* HCl. Some charcoal was added to the polyglutamic acid solution combined with the washings, and it was filtered repeatedly to give an absolutely clear solution. This solution was then dialyzed through a dialyzing membrane for 2—3 days against several portions of distilled water (with a total volume amounting to about 6—800 times that of the polyglutamic acid solution). At the end of the dialysis neither the inner nor the outer solution gave a positive chloride reaction. The dialyzed solution was then evaporated under reduced pressure to 5—10 ml and then freeze-dried. The polyacids obtained as foamy, white substances were dried in a vacuum desiccator over P_2O_5 at room temperature.

The copper salts of the mesoid poly-γ-glutamic acids were prepared as described above. After, and even during the dissolution of the copper polyglutamate in 0.1*N* HCl, the mesoid polyglutamic acid precipitated from the acid solution in the form of a white powder. After standing for a while in a refrigerator, the precipitate was centrifuged and washed several times with cold 0.1*N* HCl, water, acetone and finally with ether.

(b) The alkaline hydrolyzate of the D- or L-poly-α-methyl-glutamate was acidified to pH 2.5 by successive addition of a suspension of Amberlite IR-120 resin (H form). 10 ml of the hydrolyzate required about 7—8 ml of the resin suspension. The reaction mixture was stirred for 30 min., then the resin was filtered off. The solution (after addition of a slight amount of charcoal) was filtered clear, concentrated *in vacuo* to 5—10 ml, and freeze-dried. The polyglutamic acid was obtained in almost quantitative yield.

The procedure was the same also in the case of the mesoid poly-γ-glutamic acids, with the difference that the filtered clear solution was acidified to pH 1.5 with HCl and let to stand for several hours in a refrigerator. The precipitated mesoid polyacid was then isolated by centrifugation, and washed several times with cold water, acetone and ether. The product was an amorphous, white powder; the yield was almost quantitative.

(c) The mesoid polyglutamic acids could also be isolated by direct acidification of the alkaline hydrolyzate with HCl, without the use of an ion exchange resin. Since the precipitation of the mesoid polyacid was fairly slow, the filtration of the acid solution was possible when required.

The analytical data of a number of poly-γ-glutamic acids, prepared by different methods, are summarized in Table VII.

Table VII

Elemental analyses of poly-γ-glutamic acid samples

No.[a]	C%	H%	N%	CH_3O%
1	44.48	5.59	10.13	0.52
4	44.77	5.61	10.38	0.43
6	43.52	5.56	10.16	0.11
10	46.66	5.74	10.63	0
Calcd. for $(C_5H_7NO_3)_n$ $(129.1)_n$	46.50	5.47	10.85	0
Calcd. for $(C_5H_7NO_3 \cdot {}^1/_2\, H_2O)_n$ $(138.1)_n$	43.47	5.83	10.15	0

a) The numbers refer to those in Table II.

Solubility

(a) Racemic poly-γ-glutamic acid. — 20—20 mg (0.135 meq.) of both the D- and the L-poly-γ-glutamic acid were dissolved in 0.8 ml of water, and the resulting solution was neutralized to pH 7 with 0.27 ml of 1*N* NaOH solution. 1.07 ml of 2*N* HCl was then added, and the solution allowed to stand in a refrigerator for 20 hrs. The precipitated racemate was separated by centrifugation, washed with cold water (2×0.5 ml) and dried in a vacuum desiccator over P_2O_5. The racemic poly-γ-glutamic acid obtained weighed 33.4 mg (82%); $[\alpha]_D^{20}$ 0° (*c* 3, 1*N* NaOH).

(b) L—D *mesoid poly-γ-glutamic acid.* — 100 mg of the L—D mesoid poly-γ-glutamic acid was dissolved in 8 ml of 0.1*N* NaOH. The solution was treated with a small amount of decolourizing carbon, filtered, and acidified with 6*N* HCl to pH 1.2. After 12 hrs of cooling

the precipitated substance was separated by centrifugation, washed with cold water (2×10 ml), acetone (2×10 ml), and ether (10 ml), and dried. 85 mg of mesoid poly-γ-glutamic acid was recovered.

Determination of the molecular weight

(a) Modified van Slyke method. — The procedure of the determination has been described elsewhere [28]. Because of insolubility of the mesoid poly-γ-glutamic acids, their molecular weight could not be determined by this method (*cf.* Table II).

(b) Spectrophotometric ninhydrin method. — The reagent used [30] for the ninhydrin reaction was a 1 : 1 mixture of the following two solutions: *a)* solution of ninhydrin (3 g) in methyl cellosolve (100 g), *b)* solution of stannous chloride (1.6 g) in 4*N* sodium acetate–acetic acid buffer (1000 ml; pH 5.5). To 1 ml of the solution containing 1.0 or 1.5 mg of poly-γ-glutamic acid, 1 ml of the reagent was added, the mixture was warmed on a boiling steam bath for 20 min. and then diluted with 2.5 ml of 50% aqueous ethanol. The extinction of the sample was measured in a 10-mm cell at 570 nm. Distilled water, treated with ninhydrin in the same manner, was used for blank measurement. For the calculation of molecular weights, standard solutions of glutamic acid with concentrations from 0.1 to 0.5 mmole/ml were used. The intensities of the ninhydrin reactions of these solutions were found to be proportional to their concentrations in this concentration range. The extinction of a glutamic acid solution of the original concentration of 0.35 mmole/ml was 1.220 after the procedure described above. As standard solutions of another type, those of several glutamic acid γ-oligopeptides [31] were used. The average value of the extinctions of these solutions, in the concentration of 0.35 mmole/ml, was found, after the procedure of the ninhydrin reaction, to be only 1.060, *i.e.* 87% of that of a glutamic acid solution of the same molar concentration. The molecular weights of the polypeptides were calculated on the basis of the extinction values obtained from the oligopeptide series (see text). The extinctions of the different poly-γ-glutamic acid samples of the original concentration of 1.0 and 1.5 mg/ml, and their calculated molecular weights are summarized in Table VIII.

Determination of the optical purity

Poly-γ-L-glutamic acid (No. 6 in Table II; 13.12 mg) was dissolved in 3*N* HCl (10.0 ml) and heated in a sealed tube for 3 hrs at 100°. Glutamic acid (13.78 mg) dissolved in 3*N* HCl (10.0 ml) was treated in the same manner. For determining the glutamic acid content of the polyacid hydrolyzate, three 1-ml aliquots were withdrawn and dried in a vacuum desiccator over P_2O_5 and KOH. The nitrogen content of the dry residues were determined by the micro KJELDAHL method [32]. According to these measurements, the hydrolyzate contained 1.41 ±0.04 mg of glutamic acid per ml. This corresponds to 94 ±3% of polyglutamic acid (*i.e.* 6 ±3% of water) in the original sample. The optical rotations of both the polyacid hydrolyzate and the glutamic acid solution were measured between 580 and 280 nm in a 10.0-mm polarimeter tube at 30° C on a photoelectric spectropolarimeter (OPTON REPM 12). The observed rotation at 286 nm (which was nearly the maximum value of rotation to be measured with the maximal sensitivity on the instrument) was +0.0757° ±0.001° for both solutions. The specific rotation of glutamic acid in the hydrolyzate was $[\alpha]_{286}^{30}$ +537° ±10° (calculated for the glutamic acid content determined as described above), and that of the glutamic acid in the blank was $[\alpha]_{286}^{30}$ +550° ±10°. To control accidental racemization of glutamic acid under the conditions of acid hydrolysis, the rotation of a third standard glutamic acid solution, which had not been heated, was also measured. (The concentration of this solution was 14.80 mg in 10.0 ml of 3*N* HCl.) The observed rotation at 286 nm was +0.0822° ±0.001°, corresponding to $[\alpha]_{286}^{30}$ +556° ±10°. This means that no racemization of glutamic acid took place during the hydrolysis. The optical purity of the poly-γ-glutamic acid sample calculated from the above data may be taken as 98 ±2%.

*

The microanalyses were made by Mrs. H. MEDZIHRADSZKY-SCHWEIGER, Mrs. J. KAJTÁR, Mrs. S. KUTASSY and Mrs. M. DERCSÉNYI in our Analytical Laboratory. The IR spectra were obtained by Dr. F. RUFF. Their most valuable contribution as well as the technical assistance of Mr. J. GERA is gratefully acknowledged.

Table VIII

Data of the ninhydrin reactions of poly-γ-glutamic acids

No.[a]	Concentration,[b] mg/ml	Extinction[c]	Molar concentration[d] (mmole/ml)	Number average molecular weight	
					mean value
1	1.5	1.120	0.370	4050	4100
	1.0	0.730	0.242	4150	
2	1.5	1.750	0.580	2600	2500
	1.0	1.250	0.415	2400	
3	1.5	1.250	0.415	3600	3600
	1.0	0.845	0.280	3600	
4	1.5	1.100	0 365	4150	4100
	1.0	0.750	0.248	4050	
5	1.5	0.880	0.291	5150	5000
	1.0	0.635	0.209	4800	
6	1.5	0.430	0.140	10700	9400
	1.0	0.380	0.124	8050	
7	1.5	0.930	0.308	4900	4900
	1.0	0.622	0.207	4850	
8	1.5	0.628	0.207	7300	7100
	1.0	0.440	0.144	7000	
9	1.5	0.825	0.273	5500	5900
	1.0	0.480	0.158	6300	
10	1.5	0.700	0.230	6500	6100
	1.0	0.525	0.173	5800	
11	1.5	0.640	0.210	7200	7100
	1.0	0.438	0.143	7000	

a) The numbers refer to those in Table II; b) before the ninhydrin reaction; c) extinction of the solution diluted with the reagent (see text); d) calculated for the original sample on the basis of the molar extinction of the γ-oligopeptides (see text).

REFERENCES

1. Bruckner, V., Kovács, J.: Acta Chim. Acad. Sci. Hung. **12,** 363 (1957)
2. Bruckner, V., Medzihradszky, K., Kandel, I., Kandel, M.: Acta Chim. Acad. Sci. Hung. **21,** 105 (1959)
3. Bruckner, V., Kovács, J., Nagy, H., Kajtár, M.: Acta Chim. Acad. Sci. Hung. **6,** 219 (1955)
4. Bruckner, V., Kajtár, M., Kovács, J., Nagy, H., Wein, J.: Tetrahedron **2,** 211 (1958)
5. Bruckner, V., Kajtár, M.: Acta Chim. Acad. Sci. Hung. **21,** 417 (1959)
6. Kovács, J. in "Polyamino Acids, Polypeptides and Proteins" (Ed. M. A. Stahmann) p. 37. The University of Wisconsin Press, Madison/Wis., 1962
7. Ivánovics, G. in "Comprehensive Biochemistry" (Eds. M. Florkin and E. H. Stotz), Vol. VI, p. 286. Elsevier, Amsterdam, 1965
8. Waley, S. G.: Chem. and Ind. **1954,** 1148; J. Chem. Soc. **1955,** 520
9. Kovács, J., Gianotti, R., Kapoor, A.: J. Am. Chem. Soc. **88,** 2282 (1966)
10. DeTar, D. F., Gouge, M., Honsberg, W., Honsberg, U.: J. Am. Chem. Soc. **89,** 988 (1967)
11. Katchalski, E., Sela, M.: Advan. Protein Chem. **13,** 243 (1958); Wieland, I., Bernhard, H.: Ann. **582,** 218 (1953); Wolman, Y., Gallop, P. M., Patchornik, A., Berger, A.: J. Am. Chem. Soc. **84,** 1889 (1962); Vajda, T.: Chem. and Ind. **1963,** 785; Acta Chim. Acad. Sci. Hung. **46,** 221 (1965)
12. Kovács, J., Kapoor, A.: J. Am. Chem. Soc. **87,** 118 (1965); Kovács, J., Ballina, R., Rodin, R. L., Balasubramanian, D., Applequist, J.: J. Am. Chem. Soc. **87,** 119 (1965); Kovács, J., Johnson, B. J.: J. Chem. Soc. **1965,** 6777; Johnson, B. J.: J. Chem. Soc. (C), **1967,** 2638; Kovács, J., Schmit, G. N., Ghatak, V. R.: Biopolymers **6,** 817 (1968)
13. DeTar, D. F., Honsberg, W., Honsberg, U., Wieland, A., Gouge, M., Bach, H., Takara, A., Brinigar, W. S., Rogers, F. F.: J. Am. Chem. Soc. **85,** 2873 (1963); DeTar, D. F., Vajda, T.: J. Am. Chem. Soc. **89,** 998 (1967)
14. Stewart, F. H. C.: Australian J. Chem. **18,** 887 (1965); **21,** 1935 (1968); Fraser, R. D. B., Harrap, B. S., MacRae, T. P., Stewart, F. H. C., Suzuki, E.: J. Mol. Biol. **12,** 482 (1965); **14,** 423 (1965); Bloom, S. M., Dasgupta, S. K., Patel, R. P., Blout, E. R.: J. Am. Chem. Soc. **88,** 2035 (1966)
15. Sondheimer, E., Holley, R. W.: J. Am. Chem. Soc. **76,** 2467 (1954); **79,** 3767 (1957); Battersby, A. R., Robinson, J. C.: J. Chem. Soc. **1955,** 259; Clayton, D. E., Kenner G. W., Sheppard, R. C.: J. Chem. Soc. **1956,** 371; Schellenberg, P., Ullrich, J.: Ber. **92,** 1276 (1959); Bruckner, V., Kótai, A., Kovács, K.: Acta Chim. Acad. Sci. Hung. **21,** 427 (1959); Liefländer, M.: Hoppe-Seyler's Z. physiol. Chem. **320,** 35 (1960); Adler, A. J., Fasman, G. D., Blout, E. R.: J. Am. Chem. Soc. **85,** 90 (1963)
16. Hollósi, M., Kajtár, M., Bruckner, V.: Acta Chim. Acad. Sci. Hung., in press
17. Gordon, M., Miller, J. G., Day, A. R.: J. Am. Chem. Soc. **70,** 1946 (1948); Bodánszky, M.: Acta Chim. Acad. Sci. Hung. **10,** 335 (1956); Pless, J., Boissonnas, R. A.: Helv. Chim. Acta **46,** 1609 (1963); Stich, K., Leeman, H. G.: Helv. Chim. Acta **46,** 1887 (1963)
18. Kovács, J., Ceprini, M. Q., Dupraz, C. A., Schmit, G. N.: J. Org. Chem. **32,** 3696 (1967); Kovács, J., Kisfaludy, L., Ceprini, M. Q.: J. Am. Chem. Soc. **89,** 183 (1967); Kapoor, A., Davis, E. J.: Experientia **23,** 253 (1967); Kapoor, A.: J. Pharm. Sci. **56,** 1532 (1967); Kapoor, A., Davis, E. J., Graetzer, M. J.: J. Pharm. Sci. **57,** 1514 (1968)
19. Weygand, F., Hunger, K.: Z. Naturforsch. **13b,** 50 (1958)
20. Klieger, E., Gibian, H.: Ann. **655,** 195 (1962)
21. Kajtár, M., Bruckner, V., Rihmer, Zs.: Acta Chim. Acad. Sci. Hung. **43,** 161 (1965)
22. 5th European Peptide Symposium, Oxford, 1962. (Ed. G. T. Young). The MacMillan Co., New York, 1963
23. Elliott, D. F., Russel, D. W.: Biochem. J. **66,** 49P (1957); Bodánszky, M., duVigneaud, V.: J. Am. Chem. Soc. **81,** 5688 (1959)
24. Ben-Ishai, D., Berger, A.: J. Org. Chem. **17,** 1564 (1952)
25. Kainz, G., Huber, H., Kasler, F.: Microchim. Acta (Wien) **1957,** 744
26. Thorne, C. B., Leonard, C. G.: J. Biol. Chem. **233,** 1109 (1958)
27. Utsumi, S., Torii, M., Kurimura, O., Yamamuro, H., Amano, T.: Biken's Journal **2,** 165 (1959)
28. Kajtár, J., Kajtár, M.: Acta Chim. Acad. Sci. Hung. **55,** 33 (1968)
29. Sachs, H., Brand, E.: J. Am. Chem. Soc. **76,** 3601 (1954)
30. Greenstein, J. P., Winitz, M.: Chemistry of the Amino Acids, p. 1301. John Wiley and Sons, Inc., New York, 1961

31. KAJTÁR, M., HOLLÓSI, M., BRUCKNER, V.: Acta Chim. Acad. Sci. Hung., in press
32. SCHULEK, E., FÓTI, G.: Magyar Kém. Foly. **55,** 406 (1949)
33. KAJTÁR, M., BRUCKNER, V.: Tetrahedron Letters No. **40,** 4813 (1966)
34. WARD, R. M., ANDERSON, R. F., DEAN, F. K.: Biotechnology and Bioengineering **5,** 41 (1963)

Márton KAJTÁR
Viktor BRUCKNER } Budapest VIII., Múzeum krt. 4/b.

BOOK REVIEWS—BUCHBESPRECHUNGEN—РЕЦЕНЗИИ КНИГ

Macromolecular Chemistry 3. International Symposium, Tokyo and Kyoto, 1966 (General lectures)
Butterworths, London 1967, 609 pp., 90 s.

Macromolecular Chemistry 4. International Symposium, Brussels-Louvain, 1967 (Plenary and main lectures)
Butterworths, London 1968, 490 + 26 pp., 90 s.

In each year, the annual IUPAC Symposium on Macromolecular Chemistry is the greatest event for scientific workers of this field. The publication of these papers, which were invited lectures delivered by the most acknowledged scientists, is a great help for those, who were able to be present at these meetings, because as the Romans said "verba volant, scripta manent", and a still greater help for people who could not take part at the Symposium and to listen to what the "bests" were saying there.

The publication of these two books has now a special actuality for Hungary; we are going to have this meeting this year here, in Budapest, August 25—30. This is the first time that the Symposium on Macromolecular Chemistry will be held in our country. We hope, that the sixth wolume of this series will reflect recent achievements in macromolecular chemistry just as properly as the earlier volumes do.

The third volume contains 16 general lectures and the fourth volume the five plenary lectures (Authors: H. F. MARK, A. KATCHALSKY, I. SAKURADA, C. E. H. BAWN and V. A. KARGIN) and 10 main lectures. Each of the authors is an outstanding scientist in his field, so the papers are not only very interesting, but also they deal with the most important results which were ready to print at the time of these conferences.

G. BODOR

Organic Magnetic Resonance. An International Journal, Edited by E. F. Mooney, Heyden and Son Ltd., London. One volume per annum. Published bi-monthly

Indeed, the application of nuclear magnetic resonance to the structural analysis of organic molecules is that special field of organic chemistry, the development and importance of which justifies the starting of a special journal. In hardly twenty years, this method has become indispensable in modern research laboratories of organic chemistry. There exists an international community of specialists in this field who are in urgent need of proper opportunity for publication. The initiative of Heyden and Son to start a journal of this type, must be considered therefore as fortunate. The expected high level of the journal is guaranteed by the international editorial board, under participation of renown specialists in this field of science, and by the person of the editor in chief. In supplements to the single issues, the NMR spectra discussed in the papers will be published with detailed registration data. The first number carries 46 spectra.

The new journal, the presentation of which meets all requirements, will most certainly be included in the library of every researcher concerned with NMR work.

Gy. DEÁK

Fortschritte der Arzneimittelforschung. Band 11. Herausgegeben von E. Jucker, Birkhäuser Verlag, Basel und Stuttgart, 1968, 572 Seiten

Band 11 der von E. Jucker herausgegebenen Serie »Fortschritte der Arzneimittelforschung« ist eine würdige Fortsetzung der bisher erschienenen Bände. Auch in diesem Band behandelt das Buch Probleme, die im Mittelpunkt der Arzneimittelforschung stehen. Im Abschnitt »Mescaline and Related Compounds« behandelt A. R. PATEL eingehend die Chemie, Analyse, den Metabolismus in vivo und in vitro sowie die pharmakologischen Wirkungen des wegen seiner halluzinogenen Wirkung allgemein bekannten Mescalins und der Mescalin-Analoga. Besonders wertvoll ist dieser Artikel, weil er die im Schrifttum sehr zerstreut beschriebenen Mescalin-Derivate und -Analoga einheitlich behandelt. Die Zusammenfassung von S. T. REID »The Photochemistry of Drugs and Related Compounds« befaßt sich eingehend, über etwa 70 Seiten, außer der Photochemie von Arzneimitteln auch mit der von anderen organischen Molekülen, wie z.B. Alkenen, Dienen, ja sogar stickstoffhaltigen Verbindungen. Dieser Abschnitt des Buches ist vor allem vom Gesichtspunkt der organischen Chemie von Bedeutung, schon wegen der sehr umfangreichen Literatur (500 Zitate) von überwiegend chemischen Charakter. Der etwa 100 Seiten betragende Abschnitt »Untersuchungen zur Biochemie und Pharmakologie der Thymoleptika« wurde von M. H. BICKEL geschrieben. Auch dieser Abschnitt zeichnet sich durch die sehr sorgfältige Bearbeitung der einschlägigen Literatur aus (431 Zitate), die noch mit den bis Anfang 1967 erschienenen neuesten Publikationen ergänzt wird. Obzwar in der vergangenen Zeit auf diesem Gebiet mehrere ausgezeichnete Zusammenfassungen erschienen sind, ist es ein Verdienst dieses Artikels, daß die wichtigen Vertreter dieser neuen Arzneimittelgruppe sowie deren pharmakologische Untersuchungsmethoden ausführlich, doch gleichzeitig mit richtigem Proportionssinn besprochen werden. Dabei wird der Metabolismus der Thymoleptika und der Zusammenhang zwischen chemischer Struktur und antidepressiver Wirkung besonders eingehend behandelt. Der sich mit dem Wirkungsmechanismus befassende Teil des Abschnittes ist ausgezeichnet. Der nächste Abschnitt von nahezu 130 Seiten wurde von E. RENK und W. G. STOLL unter dem Titel »Orale Antikoagulantien« geschrieben. Auch dieser zusammenfassenden Arbeit verleihen die vielen Literaturstellen (899 Zitate) besonderen Wert. Der Abschnitt befaßt sich eingehend mit der Chemie, Pharmakologie und dem Metabolismus der 4-Hydroxykumaron- und 1,3-Indandion-Derivate. Auch für die mit Arzneimittelforschung sich beschäftigenden Chemiker und Pharmakologen wird ein Studium des mit klinischen Anwendungen sich befassenden Abschnittes sehr Lehrreich sein, besonders vom Gesichtspunkt der Behandlung der Erkrankungen der Koronarien. Die bekanntesten im Handel erhältlichen Präparate für solche Behandlungen werden in einer separaten Tabelle angeführt.

Der letzte Abschnitt des Buches hat einen von den vorangehenden vollkommen verschiedenen Charakter. KREUTZBERGER behandelt in diesem Abschnitt von etwa 90 Seiten — »Die Amidinstruktur in der Arzneimittelforschung« — nicht einen gegebenen Arzneityp, sondern die Rolle einer funktionellen Gruppe auf dem Gebiete der Arzneimittelforschung. Ein sehr übersichtlicher und ausführlicher Teil befaßt sich mit der Chemie der Ausbildung der Amidingruppe, sodann werden kurz die in der Natur vorkommenden Amidine besprochen. Der zweite Teil behandelt die zu Gruppen von verschiedener pharmakologischer Wirkung gehörigen Amidine, undzwar auf Grund der erzielten Resultate vor allem vom chemotherapeutischem Gesichtspunkt aus gesehen, da ja die meisten Amidine in dieser Richtung ihre Wirkung ausüben. Es werden aber auch Amidinderivate mit antidiabetischer, lokalanästhetischer, antiviraler und cytostatischer usw. Wirkung angeführt. Auch in diesem Abschnitt werden viele Zitate (513) aus der Literatur angeführt.

Der Wert des neu erschienene Bandes wird durch das mehr als 100 Seiten betragende Inhaltsverzeichnis nur noch erhöht. Dieses Inhaltsverzeichnis enthält nicht nur das Sachwortverzeichnis dieses Bandes, sondern auch die wichtigsten Sachwörter der vorangehenden Bände. Die Ausrichtung des Buches, ähnlich wie die der vorangehenden Bände, ist ausgezeichnet, die Typographie macht das Buch leicht lesbar, und es ist sehr erfreulich, daß die sich mit Arzneimittelforschung beschäftigende Literatur mit einem neuen ausgezeichneten Werk bereichert wurde. Nun schließt sich auch dieses Buch der ganzen Serie an, welche unentbehrlich für jeden ist, der sich mit Arzneimittelforschung beschäftigt oder die neuesten Ergebnisse auf diesem Gebiet von chemischem oder medizinischem Gesichtspunkt zu verfolgen wünscht.

K. NÁDOR

A. CORNU and R. MASSOT: *List of Conversion Factors for Atomic Impurities to ppm by Weight*

Heyden and Son, 1968

The book consists of tables which make possible the conversion of results obtained by different analytical methods (mass spectrometry, gamma-spectrometry, activation analysis, etc.) and expressed in number of atoms/million atoms into ppm by weight units, by means of the conversion factors calculated by the authors. These conversion factors have been calculated by means of a computer, using the atomic weights given by the International Union of Pure and Applied Chemistry in 1961 (Bulletin d'Information N° 14 de septembre 1961), based on $^{12}C = 12$. These atomic weights are listed on pages IX and X.

On pages V—VIII directions are given, in English and in French, for the use of the tables. The following part of the book essentially consists of two sections. Section *A* contains tables referring to pure matrix elements (42 pages) specifying the atomic number, name and atomic weight M_1 of the matrix and the symbols, atomic numbers and names of all contaminant elements with the conversion factors M_2/M_1 calculated using the values of M_2 listed on the separate table. Thus, if an analytical method shows, e.g., in metallic beryllium the presence of 1.1 atom of Li per 1 million atoms of Be, this value multiplied by the factor M_2/M_1 yields the result in ppm by weight units.

Section *B*, the second part, comprises 90 pages; it is to be used if the matrix is a chemical compound. In such cases the molecular weight (M) of the compound is calculated, and a conversion factor taken from the tables and corresponding to the nearest M_1 value is used in the above described manner.

The data listed in the tables are very helpful, because they provide a fast method of conversion of results into ppm by weight units generally used nowadays.

M. ÖRDÖGH

Annual Review of NMR Spectroscopy. Vol. 1

Edited by E. F. Mooney, Academic Press, London and New York, 1968, 353 pp.

In the last 10 years NMR spectroscopy has become a routine method for chemists. One of the several consequences of this is the exponential increase in the amount of information produced in various branches of chemistry. Therefore, chemists who wish to keep abreast of the theoretical and technical developments in NMR spectroscopy are greatly assisted by an annual monograph summarizing the most important results.

The "Annual Review of NMR Spectroscopy" serves this end. It is intended to survey annually the developments and application of proton magnetic resonance and to summarize the results on other nuclei (*e.g.*, F^{19}) in each 2 or 3 years, depending on the amount of accumulated material.

Volume 1 contains general reviews on proton magnetic resonance (RICHARD A. Y. JONES 32 pp.), the application of NMR in conformational analysis (W. A. THOMAS, 40 pp.), high resolution NMR (E.O. BISHOP, 42 pp.), heteronuclear magnetic double resonance (W. MCFARLANE, 26 pp.), (P. R. SEWELL, 54 pp.), the problem of the signal to noise ratio (G. E. HALL, 12 pp.), and finally on F^{19} NMR spectroscopy (E. F. MOONEY and P. H. WINSON, 36 pp.).

Each chapter is followed by extensive references. Chapter 1, for example, cites 376 references. The thorough author and subject indexes further increase the usefulness of the book.

The book is a very useful reading material for organic and analytical chemists who are in contact with this interesting domain of spectroscopy. Any chemist may have encountered *(e.g.)* the annoying problem of the signal to noise ratio, treated in the brief and excellent review by G. E. HALL.

Well prepared drawings of the spectra facilitate thorough understanding of the subject matter.

The typographic make-up is excellent, in accordance with the traditions of Academic Press.

CS. SZÁNTAY

INDEX

ACTA CHIMICA

ТОМ 62 — ВЫП 2

РЕЗЮМЕ

Некоторые данные к химии селена и селеновых соединений, XVI

Определение селена в теллуре и двуокиси теллура высоких чистот

Ш. ЖИНДЕЛЬ и Л. БАРЦА

Для определения содержания селена в теллуре предлагается реакция образования Se(IV)-о-фенилен-диамина. В случае теллура высокой чистоты нет необходимости разделять, достаточно лишь держать теллур (IV) в растворе лимонной кислоты при нужной величине pH (pH = 1—2). Продукт реакции определяется спектрофотометрически на длине волны 335 ммк. Нижний предел чувствительности составляет $2 \cdot 10^{-4}$% селена. Данный метод намного проще, быстрее и надежнее, нежели определение селена с помощью 3,3′-диамина-бензинида.

Применение комплексообразователей в ионообменной хроматографии, III

Связывание аминовых комплексов металлов на ионообменных смолах

Й. ИНЦЕДИ

Изучалось связывание ионов никель(II), кобальт(II), медь(II), кадмий(II) и цинк(II) из растворов хлористого аммония, содержащих различное количество свободного аммония, на катионообменных смолах.

Было установлено, что среди образующихся комплексов, комплексные ионы тетрааммина и гексааммина отличаются особенно сильными связями. Были рассчитаны также приблизительные значения констант ионообменного равновесия, характерные для данных комплексов.

Ионообменные мембраны, XI

Потенциал мембраны и внутренняя активность

Ю. Х. ШИПОШ, И. КАЛМАН и Я. МИКЕШ

Суммируя вышеизложенное авторы делают заключение о том, что количество электролита, находящееся в фазе мембраны, складывается из двух частей: пары фиксированных ионов и их противоионы составляют неизменное количество ионов, а соионы, диффундирующие из внешнего раствора, и соответствующее им количество противоионов представляют собой переменный член концентрации. Количество последнего зависит от концентрации внешнего электролита и, к тому же, не только из-за количества диффундирующего электролита, но и вследствие образования ионного слоя на поверхности раздела в условиях электродиализа. Понятие внутренней активности необходимо для того, чтобы мембранную фазу можно было бы рассматривать как такой раствор, в котором количественное и кинетическое движение ионов оценивается на основе известных зависимостей.

В приближении, электродиализирующуюся ячейку можно рассматривать как пару растворов, между членами которой находится — треть электролитного поля с определенной концентрацией ионов, ограниченное в приближении математической плоскости.

Это внутреннее поле обладает характером Доннана, поскольку один тип ионов не может изменять своего положения, а имеются свободно движущиеся противоионы и какое-то дополнительное количество ионов, зависящее от внешнего раствора. Диффузионные условия регулируются ионным слоем, образовавшимся на границе раздела — опять абстрактируя математической плоскостью — через который ионы должны проникнуть во время их движения.

Таким образом, потенциал, регулирующий движение, состоит из движущего и препятствующего компонентов, где движущий компонент представляет собой внешнее силовое поле и диффузионный потенциал, а препятствующий компонент — ионообменный потенциал мембраны. Они находятся в зависимости друг от друга, однако, именно вследствие влияния внутреннего фиксированного количества ионов, не находятся в линейной корреляции. Зависимость измеряемых условий и известных законов растворов авторы пытались заключить в рамки этой физической картины.

Изучение ионообменных равновесий с помощью метода радиоактивных индикаторов, XVI

Определение констант стабильности отрицательно заряженных комплексов хлористого цинка с помощью жидкого ионообменника

Т. ЛЕНДЬЕЛ и Й. ТЁРКЁ

С помощью жидкого ионообменника Amberlite LA—2 определялись константы образования отрицательно заряженных комплексов хлористого цинка. Был разработан новый графический метод для оценки экспериментальных данных.

Значения $\log K_3 = -0{,}30$ и $\log K_4 = -0{,}07$ кажутся вполне надежными; однако сравнение их с литературными данными, вследствие сильного расхождения последних, затруднено.

Использование потенциостата для определения максимального коррозионного тока гальванических элементов, I

Й. ДЕВАИ, Б. ЛЕНДЬЕЛ и Л. МЕСАРОШ

С помощью потенциостата измерялся максимальный коррозионный ток различных гальванических элементов. Правильность измерительного метода измерения было доказано сравнительными измерениями, причем снималась диаграмма Эванса для изучаемых гальванических элементов, а также измерялась с помощью амперметра зависимость коррозионного тока от времени. Было установлено, что, при условии подходящего включения в схему, потенциостат может быть использован и для измерения максимального коррозионного тока. Преимущество данного метода, по сравнению с остальными методами, заключается в том, что и в случае гальванических элементов с небольшим внутренним сопротивлением, величина максимального коррозионного тока и его изменения во времени измеряются непосредственно; таким образом, устраняются возможные погрешности, связанные с экстраполяцией.

Получение новых производных бензо(а)хинолизина, I

П. БИТЕ, Э. ДИСЛЕР, М. ФЕКЕТЕ, А. ВИЛЛАНИ и М. КЮРТИ

Для более глубокого изучения фармакологического действия соединений, содержащих скелет бензо(а)-хинолизина, было синтезировано большое число оксимовых эфиров и кислотных амидов, а также несколько из их эфирных и аминовых производных исходя из 2-окси- и 2-имино-соединений.

Гетероциклические соединения из сахаров, II

Получение производных 2-полигидроксиалкил-тиазола и -бензтиазола

Р. БОГНАР, И. ФАРКАШ, Л. СИЛАДЬИ, М. МЕНЬХАРТ, Е. Н. НЕМЕШ и И. Ф. САБО

На основе присоединения сероводорода к нитрилам ацетилированных альдоновых кислот, удалось получить некоторые новые производные амида тиокислот. Тиоамид пентаацетил-D-глюконовой кислоты с хлорацетоном, а тиоамид пентаацетил-D-галактоновой кислоты с фенацил-бромидом конденсируются в соответствующие замещенные производные тиазола.

При конденсации хлоридов ацетилированных альдоновых кислот с 2-амино-тиофенолом и 2-амино-4-хлор-тиофенолом образуются производные 2-полиацетокси-алкил-бензтиазола и 2-полиацетокси-алкил-5-хлор-бензтиазола. Полиацетокси-производные омыляются метилатом натрия в 2-полигидрокси-алкил-бензтиазолы. Нитрилы ацетилированных альдоновых кислот также конденсируются с 2-амино-тиофенолом, и таким путем с хорошим выходом могут быть получены 2-полиацетокси-алкил-бензтиазолы.

Между оптическим вращением 2-полигидрокси-алкил-бензтиазолов и пространственным положением гидроксильной группы на атоме углерода полигидрокси-алкильной цепочки, примыкающей к кольцу, наблюдается зависимость, подобная «бензимидазольному правилу».

Синтез стереоизомерных γ-полиглутаминовых кислот, I

М. КАЙТАР и В. БРУКНЕР

Описанные ранее методы получения γ-полиглутаминовой кислоты [4] не пригодны для практического получения этих соединений в больших количествах. Оценка возможностей разработки более подходящего синтеза привела к заключению о применимости теоретической последовательности синтезов, разработанных ранее, но на каждой основной ступени необходимо заменить старые методы более новыми. Новый способ синтеза метилового эфира γ-полиглутаминовой кислоты основан на реакции полиавтоацилирования солей α' α'-диметил-γ'-п-нитрофениловых и пентахлор-фениловых эфиров γ-глутамил-глутаминовой кислоты (X и XI) под действием оснований. Новым методом были получены стереоизомеры солей дипептидных активных эфиров (X и XI); с помощью данного метода удалось получить структурно однородные, оптически чистые продукты. Метиловые эфиры γ-полиглутаминовой кислоты удалось получить с гораздо лучшими выходами (40—90%), по сравнению с ранними работами. Путем щелочного гидролиза полиэфиров и изолирования их продуктов различными способами могут быть получены с очень хорошими выходами (65—98%) стереоизомеры γ-полиглутаминовой кислоты: γ-поли-L-глутаминовая кислота, γ-поли-D-глутаминовая кислота, а также D—L- и L—D-*мезоиды* γ-полиглутаминовой кислоты.

Определенный двумя методами молекулярный вес полиэфиров и поликислот, полученных при различных экспериментальных условиях, равен 6—8000 и 4—9000, соответственно. Проверялись структурная однородность и оптическая чистота поликислот.

Синтетический *рацемат* γ-полиглутаминовой кислоты (что означает эквимолекулярную смесь D- и L-изомеров γ-полиглутаминовой кислоты) практически не растворяется в воде; на основе этого наблюдения, более ранние представления о структуре *субтильных полипептидов* получили подтверждение и с синтетической стороны.

Мезоиды γ-полиглутаминовой кислоты также плохо растворимы в воде.

The AALC collection, including approx. 5500 punched cards gives the individual the advantages of modern data processing, without the need for expensive machines.

The advantages of cards!

The AALC collection of cards offers many advantages to its user. First, because only a card-file can be kept complete and up-to-date at any time. Book-form bibliographies are difficult to handle and are not apt for cross-indexing. Secondly with a card-file you do not have to make personal notes. If you wish to retain items of information from a book-bound bibliography, you cannot avoid noting them down (if you don't want to tear out the relevant pages!); with the AALC-file, however, you can indulge in the luxury of picking out the cards you are looking for.

The advantages of p u n c h e d cards!

By having the AALC collection on *punched* cards, you never have to replace cards in any particular order. Through the selection operation the cards you are looking for fall unerringly from the whole pack, irrespective of the place they occupy in the card-file. Using simple methods, you can collect all the cards that are particularly important for the topical field you are engaged in at a given time. A punched card file allows any questions to be combined according to the nature of your problem: it allows cross-indexing as well.

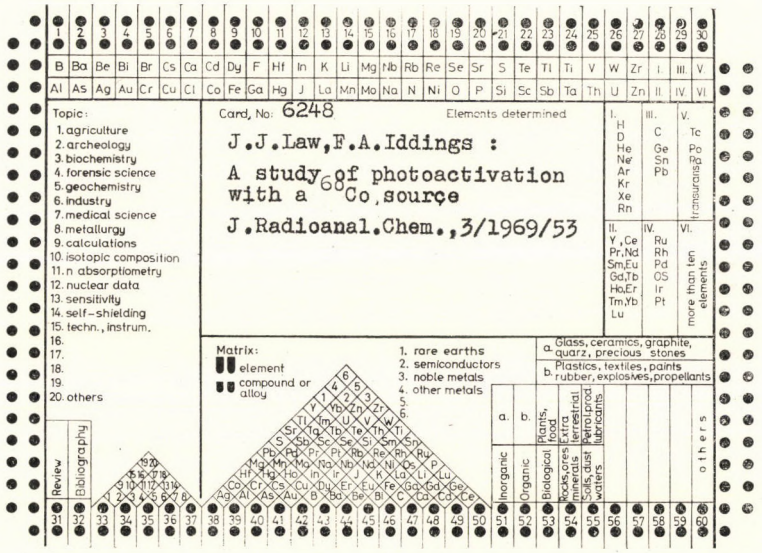

AALC—File
ACTIVATION
ANALYSIS
LITERATURE
CARDS
1935—1968

Unslotted:
US$ 0.05/card

Slotted:
US$ 0.06/card

IN PREPARATION

Ask for leaflets at the following address

AKADÉMIAI KIADÓ

Publicity Department, Budapest 502. P.O.B. 24

ACTIVATION ANALYSIS DOCUMENTATION CENTER

AKADÉMIAI KIADÓ

PUBLISHING HOUSE OF THE HUNGARIAN ACADEMY OF SCIENCES

Printed in Hungary

A kiadásért felel az Akadémiai Kiadó igazgatója — Műszaki szerkesztő: Farkas Sándor

A kézirat nyomdába érkezett: 1969. VII. 4. — Terjedelem: 8,25 (A/5) ív, 26 ábra

69.67926 Akadémiai Nyomda, Budapest — Felelős vezető: Bernát György

The Acta Chimica publish papers on chemistry in English, German, French and Russian.

The Acta Chimica appear in volumes consisting of four parts of varying size, 4 volumes being published a year.

Manuscripts should be addressed to

Acta Chimica
Budapest 112/91 Műegyetem

Correspondence with the editors should be sent to the same address.

The rate of subscription is 165 forints a volume. Orders may be placed with "*Kultúra*" Foreign Trade Company for Books and Newspapers (Budapest I., Fő utca 32. Account No. 43-790-057-181) or with representatives abroad.

Les Acta Chimica paraissent en français, allemand, anglais et russe et publient des mémoires du domaine des sciences chimiques.

Les Acta Chimica sont publiés sous forme de fascicules. Quatre fascicules seront réunis en un volume (4 volumes par an).

On est prié d'envoyer les manuscrits destinés à la rédaction à l'adresse suivante:

Acta Chimica
Budapest 112/91 Műegyetem

Toute correspondance doit être envoyée à cette même adresse.

Le prix de l'abonnement est de 165 forints par volume.

On peut s'abonner à l'Entreprise pour le Commerce Extérieur de Livres et Journaux «*Kultúra*» (Budapest I., Fő utca 32. Compte-courant No. 43-790-057-181) ou à l'étranger chez tous les représentants ou dépositaires.

«*Acta Chimica*» издают трактаты из области химической науки на русском, французском, английском и немецком языках.

«*Acta Chimica*» выходят отдельными выпусками разного объема. 4 выпуска составляют один том. 4 тома публикуются в год.

Предназначенные для публикации рукописи следует направлять по адресу:

Acta Chimica
Budapest 112/91 Műegyetem

По этому же адресу направлять всякую корреспонденцию для редакции.

Подписная цена «*Acta Chimica*» — 165 форинтов за том. Заказы принимает предприятие по внешней торговле книг и газет «*Kultúra*» (Budapest I., Fő utca 32. Текущий счет № 43-790-057-181) или его заграничные представительства и уполномоченные.

38,— Ft

Reviews of the Hungarian Academy of Sciences are obtainable at the following addresses:

ALBANIA

Ndermarja Shtetnore e Botimeve
Tirana

AUSTRALIA

A. Keesing
Box 4886, GPO
Sydney

AUSTRIA

Globus Buchvertrieb
Salzgries 16
Wien I

BELGIUM

Office International de Librairie
30, Avenue Marnix
Bruxelles 5

Du Monde Entier
5, Place St. Jean
Bruxelles

BULGARIA

Raznoiznos
1, Tzar Assen
Sofia

CANADA

Pannonia Books
2, Spadina Road
Toronto 4, Ont.

CHINA

Waiwen Shudian
Peking
P. O. B. 88

CZECHOSLOVAKIA

Artia
Ve Směčkách 30
Praha 2

Poštovná Novinová Služba
Dovoz tisku
Vinohradská 46
Praha 2

Mad'arská Kultura
Václavské nám. 2
Praha I

Poštová Novinová Služba
Dovoz tlače
Leningradská 14
Bratislava

DENMARK

Ejnar Munksgaard
Nörregade 6
Copenhagen

FINLAND

Akateeminen Kirjakauppa
Keskuskatu 2
Helsinki

FRANCE

Office International de Documentation et Librairie
48, rue Gay Lussac
Paris 5

GERMAN DEMOCRATIC REPUBLIC

Deutscher Buch-Export und Import
Leninstraße 16
Leipzig 701

Zeitungsvertriebsamt
Fruchtstrasse 3—4
1004 Berlin

GERMAN FEDERAL REPUBLIC

Kunst und Wissen
Erich Bieber
Postfach 46
7 Stuttgart S.

GREAT BRITAIN

Collet's Holdings Ltd.
Dennington Estate
London Rd.
Wellingborough. Northants.

Robert Maxwell and Co. Ltd.
Waynflete Bldg. The Plain
Oxford

HOLLAND

Swetz and Zeitlinger
Keizersgracht 471—487
Amsterdam C

Martinus Nijhof
Lange Voorhout 9
The Hague

INDIA

Current Technical Literature
Co. Private Ltd.
India House OPP
GPO Post Box 1374
Bombay I

ITALY

Santo Vanosia
Via M. Macchi 71
Milano

Libreria Commissionaria Sansoni
Via La Marmora 45
Firenze

JAPAN

Nauka Ltd.
92, Ikebukur O-Higashi 1-chome
Toshima-ku
Tokyo

Maruzen and Co. Ltd.
P. O. Box 605
Tokyo-Central

Far Eastern Bookseller:
Kanda P. O. Box 72
Tokyo

KOREA

Chulpanmul
Phenjan

NORWAY

Johan Grundt Tanum
Karl Johansgatan 43
Oslo

POLAND

RUCH
ul. Wronia 23
Warszawa

ROUMANIA

Cartimex
Str. Aristide Briand 14—18
Bucureşti

SOVIET UNION

Mezhdunarodnaya Kniga
Moscow G—200

SWEDEN

Almquist and Wiksell
Gamla Brogatan 26
Stockholm

USA

International Arts and Sciences Press
108, Grand Street
White Plains, N. Y. 10601

VIETNAM

Xunhasaba
19, Tran Quoc Toan
Hanoi

YUGOSLAVIA

Forum
Vojvode Mišića broj 1
Novi Sad

Jugoslovenska Knjiga
Terazije 27
Beograd

3. XII. 1969.

Index: 26.007

ACTA CHIMICA

ACADEMIAE SCIENTIARUM HUNGARICAE

TOMUS 62 FASCICULUS 3

AKADÉMIAI KIADÓ, BUDAPEST

1969

ACTA CHIM. ACAD. SCI. HUNG.

ACTA CHIMICA

A MAGYAR TUDOMÁNYOS AKADÉMIA KÉMIAI TUDOMÁNYOK OSZTÁLYÁNAK IDEGEN NYELVŰ KÖZLEMÉNYEI

Az Acta Chimica német, angol, francia és orosz nyelven közöl értekezéseket a kémiai tudományok köréből.

Az Acta Chimica változó terjedelmű füzetekben jelenik meg, egy-egy kötet négy füzetből áll. Évente átlag négy kötet jelenik meg.

A közlésre szánt kéziratok a szerkesztőség címére (Budapest 112/91 Műegyetem) küldendők.

Ugyanerre a címre küldendő minden szerkesztőségi levelezés. A szerkesztőség kéziratokat nem ad vissza.

Az Acta Chimica előfizetési ára kötetenként belföldre 120 Ft, külföldre 165 Ft. Megrendelhető a belföld számára az „Akadémiai Kiadó"-nál (Budapest V., Alkotmány utca 21. Bankszámla 05-915-111-46), a külföld számára pedig a „Kultúra" Könyv- és Hírlap Külkereskedelmi Vállalatnál (Budapest I., Fő utca 32. Bankszámla: 43-790-057-181) vagy annak külföldi képviseleteinél és bizományosainál.

Die Acta Chimica veröffentlichen Abhandlungen aus dem Bereiche der chemischen Wissenschaften in deutscher, englischer, französischer und russischer Sprache.

Die Acta Chimica erscheinen in Heften wechselnden Umfanges. Vier Hefte bilden einen Band. Jährlich erscheinen 4 Bände.

Die zur Veröffentlichung bestimmten Manuskripte sind an folgende Adresse zu senden:

Acta Chimica
Budapest 112/91 Műegyetem

An die gleiche Anschrift ist auch jede für die Redaktion bestimmte Korrespondenz zu richten.

Abonnementspreis pro Band: 165 Forint. Bestellbar bei dem Buch- und Zeitungs-Außenhandels-Unternehmen »*Kultúra*« (Budapest I., Fő utca 32. Bankkonto Nr. 43-790-057-181) oder bei seinen Auslandsvertretungen und Kommissionären.

Acta Chimica Academiae Scientiarum Hungaricae, Tomus 62 (3), pp. 217—228 (1969)

THERMOLYSE VON CYANOKOMPLEXEN II*

DIE THERMISCHE ZERSETZUNG EINIGER CYANOMETALLAT-SÄUREN

B. MOHAI

(Institut für Allgemeine und Anorganische Chemie der Universität für Chemische Industrie, Veszprém)

Eingegangen am 29. September 1968

Die thermische Zersetzung der folgenden Cyanometallat-Säuren wurde untersucht: $H_4[Fe(CN)_6]$, $H_3[Fe(CN)_6]$, $H_2[Fe(CN)_5NO]$, $H_3[Co(CN)_6]$. Den einzelnen Zersetzungsstufen konnten wohldefinierte Reaktionen zugeordnet werden. Außer den Zersetzungstemperaturen und Gewichtsverlusten wurden auch die Enthalpieänderungen im Laufe der Zersetzungsprozesse bestimmt. Durch die erhaltenen ΔH-Werte konnten die thermischen Stabilitäten der Verbindungen direkt verglichen werden. Zersetzungstemperatur, Wärmetönung und Reaktionswärme stehen mit der Elektronenstruktur des Zentralatoms in engem Zusammenhang.

Einleitung

Die im Zusammenhang mit der thermischen Stabilität und Zersetzung der Übergangsmetall-Cyanokomplexe früher erschienenen Mitteilungen beschäftigen sich mit der Wasserabgabe von Cyanokomplex-Hydraten [1, 2] bzw. mit der Dehydratation von wasserhaltigen Niederschlägen [3]. Über den Abbau der eigentlichen Komplexstruktur wurden die ersten thermischen und stöchiometrischen Daten — am Beispiel des Kaliumferricyanids — von CUTTICA angegeben [4]. PERRET und GILSON [5] untersuchten die Cyanoferrate der Elemente der ersten und zweiten Gruppe des Periodensystems und machten einen Unterschied zwischen Cyanid bzw. Cyanamid bildenden Kationen.

In den späteren Arbeiten von R. DUVAL und C. DUVAL wurde unter anderen analytischen Niederschlägen auch die thermische Stabilität von schwerlöslichen Übergangsmetall-Cyanokomplexen untersucht [6, 7] und in einigen Fällen wurden die Kurven der Thermolyse (beispielsweise die des Kaliumferro- und -ferricyanids) mit den IR-Spektren verglichen [8]. CHAMBERLAIN und GREENE [9] stellten auf Grund der DTA-Kurven 15 verschiedener Cyanometallate (zunächst Cyanoferrate) fest, daß deren Hydrate ihren Wassergehalt bei etwa 100 °C abgeben. Die weitere Zersetzung der dehydratierten Substanzen wurde durch Untersuchung der Gasphase verfolgt.

Die Kenntnisse über die thermischen Prozesse der Cyanokomplexe wurden in letzter Zeit besonders von SEJFER und Mitarbeitern erweitert. Außer

* I. Mitteilung, MOHAI, B.: J. inorg. nucl. Chem. 31, 885 (1969)

der Thermolyse der Ferrocyanide der Alkali- und Erdalkalimetalle [10, 11], zahlreicher Übergangs- [12, 13] bzw. Metametalle [14—16] und einiger seltener Elemente [17—19] wurde auch die thermische Zersetzung solcher Cyanide untersucht, die andere Zentralatome enthielten [20]. Die Abweichungen im Mechanismus der entsprechenden Phasen der Zersetzung und in der Zusammensetzung der festen Rückstände konnten in Einklang mit den strukturchemischen Eigenschaften der Atomkomponenten erklärt werden [21].

Über die Thermolyse der »Grundverbindungen«, d. h. der freien Cyanometallat-Säuren sind in der Literatur keine Angaben zu finden.

Die vorliegende Arbeit befaßt sich mit dem thermischen Abbau einiger bekannter Cyanometallat-Säuren, namentlich mit den Zersetzungsreaktionen von wasserfreiem $H_4[Fe(CN)_6]$, $H_3[Fe(CN)_6]$, $H_2[Fe(CN)_5NO]$ und $H_3[Co(CN)_6]$. Im Gegensatz zu den genannten Autoren wurden sowohl die TG- als auch die DTA-Kurven quantitativ ausgewertet, mit anderen Worten: statt der üblichen qualitativen Angabe der Wärmetönung wurden die im Laufe der Zersetzungsprozesse auftretenden Enthalpieänderungen bestimmt und zahlenmäßig angegeben. Diese Untersuchungen lieferten charakteristische Meßwerte, mit denen die thermische Stabilität der untersuchten Verbindungen unmittelbar verglichen werden kann.

Meßergebnisse

Die zur Untersuchung der Thermolyse von Cyanometallat-Säuren ausgewählten Modellverbindungen ermöglichen den Vergleich einerseits von zwei- und dreiwertiges Eisen enthaltenden, andererseits von Hexa- und Pentacyano-Eisenkomplexen. Weiterhin sollten die thermischen Vorgänge in der Hexacyanokobaltat(III)-Säure mit jenen der entsprechenden Eisenverbindungen (entweder gleiche Oxydationszahl oder isoelektronische Struktur des Zentralatoms) verglichen werden.

Die untersuchten Komplexsäuren sind in der ersten Spalte der Tabelle I dargestellt. Die zweite Spalte enthält die *Zersetzungstemperaturen*. Bei Reaktionen, die sowohl stöchiometrisch als auch thermisch quantitativ ausgewertet werden konnten (steile TG-Stufe, scharfe DTA-Spitze), wurde die zum Beginn der Zersetzung und auch die zur maximalen Reaktionsgeschwindigkeit gehörende Temperatur angegeben. Der allgemeinen Konvention entsprechend wurde bei endothermischen Vorgängen die sog. Spitzentemperatur, bei exothermischen Reaktionen die Anfangstemperatur der Gewichtsabnahme als Zersetzungstemperatur betrachtet (kursiv). Bei in einem breiteren Temperaturbereich ablaufenden Zersetzungsprozessen (kontinuierliche Gewichtsänderung) stehen einfach die Temperaturgrenzen statt der obigen Daten.

Die dritte Spalte der Tabelle gibt die von den TG-Kurven abgelesenen *Gewichtsabnahmen* bezogen auf 1 Mol des Ausgangskomplexes an. Wird diese

Tabelle I

Thermolyse der Cyanometallat-Säuren: stöchiometrische und thermische Kennwerte

Verbindung	Zersetzungstemperatur (°C)	Gewichtsabnahme (g · Mol^{-1})	Gasförmiges Zersetzungsprodukt (Mol^{-1})	ΔH (Kcal · Mol^{-1})	$\frac{\Delta H}{n}$	Bemerkung
$H_4[Fe(CN)_6]$	170, *190*	108,7	4 HCN (108)	24,5	6,1	stark, scharf: endoth.
	~600	—	$(CN)_2$	—	—	schwach, stumpf: endoth.
	~650	—	N_2	—	—	schwach, scharf: exoth.
$H_3[Fe(CN)_6]$	*120*, 140	26,5	$^1/_2\,(CN)_2$ (26)	—10,5	—21,0	stark, scharf: exoth.
	155, *165*	~80	3 HCN (81)	~13	4—5	mittelm. scharf: endoth.
$H_2[Fe(CN)_5NO]$	150, *175*	84,3	2 HCN + 1 NO (84)	30,0	(—)	stark, scharf: endoth.
	235, 265	25,8	$^1/_2\,(CN)_2$ (26)	— 8,5	~—17	mittelm. stumpf: exoth.
$H_3[Co(CN)_6]$	190, *225*	81,3	3 HCN (81)	32,5	10,8	stark, scharf: endoth.
	290—410	26,3	$^1/_2\,(CN)_2$ (26)	~14	25—30	mittelm. stumpf: endoth.
	430—510					
	~530					schwach, scharf: exoth.
	560	25,8	$^1/_2\,(CN)_2$ (26)	—	—	Depolymerisation: endoth.
	570, 580					stark, scharf: exoth.
	600—	—	N_2	—	—	(?)

Komponente in mehreren Stufen abgespalten (DTG-Kurve), so wurde nur der mit größerer Genauigkeit meßbare, auf die vollständige Stufe bezügliche Gesamtgewichtsverlust aufgeführt; im Falle des $H_3[Co(CN)_6]$ z. B. wird Dicyan in vier Stufen freigesetzt, von denen je zwei verschmelzen und genau einem halben Mol Dicyan entsprechen.

Die im Laufe der Zersetzung gebildeten *gasförmigen Produkte* sind in der vierten Spalte angeführt. Sofern der fraglichen thermischen Stufe eine Reaktion eindeutig zugeordnet werden kann, wurde auch die Molzahl des Zersetzungsproduktes bezogen auf 1 Mol des ursprünglich eingewogenen Komplexes angegeben. (Z. B. 4 $HCN/H_4[Fe(CN)_6]$, nachstehend in Klammern der berechnete theoretische Wert.)

Die auf Grund der DTA-Kurven bestimmten *Reaktionswärmen* sind in der fünften Spalte angegeben. Zum direkten Vergleich wurde auch die auf 1 Mol des Zersetzungsgases entfallende Enthalpieänderung ($\Delta H/n$) aufgetragen. Letztere darf aber — besonders bei mehrstufigen Zersetzungsprozessen — nur als Annäherungswert betrachtet werden. Bilden sich in derselben Stufe verschiedene gasförmige Produkte, so wäre die Angabe der erwähnten Durchschnittswerte formell, darum wurden sie auch weggelassen. Im Falle von $H_2[Fe(CN)_5NO]$ werden z. B. in der ersten Stufe 2 Mol HCN und 1 Mol NO gleichzeitig abgespalten. Offenbar verteilt sich aber der dort angegebene Wärmeeffekt (30,0 Kcal/Mol) auf die zweierlei Liganden nicht gleichmäßig: der Energiebedarf der Freisetzung von 1 Mol NO ist aller Wahrscheinlichkeit nach größer als der von 1 Mol HCN.

In der letzten Spalte wird der Ablauf der DTA-Kurven — genauer gesagt, die Form und Größe der Spitzen — kurz charakterisiert.

Aus Tabelle I ist ersichtlich, daß es sich überwiegend um Eisenverbindungen handelt, die im Laufe der Thermolyse — unabhängig vom Ausgangsstoff — zur gleichen Zersetzungsphase gelangen: es bildet sich nämlich in jedem Fall Eisen(II)cyanid. Von hier angefangen ist die weitere Zersetzung schon bei allen Eisenkomplexen die gleiche, daher wurden diese wiederkehrenden Reaktionen nur bei der erstangeführten Verbindung, also beim $H_4[Fe(CN)_6]$ angegeben. Da die Zersetzungsvorgänge der untersuchten Cyanometallat-Säuren (neben einigen erwartungsgemäßen Ähnlichkeiten) vor allem grundlegende Abweichungen zeigten, wurden in Abbildung 1 die Derivatogramme sämtlicher Verbindungen dargestellt.

Zuletzt soll im Zusammenhang mit der Genauigkeit der Meßergebnisse noch folgendes bemerkt werden: Die Zersetzungstemperaturen waren in jedem Fall innerhalb von 5 °C reproduzierbar. Die Reproduzierbarkeit der Zersetzungswärmen war im allgemeinen etwa 5% und blieb auch bei dem am wenigsten stabilen Komplex — $H_3[Fe(CN_6)]$ — weit unter 10%. Natürlich konnte der ΔH-Wert einer zweiten Stufe schlechter reproduziert werden als einer ersten. Wenn die Unsicherheit der Enthalpiewerte die obigen Fehlergrenzen

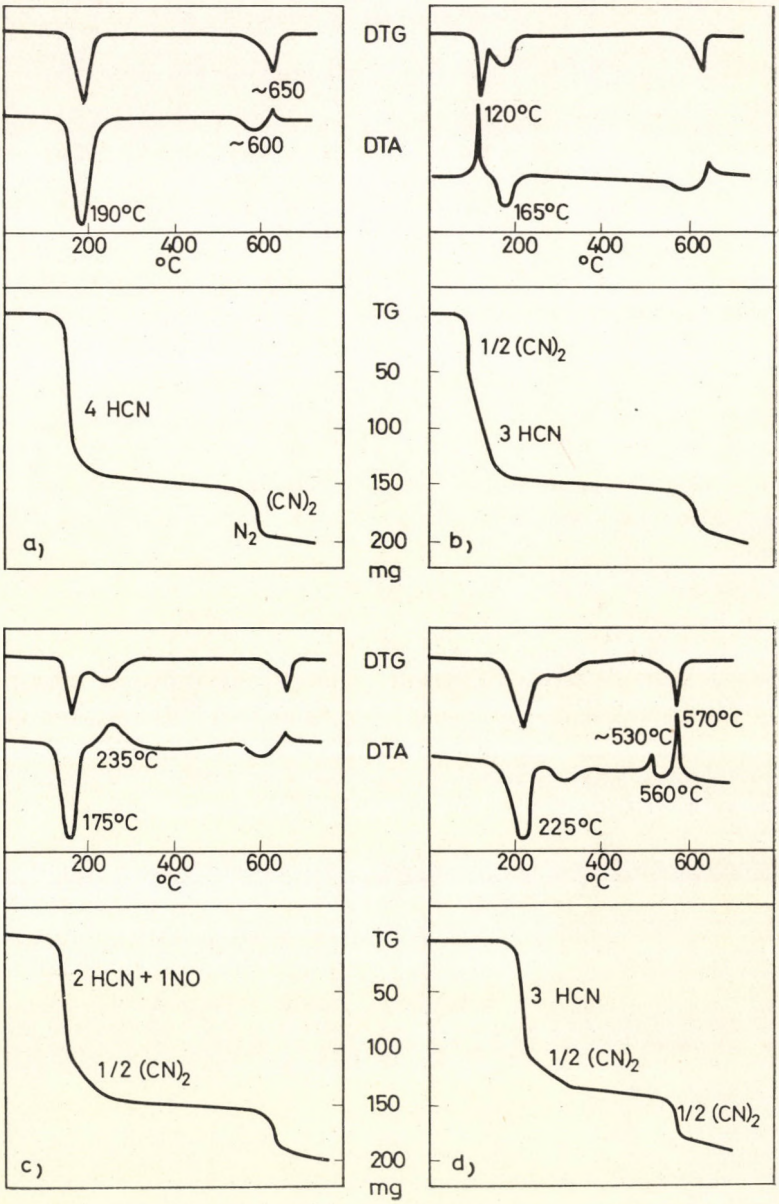

Abb. 1. Derivatogramme der Cyanometallat-Säuren:
a) $H_4[Fe(CN)_6]$; *b)* $H_3[Fe(CN)_6]$; *c)* $H_2[Fe(CN)_5NO]$; *d)* $H_3[Co(CN)_6]$

übertraf, so wurde dies in der Tabelle vermerkt. Übrigens sind die angegebenen Daten Mittelwerte von 3 bis 5 Parallelversuchen, wobei jedes einzelne Derivatogramm mit separat hergestellter Probe aufgenommen wurde.

Zersetzungsreaktionen

Unter den in Tabelle I angeführten komplexen Säuren erwies sich das in Kryptonkonfiguration ein dreivertiges Kobaltatom enthaltende $H_3[Co(CN)_6]$ als die stabilste. Die thermische Stabilität des ebenfalls diamagnetischen, mit dem obigen isoelektronischen $H_4[Fe(CN)_6]$ ist schon entschieden kleiner. Dies ist außer der niedrigeren Zersetzungstemperatur (190 gegenüber 225 °C) besonders aus den Zersetzungswärmen (24,5 bzw. 32,5 Kcal/Mol) oder noch mehr aus dem Vergleich der zur Abspaltung von 1 Mol HCN nötigen durchschnittlichen Energiebedarfe ersichtlich (6,1 bzw. 10,8 Kcal/Mol Komplex/Mol HCN). Innerhalb der dreiwertiges Eisen enthaltenden Säuren ist das edelgaskonfigurierte $H_2[Fe(CN)_5NO]$ viel stabiler als das paramagnetische $H_3[Fe(CN)_6]$, bzw. letzteres ist unter den hier behandelten Verbindungen am wenigsten wärmebeständig.

Auf Grund der gemessenen Gewichtsabnahmen und der Zusammensetzung der gasförmigen Produkte konnten den einzelnen thermischen Stufen die folgenden Reaktionen zugeordnet werden.

a) $H_4[Fe(CN)_6]$

In der ersten Zersetzungsstufe von Wasserstoffhexacyanoferrat(II) werden in einer stark endothermischen Reaktion* vier Mol Wasserstoffcyanid frei:

$$H_4[Fe(CN)_6] \xrightarrow{190\ °C} 1/3\ Fe_2^{II}[Fe^{II}(CN)_6] + 4\ HCN + 24{,}5\ Kcal. \qquad (1)$$

Was die weiteren Zersetzungsvorgänge des Eisen(II)ferrocyanids betrifft, konnte man sich zum Teil auf die Resultate von SEJFER stützen. Nach seinen mit verschiedenen Eisenhexacyanoferraten durchgeführten und durch röntgenographische Untersuchungen ergänzten Versuchen [12] findet von etwa 400 °C angefangen die stufenweise Depolymerisation des Eisen(II)-Komplexes statt:

$$Fe_2[Fe(CN)_6] \rightarrow 3\ Fe(CN)_2. \qquad (2)$$

Bei weiterem Erhitzen zersetzt sich auch das einfache Eisen(II)cyanid nach der Gleichung

$$3\ Fe(CN)_2 \rightarrow Fe_3C + 5\ C + 3N_2. \qquad (3)$$

Bei 660 °C beobachtete SEJFER noch eine polymorphe Umwandlung des gebildeten Zementits.

*Die Koeffizienten sind in den Gleichungen in jedem Fall so angegeben worden, daß die Zersetzungswärmen und gasförmigen Produkte sich immer auf 1 Mol des ursprünglichen Komplexes beziehen.

Auch unsere eigenen Untersuchungen zeigten, daß die nach dem Austritt des Wasserstoffcyanids zurückbleibende feste Phase zwischen 250 und 550 °C praktisch gewichtskonstant ist. Die weitere Zersetzung beginnt erst um etwa 600 °C: am Anfang wird in langsamer endothermischer Reaktion Dicyan gebildet, bald meldet sich zwischen 640—660 °C eine scharfe exothermische Spitze. Letztere kann aber nicht bloß als Folge der Modifikationsänderung des Zementits betrachtet werden, da eben bei dieser Reaktion eine gesteigerte Gewichtsabnahme eintritt. Daher wurde angenommen, daß der anfänglich verlaufenden Zersetzung

$$Fe(CN)_2 \xrightarrow{\sim 600\ ^\circ C} Fe + (CN)_2 \qquad (4)$$

(endotherm) um etwa 650 °C die Reaktion (3) folgt (exotherm). Der Vorzeichenwechsel der Wärmetönung ist damit zu erklären, daß die Reaktion (3) im Vergleich zur Reaktion (4) letzten Endes auch die Zersetzung des Dicyans beinhaltet, dessen Bildungswärme bekanntlich stark endotherm ist. Diese Erklärung steht auch mit der plötzlichen Geschwindigkeitszunahme der träge beginnenden Reaktion in Einklang.

b) $H_3[Fe(CN)_6]$

Beim thermischen Abbau von Wasserstoffhexacyanoferrat(III) bildet sich Wasserstoffcyanid nur in der zweiten Zersetzungsstufe. In der ersten wird in einer heftigen exothermischen Reaktion Dicyan abgespalten, wobei der Eisen(III)-Komplex sich zu Eisen(II)-Verbindungen umsetzt:

$$H_3[Fe(CN)_6] \xrightarrow{120\ ^\circ C} 3/4\, H_4[Fe(CN)_6] + 1/12\, Fe_2^{II}[Fe^{II}(CN)_6] + \\ + 1/2\, (CN)_2 - 10{,}5\ \text{Kcal}. \qquad (5)$$

Die weiteren Zersetzungsprozesse des $H_3[Fe(CN)_6]$ stimmen im wesentlichen mit denen des $H_4[Fe(CN)_6]$ überein. Demgemäß gibt das im Laufe des intramolekularen Redoxvorganges gebildete $H_4[Fe(CN)_6]$ Wasserstoffcyanid ab und es bildet sich das schon bekannte Eisen(II)cyanoferrat(II):

$$3/4\, H_4[Fe(CN)_6] \xrightarrow{165\ ^\circ C} 1/4\, Fe_2[Fe(CN)_6] + 3\, HCN + 13\ \text{Kcal}. \qquad (6)$$

Im Zusammenhang mit der letzteren Reaktion müßte auffallen, daß der Wärmeeffekt kaum die Hälfte des entsprechenden Wertes der Cyanoferrat-(II)-Säure erreicht (24,5 bzw. 13 Kcal/Mol). Der verhältnismäßig große Unterschied läßt sich zum Teil damit erklären, daß hier statt 4 nur 3 Mol HCN freigesetzt werden. Die Differenz ist aber vielmehr die Folge jener Tatsache, daß das Wasserstoffcyanid beim $H_3[Fe(CN)_6]$ nicht mehr aus einer intakten

Struktur (erste Stufe), sondern aus einem Zwischenprodukt (zweite Stufe) abgespalten wird. Vergleicht man nun die Stabilitäten der betreffenden Säuren auf Grund der auf 1 Mol HCN entfallenden Wärmebedarfe, so wird der obige Unterschied wesentlich kleiner (etwa 6 bzw. 4—5 Kcal).

c) $H_2[Fe(CN)_5NO]$

Das Wasserstoffpentacyanonitrosylferrat(III) kann gewissermaßen als Übergang zwischen $H_4[Fe(CN)_6]$ und $H_3[Fe(CN)_6]$ angesehen werden. Es enthält nämlich ein dreiwertiges Zentralatom, zugleich besitzt es — ähnlich den Eisen(II)-Cyanokomplexen — eine diamagnetische Elektronenstruktur. Dementsprechend verlaufen auch seine Zersetzungsreaktionen. Die Temperatur der beginnenden Zersetzung fällt z. B. zwischen die den erwähnten Säuren entsprechenden Werte. Die Thermolyse setzt übrigens unter Abgabe von Wasserstoffcyanid ein (Analogie zur Hexacyanoferrat(II)-Säure), es schließt sich aber sofort die Abspaltung von Stickoxyd an:

$$H_2[Fe(CN)_5NO] \xrightarrow{175\,^{\circ}C} 1/2\,Fe^{III}[Fe^{III}(CN)_6] + 2\,HCN + NO + 30{,}0\ Kcal. \quad (7)$$

Das in einer stark endothermischen Reaktion gebildete Eisen(III)cyanoferrat(III) setzt sich unter exothermischer Entwicklung von Dicyan (Analogie zur Hexacyanoferrat(III)-Säure) zu Eisen(II)ferrocyanid um:

$$1/2\,Fe^{III}[Fe^{III}(CN)_6] \xrightarrow{235\,^{\circ}C} 1/3\,Fe_2^{II}[Fe^{II}(CN)_6] + 1/2\,(CN)_2 - 8{,}5\ Kcal. \quad (8)$$

Der weitere Abbau der Nitroprussidsäure findet nach den bei der Thermolyse des $H_4[Fe(CN)_6]$ beschriebenen Teilreaktionen statt.

Bezüglich der Dicyanbildung aus $H_2[Fe(CN)_5NO]$ soll noch bemerkt werden, daß diese unter entschieden geringerer Wärmeentwicklung verläuft als im Falle des $H_3[Fe(CN)_6]$ (—8,5 bzw. —10,5 Kcal/Mol Komplex). Die Ursache ist wiederum darin zu suchen, daß hier die Abgabe von Dicyan gegenüber $H_3[Fe(CN)_6]$ nur in der zweiten Zersetzungsstufe eintritt.

d) $H_3[Co(CN)_6]$

Die thermischen Prozesse von Wasserstoffhexacyanokobaltat(III) beginnen mit einer scharfen endothermischen Reaktion, in welcher 3 Mol HCN freigesetzt werden:

$$H_3[Co(CN)_6] \xrightarrow{225\,^{\circ}C} 1/2\,Co^{III}[Co^{III}(CN)_6] + 3\,HCN + 32{,}5\ Kcal. \quad (9)$$

Von hier angefangen weichen die Zersetzungsreaktionen des $H_3[Fe(CN)_6]$ von denen der Eisenkomplexe stark ab. Am auffallendsten ist jener Unter-

schied, daß die Dicyanbildung im Falle der Kobaltverbindung in vier Stufen verläuft, von denen je zwei verschmelzen. Die Wärmetönung des ersten Stufenpaares ist endotherm; die dritte und vierte Stufe stellt exothermische Reaktionen dar. Die mehrstufige Dicyanabspaltung ist offenbar die Folge der bekanntlich großen Stabilität der Kobalt(III)-Komplexe, die gerade deshalb nur schwer zu niedrigeren Oxydationsstufen reduziert werden können. Der Vorzeichenwechsel der Wärmetönung ist darauf zurückzuführen, daß die kryptonkonfigurierten diamagnetischen Kobaltkomplexe das Dicyan in endothermischer, die ein ungepaartes Elektron enthaltenden paramagnetischen hingegen in exothermischer Reaktion abgeben (vgl. mit Cyanoferrat(III)-Säuren).

Während der endothermischen Dicyanstufen setzt sich das Kobalt(III)-cyanokobaltat(III) allmählich zu Kobalt(II)cyanid um. In der ersten Stufe, die sich meist nur beim Ammoniumhexacyanokobaltat(III) separieren läßt (s. nachstehende Mitteilung), bilden sich verschiedene Kobalt(II)kobalt(III)-Intermediäre, z. B. $Co_3^{II}[Co^{III}(CN)_6]_2$, die dann bei dauernd abnehmender Reaktionsgeschwindigkeit vollkommen zu Kobalt(II)* reduziert werden.

Die Zersetzung des ebenfalls intermediären Kobalt(II)-Cyanokomplexes beginnt bei etwa 530 °C: darauf weist außer der schnelleren Gewichtsabnahme auch eine kleine exothermische Spitze hin. Diese Reaktion wird aber von einem bei 560 °C ablaufenden Vorgang stark gehemmt, sogar unterbrochen. Letzterer konnte an der DTA-Kurve des $K_3[Co(CN)_6]$ auch von CHAMBERLAIN und GREENE beobachtet werden und wurde als Strukturumwandlung gedeutet [9]. Unserer Meinung nach findet im Laufe des endothermischen Prozesses die nach

$$Co_3^{II}[Co_2^{II}(CN)_{10}] \xrightarrow{560\ °C} 5\ Co(CN)_2 \qquad (10)$$

verlaufende Depolymerisation des bis zu einem bestimmten Grade schon aufgelockerten Kobalt(II)-Komplexes statt und es bildet sich einfaches (jetzt schon paramagnetisches) Kobalt(II)cyanid, das im weiteren in nicht gehemmter exothermischer Reaktion zu Kobalt(I)cyanid zersetzt wird. Diese Erklärung wird auch durch die Tatsache gestützt, daß die Reaktion bei 570 °C sehr heftig, fast explosionsartig wird, gleichzeitig erscheint in der DTA-Kurve eine in diesem Temperaturbereich beispiellos starke und scharfe exothermische Spitze (s. Abb. 1d). Schließlich zersetzt sich von 600 °C angefangen auch das Kobalt(I)cyanid, wobei nach SEJFER [20] metallisches Kobalt sowie Kohlenstoff und Stickstoff gebildet werden.

*Der Cyanokomplex des zweiwertigen Kobalts existiert nach den Untersuchungen von NAST [22] und anderen Verfassern [23—25] nur in Form des dimeren Pentacyanokobaltats, $[Co_2(CN)_{10}]^{6-}$. Die Kobaltatome werden von einer kovalenten σ-Bindung zusammengehalten, so enthält der dimere Kobalt(II)-Komplex kein ungepaartes Elektron und ist ähnlich den Kobalt(III)-Komplexen diamagnetisch.

Aus den obigen Ausführungen folgt, daß die Thermolyse des $H_3[Co(CN)_6]$ sich aus zahlreichen Teilprozessen zusammensetzt. Deswegen sollen die Zersetzungsvorgänge statt ausführlicher stöchiometrischer Gleichungen (obwohl die bei den Dicyan-Stufenpaaren gemessenen Gewichtsverluste genau einem halben Mol Dicyan entsprechen) doch an Hand eines viel übersichtlicheren Reaktionsschemas zusammengefaßt werden (Abb. 2).

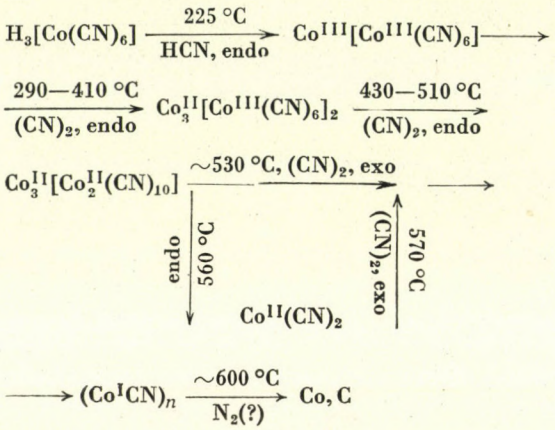

Abb. 2. Schema der Thermolyse von $H_3[Co(CN)_6]$

Die Zersetzungsreaktionen der Cyanometallat-Säuren sollen später, im Vergleich zu den thermischen Prozessen ihrer Ammoniumsalze, noch eingehend diskutiert werden.

Experimenteller Teil

1. Meßmethode

Die thermischen Zersetzungsvorgänge der Cyanometallat-Säuren wurden mit einem Derivatographen System PAULIK—PAULIK—ERDEY untersucht [26, 27]. Die Auswertung der TG-Kurven geschah auf die übliche Weise. Wie schon erwähnt wurde, dienten die DTA-

Tabelle II

Kalibrierung: Wärmeeffekt — Fläche Äquivalentfaktoren

Substanz	Benzoesäure	$AgNO_3$	$NaNO_3$
Schmelzpunkt (°C)	122	212	314
Äquivalentfaktoren	4,12	5,50	6,68
(cal/cm²)	4,08	5,51	6,62
Mittelwert	4,10	5,50	6,65

Kurven diesmal nicht nur zur Bestimmung der Richtung der Enthalpieänderungen, sondern auch der zahlenmäßigen Werte der Reaktionswärmen. Vor diesen quantitativen Untersuchungen wurde die Meßeinrichtung auf Grund von Prozessen mit bekanntem Wärmeeffekt kalibriert: dazu dienten die Schmelzwärmen von Benzoesäure, Silbernitrat und Natriumnitrat.

Die Angaben der Tabelle II zeigen, daß die Wärmeeffekt—Fläche Äquivalentfaktoren mit dem gleichen Eichmaterial vorzüglich reproduziert werden konnten: andererseits sind sie aber von der Temperatur (Schmelzpunkt des Eichmaterials) abhängig. Da die Darstellung der Faktoren als Funktion der Temperatur einen fast linearen Zusammenhang zeigte, konnten diese zwischen 80 und 350 °C durch Inter- bzw. Extrapolation für beliebige Temperaturwerte berechnet werden.

Die zur Kalibrierung und Bestimmung der Enthalpieänderungen angewandten Derivatogramme wurden auf Grund zahlreicher Vorversuche — unter Berücksichtigung der verschiedensten Anforderungen der auf dem Gebiet der Cyanokomplexe zu erwartenden Zersetzungsreaktionen — jedesmal mit den folgenden Parametern aufgenommen:

T_{max}: 900 °C
Aufheizgeschwindigkeit: 5°/Min.
TG-Empfindlichkeit: 200 mg
DTG-Empfindlichkeit: 1/15
DTA-Empfindlichkeit: 1/10
Inertstoff: bei 1200 °C geglühtes Al_2O_3 in Platintiegel (Gewicht: etwa 4,5 g).
Inertgas: sauerstofffreier Stickstoff mit einem Überdruck von 5 bis 10 Torr.

Um die Genauigkeit der Messungen zu steigern, wurden aus dem thermisch aktiven Stoff solche Mengen eingewogen, daß die von den erhaltenen DTA-Kurven begrenzten Flächen annähernd denen der Kalibrationskurven entsprachen. Im Falle der untersuchten Verbindungsgruppe waren dazu Probemengen zwischen 200 und 300 mg (0,75—1,25 mMol) notwendig. Zur weiteren Erhöhung der Meßgenauigkeit wurden die Derivatogramme der Kalibrationsstoffe sowie die der Versuchsmaterialien immer mit gleichen Interstoffmengen (500 mg) aufgenommen [28].

2. Präparation und Analyse

Die zu den thermischen Untersuchungen verwendeten Cyanometallat-Säuren wurden aus den entsprechenden Alkalisalzen hergestellt. Dabei wurde einerseits die gewöhnliche Methode verwendet, nach welcher die Säuren aus ihren Salzen freigesetzt und in Form des Ätherats isoliert werden können. Andererseits wurden auch auf Ionenaustausch beruhende Verfahren angewendet [29, 30]. Durch ihre Kombination und mehrmaliges Wiederholen gelangten wir schließlich zu alkalifreien Substanzen.

Die Präparate wurden durch Bestimmung ihres Wasserstoff- und Eisen- bzw. Kobaltgehaltes identifiziert. Die Resultate der analytischen Untersuchungen sind in Tabelle III zusammengestellt.

Tabelle III

Analysendaten der Cyanometallat-Säuren

Verbindung	H^+/Mol	Konv. (%)	Fe bzw. Co (Gew.-%)	
			ber.	gef.
$H_4[Fe(CN)_6]$	3,93	98,3	25,9	25,7
$H_3[Fe(CN)_6]$	2,88	96,1	26,0	25,3
$H_2[Fe(CN)_5NO]$	1,95	97,5	25,65	25,3
$H_3[Co(CN)_6]$	3,02	100	27,05	26,9

a) *Bestimmung des Wasserstoffgehaltes*

Da die betreffenden Cyanometallat-Säuren — mit Ausnahme des $H_4[Fe(CN)_6]$ — selbst auf Grund ihrer letzten Dissoziationsstufe sehr starke Säuren sind, konnte ihr Wasserstoffgehalt durch einfache Titration mit 0,1 *n* NaOH-Lösung bestimmt werden. Die Ergebnisse der direkten und indirekten azidimetrischen Bestimmungen stimmten überein.

b) *Bestimmung des Eisen- und Kobaltgehaltes*

Die Cyanokomplexe wurden durch mehrmaliges Abrauchen mit konzentrierter Schwefelsäure zerstört. Nach Auflösung in angesäuertem Wasser wurde der unlösliche Anteil des Rückstandes herausfiltriert. Im Filtrat wurde der Eisengehalt der Cyanoferrate titrimetrisch (Permanganometrie), der Kobaltgehalt des $H_3[Co(CN)_6]$ gravimetrisch mit α-Nitroso-β-naphthol bestimmt.

LITERATUR

1. GAUDEFROY, C.: C.r.d. l'Akad. Sci. **158,** 722 (1914)
2. GUARESCHI, I.: Gazz. chim. ital. **49,** I. 134 (1919)
3. WEISER, H. B., MILLIGAN, W. O., BATES, J. B.: J. phys. Chem. **45,** 701 (1941)
4. CUTTICA, V.: Gazz. chim. ital. **52,** I. 20 (1922)
5. PERRET, A., GILSON, A.: Bull. Soc. chim. France (4) **53,** 283 (1933).
6. DUVAL, R., DUVAL, C.: Anal. chim. Acta (Amsterdam) **5,** 84 (1951)
7. DUVAL, C.: *Ibid.* **5,** 506 (1951)
8. DUVAL, C.: *Ibid.* **16,** 545 (1957)
9. CHAMBERLAIN, M. M., GREENE, A. F.: J. inorg. nucl. Chem. **25,** 1471 (1963)
10. SEJFER, G. B.: J. anorg. Chem. (UdSSR) **7,** 1242 (1962)
11. SEJFER, G. B.: *Ibid.* **7,** 2290 (1962)
12. SEJFER, G. B.: *Ibid.* **5,** 68 (1960)
13. SEJFER, G. B., MAKAROWA, S. A.: *Ibid.* **9,** 2085 (1964)
14. SEJFER, G. B.: *Ibid.* **7,** 482 (1962)
15. SEJFER, G. B.: *Ibid.* **8,** 1172 (1963)
16. SEJFER, G. B., MAKAROWA, S. A.: *Ibid.* **10,** 1022 (1965)
17. SEJFER, G. B.: *Ibid.* **8,** 1525 (1963)
18. SCHEWTSCHENKO, G. W., TANANAJEW, I. W.: *Ibid.* **10,** 421 (1965)
19. SEJFER, G. B., MAKAROWA, S. A.: *Ibid.* **11,** 1056 (1966)
20. SEJFER, G. B., BJELOWA, W. I., MAKAROWA, S. A.: *Ibid.* **9,** 1556 (1964)
21. SEJFER, G. B. MAKAROWA, S. A.: Dokl. Akad. Nauk SSSR **169,** 358 (1966)
22. NAST, R. et alii: Z. anorg. allg. Chem. **312,** 314 (1961)
23. HUME, E. M., KOLTHOFF, I. M.: J. Amer. chem. Soc. **72,** 4423 (1950)
24. ADAMSON, A. W.: *Ibid.* **73,** 5710 (1951)
25. GRIFFITH, W. P., WILKINSON, G.: J. chem. Soc. (London) **1959,** 2757
26. ERDEY, L., PAULIK, F.: Acta chim. Acad. Sci. Hung. **7,** 27 (1955)
27. ERDEY, L. PAULIK, F., PAULIK, J.: *Ibid.* **10,** 61 (1957)
28. ROKOSZ, A., PAULIK, J., PAULIK, F., ERDEY, L.: *Ibid.* **56,** 221 (1968)
29. MOHAI, B., PAPP, S., SÁNDOR, M.: Veszprémi Vegyipari Egyetem Közleményei (Mitt. Univ. Chem. Ind. Veszprém) **8,** 107, 121 (1964)
30. HEIN, F., LILIE, H.: Z. anorg. allg. Chem. **270,** 45 (1952)

Béla MOHAI; Veszprém, Nárcisz u. 16, Ungarn

Acta Chimica Academiae Scientiarum Hungaricae, Tomus 62 (3), pp. 229—240 (1969)

THERMOLYSE VON CYANOKOMPLEXEN, III

DER THERMISCHE ABBAU VON AMMONIUM-CYANOMETALLATEN

B. MOHAI

(Institut für Allgemeine und Anorganische Chemie der Universität für Chemische Industrie, Veszprém)

Eingegangen am 29. September 1968

Die Reaktionen des thermischen Abbaus von Ammonium-hexacyanoferrat(II), -Hexacyanoferrat(III), -Pentacyanonitrosylferrat(III) und -Hexacyanokobaltat(III) wurden auf Grund der Gewichtsverluste und Zusammensetzung der gasförmigen Produkte aufgeklärt. Außer den Zersetzungstemperaturen wurden auch die Zersetzungswärmen bestimmt und mit denen der entsprechenden freien Säuren verglichen. Die Abspaltungsenergie von NH_4CN ist etwa das Vierfache der des HCN. Der ein- oder mehrstufige Verlauf der entsprechenden Reaktionen sowie die Wärmetönung und Reihenfolge der Teilprozesse konnten in Einklang mit den strukturchemischen Eigenschaften gedeutet werden.

Einleitung

Ähnlich wie die in der II. Mitteilung behandelten Cyanometallat-Säuren, sind auch die thermischen Zersetzungsvorgänge ihrer Ammoniumsalze bisher noch nicht untersucht worden. Die Thermolyse der Übergangsmetall-Cyanokomplexe, die ein flüchtiges — folglich dissoziables — Kation enthalten, ist in erster Linie wegen der Mannigfaltigkeit ihrer gasförmigen Zersetzungsprodukte interessant. Gegenüber den am eingehendsten untersuchten Alkali- und Erdalkali-Cyanometallaten (besonders Cyanoferraten), die Stickstoff und Dicyan abgeben [1—3], bildet sich bei der Zersetzung der Ammoniumverbindungen außer diesen auch noch Wasserstoffcyanid und Ammoniak. Deshalb sind die Zersetzungsprozesse der Ammonium-Cyanometallate einerseits komplizierter als die der schon früher untersuchten Cyanokomplexe, andererseits kann aber der Zersetzungsverlauf, gerade auf Grund der Zusammensetzung der Gasphase, verhältnismäßig einfach aufgeklärt werden.

Die vorliegende Mitteilung dieser Reihe befaßt sich mit den Ammoniumsalzen der schon früher untersuchten Säuren. Diese Ammonium-Cyanometallate sind in Tabelle I angeführt. Wie ersichtlich, kommen unter ihnen wasserfreie sowie Kristallwasser enthaltende Modifikationen vor. Das Ammoniumhexacyanoferrat(II) wurde in beiden Formen; beim Ammoniumhexacyanoferrat(III) und -kobaltat(III) nur die wasserfreie Modifikation und beim Ammoniumpentacyanonitrosylferrat(III) nur das Hydrat untersucht. Es konnte nämlich entweder kein wohldefiniertes Hydrat* hergestellt, oder andererseits das Präparat nicht vollständig entwässert werden.

* Die wasserhaltige Modifikation des Ammoniumferrocyanids, obwohl sie aus der Literatur als Trihydrat bekannt ist [4], konnte reproduzierbar nur mit 1,5 Mol Wassergehalt hergestellt werden.

Meßergebnisse, Zersetzungsreaktionen

Die Resultate der Untersuchungen über die thermischen Zersetzungsprozesse der Ammonium-Cyanometallate sind in Tabelle I zusammengefaßt. Die Einzeldaten der Tabelle sind wie in der II. Mitteilung zu deuten. Einige Reaktionen der Ammonium-Cyanoferrate verlaufen gegenüber den entsprechenden Säuren (besonders in der ersten Phase der Zersetzung) mehrstufig ab. Bei diesen wurden die Gewichtsabnahmen und Enthalpieänderungen der Teilvorgänge auch summiert angegeben (Σ). Ähnlich wie aus den freien Säuren bildet sich auch aus den Ammonium-Cyanoferraten der gleiche feste Rückstand (Eisen(II)cyanid). Von hier angefangen stimmen die Zersetzungsreaktionen der Eisenkomplexe schon überein, daher wurden sie nur bei der erstangeführten Verbindung angegeben.

Die Zersetzungsvorgänge der untersuchten Ammonium-Cyanometallate beginnen — sofern sie Kristallwasser enthalten — mit Abgabe von Wasser. Diese verhältnismäßig schwach endothermischen Reaktionen finden etwas über 100 °C statt. Da die Entwässerungsenthalpien der Cyanoferrat-Hydrate kürzlich [5] schon behandelt wurden, soll an dieser Stelle nur so viel bemerkt werden, daß die Pentacyanokomplexe (Prussiate) immer wesentlich stärker hydratiert sind als die Hexacyanoverbindungen (im vorliegenden Fall 11,0 gegenüber 6,2 Kcal/Mol Komplex/Mol Wasser).

Die Thermolyse der wasserfreien bzw. der bereits entwässerten Ammonium-Cyanometallate setzt sich im allgemeinen mit einer stark endothermischen Reaktion fort. In dieser Zersetzungsphase werden Ammoniak und Wasserstoffcyanid (oft gemeinsam mit Dicyan) abgespalten. Da das Molverhältnis der gasförmigen Komponenten sich im Laufe der Thermolyse fortwährend ändert (s. Tabelle II), mußte angenommen werden, daß gleichzeitig verschiedene Reaktionen ablaufen. Auf Grund der Zusammensetzung der gasförmigen Produkte konnten den einzelnen Zersetzungsstufen in Einklang mit den gemessenen Gewichtsverlusten die folgenden Reaktionen zugeordnet werden.

1. $(NH_4)_4[Fe(CN)_6]$

Bei der Thermolyse von Ammoniumhexacyanoferrat(II) wird das insgesamt 4 Mol NH_4CN entsprechende Gasgemisch in drei Stufen freigesetzt. Aus den thermischen Kurven der Abbildung 1a ist zu ersehen, daß die Geschwindigkeit der Reaktion stufenweise abnimmt. Die erste Stufe (200 °C) läßt sich gut separieren, die zweite und dritte (330 bzw. 410 °C) konnte aber nur zusammen ausgewertet werden.

Wie schon erwähnt, wurden im Falle des Ammoniumferrocyanids beide Modifikationen untersucht. Dies machte es möglich, die stöchiometrischen und thermischen Angaben hinsichtlich ihrer Reproduzierbarkeit zu verglei-

Tabelle I

Thermolyse der Ammonium-Cyanometallate: stöchiometrische und thermische Kennwerte

Verbindung	Zersetzungstemperatur (°C)	Gewichtsabnahme (g · Mol^{-1})	Gasförmiges Zersetzungsprodukt (Mol^{-1})	ΔH (Kcal · Mol^{-1})	$\frac{\Delta H}{n}$	Bemerkung
$(NH_4)_4[Fe(CN)_6] \cdot 1{,}5\ H_2O$	70, *115*	26,3	1,5 H_2O (27)	9,3	6,2	schwach, stumpf: endoth.
	160, *200*	120,0	NH_3, HCN	57,3	—	stark, scharf: endoth.
	330 410	57,5	NH_3, HCN	32,2	—	mittelm. breit: endoth.
	Σ	177,5	4 NH_4CN (176)	89,5	22,4	Dreierstufe: endoth.
	~620	—	$(CN)_2$	—	—	schwach, stumpf: endoth.
	~660	—	N_2	—	—	schwach, scharf: exoth.
$(NH_4)_4[Fe(CN)_6]$	160, *200*	118,5	NH_3, HCN	55,7	—	stark, scharf: endoth.
	330 410	58,1	NH_3, HCN	33,3	—	mittelm. breit: endoth.
	Σ	176,6	4 NH_4CN (176)	89,0	22,2	Dreierstufe: endoth.
$(NH_4)_3[Fe(CN)_6]$	*150*—200 *220*	99,6	$(CN)_2$, NH_3, HCN NH_3, HCN	26,3	—	stark, breit; result. Wärmetönung: endoth.
	340 415	58,8	NH_3, HCN	28,0	—	mittelm. breit: endoth.
	Σ	158,4	1/2$(CN)_2$ + 3 NH_4CN (158)	54,3	(—)	Viererstufe; result. Wärmetönung: endoth.
$(NH_4)_2[Fe(CN)_5NO] \cdot H_2O$	75, *120*	18,1	1 H_2O (18)	11,0	11,0	mittelm. stumpf: endoth.
	220, 250	~90	NH_3, HCN, $(CN)_2$, N_2	—18,0	(—)	stark, scharf: exoth.
	330 420	~55	NH_3, HCN	—	—	schwach, breit: endoth.
	Σ	~145	2 NH_4CN + 1 NO + + 1/2$(CN)_2$ (144)	—	—	Dreierstufe mit Sekundärreaktion
$(NH_4)_3[Co(CN)_6]$	280, *330*	130,5	3 NH_4CN (132)	120	40	sehr stark, breit: endoth.
	400, *415*	15,5	0,3 $(CN)_2$ (15,6)	~8	25—30	schwach, scharf: endoth.
	440—530	10,7	0,2 $(CN)_2$ (10,4)	—	—	schwach, breit: endoth.
	~550					schwach, scharf: exoth.
	565	25,7	1/2 $(CN)_2$ (26)	—	—	Depolymerisation: endoth.
	575, 590					stark, scharf: exoth.
	600—	—	N_2	—	—	(?)

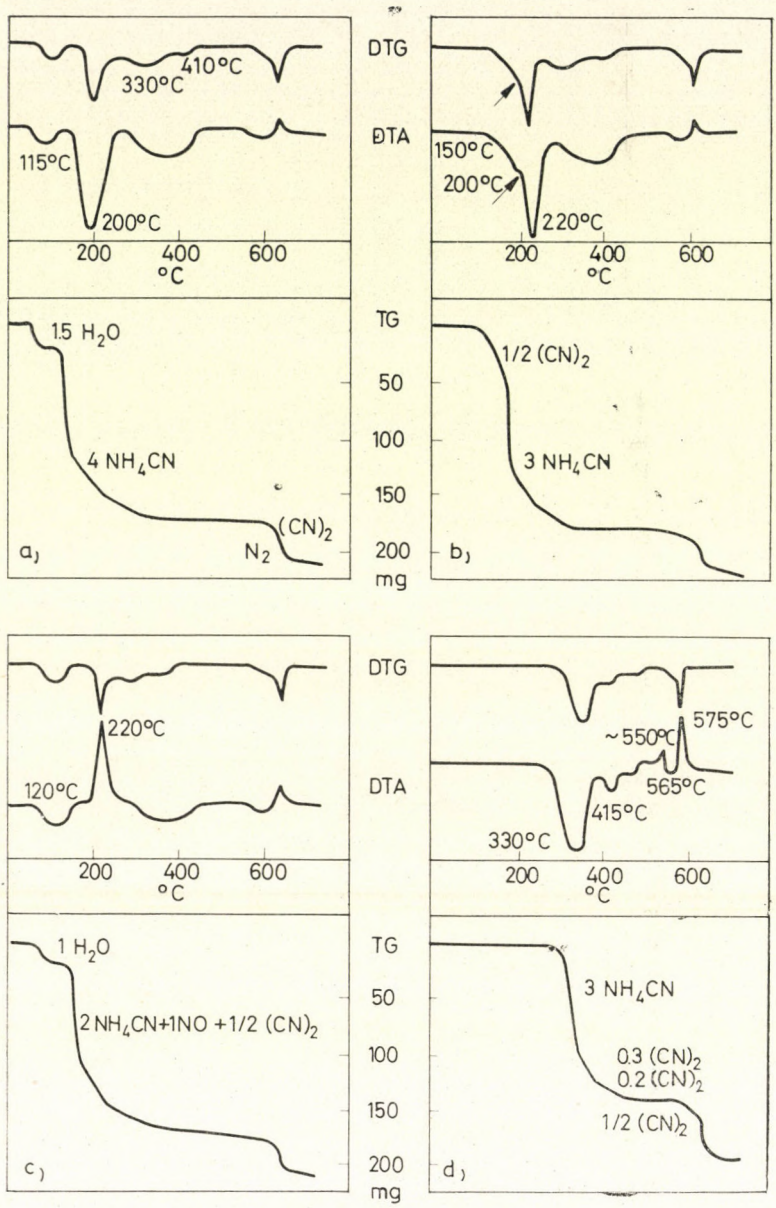

Abb. 1. Derivatogramme der Ammonium-Cyanometallate: *a)* $(NH_4)_4[Fe(CN)_6] \cdot 1{,}5\ H_2O$, *b)* $(NH_4)_3[Fe(CN)_6]$, *c)* $(NH_4)_2[Fe(CN)_5NO] \cdot H_2O$, *d)* $(NH_4)_3[Co(CN)_6]$

chen. Die Tabellendaten zeigen, daß die zu den entsprechenden Zersetzungs, stufen gehörenden Temperaturwerte identisch sind und auch die den einzelnen Teilprozessen entsprechenden Gewichtsabnahmen und Enthalpieänderungen (besonders summiert) vorzüglich übereinstimmen. Aus der Tatsache-

Tabelle II

Analysendaten des Zersetzungsgases von Ammonium-Cyanometallaten

Verbindung	Gasförmiges Produkt (Mol^{-1}) Molverhältnis	Temperatur der Unterbrechung der Thermolyse (°C)								
		150	175	210	240	260	300	330	360	550
$(NH_4)_4[Fe(CN)_6]$	NH_3	0,56	1,16	2,37		3,15		3,74		3,96
	HCN	0,34	0,81	2,03		2,97		3,77		4,04
	NH_3/HCN	1,65	1,43	1,17		1,06		0,99		0,98
$(NH_4)_3[Fe(CN)_6]$	NH_3		0,76	1,18	2,02				2,76	2,94
	$HCN+(CN)_2$		0,84	1,36	2,38				3,38	3,54
	$\frac{NH_3}{HCN+(CN)_2}$		0,91	0,87	0,85				0,82	0,83
$(NH_4)_2[Fe(CN)_5NO]$	NH_3		0			0,80			1,14	*1,31*
	$HCN+(CN)_2$		0			1,77			2,32	2,47
	$\frac{NH_3}{HCN+(CN)_2}$		(—)			0,45			0,49	0,53
	NO		0			0			0	0
$(NH_4)_3[Co(CN)_6]$	NH_3						1,83		2,48	2,93
	$HCN+(CN)_2$						1,87		2,96	3,59
	$\frac{NH_3}{HCN+(CN)_2}$						0,98		0,84	0,82

daß die Knickpunkte der TG-Kurven wiederholt bei den gleichen Temperaturwerten, nach etwa den gleichen Gewichtsverlusten auftreten und auch die Teilenthalpien befriedigend übereinstimmen, konnte gefolgert werden, daß die Brüche von wohldefinierten Teilvorgängen hervorgerufen werden. Da am Anfang der Zersetzung des Ammoniumferrocyanids ein *an Ammoniak reiches* Gasgemisch gebildet wird, in dem die Konzentration des Wasserstoffcyanids rasch zunimmt, mußte die nachstehende Reihenfolge der Teilreaktionen angenommen werden. Anfänglich dominiert die Reaktion

$$(NH_4)_4[Fe(CN)_6] \xrightarrow[\text{endo}]{200\ ^\circ C} (NH_4)_2H_2[Fe(CN)_6] + 2\,NH_3, \qquad (1)$$

dann rückt der Prozeß

$$(NH_4)_2H_2[Fe(CN)_6] \xrightarrow[\text{endo}]{330\ ^\circ C} 1/3\,Fe_2[Fe(CN)_6] + 2\,NH_3 + 4HCN \qquad (2)$$

in Vordergrund. Schließlich findet die das Molverhältnis NH_3 : HCN nicht mehr beeinflussende Reaktion

$$(NH_4)_4[Fe(CN)_6] \xrightarrow[\text{endo}]{410\ ^\circ C} 1/3\,Fe_2[Fe(CN)_6] + 4\,NH_4CN \qquad (3)$$

statt.

Die angegebenen Reaktionen verlaufen (wie das schon aus dem bisherigen hervorgeht) mit einer gewissen Überlappung. Darum sind die erwähnten Knickpunkte nur mäßig scharf und ebendeswegen dürfen die zu ihnen gehörenden Temperaturwerte bloß als Stellen betrachtet werden, an denen die obigen Reaktionen das Übergewicht erlangen.

Aus dem Ammoniumferrocyanid bildet sich im Laufe der Zersetzung — obgleich in mehreren Stufen — das gleiche Eisen(II)ferrocyanid wie aus der freien Säure. Auch seine weiteren Zersetzungsreaktionen stimmen mit denen von Wasserstoffhexacyanoferrat(II) überein, doch treten sie bei etwas höheren Temperaturen und vielleicht deshalb auch schärfer ein.

2. $(NH_4)_3[Fe(CN)_6]$

Die Zersetzung von Ammoniumhexacyanoferrat(III) beginnt, ähnlich wie bei der Eisen(II)-Verbindung, mit einer stark endothermischen Reaktion. Die Abgabe von Ammoniak und Wasserstoffcyanid verläuft aber gegenüber dem dreistufigen Prozeß des Ammoniumferrocyanids in vier Stufen, obwohl im Falle der Ferriverbindung weniger NH_4CN abgespalten werden kann. Ein weiteres Problem stellt die Tatsache dar, daß die bei der ersten Zersetzungsstufe des $H_3[Fe(CN)_6]$ beobachtete exothermische Spitze (Dicyanbildung) aus dem Derivatogramm seines Ammoniumsalzes fehlt.

Dies sind aber nur scheinbare »Unregelmäßigkeiten«. Bei näherer Betrachtung der ersten Doppelstufe ist nämlich wahrzunehmen, daß die zu ihr gehörende endothermische DTA-Spitze gewissermaßen gehemmt beginnt, dann ist ab 200 °C eine sprunghafte Änderung der Reaktionsgeschwindigkeit und der Wärmetönung zu beobachten. Unter Berücksichtigung der gasanalytischen Angaben der Tabelle II, nach welchen am Anfang der Zersetzung ein *an Cyankomponenten reiches* Gasgemisch freigesetzt wird, gelangten wir zu den nachstehenden Schlußfolgerungen:

In der ersten Zersetzungsstufe des Ammoniumferricyanids werden Dicyan, Ammoniak und Wasserstoffcyanid parallel abgegeben. Die im Falle des $H_3[Fe(CN)_6]$ gut separierbare exothermische Dicyanstufe ist daher bei seinem Ammoniumsalz mit den endothermischen NH_4CN-Stufen verschmolzen. Demzufolge bildet sich die erwähnte endothermische Spitze als die Resultierende von Prozessen entgegengesetzter Wärmetönung aus. Der in der DTA- und DTG-Kurve in Abbildung 1b sichtbare Bruch (Pfeile) bezeichnet also den Endpunkt der exothermischen Reaktion, d.h. die Beendigung der Dicyanbildung. Danach gelangt nur mehr der endothermische Wärmeeffekt der Abspaltung von NH_4CN zur Geltung, welche — ähnlich wie beim Ammoniumferrocyanid — ungefähr bei gleichen Temperaturen (220, 340 und 415 °C) ebenfalls in drei Stufen verläuft. Letzten Endes kann die erste Phase der Thermolyse des Ammoniumferricyanids also mit der folgenden Bruttogleichung beschrieben werden:

$$(NH_4)_3[Fe(CN)_6] \xrightarrow{150-415\,^{\circ}C} 1/3\ Fe_2^{II}[Fe^{II}(CN)_6] + 3\ NH_4CN + \\ + 1/2\ (CN)_2 + 54{,}3\ \text{Kcal.} \qquad (4)$$

Die weiteren Zersetzungsreaktionen sind mit denen von Ammonium- bzw. Wasserstoffhexacyanoferrat(II) identisch.

In der II. Mitteilung wurden die auf 1 Mol HCN berechneten Zersetzungswärmen von $H_4[Fe(CN)_6]$ und $H_3[Fe(CN)_6]$ verglichen. Ein solcher Vergleich der entsprechenden Werte ihrer Ammoniumsalze ist infolge des beim Eisen(III)-Komplex gleichzeitig abgespaltenen Dicyans nicht ohne weiteres möglich. Da aber — gerade aus den Zersetzungsreaktionen der Ferricyanidsäure — die bei der Entwicklung von 0,5 Mol Dicyan freiwerdende Wärme bekannt ist (−10,5 Kcal), kann der Enthalpiewert des *Ammoniumferricyanids* korrigiert werden:

$$\frac{54{,}3 + 10{,}5}{3} = 21{,}6\ \text{Kcal/Mol Komplex/Mol}\ NH_4CN\,.$$

Letzterer unterscheidet sich kaum von dem für *Ammoniumferrocyanid* erhaltenen Durchschnittswert von 22,3 Kcal. Folglich sind die Stabilitäten der Ammoniumhexacyanoferrate praktisch gleich, obwohl die entsprechenden

Säuren einen bedeutenden Unterschied zugunsten der diamagnetischen Verbindung zeigten. Diese Erfahrung ist gar nicht überraschend, denn es können auch instabile Säuren stabile Salze bilden und man findet zahlreiche Beispiele auch dafür, daß die Differenz zwischen den Stabilitäten von dasselbe Zentralatom in verschiedenen Oxydationsstufen enthaltenden Säuren viel größer ist als die ihrer Salze.

3. $(NH_4)_2[Fe(CN)_5NO]$

Nach der Abgabe des Wassergehaltes setzt sich die Thermolyse von Ammoniumpentacyanonitrosylferrat(III) mit einer heftigen, *exothermischen* Reaktion fort (– 18,0 Kcal/Mol). Dies ist um so überraschender, da die Zersetzung des $H_2[Fe(CN)_5NO]$ in der entsprechenden Phase unter stark *endothermischen* Umständen verläuft (30,0 Kcal/Mol, s. voranstehende Mitteilung). Im Falle der Säure wurden zwar ausschließlich endothermische Wärmetönung hervorrufende Komponenten (HCN und NO) freigesetzt, dagegen bildet sich bei ihrem Ammoniumsalz außer Ammoniak, Wasserstoffcyanid und Stickoxyd (endotherm) auch Dicyan (exotherm). Aus der gemeinsamen Bildung dieser Stoffe kann aber keineswegs ein exothermischer Bruttovorgang resultieren, da — auf Grund der bereits zur Verfügung stehenden Ergebnisse — bei der Dicyanbildung die Freisetzung einer etwa um eine halbe Größenordnung kleineren Wärmemenge zu erwarten ist, als die Abspaltung der erwähnten Komponenten beanspruchen würde.

Hierzu kommt noch, daß Stickoxyd im Zersetzungsgas des Ammoniumnitroprussiats in keinem Fall nachgewiesen werden konnte, weiterhin ergab sich nach der vollständigen Zersetzung der Substanz ein etwa 2/3 Mol betragender Mangel an Ammoniak (s. Tabelle II). Deshalb wurde angenommen, daß zwischen den primären Zersetzungsprodukten die Sekundärreaktion

$$2/3\,NH_3 + NO \xrightarrow{exo} H_2O + 5/6\,N_2 \qquad (5)$$

abläuft [6]. Da diese Reaktion schon stark exotherm ist, kann der Wärmebedarf der primären Zersetzung beträchtlich überkompensiert werden.

Die obige Annahme wurde im weiteren (in erster Reihe durch die Massen- und Wärmebilanz der primären und sekundären Prozesse) mehrfach bewiesen. Über diese Untersuchungen soll an anderer Stelle berichtet werden.

4. $(NH_4)_3[Co(CN)_6]$

Das Ammoniumhexacyanokobaltat(III) erwies sich sowohl auf Grund seiner hohen Zersetzungstemperatur (330 °C) als auch seiner großen Zersetzungswärme (120 Kcal/Mol) als der stabilste Vertreter dieser Verbindungs-

gruppe. Der Kobaltkomplex gibt gegenüber den Ammonium-Cyanoferraten seinen vollständigen Ammoniak- und Wasserstoffcyanid-Gehalt in einer einzigen, sehr stark endothermischen Stufe ab:

$$(NH_4)_3[Co(CN)_6] \xrightarrow{330\,^\circ C} 1/2\,Co^{III}[Co^{III}(CN)_6] + 3\,NH_4CN + 120\ Kcal. \quad (6)$$

Von hier angefangen stimmen seine Zersetzungsprozesse im wesentlichen mit denen des $H_3[Co(CN)_6]$ überein, nur setzen sie bei etwas höheren Temperaturen (5 bis 20 °C) und viel plötzlicher ein. Z. B.: die erste *endothermische* Dicyanstufe, die bei der freien Säure mit der zweiten verschmolzen war, konnte gut separiert und deshalb auch gesondert ausgewertet werden (vgl. die diesbezüglichen Angaben der II. Mitteilung). Der gemessene Gewichtsverlust scheint die frühere Annahme, nach welcher die Thermolyse des $H_3[Co(CN)_6]$ durch vorübergehende Ausbildung von Kobalt(II)kobalt(III)-Komplexen verläuft, zu beweisen:

$$1/2\,Co^{III}[Co^{III}(CN)_6] \xrightarrow{415\,^\circ C} 1/5\,Co_3^{II}[Co^{III}(CN)_6]_2 + 3/10\,(CN)_2 + 8\ Kcal. \quad (7)$$

Letzteres setzt sich in einem langsamen endothermischen Vorgang zu dem nur Kobalt(II) enthaltenden Komplex um:

$$1/5\,Co_3^{II}[Co^{III}(CN)_6]_2 \xrightarrow[endo]{440-530\,^\circ C} 1/5\,Co_3^{II}[Co_2^{II}(CN)_{10}] + 2/10\,(CN)_2. \quad (8)$$

Vergleicht man die im Falle der Ammoniumverbindung separat gemessene und auf 1 Mol Dicyan bezogene Zersetzungswärme mit dem aus der gemeinsamen Auswertung der Doppelstufe von $H_3[Co(CN)_6]$ erhaltenen Wert, so ist eine befriedigende Übereinstimmung festzustellen (25—30 Kcal/Mol Komplex/Mol Dicyan).

Die *exotherm* verlaufenden Reaktionen der weiteren Dicyanbildung sowie die inzwischen stattfindende endothermische Modifikationsänderung sind mit den Teilvorgängen der Säureverbindung identisch.

Diskussion

Den HCN-Stufen der Cyanometallat-Säuren entsprechen bei ihren Ammoniumsalzen die NH_4CN-Stufen. Da der thermische Abbau der untersuchten Komplexe im allgemeinen mit der Abgabe dieser Produkte beginnt, kann die Wärmebeständigkeit der Säure-Salzpaare zumeist auf Grund der erwähnten Zersetzungsstufen verglichen werden.

Die Versuchsergebnisse zeigten, daß die *thermische Stabilität* der Ammonium-Cyanometallate in jedem Fall größer ist, als die der entsprechenden freien

Säuren. Bei der Gegenüberstellung der *Abspaltungstemperaturen* von HCN und NH_4CN ergab sich die kleinste Differenz zwischen $H_4[Fe(CN)_6]$ und seinem Ammoniumsalz (10 °C); der größte Unterschied konnte zwischen $H_3[Co(CN)_6]$ und seinem Ammoniumsalz beobachtet werden (105 °C). Vergleicht man nun die *Zersetzungswärmen* dieser Verbindungspaare, so ist festzustellen, daß der Energiebedarf der Freisetzung des Ammoniumcyanids (22,3 bzw. 40 Kcal/Mol) in beiden Fällen fast das Vierfache des Wasserstoffcyanids erreicht (6,1 bzw. 10,8 Kcal/Mol). Schon aus diesem einzigen Beispiel ist zu ersehen, daß allein die Zersetzungstemperaturen nicht viel über die thermischen Verhältnisse aussagen, bzw. darüber inwiefern die bisher außer acht gelassenen Enthalpieänderungen zur genaueren Kenntnis des thermischen Gesamtbildes einer Verbindungsgruppe beitragen können.

Die Zersetzungstemperaturen gestalten sich auch beim Ferricyanid- und Nitroprussiat-Säure-Salzpaar den obigen entsprechend, ihre Zersetzungswärmen können aber nicht mehr verglichen werden. Es bildet sich nämlich im Falle des Ammoniumferricyanids neben Ammoniumcyanid auch Dicyan, beim Ammoniumnitroprussiat außerdem noch Stickoxyd (es findet sogar eine Sekundärreaktion statt), deshalb kann bei diesen Verbindungen nur die Resultierende der die Teilvorgänge begleitenden Enthalpieänderungen wahrgenommen werden.

Die Erfahrung, wonach das schwächer gebundene *Wasserstoffcyanid* bei sämtlichen Säuren in einer *einzigen Stufe* freigesetzt wird, steht mit den gemessenen Zersetzungswärmen in Einklang. Dagegen ist die Abspaltung des viel stärker gebundenen *Ammoniumcyanids* im Falle der Ammonium-Cyanoferrate ein *mehrstufiger* Prozeß. Es dürfte auch erwähnenswert sein, daß die *Dicyanstufen* der freien Säuren — unabhängig davon, ob sie vor oder nach der Wasserstoffcyanidstufe auftreten — meistens gut *separiert* werden können; demgegenüber ist die Dicyanbildung bei den Ammonium-Cyanoferraten immer mit den Ammoniumcyanidstufen *verschmolzen*.

Von diesen Feststellungen bilden die Kobaltkomplexe zum Teil eine Ausnahme, da bei diesen sowohl das Wasserstoffcyanid als auch das Ammoniumcyanid in einer einzigen Stufe entweicht. Die Abgabe von Dicyan verläuft aber mehrstufig und läßt sich manchmal in Teilvorgänge trennen.

Auch im Zusammenhang mit der *Wärmetönung* der Zersetzungsreaktionen kann einiges verallgemeinert werden. Die Freisetzung von *Wasserstoffcyanid* und *Ammoniumcyanid* findet — abhängig von der Stabilität des betreffenden Komplexes — in einer mehr oder weniger deutlich aber immer *endothermischen* Reaktion statt. Ebenso ist die primäre (!) Abspaltung des *Stickstoffmonoxyds* immer ein *endothermischer* Prozeß. Dagegen kann die Entwicklung von *Dicyan* endo- bzw. exothermische Wärmeeffekte hervorrufen. Die Wärmetönung der Dicyanbildung ist natürlich kein Zufall, sondern sie ist mit der Elektronenstruktur des sich zersetzenden Komplexes verbunden.

Die Abgabe von Dicyan verläuft bei den *paramagnetischen* Eisen(III)- und Kobalt(II)-Verbindungen unter *exothermischen*, bei den *diamagnetischen* Kobalt(III)- und Eisen(II)-Komplexen unter *endothermischen* Umständen.

Noch eine Erfahrung, namentlich die *Reihefolge* der Reaktionen (genauer gesagt die »Stelle« der Dicyanreaktion während der Thermolyse) steht mit den obigen Feststellungen in engem Zusammenhang. Bei den *paramagnetischen* Eisen(III)-Komplexen findet nämlich die Dicyan liefernde intramolekulare Redoxreaktion — unabhängig davon, ob sie separiert (Wasserstoffferricyanid) oder mit anderen Reaktionen verschmolzen (Ammoniumferricyanid) verläuft — immer in der *ersten* Stufe statt. Demgegenüber spielt sich die Dicyanbildung im Falle der *diamagnetischen* Eisen(III)-Verbindungen (Nitroprussiatsäure) nur in der *zweiten* Zersetzungsstufe ab. Diese Erscheinung läßt sich damit erklären, daß die diamagnetischen Eisen(III)-Komplexe durch Abgabe des dreielektronisch gebundenen Stickoxydligands erst ein ungepaartes Elektron erhalten müssen, denn sie sind zur intramolekularen Oxydation nur in diesem Zustand fähig. Mit ähnlichen Überlegungen können auch die wechselnde Wärmetönung aufweisenden Dicyanreaktionen der Cyanokobaltate erklärt werden.

Experimenteller Teil

Die angewandte Meßmethode wurde (mit besonderer Rücksicht auf die Bestimmung der Enthalpieänderungen) schon in der II. Mitteilung erörtert.

Die untersuchten Komplexsalze wurden aus den entsprechenden Säuren durch Neutralisation mit Ammoniumhydroxyd und anschließende Kristallisation hergestellt. Da die genaue Zusammensetzung der Säureverbindungen bekannt war, konnten die Ammonium-Cyanometallate einfach auf Grund ihres Ammoniakgehaltes identifiziert werden. Das Ammoniak wurde aus den Präparaten mit 10%iger NaOH-Lösung freigesetzt und mit Luft in eine Salzsäurelösung getrieben. Der Säureüberschuß wurde mit 0,1 *n* NaOH-Lösung zurücktitriert. Die Ergebnisse sind in Tabelle III dargestellt.

Tabelle III

Analysendaten der Ammonium-Cyanometallate

Verbindung	NH_4^+/Mol	Konv. (%)
$(NH_4)_4[Fe(CN)_6]$	3,895	97,5
$(NH_4)_3[Fe(CN)_6]$	3,08	100
$(NH_4)_2[Fe(CN)_5NO]$	1,96	98,0
$(NH_4)_3[Co(CN)_6]$	3,05	100

Die Zusammensetzung des im Laufe der Thermolyse gebildeten Gasgemisches wurde mit absatzweiser Aufheizung separat untersucht. Die Temperaturstellen der Unterbrechung des Zersetzungsvorganges wurden so gewählt, daß sie die Spitzen der DTA-Kurven um etwa ±20 °C in die Mitte nehmen. Das freigesetzte Gasgemisch wurde mit Stickstoff ausgetrieben und sein Ammoniakgehalt in Salzsäure-, die Cyankomponenten in Natriumhydroxyd-Lösung aufgefangen. Ersterer wurde mit azidimetrischer Rücktitration der überschüssigen Säure, letzterer — mit Rücksicht auf die Disproportionierung des Dicyans — argentometrisch bestimmt. Die Resultate dieser Untersuchungen sind aus Tabelle II schon bekannt.

LITERATUR

1. CHAMBERLAIN, M. M., GREENE, A. F.: J. inorg. nucl. Chem. **25**, 1471 (1963)
2. SEJFER, G. B.: J. anorg. Chem. (UdSSR) **7**, 1242 (1962)
3. SEJFER, G. B.: *Ibid.* **7**, 2290 (1962)
4. BRAUER, G.: Handbuch der präparativen anorganischen Chemie. Verlag: F. ENKE, Stuttgart, 1954.
5. MOHAI, B.: J. inorg. nucl. Chem. **31**, 885 (1969).
6. MOHAI, B., BAGYIN, L.: Vorlesungen der Konferenz der wissenschaftlichen Institute in Veszprém, 1968, S. 76.

Béla MOHAI; Veszprém, Nárcisz u. 16, Ungarn

Acta Chimica Academiae Scientiarum Hungaricae, Tomus 62 (3), pp. 241—252 (1969)

THE USE OF COMPLEX FORMING AGENTS IN ION EXCHANGE CHROMATOGRAPHY, IV

SEPARATION OF AROMATIC ACIDS BY MEANS OF ANION EXCHANGE COLUMN USING NICKEL(II) IONS AS COMPLEXANTS

J. INCZÉDY and L. GLÓSZ

(Institute for General and Analytical Chemistry, Technical University, Budapest)

Received November 27, 1968

A method was developed for chromatographic separation of some aromatic acids using lithium chloride and nickel(II) chloride solutions as eluents. The experimentally found peak eluent volume data were compared to those obtained by calculation based on literary and experimentally found equilibrium constant data. The separated acids were determined by direct spectrophotometric methods.

In earlier papers [1, 2] the calculation of the optimum conditions for the separation of bivalent metal ions using complex forming agents has been reported.

Anion exchange equilibria can be treated similarly to those of cation exchange. However, at the adsorption of the anions of polybasic weak acids the protonation of the anions depending on the pH of the solution must also be considered. Thus, in pH ranges, where the weak acid is not completely dissociated, the distribution coefficient depends on the adsorption strength of the different protonated anionic species. For the description of the overall distribution coefficient (D) of a dibasic acid two independent parameters or constants are necessary.

$$D_A = \frac{(A) + (HA)}{C_A} \tag{1}$$

With round brackets are denoted the concentrations of the mono- and bivalent species, in the resin phase, while C_A means the total concentration of acid in the solution, without any respect to the form of the species.

$$C_A = [H_2A] + [HA] + [A]$$

Introducing the individual partition coefficients of the adsorbable species,

$$d_A = \frac{(A)}{[A]}; \; d_{HA} = \frac{(HA)}{[HA]}$$

and the k_1 and k_2 dissociation constants of the acid, Equation (1) can be transformed:

$$D_A = \frac{d_A[A] + d_{HA}[H][A]\frac{1}{k_2}}{[A] + [A][H]\frac{1}{k_2} + [A][H]^2\frac{1}{k_1k_2}} = \frac{d_A + d_{HA}[H]\frac{1}{k_2}}{1 + [H]\frac{1}{k_2} + [H]^2\frac{1}{k_1k_2}} \tag{2}$$

Equation (2) is applicable to the calculation of the distribution coefficient, when the partition coefficients or the concentration constants of the adsorbable species and the eluent concentration are known. If the amount of the eluted A^{2-} or HA^- ions is small compared to that of the eluent chloride ions, the partition coefficients can be calculated using the following equations [1]:

$$\lg d_A = \log K_A^x Q^2 - 2\log[Cl] \tag{3}$$

$$\lg d_{HA} = \log K_{HA}^x Q - \log[Cl] \tag{4}$$

In Equations (3) and (4) Q is the volume capacity of the resin in mequ/ml; K^x the concentration constant of the anionic species referring to the eluent (chloride) ion.

$$K_{HA}^x = \frac{(HA)[Cl]}{[HA](Cl)} \; ; \; K_A^x = \frac{(A)[Cl]^2}{[A](Cl)^2}$$

Fortunately, there are some possibilities for simplifications, because in certain pH ranges only one species is predominant and usually the adsorption strength of the bivalent ion is much higher than that of the monovalent one, and the adsorption of the latter can be neglected.

The distribution coefficient of polybasic weak acids can be influenced by the concentration of the competing eluent ion and by the pH of the eluent solution but only to a limited extent. Unfortunately in the case of the separation of weak acids of similar character the change of the eluent concentration acts in the same way, and by selecting the best pH value also the selectivity of the separations can be increased but only to a limited extent. The selectivity can be increased effectively by the use of complex forming metal ions. SAMUELSON *et al.* [3, 4] used successfully zinc and magnesium acetate as eluent for separation of some aliphatic acids. Similarly other complex forming metal

ions *e.g.* nickel(II) ions can be advantageously used if acids of different complex forming properties are to be separated.

The distribution coefficient of a dibasic weak acid in the presence of complex forming bivalent metal ions is calculated by the following equation:

$$\lg D_A = \lg (K^x Q^2) - \lg \alpha_{A(M)} - 2 \log [Cl] \tag{5}$$

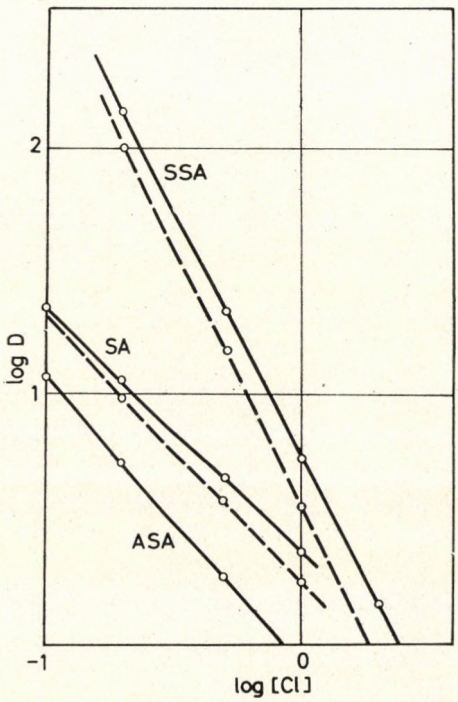

Fig. 1. Logarithmic diagram of the distribution coefficients of sulphosalicylic (SSA), salicylic (SA) and acetyl-salicylic (ASA) acids in absence (full line) and presence (broken line) of nickel(II) ions, obtained by static measurements

This equation, which is very similar to that deduced by RINGBOM [5] can be used in most cases, since for the complexation of dibasic acids bi- or trivalent metal ions are used and usually do not form any new negatively charged adsorbable species. α is the complexation coefficient, which can be calculated if the concentration of the free metal ions and the stability constant of the 1 : 1 complex (or rather the apparent stability constant K_1' taking into consideration the partial protonization of the ligand at given pH) are known.

$$\alpha_{A(M)} = 1 + [M] K_1' \tag{6}$$

K_1' is calculated using the dissociation constants of the acid.

$$K_1' = \frac{K_1}{\alpha_{A(H)}};$$

$$\alpha_{A(H)} = 1 + [H]\frac{1}{k_2} + [H]^2\frac{1}{k_1 k_2}$$

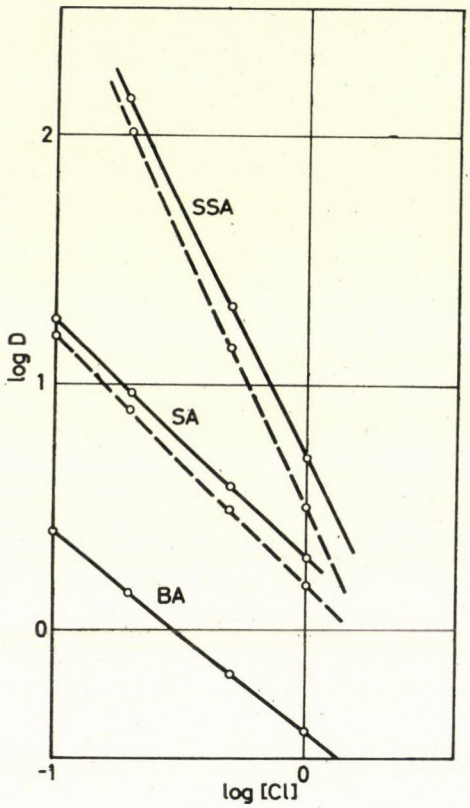

Fig. 2. Logarithmic diagram of the distribution coefficients of sulphosalicylic (SSA), salicylic (SA) and benzoic (BA) acids in absence (full line) and presence (broken line) of nickel(II) ions obtained by dynamic measurements

For separating various types of aromatic acids preliminary experiments were carried out to select the appropriate ion exchange resin, solvent and complex forming metal ion. It was found that macroporous strongly basic anion exchange resin of small particle size is suitable for the separation of the aromatic acids of small molecular weight if an ethanol–water mixture of 1 : 1 composition is used as solvent. As eluent chloride and as complexant nickel(II) ions were chosen. Nickel(II) ion forms stable complexes with many

organic ligands, does not form, however, hydroxo complexes in the pH range 4 to 7. Nickel(II) chloride is soluble in the ethanol—water solvent mixture up to 1 *M*, and the solution exhibits minimum light absorption in the region between 250 and 300 nm, so that several aromatic acids can be measured photometrically in the presence of nickel(II) ion.

To develop a method for the separation of organic aromatic acids first batch experiments were carried out to determine the ion exchange constants

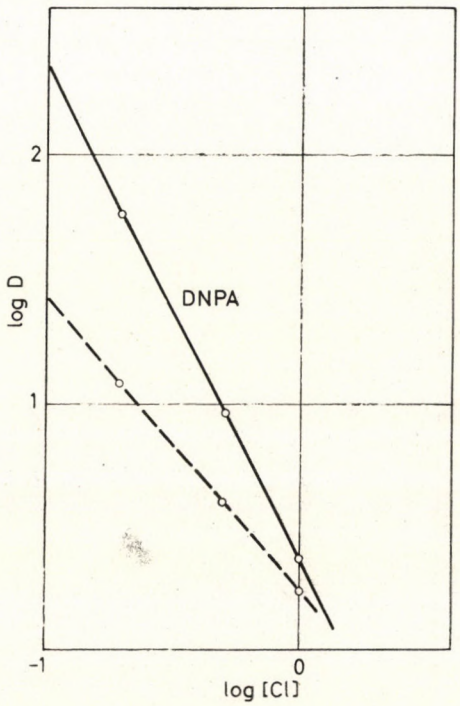

Fig. 3. Logarithmic diagram of the distribution coefficients of dinitrophthalic acid, obtained by static measurements, in absence (full line) and in presence (broken line) of nickel(II) ions

of the corresponding anions. As reference ion chloride ion — as generally accepted — and as solvent 1 : 1 ethanol — water mixture were used. All experiments were carried out at pH 5.5. Since the logarithm of the dissociation constants of the carboxylic groups of the acids are usually greater than —4, at the pH chosen they were assumed to be completely dissociated, while the phenolic groups being much weaker acids, practically undissociated.

By means of batch experiments the volume distribution coefficients of trace amounts of acids were determined, at varying concentrations of lithium chloride or nickel(II) chloride. The found volume distribution coefficient data are summarised in Figs 1 and 3.

By means of ion exchange column also elution experiments were carried out using lithium chloride or nickel(II) chloride of varying concentration as eluents. From the obtained peak eluent volume and column volume data also the volume distribution coefficients were calculated. The D values obtained

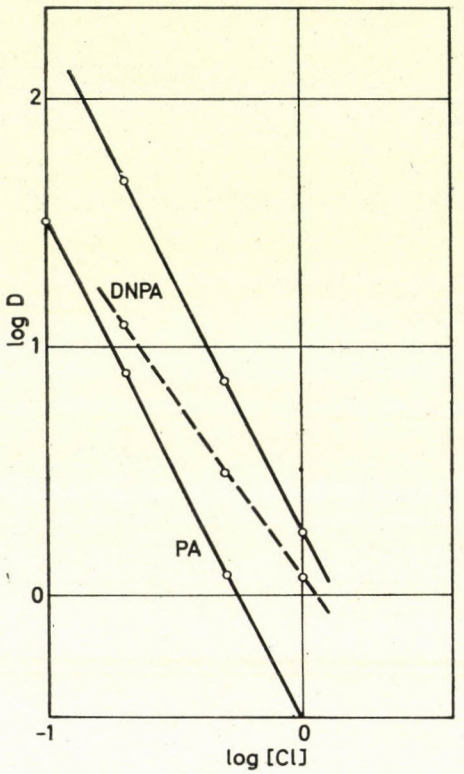

Fig. 4. Logarithmic diagram of the distribution coefficients of dinitrophthalic (DNPA) and phthalic (PA) acids, obtained by dynamic measurements, in absence (full line) and in presence (broken line) of nickel(II) ions

by column measurements were found in all cases somewhat lower than those calculated from static measurements. The distribution coefficients obtained by column measurements are summarised in Figs 2 and 4.

For the calculation of the K^x values of the anionic species the curves obtained in the absence of nickel(II) ions by static measurements, while in the cases of benzoate and phthalate ions the curves of the column measurements were used. As can be seen, the full line curves in Figs 1 and 3 (and in Figs 2 and 4) can be approximated with the following equations:

Benzoic acid (Fig. 2)

$$\lg D_{BA} = -0.4 - 0.8 \lg [Cl]$$

Salicylic acid (Fig. 1)

$$\lg D_{SA} = 0.3 - 0.9 \lg [Cl]$$

Acetylsalicylic acid (Fig. 1)

$$\lg D_{ASA}\ 2.0 - \lg [Cl]$$

Sulphosalicylic acid (Fig. 1):

$$\lg D_{SSA} = 0.76 - 2 \lg [Cl]$$

Phthalic acid (Fig. 4):

$$\lg D_{PA} = -0.4 - 2 \lg [Cl]$$

Dinitrophthalic acid (Fig. 3)

$$\lg D_{DNPA} = 0.38 - 2 \lg [Cl]$$

On the basis of the above equations one can establish that under the conditions prevailing in the experiments the acids are present as completely dissociated mono- and bivalent anions except benzoic and salicylic acids, in case of which the dissociation is not complete owing to their lower first dissociation constants.

Using the capacity of the resin, the K^x values were calculated directly by Equations (3) and (4), but in the case of benzoic and also salicylic acid a correction for incomplete dissociation was made. The calculated apparent constants were multiplied by the protonation coefficient ($\alpha_{A(H)}$) to obtain the real K^x values. The calculated ion exchange constants are summarised in Table I.

Table I

Volume ion exchange constants of some mono- and bivalent aromatic anions referred to chloride ion, in 1 : 1 ethanol—water mixture, calculated from distribution data obtained at pH 5.5, at room temperature Ion exchange resin Lewatit MP—500

Ligand	Anion formed at pH 5.5	K_{A-Cl}
Benzoate	A^-	0.46*
Salicylate	A^-	2.75
Acetyl-salicylate	A^-	1.1
Sulpho-salicylate	A^{2-}	6.9
Phthalate	A^{2-}	0.48*
Dinitrophthalate	A^{2-}	2.9

* from column measurements

The distribution coefficients in the presence of increasing nickel(II) chloride concentration were found to be lower than those obtained in the absence of complex forming ions (*i. e.* in equivalent lithium chloride solution) corresponding to the extents of complexation of the individual acids. (See broken line curves in Figs 1—4.)

However, in the case of dinitrophthalic acid the difference between the distribution coefficients measured in the absence and presence of nickel(II) ions do not increase, but decrease with increasing ion concentration of nickel(II).

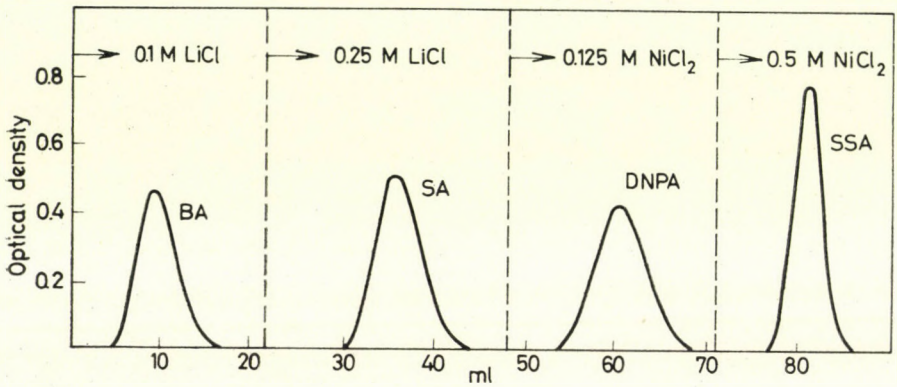

Fig. 5. Chromatographic separation of benzoic (BA), salicylic (SA), dinitrophthalic (DNPA), sulphosalicylic (SSA) acid mixture using also nickel(II) ions as complexant. Ion exchange column: Lewatit MP 500 (150—300 mesh); 5×180 mm; flow rate: 0.1 ml/min

This anomalous phenomenon, which is inconsistent with the basic principle (*i. e.* that only the negatively charged species are adsorbed on the resin), can be explained probably by a salting out effect; namely the increasing concentration of the salt was responsible for the increasing adsorption strength of the non ionic dinitrophthalato nickel(II) complex molecule.

On the basis of the obtained distribution coefficient data and K^x values separations of the acids were planned and carried out using an anion exchange column and an eluent the composition of which was changed stepwise during chromatography.

Two chromatograms of the separations obtained with Lewatit MP 500 resin column using lithium chloride and nickel(II) chloride as eluent solutions can be seen in Figs 5 and 6.

The calculation of the peak eluent volume values, using the obtained K^x values, and stability constant, dissociation constant data given in the literature, and Equations (3), (4), (5) and (6), can be given briefly as follows. (The constants were used without any correction, assuming that the errors of the approximate calculations were in similar order of magnitude as the deviations of the constants in aqueous and in mixed solvent solutions.)

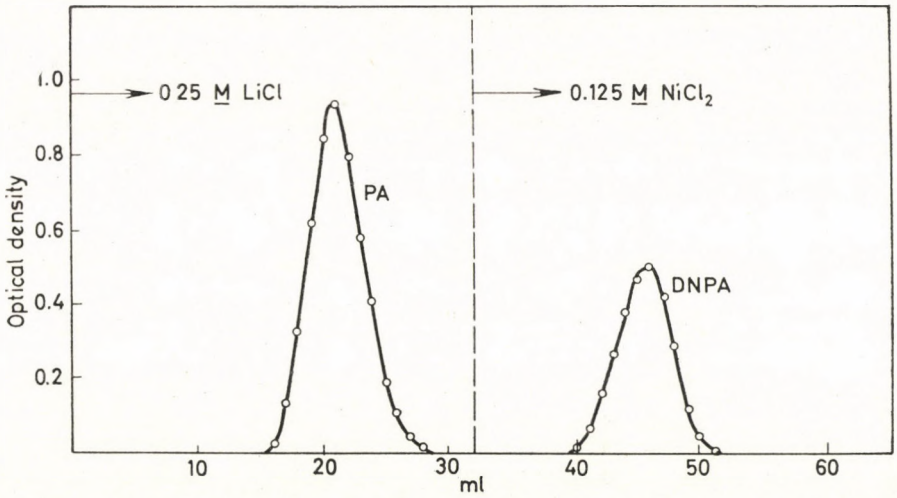

Fig. 6. Chromatographic separation of phthalic (PA) and dinitrophthalic (DNPA) acids, using nickel(II) ions as complexant. Ion exchange column: Lewatit MP 500 (150—300 mesh); 5×180 mm; flow rate: 0.1 ml/min

Acid dissociation constants and first stability of the Ni-complex used:

Benzoic acid: $\lg k_1 = -4.0$; $\lg K_1 = 0.9$ [6]
Salicylic acid: $\lg k_1 = -2.9$, $\lg k_2 = -13.1$: [7]; $\lg K_1 = 7.0$ [8]
Sulphosalicylic acid: $\lg k < 1$; $\lg k_2 = -2.6$, $\lg k_3 = -11.6$ [7]; $\lg K_1 = 6.4$ [9]
Phthalic acid: $\lg k_1 = -2.8$, $\lg k_2 = -5.1$ [7]; $\lg K_1 = 2.1$ [6]
Dinitrophthalic acid: $\lg k_1 = -1.7$, $\lg k_2 = -3.2$ [10]; $\lg K_1 = 1.78$ (estimated)
Resin column volume, $X = 3.52$ ml; Void fraction, $a = 0.4$.

Separation I (See Fig. 5)

Benzoic acid (Eluent 0.1 *M* LiCl)
$\lg D_{BA} = -0.4 + 0.8 = 0.4$; $D_{BA} = 2.5$
$v_{max,\,BA} = X(D_{BA} + a) = 3.52 \cdot 2.9 \approx 10.2$ ml
Salicylic acid (Eluent: 22 ml 0.1 *M* LiCl + 0.25 *M* LiCl)
$\lg D^1_{SA} = 0.3 + 0.9 = 1.2$; $D^1_{SA} = 16$
$22 = x_1(D^1 + a) = x_1 \cdot 16.4$; $x_1 = 1.34$ ml
$\lg D^2_{SA} = 0.3 + 0.54 = 0.8$; $D^2_{SA} = 7$
$v_{max,\,SA} = 22 + (3.52 - 1.34)(7 + 0.4) \approx 38.1$ ml
Dinitrophthalic acid (Eluent: 22 ml 0.1 *M* LiCl + 26 ml 0.25 *M* LiCl + 0.125 *M* $NiCl_2$)
$\lg D^1_{DNPA} = 0.38 + 2 = 2.38$; $D^1_{DNPA} = 240$
$\lg D^2_{DNPA} = 0.38 + 1.2 = 1.58$; $D^2_{DNPA} = 38$
$\alpha_{DNPA(Ni)} = 1 + 0.125 \cdot 60 \approx 8.5$; $\lg \alpha = 0.93$
$\lg D^3_{DNPA} = 0.38 - 0.93 + 1.2 = 0.65$; $D^3_{DNPA} = 4.5$
$22 = x_1 \cdot 240$; $x_1 = 0.092$ ml
$26 = x_2 \cdot 38.4$; $x_2 = 068$ ml; $x_1 + x_2 = 0.77$ ml
$v_{max,\,DNPA} = 48 + (3.52 - 0.77)(4.5 + 0.4) \approx 61.5$ ml
Sulphosalicylic acid (Eluents: 22 ml 0.1 *M* LiCl + 26 ml 0.25 *M* LiCl + 23 ml 0.125 *M* $NiCl_2$ + 0.5 *M* $NiCl_2$)
$\lg D^1_{SSA} = 0.76 + 2 = 2.76$; $D^2_{SSA} = 580$
$\lg D^2_{SSA} = 0.76 + 1.2 = 1.96$; $D^2_{SSA} = 92$

$$\alpha_{SSA(Ni)} = 1 + [Ni]\frac{K}{\alpha_{SSA\,(H)}} = 1 + 0.125\,\frac{10^{6.4}}{10^{6.1}} = 1.25$$

$\lg \alpha_{SSA(Ni)} = 0.1$
$\lg D^3_{SSA} = 0.76 - 0.1 + 1.2 = 1.86$; $D^3_{SSA} = 72$

$\alpha_{SSA(Ni)} = 1 + 0.5 \cdot 2 = 2$; $\lg \alpha_{SSA} = 0.3$
$\lg D^4_{SSA} = 0.76 - 0.3 - 0 = 0.46$; $D^1_{SSA} = 2.9$
$22 = 580\ x_1$; $x_1 = 0.038$
$26 = 92.4\ x_2$; $x_2 = 0.28$
$23 = 72.4\ x_3$; $x_3 = 0.32$
$v_{max,\ SSA} = 71 + (3.52 - 0.64)(2.9 + 0.4) \approx 80.5$ ml

Separation II (See Fig. 6)

Phthalic acid (Eluent: 0.25 *M* LiCl)
$\lg D_{PA} = -0.4 + 1.2 = 0.8$; $D_{PA} = 6.3$
$v_{max,\ PA} = 3.52\ (6.3 + 0.4) = 23.5$ ml

Dinitrophthalic acid (Eluent: 32 ml 0.25 *M* LiCl + 0.125 *M* $NiCl_2$)
$\lg D^1_{DNPA} = 0.38 + 1.2 = 1.58$; $D^1_{DNPA} = 38$
$\alpha_{DNPA(Ni)} = 1 + 0.125 \cdot 60 = 8.5$; $\lg \alpha_{DNPA} = 0.93$
$\lg D^2_{DNPA} = 0.38 - 0.93 + 1.2 = 0.65$; $D^2_{DNPA} = 4.5$
$32 = 38.4\ x_1$; $x_1 = 0.84$
$v_{max,\ DNPA} = 32 + (3.52 - 0.84)(4.5 + 0.4) = 45.2$ ml

The calculated v_{max} values and those obtained from the chromatograms are summarised in Table II. As it can be seen from the table, there are no high deviations between the calculated and experimentally found peak eluent volumes.

Experimental

Reagents. In all experiments a.g. reagents were used.

0.01 *M* stock solutions of benzoic, salicylic, acetylsalicylic, sulphosalicylic, phthalic, dinitrophthalic acids were prepared by weighing the solid substances and dissolving in ethanol, and after adjusting with ethanolic 0.1 *M* lithium hydroxyde solution to pH 5.5, diluted to the required volume.

2 *M* lithium chloride stock solution. The solid salt was weighed and dissolved in 1 : 1 ethanol–water mixture and diluted to the required volume. The chloride concentration of the solution was checked by argentometric titration.

Table II

Calculated and experimentally found peak eluent volumes of some aromatic acids, using eluent solution of stepwise varied composition, of pH 5.5

Acid	Eluent used	v_{max} (ml)	
		calculated	found
Benzoic acid	0.1 *M* LiCl	10.2	9
Salicylic acid	22 ml 0.1 *M* LiCl + 0.25 *M* LiCl	38.1	37
Dinitrophthalic acid	22 ml 0.1 *M* LiCl + + 26 ml 0.25 *M* LiCl + + 0.125 *M* $NiCl_2$	61.5	60
Sulphosalicylic acid	22 ml 0.1 *M* LiCl + + 26 ml 0.25 *M* LiCl + 23 ml 0.125 *M* $NiCl_2$ + 0.25 *M* $NiCl_2$	80.5	82
Phthalic acid	0.25 *M* LiCl	23.5	21
Dinitrophthalic acid	32 ml 0.25 *M* LiCl + + 0.125 *M* $NiCl_2$	45.2	46

1 *M* nickel(III) chloride stock solution. The solid crystalline salt was weighed and dissolved in 1 : 1 ethanol–water mixture and diluted to the required volume. The pH and the chloride concentration of the solution were determined.

Ion exchange resin. Lewatit MP 500 commercially available resin was sieved and the fraction of 0.3—0.5 mm particle size was treated with acid and alkali in the usual way, then transformed to the chloride form and washed with deionised water and finally extracted in a Soxleth apparatus with 96% ethanol. The extracted resin was dried at room temperature and stored in glass bottle. The capacity of the resin was determined by the usual method [11] and found to be 3.15 mequ/g air dried resin. The column density of the resin was $\sigma = 0.29$.

For elution experiments the pretreated resin was ground and fractionated by sedimentation until a fraction of 150—300 mesh particle size was obtained.

Instruments. For quantitative determination of aromatic acids a Spektromom 201 (MOM, Hungary) spectrophotometer; for the determination of pH an Universal pH-meter Typ 204 (Radelkisz, Hungary); in the elution experiments Fractomat Y 3 (Hako, Germany) fraction collector were used.

Determination of distribution coefficients by static method. 0.25 g air dried pretreated resin sample of the chloride form was weighed in a glass stoppered bottle. The solution containing lithium chloride or nickel(II) chloride and aromatic acid of required concentration in 1 : 1 ethanol–water mixture was prepared from known portions of the stock solutions and filled up to 50 ml in volumetric flasks. The amounts in μmoles of the aromatic acids used in the experiments (50 ml final volume) were as follows: Benzoic acid 25, salicylic acid 10, acetylsalicylic acid 25, sulphosalicylic acid 25, phthalic acid 5, and dinitrophthalic acid 12.5. 25 ml of the solution prepared was added to the resin sample by a pipette and after closing the bottle, it was allowed to stand 24 hours, shaked periodically to reach the equilibrium. After equilibration a fraction of the original solution and a fraction of the equilibrated solution was analysed spectrophotometrically. The optical density was measured at the following wave lengths for the determination of the individual acids: Benzoic acid 272, salicylic and sulphosalicylic acid: 300, acetylsalicylic acid 295, phthalic acid 225, dinitrophthalic acid 305 nm. The concentration was determined using calibration graphs and the D_s weight- and D volume distribution coefficients calculated:

$$D_s = \frac{\text{mequ. ion/g air dried resin}}{\text{mequ. ion/ml solution}}$$

$$D = D_s \cdot \sigma$$

Elution experiments. For elution experiments an ion exchange column of size 5 × 100 mm was prepared from the pretreated finely ground ion exchange resin. A small portion of the stock solution was poured on the resin column and the elution was carried out with lithium or nickel(II) chloride eluent solution made with 1 : 1 water–ethanol mixture. The flow rate of the eluent was kept constant, 0.1 ml/min. The effluent was collected in 1 or 2 ml fractions using an automatic fraction collector, and the fractions filled up to 5 ml with solvent mixture and analysed. From the obtained data elution graphs were constructed and the peak eluent volume (v_{max}) in ml determined. The volume distribution coefficient was also calculated [12]:

$$D = \frac{v_{max}}{X} - a$$

X = column volume in ml; a = void fraction of the column.

Separation of acids. Ion exchange column of size 5 × 180 mm was prepared from the pretreated finely ground ion exchange resin. Small portions of the stock solutions of the acids were pipetted on the column, washed with some drops of ethanol–water solvent mixture. The total amounts of the acids separated were: Benzoic acid: 25, salicylic acid 5, dinitrophthalic acid 5, sulphosalicylic acid 7.5, phthalic acid 2.75 μmol. The elution was carried out with eluents given in Figs 5 and 6, with a flow rate of 0.1 ml/min. The effluent was collected in 1 ml fractions. The optical density of the fractions after dilution to 5 ml was measured at the proper wave length (given before).

*

The authors express their thanks to Prof. L. ERDEY, Head of the Institute, for his support and attention concerning the work.

REFERENCES

1. INCZÉDY, J., GÁBOR-KLATSMÁNYI, P., ERDEY, L.: Acta Chim. Acad. Sci. Hung. **61,** 261 (1969).
2. INCZÉDY, J., GÁBOR-KLATSMÁNYI, P., ERDEY, L.: Acta Chim. Acad. Sci. Hung. **62,** 1 (1969).
3. LARSSON, V. B., ISAKSSON, T., SAMUELSON, O.: Acta Chem. Scand. **20,** 1965 (1966).
4. LEE K. S., SAMUELSON, O.: Anal. Chim. Acta **37,** 359 (1967).
5. RINGBOM, A.: Complexation in Analytical Chemistry. Wiley, New York, 1963.
6. YASUDA, M., YAMASAKI, K., OHTAKI, H.: Bull. Chem. Soc. Japan **33,** 1067 (1960).
7. KORTÜM, G., VOGEL, W., ANDRUSSOW, K.: J. of IUPAC 1, No 2—3. Butterworths, London, 1961.
8. PERRIN, D. D.: Nature 182, 741 (1958).
9. BANKS, C. V., SING, R. S.: J. Inorg. Nucl. Chem. **15,** 125 (1960).
10. INCZÉDY, J., ÁKOS-SZABÓ, Zs.: Unpublished data
11. INCZÉDY, J.: Analytical Application of Ion Exchangers. Pergamon Press, Oxford, 1966.
12. KRAUS, K. A., NELSON, F.: Symposium of Ion Exchange and Chromatography in Analytical Chemistry. P. 27. ASTM spec. Publ. No. 195, 1958.

János INCZÉDY
László GLÓSZ
} Budapest XI, Gellért tér 4

Acta Chimica Academiae Scientiarum Hungaricae, Tomus 62 (3), pp. 253—262 (1969)

INVESTIGATIONS IN THE FIELD OF RADIATION-INDUCED SOLID STATE POLYMERIZATION, XXV*

INFLUENCE OF A SECOND COMPONENT ON THE SOLID STATE POLYMERIZATION OF CETYL VINYL ETHER

GY. HARDY, K. NYITRAI and F. CSER

(Research Institute for Plastics, Budapest)

Received March 15, 1968

The kinetics of the solid state polymerization were investigated in the binary systems cetyl vinyl ether–*p*-benzoquinone and cetyl vinyl ether–dimethyl oxalate. It was found that the additives somewhat retard polymerization up to the eutectic composition, but at higher concentrations their effect remains unchanged.

The solid state polymerization of cetyl vinyl ether occurs by cationic mechanism; this has been confirmed by its solid state polymerization initiated with iodine vapour.

In our previous communication [1] we have reported on the laws governing the liquid-crystalline and solid state polymerization of cetyl vinyl ether. The polymerization rates have been found to change proportionally to the first power of dose rate, which is generally an indication of polymerization occurring by ionic mechanism. Considering the tendency of aliphatic vinyl ethers to polymerization by cationic mechanism, the process in all probability takes place according to this mechanism. In the present work we have investigated the effects of benzoquinone and dimethyl oxalate additives on the solid state polymerization of cetyl vinyl ether. Benzoquinone is a free radical acceptor, while dimethyl oxalate was chosen as an inert additive having almost the same phase diagram as benzoquinone. In previous papers [2, 3] we have pointed out that the mechanism of solid state polymerization can be determined with great certainty by studying the effect of additives, mainly for monomers polymerizing according to accelerating kinetical curves, provided the phase diagrams are known.

Experimental

The experimental method was the same as described previously [1]. The phase diagrams of the binary systems were determined by a polarization-optical method [4]. To avoid anomalies due to co-crystallization [5], the binary systems of various compositions were melted prior to irradiation and crystallized at a temperature 1—2 °C below the melting point of the eutectic composition. Polymerization was carried out in the presence of iodine by applying an about 0.02 mm thick layer of 0.5 g of cetyl vinyl ether to the walls of normal test tubes. In another small open glass vessel 1 g of iodine was weighed and this vessel was then placed into the test tube containing the cetyl vinyl ether which was maintained at the temperature of polymerization. The beginning of polymerization was counted from the time the iodine was placed into the test tube. After the end of polymerization, first the vessel containing the iodine was removed from the test tube and the unchanged cetyl vinyl ether monomer extracted, without dissolution, with acetone at the temperature of polymerization. In acetone solution no polymerization of the monomer takes place in the presence of iodine.

*Part XXIV: European Polym. Journ. 5, 133 (1969)

Results and discussion

Fig. 1 shows the phase diagram of the system cetyl vinyl ether–benzoquinone, which is characterized by an eutectic mixture containing 4.5 mole-% of benzoquinone and having a melting point of 14 °C. Similar phase diagrams were obtained for the systems allyl palmitate–benzoquinone [6] and vinyl

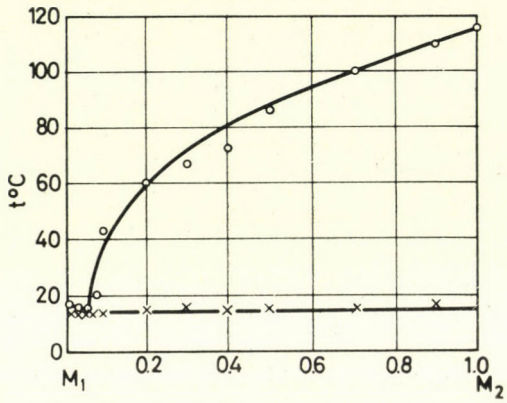

Fig. 1. Phase diagram of the binary system cetyl vinyl ether (M_1) and benzoquinone (M_2)

laurate–benzoquinone [7]. Even these monomers with long aliphatic substituents form an eutectic mixture with relatively small amounts of benzoquinone. The polymerization kinetical curves in Fig. 2 were determined at 0 °C for systems with various benzoquinone contents. It appears quite clearly that with increasing quantities of benzoquinone, up to the eutectic composition, the length of the induction period increases and the slope of the steep section of accelerating kinetical curves decreases, *i. e.* even the accelerated section will be somewhat slower than in the case of the pure monomer. It was established in our earlier work [1] that the accelerating kinetical curve in the case of cetyl vinyl ether was characteristic of the monomer in the smectic liquid crystal state. As indicated by the phase diagram, the liquid crystalline phase of cetyl vinyl ether forms with benzoquinone an eutectic mixture at 14 °C, thus at 0 °C cetyl vinyl ether is in a liquid crystalline state. This is confirmed by polaroptical patterns taken at 0 °C. Consequently, the benzoquinone molecules display their action on the cetyl vinyl ether plates along the plane formed by the vinyl groups. They may either block the emerging of vinyl groups from the plane, or alter the dielectric conditions in the polymerization area. The first effect would lead to the acceleration of polymerization (see Part XXIV of this series), so that the second assumption appears to be more likely. The maximum size of the contacting surfaces develops up to the

eutectic composition; after this, the separate benzoquinone crystals have no effect on the kinetic process of polymerization. It appears from Table I that benzoquinone has no unambiguous effect on the molecular weight, and on the intrinsic viscosity of the value of limit conversion. This is in good agreement with the above explanation. In the case of other monomers investigated so far, which polymerize in the solid phase according to accelerating kinetical curves, in agreement with a radical mechanism, an unambiguous retarding effect of

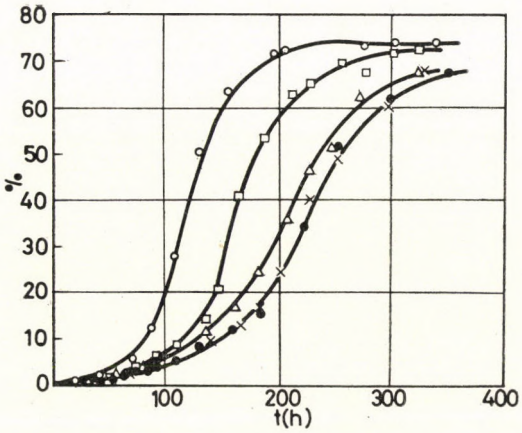

Fig. 2. Polymerization kinetical curves of cetyl vinyl ether irradiated with a constant dose rate of 5.26×10^4 rad/hour at 0 °C, in the presence of various quantities of benzoquinone: ○ = 0%, □ = 2.25 mole-%, △ = 2.5 mole-%, × = 4.5 mole-% (eutectic composition), ● = 15 mole-% benzoquinone

benzoquinone was observed, *e.g.*, for N-vinylsuccinimide [2], N-vinylcarbazole [8, 9] and acrylamide [3] monomers; at the same time, the presence of benzoquinone considerably lowered the molecular weights of the formed polymers and the limit conversion of solid state polymerization was markedly decreased. Fig. 3 shows the polymerization kinetical curves of pure cetyl vinyl ether and of a system containing 15 mole-% of benzoquinone at −10 °C. The system was prepared by storing the samples at −10 °C for 72 hrs prior to irradiation, to complete the slow crystallization process [1]. At this temperature cetyl vinyl ether forms solid three-dimensional crystals and its solid state polymerization kinetical curve has linear character. It is obvious that benzoquinone concentrations much above the eutectic composition result in a mild retarding action. In Fig. 4 are plotted the results obtained at −20 °C, under otherwise unchanged conditions, that is in the temperature range of the second crystalline modification of cetyl vinyl ether [1]. Here, too, a benzoquinone concentration three times higher than in the eutectic mixture has only a mild retarding effect.

Table I

Intrinsic viscosity values of the polymers formed in the binary systems cetyl vinyl ether (CVE)–rate of 5.26 × 10⁴, as a function of the

Conversion of pure poly-CVE %	[η]	0.25 mole-% BQ	[η]	2.5 mole-% BQ	[η]	4.5 mole-% BQ
		conversion %		conversion %		conversion %
5.2	0.060	5.9	0.060	10.0	0.096	12.7
12.0	0.042	14.0	0.071	17.0	0.078	15.6
27.5	0.050	39.0	0.068	24.5	0.078	24.6
39.5	0.082	42.0	0.041	46.2	0.064	39.9
50.1	0.070	63.0	0.078	52.0	0.063	49.3
65.1	0.048	65.1	0.070	43.0	0.088	60.1
69.4	0.052	68.3	0.085	68.0	0.062	67.3
72.0	0.070	70.0	0.076			
73.1	0.076	77.0	0.070			

The effect of crystallization time on the behaviour of the binary systems was also investigated. The kinetical curves shown in Fig. 5 were measured on systems irradiated immediately after cooling down to −10 °C. These results differ essentially from those plotted in Fig. 2, since the induction periods do not become longer at higher benzoquinone concentrations. Systems containing benzoquinone are retarded only after a conversion of about 35% has been attained, and subsequently the kinetical curve is independent of the benzo-

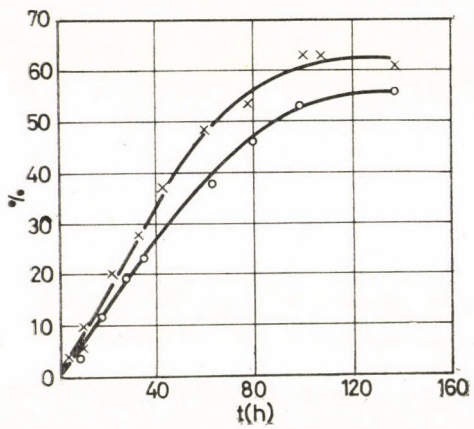

Fig. 3. Polymerization kinetical curves of cetyl vinyl ether irradiated with a constant dose rate of 5.26×10^4 rad/hour at −10 °C: × = pure monomer; ○ = 15 mole-% benzoquinone

benzoquinone (BQ) and cetyl vinyl ether–dimethyl oxalate (DMO) by irradiation at 0 °C with a do s composition and the degree of conversion

[η]	15 mole-% BQ conversion %	[η]	5.5 mole-% DMO conversion %	[η]	15 mole-% DMO conversion %	[η]
0.078	11.2	0.060	5.2	0.060	5.0	0.060
0.075	15.8	0.054	9.2	0.040	6.7	0.060
0.085	25.0	0.081	15.5	0.056	11.0	0.076
0.064	42.0	0.070	19.2	0.043	28.5	0.080
0.058	49.0	0.064	30.0	0.071	56.0	0.056
0.074	68.5	0.053	40.0	0.068	60.5	0.069
0.070			52.0	0.078	67.5	0.086
			65.1	0.060	78.5	0.080
			70.2	0.052		
			76.0	0.086		

quinone concentration with an about 10% reduction in the value of limit conversion. In the above cases, the retarding effect may be attributed rather to the lattice destroying action of the benzoquinone crystals which in the case of linear kinetical curves, that is of monomers polymerizing in the lattice, brings about a retardation of the process [3]. Here again it is possible to interpret the effect of benzoquinone by the above described mechanism. The only difference between the two structures appears to be that in the true crystal-

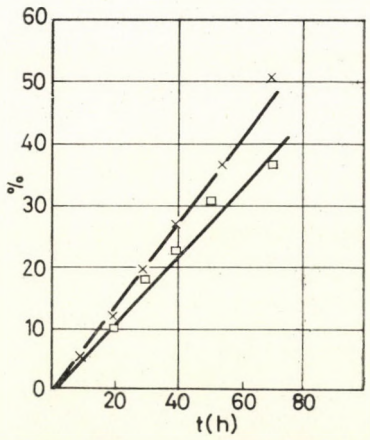

Fig. 4. Polymerization kinetical curves of cetyl vinyl ether irradiated with a constant dose rate of 5.26×10^4 rad/hour at −20 °C: × = pure monomer; □ = 15 mole-% benzoquinone

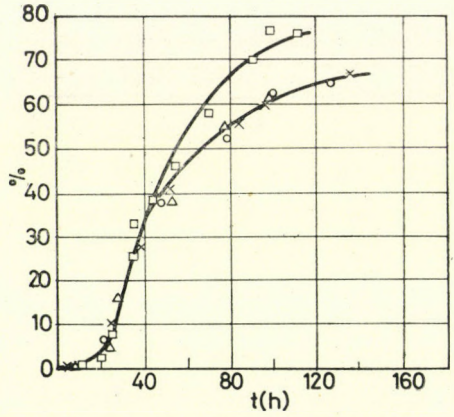

Fig. 5. Polymerization kinetical curves of cetyl vinyl ether irradiated immediately after cooling to $-10\,°C$ with 9.3×10^4 rad/hour dose rate: □ = pure monomer; × = 2.5 mole-% benzoquinone; ○ = 4.5 mole-% benzoquinone (eutectic composition); △ = 15 mole-% benzoquinone

line state the vinyl groups are situated in a well-defined plane and this plane is not disturbed by the presence of foreign molecules. Thus the kinetics of the process remains linear. In the case of rapid crystallization, an undercooled, liquid crystalline eutectic system is formed, so that the effect will be similar to that observed before. On the other hand, rapid cooling in the less mobile system does not leave time for the benzoquinone crystals to get inserted gradually and in accordance with the composition in between the plates consisting of clusters of molecules. Consequently, the effect on the polymerization

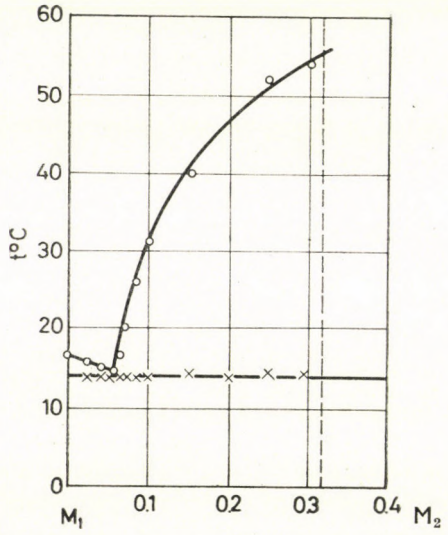

Fig. 6. Phase diagram of the binary systems cetyl vinyl ether (M_1) and dimethyl oxalate (M_2)

kinetical curve will be practically independent of the benzoquinone concentration, and kinetical retardation is observed in practice only after 35% conversion.

In order to show that the effects observed with benzoquinone are independent of the radical capturing nature of this substance, a compound was sought, to be used as an additive, whose phase diagram was similar to and the polarity roughly identical with those of benzoquinone. Dimethyl oxalate seemed to meet these requirements. Fig. 6 shows the phase diagram of the binary system cetyl vinyl ether–dimethyl oxalate, which is again characterized by the formation of an eutectic mixture with a melting point of 13.5 °C

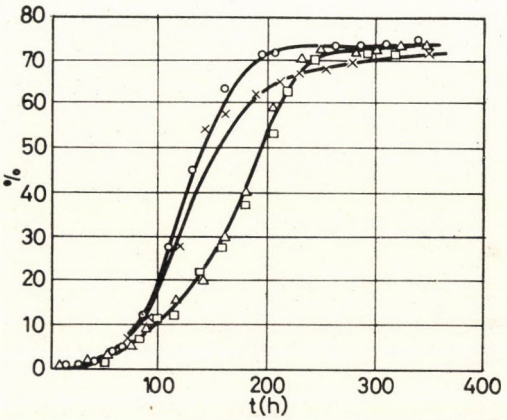

Fig. 7. Polymerization kinetical curves of cetyl vinyl ether irradiated with a constant dose rate of 5.26×10^4 rad/hour at 0 °C in the presence of various quantities of dimethyl oxalate: ○ = pure monomer; × = 1 mole-% dimethyl oxalate; △ = 5.5 mole-% dimethyl oxalate (eutectic composition); □ = 15 mole-% dimethyl oxalate

at 5.5 mole-% dimethyl oxalate content. At the melting point of dimethyl oxalate (54 °C), this compound mixes when melted with cetyl vinyl ether only up to 30 mole-% of dimethyl oxalate content, hence the examination of the phase diagram also ends at this composition. Fig. 7 shows the polymerization kinetical curves of cetyl vinyl ether with various dimethyl oxalate contents measured at 0 °C. Here again the trends are the same as in the case of benzoquinone. The induction period becomes longer, and the slope of the accelerating section smaller in the presence of dimethyl oxalate, and at concentrations higher than the eutectic, the degree of changes is the same as observed for the eutectic composition.

The data in Table I show no unambiguous effect of dimethyl oxalate on the intrinsic viscosity of the formed polymers and on the values of limit conversion. Thus the results support the assumption that in the given case the molecules of the foreign substance alter the dielectric conditions in the area of ionic polymerization and influence the course of polymerization in this way.

Consequently, the effect of both benzoquinone and dimethyl oxalate on the course of the polymerization of cetyl vinyl ether may be unequivocally explained by dielectric effects.

To find further confirmation of the validity of the polymerization mechanism of cetyl vinyl ether suggested earlier [1], the effects of various initiators and catalyst systems were investigated. The results are shown in Table II. It

Table II

Dependence of the polymerization tendency of cetyl vinyl ether on the initiator and the catalyst system applied

No.	Initiation	Polymerization temperature, °C	Polymerization	Note
1.	Azo-bis-isobutyronitrile	70	—	6 hrs polymerization
2.	Benzoyl peroxide	70	—	6 hrs polymerization
3.	Ultra-violet irradiation	25	—	5 hrs irradiation in quarz tube
4.	Gamma rays	25	—	22.6 Mrad total dose
5.	$FeCl_3$*	25	+	20 min; yield about 64%
6.	$AlCl_3$*	25	+	20 min; yield about 71%
7.	BF_3*	25	+	20 min; yield about 86%
8.	$TiCl_4$*	25	+	20 min; yield about 68%
9.	Iodine	25	+	35 min; yield about 61%

* diethyl ether solution
\+ polymerization
— no polymerization

appears that liquid phase polymerization is initiated only by the known catalysts of polymerizations occurring by cationic mechanism. In further work the kinetics of the solid phase polymerization of cetyl vinyl ether was studied. The polymerization was initiated at various temperatures by iodine vapours (Fig. 8). The kinetical curves are linear and later tend to a limit conversion. This inflection is more pronounced on the kinetic curve measured at 0 °C and is similar to the retarded kinetical curve.

In this case, the kinetical curves express beyond the polymerization kinetics also the diffusion properties of iodine vapours in both the gaseous and the solid monomeric phase. Thus, *e.g.*, in the solid phase (−10 °C, −78 °C) the diffusion rate of iodine does not change as a function of the quantity of the formed polymer, while at 0 °C, in the liquid crystalline state, it must decrease owing to the higher viscosity (lower mobility).

As shown by the data in Table III, no unequivocal correlation analogous to radiation initiation was found between the intrinsic viscosity of the

polymers (*i.e.* their molecular weights), and the polymerization temperature and conversion.

The effectual polymerizing action of iodine, together with the other facts described, prove the cationic mechanism of polymerization. The first step of iodine-initiated polymerization is in all probability the absorption of iodine vapours on the surface of the monomer, followed by the formation of a charge-transfer complex [10], which then initiates ionic polymerization [11]. In the following step iodine diffuses towards deeper layers where it displays the same

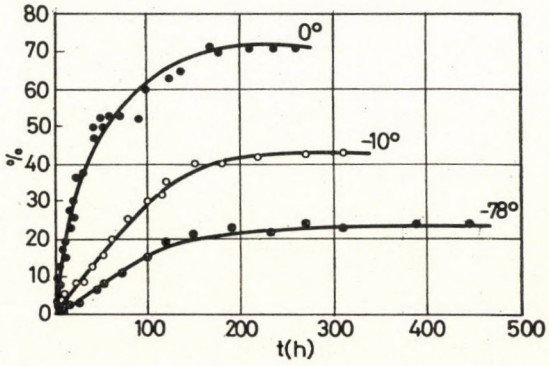

Fig. 8. Polymerization kinetical curves of the solid phase polymerization of cetyl vinyl ether at various temperatures initiated with iodine

action. Owing to the known structure of paraffins, diffusion proceeds at a preferred rate along the plane of the molecular chain terminals — thus of the vinyl groups — compared with the diffusion between the chains. This explains the formation of the polymer at temperatures as low as —78 °C, which, at the same time, excludes the possibility of iodine acting according to some kind of radical mechanism.

Table III

Intrinsic viscosity of the polymers formed in the solid state polymerization of cetyl vinyl ether initiated with iodine vapour, as a function of the temperature and the degree of conversion

0 °C		−10 °C		−78 °C	
Conversion %	$[\eta]$	Conversion %	$[\eta]$	Conversion %	$[\eta]$
11.4	0.080	7.8	0.066	11.5	0.071
18.3	0.080	13.7	0.066	15.0	0.073
23.3	0.058	32.0	0.054	16.0	0.047
30.0	0.062	36.0	0.061	18.0	0.071
55.0	0.082	43.4	0.073	24.0	0 062
62.0	0.072				
70.1	0.065				

REFERENCES

1. HARDY, GY., NYITRAY, K., CSER, F., CSELIK, GY., NAGY, I.: Magyar Kém. Foly. **74,** 602 (1968)
2. HARDY, GY., VARGA, J., CSER, F., DETREKŐY, E.: Magyar Kém. Foly. **72,** 74 (1966)
3. HARDY, GY., VARGA, J., NAGY. G., VARIA, E., SÁRA, L.: Magyar Kém. Foly. **73,** 43 (1967)
4. KOFFLER, L., KOFFLER, A.: Mikro-Methoden zur Kennzeichnung organischer Stoffe und Stoffgemische. Universitätsverlag, Innsbruck, 1948
5. HARDY, GY., NAGY, G., VARGA, J., JUHOS, S.: Magyar Kém. Foly. **73,** 257 (1967)
6. HARDY, GY., NAGY, L., CSER, F.: Magyar Kém. Foly. **72,** 112 (1967)
7. HARDY, GY., VARGA, J., NAGY, G., NYITRAI, K., VARGA, E.: Proc. Second Tihany Symposium on Radiation Chemistry. Akadémiai Kiadó, 1967
8. CHAPIRO, A., HARDY, GY.: J. Chim. Phys. **59,** 993 (1963)
9. TÜDŐS, F., BOROS-GYEVI, E.: Magyar Kém. Foly. **73,** 60 (1967)
10. ELEY, D. D., SAUNDERS, J.: Chem. Soc. **1954,** 1672
11. ELEY, D. E., RICHARDS, A. W.: Trans. Faraday Soc. **45,** 436 (1949)

Gyula HARDY
Károly NYITRAI
Ferenc CSER
Budapest XIV, Hungária krt. 114

Acta Chimica Academiae Scientiarum Hungaricae, Tomus 62 (3), pp. 263—282 (1969)

DETERMINATION OF THE TRUE COMPOSITION OF ACETIC ACID—CARBON TETRACHLORIDE MIXTURE FROM DIELECTRIC PROPERTIES USING THE A—A_2—B TERNARY MIXTURE MODEL, I

J. Liszi

(Department of Physical Chemistry, University of Veszprém)

Received March 4, 1968

The true composition of the nominally binary acetic acid—carbon tetrachloride mixture has been determined from dielectric properties using the A—A_2—B ternary mixture model. The density and dielectric constant of the mixture have been measured as functions of the nominal composition. The frequency dependence of the refractive index of acetic acid has been determined in the visible region. The results combined with the IR spectrum of liquid acetic acid have been used to determine the refractive index of the mixture extrapolated to infinite wave-length, as a function of the nominal composition. In order to calculate the dielectric constant of the mixture, the monomeric and dimeric acetic acid molecules were modeled by means of an ideal dipole located in an ellipsoidal cavity with half-axes a, b, and c. According to the results, the permanent dipole moment of the dimeric acetic acid molecule varies with dilution. The apparent equilibrium constant (expressed in mole fractions) for the dimerization of acetic acid at 20° is given by the following equation:

$$\lg K = 1.8261 + 2.4549\, x_B$$

where x_B is the nominal mole fraction of carbon tetrachloride.

Introduction

In the last three decades increasing space has been devoted in chemical literature to the study of physico-chemical properties of substances which undergo association. The introduction of computers into chemical engineering strongly increased the interest in such problems since now the lengthy and time-consuming calculations do not present obstacles. Well-established and uniform calculation methods are available for non-polar substances [1, 2, 3] which, however, introduce a high degree of uncertainty and various errors when used for the calculation of thermodynamic properties of polar substances or mixtures containing polar components. The error of the calculated values is usually due to the difference between true and nominal compositions. In this context the determination of the true composition of associating substances or mixtures containing such components is of considerable importance.

In principle, the true composition of mixtures containing associating components can be determined by measuring any property of the mixture that is a function of the degree of association.

The following methods are widely used: IR and Raman spectroscopy [4—12], NMR [13—19], analysis of pressure-volume-temperature data [20—27], study of dielectric properties [28—34].

In the present work, the true compositions of acetic acid—carbon tetrachloride liquid mixtures corresponding to the A—A_2—B ternary model were determined from the composition dependence of the dielectric constant.

1. Dielectric constant of polar liquids

Several approaches have been described for the determination of the dielectric constant of mixtures containing polar components [35—38]. Of basic importance is the theory of ONSAGER [39] in which for dielectric purposes the polar molecule is replaced by a point dipole in a *spherical cavity*. The cavity representing the dimensions of the molecule is in a homogeneous medium with dielectric constant ε. If the dipole is removed from the cavity, the external electric field **F** will give rise to an electric field **G** inside the cavity. The permanent dipole moment of the molecule (an ideal dipole inside the cavity) polarizes the surrounding medium which, in turn, acts upon the molecule. Therefore, a reaction field **R** is superimposed on **G** and the resulting field is

$$\mathbf{F} = \mathbf{G} + \mathbf{R} \tag{1}$$

Thus reaction field **R** is the field inside the cavity, *i.e.* the model of the molecule, with zero external field if the medium polarized by the dipole is fixed and the dipole removed from the cavity. The reaction field is proportional to the dipole moment of the molecule, *i.e.*

$$\mathbf{R} = f\mathbf{m} \tag{2}$$

The dipole moment of the molecule **m** is a sum of the permanent (μ) and induced dipole moments:

$$\mathbf{m} = \mu + \alpha\mathbf{F} \tag{3}$$

where α — the average polarizability of the molecule. Proportionality factor f in Eq. (2), called the reaction field factor, is a function of the dielectric constant of the mixture (ε) and the radius of the spherical molecule (r):

$$f = \frac{1}{r^3}\,\frac{2\varepsilon - 2}{2\varepsilon + 1} \tag{4}$$

Field **G** in Eq. (1) is given by the expression

$$\mathbf{G} = \frac{3\varepsilon}{2\varepsilon + 1}\,\mathbf{E} \tag{5}$$

In the calculation of the dielectric constant of polar liquids, one should take into account that the dipoles do not have fixed positions in space but are randomly moving as a result of the thermal motion. Therefore, one should use the average value for the component of the dipole moment in the direction of the external electric field, given by the following expression:

$$\bar{\mu} = \frac{3\varepsilon}{2\varepsilon + 1} \quad \frac{\mu^2}{3kT(1 - f\alpha)^2} \tag{6}$$

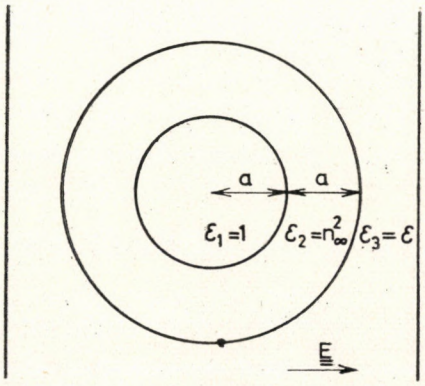

Fig. 1. Dielectric model of a dipolar liquid

The dielectric constant of a pure liquid consisting of spherical molecules can thus be written as

$$\frac{\varepsilon - 1}{\varepsilon + 3} = \frac{4\pi}{3} N \left(\alpha + \frac{\mu^2}{3kT + f\mu^2} \right) \tag{7}$$

where N — the number of molecules in 1 cm^3 of the liquid;
k — the Boltzmann constant;
T — the absolute temperature (°K).

The Onsager theory was modified by SCHOLTE [40] who considered the dielectric constant of the actual environment of the cavity representing the geometry of the molecule. The proposed model is schematically shown in Fig. 1. The point dipole is located in the center of a sphere with radius a. There is vacuum inside the sphere, therefore $\varepsilon_1 = 1$, the static dielectric constant. Since the radius of the molecule (*i.e.*, of the cavity representing the molecule) equals a, the nearest polarizable medium is at a distance a from the dipole and the nearest neighbouring dipole at a distance of $2a$. Therefore, between a and $2a$ there is a medium without dipoles of the sort under consideration,

characterized by a static dielectric constant

$$\varepsilon_2 = n_\infty^2$$

where n_∞ —the refractive index of the polar liquid extrapolated to infinite wave-length of light (*cf.* Section 4). Beyond distance $2a$, the dielectric constant is identical to that of the polar liquid: $\varepsilon_3 = \varepsilon$.

The theory was extended by SCHOLTE to molecules other than spherical. In such cases the model of the molecule is a dipole located inside an ellipsoid with half-axes a, b, and c.

On the basis of the model shown in Fig. 1, SCHOLTE has derived the following expressions for an ellipsoidal cavity with half-axes a, b, and c:

$$\mathbf{G} = \frac{36\varepsilon n_\infty^2}{17\varepsilon n_\infty^2 + 7n_\infty^4 + 7\varepsilon + 5n_\infty^2}\mathbf{E} \tag{8}$$

$$f = \frac{1}{abc}\,\frac{2n_\infty^2 - 2 + \dfrac{3(\varepsilon - n_\infty^2)}{17\varepsilon + 7n_\infty^2}}{2n_\infty^2 + 1 - \dfrac{3(\varepsilon - n_\infty^2)}{17\varepsilon + 7n_\infty^2}} \tag{9}$$

$$\bar{\mu} = \frac{\varepsilon}{\varepsilon + (1-\varepsilon)A}\;\frac{\mu^2}{3kT}\;\frac{pq^2}{(1 - f_\mu \alpha_\mu)^2} \tag{10}$$

where α_μ —the polarizability of the molecule in the direction of the dipole, and

$$f_\mu = \frac{3}{abc}\,\frac{A(1-A)(n_\infty^2 - 1)}{\varepsilon + (1-\varepsilon)A} \tag{11}$$

$$p = \frac{36\varepsilon n_\infty^2}{17\varepsilon n_\infty^2 + 7n_\infty^4 + 7\varepsilon + 5n_\infty^2}\,\frac{2\varepsilon + 1}{3\varepsilon} \tag{12}$$

$$q = \frac{1}{1 - f\alpha_\mu}\left(1 - \frac{\alpha_\mu}{abc}\,\frac{2n_\infty^2 - 2}{2n_\infty^2 + 1}\right) \tag{13}$$

Factor A in Eqs. (10) and (11) can be calculated from the dimensions of the molecule:

$$A = \frac{abc}{2}\int_0^\infty \frac{ds}{(s + a^2)^{3/2}(s + b^2)^{1/2}(s + c^2)^{1/2}} \tag{14}$$

if the permanent dipole moment points in the direction of half-axis a of the ellipsoid.

The above equations yield the following expression for the dielectric constant of a pure dipolar liquid:

$$\frac{\varepsilon-1}{4\pi}\frac{V}{N_A}=\frac{36\varepsilon n_\infty^2}{17\varepsilon n_\infty^2+7n_\infty^4+7\varepsilon+5n_\infty^2}\frac{\alpha}{1-f\alpha}+$$
$$+\frac{\varepsilon}{\varepsilon+(1-\varepsilon)A}\frac{\mu^2}{3kT}\frac{pq^2}{(1-f_\mu\alpha_\mu)^2} \qquad (15)$$

where V — the molar volume of the liquid and N_A — the Avogadro number.

In order that the above theory could be applied to the case of acetic acid — carbon tetrachloride mixtures, one should know the structure of the mixture, *i.e.* the true components of the nominally binary mixture and their molecular properties.

2. Model and equation for the calculation of true composition

Views have been put forward suggesting either chain-type association (Fig. 2a) or the formation of cyclic dimers (Fig. 2b) in liquid acetic acid [42, 43]. The existence of cyclic dimers is generally recognized in the vapor phase

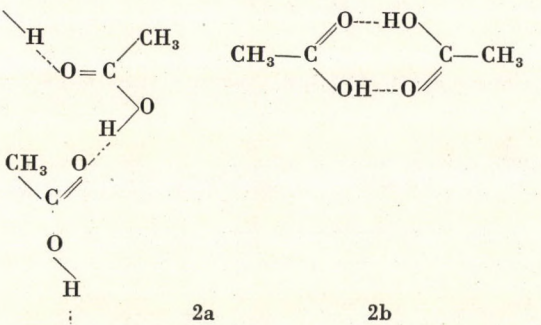

Fig. 2. Chain association (a) and cyclic (b) dimer of acetic acid

and in dilute solutions with apolar solvents. Since we need well-defined molecular properties (*e.g.* permanent dipole moment, molecular dimensions, etc.) to describe the dielectric constant of the mixture, we shall assume in the calculations that pure liquid acetic acid is a mixture of monomeric and dimeric molecules. Consequently, the nominally binary mixture acetic acid–carbon tetrachloride will be regarded as a ternary mixture consisting of components A—A_2—B. The true composition of the mixture will refer to this ternary mixture. The nominal mole fractions are x_{ac} (acetic acid) and x_B (carbon tetrachloride), while the true mole fractions — x_1 (monomeric acetic acid), x_2 (dimeric acetic acid), and x_3 (carbon tetrachloride).

Now examine the molecular characteristics of the true components, first of all the molecular dimensions. The molecular dimensions of carbon tetrachloride are precisely known [44]. Due to its high symmetry, in the calculation of the dielectric constant the molecule can be regarded as a sphere with radius $r = 3.048$ Å.

No data are available for the dimensions of monomeric and dimeric acetic acid molecules in the liquid phase. However, only negligible error is introduced if the solid state molecular dimensions are used because the temperature of the measurements (20 °C) is very close to the melting point

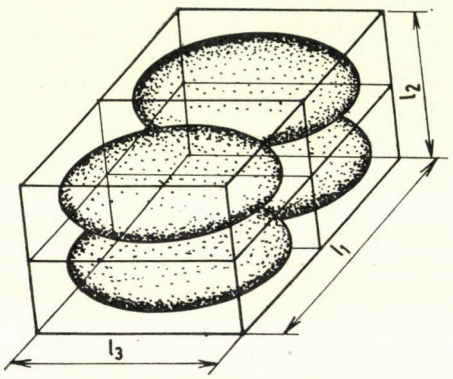

Fig. 3. The arrangement of acetic acid molecules in the solid state

(16.26 °C). By X-ray diffraction, JONES and TEMPLETON [43] determined the dimensions of the unit cell for crystalline acetic acid, containing four monomeric molecules: $l_1 = 13.32 \pm 0.02$ Å; $l_2 = 4.08 \pm 0.01$ Å; $l_3 = 5.77 \pm 0.01$ Å. According to the authors, the carbon and oxygen atoms of the molecule lie in the same plane. The arrangement of the four molecules in the unit cell is shown in Fig. 3. From the unit cell dimensions and molecular arrangement, the following dimensions are obtained for the monomeric and dimeric molecules:

$a_1 = 2.885$ Å	$a_2 = 1.02$ Å
$b_1 = 1.02$ Å	$b_2 = 6.66$ Å
$c_1 = 3.33$ Å	$c_2 = 2.885$ Å

The above dimensions define the ellipsoidal cavity which represent the molecules and include the information that the permanent dipole moment of monomeric acetic acid points in the direction of half-axis a_1, while that of the dimeric molecule — in the direction of half-axis a_2. The direction of the permanent dipole moment, of the monomeric acetic acid, has been determined from increments and molecular dimension taken from the literature [44].

The permanent dipole moment of the dimeric acetic acid will be dealt with in the discussion of the results. The references concerning the magnitude of the permanent dipole moment are contradictory. Depending on the method of determination, the permanent dipole moment of monomeric acetic acid varies between 0.84 and 2.0 D, while that of the dimer between 0.0 and 0.94 D [28]. Since the present studies are concerned with mixtures of acetic acid and an apolar component, we used the values $\mu_1 = 1.68\ D$ and $\mu_2 = 0.92\ D$, determined in n-heptane solution, an apolar solvent. However, these data give satisfactory results only for pure acetic acid. The calculations indicated that the permanent dipole moment of the dimer is not a constant but decreases with the concentration of acetic acid. This phenomenon is interpreted in Section 6.

Naturally, carbon tetrachloride has no permanent dipole moment. Its average polarizability, $\alpha_3 = 10.50 \cdot 10^{-24}\ \mathrm{cm}^3$ [45]. The average polarizabilities of monomeric and dimeric acetic acid are given by KOHLER [46] on the basis of data by POHL, HOBBS and GROSS [32]:

$$\alpha_1 = 4.85 \cdot 10^{-24}\ \mathrm{cm}^3$$
$$\alpha_2 = 15.65 \cdot 10^{-24}\ \mathrm{cm}^3$$

Using the above molecular characteristics of the components and the equations given in Section 1, one can express the dielectric constant of the mixture as a function of the composition:

$$\begin{aligned}
&\frac{\varepsilon - 1}{4\pi N_A}\ \frac{1}{\varrho}(M_1 x_1 + M_2 x_2 + M_3 x_3) = \\
&= \frac{36\varepsilon n_{\infty e}^2}{17\varepsilon n_{\infty e}^2 + 7n_{\infty e}^4 + 7\varepsilon + 5n_{\infty e}^2}\left\{x_1 \frac{\alpha_1}{1 - f_1\alpha_1} + \right. \\
&\left. + x_2 \frac{\alpha_2}{1 - f_2\alpha_2} + x_3 \frac{\alpha_3}{1 - f_3\alpha_3}\right\} + \qquad (16) \\
&+ x_1 \frac{\varepsilon}{\varepsilon + (1 - \varepsilon) A_1}\ \frac{\mu_1^2}{3kT}\ \frac{pq_1^2}{(1 - f_{\mu 1}\alpha_{\mu 1})^2} + \\
&+ x_2 \frac{\varepsilon}{\varepsilon + (1 - \varepsilon) A_2}\ \frac{\mu_2^2}{3kT}\ \frac{pq_2^2}{(1 - f_{\mu 2}\alpha_{\mu 2})^2}
\end{aligned}$$

In Eq. (16) α_1, α_2, α_3, μ_1 and μ_2 are data known from the literature. f_1, f_2, f_3 can be calculated from Eq. (9), $f_{\mu 1}$ and $f_{\mu 2}$ — from Eq. (10), A_1 and A_2 — from Eq. (13), while q_1 and q_2 — from Eq. (12). $\alpha_{\mu 1}$ and $\alpha_{\mu 2}$ are calculated from the molecular dimensions, N_A is the Avogadro number, T — the absolute temperature, M — the molecular weight, and ϱ — the density of the mixture.

The integral in Eq. (13) can be given in analytical form only for an ellipsoid of rotation (*i.e.*, if at least two half-axes are identical), therefore, the values of constants A were determined by an approximation procedure. The integral was written as a sum:

$$\int_0^\infty \frac{ds}{(s+a^2)^{3/2}(s+b^2)^{1/2}(s+c^2)^{1/2}} \simeq \int_0^{s^\circ} \frac{ds}{(s+a^2)^{3/2}(s+b^2)^{1/2}(s+c)^{1/2}} + \int_{s^\circ}^\infty \frac{ds}{s^{5/2}} \tag{17}$$

$$s^\circ = 100 \text{ Å} \gg a,\ b,\ c$$

and integration was performed graphically with an upper limit s°. The result is

$$A_1 = 0.21; \qquad A_2 = 0.73\,.$$

The molecular characteristics of the components of the A—A_2—B type mixture are listed in Table I.

Table I

	Monomeric acetic acid (A)	Dimeric acetic acid (A_2)	Carbon tetrachloride (B)
M	60	120	153.8
a	2.885 Å	1.02 Å	3.048 Å
b	1.02 Å	6.66 Å	3.048 Å
c	3.33 Å	2.885 Å	3.048 Å
α	$4.85 \cdot 10^{-24}$ cm^3	$15.65 \cdot 10^{-24}$ cm^3	$10.5 \cdot 10^{-24}$ cm^3
α_μ	$5.80 \cdot 10^{-24}$ cm^3	$4.55 \cdot 10^{-24}$ cm^3	—
A	0.21	0.73	1/3
μ	1.68 D	(variable)	0

In addition to the data in Table I, the application of Eq. (16) requires the knowledge of the density, dielectric constant, and refractive index (extrapolated to infinite wave-length) of the mixture as a function of the nominal composition.

3. Density of the mixture as a function of the nominal composition

The purest available materials were used in the experiments after additional purification. Reagent grade carbon tetrachloride was distilled on a packed column equivalent to 20 theoretical plates, the purity of the distillate was checked by refractive index measurements. The refractive index of carbon

tetrachloride used in the experiments was 1.4603 (Na_D-line) identical to the literature value [47].

Pure acetic acid is strongly hygroscopic, therefore it was freshly distilled before each experiment. The purification procedure was as follows: a mixture of 200 ml of acetic acid with 30 ml of acetic anhydride was distilled over a col-

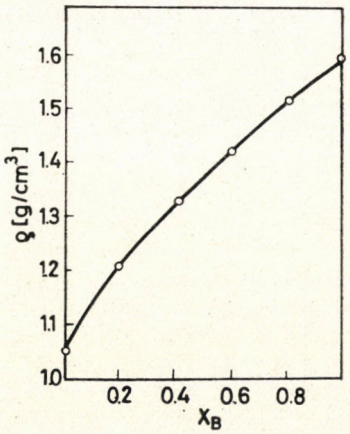

Fig. 4. The density of acetic acid–carbon tetrachloride mixtures as a function of the nominal composition

umn equivalent to 20 theoretical plates and the distillate was subjected to multiple crystallization. The melting point of the crystallized product was measured for control purposes. The sample was regarded suitable for the experiments when the melting points of two subsequent crystallization products were identical. The melting point of acetic acid used in the measurements was 16.26 °C.

The density of the mixture was determined by means of the pyknometric method. Mixtures of various compositions were prepared by weighing. The density of the acetic acid – carbon tetrachloride mixture as a function of the nominal mole fraction of CCl_4 (x_B) is shown in Table II and Fig. 4 for 20 °C.

Table II

x_B	ϱ (g/cm³)
0	1.0493
0.2065	1.2064
0.4163	1.3305
0.5995	1.4274
0.7986	1.5144
1.0000	1.5942

The results can be described with the following empirical expression obtained by a least-squares procedure:

$$\varrho_{20}\,(\mathrm{g/cm^3}) = 1.0493 + 0.7709\,x_B - 0.2259\,x_B^2 \tag{18}$$

4. Refractive index of the mixture extrapolated to infinite wave-length

The dielectric constant and refractive index of a substance with unit magnetic permeability are related, at least at low frequencies, by the following equation first given by MAXWELL [48]:

$$\varepsilon = n^2 \tag{19}$$

The magnetic permeability of dielectrics is unity, therefore, Eq. (19) holds at least for non-polar substances. Thus the square of the refractive index for CCl_4 extrapolated to infinite wave-length is

$$n^2_{\infty B} = \varepsilon_B = 2.23$$

It is necessary to remind that, in order to calculate the dielectric constant using the theory outlined in Section 1, one has to know the dielectric constant of the dipole-free mixture, *i.e.* its refractive index extrapolated to infinite wave-length (*cf.* Fig. 1). For permanent dipoles, such as acetic acid at frequencies below the relaxation frequency, the dielectric constant contains a contribution from orientation polarization, too. Therefore, the refractive index of acetic acid extrapolated to infinite wave-length cannot be calculated from Eq. (19). Instead, we used the SELLMEIER dispersion formula [37] which does not include orientation polarization due to permanent dipoles:

$$n^2 = 1 + \Sigma N_i K_i \frac{\omega_i^2}{\omega_i^2 - \omega^2} \tag{20}$$

where

$$K_i = \frac{\varphi_i}{\omega_i^2 \varrho} \tag{21}$$

n — the refractive index at angular frequency ω; ω_i — the i-th resonance frequency of the molecule; N_i — the number of oscillators per $\mathrm{cm^3}$ with angular frequency ω_i; φ_i — the force constant of the i-th oscillator; ϱ — the density of the medium; unity in the equation represents the relative refractive index

of vacuum. The calculation of φ_i is simple only for the quasy-elastic bonding of a single electron, in other cases it should be determined from spectroscopic data. Substances transparent for visible light may absorb in the UV or IR, therefore, the sum in Eq. (20) can be split in two terms:

$$n^2 = 1 + \sum_i N_i K_i \frac{\omega_i^2}{\omega_i^2 - \omega^2} + \sum_j N_j K_j \frac{\omega_j^2}{\omega_j^2 - \omega^2} \tag{22}$$

where subscripts j and i refer to resonance frequencies in the UV and IR, respectively. If the refractive index is referred to infinite wave-length, with $\omega = 0$, Eq. (22) gives:

$$n_\infty^2 = 1 + \sum_i N_i k_i + \sum_j N_j k_j \tag{23}$$

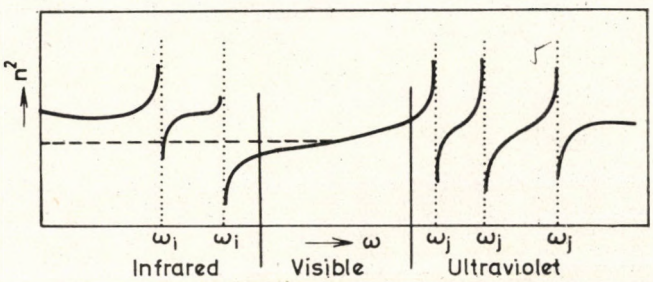

Fig. 5. The square of the refractive index as a function of the frequency (schematic)

In Eq. (22), the IR and UV contributions to n_∞^2 are represented by the second and third terms of the right-hand side, respectively. The refractive index measured with visible light includes contributions from absorption in both the IR and UV region. This is illustrated by Fig. 5 schematically showing the frequency dependence of the refractive index. The solid lines in Fig. 5 represent squares of the refractive index as calculated from Eq. (22) while the dotted lines correspond to the values derived from the CAUCHY equation [Eq. (24)].

The CAUCHY equation [37] is

$$n^2 = B + C\omega^2 + D\omega^4 + \ldots \tag{24}$$

where n — the refractive index; ω — the angular frequency; B, C, and $D \ldots$ — empirical constants. Eq. (24) gives the wave-length dependence of the refractive index from the visible region to infinite wave-length if there is no absorption in the IR, *i.e.*, it corresponds to the sum of the first and third terms in Eq. (22). Thus Eq. (22) can be written approximately as

$$n^2 \simeq B + C\omega^2 + D\omega^4 + \sum_i N_i k_i \frac{\omega_i^2}{\omega_i^2 - \omega^2} \tag{25}$$

Extrapolation of Eq. (25) to infinite wave-length yields

$$n^2 = B + \sum_i N_i K_i \tag{26}$$

According to Eqs. (26) and (24), in order to determine the refractive index referring to infinite wave-length, it is sufficient to know the IR absorptions and the wave-length dependence of the refractive index in the visible region. Accordingly, we measured the refractive index of acetic acid as a function of

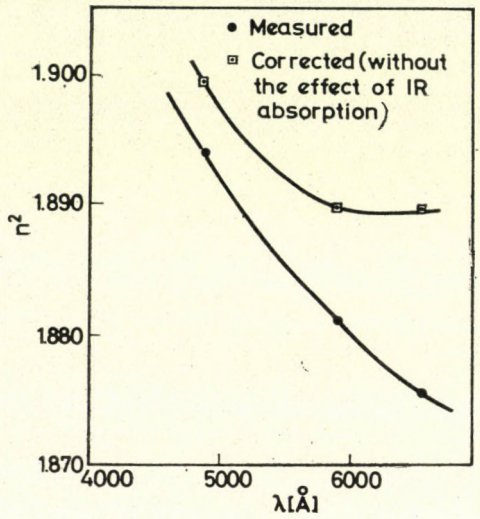

Fig. 6. The refractive index of acetic acid as a function of the wave-length

the wave-length in the visible region and subtracted the contribution by IR absorption. The corrected refractive index—wave-length values were then extrapolated to infinite wave-length using Eq. (24). The extrapolated value yields constant B of Eq. (26). The monochromatic light was obtained from a "Spectromom" spectrophotometer using a mirror system. The measurements were performed with an Abbé type refractometer, calibrating the scale with substances of known refractive index. The results are shown in Table III and Fig. 6.

Table III

λ (Å)	n	n^2	$n^2_{\text{corrected}}$
6563	1.3695	1.8755	1.8891
5893	1.3715	1.8810	1.8898
4861	1.3762	1.8939	1.8996

From the data of Table III and Eq. (24) one obtains $B = 1.8764$.

The number of oscillators per cm^3 is given by the following equation:

$$N_i = \frac{z_1 N_A x_1 + z_2 N_A x_2}{V_e} \tag{27}$$

where

$$V_e = \frac{60x_1 + 120x_2}{\varrho_{ac}} \tag{28}$$

z_1 and z_2 are the number of oscillators per molecule of acetic acid monomer and dimer, respectively. The values φ_i and ω_i and Eq. (21) have been determined from the IR absorption spectrum of liquid acetic acid. The spectra were recorded on a Type Zeiss-Jena UR–10 C. IR-spectrometer. The samples were introduced as liquid films. The identification of the absorption bands and the determination of force constant are described by BROOK and HAAS [49], HERZBERG [50], and MOELWYN-HUGHES [44]. The values for acetic acid are shown in Table IV.

Table IV

Wave-number (cm^{-1})	Bond	φ_i dyn/cm · 10^{-5}	$N_i \cdot 10^{-21}$	$N_i K_i \cdot 10^3$
3600	O—H ↔	7.265	9.5	14.3022
3050	C—H ↔	4.876	32.4	45.5868
2990	C—H ↔	4.876	32.4	47.4336
2940	C—H ↔	4.876	32.4	49.0600
1780	C=O ↔	13.45	9.5	108.3066
1435	H—C—H ↕	0.461	32.4	19.4792
1410	H—C—H ↕	0.461	32.4	28.2885
1400	H—C—C ↕	0.62	32.4	19.9131
1370	H—C—H ↕	0.461	32.4	21.3703
1290	C—O—H ↕	0.730	9.5	11.1938
1190	C—O ↔	5.046	9.5	90.8637
1060	H—C—C ↕	0.62	32.4	48.0163
1000	CH_3—	0.397	9.5	10.1278
850	C—C ↔	4.784	9.5	168.8815
650	O—H	0.055	9.5	18.5293
620	CH_3—	0.397	9.5	26.3469
564	CH_3—	0.397	9.5	31.7906
536	O=C—O ↕	0.575	9.5	51.0794
212	CH_3-torsional	0.023	9.5	12.1046

In Table IV, ↔ and ↕ denote stretching and deformations, respectively. Where there is no symbol, group vibrations are shown. The rotation of the CH_3 group appears at 235 cm^{-1}, this value is taken from the paper by BROOK and HAAS.

From Eq. (26) and the data of Table, IV, the square of the refractive index extrapolated to infinite wave-length for acetic acid is

$$n^2_{\infty ac} = 1.8764 + 0.8227 = 2.6991$$

The refractive index of the mixture was calculated from the known values of $n^2_{\infty ac}$ and $n^2_{\infty B}$, assuming additivity of molar polarisations

$$\frac{n^2_{\infty e} - 1}{n^2_{\infty e} + 2} V_e = \frac{n^2_{\infty ac} - 1}{n^2_{\infty ac} + 1} V_{ac} x_{ac} + \frac{n^2_{\infty B} - 1}{n^2_{\infty B} + 2} V_B x_B \qquad (29)$$

where subscript e refers to the mixture. The variation of $n_{\infty ac}$ with the shift of the association equilibrium was taken into account though, according to our measurements, the IR frequencies do not change significantly with dilution. The volume change upon mixing was neglected. The approximate character of the calculations is obvious especially if one considers that even the mixture of monomeric and dimeric acetic acid shows negative deviation from ideality. (These studies will be reported in a separate paper.) Nevertheless, the approximation used in connection with Eq. (29) does not introduce any appreciable error in the determination of the true composition because, according to calculations, Eq. (16) is not too sensitive towards changes of $n^2_{\infty e}$. The refractive index of the mixture extrapolated to infinite wave-length is shown as a function of the nominal CCl_4 mole fraction in Table V and Fig. 7.

Table V

x_B	$n^2_{\infty e}$
0.0	2.6991
0.2	2.5502
0.4	2.4371
0.6	2.3500
0.8	2.2740
1.0	2.23

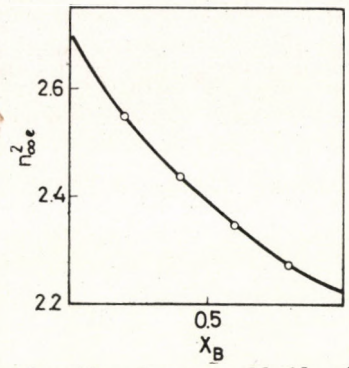

Fig. 7. Refractive index of acetic acid–carbon tetrachloride mixtures extrapolated to infinite wave-length, as a function of the nominal composition

5. Dielectric constant of the mixture

The dielectric constants were measured on a Type TR–9701 bridge at a frequency of 300 kHz. The sample holder was thermostated stainless steel cell with a capacity of 10 pF surrounded by a polyvinylchloride jacket. Since acetic acid is strongly hygroscopic, the cell was tightly covered with Teflon. The error of the dielectric constant is less than 2%. The experimental results at 20 °C are shown in Table VI and Fig. 8.

Table VI

x_B	ε	x_B	ε	x_B	ε
0.0000	6.3□	0.3051	3.42	0.6916	2.42
0.0000	6.35*	0.3099	3.37	0.7835	2.37
0.0000	6.20	0.4187	3.17	0.7919	2.36
0.0469	5.85	0.4289	2.93	0.8152	2.35
0.0473	5.83	0.4312	2.94	0.8962	2.32
0.0481	5.68	0.4978	2.74	0.9071	2.27
0.0848	4.80	0.5064	2.71	0.9608	2.25
0.1141	4.74	0.5094	2.69	0.9754	2.24
0.1224	4.76	0.5750	2.59	1.0000	2.23
0.2048	4.04	0.5898	2.53		
0.2082	3.97	0.6016	2.47		
0.2089	3.87	0.6811	2.46		
0.2838	3.60	0.6840	2.45		

The value in Table VI marked by □ is taken from the paper by DOBOS [51], the starred (*) value was reported by CONTI and FRANCONI [52]. The latter authors

also determined the dielectric constants of acetic acid–carbon tetrachloride mixtures as a function of the nominal composition but reported the data only graphically. Thus there is no way for quantitative comparison with the present results.

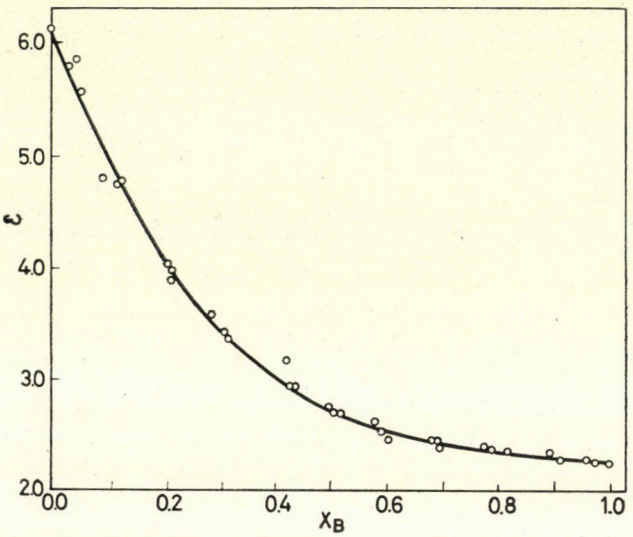

Fig. 8. Dielectric constant of acetic acid–carbon tetrachloride mixtures as a function of the nominal composition

6. Calculation of the true composition

The true composition was calculated using Eq. (16), taking into account that

$$x_1 + x_2 + x_3 = 1 \tag{30}$$

and, that the following relationship exists between nominal and true carbon tetrachloride mole fractions:

$$x_B = \frac{x_3}{1 + x_2} \tag{31}$$

Since the refractive index of acetic acid extrapolated to infinite wave-length is also a function of the composition, an iteration procedure was used in the calculations. The $n^2_{\infty ac}$ value was determined for an arbitrary composition and $n^2_{\infty e}$ was then calculated from Eq. (29). This result was combined with Eq. (16) to calculate the composition with which the procedure was repeated. Iteration was continued until two subsequent cycles yielded identical mole fractions.

As mentioned earlier, there is disagreement in the literature with respect to the permanent dipole moment of monomeric and dimeric acetic acid. In the present calculations we used the data of POHL, HOBBS and GROSS [32] obtained in a non-polar solvent, under conditions similar to our measurements:

$$\mu_1 = 1.68\ D \text{ and } \mu_2 = 0.92\ D$$

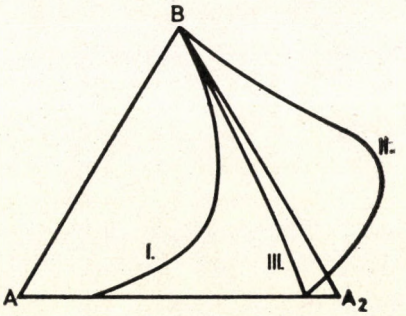

Fig. 9. The composition of the ternary mixture corresponding to the $A-A_2-B$ model

On the other hand, vapor phase measurements indicate that dimeric acetic acid has no permanent dipole moment because of its symmetrial structure (*cf.* Fig. 2b). If the calculations are performed with $\mu_1 = 1.68\ D$ and $\mu_2 = 0.00\ D$, one obtains a lower degree of dimerization for pure liquid acetic acid than that determined in the vapor phase [53] (*cf.* Fig. 9, I) while the values $\mu_1 = 1.68\ D$ and $\mu_2 = 0.92\ D$ lead to negative mole fractions (*cf.* Fig. 9, II) which obviously lack physical reality. These results indicate variation of the permanent dipole moment of dimeric acetic acid with dilution. In our view, this phenomenon can be explained by strong interaction between monomeric and dimeric molecules in concentrated solutions, resulting in the deformation of the dimer in the direction normal to the plane of the ring. Thus the dimer behaves as if it possessed a permanent dipole moment. This interaction decreases with decreasing acetic acid concentration and the dipole moment assumes zero value at infinite dilution similarly to the vapor phase. In our opinion in acetic acid—carbon tetrachloride mixtures no trimers or polymers exist. Only strongly interacting monomeric and dimeric molecules should be considered, their interaction decreasing with dilution and reaching zero at infinite dilution. In the trimer, the monomers occupy fixed positions relative to each other and the forces of interaction should be strong enough for the trimer to exist in dilute solutions. However, this would contradict the physical picture obtained from the analysis of the dielectric properties. As a first approximation, one can assume that the permanent dipole moment of dimeric acetic acid is

proportional to the concentration of acetic acid:

$$\mu_2 = 0.92(1 - x_3) \tag{32}$$

The results obtained using Eq. (32) are shown in Table VII and Fig. 9 (curve III).

Table VII

x_B	x_1	x_2	x_3	K
0	0.1149	0.8851	0	67
0.2	0.0547	0.6211	0.3242	207
0.4	0.0274	0.4090	0.5636	545
0.6	0.0120	0.2425	0.7455	1684
0.8	0.0038	0.1090	0.8872	7548
1	0	0	1	24000

The last column of Table VII contains the chemical equilibrium constant for dimerization

$$2A \rightleftharpoons A_2 \tag{33}$$

defined as

$$K = \frac{x_2}{x_1^2} \tag{34}$$

The value of $K = 67$ for pure liquid acetic acid is in good agreement with the equilibrium constant ($K = 62$) determined by FREEDMAN [54] using an ultrasonic absorption technique. (The error of the data of Table VII will be reported in the second part of this article.)

According to Fig. 10, the logarithm of the equilibrium constant for dimerization is a linear function of the nominal mole fraction of carbon tetrachloride:

$$\lg K = \lg K_{ac} + (\lg K_\infty - \lg K_{ac})\, x_B \tag{35}$$

Using the data for 20 °C, Eq. (35) can be rearranged to

$$\lg K = 1.8261 + 2.4539\, x_B \tag{36}$$

Thus Eq. (36) permits the calculation of true mole fractions for the ternary model A—A_2—B, for any arbitrary nominal composition of the acetic acid—carbon tetrachloride mixture at 20 °C.

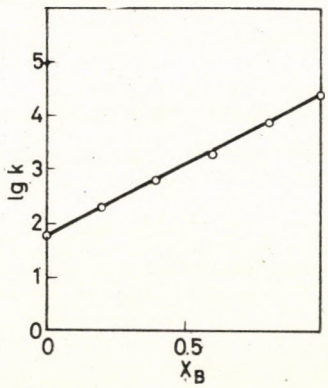

Fig. 10. The logarithm of the dimerization constant expressed in terms of mole fractions as a function of the nominal composition

The dipolar liquid model of ONSAGER and SCHOLTE is applicable to nominally binary associating mixtures of acetic acid with carbon tetrachloride. The true composition of the mixture can be determined from dielectric properties using the thermodynamic model A—A_2—B of reactive mixtures.

*

The author is indebted to Klára JÓNÁS (University of Veszprém) and György BOR (Hungarian Oil and Gas Research Institute) for helpful suggestions and recording the spectra.

REFERENCES

1. REID, R. C., SHERWOOD, T. K.: The Properties of Gases and Liquids. McGraw-Hill, 1966
2. BRETSNAÏDER, SZ.: Properties of Gases and Liquids. Moscow, 1966
3. PRAUSNITZ, J. M., ECKERT, C. A., ORYE, R. V., O'CONNELL, J. P.: Computer Calculations for Multicomponent Vapor-Liquid Equilibria. Prentice-Hall, 1967
4. COSTAIN, C. C., SRIVASTAVA, G. P.: J. Chem. Phys. **41,** 6 (1964) 1620
5. LAURENCE, C., WOJTKOWIAK, B.: C. R. Acad. Sci. Paris, t. 264. Série C 1216 (1967)
6. SINGH, S., RAO, C. N. R.: J. Phys. Chem. **71,** 4, 1074 (1967)
7. FÉNÉANT-EYMARD, S.: Sur l'état moléculaire de l'acide acétique. Paris, 1952
8. SCHWAB, G. M., GLATZER, G.: Z. Elektrochemie **61,** 1028 (1957)
9. WENOGRAD, J., SPURR, R.: J. Am. Chem. Soc. **79,** 1844 (1957)
10. GILLETTE, R. H., SHERMAN, A.: J. Am. Chem. Soc. **58,** 1135 (1936)
11. GILLETTE, R. H., DANIELS, F.: J. Am. Chem. Soc. **58,** 1139 (1936)
12. GILLETTE, R. H.: J. Am. Chem. Soc. **58,** 1143 (1936)
13. BHAR, B. N., FORSLING, W., LINDSTRÖM, G.: Arkiv för fysik **10,** 6, 59 (1955)
14. BHAR, B. N.: Il nouvo cimento **XL B,** 2, 416 (1965)
15. HUGGINS, C. M., PIMENTEL, G. C., SHOOLERY, J. N.: J. Phys. Chem. **60,** 1311 (1956)
16. REEVES, L. C., SCHEIDER, W. G.: Trans. Far. Soc. **54,** 314 (1958)
17. DAVIS, J. C., PITZER, K. S.: J. Phys. Chem. **64,** 886 (1960)

18. PARMIGIANI, A., PEROTTI, A., RIGAUTI, V.: Gaz. Chim. Italiana **91,** 1148 (1961)
19. ANDERSON, J. E.: Il nuovo cimento **XIV** B, 2, 254 (1966)
20. COOLIDGE, A. S.: J. Am. Chem. Soc. **50,** 2166 (1928)
21. MARKUZIN, N. P.: Zh. Prikl. Chim. **39,** 10, 2383 (1966)
22. JÁRÜM-AGAJEV, N. L.: Zh. Fiz. Chim. **39,** 3, 651 (1965); **39,** 7, 1614 (1965); **40,** 5, 992 (1966); **40,** 6, 1265 (1966); **40** 8, 1680 (1966)
23. JÁRÜM-AGAJEV, N. L., KOGAN, E. A., SOLDATOVA, E. D.: Zh. Fiz. Chim. **36,** 6, 1173 (1962)
24. JÁRÜM-AGAJEV, N. L., KOGAN, E. A., SLEPCOVA, C. V.: Zh. Fiz. Chim. **40,** 9, 2009 (1966)
25. LUCKIJ, A. E.: Zh. Fiz. Chim. **28,** 204 (1954)
26. MAREK, J., STANDART, G.: Coll. Czechoslov. Chem. Comm. **19,** 1074 (1954)
27. MAREK, J.: Coll. Czechoslov. Chem. Comm. **20,** 1490 (1955)
28. PIMENTEL, G. C., MYLELLAN, A. L.: The Hydrogen Bond, Freeman and Co., 1960
29. BRIEGLEB, G.: Z. Phys. Chem. **B. 10,** 205 (1930)
30. ZAHN, C. T.: Phys. Rev. **35,** 1047 (1930)
31. ZAHN, C. T.: Phys. Rev. **37,** 1516 (1931)
32. POHL, H. A., HOBBS, M. E., GROSS, P. M.: J. Chem. Phys. **9,** 408 (1941)
33. SMYTH, C. P., ROGERS, H. E.: J. Am. Chem. Soc. **52,** 1824 (1930)
34. LE FEVRE, R. J. W., VINE, H.: J. Chem. Soc. 1795 (1938)
35. FRÖHLICH, H.: Theory of Dielectrics. Oxford, 1950
36. GRANIER, J.: Les dielectriques. Paris, 1948
37. PARTINGTON, J. R.: An Advanced Treatise on Physical Chemistry, vol. V. Longmans, 1954
38. SKANAVI, G. J.: A dielektrikumok fizikája. Akadémiai Kiadó, Budapest 1953
39. ONSAGER, L.: J. Am. Chem. Soc. **58,** 7, 1486 (1936)
40. SCHOLTE, T. G.: Physica **XV,** 5—6, 437 (1949)
41. NECKEL, A., VOLK, H.: Z. Elektrochemie **62,** 1104 (1958)
42. ALLEN, G., CALDIN, E. F.: Quarterly Rev. **7** (1953)
43. JONES, R. E., TEMPLETON, D. H.: Acta Cryst. **11,** 484 (1958)
44. MOELWYN-HUGHES, E. A.: Physical Chemistry, Pergamon Press, 1964
45. ILIC, M.: Technika (Beograd) **19,** 10, 1877 (1964)
46. KOHLER, F.: Institut für Physikalische Chemie der Universität Wien, private communication
47. PARTINGTON, J. R.: An Advanced Treatise on Physical Chemistry, vol. **IV.** Longmans, 1954
48. NOVOBÁTZKY, K., NEUGEBAUER, T.: Electrodynamics and Optics. Tankönyvkiadó, Budapest 1961
49. BROOKS, W. V. F., HAAS C. M.: J. Phys. Chem. **71,** 3, 650 (1967)
50. HERZBERG, G.: Infrared and Raman Spectra of Polyatomic Molecules. New York, 1945
51. DOBOS, D.: Electrochemical Tables. Műszaki Könyvkiadó, Budapest 1965
52. CONTI, F., FRANCONI, C.: Berichte Bunzen, **71,** 2, 146 (1967)
53. RITTER, H. L., SIMONS, H. H.: J. Am. Chem. Soc. **67,** 757 (1945)
54. FREEDMAN, E.: J. Chem. Phys. **21,** 1784 (1953)

János LISZI; Veszprém, Schönherz Z. u. 12. Hungary

Acta Chimica Academiae Scientiarum Hungaricae, Tomus 62 (3), pp. 283—292 (1969)

SOLANUM GLYCOSIDES, III*

DIOSCIN

P. BITE and M. M. SHABANA**

(Research Institute for Pharmaceutical Chemistry, Budapest)

Received August 23, 1968

From fresh, unripe berries of *Solanum introsum* dioscin, a saponin earlier obtained only from Dioscoreae, has been isolated.

The identity of the isolated substance with dioscin was proved on the basis of melting point, optical rotatory power, infrared spectrum, thin-layer chromatography in several solvent systems, acetylation, qualitative investigation and quantitative determination of the aglycone and the sugar components, moreover by periodate oxidation and identification of trillin obtained by partial hydrolysis. Acetylation of dioscin at 140 °C yielded directly a homogeneous peracetate.

The presence of gracillin in the berry was confirmed by thin-layer chromatography.

In the past two decades several studies dealt with the steroid alkaloids of *Solanum* species, as a possible source of starting material for the production of steroid pharmaceuticals in countries of the temperate zone. In the course of these investigations several authors have isolated smaller amounts of steroid sapogenins from various *Solanum* species, but isolation of the corresponding saponins present in the living plant has not yet been reported in the literature.***

No steroid alkaloidal constituent was found in the dilute acid extract of the dried and grounded unripe fruits of *S. introsum*. On the other hand, thin-layer chromatography of a concentrated methanol extract of the fresh, unripe fruits of the same plant revealed the presence of some steroid glycoside in considerable amount (Fig. 1, strip *a*) (Silicagel-G; developing solvent [1] the lower phase of a 63 : 35 : 10 mixture of chloroform : methanol : water, solvent system I; detection with $SbCl_3$).

On treatment of the evaporation residue of the aqueous methanol extract with abs. methanol, the steroid glycosides fully dissolved, while the contaminants mostly remained undissolved. Thin-layer chromatography of the concentrated abs. methanol extract showed now well separated spots (Fig. 1, strip *b*), 10 of which were reddish-violet and 3 yellow after detection with $SbCl_3$. The former were designated, in order of decreasing R_f values, with

* Part II: Acta Chim. Acad. Sci. Hung. **52**, 79 (1967).

** United Arab Republic Scholar from Cairo University, Faculty of Pharmacy.

*** Subsequent to completion of the manuscript of this paper appeared the publication of H. RIPPERGER and K. SCHREIBER (Chem. Ber. **101**, 2450; July, 1968), dealing with the isolation and structure elucidation of two steroid saponins of *Solanum paniculatum*.

letters *A* to *K*, and the latter spots similarly with numbers *1*, *2* and *3*. On the basis of the chromatogram, the amounts of *A*, *E*, *F* and *1* are considerable, their respective R_f values being 0.55, 0.32, 0.25 and 0.38, while the other components are present in small amounts only (Table I).

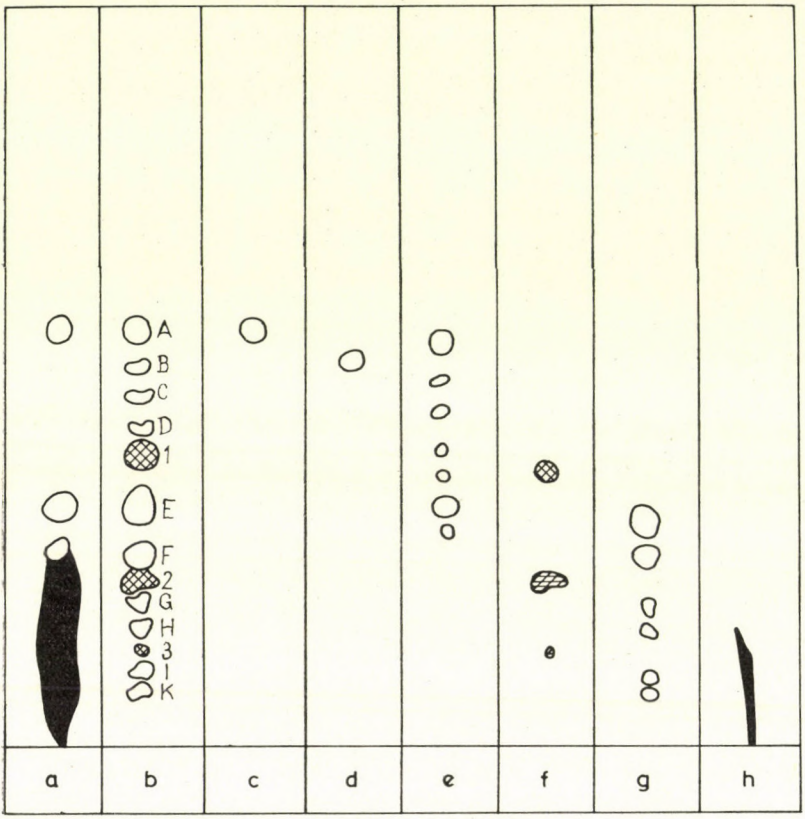

Fig. 1. Thin-layer chromatograms. Adsorbent: Silicagel-G; developing solvent: the lower phase of a $CHCl_3$–MeOH–H_2O 65 : 35 : 10 mixture; detection with $SbCl_3$ in $CHCl_3$. *a)* crude methanol extract; *b)* abs. methanol extract; *c)* authentic dioscin; *d)* authentic gracillin; *e)* $CHCl_3$–EtOH (3 : 1) extract; *f)* ethyl acetate extract; *g)* butanol extract; *h)* aqueous residue

Isolation of component *A* was achieved as shown in Fig. 2.

Component *A* accumulated fully in the chloroform–ethanol (3 : 1) extract, which was concentrated in vacuum and the residue chromatographed first on silicagel and then on aluminium oxide columns; the fractions showing the spot of *A* only were combined, concentrated and the residue subjected to repeated precipitations and then to recrystallizations to give pure *A*, in form of colourless needles. Thin-layer chromatography with four different solvent systems, elemental analysis as well as infrared spectroscopic analysis showed the product to be identical with dioscin [2], whose structure was elucidated by

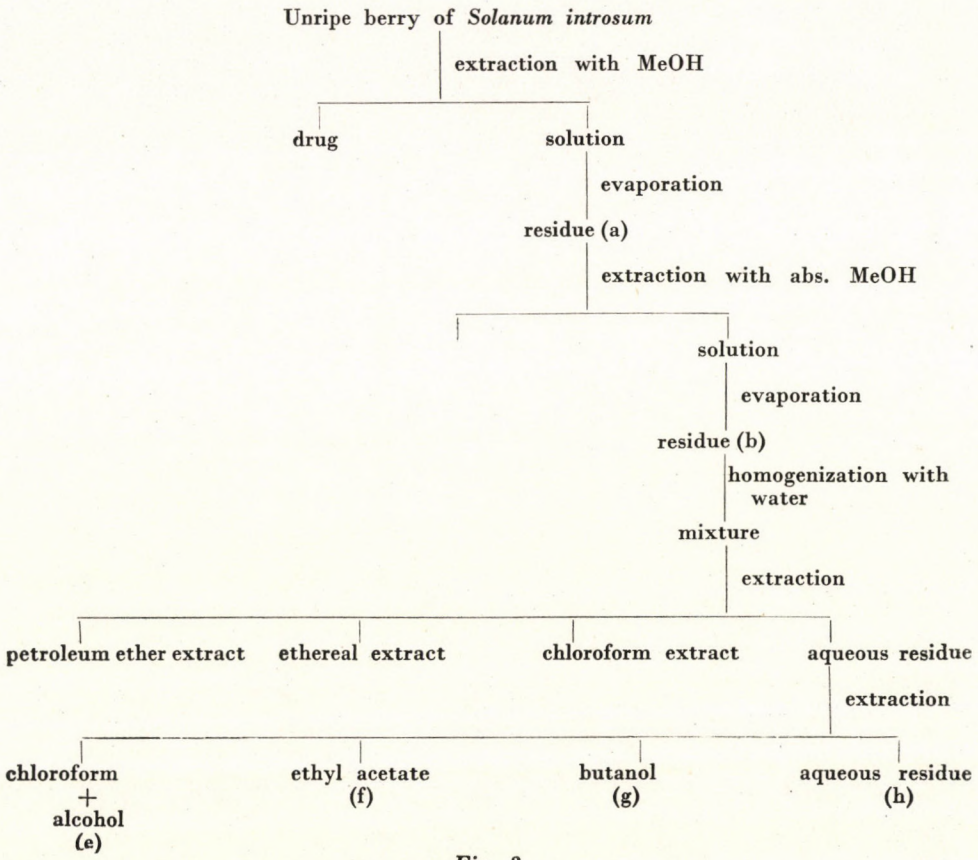

Fig. 2

KAWASAKI and YAMAUCHI [3] in 1962 as bis-α-L-rhamnopyranosyl (1 → 2 and 1 → 4)-β-D-glucopyranosyl diosgenin.

However, pure *A* melted about 20 °C higher than that given in the literature for dioscin. Also its specific rotation was about 5° lower than reported.

The Fehling reaction was negative, the Alberti reaction, and the Bial reaction were positive [4]; accordingly, *A* does not contain a free reducing group, its aglycone contains at least one double bond and methylpentose is present in its sugar moiety.

Acetylation of *A* with acetic anhydride in pyridine at room temperature yielded a product which on thin-layer chromatographic analysis according to KAWASAKI, with benzene–acetone 4 : 1 (solvent system II) (detection with $SbCl_3$) gave always two well-separated spots (R_f 0.70 and 0.63). On the other hand, acetylation at 140 °C gave a homogeneous crude product. This was chromatographed on silicagel column and purified by precipitation. On the basis of elemental analysis, and mass spectrum the pure product was dioscin

peracetate, in contrast to the finding of KAWASAKI [1], it gave one spot only on thin-layer chromatography.

In order to identify the aglycone and the sugar moiety of *A*, it was hydrolyzed with hydrochloric acid. On the basis of melting point, mixed melting point, thin-layer chromatography with a 9 : 1 mixture of cyclohexane–acetone (solvent system III) [5], infrared spectroscopy, and elemental analysis, the aglycone was identical with diosgenin.

On basis of the measured amount of diosgenin formed, the molecular weight of *A* was found to be 885, which is in agreement with the calculated molecular weight (869.15) of dioscin.

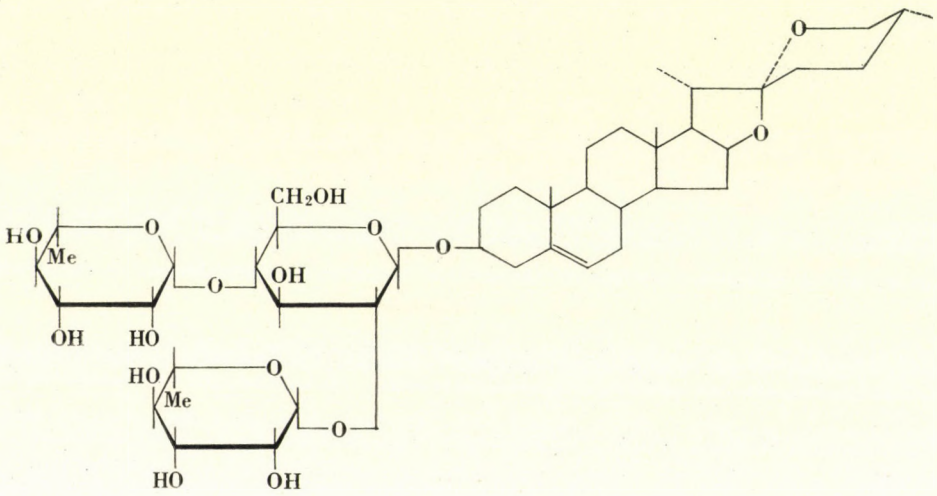

Fig. 3

After the removal of the aglycone, the acidic solution was neutralized with Amberlite IR—4B resin. The neutralized solution was run on Whatman 1 paper by the ascending technique with butanol : pyridine : water, 6 : 4 : 3 (solvent system IV) [6] and butanol : ethanol : water, 8 : 1 : 2 (solvent system V) [7], and the spots detected with aniline phthalate, in this way D-glucose and L-rhamnose were identified.

By means of the FISCHER and DÖRFEL quantitative sugar determination procedure [8] the molar ratio of L-rhamnose and D-glucose was found to be 1.95 : 1, in accordance with the ratio of 2 : 1 subsisting in dioscin.

Periodate oxidation of *A*, according to KUHN [9], and subsequent hydrolysis followed by paper chromatography showed glucose as the only surviving sugar component.

Partial hydrolysis of *A* and chromatographic purification of the crude product yielded an intermediary product A_1 in pure form, which on the basis of melting point, optical rotatory power, behaviour in thin-layer chromatography, its aglycone and sugar moiety, moreover the melting point and optical activity of its acetylated derivative, was identical with trillin (β-D-glucopyranosyl-diosgenin) [10].

Component *B* in Fig. 1, strip *b* (R_f 0.5) could not be isolated in pure form. However, when a mixture of *A* and *B* was run parallel to a mixture of authentic dioscin and gracillin as well as a common solution of these two mixtures on Silicagel-G thin-layer with solvent system I, moreover both on Whatman 1 paper with the ascending technique and cellulose powder thin-layer with benzene–butanol–water 10 : 4 : 5 (solvent system VI) [11] and butanol–5% acetic acid 10 : 4 (solvent system VII [12], respectively *B*) showed a behaviour identical with gracillin.

On the basis of these experiments, component *A* is identified with dioscin, earlier isolated from *Dioscoreae* only. Component *B* is presumably identical with gracillin, again only isolated so far from *Dioscoreae*.

Isolation and identification of components *E*, *F* and *1* are in progress.

Experimental

All melting points are uncorrected and were determined in a Boetius apparatus. The infrared spectra were obtained with a Zeiss UR—10 instrument in KBr pellets.

Thin-layer chromatography was done with Silicagel G prepared according to Stahl by Reanal Fine Chemical Factory, Budapest. Woelm silicagel (activity I) and Woelm aluminium oxide (neutral, activity II) were used as the adsorbents for column chromatography

Extraction and fractionation

Fresh, unripe berries (25 kg) of *Solanum introsum* were minced in methanol, and stirred with 100 l of methanol and then 3 × 75 l of 80% aqueous methanol for 1 hr. each, at room temperature. The combined extract was concentrated to give 1200 g of a dark greenish-brown syrupy product, whose chromatogram on silicagel thin-layer with solvent system I, after detection with antimony trichloride, is shown in Fig. 1, strip *a*.

The 1200 g syrupy product was extracted with 4 l of abs. methanol four times at boiling temperature for 1 hr. each. The combined extract gave on concentration in vacuum 630 g of a dark, thick residue. This product had a chromatogram composed of well-separated spots. The chromatogram obtained with solvent system I and various detecting agents is shown in Fig. 1, strip *b*, while respective R_f values and other data of the chromatograms are listed in Table I.

The 630 g product was homogenized with 2 l of H_2O and extracted successively with petroleum ether, ether and chloroform. The aqueous phase was then extracted with 9 l of chloroform–ethanol (3 : 1), 6 l of ethyl acetate and 8 l of butanol saturated with water. The progress of the extraction was checked by thin-layer chromatography. Chromatograms of the concentrated fractions are shown in strips *e*, *f* and *g* in Fig. 1.

Accordingly, component *A* was fully accumulated in the chloroform–ethanol solution. This fraction gave on evaporation 300 g of a dark syrupy product.

Isolation of component A

The syrupy product containing *A* was diluted with solvent system I and applied to a column of 5 cm diameter and prepared from 2 kg of silicagel and eluted with the same solvent mixture. Fractions of 15 ml were collected; the results are summarized in Table II.

Table I

R_f values, colours and colour intensities of the spots in the chromatograms shown in strips b, c and d in Fig. 1

Substance	R_f	Colour with			Colour intensity*
		Dragendorff [13]	$SbCl_3$	$AlCl_3$ [14]	
A	0.55	red	violet-red	—	+++
dioscin	0.54	red	violet-red	—	—
B	0.50	red	violet-red	—	(+)
gracillin	0.50	red	violet-red	—	—
C	0.46	red	violet-red	—	(+)
D	0.42	red	violet-red	—	(+)
1	0.38	—	yellow	yellow	++
E	0.32	red	violet-red	—	+++
F	0.25	red	violet-red	—	++
2	0.22	—	yellow	yellow	+
G	0.19	red	violet-red	—	(+)
H	0.14	red	violet-red	—	(+)
3	0.13	—	yellow	yellow	(+)
I	0.10	red	violet-red	—	(+)
K	0.07	red	violet-red	—	(+)

*(+) just observable

Table II

Chromatography on silicagel of the residue of the extract obtained with chloroform–ethanol 3 : 1

Fraction	Residue		Components (according to TLC)
	weight (g)	appearance	
1— 80	35.5	dark green resin	—
81—310	90.0	dark green syrup	*A*+(*B*)+(*C*)+(*D*)+(*E*)
311—430	20.3	dark brown syrup	(*C*)+(*D*)+*E*+*F*
431—750	60.8	dark brown syrup	(*E*)+(*F*)

The residue obtained from the combined fractions 81—310 (90 g) was extracted with 5 × 300 ml of petroleum ether by stirring under reflux; and the 72 g dark green, insoluble part was again chromatographed on aluminium oxide.

The 72 g product was homogenized with some aluminium oxide and solvent system I, and applied to a column of 5.5 cm diameter, made of 1.5 kg aluminium oxide in solvent system I. Again 15 ml fractions were taken (120 ml/hr), and the separation process was checked by thin-layer chromatography. The results are summarized in Table III.

Table III

Chromatography on aluminium oxide of the crude product containing component A

Fraction	Residue		Components (according to TLC)
	weight (g)	appearance	
1— 110	12.3	dark green resin	—
111— 200	5.0	brownish-green powder	(partially hydrolyzed products)
201— 280	10.2	dark green powder	*A*
281— 380	6.5	brownish-green powder	*A* + (*B*)
381—1060	9.6	greenish-brown powder	*A* + (*B*) + (*C*) + (*D*)

Evaporation in vacuum of the combined 201—280 fractions gave 10.2 g of a product, which was dissolved in abs. ethanol and precipitated with abs. ether several times, followed by repeated recrystallizations from abs. ethanol. The crystalline product was colourless needles, insoluble in water: it was dried over phosphorus pentoxide at 110—120 °C and 1.5 mm for 5 hrs; m.p. 298—302 °C (decomposition), $[\alpha]_D^{25}$ — 109.0° (*c* 0.373, EtOH). If the product was recrystallized from 60% ethanol and dried at room temperatur, it melted at 275—277 °C, while after drying as above, it had m.p. 278—280 °C. The corresponding data in the literature for dioscin [15] are: m.p. 275—277 °C ; $[\alpha]_D^{13}$ —115° (*c* 0.373, EtOH).
$C_{45}H_{72}O_{16}$ (869.15). Calcd. C 62.16; H 8.35. Found C 61.47; H 8.46%.

Acetylation of A

100 mg of *A*, previously dried over phosphorus pentoxide, was heated with 3 ml of acetic anhydride in dry pyridine at 140 °C for 3 hrs. The solution was evaporated in vacuum and the residue dissolved in benzene. After washing and drying, the benzene solution was treated with activated charcoal at boiling temperature, filtered, and the solvent was then evaporated. The colourless crystalline residue was chromatographed on silicagel thin-layer with solvent system II; it gave one spot only, with R_f 0.70. (When the acetylation was accomplished at room temperature or at 100 °C, two spots were detected on the chromatogram each time.)

The crude *A*-peracetate is a colourless crystalline product, m.p. 135 °C, after chromatography through a small silicagel column with benzene, it was melted at 138—142 °C, and remained unchanged on subsequent chromatography; $[\alpha]_D^{20}$ — 71.5° (*c* 1, $CHCl_3$). According to the infrared spectrum, the substance did not contain free OH group. (Data given in the literature for the acetylated dioscin consisting of 2 spots are: m.p 143—145 °C; $[\alpha]_D^{10}$ — 72° (*c* 0.389, $CHCl_3$.)
$C_{61}H_{88}O_{24}$ (1205.36). Calcd. C 60.76; H 7.36; CH_3CO 28.38. Found C 61.01; H 7.25; CH_3CO 28.10%.

Total hydrolysis of component A

0.5 g of *A* was refluxed with 40 ml of 3*N* HCl in 50% aqueous ethanol for 5 hrs, the mixture was diluted with water, the alcohol evaporated, and the residue let to stand in a refrigerator to deposit the aglycone.

Examination of the aglycone

The precipitate was filtered off, washed with water and dried at 100 °C to obtain 225 mg of a product, m.p. 192—196 °C. After chromatography on a small Al_2O_3 column and crystallization from acetone it melted at 198—200 °C and gave one spot (R_f 0.31) on silicagel thin-layer with solvent system III and $SbCl_3$. Mixed m.p. with authentic diosgenin showed no depression. The thin-layer chromatographic behaviour, infrared spectroscopic analysis and CH analysis data were in agreement with those of diosgenin.

On the basis of the amount of the crude aglycone formed (225 mg), the molecular weight of *A* was calculated to be 885; the calculated molecular weight of dioscin is 869.15.

The m.p., thin-layer chromatographic behaviour and infrared spectrum of the acetate of the aglycone were identical with those of authentic diosgenin acetate.

Examination of the sugar moiety of A

The combined mother liquor and washings of the crude aglycone was stirred with 10 g of Amberlite IR—4B resin for 10 min, then the mixture was filtered, and the resin washed.

The resulted solution was subjected to paper chromatographic analysis. Comparative experiments were carried out with authentic monosaccharides, both with parallel solutions and in mixture, on Whatman 1 paper at 24 °C, with the ascending technique, and with solvent systems IV and V, using aniline phthalate for detection. The final results of these experiments are summarized in Table IV.

Table IV

Qualitative examination of the sugars obtained by hydrolysis of A, on Whatman 1 paper

Substance	R_f			
	BuOH : C_5H_5N : H_2O 6 : 4 : 3, ascending, 18 hrs		BuOH : EtOH : H_2O 8 : 1 : 2, ascending, 20 hrs	
Hydrolyzate of *A*	0.61	0.81	0.27	0.59
D-glucose	0.61		0.27	
L-rhamnose		0.81		0.59

The quantitative determination of glucose and rhamnose was accomplished as follows: 4 mg of *A* was heated at 100 °C with 0.5 ml of 3*N* HCl in EtOH–H_2O (1 : 1) in a sealed tube for 5 hrs; the mixture was then cooled and allowed to stand in a refrigerator. The tube was opened and the aglycone removed by centrifugation. An aliquot part of the acidic solution corresponding to 100 μg of *A* was applied to Whatman 1 paper and the chromatogram was developed with solvent system IV. The amount of monosaccharides was determined by the procedure of FISCHER and DÖRFEL; the results are shown in Table V.

Table V

Quantitative determination of D-*glucose and* L-*rhamnose in the hydrolyzate of A*

D-glucose		L-rhamnose		Molar ratio	
μg	$\times 10^{-8}$ mole	μg	$\times 10^{-8}$ mole	D-glucose	L-rhamnose
17.5	9.7	30.2	18.4	1	1.8
16.5	9.2	32.0	19.5	1	2.1

After the total hydrolysis of *A*, removal of the aglycone precipitate and neutralization with an anion exchange resin, the amount of reducing sugars, expressed as glucose, was determined in an aliquot portion of the solution. The result was 566 mg glucose per 1 g of *A*; the respective value calculated for dioscin is 621 mg.

Periodate oxidation of A

30 mg of *A* in 5 ml of 0.1*N* acetic acid in ethanol was oxidized with 2.5 ml of 0.25*N* KIO_4 in 50% aq. ethanol according to KUHN [9]. The residue obtained on evaporation was chromatographed on Whatman 1 paper with solvent systems IV and V, and the spots were detected with aniline phthalate. Only one spot, corresponding to glucose, was observed.

Partial hydrolysis of A (isolation of A_1)

500 mg of *A* was refluxed in 40 ml of 1*N* H_2SO_4 in dioxan–water (1 : 3) for 2 hrs. The mixture was cooled and neutralized with $NaHCO_3$, the precipitate separated, washed with water and dissolved in chloroform–methanol (1 : 1). The solution was filtered, concentrated in vacuum and the residue chromatographed on silicagel with solvent system I. On spraying with antimony trichloride three spots were noticed with R_f values 0.97, 0.77 and 0.53. In a parallel experiment with authentic diosgenin, trillin and dioscin the respective R_f values 0.98, 0.77 and 0.54 were obtained.

According to thin-layer chromatographic examinations, the maximum amount of the product with R_f 0.77 (A_1) was achieved by refluxing for 2 hrs.

The dry crude product was refluxed twice with 30 ml of cyclohexane–acetone (9 : 1) for a few minutes, and the filtrate was concentrated in vacuum to yield 80 mg of a colourless powder consisting mostly of diosgenin. The undissolved part was dissolved in a 5 ml portion of solvent system I, and passed through a column of 2.5 cm diameter, made of 30 g aluminium oxide in the same solvent. Elution was done with solvent system I and fractions of 5 ml volume were collected. The results are summarized in Table VI.

Table VI

Chromatography on Al_2O_3 column of the crude product obtained in the partial hydrolysis of A

Fraction	Residue, mg	Components according to TLC
1— 5	23	diosgenin + (A_1)
6—18	132	A_1
19—40	82	$A_1 + A$

The residue from fractions 19—40 was subjected to a second chromatographic separation procedure just in the same way, and finally 165 mg of crude A_1 was obtained. It was twice recrystallized from methanol to obtain colourless needles, m.p. 261—263 °C (decomposition), $[\alpha]_D^{26}$ −105.3° (*c* 0.5, dioxan). Reported data for trillin [16]: m.p. 260—262 °C; $[\alpha]_D^{26}$ −103.4° (dioxan). The elementary analysis data (C, H) were also consistent with the composition of trillin.

Hydrolysis of A_1

5 mg of A_1 was heated with 0.5 ml of 1*N* HCl in 50% aqueous ethanol in a sealed tube at 100 °C for 2 hrs. By means of the previous methods only diosgenin and glucose could be detected in the hydrolyzate.

Examination of component B

Combined fractions 281—380 of Table III were concentrated in vacuum and the residue (6.5 g) crystallized from EtOH to give 1.4 g of pure *A*. All attempts to isolate pure *B* from the mother liquor failed. The *A* + *B* mixture behaved indistinguishably from a mixture of authentic dioscin and gracillin both in parallel examinations and in common solutions when chromatographed on silicagel thin-layer with solvent system I, moreover on Whatman 1 paper and cellulose powder thin-layer with solvent systems VI and VII.

*

The authors wish to express their thanks to deputy-director B. KOCH (National Institute of Agrobotany, Tápiószele) for the plant starting material. We are also indebted to the Analytical Department of our institute (Head: Mr. A. MIZSEI) for accomplishment of the various analyses and to Prof. Dr. TOSHIO KAWASAKI for authentic samples of dioscin, gracillin and trillin. Thanks are due to Miss É. SZEBENYI for her valuable technical assistance.

REFERENCES

1. KAWASAKI, T., MIYAHARA, K.: Chem. Pharm. Bull. Japan **11,** 1546 (1963)
2. HONDA, J.: ref. C. **1904,** II. 118
3. KAWASAKI, T., YAMAUCHI, T.: Chem. Pharm. Bull. Japan **10,** 703 (1962)
4. SCHREIBER, K.: Die Pharmazie **10,** 379 (1955)
5. BREWIN, D. J.: Private communication. Boots Pure Company
6. DJATLOVITZKAJA, E. V., VORONKOVA, V. V., BERGELSON, L. D.: Dokl. Akad. Nauk. SSSR **145,** 325 (1962)
7. BOLL, P. M.: Acta Chem. Scand. **16,** 1819 (1962)
8. FISCHER, F. G., DÖRFEL, H.: Hoppe-Seylers Z. physiol. Chem. **297,** 164 (1954)
9. KUHN, R., LŐW, I.: Ber. **88,** 289 (1955)
10. MARKER, R. E., KRUEGER, J.: J. Am. Chem. Soc. **62,** 2548 (1940)
11. KAWASAKI, T., YAMAUCHI, T., YAMAUCHI, R.: Chem. Pharm. Bull, Japan **10,** 698 (1962)
12. MADAJEVA, O. S., RIZHKOVA, V. K., PAN'INA, V. V.: Him. Prir. Soed. **1967,** 155
13. MERCK, E., DARMSTADT: A. G. Dyeing Reagents for Thin-Layer and Paper Chromatography 20/86
14. Cf. Reference [13], 1/2
15. TSUKAMOTO, T., KAWASAKI, T., YAMAUCHI, T.: Chem. Pharm. Bull. Japan, **4,** 35 (1956)
16. TSUKAMOTO, T., KAWASAKI, T., NARAKI, A., YAMAUCHI, T.: J. Pharm. Soc. Japan **74,** 1097 (1954)

Pál BITE
M. MARRUAN SHABANA
Budapest IV, Szabadságharcosok útja 47—49

Acta Chimica Academiae Scientiarum Hungaricae, Tomus 62 (3), pp. 293—303 (1969)

SYNTHESIS OF PROTEIN MODEL COMPOUNDS BY SIDE GROUP MODIFICATION OF POLYAMINO ACID DERIVATIVES, II

THE PREPARATION OF POLY-L-GLUTAMIC ACID DERIVATIVES CONTAINING SIMULTANEOUSLY VARIOUS FUNCTIONAL GROUPS

A. KÓTAI, GY. SZÓKÁN, I. FERENCZ and M. ALMÁS

(Institute of Organic Chemistry, L. Eötvös University, Budapest)

Received September 27, 1968

The synthesis of modified polyglutamic acid derivatives simultaneously containing various functional (dialkylamino, carboxyl, hydroxyl, imidazolyl, mercapto and ester) groups has been attempted. In the preparation of these compounds, poly-γ-methyl-L-glutamate (**I**), used as the starting material, was transformed either by different modifying reagents applied in subsequent steps, or by mixed modifying reagents. It has been observed that, using the mixed reagents for the modification, the average composition and degree of polymerization of the product depend not only on the composition of the mixed reagent, but also on the other reaction conditions (especially the temperature). It has been further established that in the preparation of polyamino acid derivatives simultaneously containing various functional groups, the character of the products is fundamentally influenced — in addition to the principal characteristics already discussed in the previous publication [2] — also by the way of working up the reaction mixture.

Polyamino acids as protein model compounds had been reviewed by KATCHALSKI *et al.* [1]. In the first paper of this series [2] a new possibility for the rather simple synthesis of a novel type of protein model compounds made by side group modification of polyamino acid derivatives was suggested.

These model compounds are similar to proteins in the respect that they have protein functional groups attached to a polypeptide backbone. However, they are different from proteins in regard of their fundamental monomeric structural units, being usually not native amino acids but modified derivatives of them.

Although the preparation of modified polyamino acids had been reported several times [3—10], a systematic investigation of side group modifying reactions of polyamino acid derivatives commenced only recently [2]. To find out the scope and limitation of this method, in our previous communication [2] the reaction of poly-γ-methyl-L-glutamate (**I**) with different diamines was examined and described. It has been shown that the average composition and average degree of polymerization of the prepared basic derivatives of poly-L-glutamic acid greatly depend both on the characteristics of the starting materials and on the reaction conditions, especially on the temperature and duration of the reaction.

The aim of the present paper was to investigate how polyamino acid derivatives, simultaneously containing two or more different kinds of functional groups, could be prepared.

There are two ways for the preparation of modified polyamino acid derivatives containing several kinds of protein functional groups: 1) The starting polyamino acid derivative is treated with a mixed modifying reagent, the components of which react with the polymer. Even if a reagent consisting only of two components is used, a great number of different compounds may be synthesised by varying the ratio of the components and some other characteristics of the reaction, as it will be shown below. 2) The individual functional groups are attached stepwise to the starting polymer. In this case, the starting polymer is transformed only partially with the first modifying reagent; this product is then further modified with a second reagent, and so on. This method is more circumstantial than the first one, but provides more opportunity for structural variations, since the compositions of the synthesised materials are independent of the relative reactivities of the different modifying reagents. As a matter of course, the two methods can also be conveniently combined, according to special needs.

To test the applicability of the mixed reagents, a part of the experiments described in the previous publication [2] has been repeated using aqueous instead of anhydrous amines as modifying reagents. In this way the ester groups of the starting poly-γ-methyl-L-glutamate (I) have been partly aminolyzed and partly hydrolyzed. Taking into account that a few per cent of glutamyl residues had already been present in the starting polymer [2], the reaction could be formulated as follows:

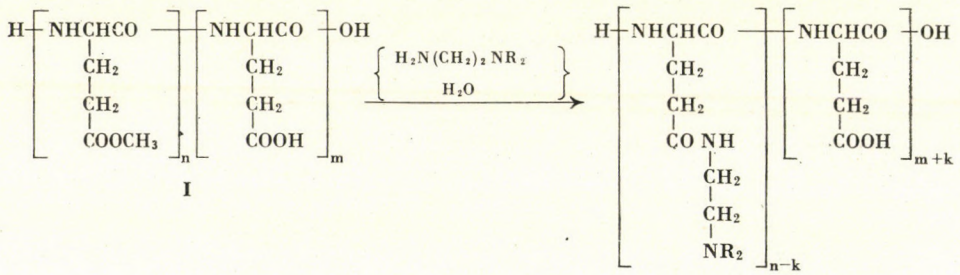

I

IIa–b

(a : R = CH_3; b : R = C_2H_5)

The characteristics of the reactions carried out under various experimental conditions and with the help of differently composed reagents, and the characteristic data of the prepared amphoteric polyamino acid derivatives are summarized in Table I.

To ensure an easy survey of the results, the same polyglutamate samples — or at least similar ones — were used as the starting materials. The compounds listed in Table I are arranged according to the increasing temperature of the preparation reactions, and within this, in the order of increasing water content of the modifying reagent. Samples, prepared with identically composed

Table I

Data of the prepared amphoteric derivatives of poly-L-glutamic acid **(II a–b)** *and the conditions of their preparation**

Characteristics of the prepared materials			Water content of the reagent		Characteristics of the reaction			
No.	Name[a] indicating composition	$\frac{\eta_{sp}}{c}$[b] dl/g	weight %	mole %	Temp.,[c] °C	Time, hours	Conversion of ester groups, %	η_{quot}[d]
1a	poly-DMAG^{25}MG^{71}Glu^{4}	1.10	0	0	20	240	26	1.06
1b	poly-DMAG^{92}MG^{4}Glu^{4}	—	0	0	20	2352	90	—
1c	poly-DMAG^{96}Glu^{4}	1.13	0	0	20	6450	100	1.09
2a	poly-DMAG^{44}MG^{52}Glu^{4}	1.03	20	52	20	240	46	0.99
2b	poly-DMAG^{95}Glu^{5}	0.92	20	52	20	2352	100	0.89
3a	poly-DMAG^{64}MG^{28}Glu^{8}	0.86	40	74	20	240	71	0.83
3b	poly-DMAG^{88}Glu^{12}	0.81	40	74	20	2800	100	0.78
4	poly-DMAG^{93}Glu^{7}	0.69	10	32	60	100	100	0.66
5	poly-DMAG^{83}Glu^{17}	0.54	40	74	60	100	100	0.52
6	poly-DMAG^{87}Glu^{13}	0.33	10	32	42; 98[e]	2; 72[e]	100	0.32
7	poly-DMAG^{84}Glu^{16}	0.21	20	52	42; 98[e]	2; 72[e]	100	0.20
8	poly-DMAG^{71}Glu^{29}	0.17	40	74	42; 98[e]	2; 72[e]	100	0.16
9	poly-DEAG^{81}Glu^{19}	0.43	20	62	75; 97[f]	2; 70[f]	100	0.34
10	poly-DEAG$^{80\pm1}$Glu$^{20\pm1}$	0.33 ±0.03	20	62	75; 97[g]	1; 70[g]	100	0.24 ±0.02
11	poly-DEAG^{77}Glu^{23}	0.34	20	62	75; 160[h]	1; 5[h]	100	0.27
12	poly-DEAG^{75}Glu^{25}	0.30	30	74	75; 97[g]	1; 70[g]	100	0.24
13	poly-DEAG^{69}Glu^{31}	0.12	30	74	75; 160[i]	1; 9[i]	100	0.10

a Names are constructed according to GILL III [15]; DMAG stands for N-(dimethylaminoethyl)-L-glutaminyl, DEAG for N-(diethylaminoethyl)-L-glutaminyl and MG for γ-methyl-L-glutamyl residues

b $c = 0.5\%$, in dichloroacetic acid

c The temperature of the heating bath is given in the Table

d $$\eta_{quot} = \frac{\frac{\eta_{sp}}{c}\text{ (product)}}{\frac{\eta_{sp}}{c}\text{ (PMG)}} \quad (c = 0.5\%,\ \text{in dichloroacetic acid})$$

e Heating at 42 °C for 2 hrs, then at 98 °C for 72 hrs

f Heating at 75 °C for 2 hrs, then at 97 °C for 70 hrs

g Heating at 75 °C for 1 hr, then at 97 °C for 70 hrs

h Heating at 75 °C for 1 hr, then at 160 °C for 5 hrs

i Heating at 75 °C for 1 hr, then at 160 °C for 9 hrs

* The characteristics of the starting polymers used for the preparation of samples Nos 1–8 were poly-MG^{96}Glu^{4} with $\frac{\eta_{sp}}{c} = 1.04$ dl/g; and for samples No. 9 and 11–13, poly-MG^{96}-Glu^{4} with $\frac{\eta_{sp}}{c} = 1.26$ dl/g. The data of six different samples were averaged as No. 10. They were prepared from different starting polymers, characterized as poly-MG^{96}Glu^{4} with $\frac{\eta_{sp}}{c}$ values from 1.29 to 1.44 dl/g.

reagents at the same temperature but with different reaction times, are listed under the same number but with different letters.

From the data of Table I the following can be seen:

1) By increasing the temperature of the reaction — but using the same reagent — the viscosity of the products decreased, as it had already been observed [2], and at the same time the amount of acidic groups increased (see, *e.g.*, the composition of samples 3b, 5 and 8). Thus, the alteration of the temperature has an influence on the relative rates of hydrolysis and aminolysis of the ester groups; the increase of temperature favours hydrolysis.

2) By increasing the water content of the reagent, not only the amount of acidic groups increased — which was especially significant at higher temperatures — but also the viscosity of the prepared products decreased (compare, *e.g.*, the viscosities of samples 1c, 2b and 3b or 6, 7 and 8).

The decrease of viscosities is caused rather by the splitting of peptide chains than by conformational changes or variations in the state of solvation, dependent on the compositions of the modified polymers. This has been proved by demonstrating — parallel to the decrease of viscosities — the appearance of increasing amounts of ninhydrin-positive amino terminals* in the materials prepared at higher temperatures with reagents of higher water content.

The presence of water in the mixed reagent gives thus rise — beside the hydrolysis of the ester groups — to partial hydrolysis of the polypeptide chains. The increase of the water content of the reagent enhances the rate of conversion of ester groups too, as it can be seen by comparing the data of samples 1a, 2a and 3a. This effect is produced in part by the observed better solubilities, but the water-catalyzed acceleration of the aminolytic reaction cannot be excluded either.

3) In the course of the preparation of sample No. 10, the reproducibility both of the preparative methods (the preparation of the starting polymer included) and of the analytical procedures has been checked. Six samples were prepared under identical conditions; the compositions and the viscosities of all of them were within the limits of error, given in Table I.

Summarizing the results obtained by the use of mixed reagents for the side group modification of polyamino acid derivatives, it can be concluded that various functional groups may be simultaneously attached to the polypeptide chain by means of reagent mixtures. It seems probable, however, that the compositions of the prepared products are not exclusively determined by the molar ratios and by the—still on other reaction conditions dependent—relative reactivities of the components of the mixed reagents, but also by the successively changing structural properties of the polyamino acid derivatives, trans-

* No ninhydrin-positive amino terminals could be found in the samples of low viscosities prepared with anhydrous reagents.

formed gradually during the reactions. If only a mixed reagent of two components is applied, the final structure of the product is determined by at least four concurrent reactions: namely, besides the side group modifying principal action of both components, chain splitting as a side effect in both cases has also to be considered. Therefore, a product with exactly prescribed characteristics (average composition and average degree of polymerization) can at present only be prepared with mixed reagents on the basis of informative preliminary experimentations.

Experiments for the preparation of amphoteric polyglutamic acid derivatives, containing hydroxyl groups as well, have also been started. Ethanolamine has been employed as the modifying reagent for building in hydroxyl groups. The preparation of α-poly-L-glutamic-γ-(2-hydroxyethyl)-amide (**IV**; l and $m = 0$), claimed to contain an appreciable amount of weakly basic oxazoline rings [11], was reported by LUPU *et al.* [4]. However, in our preliminary experiments — to be published elsewhere — the presence of such basic groups in the products, prepared according to the now described experimental conditions, could only be detected in negligible amounts or not at all.

In order to prepare amphoteric polyglutamic acid derivatives (**IV**) containing hydroxyl groups, at first poly-γ-methyl-L-glutamate samples, modified previously with 2-dimethylaminoethylamine–water mixtures (**III**), were treated with anhydrous ethanolamine. Later poly-γ-methyl-L-glutamate (**I**) was directly treated with a mixture of 2-dimethylaminoethylamine and ethanolamine (see formula on the next page).

The characteristics of these reactions and the data of the prepared materials are summarized in Table II.

Comparing the data of Table II with those of the preparation of the basic [2] and amphoteric (Table I) derivatives of polyglutamic acid, it can be seen that the periods required for the total conversion of the ester groups are now considerably shorter. This can be explained both by different solubilities and by the increased speed of aminolysis, catalyzed by hydroxyl groups [12].

The examination of the data of Table II also reveals that in the preparation of polyglutamic acid derivatives containing various functional groups, the relationship between the composition of the product and the reaction conditions is less distinct than for the compounds discussed earlier. *E.g.*, in spite of the use of pure and anhydrous ethanolamine for the preparation of samples No. 1 and 2, the amount of the basic DMAG as well as the glutamyl residues apparently increased. Similarly, it is difficult to understand, on the basis of the former connections, the differences existing between the compositions of samples No. 4 and 5. These irregularities draw attention to the fact that if modified polyamino acid derivatives — containing various functional groups and being polymolecular in character — are prepared, their compo-

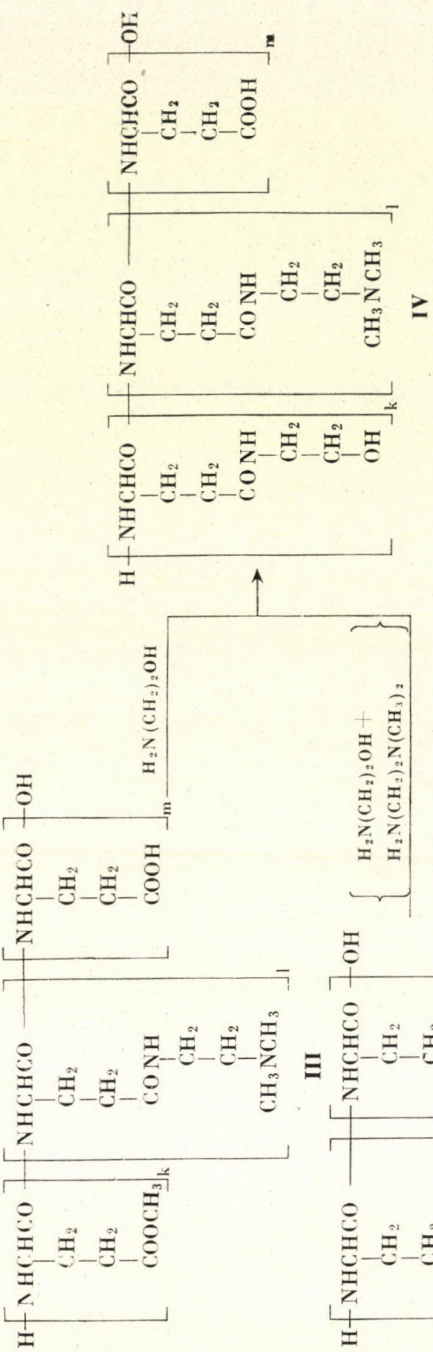
I
III
IV
$H_2N(CH_2)_2OH$ +
$H_2N(CH_2)_2N(CH_3)_2$

Table II

Data of amphoteric derivatives of poly-L-glutamic acid **(IV)** *containing hydroxyl groups and the characteristics of their preparation*

Characteristics of the prepared materials		Starting material		Characteristics of the reaction		
No.	Name[a] indicating composition	Starting polymer	Modifying reagent	Temp.,[b] °C	Time, hours	Conversion of ester groups, %
1	poly-$HG^{7}DMAG^{78}MG^{5}Glu^{10}$	poly-$DMAG^{74}MG^{18}Glu^{8}$	ethanolamine	20	120	72
2	poly-$HG^{12}DMAG^{78}Glu^{10}$			20	240	100
3	poly-$HG^{14}DMAG^{75}Glu^{11}$			97	5	100
4	poly-$HG^{41}DMAG^{47}MG^{9}Glu^{3}$	poly-$MG^{96}Glu^{4}$	ethanolamine + 2-dimethylaminoethylamine 1 : 1 (v/v)	20	72	91
5	poly-$HG^{51}DMAG^{44}Glu^{5}$			20	312	100
6	poly-$HG^{45}DMAG^{42}MG^{6}Glu^{7}$			97	5	95

a Names are constructed according to GILL III. [15]; HG stands for N-(2-hydroxyethyl)-L-glutaminyl, DMAG for N-(2-dimethylaminoethyl)-L-glutaminyl, MG for γ-methyl-L-glutamyl residues

b The temperature of the heating bath is given in the Table

sitions are also deeply influenced by inevitable molecular fractionations, occurring during the isolation and purification of the products.

The possibility of extending the scope of the synthesis of protein model compounds by side group modification of polyamino acid derivatives has also been examined. In preliminary experiments some polyamino acid derivatives **(V, VI)** have been prepared, containing imidazolyl and/or mercapto groups in addition to the hydroxyl, basic and acidic groups, discussed previously.

Modified polyamino acid derivatives containing also imidazolyl groups **(V)** have been prepared with the aid of mixed reagents including histamine. By transforming poly-γ-methyl-L-glutamate **(I)** with a reagent mixture consisting of histamine, ethanolamine and 2-dimethylaminoethylamine, the following types of modified polyamino acid derivatives can be prepared:

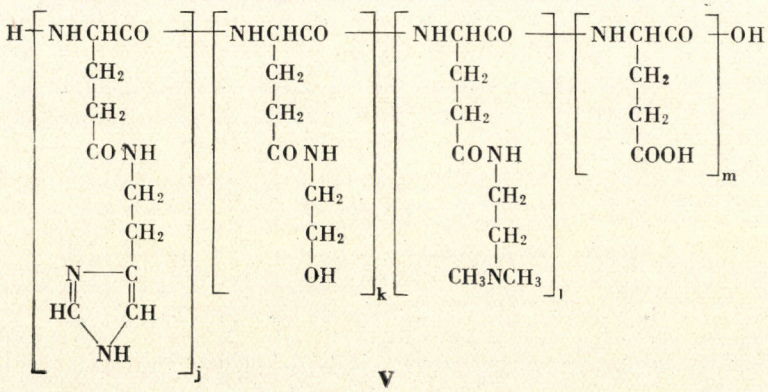

V

For the synthesis of modified polyamino acid derivatives containing also mercapto groups (**VI**), mixed reagents containing β-mercaptoethylamine have been used. The presence of free mercapto groups in these products could, however, only be demonstrated after treatment with mercaptoethanol [13], despite the applied hydrogen or nitrogen atmosphere, in which these reactions had always been carried out. Therefore, it is probable that mercapto groups underwent conversion into disulphide groups during the preparation or isolation of the products. Leaving this last mentioned process provisionally out of consideration, the general formula for the compounds, prepared with mixed reagents containing also mercaptoethylamine, can be written as follows:

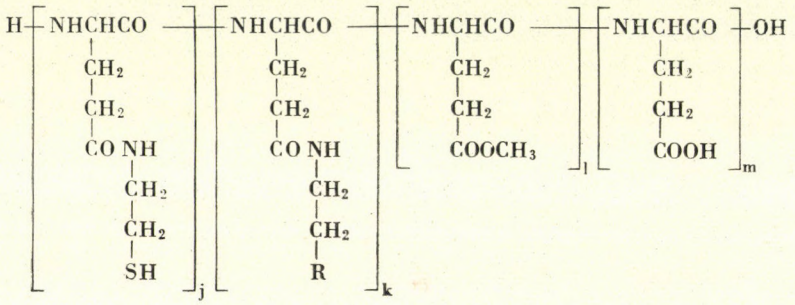

VI a–c

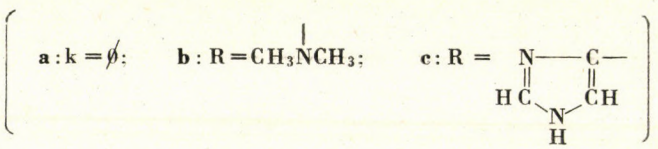

Two different products could be isolated from the same reaction mixture in the preparation of a derivative containing mercapto as well as imidazolyl groups (**VIc**). This is further evidence to support our former conclusion that during the preparation of polyamino acid derivatives, containing simultaneously various functional groups, the character of the isolated product is fundamentally influenced by the way of working up the reaction mixture.

To characterize more precisely the preparation of the last mentioned polyamino acid derivatives and to explore their biochemical properties, further experimental work is necessary.

Experimental

Preparation of amphoteric polyglutamic acid derivatives (II)

Reaction of poly-γ-methyl-L-glutamate with 2-dimethylaminoethylamine–water mixtures

Poly-γ-methyl-L-glutamate (4.0 g) was stirred with mixtures (60 ml) of 2-dimethylaminoethylamine and water. The compositions of the mixed reagents, the temperatures and the periods of the reactions were summarized in Table I. The light yellowish viscous solutions

were diluted with an amount (35–72 ml) of anhydrous ethanol, depending on the water content of the reagent, then ether (300 ml) was added. From the separated, usually greasy materials the solvents were decanted and the residues treated with several portions (50 ml each) of ether till they became powder-like. The number of these treatments (3–5) depended on the water content of the reagent. In this stage the isolated materials (4.1–4.9 g) were contaminated with dimethylaminoethylamine (1–2%), which was determined by chromatography. These impurities were removed by dissolving the materials in anhydrous ethanol (10–15 ml) and precipitating them with ether (100 ml). This last procedure was repeated 3 to 5 times until the materials contained less than 0.3% of uncombined dimethylaminoethylamine. The samples were analyzed and their purity checked by the methods described in detail in the previous publication [2] of this series.

Reaction of poly-γ-methyl-L-glutamate with 2-diethylaminoethylamine-water mixtures

The reactions were carried out according to the preceding description except that the mixed reagent contained 2-diethylaminoethylamine instead of 2-dimethylaminoethylamine. Detailed data of the compositions of the reagents, and the temperatures and durations of the reactions are summarized in Table I.

Preparation of amphoteric polyglutamic acid derivatives containing hydroxyl groups (IV)

Reaction of amphoteric polyglutamic acid derivatives, containing ester groups, with ethanolamine

A partially modified polyglutamic acid derivative (2.5 g), characterized as poly-$DMAG^{74}$-$MG^{18}Glu^{8}$ was stirred with anhydrous ethanolamine (25 ml) at temperatures and for periods given in Table II. The nearly clear solution was then rapidly concentrated in vacuum and the viscous residue dissolved in anhydrous ethanol (10 ml) and treated with ether (30–50 ml). The solvents were decanted from the precipitated material, and this procedure was repeated three times; finally, the solid material was filtered off and washed with ether. The isolated light yellowish amorphous powder (2.1–2.6 g) contained less than 0.5% of unchanged ethanolamine, as determined by paper chromatography [2]. Titrimetric methods [2] and methoxyl determinations were used to calculate the compositions of the prepared products (Table II).

Reaction of poly-γ-methyl-L-glutamate with mixtures of ethanolamine and 2-dimethylaminoethylamine

Poly-γ-methyl-L-glutamate (I)* (3.0 g) was stirred in N_2 atmosphere with a mixture of ethanolamine (25 ml) and 2-dimethylaminoethylamine (25 ml) at temperatures and for periods given in Table II. Then the reaction mixture was rapidly concentrated in vacuum and the residue diluted with anhydrous ethanol (20 ml) and treated with ether (80 ml). After decanting the solvents, this procedure was repeated three times; the residue was then treated two or three times with anhydrous ether, filtered off, and dried. The isolated white powder (3.1–3.4 g) contained an impurity of about 1% unchanged reagent, determined by paper chromatography [2]. The composition of the products (Table II) was calculated as above.

Preparation of amphoteric polyglutamic acid derivatives, containing imidazolyl, hydroxyl and dimethylamino groups (V)

Reaction of poly-γ-methyl-L-glutamate with the mixture of histamine, ethanolamine and 2-dimethylaminoethylamine

Poly-γ-methyl-L-glutamate (I)* (1.0 g) was shaken with a mixture of histamine (3.0 g), ethanolamine (3.0 g) and 2-dimethylaminoethylamine (12.0 ml) at room temperature for 10 days. The extremely viscous reaction mixture was diluted with anhydrous ethanol (40 ml),

* The composition of the starting polymer was poly-$MG^{96}Glu^{4}$, and its $\eta_{sp/c}$ value was 1.26 dl/g.

and then ligroin (60 ml; b.p. 60–80 °C) was added. After decanting the solvents from the precipitated material, the residue was repeatedly treated with a mixture of ethanol (20 ml) and ligroin (30 ml); the amorphous solid was then filtered off and dried. The nearly colourless product (1.15 g) contained some of the starting materials as shown by paper chromatography. Therefore, it was treated three times successively with mixtures of ethanol (5 ml) and ether (10 ml). The material (0.95 g) recovered after this purification contained, according to chromatographic analysis, no impurities. In the prepared methoxyl-free, modified polyglutamic acid derivatives the amount of basic groups was determined by titrimetric methods [2]. The amount of imidazolyl groups was calculated from the absorption (measured at 211 mμ) of the solution containing histamine, produced by hydrolyzing an aliquot of the product with 6*N* HCl. Identically treated, differently composed solutions, prepared from the compounds formed in the hydrolysis, were used for comparison. According to the referred analytical methods, the probable composition of the prepared material* was:
Poly-IG^{8}HG^{15}DMAG^{73}Glu^{4} ($\overline{M}_{100}$** = 19422)

	Base (total)	Histamine	OCH_3
Found	4.16 meq./g;	0.39 mmole/g;	0%
Calcd.	4.18 meq./g;	0.41 mmole/g;	0%.

Preparation of polyglutamic acid derivatives containing sulphur (VI)

Reaction of poly-γ-methyl-L-glutamate with a mixture of β-mercaptoethylamine and aqueous NaOH solutions

Poly-γ-methyl-L-glutamate (I)*** (2.1 g) was shaken at room temperature in H_2 atmosphere for 6 hrs with a mixture of β- mercaptoethylamine (1.0 g), and 0.5*N* NaOH solution (25 ml). The undissolved material (0.6 g) was then filtered off (still in H_2 atmosphere) and the solution acidified with 6*N* HCl (5.0 ml). The precipitated material was centrifuged and washed first with 0.1*N* HCl (3 × 25 ml), then with water (3 × 25 ml) in the centrifuge tube, and dried. The probable composition**** of the white amorphous powder (0.4 g) was calculated from methoxyl and sulphur determinations:
Poly-TG^{9}MG^{13}Glu^{78} ($\overline{M}_{100}$ = 13714). Found S 2.04; OCH_3 3.00; N 11.3. Calcd. S 2.10; OCH_3 2.94; N 11.1%.

Reaction of amphoteric polyglutamic acid derivatives, containing ester groups with β-mercaptoethylamine

A partially modified polyglutamic acid derivative (1.0 g) characterized as poly-DMAG^{74}-MG^{18}Glu^{8} was shaken in H_2 atmosphere at 60 °C for 25 hrs with β-mercaptoethylamine (0.5 g) dissolved in ethanol (35 ml). The undissolved material (0.26 g) was centrifuged off and the solution evaporated to dryness. The residue, dissolved in water (5 ml) was dialyzed for 3 days against distilled water. The white material (0.5 g), isolated by lyophilization did not contain uncombined reagents, as shown by paper chromatography. The composition of the material was calculated from sulphur and methoxyl determinations, assuming that the molar ratio of basic and acidic parts remained unchanged. According to this, the assumed composition is: Poly-TG^{7}DMAG^{74}MG^{11}Glu^{8} ($\overline{M}_{100}$ = 18669). Found S 1.20; OCH_3 1.86. Calcd. S 1.18; OCH_3 1.83%.

The presence of free SH groups could only be detected [14] in the compound after treatment with mercaptoethanol [13].

* IG stands for N-[2-(β-imidazolyl)-ethyl]-L-glutaminyl residues.

** $\overline{M}_{100}$ is the average molecular weight of a polymer whose degree of polymerization is 100.

*** See footnote on page 301

**** TG stands for N-(2-mercaptoethyl)-L-glutaminyl residues. For the sake of simplicity, the composition was calculated by assuming structural parts containing free mercapto groups, though their presence could only be detected with sodium *p*-chloromercurybenzoate [14] after treatment with mercaptoethanol [13].

Reaction of poly-γ-methyl-L-glutamate with a mixture of β-mercaptoethylamine and histamine

Poly-γ-methyl-L-glutamate (I)* (1.0 g) was blended with a mixture of thoroughly powdered histamine (10 g) and β-mercaptoethylamine (0.78 g), then heated in N_2 atmosphere to 95–98 °C. The viscous, molten material was stirred at this temperature for 74 hours, then cooled and diluted with anhydrous ethanol (15 ml). Finally ligroin (5 ml) was added. The solvents were decanted from the precipitated sticky amorphous material, and the residue was treated with a mixture of ethanol (7 ml) and ligroin (5 ml). After discharging also these solvents, the remainder was treated with ethanol (2 × 15 ml) until it transformed into a powder. This was filtered off and washed with ethanol. The composition of the material (0.75 g) — insoluble both in water and in acids — was calculated from methoxyl and sulphur determinations. The assumed composition is:

Poly-$TG^{19}IG^{52}MG^{25}Glu^4$ ($\overline{M}_{100}$ = 19228). Found S 3.10; OCH_3 4.08. Calcd. S 3.17; OCH_3 4.05%.

To the first mother liquor obtained in the course of working up the reaction mixture, more ligroin (10 ml) was added and the precipitated material was worked up as the former. The probable composition of this second product (0.3 g), according to methoxyl and sulphur determination, was the following:

Poly-$TG^{32}IG^{48}MG^{16}Glu^4$ ($\overline{M}_{100}$ = 19498). Found S 5.22; OCH_3 2.49. Calcd. S 5.26; OCH_3 2.55%.

The presence of free mercapto groups could only be detected [14] in both compounds after treatment with mercaptoethanol [13].

*

The authors' thanks are due to Prof. V. BRUCKNER, Director of the Institute of Organic Chemistry, for giving an opportunity to carry out the experiments and for his critical comments. We also wish to express our thanks to our Microanalytical Laboratory, supervised by Mrs. H. MEDZIHRADSZKY, for the analyses.

REFERENCES

1. KATCHALSKI, E., SELA, M., SILMAN, H. J., BERGER, A.: in "The Proteins" (Ed. Neurath, H.) IInd ed. Academic Press, New York and London, 1964, Vol. II, p. 405
2. KÓTAI, A.: Acta Chim. Acad. Sci. Hung. **54,** 65 (1967)
3. KOVÁCS, K., KÓTAI, A.: Acta Chim. Acad. Sci. Hung. **21,** 435 (1959)
4. LUPU, N., YARON, A., SELA, M., BERGER, A.: Bull. Res. Counc. of Israel **10A** (1), 47 (1961)
5. LOTAN, N., YARON, A., BERGER, A.: Biopolymers **4,** 365 (1966)
6. KULKARNI, R. K., BLOUT, E. R.: J. Am. Chem. Soc. **84,** 3971 (1962)
7. SELA, M., KATCHALSKI, E.: J. Am. Chem. Soc. **77,** 3662 (1955)
8. SZEKERKE, M.: Nature **199,** 280 (1963)
9. SZEKERKE, M., CSÁSZÁR, J., BRUCKNER, V.: Acta Chim. Acad. Sci. Hung. **46,** 379 (1965)
10. KOVÁCS, N. H., KOVÁCS, J., PISANO, M. A., SHIDLOVSKY, B. A.: J. Med. Chem. **10,** 904 (1967)
11. WENKER, H.: J. Am. Chem. Soc. **57,** 1079 (1935)
12. ARNETT, E. M., MILLER, J. G., DAY, A. R.: J. Am. Chem. Soc. **72,** 5635 (1950)
13. ANFINSEN, C. B., HABER, E.: J. Biol. Chem. **236,** 1361 (1961)
14. ISLES, T. E., JOCELYN, P. E.: Biochem. J. **88,** 84 (1963)
15. GILL III., T. J.: Biopolymers **2,** 283 (1964)

András KÓTAI
Gyula SZÓKÁN
Ilona FERENCZ
Márta ALMÁS

Budapest VIII, Múzeum krt. 4/b

* See footnote on p. 301

Acta Chimica Academiae Scientiarum Hungaricae, Tomus 62 (3), pp. 305—319 (1969)

IMPROVED SYNTHESES OF STEREOISOMERIC POLY-γ-GLUTAMIC ACIDS, II

SYNTHESES VIA POLYBENZYL AND POLY-*t*-BUTYL ESTERS

M. HOLLÓSI, M. KAJTÁR and V. BRUCKNER

(Institute for Organic Chemistry, L. Eötvös University, Budapest)

Received December 21, 1968

The synthesis of poly-γ-glutamic acid *via* its polybenzyl ester and poly-*t*-butyl ester is described. Two types of dipeptide active ester salts, α,α'-dibenzyl γ-L-glutamyl-L-glutamate *p*-nitrophenyl ester hydrochloride **(VIII)** and both the L–L and the D–D stereoisomers of α,α'-di-*t*-butyl γ-glutamyl-glutamate pentachlorophenyl ester hydrochloride **(XIII)** have been prepared by coupling suitably protected glutamic acid derivatives by the active ester method. Polyautoacylation reaction of the dipeptide derivatives **VIII** and **XIII**, carried out in dimethylformamide solution in the presence of triethylamine, resulted in poly-α-benzyl-glutamate **(XV)** and poly-α-*t*-butyl-glutamate **(XVII)**, respectively, in yields of 50—60%. Catalytic hydrogenation of the polybenzyl ester **(XV)** in a mixture of hexamethylphosphoric triamide and dimethylformamide gave a polyacid containing about 15—20% of the α-carboxyl groups still esterified. The poly-α-*t*-butyl-glutamate **(XVII)** was transformed into the polyacid by removing the *t*-butyl groups with 97% trifluoroacetic acid in nearly quantitative yield. The number average molecular weights of the poly-α-*t*-butyl-glutamate and the poly-γ-glutamic acid prepared from it were found to be 17 500 and 12 500, respectively, by amino nitrogen analysis. The polyglutamic acid obtained from the polybenzyl ester had very low molecular weight (1300). Total hydrolysis of the high molecular weight poly-γ-glutamic acid showed it to be optically pure (at least 99±3%). The optical rotations of the polyacids synthesized through the polymethyl and the poly-*t*-butyl esters have been compared and their relations explained.

In a previous communication [1] two of us reported a new synthesis of poly-γ-glutamic acid *via* its polymethyl ester. Though all our investigations carried out so far have shown the synthetic product to be built up entirely of γ-linked glutamic acid residues [1, 2], the absolute structural purity of the polyacid has remained disputable to a certain extent, because the possibility of $\gamma \rightarrow \alpha$ transpeptidation [3] in the course of the alkaline hydrolysis of the polymethyl ester could not be precluded. As the available analytical methods are not sensitive enough to detect a slight amount of α-linkages in the polymer, we wanted to solve the problem by working out new routes for the preparation of poly-γ-glutamic acid, which do not involve alkaline treatment. Two possibilities appeared suitable for this purpose, namely the synthesis of poly-α-benzyl- and poly-α-*t*-butyl-glutamates which can be converted into the polyacid by hydrogenolytic and acidolytic cleavage, respectively, instead of alkaline hydrolysis of the ester groups.

Synthesis of dipeptide active ester salts

Since fairly good results had been obtained in polymerizing the active ester salts of α,α'-dimethyl γ-glutamyl-glutamate [1], we followed the same general method in the synthesis of the two polyesters mentioned above. So we had to synthesize, first of all, the appropriate active ester salt derivatives of the α,α'-dibenzyl and α,α'-di-*t*-butyl γ-glutamyl-glutamates.

Synthesis of α,α'-dibenzyl γ-glutamyl-glutamate p-nitrophenyl ester hydrochloride (**VIII**)*. In the course of the synthesis of the dipeptide dibenzyl ester derivative, temporary protection of the amino group of the acylating component must be accomplished by a group which can be selectively removed from the dipeptide derivative without cleavage of the α-benzyl esters. In the first experiments an attempt was made to use *t*-butyloxycarbonyl group [4, 5] for this purpose. We succeeded in obtaining a crystalline dicyclohexylammonium salt (**III**) by acylating α-benzyl glutamate (**II**) [6] with the *p*-nitrophenyl ester of α-benzyl N-*t*-butyloxycarbonyl-glutamate (**I**) in the presence of dicyclohexylamine. The active ester **I** was prepared from α-benzyl N-*t*-butyloxycarbonyl-glutamate [7] and *p*-nitrophenol by the dicyclohexyl-carbodiimide method [8].

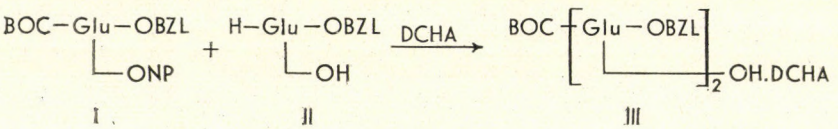

It may seem unusual to use a secondary instead of a tertiary base in a peptide bond forming reaction, but — as our experiments have shown — the NH group of dicyclohexylamine, with the two bulky cyclohexyl groups attached to it, does not significantly compete with the primary amino group of the ester component in the acylation reaction.**

Though the dicyclohexylammonium salt **III** was obtained in analytically pure state after repeated crystallizations, the free dipeptide acid liberated from it by citric acid could not be crystallized. Therefore, we gave up this way of synthesis and looked for other possibilities.

WEYGAND and HUNGER [10] have reported the application of the *p*-methoxy-benzyloxycarbonyl group — introduced into the methodics of peptide chemistry by MCKAY and ALBERTSON [4] — as a useful amino protecting group in the syntheses of N-protected benzyl ester derivatives of a series of γ-glutamyl oligopeptides. One of the compounds described by WEYGAND and

* For abbreviations, see Reference [22] of our previous article [1].

** An analogous reaction, the acylation of dicyclohexylammonium salts of amino acids with carbobenzoxy-peptide pentachlorophenyl esters, was reported recently by KAPOOR and DAVIS [9].

HUNGER, namely α,α'-dibenzyl N-*p*-methoxy-benzyloxycarbonyl-γ-glutamyl-glutamate (**VI**) promised to be an appropriate intermediate also for our purposes. We prepared, however, the above dipeptide derivative (**VI**) in a modified way by acylating α-benzyl glutamate (**II**) with α-benzyl N-*p*-methoxy-benzyloxycarbonyl-glutamate *p*-nitrophenyl ester (**V**) obtained from the protected α-benzyl ester (**IV**) [10] and *p*-nitrophenol by the usual dicyclohexyl-carbodiimide procedure [8]. Both the yield of our synthesis and the purity of the product were better than those described earlier [10].

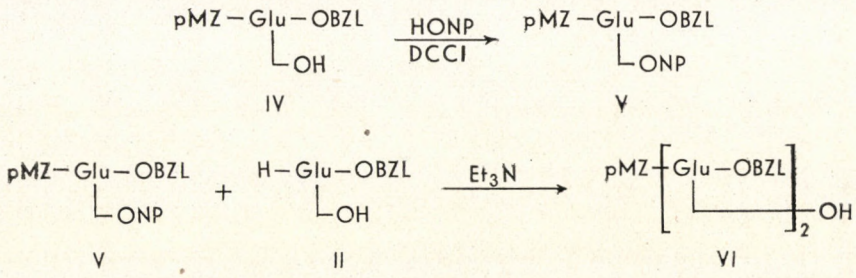

The condensation of the dipeptide acid **VI** with *p*-nitrophenol by means of dicyclohexyl-carbodiimide gave the crystalline protected dipeptide active ester **VII**, whose protecting group was removed by mild acidolysis with trifluoroacetic acid in the presence of anisole [10]. The trifluoroacetate obtained in this way could be transformed into the dipeptide *p*-nitrophenyl ester hydrochloride **VIII** by saturating a solution of the former in tetrahydrofuran with dry hydrogen chloride (*cf.* [10]).

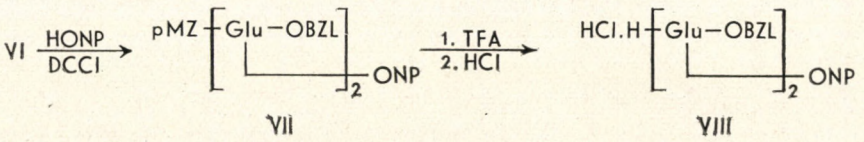

The α,α'-dibenzyl γ-glutamyl-glutamate *p*-nitrophenyl ester hydrochloride (**VIII**) was obtained, after recrystallization from acetone–ether, as a sharp-melting, both analytically and chromatographically pure substance, which proved to be an appropriate starting material for the polymerization reaction.

Synthesis of α,α'-di-t-butyl γ-glutamyl-glutamate pentachlorophenyl ester hydrochloride (**XIII**). In the synthesis of the active ester salt derivative of the dipeptide di-*t*-butyl ester (**XIII**), the carbobenzoxy group promised to be the most advantageous amino protecting group, since its hydrogenolytic cleavage

does not involve any damage to the *t*-butyl esters, which are very sensitive to acid treatment. It had to be considered, however, that the *p*-nitrophenyl ester is reducible by catalytic hydrogenation, thus it must not be applied as the active ester derivative in this case. The preparation of the dipeptide active ester salt followed the general route used in the syntheses of both the methyl [1] and the benzyl ester derivatives as summarized below.

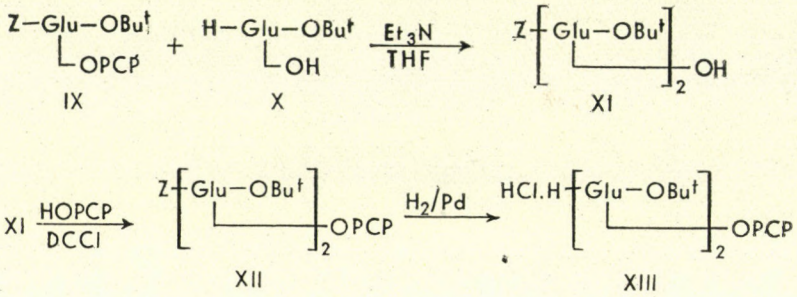

The two glutamic acid derivatives **IX** and **X** were prepared in the following way. γ-Methyl N-carbobenzoxy-glutamate [11] was converted into the α-*t*-butyl ester both by transesterification with *t*-butyl acetate according to TASCHNER *et al.* [12], and by proton-catalyzed addition of isobutylene [13]. Selective hydrolysis of the γ-methyl ester group with sodium hydroxide solution afforded the α-*t*-butyl N-carbobenzoxy-glutamate which was isolated in the form of its dicyclohexylammonium salt [12, 14]. The protected semi-ester liberated from this salt was described by TASCHNER [12] as a slowly crystallizing oil. We obtained it, after recrystallization from a mixture of ether–petroleum ether, in analytically pure, crystalline state. It was attempted to convert the protected semi-ester into different active esters (*p*-nitrophenyl ester, N-hydroxyphthalimide ester), but it was only the pentachlorophenyl ester (**IX**), described also by KOVÁCS *et al.* [15], that could be obtained as a crystalline substance.* Catalytic hydrogenation of α-*t*-butyl N-carbobenzoxy-glutamate gave the free semi-ester **X**. We did not succeed in crystallizing this substance, the solid microcrystalline powder had, nevertheless, a fairly sharp melting point and proved to be pure by both elemental analysis and thin-layer chromatography. Coupling of the protected active ester **IX** and α-*t*-butyl glutamate (**X**) was achieved — after a series of unsuccessful experiments — in tetrahydrofuran by applying triethylamine as a base. Since α-*t*-butyl glutamate (**X**) is insoluble in tetrahydrofuran, the heterogeneous reaction required very intensive stirring to go to completion. The crystalline dipeptide derivative **XI** was converted into the corresponding γ'-pentachlorophenyl ester (**XII**) by

* It is to be noted that KOVÁCS *et al.* [15] described the *p*-nitrophenyl ester, too, as a low-melting crystallline substance, but without giving any details on the preparation of either of the two active esters.

the dicyclohexyl-carbodiimide method [8]. The last step in the preparation of the dipeptide active ester salt (**XIII**) was the removal of the carbobenzoxy group from the protected dipeptide active ester **XII**. This was effected by catalytic hydrogenation in the presence of hydrogen chloride used in a slight excess above the stoichiometric quantity. Both the L–L and the D–D antipodes of the pentachlorophenyl ester hydrochloride of α,α'-di-*t*-butyl γ-glutamyl-glutamate (**XIII**) were prepared. These salts were repeatedly recrystallized from ethanol–ethylacetate–ether mixture to obtain chromatographically pure substances with sharp melting points and elemental analyses in good agreement with the calculated values. They served as appropriate starting materials for the synthesis of the two antipodes of poly-α-*t*-butyl glutamate.

Preparation of the polyesters (Polymerization)

The polymerization of the dipeptide active ester salts (**VIII** and **XIII**) was achieved by deprotonating the amino group with a tertiary base. The free dipeptide active esters (**XIV** and **XVI**) underwent a polyautoacylation reaction resulting in the corresponding polyesters (**XV** and **XVII**):

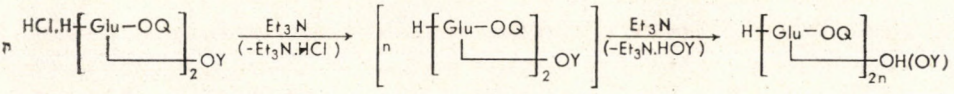

Q = BZL, Y = NP; VIII XIV XV

Q = Bu^t, Y = PCP; XIII XVI XVII

The reactions were carried out in a similar way as in the case of the preparation of poly-α-methyl-glutamate [1]. Dimethylformamide proved to be a better solvent than dimethyl sulfoxide for both starting dipeptide derivatives. The concentrations of the latter were about 0.5—1.0 mmole/ml. The polymerization was made at room temperature by stirring the solutions in the presence of 2.0—2.2 equivalents of triethylamine for several hours, and then allowing the reaction mixtures to stand for a day. Though the IR band at 1780 cm^{-1}, characteristic for the active ester group [1], could not be detected in the spectrum of the reaction mixture half an hour after the addition of the base, the polymerization reaction did possibly not end in such a short time, since the viscosity of the solutions was still in increase (*cf.* [1]).

The isolation procedure was somewhat different in the case of the two polyesters. The *polybenzyl ester*, being very scarcely soluble in every common organic solvent, was isolated by diluting the viscous reaction mixture with hot methanol and washing the precipitated substance with the same solvent. The polyester was obtained as an amorphous white powder in a yield of 51%. The *poly-t-butyl ester* is, in turn, fairly soluble in both ether and water, so the

crude product precipitated from the reaction mixture by the addition of ether was washed with water (to eliminate triethylammonium chloride) and ether (to remove the last traces of pentachlorophenol). The yield of poly-α-*t*-butyl-glutamate was between 55 and 60%.

The number average molecular weights of the different samples of poly-α-*t*-butyl-glutamate were calculated from their amino nitrogen contents determined by the modified VAN SLYKE method [16]. The amino nitrogen analysis of the polybenzyl ester could not be performed, because this substance failed to dissolve in the solvents applicable in the analytical procedure.

The reaction conditions and yields of the polymerization experiments, together with the molecular weights of the polymers are summarized in Table I.

Table I

Reaction conditions of the preparation and molecular weights of esters of poly-γ-glutamic acid

No.	Structure of the polyester		Solvent	Yield, %	Amino N, %	Number average molecular weight
	Esterifying group	Confign.				
1	BZL	L	DMFA	51	—	—
2		L	DMSO	55	0.09	15 500
3	Bu^t	L	DMFA	57	0.08	17 500
4		D	DMFA	60	0.15	9 500

As it can be seen from the data listed in Table I, the molecular weights of the poly-*t*-butyl-glutamate samples are about two or three times higher than those of the corresponding polymethyl esters [1]. This may probably be accounted for by the relatively high solubility of the poly-*t*-butyl ester allowing the polymerization reaction to proceed to a higher degree than in the case of the less soluble polymers. The practical insolubility of the polybenzyl ester made the determination of its molecular weight, unfortunately, impossible. However, since the molecular weight of the polyacid prepared from the polybenzyl ester is rather low (see below), that of the polyester cannot be very high, either.

Conversion of the polyesters into the polyacid

The benzyl groups of *poly-α-benzyl-glutamate* were removed by catalytic hydrogenation. Because of the practical insolubility of this substance in most of the common organic solvents, this preparative task was fairly difficult to perform. It was only hexamethylphosphoric triamide that proved to be an appropriate solvent for this purpose. The polyester could be dissolved in this solvent on warming, and did not precipitate even after dilution of the solution

with dimethylformamide. So the hydrogenation was carried out in a mixture of these two solvents. After the uptake of hydrogen had stopped, the catalyst was removed, and the dimethylformamide was evaporated under reduced pressure. The remaining concentrated solution of the hydrogenated polyester in hexamethylphosphoric triamide was diluted with water, and — after the addition of fresh, prehydrogenated catalyst — the hydrogenation was continued. An additional slight amount of hydrogen was still absorbed. After the evaporation of water, the polyacid was precipitated by adding ether to the remaining concentrated solution. The crude product contained a considerable amount of hexamethylphosphoric triamide that made it rather hygroscopic. Therefore, it was dissolved again in water and dialyzed. The dialyzate was concentrated, and the polyacid was finally precipitated from the concentrated water solution by ethanol and ether.

The poly-γ-glutamic acid obtained in this way still contained benzyl residues the amount of which was determined by measuring the UV absorption of the substance. (When calculating the benzyl content, the molar extinction coefficient of the benzyl groups was taken as identical with that of toluene.) According to the spectroscopic measurements, about 15—20% of the carboxyl groups remained esterified. The failure of poly-α-benzyl-glutamate to undergo complete change into poly-γ-glutamic acid is in accordance with earlier experiments [17] on poly-γ-benzyl-glutamate, whose benzyl groups could not be removed quantitatively by catalytic hydrogenation, either.

The conversion of *poly-α-t-butyl-glutamate* into the free polyacid was effected by acidolysis with trifluoroacetic acid [18]. As KOVÁCS *et al.* [15] reported in connection with the preparation of poly-glutamyl-alanyl-glutamic acid from the corresponding γ-*t*-butyl ester, they had found that the optimal conditions for the cleavage of the *t*-butyl groups consisted in a treatment with 90% trifluoroacetic acid at room temperature for 50 minutes. According to our experiments, complete removal of the *t*-butyl groups from poly-α-*t*-butyl-glutamate requires somewhat more energetic reaction conditions. We reacted the polyester with 97% trifluoroacetic acid for at least 90 minutes at room temperature and for additional 24 hours at 0 °C, or we repeated the trifluoroacetic acid treatment. Milder cleavage afforded polyacids containing more or less *t*-butyl groups determined by the usual methoxyl analysis. The poly-γ-glutamic acid was isolated by diluting the trifluoroacetic acid solution with ether, and washing the precipitated substance with several portions of a large amount of the same solvent. To eliminate the last traces of included ether, the polyacid was finally dissolved in water and freeze-dried. The conversion was almost quantitative.

Molecular weights of the polyacids. The number average molecular weights of the different poly-γ-glumatic acid samples were determined by the modified VAN SLYKE method [16, 19] and are summarized in Table II. The polyacid

prepared from poly-α-benzyl-glutamate had very low molecular weight, owing probably to the low solubility of the polyester; precipitation of the latter during the polymerization reaction might have caused chain propagation to break off too early. In contrast to this, the molecular weight of the poly-γ-glutamic acid obtained from the poly-*t*-butyl ester was even higher than that of the polyacid made *via* the polymethyl ester [1]. Since the accuracy of the amino nitrogen analysis decreases with increasing molecular weight, the high values presented in Tables I and II may be rather erroneous. It may, however, be stated with certainty that the molecular weight of the polyacid synthesized *via* the poly-*t*-butyl ester is about 10 000, *i.e.* the highest of all synthetic poly-γ-glutamic acids obtained by us so far [1, 2].

Table II

Reaction conditions of the preparation and molecular weights of poly-γ-glutamic acids

No.[a]	Structure of the starting polyester		Reaction conditions of preparation	Yield, %	Amino-N %	Number average molecular weight
	Esterifying group	Confign.				
1	BZL	L	H_2/Pd HMPA[b]—DMFA H_2O	52	1.08	1 300
3	Bu^t	L	97% TFA	95	0.12	12 500
4		D		98	0.20	7 000

a) Numbers refer to those in Table I; b) hexamethylphosphoric triamide.

Structure and optical purity. The results of elemental analysis of the poly-γ-glutamic acid (made *via* the poly-*t*-butyl ester) are in fairly good agreement with the values calculated for a polyacid containing half a mole of water per glutamyl residues (*cf.* [1, 2]). As to the structural homogeneity of the polyacid, it is to be kept in mind that the synthesis of the poly-*t*-butyl ester has proceeded in a strictly unequivocal route, therefore the possibility for accidental formation of α-glutamyl residues in the polyacid might only have arisen from acid-catalyzed transpeptidation during the acidolytic elimination of the *t*-butyl groups. However, Kovács *et al.* [15] made very accurate investigations on the possibility of this sort of isomerisation during the trifluoroacetic acid treatment of model peptides containing *t*-butyl esters of α- or γ-glutamyl residues, and concluded that no transpeptidation occurred under these conditions. Their results are in accordance with earlier views [20] concerning the resistance to transpeptidation of the *t*-butyl esters of glutamyl and aspartyl residues. As no $\gamma \rightarrow \alpha$ transpeptidation could be observed even after the alkaline hydrolysis of poly-α-methyl glutamate [1], it was thought to be justi-

fied not to reckon with this isomerization at all, and to take the structural homogeneity of poly-γ-glutamic acid for granted.

The optical purity of the polyacid was tested by total hydrolysis in the same manner as described in a previous paper [1]. According to the results of this experiment, the error of which amounts to about ±3%, the polyacid proved to be optically pure. Though the optical rotations of the acid hydrolyzates of the polyacids derived from the poly-α-methyl- and the poly-α-*t*-butyl-glutamates, respectively, were exactly identical, the specific rotations (at the sodium D line) of the two substances differed in a non-negligible extent: the polyacid prepared from the poly-*t*-butyl ester gave a value of $[\alpha]_D$ —36.9° (for the L-antipode), while the polyacid made from the polymethyl ester gave only $[\alpha]_D$ −24° to −27° (measured on different samples of the L-antipode). At first sight one may think that — since both polyacids are optically pure — the difference in specific rotation can be attributed to the occurrence of α-glutamyl residues in the polyacid synthesized *via* the polymethyl ester. However, an α-linked L-glutamic acid residue has much higher negative rotation (−79°, calculated as the difference between the molecular rotations of the α-tripeptide and α-dipeptide of L-glutamic acid [21]) than the corresponding γ-linked residue (−22° [22]), therefore the presence of α-glutamyl residues in the polyacid should have caused the rotation to shift in the direction just opposite to that observed. The difference in the rotations of the two poly-γ-glutamic acids can be interpreted on the basis of the rather great difference in their molecular weights. The even smaller value of the specific rotation of the low molecular weight polyacid obtained from the polybenzyl ester is also in agreement with this reasoning. Analysis of the optical rotatory dispersions of γ-linked oligo- and polypeptides of glutamic acid (*cf.* [22], and some other data to be published in detail later) seem also to substantiate these conclusions. It can, therefore, be stated that the poly-γ-glutamic acids synthesized by the two methods (*via* the polymethyl and the poly-*t*-butyl esters) differ only in their molecular weights and not in optical purity or structural homogeneity. Thus the scruples about the adequacy of the former syntheses [1] to yield polyglutamic acids with pure γ-linked structures may be rejected. The new synthesis *via* poly-α-*t*-butyl glutamate has, nevertheless, to be regarded as the best one, because of the higher molecular weight of the polyacid obtained by it. The polybenzyl ester proved in all respects to be the least suitable intermediate for the synthesis of poly-γ-glutamic acid.

Note added in proof. Fractionation experiments on Sephadex G-50 column have shown the poly γ-glutamic acids to contain a considerable amount of cyclopeptide impurities. Accordingly the high molecular weights calculated from amino-N analysis should be erroneous. It is very probable that the high value of the specific rotation of the polyacid may also be caused by the cyclopeptide content of the sample. Experiments are in progress and will be published later.

Experimental

All m.p.'s are uncorrected and were taken on a Tottoli apparatus (W. Büchi, Flawil/Schweiz). The optical rotations were measured with a visual polarimeter (Schmidt-Haensch) using a sodium lamp. Before microanalysis, the samples were dried in a vacuum desiccator over phosphorus pentoxide for 8—10 hrs at a temperature (50—100 °C) adjusted to the m.p. of the substance to be analyzed. Thin-layer chromatograms were made on silica gel (Kieselgel-G nach Stahl, Merck) using the following solvent mixtures:

a) ethyl acetate–pyridine–acetic acid–water (60 : 20 : 6 : 11),
b) *n*-butyl alcohol–acetic acid–water (4 : 1 : 1),
c) *n*-butyl alcohol–pyridine–acetic acid–water (30 : 20 : 6 : 24).

α-Benzyl N-*t*-butyloxycarbonyl-L-glutamate *p*-nitrophenyl ester (I)

A cold solution of α-benzyl N-*t*-butyloxycarbonyl-L-glutamate (1.60 g; 4.8 mmoles) [7] and *p*-nitrophenol (0.66 g; 4.8 mmoles) in ethyl acetate (8 ml) was mixed with dicyclohexylcarbodiimide (0.98 g; 4.8 mmoles). The reaction mixture was stirred for 2 hrs under cooling and then let to stand for a day at room temperature. After cooling for several hours, the mixture was filtered and the dicyclohexylurea (1.00 g; 94%) washed with ethyl acetate (4 ml); the ethyl acetate solution was washed with 8% $NaHCO_3$ solution (2 × 5 ml) and water (5 ml). The dried ($MgSO_4$) solution was evaporated under reduced pressure. The remaining oil crystallized (2.05 g; 94%); m.p. 90—94 °C. This crude product was recrystallized from ethyl acetate-ether (1 : 1) (2 ml) to yield 1.28 g (58%) of pure **I**, m.p. 100—102 °C, $[\alpha]_D^{20}$ −15° (*c* = 1, methanol).

$C_{23}H_{26}N_2O_8$ (485.5). Calcd. C 60.25; H 5.71; N 6.11. Found C 59.87; H 6.04; N 5.93%.

Dicyclohexylammonium salt of α,α'-dibenzyl N-*t*-butyloxycarbonyl-γ-L-glutamyl-L-glutamate (III)

A solution of α-benzyl L-glutamate (**II**) (0.88 g; 3.7 mmoles) [6], α-benzyl N-*t*-butyloxycarbonyl-L-glutamate *p*-nitrophenyl ester (**I**) (1.70 g; 3.7 mmoles), and dicyclohexyl-carbodiimide (0.67 g; 3.7 mmoles) in dimethylformamide (18 ml) was stirred for 3 hrs and then let to stand for a day. The solvent was removed under reduced pressure, and the remaining oil taken up in anhydrous ether (30 ml). The dicyclohexylammonium salt of the dipeptide derivative soon crystallized. After standing for 24 hrs, the crystals were filtered off and washed thoroughly with several portions of anhydrous ether (50 ml) to obtain 2.43 g (89%) of **III**, m.p. 116—119 °C. Recrystallization of the product from aqueous alcohol did not raise the m.p. significantly (117—119 °C); $[\alpha]_D^{20}$ −19.6° (*c* = 3, methanol).

$C_{41}H_{59}N_3O_4$ (737.9). Calcd. C 66.73; H 8.06; N 5.70. Found C 66.65; H 8.10, N 6.07%.

α,α'-Dibenzyl N-*t*-butyloxycarbonyl-γ-L-glutamyl-L-glutamate

The above dicyclohexylammonium salt (**III**) (1.1 g; 1.5 mmoles) was suspended in ethyl acetate (25 ml) and water (15 ml). Citric acid was added (to adjust to pH 3), and the mixture was shaken until the salt dissolved. After the separation of the phases, the aqueous layer was extracted with two 15-ml portions of ethyl acetate, and the combined ethyl acetate solutions were dried and evaporated under reduced pressure. A yellow oil (0.85 g; 100%) was obtained which failed to crystallize.

α-Benzyl N-(*p*-methoxybenzyloxycarbonyl)-L-glutamate *p*-nitrophenyl ester (V)

p-Nitrophenol (1.53 g; 11 mmoles) and dicyclohexyl-carbodiimide (2.26 g; 11 mmoles) were added to a cold solution of α-benzyl N-(*p*-methoxybenzyloxycarbonyl)-L-glutamate (**IV**) (4.01 g; 10 mmoles) [10] in ethyl acetate (9 ml). The resulting solution was stirred for 1 hr. at 0 °C and for 2 hrs at room temperature. Next day the dicyclohexylurea (2.04 g; 92%) was filtered off and washed with a small amount of ethyl acetate. The ethyl acetate solution was diluted with the same solvent to about 40 ml, washed with 8% $NaHCO_3$ solution (3 × 10 ml) and water (2 × 10 ml), dried over $MgSO_4$, and finally evaporated *in vacuo*. The remaining oil was rubbed with ether (40 ml) until it transformed into a powder. It was then crystallized

from ethyl alcohol (16 ml) to yield 3.7 g (71%) of the *p*-nitrophenyl ester of α-benzyl N-(*p*-methoxybenzyloxycarbonyl)-L-glutamate. The m.p. of this product (77—79 °C) raised, after two recrystallizations from alcohol, to 83—84 °C; $[\alpha]_D^{20}$ —16.0° (*c* = 5, ethyl acetate).

$C_{27}H_{26}N_2O_9$ (522.5). Calcd. C 62.10; H 5.00; N 5.40. Found C 61.75; H 5.25; N 5.50%.

α,α'-Dibenzyl N-(*p*-methoxybenzyloxycarbonyl)-γ-L-glutamyl-L-glutamate (VI)

Triethylamine (2.74 ml; 19.5 mmoles) and α-benzyl N-(*p*-methoxybenzyloxycarbonyl)-L-glutamate *p*-nitrophenyl ester (V) (10.20 g; 19.5 mmoles) were added to a suspension of α-benzyl L-glutamate (II) (4.62 g; 19.5 mmoles) [6] in dimethylformamide (32 ml), and the reaction mixture was stirred at room temperature for 2 hrs. During this time most of the semi-ester went into solution. Next day the solution was filtered from the undissolved crystals and evaporated at about 1 torr (bath temperature 40 °C). The oily residue was taken up in ethyl acetate (180 ml), and the solution was washed with two 50-ml portions of ice-cold 0.5*N* H_2SO_4. After drying ($MgSO_4$), the solvent was evaporated under reduced pressure, and the remaining crystalline substance was suspended in ether (140 ml), filtered, and washed thoroughly with several portions of warm ether. The resulting crude product (9 g; m.p. 135—140 °C) was recrystallized from ethyl acetate (150 ml) to yield 8.44 g (70%) of the pure α, α'-dibenzyl N-(*p*-methoxybenzyloxycarbonyl)-γ-L-glutamyl-L-glutamate, m.p. 143—146 °C; $[\alpha]_D^{25}$ —5.1° (*c* = 2.5, acetic acid). The physical constants of the same substance described formerly [10] are: m.p. 133—135 °C; $[\alpha]_D^{23}$ —5.15° (*c* = 2.5, acetic acid).

$C_{33}H_{36}N_2O_{10}$ (620.6). Calcd. N 4.52. Found N 4.65%.

α,α'-Dibenzyl N-(*p*-methoxybenzyloxycarbonyl)-γ-L-glutamyl-L-glutamate *p*-nitrophenyl ester (VII)

The protected dipeptide dibenzyl ester described above (VI) (6.61 g; 10.6 mmoles) was dissolved in a mixture of tetrahydrofuran (12 ml) and dimethylformamide (4 ml), and to this solution *p*-nitrophenol (1.63 g; 11.7 mmoles) and dicyclohexyl-carbodiimide (2.41 g; 11.7 mmoles) were added under stirring and cooling. Stirring was continued for 1 hr. at 0 °C and for 2 hrs at room temperature. The reaction mixture was allowed to stand for a day. The precipitated dicyclohexylurea was then filtered off and washed thoroughly with tetrahydrofuran (8—10 ml). The solvent was distilled off under reduced pressure, and the remaining oil was dissolved in ethyl acetate (80 ml). The ethyl acetate solution was washed with 3% K_2CO_3 solution (2×25 ml) and water (25 ml), dried over anhydrous $MgSO_4$, and then evaporated *in vacuo*. The oily residue was rubbed under frequently changed portions of ether until it solidified. This solid substance was finally boiled out with three 40-ml portions of ether; it weighed 6.33 g (80%) and melted at 103—106 °C. Recrystallization of the crude product first from aqueous methanol (50%) and then from aqueous ethanol (50%) raised the m.p. only slightly, and yielded 4.84 g (61%) of the pure substance; m.p. 104—106.5 °C; $[\alpha]_D^{20}$ —16.3° (*c* = 2, dimethylformamide).

$C_{39}H_{39}N_3O_{12}$ (741.8). Calcd. C 63.15; H 5.30; N 5.65. Found C 63.50; H 5.50; N 5.50%.

α,α'-Dibenzyl γ-L-glutamyl-L-glutamate *p*-nitrophenyl ester hydrochloride (VIII)

The protected dipeptide nitrophenyl ester VII (1.81 g; 2.44 mmoles) was dissolved in ice-cold trifluoroacetic acid (3.3 ml) to which anisole (0.6 ml) was added. The solution was kept for 90 min at 0 °C, and then trifluoroacetic acid was distilled off under reduced pressure (at a temperature of max. 30 °C). The residue was taken up in tetrahydrofuran (7 ml), and the solution saturated with dry hydrogen chloride under cooling. The active ester hydrochloride was precipitated by anhydrous ether (about 100 ml), filtered, washed several times with ether, and finally dried. This product weighed 1.31 g (87%) and melted at 90—92 °C with sintering from 82 °C. Recrystallization from a small amount of acetone–ether gave 0.9 g (60%) of the analytically pure α,α'-dibenzyl γ-L-glutamyl-L-glutamate *p*-nitrophenyl ester hydrochloride, m.p. 93—96 °C $[\alpha]_D^{25}$ —11.7° (*c* = 3, dimethylformamide), R_F(b) 0.39.

$C_{30}H_{32}N_3O_9Cl$ (614.0), Calcd. C 58.70; H 5.30; Cl 5.77. Found C 58.85; H 5.85; Cl 5.67%.

α-*t*-Butyl N-carbobenzoxy-L-glutamate

A suspension of the dicyclohexylammonium salt of α-*t*-butyl N-carbobenzoxy-L-glutamate (42 g; 81 mmoles) [12,14] in ether (160 ml) was cooled in ice and shaken, under continuous cooling, with the same volume of ice-cold 1*N* H_2SO_4 until all the solid dissolved. After the separation of the phases, the aqueous layer was extracted with two 80-ml portions of ether, the combined ether solutions were washed with water (80 ml), dried over $MgSO_4$ and evaporated under reduced pressure. The remaining oil (25.5 g; 94%) crystallized in a few days, m.p. 82—83.5 °C. No rise in the m.p. was observed after recrystallization of the solid substance from a mixture of ether and petroleum ether; $[\alpha]_D^{25}$ −27.3° (*c* = 3, methanol).

$C_{17}H_{23}NO_6$ (337.4). Calcd. C 60.52; H 6.87. Found C 60.81; H 7.07%.

The D-*antipode* of this substance melted at 82—83.5 °C; $[\alpha]_D^{25}$ +27.2° (*c* = 3, methanol).

α-*t*-Butyl N-carbobenzoxy-L-glutamate pentachlorophenyl ester (IX)

A solution of α-*t*-butyl N-carbobenzoxy-L-glutamate (3.37 g; 10 mmoles), pentachlorophenol (2.67 g; 10 mmoles), and dicyclohexyl-carbodiimide (2.06 g; 10 mmoles) in ethyl acetate (15 ml) was stirred for 2 hrs and then let to stand for a day at room temperature. The precipitated solid (containing, besides dicyclohexylurea, also the bulk of the active ester) was filtered off by suction and washed thoroughly with several portions of chloroform (about 40 ml). The insoluble dicyclohexylurea weighed 2.0 g (90%). The combined ethyl acetate and chloroform solutions were washed with 8% $NaHCO_3$ solution (2 × 10 ml) and water (10 ml), dried over $MgSO_4$, and evaporated under reduced pressure to obtain 5.67 (97%) of the crystalline pentachlorophenyl ester, m.p. 121—123 °C. Recrystallization from ethyl acetate (7 ml) gave an analytically pure product (4.75 g; 81%), m.p. 123—125 °C (lit. [15] m.p. 122—123 °C); $[\alpha]_D^{25}$ −18.2° (*c* = 3, dimethylformamide).

The D-*antipode* of the above active ester was prepared by the same method; m.p. 122—124 °C; $[\alpha]_D^{25}$ +18.3° (*c* = 3, dimethylformamide).

α-*t*-Butyl L-glutamate (X)

Palladium (10%) on charcoal catalyst (0.5 g) was suspended in a solution of α-*t*-butyl N-carbobenzoxy-L-glutamate (12 g; 35.6 mmoles) in methanol (200 ml), and the suspension was shaken in a stream of hydrogen until no more carbon dioxide could be detected in the leaving gas (3—4 hrs). After the removal of the catalyst by filtration, the solution was evaporated to dryness under reduced pressure. The remaining gel-like substance was dried thoroughly for several days in a vacuum desiccator over cc. H_2SO_4. The solid α-*t*-butyl glutamate could not be crystallized. The yield was 7 g (96%), m.p. 147—148 °C; $[\alpha]_D^{20}$ +13.0° (*c* = 1, water); R_F(a) 0.28.

$C_9H_{17}NO_4$ (203.2). Calcd. C 53.18; H 8.43; N 6.89. Found C 53.12; H 9.10; N 7.31%.

α-*t*-Butyl D-glutamate was prepared in the same way; m.p. 146—147 °C; $[\alpha]_D^{20}$ −12.3° (*c* = 2.2, water); R_F(a) 0.28.

α,α'-Di-*t*-butyl N-carbobenzoxy-γ-L-glutamyl-L-glutamate (XI)

A suspension of α-*t*-butyl L-glutamate (**X**) (3.75 g; 18.5 mmoles) in tetrahydrofuran (60 ml) was mixed with triethylamine (2.60 ml; 18.5 mmoles) and α-*t*-butyl N-carbobenzoxy-L-glutamate pentachlorophenyl ester (**IX**) (9.85 g; 16.8 mmoles), and the reaction mixture was stirred at room temperature until the semi-ester dissolved almost completely (about 4 hrs). The solution was allowed to stand overnight, filtered from the unchanged semi-ester, and evaporated under reduced pressure. The remaining oil was dissolved in ethyl acetate (80 ml) and washed twice with ice-cold 1*N* H_2SO_4 (30 ml) and cold water (2 × 50 ml). The ethyl acetate solution was dried over Na_2SO_4, evaporated under reduced pressure, and the oily residue was triturated with two portions of warm petroleum ether until it became a powder. This was filtered off (5.5 g; 63%) and crystallized from a mixture of ether and petroleum ether. The substance obtained (4.1 g; 47%) had m.p. 69—71 °C. Two recrystallizations from ethyl acetate–petroleum ether raised the m.p. to 72—74 °C; $[\alpha]_D^{25}$ −25.2° (*c* = 3, dimethylformamide).

$C_{26}H_{38}N_2O_9$ (522.6). Calcd. C 59.73; H 7.33; N 5.36. Found C 59.82; H 7.72; N 5.30%.

The D–D *stereoisomer* was prepared in the same way; m.p. 71—73 °C; $[\alpha]_D^{25}$ +25.0° (*c* = 3, dimethylformamide).

α,α'-Di-*t*-butyl N-carbobenzoxy-γ-L-glutamyl-L-glutamate pentachlorophenyl ester (XII)

α,α'-Di-*t*-butyl N-carbobenzoxy-α-L-glutamyl-L-glutamate **(XI)** (3.6 g; 6.9 mmoles) was dissolved in ethyl acetate (30 ml), and, after the addition of pentachlorophenol (2.0 g; 7.6 mmoles) and dicyclohexyl-carbodiimide (1.56 g; 7.8 mmoles) at 0 °C, the reaction mixture was stirred for 30 min under cooling, and then for 2 hrs at room temperature. It was allowed to stand overnight. Acetic acid (1 ml) was then added, and the solution was stirred for 1 hr. The precipitated dicyclohexylurea (1.6 g; 94%) was filtered off. The filtrate was diluted with ethyl acetate (40 ml) and washed with water (30 ml), 8% $NaHCO_3$ solution (3 × 30 ml), and again with water (30 ml). The solution was dried (Na_2SO_4) and evaporated under reduced pressure. The oily residue solidified on standing. It was crystallized from a mixture of ether and petroleum ether. The resulting crystalline product (4.20 g; 79%) melted at 62—64 °C. Recrystallization from the same solvent raised the m.p. to 63—65 °C; $[\alpha]_D^{20}$ −19.5° (*c* = 3, dimethylformamide).

$C_{37}H_{37}N_2O_9Cl_5$(770.9). Calcd. C 49.85; H 4.84; Cl 23.00. Found C 50.05; H 5.03; Cl 22.94%.

The D–D *antipode* of this compound was prepared in the same manner, m.p. 64—65 °C; $[\alpha]_D^{25}$ +19.7° (*c* = 3, dimethylformamide).

α,α'-Di-*t*-butyl γ-L-glutamyl-L-glutamate pentachlorophenyl ester hydrochloride (XIII)

The protected dipeptide derivative **XII** (3.85 g; 5 mmoles) was hydrogenated in methanol (65 ml) containing hydrogen chloride (0.22 g; 6 mmoles), in the presence of palladium(10%)-on-charcoal catalyst (0.5 g). The hydrogenation was carried out by passing hydrogen gas through the solution until no more carbon dioxide could be detected in the leaving gas. The catalyst was then filtered off, and the solution evaporated under reduced pressure. The residue was triturated with several portions of ether (100 ml). The resulting solid (2.5 g; 74%) was crystallized from a mixture of methanol, ethyl acetate, and ether to give 2.3 g (68%) of the pure substance, m.p. 150—152 °C; $[\alpha]_D^{25}$ −14.9° (*c* = 3, dimethylformamide); R_F(b) 0.69.

$C_{24}H_{22}N_2O_7Cl_6$ (673.3). Calcd. C 42.78; H 4.75; N 4.16; Cl(total) 31.59; Cl (ionic) 5.27. Found C 43.10; H 5.20; N 4.33; Cl (total) 31.65; Cl (ionic) 5.19%.

The corresponding D–D *stereoisomer* was prepared similarly; m.p. 149—151 °C; $[\alpha]_D^{25}$ +15.2° (*c* = 3, dimethylformamide); R_F(b) 0.67.

Poly-α-benzyl-L-glutamate (XV)

(No. 1 in Table I)

α,α'-Dibenzyl γ-L-glutamyl-L-glutamate *p*-nitrophenyl ester hydrochloride **(VIII)** (2.4 g; 3.9 mmoles) was dissolved in dimethylformamide (3.9 ml) under mild warming. Triethylamine (1.2 ml; 8.6 mmoles) was added, and the reaction mixture was stirred at room temperature. Triethylammonium chloride separated soon, and the solution became more and more viscous. In about 8 hrs the reaction mixture turned into an unstirrable gel; it was then set aside for a day. The viscous solution was diluted with hot methanol (50 ml), and the separated gummy substance was rubbed to give a powder. It was filtered off, washed thoroughly with several portions of hot methanol (150 ml), and finally dried in a vacuum desiccator over cc. H_2SO_4. The poly-α-benzyl-glutamate (0.87 g; 51%) was obtained in the form of an amorphous powder.

$(C_{12}H_{13}NO_3)_n$ $(219.2)_n$. Calcd. C 65.75; H 5.98; N 6.38. Found C 65.00; H 6.65; N 6.13%.

Poly-γ-L-glutamic acid

(from the polybenzyl ester; No. 1 in Table II)

Poly-α-benzyl-L-glutamate (820 mg; 3.74 meq.) was dissolved, under mild warming, in hexamethylphosphoric triamide (10 ml) and the resulting solution was diluted with dimethylformamide (25 ml). This solution was added to a prehydrogenated suspension of palladium(10%)-on-charcoal catalyst (0.4 g) in dimethylformamide (25 ml), and the mixture was hydrogenated in a closed system until no more hydrogen was absorbed (4—5 hrs; uptake of hydrogen about 60 ml). After removing the catalyst by filtration, the solution was evaporated under reduced pressure (0.5 torr; bath temperature max. 45 °C). The residue was dissolved in water (30 ml), and hydrogenation was continued in the presence of fresh prehydrogenated catalyst (0.2 g). Some more hydrogen (6—8 ml) was absorbed. The catalyst was removed by filtration, and the solution evaporated *in vacuo*. The residue was triturated with several portions of anhydrous

ether, and the resulting hygroscopic powder was dissolved in water (2 ml). The polyacid was precipitated by the addition of ethanol (100 ml) and filtered off. This procedure was repeated two times more, and the product was finally dried in a vacuum desiccator over P_2O_5. The poly-γ-glutamic acid was obtained as a slightly hygroscopic, amorphous powder which weighed 250 mg (52%); $[\alpha]_D^{23}$ −21.0° (c = 2, 0.5N HCl).

Poly-α-*t*-butyl-L-glutamate (XVII)

(*a*) Triethylamine (5.78 ml; 41.5 mmoles) was added to a solution of α,α'-di-*t*-butyl γ-L-glutamyl-L-glutamate pentachlorophenyl ester hydrochloride **(XIII)** (14.0 g; 20.75 mmoles) in dimethylformamide (38 ml), and the reaction mixture was stirred at room temperature. Triethylammonium hydrochloride precipitated soon, and the reaction mixture became too viscous to be stirred. More dimethylformamide (10 ml) was then added, and stirring was continued for 8 hrs. After standing for a day at room temperature, about one half of the dimethylformamide was distilled off under reduced pressure (1 torr, at 45 °C), and the residual gel-like solution was diluted with ether (200 ml). The precipitated solid was filtered off and washed thoroughly with ether (6 × 30 ml) and water (5 × 30 ml). It was finally dried in a vacuum desiccator over P_2O_5. The polyester (4.41 g; 57%; No. 3 in Table I) was obtained as an amorphous white powder; $[\alpha]_D^{25}$ −43.7° (c = 1.2, dimethylformamide).

$(C_9H_{15}NO_3)_n$ $(185.2)_n$. Calcd. C 58.32; H 8.17; N 7.57. Found C 58.49; H 8.24; N 7.42; Cl 0.92%.

(*b*) The dipeptide active ester salt **(XIII)** (2.20 g; 3.20 mmoles) was dissolved in dimethyl sulfoxide (3.2 ml) under mild warming, and to this lukewarm solution triethylamine (1.0 ml; 7.1 mmoles) was added. Triethylammonium chloride precipitated immediately, and the fairly viscous reaction mixture was stirred at room temperature for 8 hrs. After standing for a day, ether (100 ml) was added to the reaction mixture. The precipitated material was rubbed to obtain a powder which was separated by centrifugation. The solid substance was washed with ether (3 × 30 ml), water (3 × 30 ml) and again with ether (3 × 30 ml) in the centrifuge, and finally dried in a vacuum desiccator over cc. H_2SO_4. The amorphous white polyester (No. 2 in Table I) weighed 0.67 g (55%); $[\alpha]_D^{20}$ −43.4° (c = 1.2, dimethylformamide).

Poly-α-*t*-butyl-D-glutamate (XVII)

The D–D stereoisomer of the dipeptide active ester salt **(XIII)** (1.80 g; 2.67 mmoles) was polymerized in dimethylformamide (4.2 ml) in the presence of triethylamine (0.82 ml; 5.9 mmoles) by the same procedure as described above for the L–L antipode (method *a*). The yield of the resulting D-polyester (No. 4 in Table I) was about the same (0.59 g; 60%); $[\alpha]_D^{22}$ +46.5° (c = 1.2, dimethylformamide).

$(C_9H_{15}NO_3)_n$ $(185.2)_n$. Calcd. C 58.32; H 8.17. Found C 58.64; H 8.43; Cl 2.14%.

Poly-γ-L-glutamic acid

(from the poly-*t*-butyl ester; No. 3 in Table II)

Poly-α-*t*-butyl-L-glutamate (2.00 g; 10.8 meq.) was dissolved in ice-cold trifluoroacetic acid (97%; 40 ml) and kept for 5 min. at 0 °C. The solution was then allowed to warm up to room temperature, and after 100 min evaporated under reduced pressure. A second portion of trifluoroacetic acid (100 ml) was added to the residue, and, after standing at room temperature for 10 min, the solution was evaporated and then diluted with anhydrous ether (160 ml) and kept in a refrigerator for several hours. The precipitated polyacid was filtered off and washed with ether (3 × 50 ml). It was then dissolved in water (20 ml) and freeze-dried. The polyacid dried over P_2O_5 in a vacuum desiccator weighed 1.30 g (95%); $[\alpha]_D^{23}$ −36.9 (c = 2, 0.5N HCl).

$(C_5H_7NO_3 \cdot 1/2H_2O)_n$ $(138.1)_n$. Calcd. C 43.47; H 5.83; N 10.15. Found C 43.80; H 5.90; N 10.31%.

Poly-γ-D-glutamic acid

(No. 4 in Table II)

Poly-α-*t*-butyl-D-glutamate (300 mg; 1.6 meq.) was treated with trifluoroacetic acid (6.6 ml) for 30 min at 0 °C, then for 90 min at room temperature, and finally for 24 hrs at 0 °C again. The product was isolated in the same manner as described above. The yield of the D-polyacid was 205 mg (98%); $[\alpha]_D^{23}$ +36.0° (c = 2, 0.5N HCl).

Determination of the optical purity

The optical purity of the poly-γ-L-glutamic acid prepared from the corresponding poly-*t*-butyl ester (No. 3 in Table II) was determined by the procedure described in our previous paper [1]. — The concentration of the polyacid solution before hydrolysis was 1.285 mg/ml. The glutamic acid content of the hydrolyzate, determined by the KJELDAHL method, was 1.36 ± ± 0.05 mg/ml. Accordingly, the value of 93 ± 3% was obtained for the polyglutamic acid content of the sample. The observed rotation of the hydrolyzate measured at 286 nm in a 10.0 mm polarimeter tube at 30 °C was +0.0742° ± 0.001°, corresponding to $[\alpha]^{30}_{286}$ + 545° ± 15°. The optical purity of poly-γ-glutamic acid was calculated to be 99 ± 3%, by comparing the specific rotation of the hydrolyzate with that of a standard glutamic acid solution described in our previous paper [1].

*

We wish to thank Mrs. H. MEDZIHRADSZKY-SCHWEIGER, Mrs. J. KAJTÁR, Mrs. S. KUTASSY, Mrs. M. DERCSÉNYI and Mrs. A. LOVÁSZ for the microanalyses, and Dr. F. RUFF for obtaining the spectra. Technical assistance by Mrs. G. NÉMETH is greatly appreciated.

REFERENCES

1. KAJTÁR, M., BRUCKNER, V.: Acta Chim. Acad. Sci. Hung. **62,** 191 (1969)
2. BRUCKNER, V., KAJTÁR, M., KOVÁCS, J., NAGY, H., WEIN, J.: Tetrahedron **2,** 211 (1958)
3. BATTERSBY, A. R., ROBINSON, J. C.: J. Chem. Soc. **1955,** 259; BRUCKNER, V., KÓTAI, A., KOVÁCS, K.: Acta Chim. Acad. Sci. Hung. **21,** 427 (1959)
4. MCKAY, F. C., ALBERTSON, N. F.: J. Am. Chem. Soc. **79,** 4686 (1957)
5. ANDERSON, G. W., MCGREGOR, A. C.: J. Am. Chem. Soc. **79,** 6180 (1957)
6. SACHS, H., BRAND, E.: J. Am. Chem. Soc. **75,** 4610 (1953)
7. SCHRÖDER, E., KLIEGER, E.: Ann. **673,** 196 (1964)
8. ELLIOTT, D. F., RUSSEL, D. W.: Biochem. J. **66,** 49P (1957); BODÁNSZKY, M., DU VIGNEAUD, V.: J. Am. Chem. Soc. **81,** 5688 (1959)
9. KAPOOR, A., DAVIS, E. J.: Experientia **23,** 253 (1967)
10. WEYGAND, F., HUNGER, K.: Ber. **95,** 1, 7 (1963)
11. BRUCKNER, V., KOVÁCS, J., NAGY, H., KAJTÁR, M.: Acta Chim. Acad. Sci. Hung. **6,** 219 (1955)
12. TASCHNER, E., WASIELEWSKI, C., SOKOLOWSKA, T., BIERNAT, J. F.: Ann. **646,** 119, 127 (1961)
13. ROESKE, R. W.: Chem. and Ind. **1959,** 1121; ANDERSON, G. W., CALLAHAN, F. M.: J. Am. Chem. Soc. **82,** 3359 (1960)
14. KLIEGER, E., GIBIAN, H.: Ann. **655,** 195 (1962)
15. KOVÁCS, J., KAPOOR, A.: J. Am. Chem. Soc. **87,** 118 (1965); KOVÁCS, J., GIANOTTI, R., KAPOOR, A.: J. Am. Chem. Soc. **88,** 2282 (1966)
16. KAINZ, G., HUBER, H., KASLER, F.: Microchim. Acta (Wien) **1957,** 744
17. HANBY, W. E., WALEY, S. G., WATSON, J.: J. Chem. Soc. **1950,** 3239
18. SCHWYZER, R., RITTEL, W., KAPPELER, H., ISELIN, R.: Angew. Chem. **72,** 915 (1960)
19. KAJTÁR, J., KAJTÁR, M.: Acta Chim. Acad. Sci. Hung. **55,** 33 (1968)
20. SCHWYZER, R., KAPPELER, H.: Helv. Chim. Acta **44,** 1991 (1961); SCHWYZER, R., DIETRICH, H.: Helv. Chim. Acta **44,** 2003 (1961)
21. ROWLANDS, D. A., YOUNG, G. T.: Biochem. J. **65,** 516 (1957); SACHS, H., BRAND, E.: J. Am. Chem. Soc. **75,** 4608 (1953)
22. KAJTÁR, M., BRUCKNER, V.: Tetrahedron Letters, 4813 (1966)

Miklós HOLLÓSI
Márton KAJTÁR
Viktor BRUCKNER
Budapest VIII, Múzeum krt. 4/b

Addition Polymers: Formation and Characterization. Ed. Derek A. Smith. Butterworth, London, 1968, pp. 492

Derek A. Smith's book is based on his course of lectures, offered for many years at the National College of Rubber Technology (Northern Polytechnic, London). The structure of the book differs, therefore, in many respects from that of books treating similar subjects and emphasizes the pedagogical aspects of the mutual connection between polymer chemistry, polymer technology and polymer physics, clearly showing the unity of science and technology. Based on the fundamentals of organic and physical chemistry, the first three chapters of the book survey the kinetic laws and characteristic mechanisms of polymerization processes with radical and ionic mechanisms. The fourth chapter deals with the principles of the industrial-technological design of polymerization processes, thus completing the discussion of the preparation of polymers. The next chapters of the book are concerned with methods for the determination of the molecular weight, fractionation of polymers, and with methods for the study of microstructure and crystallinity. The last two chapters deal with problems of polymer degradation, important from the viewpoint of practical application, and with factors and laws determining the physical properties of solid polymers.

As indicated by this short survey of its chapters, the book gives an exhaustive description of polymeric plastics, including recent scientific results. A great merit of the book is the concise and lucid manner of discussion. An extensive list of references is given at the end of each chapter for those interested in original papers treating individual problems. The reviewer finds it regrettable that other reactions leading to the formation of polymers, *i.e.* polycondensation, polymerization of cyclic monomers and reactions involving polyaddition are not included in this book. Our knowledge about these reactions would also be furthered by a book treating its subject with similar clarity. Among all plastics produced world-wide, polymerization plastics are characterized by the most dynamic growth index, so that the subject orientation of the book to this field is understandable.

Although the book is intended primarily for advanced university students, it will render valuable services to those engaged in research or industrial technology and wishing to deepen their knowledge in this field.

GY. HARDY

Progress in Drug Research, Vol. 12. Ed. E. Jucker. Birkhäuser Verlag, Basel and Stuttgart, 1968, pp. 479

The latest volume of this internationally well-known series, indispensable today in the library of every medicinal chemist and pharmacologist, gives summaries, as was the custom in earlier volumes, on some of the up-to-date problems of medicinal chemistry in monographic form, written by known specialists of the field. According to the character of this field of science, the pharmacological approach has been stressed in some chapters and the chemical one in others, generally to such depth that the pharmacological knowledge of the chemist doing medicinal syntheses and the chemical background of the pharmacologist are enough to understand the subject and to use it in their practical work.

The first chapter (by C. J. CAVALLITO) deals with the contribution of medicinal chemistry to medicine from 1935 on. The next chapter is concerned with the increasingly urgent problem of pharmacological control of reproduction in women (reviewed by M. J. K. HARPER). After a discussion of the necessity for population limitation, the reproductive stages amenable to pharmacological control are enumerated and discussed.

The third chapter of the book (by M. TAUSK) is devoted to the practical results of twenty years of research in endocrinology. As the author says: "The boundaries of endocrinology . . . are fading. Most of the now known hormones were discovered in the course of this century, and they became the rewarding objects of investigations for those scientists who know what regulates their secretion, how they are transported, and by what mechanism they act and are inactivated. But hormones also became drugs and thus were subjected to the rules of operation of the pharmaceutical industry and of those who study the effects and uses of drugs irrespective of their endocrine ancestry". In this chapter the results obtained by the use of cortisone and related drugs, anabolic steroids, oestrogens, progesterone, compounds having progestational effects, gonadotropins and the recently synthesized ACTH are considered. In the subsequent part of the chapter even the problem of diabetes and pancreas and the use of thyroid are touched.

In contrast with the above method of treatment, the author of the next chapter, W. MOLL, dealing with the therapy of rheumatism, has emphasized the medicinal attitude. After a discussion of the general basic principles of rheumatology, he is concerned with the therapy of rheumatism, including psychosomatic, physical, disinfectant and immunosuppressing therapy. Following this, he comes to the anti-inflammatory, antipyretic and analgetic drugs, partly known for ages (*e.g.*, salicylates), partly synthesized recently (*e.g.*, corticosteroids). The last part of the review is of interest in the first place to physicians intending to cure rheumatism. On the whole, this is the character of the whole review.

"The great progress made in the last decade in the electrophysiology of the heart as well as in the pathophysiology and pharmacotherapy of the heart rhythm disturbances necessitates from time to time a critical evaluation of the drugs effective in cardiac arrhythmias. Although the numerous monographs dealing with cardiac arrhythmias usually contain valuable data on antiarrhythmic compounds, so far relatively few attempts have been made to give a systematic survey of the available antiarrhythmic compounds." This is why the next chapter on antiarrhythmic compounds has its great importance. One of the Hungarian co-workers, professor L. SZEKERES is well known for his contribution to the development of our national pharmacological traditions of a great past. In this small monograph, after a classification of the antiarrhythmic agents, the authors discuss their most significant structure–activity relationships, which are followed by a detailed analysis of antiarrhythmic compounds from the pharmacological aspect, dealing among others with antimalarials, local anesthetics, antihistaminics, minor and major tranquillizers, antiepileptics, antidepressive agents, spasmolytic and coronary vasodilator drugs, and drugs stimulating and depressing the adrenergic system, digitalis, etc. A very useful part of this chapter is devoted to the clinical application of antiarrhythmic compounds.

In the last two chapters of the book some special problems of chemotherapy and up-to-date results in the field of sulfonamide research are considered. The subject discussed by L. G. GARROD is the chemotherapy of enterobacterial infections. He first describes the types of infections, then older drugs (sulphonamides, benzylpenicillin, streptomycin, neomycin, chloramphenicol, tetracyclines, poly myxins), and the newer ones (ampicillin, hetacillin, carbenicillin, cephaloridine and cephalothin, gentamicin, trimethoprim). He touches upon the problem of drug resistance, and finishes his review discussing the treatment of infections in different bodily sites.

The thorough and interesting review by Th. STRULLER in the last chapter is devoted to the mechanism of action and half-life of sulfonamides and their classification on the basis of their half-lifes. A very instructive part of the compilation gives a chronological review of the more important sulfonamides. More than half of this chapter is concerned with some unsolved problems in sulfonamide research.

Owing to the great importance of these compounds, the review is very valuable and makes interesting reading even for those who are concerned in their practical work with another field of medicinal chemistry.

The usefulness of the book edited at the customary high level is further increased by the bibliographies at the end of the chapters.

GY. DEÁK

INDEX

Printed in Hungary

A kiadásért felel az Akadémiai Kiadó igazgatója — Műszaki szerkesztő: Farkas Sándor

A kézirat nyomdába érkezett: 1969. VII. 29. — Terjedelem: 9,25 (A/5) ív, 39 ábra

69.68057 Akadémiai Nyomda, Budapest — Felelős vezető: Bernát György

The AALC collection, including approx. 5500 punched cards gives the individual the advantages of modern data processing, without the need for expensive machines.

The advantages of cards!

The AALC collection of cards offers many advantages to its user. First, because only a card-file can be kept complete and up-to-date at any time. Book-form bibliographies are difficult to handle and are not apt for cross-indexing. Secondly with a card-file you do not have to make personal notes. If you wish to retain items of information from a book-bound bibliography, you cannot avoid noting them down (if you don't want to tear out the relevant pages!); with the AALC-file, however, you can indulge in the luxury of picking out the cards you are looking for.

The advantages of p u n c h e d cards!

By having the AALC collection on *punched* cards, you never have to replace cards in any particular order. Through the selection operation the cards you are looking for fall unerringly from the whole pack, irrespective of the place they occupy in the card-file. Using simple methods, you can collect all the cards that are particularly important for the topical field you are engaged in at a given time. A punched card file allows any questions to be combined according to the nature of your problem: it allows cross-indexing as well.

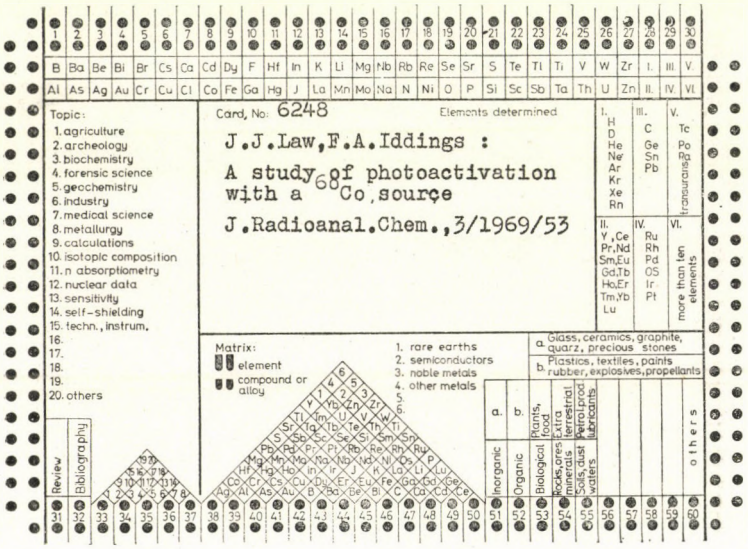

AALC—File
ACTIVATION
ANALYSIS
LITERATURE
CARDS
1935—1968

Unslotted:
US$ 0.05/card

Slotted:
US$ 0.06/card

IN PREPARATION

Ask for leaflets at the following address

AKADÉMIAI KIADÓ

Publicity Department, Budapest 502. P.O.B. 24

ACTIVATION ANALYSIS DOCUMENTATION CENTER

AKADÉMIAI KIADÓ

PUBLISHING HOUSE OF THE HUNGARIAN ACADEMY OF SCIENCES

ACTA CHIMICA

ТОМ 62 — ВЫП. 3

РЕЗЮМЕ

Термолиз цианокомплексов, II.

Термическое разложение некоторых цианометаллатных кислот

Б. МОХАИ

Изучалось термическое разложение следующих цианометаллатных кислот: $H_4[Fe(CN)_6]$, $H_3[Fe(CN)_6]$, $H_2[Fe(CN)_5NO]$ и $H_3[CO(CN)_6]$. Отдельным ступеням разложения приписывались хорошо определенные реакции. Помимо температур разложения и уменьшений в весе, определялись изменения энтальпии, сопровождающие процесс разложения. На основе полученных значений ΔH можно было непосредственно сравнивать термическую стабильность соединений. Температура разложения, термичность и теплота реакции находятся в тесной зависимости с электронным строением центрального атома.

Термолиз цианокомплексов, III

Термическое разложение цианометаллатов аммония

Б. МОХАИ

О реакциях термического разложения гексацианo-феррата (II), гексацианo-феррата (III), пентацианo-кобальта (III) аммония судили по изменению в весах и по составу газовых продуктов разложения. Помимо температур разложения определялись также и теплоты разложения, которые сравнивались с величинами, полученными для соответствующих кислот. Энергия, необходимая для отщепления NH_4CN, превышает почти в четыре раза энергию отщепления HCN. Протекание соответствующих реакций по одно- или много-ступенчатому механизму, а также термичность и порядок отдельных ступеней объяснялись в согласии со структурно-химическими свойствами.

Применение комплексообразователей в ионообменной хроматографии, IV

Хроматографическое разделение ароматических кислот на ионообменной колонке с помощью ионов никеля(II), образующих комплексы

Й. ИНЦЕДИ и Л. ГЛОС

Был разработан метод хроматографического разделения ароматических кислот. В качестве элюента использовался 50%-ый спиртовый раствор хлористого лития и хлористого никеля(II). Объемы элюента, полученные экспериментально, сравнивались с данными, полученными на основе расчетов равновесий. Определение разделенных ароматических кислот производилось непосредственно спектрофотометрическим методом.

Исследования в области твердофазной радиационной полимеризации, XXV

Влияние добавок на твердофазную полимеризацию цетилвинилового эфира

ДЬ. ХАРДИ, К. НИТРАИ и Ф. ЧЕР

Изучалась кинетика твердофазной полимеризации двухкомпонентных систем: цетилвиниловый эфир и бензохинон, а также цетилвиниловый эфир и диметилоксалат. Было установлено, что вышеупомянутые добавки для составов, меньших эвтектических, замедляют полимеризацию в небольшой мере, а для составов, больших эвтектических, степень их влияния не изменяется. Таким образом, их влияние обусловливается лишь физическими факторами. Твердофазная полимеризация цетилвинилового эфира протекает по катионному механизму, что хорошо подтверждается, помимо вышесказанным, и возможностью проведения твердофазной полимеризации под действием йодных паров.

Определение истинного состава смеси уксусная кислота-четыреххлористый углерод из диэлектрических свойств смеси, на основе модели тернарной смеси $A—A_2—B$

Й. ЛИСИ

На основе модели тернарной смеси $A—A_2—B$ и путем исследования диэлектрических свойств определялись истинные составы номинально бинарной смеси уксусная кислота-четыреххлористый углерод. Измерялись плотность и диэлектрическая постоянная смеси в зависимости от номинального состава, измерялась зависимость коэффициента преломления в видимом свете от частоты, откуда и из ИК-спектра уксусной кислоты в жидкой фазе определялся коэффициент преломления смеси, относимый к бесконечной длине волны света, в зависимости от номинального состава. Для расчета диэлектрической постоянной, молекулы мономера и димера уксусной кислоты моделировались идеальными диполями, находящимися в пространстве эллипсоидной формы с полуосями a, b и c. Согласно нашим исследованиям, перманентный дипольный момент молекулы димера уксусной кислоты изменяется с разбавлением. Согласно нашим расчетам кажущаяся константа равновесия реакции димеризации уксусной кислоты при 20° C, выраженная в молярных долях, описывается следующим уравнением:

$$\lg K = 1{,}8261 + 2{,}4549\, x_B,$$

где x_B — номинальная молярная доля четыреххлористого углерода.

Гликозиды видов Solanum, III

Диосцин

П. БИТЕ и М. М. ШАБАНА

Из свежих недозрелых ягод Solanum introsum, изолировался диосцин, который согласно литературным данным, был изолирован до сих пор лишь из видов Dioscorea.

Идентичность продукта с диосцином была доказана на основе температуры плавления, оптического вращения, ИК-спектра, тонкослойной хроматографии, ацетилирования, качественной идентификации и количественного определения аглюкона и сахарных компонентов, периодатного окисления и идентичности с триллином, полученным при частичном гидролизе продукта. С помощью ацетилирования диосцина при 140° C удалось получить непосредственно единообразный перацетат.

Присутствие грациллина в ягодах подтверждалось тонкослойной хроматографией

Получение модельных соединений белков путем модифицирования боковых цепей производных полиаминовых кислот, II

Получение производных полиглутаминовой кислоты, содержащих различные функциональные группы

А. КОТАИ, ДЬ. СОКАН, И. ФЕРЕНЦ и М. АЛМАШ

Проводились попытки синтеза модифицированных производных полиглутаминовой кислоты, содержащих одновременно различные функциональные группы (диалкиламиновые, карбоксильные, гидроксильные, имидазолильные, меркаптановые и эфирные группы). Исходным веществом синтеза был γ-метиловый эфир α-поли-L-глутаминовой кислоты (I). Последний превращался в желаемые производные с помощью различных модифицирующих реагентов, использованных либо последовательно, либо одновременно, в смеси. Было замечено, что при использовании смеси реагентов не только ее состав, но и другие условия реакции (в основном, температура) оказывают значительное влияние на средний состав образующихся продуктов и молекулярный вес полимера. Также было установлено, что при получении производных, содержащих одновременно несколько функциональных групп, оказывает и обработка реакционной смеси значительное влияние на качество образующегося продукта, кроме факторов, обсужденных подробно в предыдущем сообщении [2].

Синтез стереоизомерных γ-полиглутаминовых кислот, II

М. ХОЛЛОШИ, М. КАЙТАР и В. БРУКНЕР

Описывается синтез γ-полиглутаминовой кислоты через полибензиловый и поли-*трет.*-бутиловый эфиры. Получение L—L, а также D—D-стереоизомеров гидрохлористого α, α′-дибензил-γ′-п-нитрофенилового эфира γ-—L-глутамил-L-глутаминовой (VIII) и гидрохлористого α, α′-ди-*трет.*-бутил-γ-пентахлорфенилового эфира γ-глутамил- глутаминовой кислоты (XIII) — двух типов солей дипептидных активных эфиров, необходимых в качестве исходных материалов для реакции полимеризации, производилось из защищенных соответствующим способом производных глутаминовой кислоты путем присоединения методом активного эфира. Реакция полиавтоацилирования, протекающая в диметилформамидном растворе дипептидных производных VIII и XIII в присутствии триэтиламина, приводит к образованию α-бензилового эфира γ-полиглутаминовой кислоты (XVIII) и α-*трет.*-бутилового эфира γ-полиглутаминовой кислоты (XX), соответственно. После каталитического гидрирования полибензиливого эфира (XVIII), в смеси триамида гексаметил-фосфорной кислоты с диметилформамидом, удалось изолировать такую поликислоту, в которой 15—20% карбоксильных групп остались этерефицированными. Отщепление *трет.*-бутиловых групп от *трет.*-бутилового эфира γ-полиглутаминовой кислоты производилось с помощью 97%-ой трифторуксусной кислоты; поликислота может быть изолирована с почти количественным выходом. На основе анализа на азот аминогруппы, средний численный молекулярный вес *трет.*-бутилового эфира γ-полиглутаминовой кислоты и полученной из него γ-полиглутаминовой кислоты, равен 17 500 и 12 500, соответственно. γ-полиглутаминовая кислота, полученная из полибензилового эфира, имела очень низкий молекулярный вес (1300).

Оптическая чистота высокомолекулярной полиглутаминовой кислоты, полученная путем полного гидролиза, равна $99 \pm 3\%$. На основе сравнения оптического вращения γ-полиглутаминовых кислот, синтезированных через полиметиловый и поли-*трет.*-бутиловый эфиры, были сделаны заключения о структурных особенностях этих соединений.

The Acta Chimica publish papers on chemistry in English, German, French and Russian.

The Acta Chimica appear in volumes consisting of four parts of varying size, 4 volumes being published a year.

Manuscripts should be addressed to

Acta Chimica
Budapest 112/91 Műegyetem

Correspondence with the editors should be sent to the same address.

The rate of subscription is 165 forints a volume. Orders may be placed with "*Kultúra*" Foreign Trade Company for Books and Newspapers (Budapest I., Fő utca 32. Account No. 43-790-057-181) or with representatives abroad.

Les Acta Chimica paraissent en français, allemand, anglais et russe et publient des mémoires du domaine des sciences chimiques.

Les Acta Chimica sont publiés sous forme de fascicules. Quatre fascicules seront réunis en un volume (4 volumes par an).

On est prié d'envoyer les manuscrits destinés à la rédaction à l'adresse suivante:

Acta Chimica
Budapest 112/91 Műegyetem

Toute correspondance doit être envoyée à cette même adresse.

Le prix de l'abonnement est de 165 forints par volume.

On peut s'abonner à l'Entreprise pour le Commerce Extérieur de Livres et Journaux «*Kultúra*» (Budapest I., Fő utca 32. Compte-courant No. 43-790-057-181) ou à l'étranger chez tous les représentants ou dépositaires.

«*Acta Chimica*» издают трактаты из области химической науки на русском, французском, английском и немецком языках.

«*Acta Chimica*» выходят отдельными выпусками разного объема. 4 выпуска составляют один том. 4 тома публикуются в год.

Предназначенные для публикации рукописи следует направлять по адресу:

Acta Chimica
Budapest 112/91 Műegyetem

По этому же адресу направлять всякую корреспонденцию для редакции.

Подписная цена «*Acta Chimica*» — 165 форинтов за том. Заказы принимает предприятие по внешней торговле книг и газет «*Kultúra*» (Budapest I., Fő utca 32. Текущий счет № 43-790-057-181) или его заграничные представительства и уполномоченные.

42,— Ft

Reviews of the Hungarian Academy of Sciences are obtainable at the following addresses:

ALBANIA

Ndermarja Shtetnore e Botimeve
Tirana

AUSTRALIA

A. Keesing
Box 4886, GPO
Sydney

AUSTRIA

Globus Buchvertrieb
Salzgries 16
Wien I

BELGIUM

Office International de Librairie
30, Avenue Marnix
Bruxelles 5

Du Monde Entier
5, Place St. Jean
Bruxelles

BULGARIA

Raznoiznos
1, Tzar Assen
Sofia

CANADA

Pannonia Books
2, Spadina Road
Toronto 4, Ont.

CHINA

Waiwen Shudian
Peking
P. O. B. 88

CZECHOSLOVAKIA

Artia
Ve Směčkách 30
Praha 2

Poštovná Novinová Služba
Dovoz tisku
Vinohradská 46
Praha 2

Mad'arská Kultura
Václavské nám. 2
Praha I

Poštová Novinová Služba
Dovoz tlače
Leningradská 14
Bratislava

DENMARK

Ejnar Munksgaard
Nörregade 6
Copenhagen

FINLAND

Akateeminen Kirjakauppa
Keskuskatu 2
Helsinki

FRANCE

Office International de Documentation et Librairie
48, rue Gay Lussac
Paris 5

GERMAN DEMOCRATIC REPUBLIC

Deutscher Buch-Export und Import
Leninstraße 16
Leipzig 701

Zeitungsvertriebsamt
Fruchtstrasse 3—4
1004 Berlin

GERMAN FEDERAL REPUBLIC

Kunst und Wissen
Erich Bieber
Postfach 46
7 Stuttgart S.

GREAT BRITAIN

Collet's Holdings Ltd.
Dennington Estate
London Rd.
Wellingborough. Northants.

Robert Maxwell and Co. Ltd.
Waynflete Bldg. The Plain
Oxford

HOLLAND

Swetz and Zeitlinger
Keizersgracht 471—487
Amsterdam C

Martinus Nijhof
Lange Voorhout 9
The Hague

INDIA

Current Technical Literature
Co. Private Ltd.
India House OPP
GPO Post Box 1374
Bombay I

ITALY

Santo Vanasia
Via M. Macchi 71
Milano

Libreria Commissionaria Sansoni
Via La Marmora 45
Firenzé

JAPAN

Nauka Ltd.
92, Ikebukur O-Higashi 1-chome
Toshima-ku
Tokyo

Maruzen and Co. Ltd.
P. O. Box 605
Tokyo-Central

Far Eastern Bookseller:
Kanda P. O. Box 72
Tokyo

KOREA

Chulpanmul
Phenjan

NORWAY

Johan Grundt Tanum
Karl Johansgatan 43
Oslo

POLAND

RUCH
ul. Wronia 23
Warszawa

ROUMANIA

Cartimex
Str. Aristide Briand 14—18
Bucureşti

SOVIET UNION

Mezhdunarodnaya Kniga
Moscow G—200

SWEDEN

Almquist and Wiksell
Gamla Brogatan 26
Stockholm

USA

International Arts and Sciences Press
108, Grand Street
White Plains, N. Y. 10601

VIETNAM

Xunhasaba
19, Tran Quoc Toan
Hanoi

YUGOSLAVIA

Forum
Vojvode Mišića broj 1
Novi Sad

Jugoslovenska Knjiga
Terazije 27
Beograd

5. XII. 1969.

Index: 26.007

ACTA CHIMICA

ACADEMIAE SCIENTIARUM HUNGARICAE

TOMUS 62 FASCICULUS 4

AKADÉMIAI KIADÓ, BUDAPEST

1969

ACTA CHIM. ACAD. SCI. HUNG.

ACTA CHIMICA

A MAGYAR TUDOMÁNYOS AKADÉMIA KÉMIAI TUDOMÁNYOK OSZTÁLYÁNAK IDEGEN NYELVŰ KÖZLEMÉNYEI

SZERKESZTI

LENGYEL BÉLA

TECHNIKAI SZERKESZTŐK

DEÁK GYULA és HARASZTHY-PAPP MELINDA

Az Acta Chimica német, angol, francia és orosz nyelven közöl értekezéseket a kémiai tudományok köréből.

Az Acta Chimica változó terjedelmű füzetekben jelenik meg, egy-egy kötet négy füzetből áll. Évente átlag négy kötet jelenik meg.

A közlésre szánt kéziratok a szerkesztőség címére (Budapest 112/91 Műegyetem) küldendők.

Ugyanerre a címre küldendő minden szerkesztőségi levelezés. A szerkesztőség kéziratokat nem ad vissza.

Az Acta Chimica előfizetési ára kötetenként belföldre 120 Ft, külföldre 165 Ft. Megrendelhető a belföld számára az „Akadémiai Kiadó"-nál (Budapest V., Alkotmány utca 21. Bankszámla 05-915-111-46), a külföld számára pedig a „Kultúra" Könyv- és Hírlap Külkereskedelmi Vállalatnál (Budapest I., Fő utca 32. Bankszámla: 43-790-057-181) vagy annak külföldi képviseleteinél és bizományosainál.

Die Acta Chimica veröffentlichen Abhandlungen aus dem Bereiche der chemischen Wissenschaften in deutscher, englischer, französischer und russischer Sprache.

Die Acta Chimica erscheinen in Heften wechselnden Umfanges. Vier Hefte bilden einen Band. Jährlich erscheinen 4 Bände.

Die zur Veröffentlichung bestimmten Manuskripte sind an folgende Adresse zu senden:

Acta Chimica
Budapest 112/91 Műegyetem

An die gleiche Anschrift ist auch jede für die Redaktion bestimmte Korrespondenz zu richten.

Abonnementspreis pro Band: 165 Forint. Bestellbar bei dem Buch- und Zeitungs-Außenhandels-Unternehmen »*Kultúra*« (Budapest I., Fő utca 32. Bankkonto No. 43-790-057-181) oder bei seinen Auslandsvertretungen und Kommissionären.

Acta Chimica Academiae Scientiarum Hungaricae, Tomus 62 (4), pp. 323—334 (1969)

INVESTIGATION OF LiF—CaF_2 BASED LUMINOPHORS ACTIVATED WITH MANGANESE

I. KÁSA, É. BUZÁGH-GERE and I. TÖRÖK

(Institute for Applied Chemistry of the Technical University, Budapest, Institute for General and Analytical Chemistry of the Technical University, Budapest and Clinic for Radiology of the Medical University, Budapest)

Received October 18, 1968

The effect of manganese(II) fluoride activator on LiF—CaF_2 luminophors can be summarized as follows:

1 wt% of the activator markedly increases the height of the peak at 190—195°C, while it gradually suppresses the one at 280°C.

The presence of manganese(II)fluoride in amounts higher than 1 wt% causes a peak at about 252—255°C, which is characteristic of pure CaF_2 : Mn. This peak becomes predominating as the activator concentration increases. This makes possible to prepare a luminophor by increasing the concentration of the activator, for which only one peak appears on the heating curve at about 255°C.

It holds for every sample that the sensitivity is increased by orders of magnitude by manganese(II)fluoride activator, and also that the heating curves are the same irrespective of whether excitation was made by X-ray or β-ray.

As for the fading, the samples with 0.1—1% activator content behave most favourably, since the total light intensity decreases only very little after a fast reduction during the first 4—6 hours after excitation. With samples containing 2.5—5% activator the reduction of total intensity is greater also in later periods. Consequently the samples with 0.2—1% activator content are most suited to practical applications.

The energy dependence of every sample corresponds to that expected on the basis of the average atomic number.

A further advantage of these luminophors from the point of view of dosimetric application is, that since they contain ^6Li isotope, they can also be used in thermal neutron dosimetry.

The application of solid-body dosimetric methods has gained importance in the last years. At present the so called thermoluminescent dosimeters are most widely used. Various thermoluminescent luminophors, which are used as dosimeters, are commercially available along with the necessary instruments for estimation.

The application of thermoluminescent dosimeters is especially favourable in medical practice where, in the "in vivo" dosimetric methods which are coming into prominence, very small, wide-range dosimeters are necessary which behave similarly to the tissues of the human body from the point of view of energy dependence. Thermoluminescent luminophors meet these requirements quite well, and, besides, have high mechanical strength, and a great resistance towards the changes in chemical and other conditions.

In practical dosimetry $CaSO_4$: Mn, CaF_2 : Mn and lithium fluoride are used most frequently. All these luminophors have advantages and disadvantages [1—5]. The advantage of LiF as thermoluminescent luminophor is its

small average atomic number (8.2), and consequently small energy dependence, and also the fact that due to the reaction $^6Li\ (n,\alpha)^3He$ it can also be used in thermal neutron dosimetry. The drawback of this luminophor is its relatively small sensitivity. Several attempts have been made to increase the sensitivity of LiF. The authors of the present paper have earlier established that the sensitivity of LiF can be increased by adding CaF_2 to it [6]. This effect of CaF_2 has been studied in detail and the application of this type of thermoluminescent luminophor in dosimetry reported by JUZNIC and KOBAL [7]

In the present paper the authors deal with the investigation and application in dosimetry of LiF—CaF_2 based luminophors activated with manganese. The composition of the basic material is near to that of the eutectic, and the average atomic number of the LiF—CaF_2 mixture is 13.75. Its great advantage over luminophors which do not contain activator is its much higher sensitivity.

The phase equilibrium of the LiF—CaF_2 binary system has been investigated among others by ROAKE [8] and DEADMORE and MACHIN [9]. Different values are given for the composition of the eutectic by different research workers. According to ROAKE LiF forms an eutectic with 19.5 mole% CaF_2 which melts at 769°C, while according to DEADMORE and MACHIN the eutectic contains 23 mole% CaF_2 and melts at 760°C.

Experimental

Lithium fluoride was prepared from analytical grade lithium compound by precipitation with hydrogen fluoride solution following purification by fractionated precipitation. Calcium fluoride was prepared similarly to lithium fluoride.

Manganese(II)fluoride was prepared from analytical grade manganese(II) carbonate by means of hydrogen fluoride solution.

The properties of the pure components and of activated and non-activated mixtures with a composition near to the eutectic were studied by thermal methods with a derivatograph.

Thermoanalytical measurements were made with a PAULIK—PAULIK—ERDEY MOM derivatograph [10], at a heating rate of 10°C/min, in oxygen-free argon atmosphere, in platinum crucible, using 600 mg samples. The thermogravimetric (TG) and differential thermal analytical (DTA) curves of the basic materials are presented in Fig. 1, while those of non-activated and Mn-activated LiF—CaF_2 mixtures in Fig. 2.

Lithium fluoride is of constant weight up to about 300°C, then it exhibits a weight loss of 1.1% up to 1000°C. The melting point is indicated on the DTA curve by an endothermic peak at 860°C.

The total weight loss of calcium fluoride is 1.5% up to 1000°C, 0.3% being moisture leaving between 60 and 300°C, while 1.2% leaves between 450 and 700°C, in connection with the contraction of the substance. There appears no peak on the DTA curve, since the melting point is beyond the studied temperature interval.

Manganese(II) fluoride is of constant weight up to 200°C, then exhibits a weight loss of 1.5% up to 400°C and of 3.5% up to its melting point, 925°C.

The value of the melting point agrees with literary data (929.5°C) within the limits of accuracy of differential thermal analysis. During melting a faster weight loss starts and a further 3.2% reduction in weight occurs up to 1000°C. The probable reason for this is that manganese(II) fluoride becomes more volatile above the melting point.

Non-activated LiF—CaF_2 mixture undergoes a weight loss of 1.1% from 300°C to 1000°C.

The reduction in weight of activated mixtures increases with the amount of activator from 1.1% to 1.5%. This is in concordance with the higher volatility of manganese(II) fluoride.

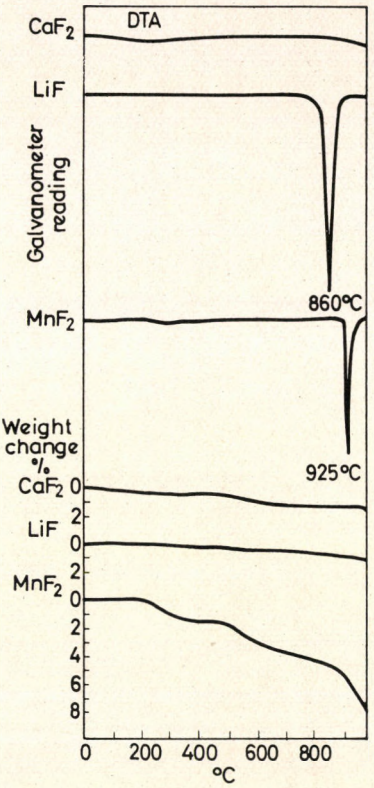

Fig. 1. Thermogravimetric (TG) and differential thermal analytical (DTA) curves of the starting materials

The melting of the eutectic is indicated by the endothermic peak at 780—790°C, for both the activated and non-activated mixtures.

The prepared luminophors were ignited at 1000°C. At this temperature both the LiF—CaF_2 eutectic and MnF_2 melt.

During the preparation of the luminophors 75 mole% LiF and 25 mole% CaF_2 were weighed and then activated with varying amounts of manganese(II) fluoride. The activated products were ignited at 1000°C, in platinum crucible in oxygen-free argon atmosphere. The samples contained the following amounts of manganese(II) fluoride:

Sample 1	0.0 wt% MnF_2
Sample 2	0.2 wt% MnF_2
Sample 3	1.0 wt% MnF_2
Sample 4	2.5 wt% MnF_2
Sample 5	5.0 wt% MnF_2

Ignited samples were crushed and the sieve fraction of smaller than 0.2 mm grain size taken. The sieved luminophors were treated with acid, washed by decantation and dried.

For the purpose of taking the heating curve the luminophors were placed into a 20 mm diameter plate made of aluminium foil and excited with X-ray in one case and with β-ray from Tl-204 isotope ($E_{max} = 0.764$ MeV) in the other.

The heating curve was taken by a d. c. valve voltmeter equipped with an electron multiplier detector (EMI 6097 S), at a heating rate of 30°C/min.

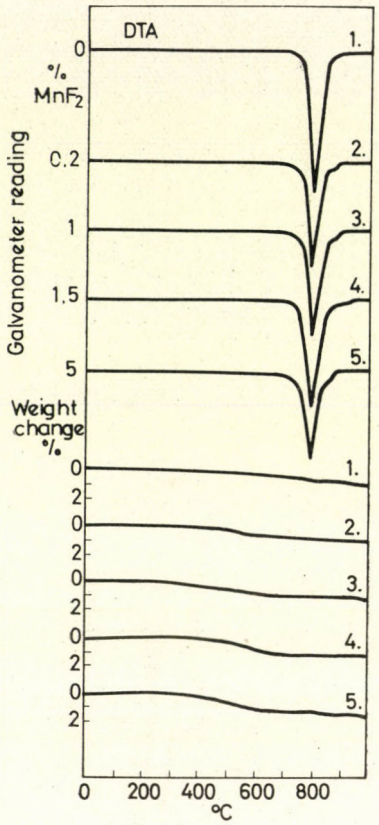

Fig. 2. Thermogravimetric (TG) and differential thermal analytical (DTA) curves of LiF—CaF_2 mixtures containing various amounts of activator. Curve 1: 0% MnF_2; Curve 2: 0.2% MnF_2; Curve 3: 1.0% MnF_2; Curve 4: 2.5% MnF_2; Curve 5: 5.0% MnF_2

In other dosimetric measurements 50 mg of the samples were weighed in 6 mm diameter steel plates and excited by normal X-ray of varying average energy, and with γ-ray from Co^{60} isotope ($E_{average} = 1.25$ MeV). Since thermoluminescent dosimeters can only be used for comparative measurements, standardization was made with a Siemens universal dosimeter.

The dosimeters were evaluated by a Vakutronik VA-M-30 type thermoluminescent dosimeter evaluator.

Discussion

The heating curves of samples containing different amounts of activator are presented in Figs 3—7.

The first curves in all five figures were taken as follows: the sample was excited by X-ray and heating started 10 minutes after irradiation. With the second curves excitation was accomplished with β-ray and heating started 10 minutes after irradiation. In the case of the third curves the samples were

excited with X-ray and heating started after 24 hours' standing at room temperature.

In Table I the temperatures belonging to the maxima of the heating curves are summarized.

Table I

Maxima of the heating curves

Number of sample	T_{max} (°C)								
	Excitation with X-ray, measurement 10 minutes after irradiation			Excitation with β-ray, measurement 10 minutes after irradiation			Excitation with X-ray, measurement 24 hours after irradiation		
1.	61	180	289	60	197	282	136	181	286
2.	52	198	—	49	197	—	130	192	—
3.	52	199	—	47	202	—	128	202	—
4.	—	194	252	—	185	253	—	192	257
5.	—	192	254	—	191	252	—	(200)	255

The following statements can be made on the basis of the curves and data in Table I.

The curves of the non-activated sample have three distinct maxima. On curves *a)* and *b)* in Fig. 3 there is also a maximum at about 130°C, which, however, partly overlaps with the peak at 180°C. After 24 hours' standing the maximum at about 60°C disappears and the one at 130°C becomes separate. The relative height of the peak at 280°C remarkably increases. The reason for this is probably that the electrons being in the lower traps are liberated and they partly recombine, and a smaller part is trapped in lower levels.

The introduction of manganese as activator modifies the situation in an extent depending on its concentration.

The analysis of the curves in Fig. 4 shows that 0.2 wt% manganese remarkably increases the "main peak" at 195—200°C, while the other peaks become relatively smaller. With heating starting 10 minutes after irradiation the peak at 280°C cannot be measured, yet some sign of a peak is observable at this temperature on the curve obtained 24 hours after irradiation. This means that traps are still present but their relative amount is smaller.

Fig. 5 shows the heating curves of luminophors containing 1 wt% manganese(II) fluoride activator. The sample behaves similarly to the former one with the difference that the peak at about 280°C is practically lacking.

Fig. 6, in which the curves obtained for samples containing 2.5 wt% manganese(II) fluoride are presented, shows a substantial change of the luminophor as compared to the previous ones. The small peak at 50—60°C has disappeared while one at 252—255°C appears the relative height of which is

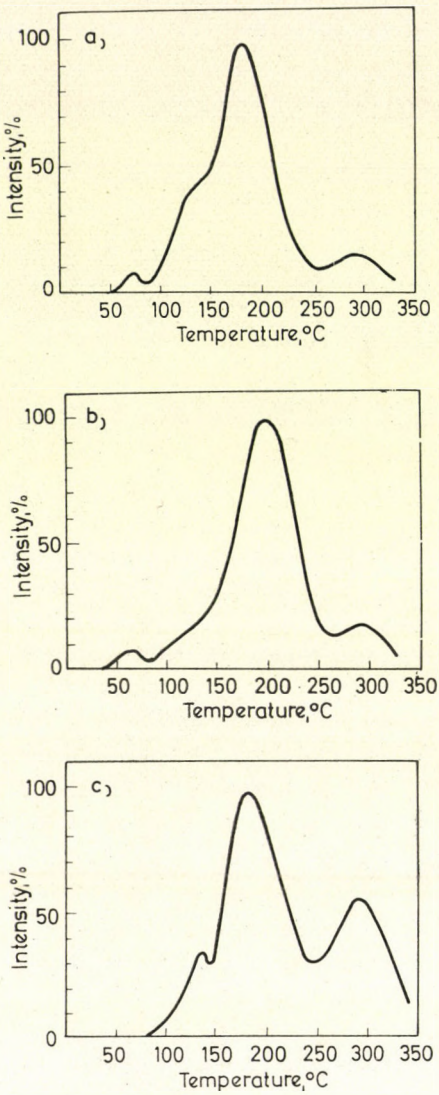

Fig. 3. Heating curves of Sample 1. *a)* Excitation with X-ray, measurement after 10 minutes; *b)* Excitation with Tl^{204} β-ray, measurement after 10 minutes; *c)* Excitation with X-ray, measurement after 24 hours

similar to that of the peak at 190—195°C on the curve taken 10 minutes after irradiation. After standing for 24 hours the height of the peak at the lower temperature becomes remarkably smaller as compared to that at about 252—255°C (Fig. 6, curve *c)*).

Fig. 7 shows the heating curves of samples containing 5 wt% manganese(II) fluoride. The height of the peak at about 190—195°C remarkably decreases even 10 minutes after irradiation, while it does not appear separately

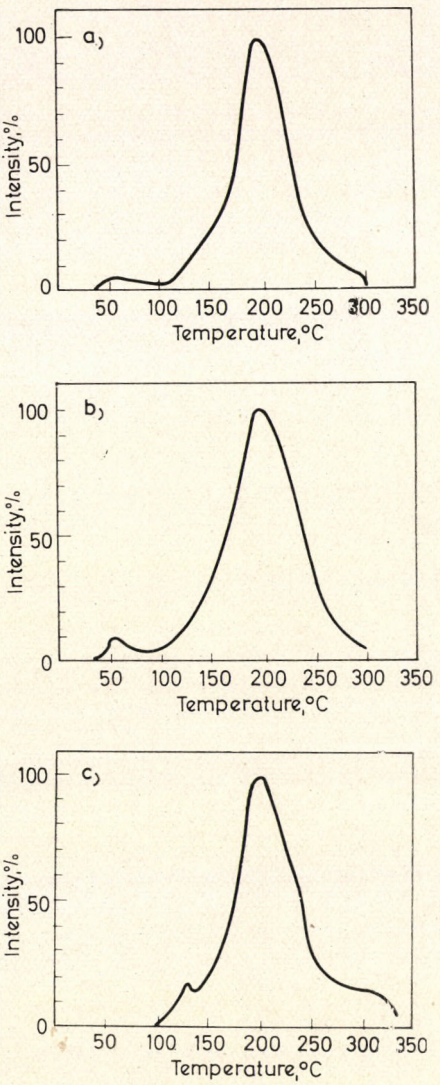

Fig. 4. Heating curves of Sample 2. *a)* Excitation with X-ray, measurement after 10 minutes; *b)* Excitation with Tl^{204} β-ray, measurement after 10 minutes; *c)* Excitation with X-ray, measurement after 24 hours

24 hours after irradiation, although it is still present. The peak at 252—255°C is predominating.

According to our experience with manganese-activated LiF—CaF_2 based luminophors of nearly eutectic composition the peak belonging to the higher temperature becomes predominating as the activator content increases.

Fig. 8 shows the decrease of the amount of thermoluminescent light as function of the time of storing at room temperature. The average of the values

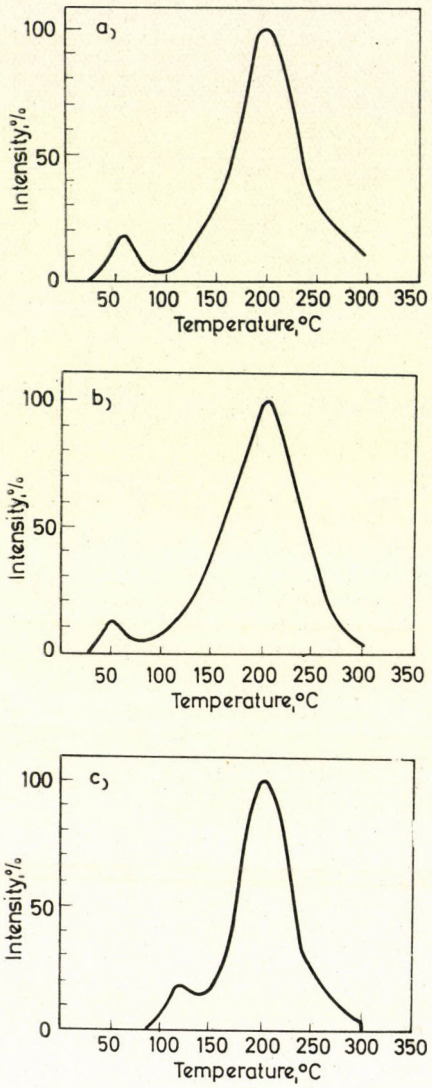

Fig. 5. Heating curves of Sample 3. *a)* Excitation with X-ray, measurement after 10 minutes; *b)* Excitation with Tl^{204} β-ray, measurement after 10 minutes; *c)* Excitation with X-ray, measurement after 24 hours

measured within some minutes after irradiation was taken as 100%. Total light was measured every hour in the first six hours, then only every 24 hours.

The measured values are in good agreement with the conclusions drawn from the heating curves.

With Samples 2 and 3 the decrease is remarkable during the initial 4—5 hours (24—34%). In this case the electrons leave the traps of small energy depth relatively quickly. Later the curve descends smoothly and only very

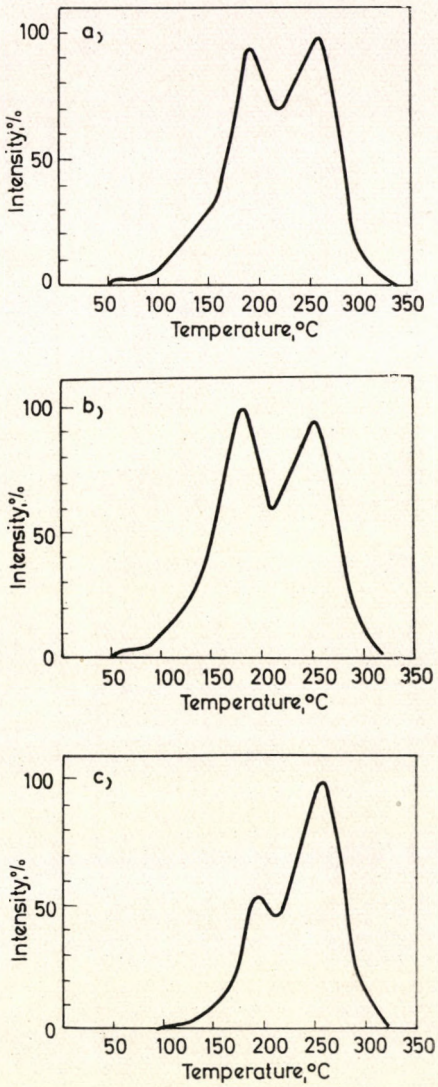

Fig. 6. Heating curves of Sample 4. *a)* Excitation with X-ray, measurement after 10 minutes; *b)* Excitation with Tl^{204} β-ray, measurement after 10 minutes; *c)* Excitation with X-ray, measurement after 24 hours

slowly. This means that the probability of the electrons being in the trap belonging to the peak at 200°C to leave is very small at room temperature.

With Sample 4 the decrease is much greater. This is also in agreement with the data of the heating curve (Fig. 6 curve *c)*). In this case, however, it is striking that the probability of electrons being in the trap corresponding to the peak at 190—200°C to leave is much higher than for the previous two

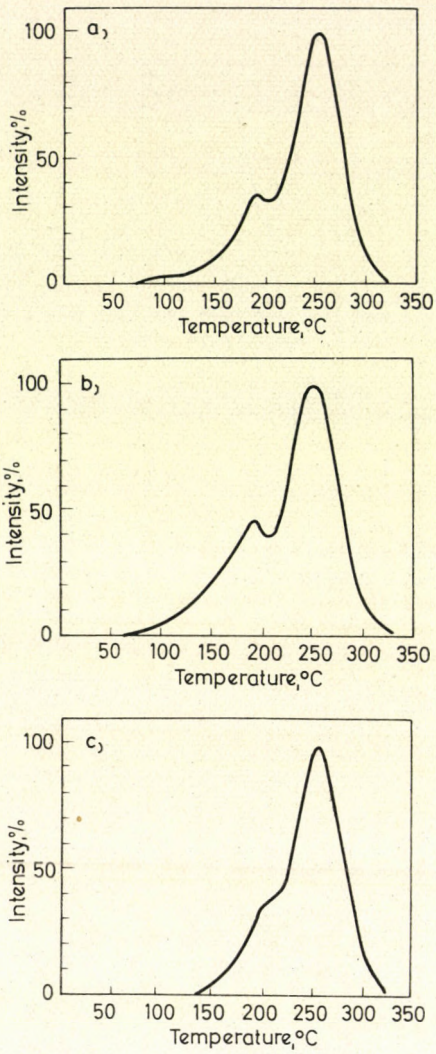

Fig. 7. Heating curves of Sample 5. *a)* Excitation with X-ray, measurement after 10 minutes; *b)* Excitation with Tl^{204} β-ray, measurement after 10 minutes; *c)* Excitation with X-ray, measurement after 24 hours

samples. Consequently the absolute value of the fading is greatest for this sample.

The fading of Sample 5 agrees with that expected on the basis of the heating curve.

The energy dependence of activated samples is shown in Fig. 9. The sensitivity of luminophors increases with decreasing energy of photons. If the sensitivity for the γ-radiation from Co^{60} is taken as unity, then the sensitivity increases about five times on irradiation with 30 KeV X-ray.

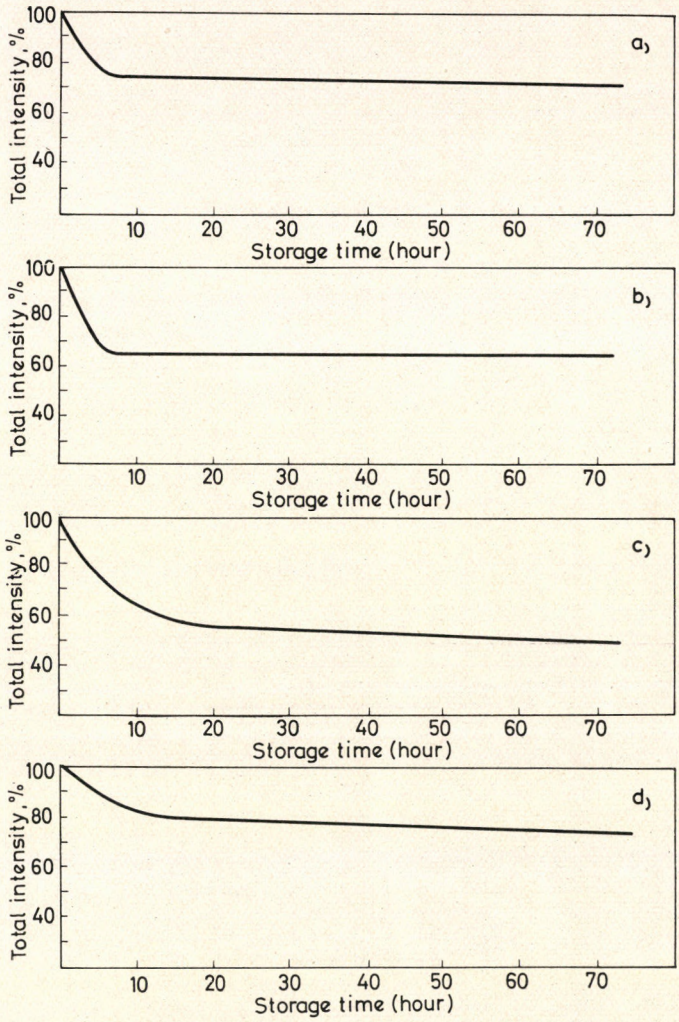

Fig. 8. Decrease of total light intensity of activated luminophors as function of time elapsed after irradiation. *a)* activator content: 0.2% MnF_2; *b)* activator content: 1.0% MnF_2; *c)* activator content: 2.5% MnF_2; *d)* activator content: 5.0% MnF_2

REFERENCES

1. Attix, F. H.: AEC Accession No 777 Rept. No. NRL—6145 (1964).
2. Endress, G. W. R.: U. S. At. Energy Comm. BUWL—SA—23 (1965).
3. Watson, R. C.: U. S. At. Energy Comm. TID—21945 (1965).
4. Con-Rad TDL System, Controls for Radiation Inc. Cambridge 40 (Mass) (Firmenprospect).
5. Lumivad VA—M—30, VEB Vakutronik WIB Dresden (Firmenprospect).
6. Erdey, L., Kása, I., Kovács, L.: Acta Chim. Acad. Sci. Hung. **45,** 95—100 (1965).
7. Juznic, K., Kobal, I.: International Conference on Luminescence, Budapest 23—30 August 1966. Preprints **11,** Application of Luminescence 33—40 (1966).

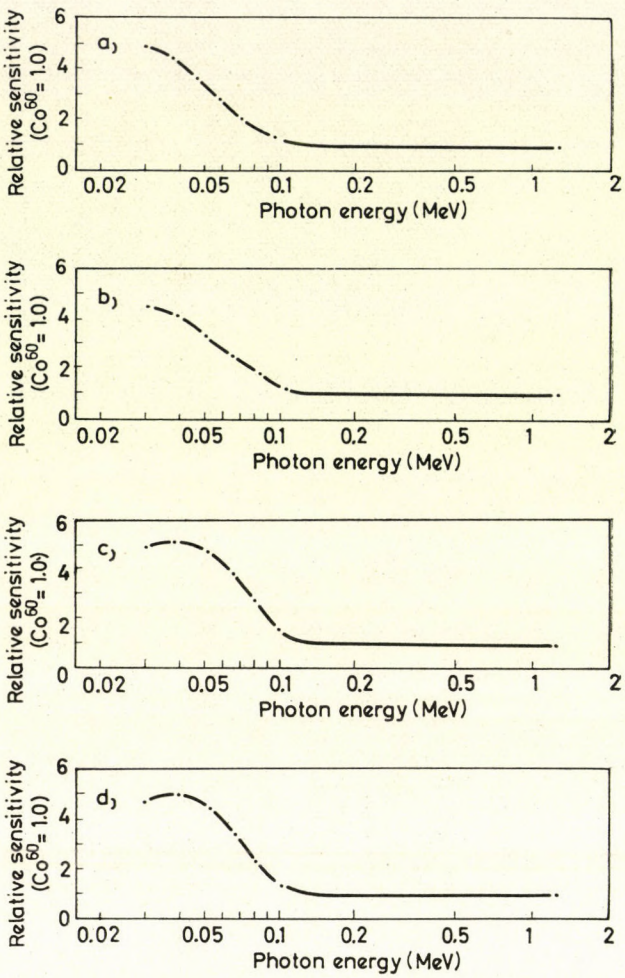

Fig. 9. Energy dependence of activated luminophors. *a)* activator content: 0.2% MnF_2; *b)* activator content: 1.0% MnF_2; *c)* activator content: 2.5% MnF_2; *d)* activator content: 5.0% MnF_2

8. ROAKE, W. E.: J. Electrochem. Soc. **104,** 661—662 (1957).
9. DEADMORE, D. L., MACHIN, J. S.: J. Phys. Chem. **64,** 824 (1960).
10. PAULIK, F., PAULIK, J., ERDEY, L.: Z. analyt. Chem. **160,** 241 (1958).
11. KOGLIN, W.: Kurzes Handbuch der Chemie (1954) 3. Teilband, 1043 p.

Imre KÁSA; Budapest XI., Egry József u. 20—22.
Éva BUZÁGH-GERE; Budapest XI., Gellért tér 4.
István TÖRÖK; Budapest VIII., Üllői út 78.

Acta Chimica Academiae Scientiarum Hungaricae, Tomus 62 (4), pp. 335—355 (1969)

CORRELATION BETWEEN MASS SPECTRA AND MOLECULAR STRUCTURE OF SOME ORGANOSILICON COMPOUNDS WITH TWO SILICON ATOMS

J. TAMÁS,* K. UJSZÁSZY,* T. SZÉKELY** and G. BUJTÁS*

* *Centre for Chemica-Structural Studies, Hungarian Academy of Sciences and*
** *Research Group of Inorganic Chemistry, Hungarian Academy of Sciences, Budapest*

Received May 23, 1968

The mass spectra of hexamethyldisilane, hexamethyldisilylmethylene, hexamethyldisiloxane, hexamethyldisilazane and N-methyl-hexamethyldisilazane have been studied and the fragmentation processes of these compounds are discussed. The chemical formulas of the significant ions present in the mass spectra and the main fragmentation modes were determined by comparing the computed and observed ratios of isotopic species, using ^{18}O labelling, further by observing the metastable peaks. Correlations between the molecular structure and the mass spectra, *i.e.* the types and quantities of the significant ions, the fragmentation modes, the relative stabilities of the molecular ions and especially the relative abundance of ions containing the Si—X—Si skeleton have been studied.

Among the great number of rearrangement reactions observed, several cases of molecular skeleton rearrangements were found. One type of the fission processes of the Si—X—Si skeleton is supposed to be heterolytic, including charge shift.

The origin and decomposition of the double-charged ions is shown in a fragmentation scheme. The relative quantity of the double-charged ions allows conclusions concerning the charge distribution within the ions.

I. Introduction

As a rule, in the mass spectra of organosilicon compounds there are several rearrangement ion peaks (*cf.* [1]—[7]). This is supported by earlier results obtained in a study [8] of the fragmentation pattern of tetramethylsilane, for the mass spectrum of this compound indicates the presence of the SiH^+, SiH_3^+, $SiCH_4^+$, $SiCH_5^+$ and $SiC_2H_7^+$ ions, which are formed from tetramethylsilane by H-atom rearrangement during unimolecular decomposition. Obviously, in such cases the correlation between mass spectrum and molecular structure is rather complex. Therefore, the occurrence of numerous rearrangement processes justifies detailed studies on the correlation between mass spectra and molecular structure, which are required for successful mass spectrometric studies of the molecular structure in the case of unknown members in a given group of compounds.

As an extension of earlier studies on tetramethylsilane, the following molecules, each containing two silicon atoms, have been subjected to mass spectrometric analysis.

Compound	Structure	Mol. wt.	Symbol
Hexamethyldisilane	$(CH_3)_3Si-Si(CH_3)_3$	146	**I**
Hexamethyldisilylmethylene	$(CH_3)_3Si-CH_2-Si(CH_3)_3$	160	**II**
Hexamethyldisilazane	$(CH_3)_3Si-NH-Si(CH_3)_3$	161	**III**
Hexamethyldisiloxane	$(CH_3)_3Si-O-Si(CH_3)_3$	162	**IV**
N-methylhexamethyldisilazane	$(CH_3)_3Si-N(CH_3)-Si(CH_3)_3$	175	**V**

The results of this study yield fundamental information on the stability of these molecules under electron impact, as well as on the relative strength of the various silicon bonds.

From the viewpoint of silicon chemistry, this is especially interesting because these compounds can be regarded as the first members of a homologous polymer series important both practically and theoretically. It can be assumed that these studies provide information about the nature of much larger molecules, too.

In this paper, the poly-isotopic spectra of the listed compounds and mono-isotopic spectra calculated from experimental data are reported. The empirical formulas assigned to the more important ion fragment peaks will be given together with the decomposition pathways deduced from the observed metastable peaks. The present study is aimed at the elucidation of correlations between decomposition pathways and molecular structure. The main types of rearrangement reactions will be summarized and the correlation between the abundance of doubly-charged ions, the stability of molecular skeleton, and the structure of the molecules will be interpreted.

II. Experimental

Hexamethyldisilazane, N-methylhexamethyldisilazane, hexamethyldisiloxane have been prepared by well known methods.

^{18}O-labelled hexamethyldisiloxane has been prepared using water containing 25% of heavy oxygen. Hexamethyldisilylmethylene and hexamethyldisilane were synthesized in the Institute of Organic Chemistry, Academy of Sciences of the U. S. S. R.* The latter was used after purification with a preparative gas chromatograph. Gas chromatographic analyses have shown that compounds **I**—**IV** are uniform and do not contain impurities. As shown by mass spectra, in compounds **III** and **V** the trimethylchlorosilane contamination was not more than 10^{-2}%. In compound **V** about 0.3% of compound **III**, and traces of compound **IV** were present. Spectra were corrected accordingly.

Mass spectra have been recorded with an MH-1303 type instrument at an ion accelerating voltage of 2 kV. The ion source and ionization chamber were operated at 200°C, the temperature of the all-metal inlet system was 100°C. A tungsten filament served as the cathode of

* We wish to express our thanks to Dr. P. GÖMÖRI, L. EÖTVÖS University, Dept. of General and Inorganic Chemistry, for the preparation of ^{18}O-hexamethyldisiloxane, and to Dr. O. M. N'EFIODOV, Institute of Org. Chem. Academy of Sciences, U. S. S. R., for the preparation and gift of hexamethyldisilylmethylene and hexamethyldisilane.

the ion source, with a constant emission current of 1.5 mA. A source slit of 0.1 mm was used and the slit of the ion collector was set as required during operation.

With a 0.2 mm collector slit already suitable for quantitative measurements, the resolution of the instrument $(M/\Delta M)_{5\%}$ was about 650. This is nearly three times better than the original resolution and has been achieved by fine positioning of the ion source cathode. For this purpose the cathode holder has been modified in such a manner that it permitted extremely precise and reproducible positioning. A further modification involved an increase of the maximum voltage applied to the repeller electrode in the ion source to 14 V from the original 9 V, with respect to the ionization chamber. Both modifications helped the detection of metastable peaks and the determination of the corresponding mass numbers, thus permitting the study of metastable transitions.

III. Experimental results

The mass spectra of the substances studied are listed in Table I, as recorded at a nominal ionization energy of 50 eV. The abundance (intensities) of ions corresponding to various m/e (mass to charge) ratios are expressed in per cents of the ion-current of the most intensive peak (reference peak) within the spectrum. In the case of compound **I** the reference peak is at $m/e = 73$, in the case of the other compounds this is at a mass to charge ratio of M-15, where M is the mass number of the molecule. All ion peaks more intensive than 0.2% are listed; double charge peaks are listed if more intensive than 0.01%.

In the case of all substances, the relative intensities were, within $\pm 2\%$, independent of the vapor pressure of the sample in the ionization chamber.

No mass spectral data for compounds **I** and **V** were found in the literature. For the other three compounds, 70 eV spectra have been reported: by FRITZ *et al.* [4] for compound **II** (practically the whole spectrum), by DIBELER *et al.* [9] for compound **IV** (a few intensive ion peaks), and by SHARKEY *et al.* [1] for compounds **III** and **IV** (parts of spectra).

For purposes of comparison, spectra at 70 eV have also been recorded (not listed in this paper). Apart from doubly-charged ion peaks, peak intensities in the 70 eV spectra did not differ greatly from these in the 50 eV spectra. The ion peak intensities of the 70 eV spectra recorded by us agree within 2—5% with the corresponding peak intensities mentioned in the literature. Exceptions were found in the following cases.

a) The molecule-ion intensity at 70 eV referring to **II** was found to be much higher (0.09% instead of 0.03%) than the reported value [4].

b) The region between mass numbers 99 and 117 in the spectrum **III** does not even qualitatively agree with that found in the literature [1]. However, agreement within the stated limits is found if each one of SHARKEY's m/e values assigned in this section to the given intensity values is reduced by one unit.

A number of metastable peaks were observed in the mass spectra. In order to establish the ion peak intensity values, in some cases the base line-modifying effect of metastable peaks had to be taken into consideration.

Table I

m/e	I.	II.	III.	IV.	V.
177	—	—	—	—	1.12
176	—	—	—	—	2.51
175	—	—	—	—	13.64(M)
174	—	—	—	—	0.27
163	—	—	—	—	0.85
162	—	—	0.39	0.02(M)	7.93
161	—	—	2.29(M)	—	17.50
160	—	0.13(M)	—	—	**100.00**
150	—	—	—	0.77	—
149	—	—	0.79	7.85	—
148	0.76	0.80	7.70	15.70	—
147	1.71	7.80	16.10	**100.00**	—
146	9.91(M)	16.70	**100.00**	—	0.23
145	—	**100.00**	—	—	0.49
144	—	—	—	—	3.02
134	—	—	—	0.27	—
133	1.59	—	0.38	2.07	—
132	3.30	0.23	3.93	1.04	0.35
131	21.30	1.66	6.64	—	0.80
130	0.29	1.46	44.24	—	2.12
129	0.99	9.43	0.43	—	—
119	—	—	—	0.42	0.62
118	—	—	0.25	—	1.25
117	0.25	1.36	0.43	1.13	8.30
116	0.39	0.26	2.53	0.26	1.26
115	2.19	1.57	0.86	0.76	0.90
114	—	—	2.13	—	1.18
113	0.34	1.07	3.30	0.37	0.54
105	—	—	—	0.90	—
104	—	—	0.35	—	0.27
103	0.34	0.67	0.31	1,20	1.48
102	—	0.30	1.74	0.47	1.26
101	0.70	2.10	1.34	0.58	1.84
100	—	0.3	8.77	—	5.83
99	1.05	1.44	0.46	—	0.88
89	—	—	—	0.25	0.39
88	—	—	0.36	0.20	4.15
87	0.37	0.54	0.60	1.20	9.12

Table I (cont.)

m/e	I.	II.	III.	IV	V.
86	0.21	0.42	2.78	—	95.90
85	1.06	2.70	1.04	—	1.08
84	0.21	0.20	—	—	0.24
83	0.52	0.71	—	—	—
81	0.20	—	—	—	0.02
80.5	—	—	—	—	0.02
80	—	—	—	—	0.12
75	3.60	1.60	0.66	1.28	1.92
74	8.39	3.87	3.31	1.24	4.44
73.5	—	—	0.02	0.04	0.55
73	**100.00**	42.67	11.32	14.35	50.20
72.5	—	0.02	—	—	7.41
72	2.44	1.16	2.02	0.85	3.64
71	1.18	0.98	0.84	0.47	0.75
70	0.51	0.32	1.32	—	1.09
69	—	0.65	—	—	—
67	—	—	—	0.67	—
66.5	—	—	0.76	1.20	—
66	—	0.44	1.56	8.33	—
65.5	—	0.85	10.21	—	—
65	—	5.42	—	—	0.14
64.5	—	—	—	—	0.89
61	—	0.27	0.24	0.36	1.14
60	0.34	0.56	1.06	0.47	2.51
59	4.16	7.28	5.53	5.96	32.07
58.5	—	—	0.74	0.02	0.05
58	2.14	0.92	0.97	0.66	1.54
57.5	—	0.05	2.73	—	—
57	1.07	1.10	0.53	0.43	121.00
56	0.22	0.19	0.30	—	0.84
55	1.01	0.76	0.26	0.23	0.48
53	0.36	0.21	—	0.24	—
52.5	—	—	0.27	0,33	—
52	—	—	0.48	2.67	—
51.5	—	0.14	3.85	0.04	—
51	—	1.00	—	—	—
47	0.54	0.42	0.32	0.64	0.60
46	1.09	0.86	1.21	0.46	1.03

Table I (cont.)

m/e	I.	II.	III.	IV.	V.
45	16.94	13,52	7.75	6.14	16.22
44	2.69	2.61	1.53	1.79	1.81
43	7.33	3.23	2.12	1.53	3.95
42	0.42	0.21	—	—	0.46
31	1.25	1.76	0.87	0.46	2.73
29	1.55	1.04	0.47	0.43	0.96
28	2.37	1.16	1.41	1.99	1.47

Metastable peaks, as known, (*cf.* [2] or [10]) are utilized in determining the origin of mass spectra, *i.e.* in the elucidation of the formation and the decomposition sequence of the ionic species.

For this purpose, equation

$$m^* = \frac{m_1^2}{m_0} \tag{1}$$

can be used, which correlates the mass number of the metastable peak (m^*) with those of the decaying ion (m_0) and the ion (m_1) formed [11].

In order to improve the detection of these low intensity metastable peaks and to elucidate the transitions assignable to them, several parameters have been varied. Thus, the vapor pressure of the sample substance in the ionization chamber was increased two- and four-fold with respect to the usual value; a comparatively wide and variable collector slit was used during the measurements and the ionization voltage was varied, too. The potential of the repeller electrode was also varied in a wide interval. In certain cases the ion-optics (repeller, attractor, focusing voltages) and the ionization energy were adjusted according to the maximum intensity metastable peaks. By this technique, the intensity of metastable peaks could be raised 3 to 6 times with respect to the intensity measured with ion optics adjusted to the first maximum of the repeller potential (for Hg^+ ions) and the intensity relative to the normal peaks could be raised by one order of magnitude. Metastable peak intensities with varying sample pressure were always measured with respect to normal ion peak intensities unequivocally due to monomolecular decomposition of the molecule. Only those metastable peaks were taken into consideration for which this intensity was found to be independent of the sample pressure. Thus, the metastable peaks which appeared at higher sample pressures at $m^*/e = = 91.5$ in the spectrum of **III**, and at $m^*/e = 26.5$ in the spectrum of **IV** were found to be due to secondary processes, therefore, these were not included in Table II.

Table II

I. (M = 146)		II. (M = 160)		III. (M = 161)		IV. (M = 162)		V. (M = 175)	
m^*/e	transition	m^*/e	transition	m^*/e	transition	m^*/e	transition	m^*/e	transition
127.0	$131 \xrightarrow{-2} 129$	131.4	$160 \xrightarrow{-15} 145$	132.4	$161 \xrightarrow{-15} 146$	116.7	$147 \xrightarrow{-16} 131$	146.3	$175 \xrightarrow{-15} 160$
117.5	$146 \xrightarrow{-15} 131$	114.8	$145 \xrightarrow{-16} 129$	115.7	$146 \xrightarrow{-16} 130$	102.9	$133 \xrightarrow{-16} 117$	129.6	$160 \xrightarrow{-16} 144$
111.0	$115 \xrightarrow{-2} 113$	100.9	$131 \xrightarrow{-16} 115$	101.9	$132 \xrightarrow{-16} 116$	101.0	$131 \xrightarrow{-16} 115$	95.1	$144 \xrightarrow{-27} 117$
100.9	$131 \xrightarrow{-16} 115$	99.0	$129 \xrightarrow{-16} 113$	98.4	$130 \xrightarrow{-17} 113$	97.5	$131 \xrightarrow{-18} 113$	81.6	$130 \xrightarrow{-27} 103$
97.0	$101 \xrightarrow{-2} 99$	97.0	$101 \xrightarrow{-2} 99$	80.0	$130 \xrightarrow{-28} 102$	96.3	$147 \xrightarrow{-28} 119$	65.7‡	$80 \xrightarrow{-15} 72.5$
81.0	$131 \xrightarrow{-28} 103$	94.4	$145 \xrightarrow{-28} 117$	76.9	$130 \xrightarrow{-30} 100$	84.2	$131 \xrightarrow{-26} 105$	62.5	$160 \xrightarrow{-60} 100$
79.1	$129 \xrightarrow{-28} 101$	82.2	$129 \xrightarrow{-26} 103$	58.8‡	$73 \xrightarrow{-15} 65.5$	81.0	$131 \xrightarrow{-28} 103$	57.4‡	$72.5 \xrightarrow{-16} 64.5$
71.5	$101 \xrightarrow{-16} 85$	79.1	$129 \xrightarrow{-28} 101$	51.9	$100 \xrightarrow{-28} 72$	59.3‡	$73.5 \xrightarrow{-15} 66$	53.3	$100 \xrightarrow{-27} 73$
68.0	$72 \xrightarrow{-2} 70$	50.0‡	$65 \xrightarrow{-16} 57$	50.6	$146 \xrightarrow{-60} 86$	57.8	$131 \xrightarrow{-44} 87$	46.2	$160 \xrightarrow{-74} 86$
52.8	$101 \xrightarrow{-28} 73$	49.8	$145 \xrightarrow{-60} 85$	50.5‡	$65.5 \xrightarrow{-16} 57.5$	51.0‡	$66 \xrightarrow{-16} 58$	40.5	$86 \xrightarrow{-27} 59$
46.3	$115 \xrightarrow{-42} 73$	46.3	$115 \xrightarrow{-42} 73$	45.9	$116 \xrightarrow{-43} 73$	45.5	$117 \xrightarrow{-44} 73$	39.6	$85 \xrightarrow{-27} 58$
40.7	$131 \xrightarrow{-58} 73$	40.9	$85 \xrightarrow{-26} 59$	40.5‡	$65.5 \xrightarrow{-28} 51.5$	41.0‡	$66 \xrightarrow{-28} 52$	33.3	$160 \xrightarrow{-87} 73$
36.5	$146 \xrightarrow{-73} 73$	40.0‡	$65 \xrightarrow{-28} 51$	40.5	$86 \xrightarrow{-27} 59$	40.0	$87 \xrightarrow{-28} 59$	32.4	$160 \xrightarrow{-88} 72$
31.9	$58 \xrightarrow{-15} 43$	36.8	$145 \xrightarrow{-72} 73$	31,9	$58 \xrightarrow{-15} 43$	36.2	$147 \xrightarrow{-74} 73$	31.9	$58 \xrightarrow{-15} 43$
27.7	$73 \xrightarrow{-28} 45$	34.5	$101 \xrightarrow{-42} 59$	28.6	$74 \xrightarrow{-28} 46$	33.8	$103 \xrightarrow{-44} 59$	27.7	$73 \xrightarrow{-28} 45$
26.9	$72 \xrightarrow{-28} 44$ $129 \xrightarrow{-70} 59$	31.9	$58 \xrightarrow{-15} 43$	27.7	$73 \xrightarrow{-28} 45$	31.9	$58 \xrightarrow{-15} 43$	16.3	$59 \xrightarrow{-28} 31$
		27.7	$73 \xrightarrow{-28} 45$	26.9	$72 \xrightarrow{-28} 44$ $129 \xrightarrow{-70} 59$	29.4	$75 \xrightarrow{-28} 47$		
16.3	$59 \xrightarrow{-28} 31$	26.9	$72 \xrightarrow{-28} 44$ $129 \xrightarrow{-70} 59$	16.3	$59 \xrightarrow{-28} 31$	27.7	$73 \xrightarrow{-28} 45$		
		16.3	$59 \xrightarrow{-28} 31$			26.9	$72 \xrightarrow{-28} 44$		
						16.3	$59 \xrightarrow{-28} 31$		

The intensities of metastable peaks were strongly dependent on the electron energy used for ionization. The most intensive metastable peaks were obtained in the 25—35 eV region, with the exception of double-charge metastable peaks the intensity of which was the highest between 50 and 60 eV. These experimental results are in good agreement with the assumptions about metastable ions [10] in the quasiequilibrium theory of mass spectra.

The variation of the slit width and the increased resolution (*cf.* above), permitted the determination of the mass to charge ratio with an accuracy of $\pm 0.1-0.2$ units, as a rule. This has significantly reduced the number of m_1-m_0 mass number pairs consistent with a given metastable peak on the basis of Eq. (1).

The m^*/e values of metastable peaks detected and studied are collected in Table II, together with the dissociation processes selected by means of Eq. (1). Dissociation processes are written in the form $m_0/e \xrightarrow{m_2} m_1/e$. Metastable peaks marked by ‡ in Table II correspond to the dissociation of doubly-charged ions. Metastable peaks which proved to be connected with the transition of heavier isotopes are not included in this Table.

Often, more than one transition process could be assigned to a given metastable peak on the basis of Eq. (1). The actual dissociation process could only be determined by further studies. The identification of metastable peaks corresponding to the transition of doubly-charged ions was possible on the basis of their dependence on the ionization energy studied in a wide range, even in cases when it overlapped with a metastable peak corresponding to the transition of a single charged ion, *i.e.* when they appeared at practically the same m^*/e value in the spectrum. As an example the peak at $m^*/e = 40.5$ in the spectrum of compound **II** may be mentioned. In the case of more intensive metastable peaks the identification of the true transition process was assisted by the metastable peak that corresponded to the transition of heavier isotope ions. For example, on the basis of Eq. (1), both the $73 \xrightarrow{-28} 45$ and the $117 \xrightarrow{-60} 57$ transition can be assigned to the metastable peak at 27.7 in the spectrum of compound **II**. However, only the first alternative is acceptable because the second isotopic peak of the metastable peak at 27.7 has been found at mass number 29.4 in agreement with the first transition ($47^2/75 = 29.4$), while no peak is observed at $59^2/119 = 29.2$ corresponding to the second possible transition. The intensity of metastable isotope peaks obtained in the spectrum of compound **IV** as a result of ^{18}O labelling helped to elucidate the transition process in a similar way.

In the case of compounds **I**, **II** and **III**, two transitions corresponded, on the basis of Eq. (1), with the metastable peak at mass number 26.9 and since neither of them could be excluded, both were listed in Table II. Pathway $72 \xrightarrow{-28} 44$ seems to be more likely because this transition is observed with both compound **IV** and tetramethylsilane [8].

All metastable peaks and the corresponding transitions reported in the literature have been observed in the present study, thus these, too, are included in Table II. For compound **II** these are the metastable peaks at mass to charge ratio 79.1, 49.8, 40.9, 36.8, 27.7 and 16.3 [3] and the metastable peak at $m^*/e = 115.7$ [12] for hexamethyldisilazane.

IV. Interpretation of the experimental results

On the basis of the known poly-isotopic spectra and metastable transitions we attempted the determination of the chemical composition (empirical formula) of the ionic species corresponding to the most intensive ion peaks in the individual spectra, the elucidation of the main transition processes, including the determination of the chemical composition of neutral fragments produced by dissociation.

In the determination of empirical formulas corresponding to relatively high intensity peaks poly-isotopic spectra, *i.e.* the measured isotope ratios, were used because the natural abundance of the heavy Si-isotopes is significant. Information gathered from the study of metastable peaks were largely used for control purposes.

In the case of compounds **I** and **II**, the determination of the empirical formula corresponding to a peak at a given mass number is equivalent to answering the question whether the ionic species contains one or two silicon atoms. This question could be answered on the basis of isotope ratios in poly-isotopic spectra for the more intensive peaks, with the exception of the peak at $m/e = 85$ since at mass number 86 an independent (non-isotopic) peak is also observed. The empirical formulas of ions, at least of those responsible for a significant part of the peak intensity, have been determined on the basis of metastable transitions, both in the case of compounds **I** and **II**.

In the spectra of compound **IV**, only the question whether or not the individual ionic species contained oxygen could only be answered by ^{18}O-labelling. Once the problem of oxygen content settled, the question of empirical formulas was reduced essentially to determining the number of silicon atoms. In the case of intensive peaks, this was possible on the basis of the poly-isotopic spectra and metastable transitions. The nitrogen content for ion peaks in spectra of compounds **III** and **V** could not be studied on the basis of isotope ratios, only by utilizing metastable transitions. The empirical formulas deduced in the above manner and from isotope ratios, were checked using the generally observed phenomenon that the more important fragment peaks of compounds containing a nitrogen atom appear, as a rule, at even mass numbers [2].

The main types of ions detected in this way are listed in Table III. Empirical formulas are given in a generalized form. X stands for moieties:—, CH_2, NH, O, NCH_3 which link the two Si atoms. "+" indicates the presence and "—"

Table III

m/e	formulae	I.	II.	III.	IV.	V.
M	$(Si_2C_6H_{18}X)^+$	+	+	+	+	+
M−15	$(Si_2C_5H_{15}X)^+$	+	+	+	+	+
M−29	$(Si_2C_4H_{13}X)^+$	−	+r	+r	+r	−
M−30/2	$(Si_2C_4H_{12}X)^{++}$	−	+	+	+	+
M−31	$(Si_2C_4H_{11}X)^+$	+	+	+	+	+
M−43	$(Si_2C_3H_{11}X)^+$	+r	+r	−	+r	−
M−45	$(Si_2C_3H_9X)^+$	+	+	+	+	+
M−46/2	$(Si_2C_3H_8X)^{++}$	−	+	+	+	+
M−47	$(Si_2C_3H_7X)^+$	+	+	+	+	−
M−57	$(Si_2C_2H_9X)^+$	−	+r	+r	+r	−
M−58/2	$(Si_2C_2H_8X)^{++}$	−	+r	+r	+r	+r
M−59	$(Si_2C_2H_7X)^+$	+r	+r	+r	+r	+r
M−61	$(Si_2C_2H_5X)^+$	+	+	+	+	−
M−75	$(SiC_3H_7X)^+$	−	+	+	+	+
M−87	$(SiC_2H_7X)^+$	+r	+	+r	+r	−
M−101	$(SiCH_5X)^+$	+r	+r	+r	+r	−
M−115	$(SiH_3X)^+$	+r	+r	+r	+r	−
113	$(Si_2C_4H_9)^+$	+	+	+r	+r	−
73	$(SiC_3H_9)^+$	+	+	+	+	+
59	$(SiC_2H_7)^+$	+r	+r	+r	+r	+r
45	$(SiCH_5)^+$	+r	+r	+r	+r	+r
31	$(SiH_3)^+$	+r	+r	+r	+r	+r
29	$(SiH)^+$	+r	+r	+r	+r	+r
28	$(Si)^+$	+	+	+	+	+

the absence of a certain type ion. No mark is given in ambiguous cases. Ions to which a rearranged structure has to be attributed on the basis of their empirical formulas, are marked with an *r*. The empirical formula for the peak at mass number 117 in the spectrum of compound **V** was proved to be $Si_2C_4H_{13}^+$ on the basis of metastable transitions. Similarly, the empirical formula for the peak at mass number 103 has been found to be $Si_2C_3H_{14}^+$. These formulas are not listed in Table III. Similarly to ions at mass number 113 in the spectra of compounds **III** and **IV**, these ions can only be formed by rearrangement of the skeleton of the parent molecule (*cf.* later).

From the ion peaks in the low mass number region of the spectra only those ions exhibiting the highest intensities are listed in Table III. In the Table, ions with mass number 59, 45 and 31 (in the case of compound **I**), and those with mass number 73, 59 and 45 (in the case of compound **II**) are listed

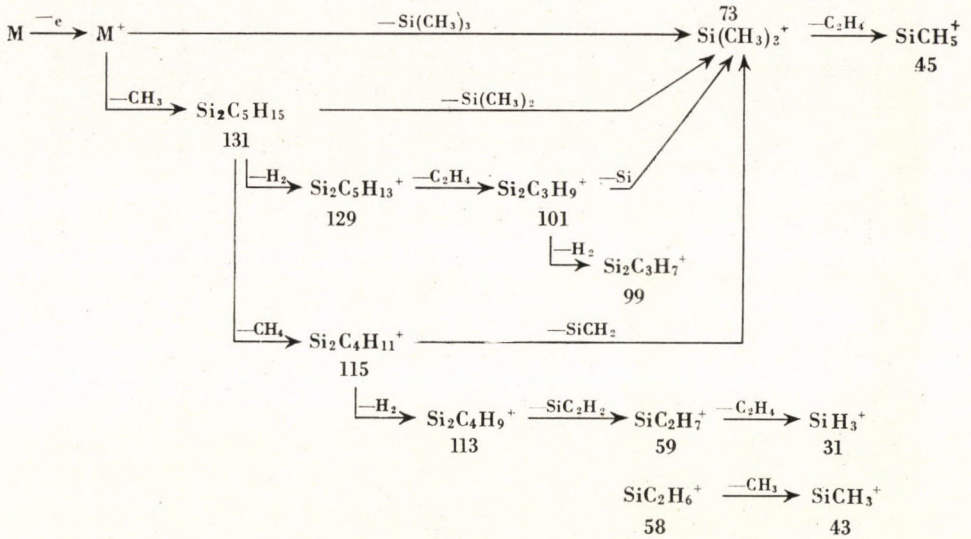

Fig. 1. Partial decomposition scheme of hexamethyldisilane

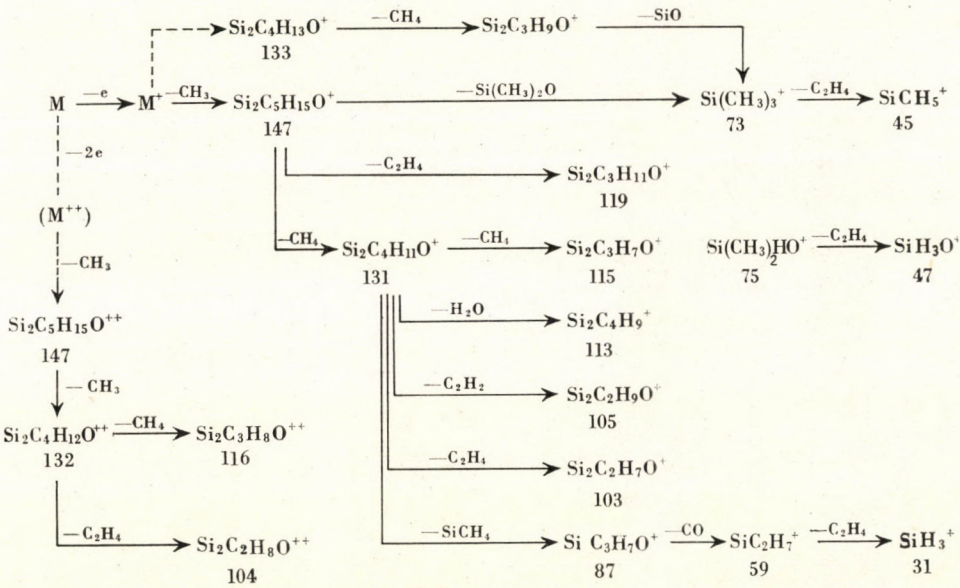

Fig. 2. Partial decomposition scheme of hexamethyldisiloxane. - - - - - assumed pathways; M++ not observed in the spectra

twice. For example, in the case of compound **II** (X = CH_2) SiC_2H_7 is the same as $SiCH_5X$, etc.

A consistent decomposition scheme including the more important ionic species can be given for each substance on the basis of transitions deduced from the metastable peaks, using properly determined empirical formulas.

Table IV

Type of reaction $e = 1$	Neutral fragments					
	I.	II.	III.	IV.	V.	
M → M− 15	CH_3	CH_3	CH_3	—	CH_3	CH_3
M−15 → M− 31	CH_4	CH_4	CH_4	CH_4	CH_4	CH_4
→ M− 43	C_2H_4	C_2H_4	—	C_2H_4	—	C_2H_4
→ M− 75	—	SiC_2H_8	SiC_2H_8	—	SiC_2H_8	SiC_2H_8
→ 73	SiC_2H_6	SiC_3H_8	—	SiC_2H_6O	SiC_3H_9N	SiC_2H_6X
M−29 → M− 45	—	CH_4	CH_4	CH_4	—	CH_4
M−31 → M− 57	—	C_2H_2	—	C_2H_2	—	C_2H_2
→ M− 59	—	C_2H_4	C_2H_4	C_2H_4	—	C_2H_4
→ 113	—	CH_4	NH_3	H_2O	—	H_2X
M−45 → 73	Si	$SiCH_2$	SiNH	SiO	—	SiX
M−59 → 59	—	$SiCH_2$	—	SiO	—	SiX
M−75 → 59	—	C_2H_2	HCN	CO	—	CX
M−87 → M−115	C_2H_4	C_2H_4	C_2H_4	C_2H_4	—	C_2H_4
73 → 45	C_2H_4	C_2H_4	C_2H_4	C_2H_4	C_2H_4	C_2H_4
59 → 31	C_2H_4	C_2H_4	C_2H_2	C_2H_4	C_2H_4	C_2H_4
58 → 43	CH_3	CH_3	CH_3	CH_3	CH_3	CH_3
$e = 2$						
M−15 → M− 30	—	—	CH_3	CH_3	CH_3	CH_3
M−30 → M− 46	—	CH_4	CH_4	CH_4	CH_4	CH_4
→ M− 58	—	C_2H_4	C_2H_4	C_2H_4	—	C_2H_4

In Figs 1 and 2, the decomposition schemes of compounds **I** and **IV**, respectively, are presented.

Table IV contains those among the principal dissociation processes which are found in the mass spectra of at least two compounds. In this Table, the empirical formulas of neutral fragments removed in the process are also listed. This is also given as a general formula, X standing for an atom or radical that links the two Si atoms. In most cases, the composition of neutral fragments has been deduced from the mass numbers of metastable transitions. In some instances, we have used the empirical ion formulas determined with the aid of isotopes.

In the bottom of the Table IV the metastable transitions found for doubly-charged ions are summarized.

After the empirical formulas for the higher intensity ion peaks had been determined the approximate calculation of the so-called mono-isotopic spectra was performed in order to determine the ratio of the abundance of individual ionic species. These are spectra which would be observed if the atoms of chem-

ical elements which form the compound would consist of only a single isotope (preferably of those with the highest natural abundance, *i.e.* ^{28}Si, ^{12}C, ^{16}O, ^{14}N, ^{1}H, in the cases under consideration). Exact calculations require that the empirical formulas of all ionic species be accurately known. Therefore, in the case of peaks for which we could not determine the empirical formula by the above method, we used the average isotope ratio of all compositions consistent with a given mass number. In the recalculation of the poly-isotopic spectra, this approximation results in an average error of $\pm 2\%$ in the peaks of mono-isotopic spectra, but never exceeds $\pm 5\%$, because this approximation had to be used only in the case of low intensity peaks.

The isotope ratio data used in the calculations have been taken from reference [2] for Si and from [13] for C, H, N and O. Table V contains the data for mono-isotopic spectra obtained by the above approximate calculations. Within one spectrum, the abundance of ions corresponding to the individual m/e values are given as % of the number of all ions. Data referring to doubly-charged ions are marked with x, while the + sign marks those for which average isotope ratios were used in the calculations. In the calculation of the amount of doubly-charged ions we have utilized the fact that in a poly-isotopic spectrum either the main peak corresponding to a given ionic species, or the first isotope peak appears always at a half mass number.

V. Conclusions

In Tables II—V constructed in the way described, the empirical formulas and relative abundances of the more important ionic species are shown. In most cases the decomposition pathways caused by electron bombardment are also presented, as deduced from the observed metastable transitions. The Tables indicate that, with some exceptions, all high intensity ions in the spectra of these compounds belong to the same type. A number of rearrangement peaks are observed in all spectra (on the basis of the empirical formulas). The decomposition and formation pathways for compounds **II**, **III** and **IV** are very similar. At the same time, as shown by Table V, the amount of the individual ion-types varies strongly and numerous specific transitions are encountered, especially in the fragmentation of compounds **I** and **V**.

On the basis of the proposed decomposition pathways, molecular ions with an odd number of electrons are transformed (mainly by the loss of methyl radicals) into ions with an even number of electrons in the first fragmentation step while as a result of further fission, ions with an even number of electrons will be formed and neutral species with an even number of electrons will be expelled.

Data in Table V show that the relative abundance of molecular ions varies between very low and medium values, significant differences being ob-

Table V

m/e	I.	II.	III.	IV.	V.
175	—	—	—	—	4.10
162	—	—	—	0.01	—
161	—	—	1.09	—	—
160	—	0.07	—	—	29.7
147	—	—	—	65.4	—
146	5.94	—	46.9	—	—
145	—	51.1	—	—	—
144	—	—	—	—	0.89
133	—	—	—	0.99	—
132	—	—	0.26	—	—
131	12.6	0.47	—	4.54	0.14+
130	—	—	20.5	—	0.62
129	0.58	4.76	0.20+	—	—
119	—	—	—	0.22	—
117	—	0.63	—	0.67	2.34
116	—	—	1.08	—	0.30
115	1.27	0.70	1.18+	0.47	0.20+
114	—	—	0.77	—	0.31
113	0.19	0.54	1.52	0.24	0.15+
105	—	—	—	0.52	—
104	—	—	0.11+	—	—
103	0.14	0.25	—	0.70	0.36
102	—	—	0.54	0.25+	0.22+
101	0.36	0.98	0.13+	0.36	0.31+
100	—	—	3.87	—	1.59
99	0.61	0.71	0.20+	—	0.24+
89	—	—	—	0.11	—
88	—	—	—	—	0.17+
87	0.16+	0.20+	0.13+	0.70+	0.15+
86	—	—	1.13	—	25.6
85	0.58	1.23	0.46+	—	0.29+
83	0.28+	0.33+	—	—	—
80	—	—	—	—	0.01×
75	—	—	—	0.47	—
74	—	—	0.99	—	—
73.5	—	—	—	0.01×	—
73	53.6	19.5	0.03× 4.67	8.42	12.9

Table V (cont.)

m/e	I.	II.	III.	IV.	V.
72.5	—	0.004×	—	—	1.09×
72	1.27×	0.50+	0.82+	0.49+	0.96+
71	0.63+	0.43+	0.31+	0.28+	0.18+
70	0.28+	0.12+	0.58+	—	0.29+
69	—	0.30+	—	—	—
66	—	—	—	2.69×	—
65.5	—	—	2.37×	—	—
65	—	1.38×	—	—	—
64.5	—	—	—	—	0.12×
61	—	—	—	0.10	—
60	—	—	0.27	—	—
59	2.08	3.25	2.28	3.45	8.38
58.5	—	—	0.12×	—	0.005×
58	1.11	0.38	0.23	0.09× 0.21	0.37
57.5	—	—	0.68×	—	—
57	0.56+	0.33+ 0.08×	0.21+	0.25+	0.30+
56	—	—	0.12+	—	0.21+
55	0.53	0.33	0.10+	0.13+	0.12+
53	0.19	—	—	—	—
52	—	—	—	0.84×	—
51.5	—	—	0.88×	—	—
51	—	0.25×	—	—	—
47	—	—	—	0.25	—
46	—	—	0.29	—	—
45	8.71	5.95	3.16	3.46	4.16
44	1.16	1.07	0.58+	0.97+	0.40+
43	3.84	1.45	0.88	0.89	1.01
42	0.22	—	—	—	0.12+
31	0.62	0.76	0.34	0.26	0.70
29	0.74	0.44	0.17	0.19	0.22
28	1.23	0.52	0.58	1.14	0.37

served in the case of compounds under consideration. The sequence in this respect is **I** > **V** > **III** > **II** > **IV**. Since the data in Table V are in % of the total abundance of ions present, this sequence can be regarded as the stability order of the molecular ions. In every case, the loss of a methyl radical from the

molecular ion leads to the formation of M—15 ions which generate very intense peaks in the spectra. Their relative abundance increases in a sequence opposite to that observed for molecular ions (*cf.* Table V).

Interesting further conclusions can be drawn from the ratio of the amounts of ionic species containing and not containing the Si—X—Si moiety. This ratio can be regarded as a measure of the resistance to electron bombardment of the structure involved. The approximate calculation of this ratio was based on the mono-isotopic spectra. In addition to the fragments, containing one Si-atom, also those ions were regarded as decomposed whose empirical formula could be interpreted only on the basis of skeleton rearrangements, *i.e.* the ions with mass numbers 117 and 103 in the spectrum of compound **V** and that with 113 in the spectrum of **III** and **IV**. The ionic species with ambiguous empirical formulas have been taken into account twice, *i.e.* as ions containing both one and two Si atoms. Consequently, two limiting per cent figures were obtained for every substance. According to the above method of calculation, the Si—X—Si moiety remains intact in the following fractions of the total amount of ions

I	**II**	**III**	**IV**	**V**
22—25%	61—63%	81—84%	78—79%	39—45%

As shown by these figures, the random deviation due to peaks associated with inaccurate empirical formulas does not invalidate the sequence deduced from the ratios obtained for the individual compounds. The order of decreasing stability of the Si—X—Si skeleton is the following: **III** > **IV** > **II** > **V** > **I**. Thus, the Si—NH—Si structure proved to be the most resistant towards electron bombardment, while the relative frequency of the Si—Si bond rupture is very high in compound **I**.

It is very interesting to compare this order of skeleton stability with the decomposition pathways found for the individual compounds. For the decomposition of the Si—Si skeleton a number of pathways were found which involve the fission of only one bond. Such are the reactions (*cf.* Fig. 1) leading to the formation of the trimethylsilyl ion ($m/e = 73$), occurring in nearly all the possible combinations in the case of this compound. In other compounds, decomposition without skeleton rearrangement is much less frequent, as indicated by abundance ratio of the ions with mass number 73.

The stability of the Si—NCH_3—Si skeleton is much lower than that of the Si—NH—Si moiety, *i.e.* the substitution of an N-hydrogen by a methyl group greatly reduces the stability of the original structure. This can be attributed to an enhanced possibility of rearrangement reactions, as a result of substitution (*cf.* Table II).

Ions formed *via* skeletal rearrangements are present in greatest abundance in the spectrum of compound **V**. According to metastable peaks at $m^*/e = 95.1$ and 81.6, such ions are formed in the following dissociation process:

$$\underset{144}{[Si_2C_4H_{11}NCH_3]^+} \xrightarrow{-HCN} \underset{117}{[Si_2C_4H_{13}]^+}$$

and

$$\underset{130}{[Si_2C_3H_9NCH_3]^+} \xrightarrow{-HCN} \underset{103}{[Si_2C_3H_{11}]^+}$$

In the case of hexamethyldisilazane (**III**) skeletal rearrangement is also observed ($m^*/e = 98.4$)

$$\underset{130}{[Si_2C_4H_{11}NH]^+} \xrightarrow{-NH_3} \underset{113}{[Si_2C_4H_9]^+}$$

A similar process can be detected in the case of compound **IV** ($m^*/e = 97.5$)

$$\underset{131}{[Si_2C_4H_{11}O]^+} \xrightarrow{-H_2O} \underset{113}{[Si_2C_4H_9]^+}$$

On the basis of analogies, it can be assumed that the following transition in the case of compound **II**, involves a skeletal rearrangement ($m^*/e = 99.0$)

$$\underset{129}{[Si_2C_4H_{11}CH_2]^+} \xrightarrow{-CH_4} \underset{113}{[Si_2C_4H_9]^+}$$

Similar expulsion reactions were recently observed by GILLIS and OCCOLOWITZ [14] in the case of organic sulfur compounds.

For practical purposes, only those processes are regarded as rearrangement processes in mass spectrometry in which the ions detected in the spectrum contain new bonds between atoms. However, if also the dissociation processes in which, instead of the ion formed, it is the expelled neutral particle that contains new bonds (*i.e.* one not present in the parent structure) are regarded as rearrangements then the empirical formulas indicate that the majority of reactions involving the destruction of the skeleton belong into the class of rearrangement processes. Among the reactions in which the skeleton is destroyed, the most important series of this category is the following.

For compound **II**:

$$\underset{145}{[Si_2(CH_3)_5CH_2]^+} \xrightarrow{-Si(CH_3)_2H_2} \underset{85}{[SiC_4H_9]^+} \xrightarrow{-C_2H_2} \underset{59}{[Si(CH_3)_2H]^+}$$

For compound **III**:

$$\underset{146}{[Si_2(CH_3)_5NH]^+} \xrightarrow{-Si(CH_3)_2H_2} \underset{86}{[SiC_3H_8N]^+} \xrightarrow{-HCN} \underset{59}{[Si(CH_3)_2H]^+}$$

and for compound **IV**, where instead of the M—15 ion the M—31 one is decomposed in a similar way:

$$\underset{131}{[Si_2C_4H_{11}O]^+} \xrightarrow{-SiCH_4} \underset{87}{[SiC_3H_7O]^+} \xrightarrow{-CO} \underset{59}{[Si(CH_3)_2H]^+}$$

In the case of compound **V**, there are two possible transitions resulting in very intensive ion peaks.

$$\underset{160}{[Si_2(CH_3)_5NCH_3]^+} \xrightarrow{-Si(CH_3)_3H} \underset{86}{[SiC_3H_8N]^+} \xrightarrow{-HCN} \underset{59}{[Si(CH_3)_2H]^+}$$

$$\xrightarrow{-Si(CH_3)_2H_2} \underset{100}{[SiC_4H_{10}N]^+} \xrightarrow{-HCN} \underset{73}{[Si(CH_3)_3]^+}$$

In the spectra of compounds **III**, **IV** and **V**, among the ions resulting from decomposition without rearrangement of the Si—X—Si skeleton, only small amounts of ions are present which carry the atom or atom group that linked the two silicon atoms in the parent molecule (*cf.* Tables III and V). In other words, if the skeleton is disrupted without rearrangement, this is usually not the fragment that carries the charge.

Since, in compounds **III**, **IV** and **V** the linking atom bonded to Si is strongly electronegative, the Si—X bond is strongly ionic. In these compounds, the original electron distribution along the Si—X bond is inhomogeneous. Presumably, this is further enhanced by the positive charge generated on one of the Si atoms as a result of the ionization of the molecule. Thus, in the case of the M—15 ion of compound **IV**, the following situation may be expected

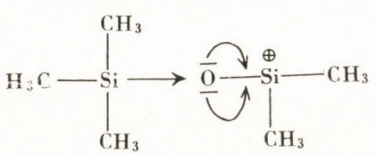

Arrows indicate the expected shift of electron density on the σ, and $p_\pi - d_\pi$ levels.

It follows from the above structure that disruption of the skeleton without rearrangement occurs heterolytically which means that it is very likely

that the oxygen-free fragment will be the one carrying the charge, thus in the reaction the following fragments

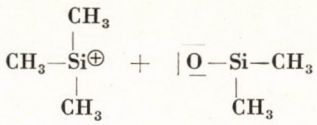

will be formed. This process is responsible also for the phenomenon that the spectrum mainly contains fragments with an even number of electrons.

Among ions with one Si atom, ionic species with hetero-atoms are generally present in small amounts. Such ions are also found among those formed by H-rearrangement, presumably containing Si—H bonds. Thus, *e.g.* the

$$\underset{31}{[SiH_3]^+},\ \underset{45}{[SiCH_3H_2]^+},\ \underset{59}{[Si(CH_3)_2H]^+}$$

series leading to intensive peaks in the spectrum of tetramethylsilane [8] as well as in spectra of the compounds under consideration occurs also in the spectrum of compounds **III** and **IV** as a series complete with NH and O but in relatively low abundance (*cf.* Tables III and V):

$$\underset{46}{[SiH_4N]^+},\ \underset{60}{[SiCH_6N]^+},\ \underset{74}{[SiC_2H_8N]^+}$$

and

$$\underset{47}{[SiH_3O]^+},\ \underset{61}{[SiCH_5O]^+},\ \underset{75}{[SiC_2H_7O]^+}$$

SHARKEY *et al.* have detected [1] the latter series, *i.e.* the ions corresponding to the oxygen variant of this type of rearrangement, in the mass spectra of trimethylsilyl ethers. As shown by Tables II and IV, the similarity of series with and without a hetero-atom is maintained also with respect to pathways of formation:

$$\underset{59}{[Si(CH_3)_2H]^+} \xrightarrow{-C_2H_4} \underset{31}{[SiH_3]^+},\ \text{and}$$

$$\underset{74}{[SiC_2H_8N]^+} \xrightarrow{-C_2H_4} \underset{46}{[SiH_4N]^+},\ \text{and}$$

$$\underset{75}{[SiC_2H_7O]^+} \xrightarrow{-C_2H_4} \underset{47}{[SiH_3O]^+}.$$

On the basis of empirical formulas, H-rearrangement ions can also be observed in the upper section of the spectra (*cf.* Table III). In these ions, the

Si—X—Si skeleton is presumably intact. The lowest amount of this ionic species is present in the case of compound **V**. The neutral particle expelled during the formation of this species also has a rearranged structure (*cf.* Table IV).

On the basis of empirical formulas, the neutral species removed as a result of decomposition with rearrangement, can be assumed to be stable products, *e.g.* trimethylsilane, dimethylsilane, methylsilane, methane, ethylene, acetylene, ammonia, hydrogen cyanide, carbon monoxide and water.

In the spectra of compounds **II**—**V** doubly-charged ions are present in significant amounts. The most probable pathway of their formation and decomposition is the following. Doubly-charged molecular ions formed as a result of electron bombardment are stabilized by the successive loss of two methyl groups. Further decomposition involves the loss of CH_4 or C_2H_4. Thus, the fragmentation pattern of these species involves the loss of one methyl radical more than that of molecular ions (*cf.* Table II) with a single positive charge.

The appearance of multi-charged ions in substantial abundance in the mass spectra of hexamethyldisiloxane and octamethyltrisiloxane has been first observed and interpreted [9] by DIBELER *et al.* In accordance with their observation that in the spectrum of tetramethylsilane there are only single charged positive ions, while those of hexamethyldisiloxane and octamethyltrisiloxane contain at most doubly and triply charged ions, respectively, the authors assume that in multi-charged ions one Si atom carries only one charge and releases one methyl radical. In the mass spectra of linear and cyclic silicon-methylene compounds, AULINGER has found a substantial amount of multiply charged ions and attributed their formation to the mechanism postulated by DIBELER [15]. The present study provides further data concerning this theory, since no ions with more than two charges have been found in the spectra of the compounds which contained two silicon atoms. On the other hand, the abundance of doubly-charged ions increases in the order **I** < **V** < **II** < **IV** < < **III** as shown by the mass spectra. This sequence is identical with the stability order of the Si—X—Si skeleton. This supports the assumption that the presence of two silicon atoms in these compounds is a necessary condition for the formation of doubly-charged ions. At the same time, in the spectra of compound **I**, no doubly-charged ions have been detected even at the highest instrument sensitivity and high ionizing-electron energies (70—90 eV). Thus DIBELER's interpretation may be extended by the statement that multiply charged species can occur only with skeletons containing isolated silicon atoms.

Since in the case of compounds **III**, **IV** and **V**, the interaction between the two Si atoms and the linking X moiety is presumably of the p_π—d_π type it is probable that this stabilizes the isolated positive charge because the electron defect can be compensated by the electrons of the coupling atom or atom group. This effect in compound **II** can only be due to hyperconjugation.

No doubly-charged ions can be formed from compound **I**. This is in agreement with the above considerations, since there is no linking atom in this compound functioning as an electron donor. Also the fact is to be taken into account that among the compounds in question the lowest effective nuclear charge (the sum of electronegativities being equal to 3.8) is associated with the Si—Si bond so that the assumption of a certain degree of charge and energy delocalization seems justified.

REFERENCES

1. SHARKEY, A. G. jr., FRIEDEL, R. A., LANGER, S. R.: Anal. Chem. **29,** 770 (1957).
2. BEYNON, J. H.: Mass Spectrometry and its Applications to Organic Chemistry. Elsevier Publ. Co., London, 1960.
3. AULINGER, F., REERINK, W.: IX. Colloquium Spectroscopium Internationale, Lyon, June 5, 1961. Tome III., p. 556.
4. FRITZ, G., GROBE, J.: Z. anorg. allg. Chem. **309,** 77 (1961).
5. AGAFONOW, J. L., LYARIN, N. V.: Zhurn. Organ. Khim. **33,** 2626 (1963).
6. CHERNYAK, N. Ya., KHMEL'NITSKIĬ, R. A., DYAKOWA, J. V., VDOVIM, V. M.: Zhurn. Org. Chim. **36,** 89 (1966).
7. POLYAKOVA, A. A., KHMEL'NITSKIĬ, R. A.: Vvedenie v massspektrometriyu organicheskikh soedineniĭ (Introduction to the Mass Spectrometry of Organic Compounds). Izd. Khimiya, Moscow, 1966.
8. TAMÁS, J., UJSZÁSZY, K.: Acta Chim. Acad. Sci. Hung. **56,** 125 (1968).
9. DIBELER, V. H., MOHLER, F. H., REESE, R. M.: J. Chem. Phys. **21,** 180 (1953).
10. MCLAFFERTY, F. W.: Mass Spectrometry of Organic Ions. Academic Press, New York, 1963.
11. HIPPLE, J. A., FOX, R. E., CONDON, E. U.: Phys. Rev. **69,** 347 (1946).
12. SILBIGER, J., LIFSHITZ, C., FUCHS, J., MANDELBAUM, A.: J. Amer. Chem. Soc. **89,** 4308 (1967).
13. BEYNON, J. H., WILLIAMS, A. E.: Mass and Abundance Tables for Use in Mass Spectrometry. Elsevier, London, 1963.
14. GILLIS, R. G., OCCOLOWITZ, J. L.: Tetrahedron Letters, 1997 (1966).
15. AULINGER, F.: VIII. Coll. Spectrosc. Internat., p. 267 (1959).

József TAMÁS
Kálmán UJSZÁSZY } Budapest VIII., Puskin u. 11—13.
György BUJTÁS

Tamás SZÉKELY, Budapest VIII., Múzeum krt. 6—8.

Acta Chimica Academiae Scientiarum Hungaricae, Tomus 62 (4), pp. 357—369 (1969)

DIPHENYL PICRYL HYDRAZIL IN MO-LCAO APPROXIMATION

M.-M. HEGYHÁTI

(Central Research Institute for Physics, Budapest)

Received October 11, 1968

The unpaired electron density distribution in DPPH as a function of a range of values of the Coulomb integral α_N for the central nitrogen atoms has been evaluated by Hückel-type molecular orbital (MO) calculations without and with overlap and McLachlan-type approximate unrestricted SCF LCAO MO calculations without and with overlap. It was assumed that the NO_2 groups of the picryl ring are not involved in the formation of the conjugated pi-electron system and that the DPPH molecule is formed by a five step "systematic perturbation" of the triphenylethyl "basic skeleton". The MO calculations with input parameters whose values lie in a reasonable range ($\alpha_N = 0.3$——0.5) will give for the ratio of unpaired electron spin densities on the hydrazine nitrogen atoms 0.76—0.86 a good agreement with the measured ratio (0.77—0.84) [1, 2] only if the McLACHLAN's spin densities are taken to be proportional to the measured values, since the splittings depend rather critically on the signs of the unpaired spin densities.

1. Introduction

The α,α-diphenyl-β-picrylhydrazil (DPPH, see Fig. 1), is one of the stable free radicals most frequently observed by paramagnetic resonance (PMR) technique.

The first MO calculation for DPPH was reported by BERSOHN [3] in 1958. The VB approach was used by BROWN *et al.* [4] in 1960 with the special aim to account for the negative spin densities, too.

The MO and VB methods, though fundamentally different in viewpoint, lead to essentially the same molecular wave function [5, 6]. However to see whether the results are truly the same, both types of calculation should be carried through step by step. For molecules sized like DPPH this seems to be impossible owing to the large number of independent canonical structures [7] and the difficulties involved in the treatment of the unpaired electron on the bonding or antibonding molecular orbitals [8] in the VB approach. Additional difficulties are presented in the VB method by the uncertainty of the resonance structures to be taken into account, since already the results of the earliest DPPH measurements [9] made WHELAND [10] to question the existence of contributions from resonance structures of the type illustrated in Fig. 2, considering that the average distances of the unpaired electron from the two nitrogen atoms of the hydrazyl grouping were found to be equal and considerably

shorter than would have been expected if this radical receives important contributions of this type.

The present computations were performed using Hückel's LCAO-MO method. In order to account for the negative spin densities, a modification of the unrestricted SCF treatment suggested by McLachlan [11] for the estimation of the pi electron densities was applied. The following calculation procedures were used: Hückel-type calculation without and with overlap and McLachlan-type treatment without and with overlap. The relationships

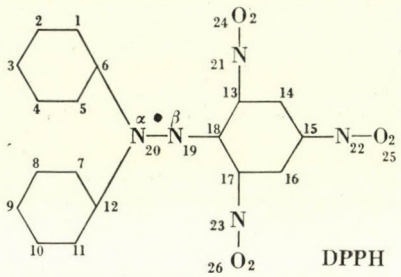

Fig. 1. Schematic representation of the molecular structure of DPPH free radical (the dot represents the odd electron)

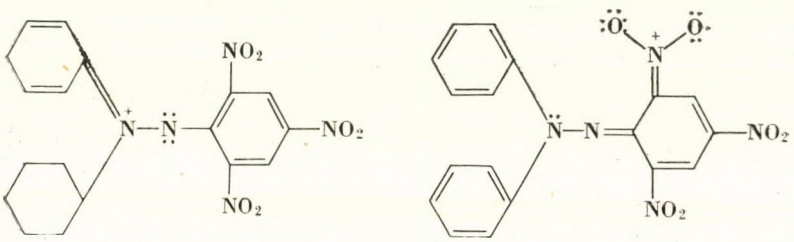

Fig. 2. Two resonant structures to DPPH free radical

between the parameters of the different procedures are discussed and the calculated values are compared with the reported experimental data on spin densities.

2. Methods of calculation

a) *Hückel-type calculation without overlap*

In this case

$$S_{ij} = (\varepsilon_i \mid \varepsilon_j) = \delta_{ij} \text{ (the unit matrix)} \qquad (1)$$

i.e. the basic AO-s are supposed to be orthonormal, thus the overlap integrals may be entirely neglected.

In the case of conjugated molecules with heteroatoms the parameters α_i and β_{ij} are written, as suggested by [12] in the form

$$\alpha_X = \alpha_{CC} + a_X\beta_{CC} \text{ and} \qquad (2)$$
$$\beta_{CX} = b_{CX}\beta_{CC} \qquad (X = \text{heteroatom}).$$

The value of α_{CC} for the carbon $2p$ orbital in unsubstituted benzene is taken as a reference point and the deviation of the Coulomb integral of the heteroatom from α_{CC} is expressed in units of the resonance integral β_{CC} characterizing a pair of carbon atoms in unsubstituted benzene. The resonance integral between a heteroatom and an adjacent carbon atom is also measured in units of β_{CC}.

b) *Hückel-type calculation with overlap*

In this case

$$S_{ij} \neq 0, \; i \neq j \; (i \text{ and } j \text{ are nearest neighbours}) \qquad (3)$$

The basic AO-s are assumed to be overlapping. It was shown [13] that in calculations with heteromolecules both the charges P_{ii} and the atom-atom (or mutual) polarizabilities π_{ij} are sensitive to the values of S_{ij}, no reliable results are to be expected unless the overlap integrals are included right from the beginning. This can be done provided that the basis functions are understood to be orthogonalized atomic orbitals Φ_i constructed from the atomic orbitals ε_j according to the criteria

$$\sum_i |\, \Phi_i - \varepsilon_i \,|^2 = \text{minimum}, \; (\Phi_i \mid \Phi_j) = \delta_{ij}. \qquad (4)$$

The solution of Eq. (4) is the so-called symmetric orthogonalization proposed by LÖWDIN [14], where the orthogonalized orbital Φ_i is the following linear combination of the AO-s ε_j

$$\Phi_i = \varepsilon_i - \frac{1}{2}\sum_{j \neq i} \varepsilon_j S_{ji} + \frac{3}{8}\sum_{jk} \varepsilon_j S_{jk} S_{ki} - + \ldots \qquad (5)$$

Thus, each Φ_i contains one main term arising from the corresponding ε_i and a small amount of the others in order to ensure the orthogonality.

c) *McLachlan-type calculation without overlap*

MCLACHLAN [11] developed a SCF MO theory of electron spin distribution which yields the observed negative spin densities. The SC wave function has the form proposed by POPLE and NESBET [15], as

$$\Psi = \| \psi_1^\alpha \psi_1'^\beta \ldots \psi_n^\alpha \psi_n'^\beta \psi_0^\alpha \| \qquad (6)$$

in which electrons of α and β spin occupy independent sets of orbitals. The spin density ϱ is then given by

$$\varrho = |\psi_0|^2 + \sum_{j=1}^{n} \{|\psi_j|^2 - |\psi'_j|^2, \tag{7}$$

or, using the LCAO semi-empirical method of PARISER and PARR [16] and introducing further neglections which, however, do not cause significant errors, as it was shown by MCLACHLAN [11], one may write for the spin density at atom i

$$\varrho_i = C_{0i}^2 - \lambda \sum_j \pi_{ij} C_{0j}^2, \tag{8}$$

where λ is an adjustable parameter. (π_{ij} is the mutual polarizability and C_{ij} are the coefficients).

MCLACHLAN further has shown that we can obtain the spin densities ϱ_i directly from (7) if we determine the coefficients in the MO-s ψ_0 and ψ_j-s from a Hückel matrix and those in the MO-s ψ'_j from a modified Hückel matrix with the off-diagonal elements β_{rs} unchanged but substituting for the diagonal elements $\alpha_r = 2\lambda C_{0r}{}^2 \beta_{CC}$.

d) *McLachlan-type calculation with overlap*

Considering the fact that for heteromolecules the overlap effects must be taken into account right from the beginning, the idea has arisen to work with atomic orbitals of the type (5) for the calculation of spin densities by MCLACHLAN's method described in *c*, since the transformation of the atomic orbitals ε_i into the orthogonalized Löwdin atomic orbitals (LAO) Φ_i takes account of the overlap.

3. Outline of the calculations on DPPH

ESR measurements show that the unpaired electron left on the β-nitrogen of the DPPH molecule upon the removal of the hydrogen is delocalized through the aromatic rings and also through the picryl ring [4]. It follows that the DPPH free radical can be treated by the MO method as a conjugated pi-electron system with the bond between α-N and β-N behaving as a quasi-double bond. In the calculations the hydrazine bond length was taken to be $\sim$1.31 Å, the length of the single bond C—N to be 1.43 Å. Both N_{19} and N_{20} are assumed to involve sp^2 hybrid orbitals. Such bonds must necessarily lie nearly in a plane perpendicular to the conjugated pi-electron orbitals so that the molecule should be as a whole (except the NO_2 groups) also planar.

It is assumed that in DPPH the NO_2 groups of the picryl ring are not involved in the formation of the conjugated pi-electron system. Though, it follows that the NO_2 groups cannot be regarded as direct centres for pi-electrons, the electrostatic effect of the nitro groups inductively still remains.

Since the nitro group removes electrons from and so increases the electron affinity of the carbon atom to which it is attached, this inductive effect can be expressed by the change of the Coulomb integral α, it can be estimated by making use of the auxiliary inductive parameter (AIP) introduced by WHELAND and PAULING [12], as

$$a_{Cn} = \delta a_{N_l}, \text{ where } \alpha_{Cn} = \alpha_C + a_{Cn}\beta_{CC}$$

$$n = 13, 15, 17 \text{ and} \qquad (9)$$

$$l = 21, 22, 23 \text{ (Fig. 1).}$$

Assuming the nitrogen of the NO_2 group to contribute two electrons to the system, $a_{\dot{N}} \approx 3a_{\dot{N}}$. If the pi-electrons of the substituent do not take part in the delocalization, the values of δ has to be taken as one third of the 1/3 characterizing the conjugated system, that is about 1/10 [17]. For the carbon atoms adjacent to N_{19} and N_{20} we take $\delta = 1/3$.

To obtain consistent results it seems, however, insufficient to calculate with even the most carefully chosen optimum possible parameter values, the present calculations were performed therefore systematically, with the aim to evaluate individually the effect of each of the assumed parameters on the same basic skeleton. As seen above, the DPPH molecule can be approximated in the Hückel-type MO approach to a system of C_{2V} symmetry with 20 atomic centres, each with a pi-electron, thus the corresponding "unperturbed" basic skeleton is the triphenylethylene (TPE) molecule of the same symmetry. As compared with DPPH the TPE molecule represents the case with $a_N = 0$, $b_N = 1$, AIP $= 0$ and $S_{ij} = 0.25$. The sequence of "perturbations" leading from TPE to DPPH is the following.

1. Introduction of the inductive effect of the NO_2 groups ($\delta = 1/10$) giving rise to diphenyl-picryl-ethylene (DPPE).

2. Introduction of a_N at the atoms 19 and 20 giving rise to triphenylhydrazine TPH (1).

3. The simultaneous introduction of AIP ($\delta = 1/3$) with a_N at the atoms 6, 12 and 18 leading to TPH (2).

4. The simultaneous introduction of perturbations 1 and 2 lead to DPPH (1).

5. Finally, the simultaneous introduction of the perturbations 1, 2 and 3 leads to DPPH (2).

It has to be noted that in the cases 2/a and 2/b (Hückel-type calculation without and with overlap) the value of the Coulomb integral $\alpha_N = \alpha_C + a_N \beta_{CC}$ for nitrogen was taken, as suggested by LAFORGUE [18], by using PAULING's scale for electronegativities: $a_N = \chi_N - \chi_C = 3.0-2.5$. In order to take account of the dependence of β_{ij} on bond length, the values of β_{ij} were estimated from the overlap integrals, as proposed by WHELAND for the carbon-carbon bonds [19]:

$$b_{ij}(r) = \frac{S_{ij}(r)}{S_{CC}(r = 1.397\,\text{Å})} . \tag{10}$$

The overlap integrals can be evaluated as shown in [20]. In the evaluation of the parameters no attempt has been made to work with values of b_{ij} computed to two decimal accuracy. According to the estimations of the bond length it was taken to be uniformly $b_{CN} = b_{NN} = 0.80$. The values of AIP corresponding to NO_2 for the carbon atoms 13, 15 and 17 were obtained by considering that $a_N = 0.5$, $a_{\ddot{N}} \simeq 1.5$ and $\delta = 1/10$, thus $a_{C_n} \simeq 0.10-0.20$. In the five steps perturbation sequence the lower limit of this value has been taken, since

Table I

Parameters of the systematic perturbation of TPE

Values of	*i, j*	TPE	DPPE	TPH(1)	TPH(2)	DPPH(1)	DPPH(2)
	19	0.0	0.0	0.5	0.5	0.5	0.5
increments	20	0.0	0.0	0.5	0.5	0.5	0.5
in α_i	6	0.0	0.0	0.0	0.1	0.0	0.1
(in β_{CC})	18	0.0	0.0	0.0	0.1	0.0	0.1
	13	0.0	0.1	0.0	0.0	0.1	0.1
β_{ij}	19—20	1.0	1.0	0.8	0.8	0.8	0.8
	6—20	1.0	1.0	0.8	0.8	0.8	0.8
(in β_{CC})	18—19	1.0	1.0	0.8	0.8	0.8	0.8

according to the SCF calculations $a_N = 0.5$ is an upper limit [21]. For the carbon atoms 6, 12 and 18 one gets with $a_N = 0.5$ and $\delta = 1/3$, $a_{C_n} \simeq 0.10-20$, again the lower limit has been taken. After having performed the computations with these values (Table I), the influence of the so-called α-effect on DPPH (2) was investigated by varying the values of α_N while the values of β and AIP were left unchanged. In the MCLACHLAN-type calculations the value of λ was also varied to see its effect on the spin density.

4. Results and discussion

In the tables and discussion the symbols q_k^H, q_k^L and ϱ_k^H, ϱ_k^L are the charges and spin densities obtained from the calculations 2/a and 2/b, respectively, while the spin densities obtained from the McLACHLAN calculations 2/c and 2/d without and with overlap are denoted by $\varrho_k^{H,M}$ and $\varrho_k^{L,M}$.

In Tables II and III are summarized the values of energy, charge, and spin density, as obtained for the "systematical perturbation" of the TPE skeleton.

Table II

Energy levels x_k^H of systematically perturbed TPE
(parameters are listed in Table I)

	k	TPE	DPPE	TPH(1)	TPH(2)	DPPH(1)	DPPH(2)
	1	2.35829	2.36408	2.29084	2.32172	2.29739	2.32796
	2	2.08397	2.12063	2.06800	2.09150	2.10423	2.12728
	3	2.00000	2.00000	2.00000	2.01751	2.00000	2.01751
	4	1.57184	1.58065	1.60235	1.60545	1.61086	1.61422
	5	1.19935	1.22684	1.19190	1.21983	1.21707	1.24481
	6	1.00000	1.05125	1.00000	1.03349	1.05125	1.05125
	7	1.00000	1.00000	1.00000	1.00000	1.00000	1.03349
x_k^H	8	1.00000	1.00000	1.00000	1.00000	1.00000	1.00000
(in β)	9	1.00000	1.00000	1.00000	1.00000	1.00000	1.00000
	10	0.43173	0.45526	0.62427	0.63892	0.64810	0.66179
	11	−0.43173	−0.40875	−0.17303	−0.17208	−0.15809	−0.15683
	12	−0.00000	−0.95125	−1.00000	−0.96688	−0.95125	−0.95125
	13	−1.00000	−1.00000	−1.00000	−1.00000	−1.00000	−0.96688
	14	−1.00000	−1.00000	−1.00000	−1.00000	−1.00000	−1.00000
	15	−1.00000	−1.00000	−1.00000	−1.00000	−1.00000	−1.00000
	16	−1.19935	−1.17355	−1.11291	−1.08103	−1.07965	−1.04711
	17	−1.57184	−1.56332	−1.31826	−1.29662	−1.31314	−1.29149
	18	−2.00000	−2.00000	−2.00000	−1.98412	−2.00000	−1.98013
	19	−2.08397	−2.04783	−2.04340	−2.02377	−2.00041	−1.98412
	20	−2.35829	−2.35400	−2.12974	−2.10391	−2.12636	−2.10051

Let us first consider the energies (Table II). The schematic representation of the MO's of these systems (Fig. 4 and Table II) shows that the fourfold degeneracy of TPE ($k = 6$, 7, 8 and 9) is eventually removed in DPPH (2) by the introduction of the NO_2 groups ($k = 6$) and the AIP parameters ($k = 7$). The AIP parameters remove also the characteristic values of 2β ($k = 3$). The orbital energy of the unpaired electron ($k = 11$) gradually decreases to attain

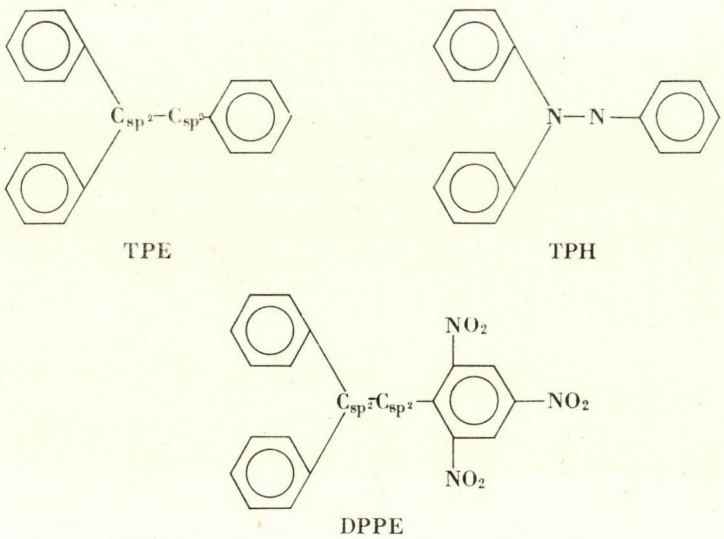

Fig. 3. Systematic perturbation of the "basic skeleton" TPE

AO / MO	1	2	3	4	5	6	7	8	9	10	11	12	13	14	15	16	17	18	19	20
1	+	+	+	+	+	+	+	+	+	+	+	+	+	+	+	+	+	+	+	+
2	+	+	+	+	+	+	+	+	+	+	+	+	−	−	−	−	−	−	−	+
3	+	+	+	+	+	+	−	−	−	−	−	−	○	○	○	○	○	○	○	○
4	−	−	−	−	−	+	−	−	−	−	−	+	−	−	−	−	−	+	+	+
5	+	−	−	−	+	+	+	−	−	−	+	+	−	+	+	+	−	−	−	+
6	○	○	○	○	○	○	○	○	○	○	○	○	+	+	○	−	−	○	○	○
7	−	+	+	+	−	−	+	−	−	−	+	+	○	○	○	○	○	○	○	○
8	−	−	○	+	+	○	○	○	○	○	○	○	○	○	○	○	○	○	○	○
9	○	○	○	○	○	○	+	+	○	−	−	○	○	○	○	○	○	○	○	○
10	+	−	−	−	+	+	+	−	−	−	+	+	+	−	−	−	+	+	−	−
11	−	−	+	−	−	+	−	−	+	−	−	+	+	+	−	+	+	−	−	+
12	○	○	○	○	○	○	○	○	○	○	○	○	−	+	○	−	+	○	○	○
13	+	+	−	+	+	−	−	−	+	−	−	+	○	○	○	○	○	○	○	○
14	+	−	○	+	−	○	+	−	○	+	−	○	○	○	○	○	○	○	○	○
15	−	+	○	−	+	○	+	−	○	+	−	○	○	○	○	○	○	○	○	○
16	+	+	−	+	+	−	+	+	−	+	+	−	+	+	−	+	+	−	+	+
17	+	+	−	+	+	−	+	+	−	+	+	−	−	−	+	−	−	+	−	+
18	−	+	−	+	−	+	+	−	+	−	+	−	○	○	○	○	○	○	○	○
19	+	−	+	−	+	−	+	−	+	−	+	−	+	−	+	−	+	−	+	+
20	+	−	+	−	+	−	+	−	+	−	+	−	−	+	−	+	−	+	−	+

Fig. 4. Schematic representation of molecular orbitals of TPE, DPPE, TPH and DPPH

its smallest (that is the most stable) value in DPPH. Also the other orbitals are getting stabilized ($k = 1, 2, 4, 5$ and 10) on going towards DPPH (2). For the better understanding of symmetry relations, the molecular orbitals are shown for benzene too (Fig. 5).

It is apparent from Table III that in the TPE skeleton the spin density at carbon 19 is not the same as that at carbon 20. In the introduction of the NO_2 groups (DPPE), the charge distribution changes according to the ori-

AO / MO	1	2	3	4	5	6
1	+	+	+	+	+	+
2	−	+	○	−	−	○
3	+	−	−	−	+	+
4	−	−	+	−	−	+
5	+	−	○	+	−	○
6	−	+	−	+	−	+

Fig. 5. Schematic representation of MO-s of benzene

entation effect of the NO_2 substituents. On the introduction of the N-s (TPH), both the charge and the spin density at the atoms 19 and 20 attain the orders of magnitude characteristic of DPPH.

The results of the calculations are given in such detail because the data seem to suggest a possible direct relationship between the calculated spin densities and the measured coupling constants. It seems that the uncertainties, referred to by R. J. WALTER [22] as being "so great that one cannot be certain that the larger coupling constant associated with nitrogen 19 really means that the unpaired electron density in the $2p_z$ orbital at atom 19 is greater than that at 20", are not so great after all. The uncertainty of [22] seems to be due to the unsuitable inclusion of the NO_2 groups. Reproducing the calculation with the artificial parameter used in [22] the system was found to be overstabilized since 16 from the 26 MO-s are bonding and only 10 antibonding.

The variations of spin densities in DPPH with the values of α_N and λ are listed in Table IV. The trend of the variations is well apparent. Any further analysis, however, would seem purely speculative in lack of sufficiently accurate experimental data.

Summarizing, it can be said that results in fair agreement with the measured values are obtained by the DPPH calculations performed with the following assumptions:

a) In DPPH free radical the pi-electronic structure is affected by the NO_2 substituents primarily through the inductive effect, but they do not enter into conjugation with the pi-electron system.

b) Both of the central nitrogens in DPPH are in the sp^2 hybrid state.

Table III

Charges and spin densites of systematically perturbed TPE
(parameters are listed in Table I)

	k	TPE	DPPE	TPH(1)	TPH(2)	DPPH(1)	DPPH(2)
q_k^L	1	1.0000	0.9964	0.9804	0.9685	0.9776	0.9658
	2	1.0000	1.0001	0.9998	1.0005	0.9998	1.0005
	3	1.0000	0.9967	0.9789	0.9705	0.9762	0.9678
	6	1.0000	1.0006	0.9934	1.0263	0.9936	1.0264
	13	1.0000	1.0453	0.9870	0.9758	1.0318	1.0203
	14	1.0000	0.9606	0.9994	1.0001	0.9600	0.9607
	15	1.0000	1.0452	0.9838	0.9758	1.0288	1.0215
	18	1.0000	0.9695	0.9879	1.0199	0.9566	0.9887
	19	1.0000	1.0092	1.1330	1.1308	1.1415	1.1393
	20	1.0000	0.9837	1.0568	1.0519	1.0404	1.0358
ϱ_k^H	1	0.0491	0.0502	0.0448	0.0455	0.0458	0.0463
	2	0.0028	0.0025	0.0004	0.0004	0.0003	0.0003
	3	0.0597	0.0598	0.0462	0.0469	0.0469	0.0475
	6	0.0220	0.0200	0.0031	0.0031	0.0026	0.0026
	13	0.0724	0.0697	0.0499	0.0507	0.0485	0.0498
	14	0.0041	0.0056	0.0004	0.0004	0.0009	0.0009
	15	0.0881	0.0869	0.0514	0.0522	0.0505	0.0518
	18	0.0325	0.0438	0.0034	0.0034	0.0074	0.0075
	19	0.2120	0.1959	0.2978	0.2946	0.2847	0.2808
	20	0.1436	0.1523	0.2677	0.2646	0.2754	0.2721
ϱ_k^L	1	0.0491	0.0504	0.0482	0.0489	0.0494	0.0499
	2	0.0028	0.0025	0.0004	0.0004	0.0004	0.0004
	3	0.0597	0.0601	0.0498	0.0505	0.0507	0.0513
	6	0.0220	0.0204	0.0041	0.0040	0.0035	0.0034
	13	0.0724	0.0687	0.0541	0.0549	0.0516	0.0528
	14	0.0041	0.0055	0.0005	0.0005	0.0010	0.0010
	15	0.0881	0.0854	0.0559	0.0567	0.0539	0.0552
	18	0.0325	0.0427	0.0045	0.0044	0.0089	0.0088
	19	0.2120	0.1987	0.2794	0.2762	0.2684	0.2646
	20	0.1436	0.1523	0.2486	0.2456	0.2566	0.2535

c) ϱ_k^H is not directly proportional to the measured splitting constant owing to the negative spin densities. However, the spin densities $\varrho_k^{H,M}$ or $\varrho_k^{L,M}$ obtained by the McLACHLAN method can be directly related to the measured values. According to [23] the nitrogen splitting A_N seems to be proportional to the calculated unpaired electron density on the nitrogen and the theoretical

Table IV

Variations of McLachlan's *spin densities* $\varrho_k^{H,M}$ *and* $\varrho_k^{L,M}$ of DPPH *with* α_N *and* λ

		$\alpha_N = 0{,}3$			$\alpha_N = 0{,}4$			$\alpha_N = 0{,}5$		
	k \ λ	1.00	1.10	1.20	1.00	1.10	1.20	1.00	1.10	1.20
$\varrho_k^{H,M}$	1	0.0532	0.0538	0.0544	0.0536	0.0543	0.0549	0.0541	0.0547	0.0552
	2	−0.0184	−0.0203	−0.0223	−0.0189	−0.0209	−0.0229	−0.0195	−0.0216	−0.0236
	3	0.0563	0.0567	0.0571	0.0541	0.0543	0.0544	0.0520	0.0520	0.0519
	6	−0.0126	−0.0148	−0.0172	−0.0179	−0.0206	−0.0234	−0.0229	−0.0260	−0.0292
	13	0.0689	0.0705	0.0721	0.0665	0.0681	0.0696	0.0642	0.0657	0.0673
	14	−0.0202	−0.0224	−0.0246	−0.0201	−0.0222	−0.0244	−0.0199	−0.0220	0.0241
	15	0.0753	0.0759	0.0786	0.0695	0.0709	0.0723	0.0644	0.0656	0.0668
	18	−0.0040	−0.0061	−0.0082	−0.0106	−0.0129	−0.0153	−0.0162	−0.0188	−0.0213
	19	0.3428	0.3509	0.3591	0.3519	0.3605	0.3693	0.3589	0.3680	0.3775
	20	0.2617	0.2643	0.2672	0.2852	0.2890	0.2932	0.3079	0.3130	0.3185
	$\frac{20}{19}$	0.76	0.75	0.74	0.81	0.80	0.79	0.86	0.85	0.84
$\varrho_k^{L,M}$	1	0.0561	0.0568	0.0576	0.0582	0.0590	0.0598	0.0605	0.0613	0.0622
	2	−0.0190	−0.0210	−0.0231	−0.0199	−0.0220	−0.0241	−0.0208	−0.0230	−0.0252
	3	0.0605	0.0611	0.0616	0.0599	0.0603	0.0607	0.0596	0.0599	0.0602
	6	−0.0110	−0.0132	−0.0155	−0.0165	−0.0191	−0.0218	−0.0218	−0.0248	−0.0278
	13	0.0714	0.0730	0.0747	0.0703	0.0719	0.0736	0.0693	0.0709	0.0726
	14	−0.0214	−0.0237	−0.0259	−0.0216	−0.0239	−0.0261	−0.0218	−0.0240	−0.0262
	15	0.0792	0.0809	0.0826	0.0748	0.0764	0.0779	0.0704	0.0718	0.0731
	18	−0.0030	−0.0051	−0.0072	−0.0095	−0.0118	−0.0141	−0.0153	−0.0178	−0.0203
	19	0.3298	0.3374	0.3452	0.3325	0.3405	0.3486	0.3328	0.3411	0.3497
	20	0.2469	0.2491	0.2615	0.2652	0.2684	0.2719	0.2825	0.2869	0.2915
	$\frac{20}{19}$	0.75	0.74	0.73	0.80	0.79	0.78	0.85	0.84	0.83

Table V

Computed and measured unpaired electron densities ϱ_k on two central N atoms of DPPH free radical

k	Bersohn [3]	Brown [4a] *et al.*	Anderson [4b]	Walter*[22] "systematic"	Walter*[22] "optimum"	DPPH**		Experimental values	
	ϱ_k^H	ϱ_k^H	ϱ_k^H	ϱ_k^H		ϱ_k^H	$\varrho_k^{H,M}$	[1] (in gauss)	[2] (in gauss)
19	0.1518	0.300	0.464	0.432	0.191	0.277	0.352	9.35±0,20	9.90±0.20
20	0.1416	0.266	0.464	0.109	0.147	0.259	0.285	7.85±0.20	7.63±0.20
$\frac{20}{19}$	0.93	0.89	1.00	0.25	0.77	0.94	0.81	0.84	0.77

(ϱ^H = Hückel-type calc., $\varrho^{H,M}$ = McLachlan-type calculation)

* Including the NO_2 groups of the picryl ring.

** This paper (McLachlan's $\lambda = 1.00$, Coulomb parameter $\alpha_N = 0.4$, resonance parameter $\beta_{CN} = 0.80$, AIP values $a_{13,\,15,\,17} = 0.10$, $a_{6,\,12,\,18} = 0.10$).

estimates of the contributions to the splitting from spin densities on adjacent atoms indicate that they should be small. Then the McConnell relation $A_N = Q\varrho_k^{H,M}$ or $A_N = Q\varrho_k^{L,M}$, $k = 19, 20$, see [24]) gives for the proportionality factor $Q = 26-28$ (see Table V and [26]). As far as we know, the measured splittings of the ring-protons has not been specified so far, even the first partial resolution of the proton hyperfine splittings reported by Deguchi [25] has not been included in the Atlas of Electron Spin Resonance Spectra edited by B. H. J. Bielski and J. M. Gebicki in 1967.

The calculations were performed on the ICT 1905 computer of the Central Research Institute for Physics with the use of a Fortran IV program. The listing of the Fortran program was made available by the courtesy of Professor R. J. Myers (D. H. Levy, Ph. D. Thesis, UCRL 11864, January 1965). The original program written for IBM 7094 computer was rewritten and slightly modified for ICT 1905 computer.

*

Thanks are due to Drs. I. Kósa-Somogyi and M. Gécs-Erő for suggesting the problem and for their helpful interest. Author is greatly indebted to Dr. J. Ladik for reading the manuscript.

REFERENCES

1. Lord, N. W., Blinder, S. M.: J. Chem. Phys. **34,** 1693 (1961).
2. Sane, K. V., Weil, J. A.: 1963, Proc. Colloq. AMPERE, 11th 1962, p. 431.
3. Bersohn, R.: Arch. sci. (Geneva) **11,** 12 (1958).
4.a. Brown, T. H., Anderson, D. H., Gutowsky, H. S.: J. Chem. Phys. **33,** 720 (1960).
4.b. Anderson, D. H.: Thesis, University of Illinois, Urbana, Illinois, 1959.
5. Wheland, G. W.: J. Chem. Phys. **2,** 474 (1934).
6. Roothaan, C. C.: Rev. Mod. Phys. **23,** 69 (1951).

7. RUMER, G.: Göttinger Nachr. p. 377 (1932).
8. WHELAND, G. W.: J. Chem. Phys. **3,** 356 (1935).
9. HUTCHISON, C. A., Jr. PASTOR, R. C., KOWALSKY, A. G.: J. Chem. Phys. **20,** 534 (1952).
10. WHELAND, G. W.: Resonance in Organic Chemistry. John Wiley et Sons New York, p. 393/a, p. 370/b (1955).
11. MCLACHLAN, A. D.: Mol. Phys. **3,** 233 (1960).
12. PAULING, L., WHELAND, G. W.: J. Am. Chem. Soc. **57,** 2086 (1935).
13. CHIRGWIN, B. H., COULSON, C. A.: Proc. Roy. Soc. (London) A**201,** 196 (1950).
14. LÖWDIN, P.-O.: J. Chem. Phys. **18,** 365 (1950).
15. POPLE, J. A., NESBET, R. K.: J. Chem. Phys. **22,** 571 (1954).
16. PARISER, R., PARR, R. G.: J. Chem. Phys. **21,** 466, 767 (1953).
17. STREITWIESER, A.: Molecular Orbital Theory for Organic Chemists, John Wiley et Sons, New York, 1961.
18. LAFORGUE, A.: J. Chem. Phys. **46,** 568 (1949).
19. OHNO, K.: Advan. Quantum Chem. **3,** 239 (1967).
20. MULLIKEN, R. S., RIECKE, A., ORLOFF, D., ORLOFF, H.: J. Chem. Phys. **17,** 1248 (1949).
21. DAUDEL, R., LEFEBVRE, R., MOSER, C.: Quantum Chemistry. Interscience Publ., New York, p. 531 (1959).
22. WALTER, R. J.: J. Am. Chem. Soc. **88,** 1930 (1966).
23. CARRINGTON, A. dos SANTOS-VEIGA, J.: Mol. Phys. **5,** 285 (1962).
24. MCCONNELL, H. M.: J. Chem. Phys. **24,** 632 (1956).
25. DEGUCHI, Y.: J. Chem. Phys. **32,** 1584 (1960).
26. HEGYHÁTI, M.-M.: J. Chem. Phys. **50,** 3123 (1969).

Magdolna M. HEGYHÁTI, Budapest, XII., Konkoly-Thege M. u.

Acta Chimica Academiae Scientiarum Hungaricae, Tomus 62 (4), pp. 371—393 (1969)

THE CRYSTAL STRUCTURE OF POTASSIUM THIOSULPHATE 1/3 HYDRATE

L. CSORDÁS

(Institute of Experimental Physics, L. Eötvös University, Budapest)

Received October 24, 1968

The structure of potassium thiosulphate 1/3 hydrate, $K_2S_2O_3 \cdot 1/3\ H_2O$ was determined. The crystals are monoclinic, space group $P\ 2_1/c$. The unit cell parameters are

$a = 9.389 \pm 0.005$ Å $\quad b = 6.006 \pm 0.006$ Å
$c = 30.98 \pm 0.01$ Å $\quad \beta = 98° 22' \pm 3'$, $Z = 12$

The (010) projection of the structure was determined by direct methods, the y_j coordinates of the atoms were determined with the aid of the system of linear structure factor equations and of the generalized projection of the electron density. The three dimensional refinement was carried out by the CRUICKSHANK $(\varrho_0 - \varrho_c)$ synthesis from 2500 independent reflections. Anisotropic temperature factor was calculated. The final R factor was 0.13 and 0.15 including the unobserved reflections too. The bond distances and bond angles of the S_2O_3 tetrahedra are in good agreement with the mean values found in other known thiosulphate structures. The H_2O molecules form a screw line around the screw axes.

Introduction

Although crystal structures of several thiosulphates have been published (TAYLOR and BEEVERS, 1952; SÁNDOR and CSORDÁS, 1961; NARDELLI, FAVA and GIRALDI, 1962; NARDELLI and FAVA, 1962) [1—4], in these crystals the asymmetric unit of the unit cell contains only one S_2O_3 group. In the Institute of Experimental Physics the structure analysis of $K_2S_2O_3 \cdot 1/3\ H_2O$ was performed. The volume of the unit cell for this crystal is larger than for any of the others, and the asymmetric unit contains three S_2O_3 groups.

Experimental procedure and crystal data

The single crystals of $K_2S_2O_3 \cdot 1/3\ H_2O$ were grown by the slow evaporation of the aqueous solution in a thermostat set at 70°C. The material was purified by repeated crystallization. The single crystals were colourless, a little elongated prisms.

The density of the crystals was determined by flotation in a mixture of bromoform and ethylene bromide at 24°C. The measured density is $2.262 \pm \pm 0.002\ g cm^{-3}$.

The unit cell dimensions and space group were obtained from Laue, oscillation and Weissenberg photographs (with Cu K_α radiation).

Crystal data [5]:

$K_2S_2O_3 \cdot 1/3\ H_2O$, $M = 196.32$

$a = 9.389 \pm 0.005$ Å
$b = 6.006 \pm 0.006$ Å
$c = 30.98 \pm 0.01$ Å
$\beta = 98° 22' \pm 3'$
$V = 1728 \pm 1$ Å^3
$Z = 12$
$D_m = 2.262 \pm 0.002$ gcm^{-3}
$D_x = 2.263$ gcm^{-3}
$\mu = 275$ cm^{-1}
$F\ (000) = 1168$

Space group $P2_1/c - C_{2h}^5$ (uniquelly determined from systematic absences).

The intensity data were obtained photometrically and by visual estimation from 3—3 levels around [100] and [010] axes, from integrated and usual equi-inclination Weissenberg photographs with multiple-film method. From these photographs 2500 independent reflections were determined with 1560 non-zero intensities. The limits of the intensities for the non-observed reflections were estimated in the usual form.

The set of the relative intensities was corrected for Lorentz and polarization factor and converted to absolute values by the statistical method of Wilson. The isotropic temperature factor was found $B = 1.86$ Å^{-2}.

Structure analysis

First the $P(u, w)$, $P(v, w)$ Patterson projections and the two Harker sections [$(u, 0, w)$ and $(u, 1/2, w)$] were calculated. The first section showed 4 great peaks and the second section showed 6 great peaks together with many lower maxima. From these patterns we could not find the positions of the S_2O_3 groups and the potassium atoms.

The structure analysis was solved by the direct phase determination. As the crystal has a centre of symmetry, we had to find only the signs of the structure factors. The Harker—Kasper inequalities were not useful for the sign determination, as the average value of the absolute values of the unitary structure factors was very small. Next the signs of the structure factors of the $(2h, 0, 2l)$ type were derived using the formula Σ_1 given by HAUPTMAN and KARLE for the space group $P2_1/c$ [6]. In this way four signs could be determined with the probability, greater than 0.9. In our space group three signs can be specified arbitrarily, which are linearly independent. Investigating the triple products of the normalized structure factors for the statistical equation of SAYRE and ZACHARIASEN [7, 8], three large structure factors [(2, 1, 4), (1, 0,

$\bar{1}0)$, $(1, 2, \bar{5})$] most often appearing in the triple products were assigned by positive signs. With the aid of these seven known signs the statistical equations gave two new signs. In this calculation and in the following one only those signs were accepted for which the probability was greater than 0.98. At this stage the signs of 12 other structure factors were specified with letters. Writing these into the table of the triple products, first we got signs in letter form, the meaning of which could be fixed step by step later from the relations found among them. As the meaning of each letter was determined, we knew altogether 55 signs. Further the investigation of this statistical equation was carried out on the computer type Ural-2, first for 350 structure factors of unknown sign. The computer printed the new signs, their probability, the number of the positive and negative relations found, transferred the data of these reflections into the set of the known reflections and striked them out from the unknown one. In this way 132 new signs were determined. Later from 150 other structure factors we got 28 further new signs, so finally we had altogether 215 known signs. From these 93 signs belonged to the (010) projection and 46 signs to the (100) projection. Knowing the final calculated structure factors, it seemed, that only 4 signs were incorrect among the 215 ones.

Using the signs determined and the absolute values of the observed structure factors, we calculated the (010) Fourier projection of the electron density. After a few attempts we could build up from this projection an approximate model of the structure in two dimensions. It was refined first by calculating the structure factors, the projection of the electron density and of the $(F_0 - F_c)$ synthesis and later by the differential synthesis in six cycles. In this stage the value of the reliability index was 0.18 for all $(h0l)$ reflections.

The determination of the third (y_j) coordinates of the atoms was not successful from the (100) projection of the electron density. The 46 known signs were very few for the good resolution, though each sign was correct. This problem was solved with two methods:

a) The system of the linear structure factor equations [9, 10]. In the space group $P\,2_1/c$ the structure factor has the form

$$F(hkl) = 4 \cdot \sum_{j=1}^{N/4} f_j \cos 2\pi(hx_j + lz_j) \cdot \cos 2\pi k y_j$$

$$k + l = 2n$$

and

$$F(hkl) = -4 \cdot \sum_{j=1}^{N/4} f_j \sin 2\pi(hx_j + lz_j) \cdot \sin 2\pi k y_j$$

$$k + l = 2n + 1.$$

If we know two coordinates of the atoms (x_j, z_j) and if we hold $k = \text{const.}$, then we can write a system of linear equations for $\cos 2\pi\, ky_j$ and for $\sin 2\pi\, ky_j$. The constants of the equations are the observed structure factors. If we don't

know their signs, we choose the unobserved reflections (puting $F = 0$) except one, the sign of which can be specified arbitrarily. If we know the signs of some of the structure factors (for instance from the direct method), then we can write those into the equations. As the observed structure factors have errors from the measurements, we used not only 22 equations for the 22 unknown coordinates, but 48 equations and the system of this linear equations was solved by the least square method.

b) The generalized projection of the electron density. As it is well known, the (010) projection of the electron density can be calculated from the $F(h0l)$ structure factors. If we put $F(hKl)$ as amplitudes into the Fourier series (where K is a const., in our case $K = 1$), we get the generalized projection of the electron density. The original maxima appear here weightened by $\cos 2\pi K y_j$. So from the conventional and from the generalized projections we can obtain the third coordinates (y_j) of the atoms.

Comparing the results of these two methods, we could find the approximate coordinates, *i.e.* the whole three-dimensional model.

Table I

Final atomic coordinates and their standard deviations

	x/a		y/b		z/c	
S_1	0.8337	(8)	0.1770	(9)	0.0094	(2)
S_2	0.2625	(9)	0.9678	(9)	0.1202	(2)
S_3	0.6796	(8)	0.7442	(11)	0.1686	(2)
S_4	0.7185	(7)	0.3256	(9)	0.0507	(2)
S_5	0.2602	(7)	0.6377	(9)	0.1261	(2)
S_6	0.8405	(7)	0.9066	(10)	0.2049	(2)
O_1	0.5700	(37)	0.2707	(39)	0.0443	(8)
O_2	0.7341	(36)	0.5630	(49)	0.0453	(7)
O_3	0.7852	(30)	0.2726	(37)	0.0948	(7)
O_4	0.1247	(23)	0.5542	(36)	0.1058	(6)
O_5	0.2809	(21)	0.5776	(30)	0.1730	(10)
O_6	0.3699	(27)	0.5495	(25)	0.1046	(6)
O_7	0.8753	(24)	0.7928	(49)	0.2468	(9)
O_8	0.9625	(25)	0.8923	(35)	0.1808	(6)
O_9	0.7928	(17)	0.1422	(31)	0.2102	(5)
K_1	0.5569	(7)	0.2488	(9)	0.1524	(2)
K_2	0.9114	(7)	0.8605	(9)	0.0939	(2)
K_3	0.2495	(7)	0.9203	(9)	0.2274	(2)
K_4	0.4950	(7)	0.8079	(9)	0.0527	(2)
K_5	0.1930	(8)	0.3181	(8)	0.0365	(2)
K_6	0.9904	(7)	0.3916	(9)	0.1731	(2)
H_2O	0.4590	(21)	0.3082	(34)	0.2358	(5)

Refinement of the structure

In the three-dimensional model the (x_j, z_j) coordinates of the atoms were more accurate than y_j, therefore first only the y_j coordinates were refined by the three-dimensional differential synthesis in three cycles. After this the refinement of the whole structure was performed in three steps. First the x_j, y_j, z_j coordinates were refined by the CRUICKSHANK $(\varrho_0 - \varrho_c)$ synthesis [11] independently (*i.e.* from the diagonal of the matrix) in four cycles, thereafter the calculation of the refinement from the full matrices of the coordinates was made again in four cycles. Finally anisotropic temperature factors were calculated. The final reliability index was $R = 0.13$ for the observed reflections only and $R' = 0.15$ including the unobserved reflections too. The final atomic coordinates and their standard deviations [12] are reported in Table I. Table II

Table II

Anisotropic thermal parameters

	b_{11}	b_{22}	$b_{33} \cdot 10^4$	b_{12}	b_{13}	b_{23}
S_1	36.80	50.89	−1.35	20.34	12.31	−3.58
S_2	14.30	15.70	−2.20	35.49	4.57	−4.79
S_3	11.05	2.00	−0.57	178.2	−4.04	2.60
S_4	2.95	21.60	−2.45	33.35	5.85	−3.06
S_5	10.03	73.62	−4.75	−33.05	6.32	−2.30
S_6	−6.00	28.66	−5.22	131.7	1.52	−1.29
O_1	19.29	147.8	1.79	−6.04	−4.99	9.01
O_2	76.29	70.90	0.19	−231.6	7.02	24.53
O_3	16.58	186.5	−1.44	179.6	20.45	−22.10
O_4	−20.23	66.14	2.74	−20.74	11.27	−10.73
O_5	−61.54	−35.53	0.72	316.2	11.48	3.47
O_6	−5.77	64.19	0.0	−175.4	−31.93	−9.77
O_7	13.32	95.64	5.17	40.61	6.21	−30.97
O_8	−46.61	−81.04	0.0	381.4	36.09	52.30
O_9	−43.50	−60.63	−1.00	279.0	−1.43	5.13
K_1	−5.02	14.37	0.10	139.7	−12.19	7.59
K_2	10.63	75.79	−2.64	91.96	−10.20	6.80
K_3	10.70	67.46	−2.15	102.9	−1.23	2.54
K_4	−5.61	65.83	1.22	173.8	14.19	1.11
K_5	46.31	46.71	−1.52	124.9	6.53	4.07
K_6	14.96	67.93	−0.75	86.45	−20.30	12.17
H_2O	−6.37	115.9	4.32	−101.2	8.87	−16.26

shows the anisotropic thermal parameters, which are the differences compared to the isotropic value, as they were calculated from the structure factors corrected by the isotropic temperature factor. The b's were used in the expression:

$$\exp[-(b_{11}h^2 + b_{22}k^2 + b_{33}l^2 + b_{12}hk + b_{13}hl + b_{23}kl)].$$

Discussion of the structure

The structure is shown in projection along the b axis in Fig. 1. The dimensions of the three S_2O_3 groups are reported in Table III. The mean values of the bond distances and bond angles with their mean errors [13] are:

S_1-S_2:	1.998 ± 0.01 Å
S_1-O:	2.820 ± 0.02 Å
S_2-O:	1.450 ± 0.02 Å
$O-O$:	2.378 ± 0.03 Å
S_1-S_2-O:	$108.8 \pm 1.0°$
$O-S_2-O$:	$110.1 \pm 1.3°$

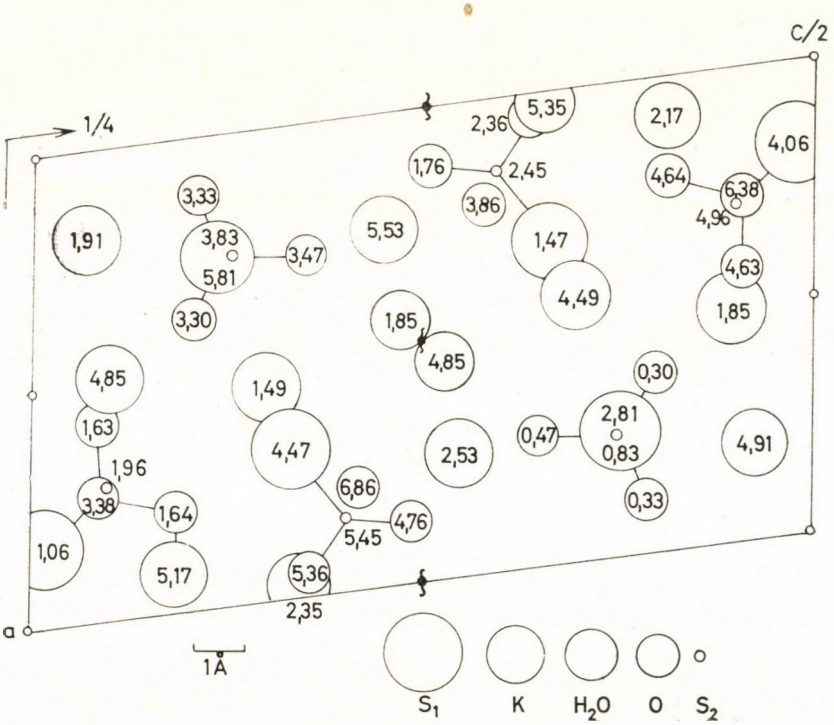

Fig. 1. The arrangement of atoms in the half of the unit cell viewed along [010]. The y_j coordinates are indicated in Å units. The full lines show the inner bonds of the S_2O_3 tetrahedra

As Table IV shows, our results are in a good agreement with the mean values found in the other thiosulphates of known structures. The deviations from the regular tetrahedron are less than in the earlier investigations, so they do not seem to be significant.

The nearest neighbours around the K atoms do not form any regular arrangement. The distances between the K atoms and their nearest neighbours

Table III

The bond distances and the bond angles in the three S_2O_3 groups

	$(S_2O_3)_1$	$(S_2O_3)_2$	$(S_2O_3)_3$
S_1-S_2	2.001 Å	2.001 Å	1.992 Å
S_1-O_1	2.790	2.775	2.775
S_1-O_2	2.808	2.835	2.806
S_1-O_3	2.898	2.848	2.848
S_2-O_1	1.419	1.459	1.409
S_2-O_2	1.446	1.461	1.425
S_2-O_3	1.452	1.500	1.481
O_1-O_2	2.325	2.386	2.308
O_1-O_3	2.334	2.456	2.369
O_2-O_3	2.368	2.458	2.393
$S_1-S_2-O_1$	107.0°	105.6°	108.1°
$S_1-S_2-O_2$	107.8	108.0	109.3
$S_1-S_2-O_3$	114.8	109.0	109.3
$O_1-S_2-O_2$	106.7°	109.6°	109.1°
$O_1-S_2-O_3$	109.1	112.1	109.2
$O_2-S_2-O_3$	111.1	112.3	111.7

Table IV

Distances and angles in the S_2O_3 group of the known thiosulphate structures

	$Na_2S_2O_3 \cdot 5H_2O$	$Na_2S_2O_3$	$MgS_2O_3 \cdot 6H_2O$	$BaS_2O_3 \cdot H_2O$	$K_2S_2O_3 \cdot 1/3H_2O$
S_1-S_2	1.97 Å	2.01 Å	2.02 Å	1.96 Å	2.00 Å
S_1-O	2.78	2.84	2.85	2.75	2.82
S_2-O	1.48	1.47	1.48	1.51	1.45
$O-O$	2.45	2.41	2.44	2.34	2.38
S_1-S_2-O	104°	108.4°	108.5°	110.1°	108.8°
$O-S_2-O$	—115	110.6	111.0	108.6	110.1

are as follows (when the coordinates are not indicated the atom is at x, y, z):

$K_1—S_3$:	3.20 Å
$K_1—S_2$ $(x, y+1, z)$:	3.27 Å
$K_1—S_3$ $(x, y+1, z)$:	3.26 Å
$K_1—O_3$:	2.99 Å
$K_1—O_6$:	2.79 Å
$K_1—O_9$ $(x, y+1, z)$:	2.71 Å
$K_1—H_2O$:	2.89 Å
$K_2—S_3$:	3.47 Å
$K_2—S_1$ $(x, y+1, z)$:	3.23 Å
$K_2—S_2$ $(x-1, y, z)$:	3.34 Å
$K_2—O_2$:	2.74 Å
$K_2—O_8$:	2.67 Å
$K_2—O_3$ $(x, y+1, z)$:	2.75 Å
$K_2—O_4$ $(x-1, y, z)$:	2.71 Å
$K_3—S_2$:	3.35 Å
$K_3—S_3$ $(1-x, 1/2+y, 1/2-z)$:	3.74 Å
$K_3—O_5$:	2.70 Å
$K_3—O_7$ $(1-x, 1/2+y, 1/2-z)$:	2.70 Å
$K_3—O_9$ $(1-x, 1/2+y, 1/2-z)$:	2.63 Å
$K_3—O_8$ $(x-1, y, z)$:	2.87 Å
$K_3—H_2O$ $(x, y+1, z)$:	3.04 Å
$K_3—H_2O$ $(1-x, 1/2+y, 1/2-z)$:	2.89 Å
$K_4—S_2$:	3.37 Å
$K_4—S_3$:	3.77 Å
$K_4—O_2$:	2.72 Å
$K_4—O_6$:	2.63 Å
$K_4—O_1$ $(x, y+1, z)$:	2.89 Å
$K_5—S_2$ $(x, y+1, z)$:	3.33 Å
$K_5—S_1$ $(x-1, y, z)$:	3.46 Å
$K_5—S_1$ $(1-x, \bar{y}, \bar{z})$:	3.29 Å
$K_5—O_4$:	2.73 Å
$K_5—O_6$:	2.85 Å
$K_6—S_3$:	3.59 Å
$K_6—O_9$ $(x, y+1, z)$:	2.76 Å
$K_6—O_4$ $(x-1, y, z)$:	2.77 Å
$K_6—O_5$ $(x-1, y, z)$:	2.95 Å
$K_6—O_8$:	3.03 Å
$K_6—O_8$ $(x, y+1, z)$:	3.02 Å

The mean errors in the distances between the K—S are: $\pm$ 0.01 Å, between the K—O: $\pm$0.02 Å.

Table V

Observed and calculated structure factors (x10)

The signs of the observed structure factors were determined by the direct method. Unobserved reflections are indicated by an asterisk

	$10 \cdot F_o$	$10 \cdot F_c$
l	0 0 *l*	
2	—	— 88
4	300	— 402
6	200	145
8	400	— 453
10	600	— 719
12	552	— 475
14	1760	—1793
16	545	— 643
18	+1880	1884
20	535	525
22	+1050	1068
24	+1260	1259
26	593	— 596
28	— 944	—1072
30	* 160	165
32	* 160	— 291
34	+ 780	891
36	—1190	—1339
38	— 975	— 901
	0 1 *l*	
1	400	— 275
2	580	386
3	302	— 198
4	500	— 364
5	600	508
6	— 840	— 798
7	880	— 857
8	—1540	—1572
9	+1740	1743
10	471	— 516
11	* 100	— 199
12	* 80	178
13	+ 707	757
14	635	— 630
15	850	852
16	412	— 442
17	425	— 426
18	735	727
19	* 110	179
20	* 110	190
21	* 120	17
22	420	— 540
23	405	— 416
24	354	352
25	242	159
26	268	396
27	* 140	— 180
28	—1080	—1151
29	820	— 671
30	— 925	—1022
31	* 170	128
32	* 160	— 19
33	500	437
34	565	— 616
35	392	540
36	* 140	— 5
37	— 850	— 862
38	— 655	— 609
	0 2 *l*	
0	1870	—1667
1	+1680	1657
2	—1060	— 912
3	* 60	55
4	845	— 674
5	+1420	1417
6	680	— 603
7	+ 775	683
8	550	593
9	484	— 407
10	1950	1738
11	565	— 541
12	653	— 685
13	214	215
14	* 90	38
15	435	— 553
16	455	521
17	— 988	—1264
18	* 110	31
19	— 555	— 755
20	—1060	—1176
21	396	— 494
22	— 388	— 408
23	395	421
24	— 400	— 363
25	* 140	196
26	* 140	301
27	* 150	— 113
28	* 150	232
29	— 518	— 491
30	* 170	174
31	* 160	42
32	* 170	— 227
33	—1060	—1163
34	* 150	329
35	340	392
36	* 130	38
37	394	390
	0 3 *l*	
1	* 90	38
2	+1590	1507
3	405	— 316
4	314	220
5	* 90	— 163
6	* 90	— 54
7	590	469
8	— 860	— 886
9	— 556	— 538
10	1540	1428
11	—1420	—1296
12	* 110	— 69
13	— 755	— 899
14	* 110	32
15	226	— 313
16	* 170	201
17	468	576
18	537	— 717
19	— 695	— 908
20	278	— 346
21	— 658	— 701
22	490	520
23	471	509
24	465	— 438
25	+ 828	910
26	* 150	186
27	341	266
28	665	653
29	227	— 251
30	— 640	— 557
31	* 160	259
32	* 150	133
33	* 140	155
34	822	810
35	* 120	53
36	550	663
	0 4 *l*	
0	— 565	— 591
1	189	162
2	268	225
3	—1450	—1315
4	443	— 443
5	—1360	—1279
6	338	252
7	468	— 534
8	342	368
9	366	— 323
10	876	— 937
11	627	672
12	420	421
13	* 130	— 75
14	* 130	— 85
15	955	1099
16	* 140	— 188
17	+ 888	1054
18	* 140	194
19	+1300	1374
20	* 150	299
21	* 150	— 51
22	— 547	— 696
23	242	— 472
24	292	— 371
25	* 160	— 85
26	740	804
27	328	410
28	* 160	189
29	* 150	— 114
30	540	— 510
31	* 120	286
32	* 120	105
33	* 110	9

	$10 \cdot F_o$	$10 \cdot F_c$
	0 5 *l*	
1	* 140	77
2	* 140	253
3	* 140	16
4	* 140	− 199
5	422	− 361
6	+1020	883
7	1050	954
8	* 140	124
9	242	− 292
10	348	329
11	+ 532	496
12	* 160	296
13	* 160	91
14	* 150	− 119
15	435	411
16	765	− 853
17	920	979
18	415	443
19	* 160	− 78
20	650	664
21	390	− 406
22	528	− 423
23	276	149
24	* 150	66
25	* 150	− 197
26	* 140	193
27	* 130	− 160
28	* 120	123
29	355	− 366
30	+1030	987
	0 6 *l*	
0	* 150	− 276
1	* 150	39
2	+1520	1431
3	* 150	245
4	242	407
5	294	479
6	680	− 634
7	292	− 242
8	445	377
9	848	818
10	* 160	− 6
11	326	185
12	664	− 737
13	1120	− 966
14	* 170	− 117
15	710	− 621
16	760	669
17	* 150	184
18	* 150	− 204
19	* 150	101
20	544	374
21	242	236
22	495	477
23	565	− 453
24	* 110	253

	$10 \cdot F_o$	$10 \cdot F_c$
	0 7 *l*	
1	* 150	142
2	* 150	131
3	* 150	2
4	* 150	8
5	* 150	− 218
6	−1020	− 942
7	* 140	56
8	* 140	− 60
9	* 140	− 85
10	* 130	− 144
11	822	675
12	* 120	− 213
13	* 120	− 50
14	* 110	− 124
15	566	− 470
16	* 90	− 115
	1 0 *l*	
−38	−1090	−1087
−36	* 290	− 156
−34	660	878
−32	624	627
−30	* 300	− 333
−28	1300	1404
−26	2060	−1950
−24	540	− 679
−22	−1300	−1151
−20	1310	−1408
−18	+ 970	943
−16	−1030	−1123
−14	−1050	−1195
−12	655	786
−10	+4300	4300
− 8	465	− 445
− 6	1210	−1172
− 4	* 170	160
− 2	610	− 604
0	—	300
2	631	− 446
4	* 150	50
6	1630	1513
8	445	559
10	408	424
12	+ 960	1067
14	333	− 268
16	885	841
18	−2110	−2225
20	* 240	158
22	+1610	1586
24	+1580	1656
26	* 250	240
28	* 300	− 51
30	+1900	1919
32	+ 575	− 644
34	* 300	52
36	925	− 890
38	820	− 828

	$10 \cdot F_o$	$10 \cdot F_c$
	1 1 *l*	
−38	+1080	1264
−37	* 140	106
−36	* 160	− 165
−35	−1070	−1111
−34	916	− 990
−33	* 180	− 143
−32	324	535
−31	487	− 456
−30	352	− 508
−29	* 160	99
−28	+1190	−1087
−27	796	616
−26	221	289
−25	605	− 621
−24	* 140	223
−23	290	352
−22	* 130	− 102
−21	* 120	− 104
−20	650	627
−19	763	750
−18	+1600	1599
−17	970	− 990
−16	* 90	127
−15	174	− 227
−14	302	390
−13	550	− 562
−12	* 90	− 31
−11	380	− 297
−10	* 70	123
− 9	+1470	1531
− 8	+1560	1549
− 7	670	− 640
− 6	625	627
− 5	660	496
− 4	* 50	50
− 3	302	− 253
− 2	270	81
− 1	358	− 166
0	890	766
1	720	443
2	745	573
3	* 90	188
4	880	− 678
5	569	− 565
6	802	− 810
7	118	− 135
8	* 90	84
9	129	191
10	615	667
11	900	882
12	645	− 750
13	705	751
14	+1400	1502
15	540	593
16	1200	1210
17	224	− 190
18	127	4

	$10 \cdot F_o$	$10 \cdot F_c$
19	598	— 543
20	590	— 518
21	870	931
22	1080	1110
23	626	— 655
24	1100	—1080
25	720	733
26	172	— 36
27	1140	—1096
28	705	— 666
29	* 180	— 150
30	—1400	—1359
31	840	756
32	* 200	— 137
33	641	588
34	480	310
35	401	402
36	420	— 402
37	595	— 681
	1 2 *l*	
—37	380	— 158
—36	351	250
—35	445	— 562
—34	* 100	— 107
—33	352	— 340
—32	372	— 391
—31	* 110	— 8
—30	642	— 700
—29	* 110	253
—28	* 110	55
—27	+2020	2229
—26	389	417
—25	* 100	— 196
—24	381	456
—23	205	170
—22	154	193
—21	465	566
—20	856	1201
—19	* 80	— 49
—18	770	1031
—17	234	294
—16	825	— 912
—15	466	— 505
—14	701	785
—13	410	— 547
—12	* 60	— 34
—11	862	— 807
—10	1230	—1149
— 9	1450	1269
— 8	1270	—1051
— 7	210	— 208
— 6	148	— 129
— 5	+2040	2063
— 4	845	— 778
— 3	1090	943
— 2	1610	1240
— 1	1230	—1008
0	1260	1158
1	1050	830
2	2060	—1709
3	1170	937
4	* 50	11
5	372	296
6	1440	1168
7	214	229
8	494	— 410
9	390	— 455
10	1080	—1053
11	536	— 607
12	138	— 145
13	+1650	1690
14	576	— 480
15	482	— 409
16	546	573
17	* 130	— 76
18	* 130	96
19	705	— 602
20	475	— 357
21	742	— 713
22	352	— 346
23	580	— 533
24	701	— 537
25	630	425
26	422	— 364
27	836	652
28	585	— 706
29	264	— 430
30	* 170	15
31	493	468
32	246	— 259
33	451	— 445
34	565	633
35	725	1044
36	270	— 256
	1 3 *l*	
—36	335	542
—35	+1810	1864
—34	* 90	— 224
—33	715	750
—32	* 100	108
—31	* 110	— 134
—30	455	501
—29	* 110	55
—28	* 120	236
—27	656	594
—26	* 110	22
—25	* 110	266
—24	* 110	— 298
—23	706	— 680
—22	* 100	91
—21	729	— 748
—20	1510	—1466
—19	202	315
—18	860	889
—17	798	800
—16	* 80	— 14
—15	* 80	180
—14	* 80	— 98
—13	213	— 281
—12	310	— 343
—11	430	517
—10	314	— 263
— 9	266	— 270
— 8	+1580	1409
— 7	286	— 282
— 6	312	— 357
— 5	107	123
— 4	911	— 698
— 3	471	356
— 2	770	— 580
— 1	1040	698
0	1040	789
1	1020	— 773
2	1040	— 974
3	* 60	— 65
4	296	303
5	* 60	83
6	350	302
7	288	291
8	* 70	— 42
9	—1900	—1575
10	203	— 178
11	—1650	—1443
12	607	565
13	455	— 470
14	930	— 965
15	120	— 156
16	334	471
17	278	— 362
18	571	653
19	* 90	— 136
20	1460	—1425
21	140	178
22	141	225
23	775	795
24	306	308
25	304	— 340
26	535	614
27	202	— 167
28	510	— 546
29	* 120	117
30	* 110	177
31	* 110	— 170
32	292	340
33	900	—1150
34	250	— 405
35	972	—1120
36	636	621
	1 4 *l*	
—33	413	486
—32	386	— 565

	$10 \cdot F_o$	$10 \cdot F_c$
−31	* 100	− 4
−30	411	424
−29	−1290	−1604
−28	* 110	− 86
−27	448	− 362
−26	351	476
−25	725	− 722
−24	* 120	− 156
−23	238	− 208
−22	304	265
−21	* 110	− 62
−20	* 110	46
−19	489	− 523
−18	445	− 688
−17	541	788
−16	880	917
−15	238	299
−14	157	− 139
−13	404	375
−12	* 90	− 128
−11	680	− 756
−10	* 90	148
− 9	* 90	85
− 8	268	− 144
− 7	−1310	−1011
− 6	248	− 383
− 5	−1080	−1010
− 4	925	836
− 3	133	− 204
− 2	* 80	148
− 1	545	− 462
0	1720	−1463
1	344	309
2	489	442
3	302	− 155
4	247	194
5	497	− 387
6	1010	− 879
7	326	207
8	1200	1080
9	* 90	− 28
10	* 90	− 106
11	1080	− 974
12	− 828	− 909
13	* 90	− 254
14	620	618
15	311	− 300
16	171	129
17	705	653
18	173	181
19	188	137
20	595	− 476
21	592	588
22	535	− 505
23	650	622
24	200	− 176
25	355	338
26	* 120	181
27	* 110	11
28	* 110	12
29	1210	−1277
30	424	− 510
31	348	394
32	576	663

1 5 *l*

−29	* 100	− 67
−28	* 110	− 218
−27	* 120	− 109
−26	585	712
−25	461	757
−24	185	− 327
−23	249	− 291
−22	* 140	− 123
−21	* 140	105
−20	256	− 343
−19	440	− 284
−18	* 150	99
−17	415	447
−16	760	− 811
−15	591	− 699
−14	242	− 223
−13	188	− 122
−12	488	456
−11	550	439
−10	* 100	27
− 9	421	− 476
− 8	140	− 217
− 7	383	397
− 6	625	− 664
− 5	440	− 353
− 4	* 100	− 115
− 3	220	216
− 2	170	− 180
− 1	* 100	71
0	* 100	− 7
1	440	− 449
2	* 100	0
3	382	− 484
4	441	− 523
5	626	683
6	384	− 405
7	385	439
8	835	890
9	545	563
10	448	466
11	189	128
12	244	− 305
13	910	843
14	460	− 430
15	* 110	124
16	455	− 343
17	204	393
18	262	− 275
19	256	− 241
20	* 110	164
21	645	− 550
22	* 110	186
23	540	487
24	1039	−1014
25	717	− 742
26	625	592
27	* 90	201
28	565	751
29	658	523

1 6 *l*

−25	895	1031
−24	833	− 851
−23	738	838
−22	874	− 857
−21	261	− 362
−20	* 120	176
−19	178	− 183
−18	461	− 500
−17	* 130	63
−16	556	− 450
−15	256	− 223
−14	* 140	− 128
−13	206	− 126
−12	661	578
−11	* 140	− 293
−10	* 140	− 224
− 9	* 140	20
− 8	954	817
− 7	650	556
− 6	* 150	6
− 5	* 150	− 61
− 4	508	− 472
− 3	* 150	75
− 2	535	495
− 1	958	904
0	169	163
1	207	103
2	206	− 141
3	460	− 462
4	205	90
5	205	− 169
6	526	529
7	* 140	110
8	* 140	− 52
9	536	504
10	* 140	− 20
11	* 140	− 162
12	* 150	112
13	518	− 401
14	444	431
15	193	330
16	589	− 598
17	461	385
18	* 130	200
19	520	− 448
20	512	210

	$10 \cdot F_o$	$10 \cdot F_c$
21	190	— 302
22	684	709
23	119	7
24	651	686
	1 7 *l*	
—16	921	855
—15	* 90	— 231
—14	* 100	— 133
—13	* 110	140
—12	* 110	— 111
—11	* 110	— 10
—10	906	630
— 9	* 120	— 89
— 8	* 120	143
— 7	* 120	142
— 6	222	293
— 5	229	— 326
— 4	* 130	17
— 3	* 130	37
— 2	* 130	316
— 1	* 130	— 37
0	472	526
1	462	447
2	* 130	— 166
3	* 130	133
4	397	— 386
5	222	— 196
6	* 120	15
7	379	— 317
8	* 120	— 146
9	* 120	102
10	* 110	107
11	* 110	141
12	273	100
13	* 100	— 132
14	290	169
15	206	109
	2 0 *l*	
—38	1130	1087
—36	* 290	— 203
—34	* 290	— 342
—32	* 300	— 9
—30	605	— 661
—28	+1200	1388
—26	—1390	—1359
—24	—1980	—1950
—22	675	— 623
—20	605	718
—18	— 815	— 821
—16	—1010	—1039
—14	362	— 453
—12	862	849
—10	706	— 934
— 8	890	892
— 6	498	576
— 4	* 170	— 203

	$10 \cdot F_o$	$10 \cdot F_c$
— 2	596	— 475
0	—1660	—1546
2	* 160	45
4	970	— 770
6	515	340
8	—3190	—3294
10	418	— 507
12	+2760	2801
14	* 260	176
16	681	745
18	* 280	— 62
20	+1060	1176
22	496	483
24	476	— 379
26	* 280	9
28	* 300	— 70
30	* 320	— 323
32	* 320	— 239
34	+ 730	809
36	+ 714	897
38	* 230	— 117
	2 1 *l*	
—38	1060	— 990
—37	885	741
—36	+1010	1044
—35	—1640	—1599
—34	446	— 504
—33	* 180	292
—32	* 180	— 216
—31	* 180	— 97
—30	* 160	— 5
—29	* 160	— 101
—28	247	— 253
—27	480	— 401
—26	274	— 232
—25	655	— 682
—24	1160	— 943
—23	428	412
—22	1180	—1077
—21	400	485
—20	645	— 555
—19	716	650
—18	+1820	1703
—17	333	— 280
—16	435	439
—15	* 90	— 82
—14	1320	1250
—13	663	— 755
—12	183	182
—11	702	— 655
—10	725	774
— 9	1090	—1152
— 8	642	640
— 7	* 60	— 70
— 6	545	— 447
— 5	—1260	—1182
— 4	2230	—2025

	$10 \cdot F_o$	$10 \cdot F_c$
— 3	845	636
— 2	332	313
— 1	241	— 186
0	1210	— 979
1	1170	1110
2	990	— 637
3	1530	1284
4	2680	2532
5	220	— 155
6	1860	1789
7	* 100	199
8	256	217
9	1620	—1463
10	551	666
11	590	559
12	1050	1200
13	652	— 729
14	338	— 371
15	158	323
16	546	752
17	356	— 518
18	* 120	— 263
19	179	— 292
20	1010	—1115
21	1040	1094
22	815	807
23	* 150	171
24	606	676
25	355	421
26	* 160	— 142
27	* 160	— 201
28	* 160	234
29	* 170	— 164
30	410	314
31	* 180	302
32	870	— 696
33	* 160	108
34	* 160	— 264
35	* 140	— 169
36	* 130	220
37	663	680
	2 2 *l*	
—37	655	959
—36	* 160	69
—35	626	— 717
—34	* 170	— 181
—33	535	— 536
—32	* 190	— 5
—31	* 190	140
—30	656	523
—29	* 170	— 185
—28	730	647
—27	+1180	1169
—26	625	— 684
—25	1110	—1096
—24	784	825
—23	* 150	— 8

	$10 \cdot F_o$	$10 \cdot F_c$
−22	794	656
−21	* 140	67
−20	* 140	− 273
−19	740	− 642
−18	270	250
−17	120	7
−16	288	281
−15	622	779
−14	329	− 215
−13	662	− 745
−12	758	835
−11	165	− 200
−10	871	914
− 9	* 120	106
− 8	1590	1308
− 7	252	249
− 6	246	263
− 5	+1670	1391
− 4	821	588
− 3	744	469
− 2	685	− 388
− 1	680	− 638
0	1130	− 849
1	1140	889
2	1220	1161
3	+1540	1334
4	390	− 237
5	444	− 369
6	550	678
7	+1510	1169
8	444	500
9	550	− 630
10	326	330
11	877	− 846
12	258	321
13	465	571
14	397	− 509
15	258	− 279
16	288	− 461
17	705	909
18	675	− 894
19	300	412
20	* 140	5
21	319	− 281
22	275	− 242
23	* 160	199
24	* 160	7
25	+1230	1208
26	731	− 640
27	* 170	280
28	464	380
29	304	− 362
30	731	700
31	* 180	− 161
32	* 180	− 249
33	* 170	− 133
34	626	− 628
35	* 140	95

	$10 \cdot F_o$	$10 \cdot F_c$
	2 3 *l*	
−36	690	843
−35	670	683
−34	908	− 924
−33	* 160	− 158
−32	582	603
−31	* 180	− 105
−30	803	− 709
−29	+1260	1121
−28	248	218
−27	472	485
−26	1050	1142
−25	236	280
−24	* 170	50
−23	* 150	− 152
−22	483	− 496
−21	* 150	− 58
−20	* 150	176
−19	481	− 470
−18	469	507
−17	487	− 608
−16	758	− 780
−15	* 120	136
−14	435	− 460
−13	+1510	1468
−12	163	− 218
−11	+1440	1303
−10	251	− 278
− 9	372	383
− 8	* 90	− 73
− 7	421	498
− 6	355	500
− 5	+1460	1618
− 4	302	335
− 3	302	313
− 2	1020	907
− 1	820	− 691
0	345	− 337
1	−1800	−1571
2	349	− 329
3	554	− 639
4	* 80	9
5	311	301
6	465	− 540
7	* 90	− 183
8	445	625
9	350	240
10	1700	−1548
11	477	653
12	* 110	− 170
13	469	611
14	412	532
15	244	− 222
16	522	670
17	* 130	− 138
18	670	− 777
19	274	307
20	* 150	133

	$10 \cdot F_o$	$10 \cdot F_c$
21	398	− 422
22	530	613
23	680	− 810
24	748	− 837
25	750	− 897
26	* 190	295
27	* 180	334
28	* 190	248
29	630	749
30	511	− 485
31	405	− 607
32	* 150	205
33	827	− 814
34	* 140	52
	2 4 *l*	
−33	* 120	78
−32	* 140	213
−31	* 150	− 14
−30	* 160	− 70
−29	690	− 700
−28	692	− 799
−27	655	501
−26	826	923
−25	454	− 462
−24	* 180	152
−23	* 160	7
−22	* 160	− 150
−21	382	325
−20	585	711
−19	308	428
−18	626	− 678
−17	217	443
−16	* 150	10
−15	* 150	25
−14	1210	1323
−13	* 140	− 69
−12	710	− 723
−11	609	574
−10	776	− 795
− 9	* 130	53
− 8	585	463
− 7	1300	−1033
− 6	* 130	− 75
− 5	510	− 506
− 4	* 120	− 78
− 3	883	− 762
− 2	990	870
− 1	* 120	− 104
0	168	183
1	985	−1019
2	832	− 762
3	* 130	− 57
4	940	839
5	751	− 650
6	* 130	− 225
7	965	843
8	246	247

	$10 \cdot F_o$	$10 \cdot F_c$
9	* 130	— 149
10	* 130	— 182
11	* 140	— 105
12	1065	— 917
13	611	743
14	392	401
15	686	— 660
16	* 150	— 188
17	* 170	— 227
18	* 170	244
19	1060	— 985
20	* 170	191
21	* 180	— 123
22	* 180	— 27
23	480	— 350
24	* 170	— 267
25	461	— 344
26	* 170	47
27	715	— 631
28	* 150	42
29	376	285
30	354	— 232
31	520	471
32	359	257
	2 5 *l*	
—29	273	— 143
—28	490	412
—27	258	— 476
—26	* 150	— 170
—25	415	— 242
—24	254	316
—23	* 170	115
—22	655	651
—21	521	341
—20	* 180	35
—19	* 180	225
—18	466	— 546
—17	* 180	26
—16	670	— 756
—15	* 170	— 206
—14	471	— 370
—13	305	— 226
—12	* 170	— 165
—11	263	— 314
—10	* 150	130
— 9	1260	—1214
— 8	* 150	22
— 7	1190	— 932
— 6	351	261
— 5	392	227
— 4	* 150	— 115
— 3	* 150	— 190
— 2	1040	913
— 1	555	461
0	* 150	83
1	279	252
2	555	— 617

	$10 \cdot F_o$	$10 \cdot F_c$
3	392	318
4	350	— 324
5	759	655
6	— 990	— 843
7	488	— 372
8	630	— 639
9	* 170	— 77
10	* 170	— 120
11	610	— 585
12	427	291
13	* 170	212
14	738	— 670
15	670	— 671
16	* 180	282
17	* 180	34
18	555	498
19	625	663
20	415	— 444
21	* 170	71
22	* 160	182
23	430	390
24	* 150	149
25	* 150	— 204
26	551	— 573
27	* 120	113
28	690	— 739
	2 6 *l*	
—24	585	— 496
—23	321	— 208
—22	245	— 168
—21	251	— 356
—20	465	— 396
—19	568	466
—18	* 160	— 23
—17	* 160	— 88
—16	382	— 270
—15	545	— 418
—14	640	— 502
—13	* 180	68
—12	* 180	262
—11	700	612
—10	550	354
— 9	* 180	76
— 8	455	— 319
— 7	565	— 357
— 6	* 180	— 47
— 5	419	— 479
— 4	333	361
— 3	575	399
— 2	811	— 682
— 1	938	767
0	254	— 286
1	254	— 191
2	254	— 252
3	254	— 159
4	318	170
5	663	502

	$10 \cdot F_o$	$10 \cdot F_c$
6	1094	— 810
7	* 180	166
8	* 170	79
9	* 170	— 41
10	* 180	129
11	* 180	— 164
12	* 180	232
13	* 170	— 141
14	606	663
15	* 160	138
16	300	— 245
17	410	— 346
18	387	335
19	* 140	— 139
20	* 130	11
21	918	742
22	398	341
23	680	531
	2 7 *l*	
—16	554	370
—15	* 100	— 132
—14	500	311
—13	* 130	— 49
—12	415	456
—11	* 130	— 152
—10	610	545
— 9	864	626
— 8	497	— 501
— 7	* 150	146
— 6	512	— 490
— 5	* 150	— 100
— 4	* 150	113
— 3	485	— 344
— 2	560	— 596
— 1	* 150	12
0	* 150	97
1	* 150	— 23
2	477	372
3	* 150	21
4	* 150	91
5	* 150	— 121
6	1000	823
7	* 140	— 211
8	1063	893
9	332	292
10	* 140	57
11	286	— 201
12	270	— 181
13	387	311
14	655	670
	3 0 *l*	
—38	+ 725	842
—36	768	— 601
—34	—1540	—1499
—32	562	— 467
—30	+1130	1087

	$10 \cdot F_o$	$10 \cdot F_c$
−28	* 300	− 366
−26	736	− 683
−24	* 300	350
−22	1550	1388
−20	−1180	−1361
−18	* 290	93
−16	415	673
−14	−1590	−1674
−12	1280	1329
−10	− 995	− 832
− 8	930	− 944
− 6	1700	1820
− 4	− 975	− 924
− 2	−2730	−2778
0	−1240	−1199
2	+ 830	549
4	−2940	−2890
6	* 240	370
8	596	− 512
10	747	643
12	986	994
14	441	− 470
16	475	425
18	1310	1279
20	−2050	−2159
22	* 260	− 373
24	* 280	− 193
26	* 300	− 413
28	* 300	401
30	−1120	−1121
32	* 300	− 135
34	920	881
36	+2240	2230
	3 1 *l*	
−38	865	− 683
−37	* 150	154
−36	213	− 233
−35	* 160	− 424
−34	−1320	−1313
−33	396	568
−32	−1340	−1392
−31	803	829
−30	* 180	− 330
−29	* 160	− 304
−28	637	537
−27	214	363
−26	955	938
−25	475	342
−24	209	224
−23	−1230	−1078
−22	* 130	− 281
−21	* 130	59
−20	567	519
−19	913	− 745
−18	508	− 292
−17	605	547
−16	1060	− 807

	$10 \cdot F_o$	$10 \cdot F_c$
−15	139	− 118
−14	1280	−1190
−13	131	− 264
−12	564	− 565
−11	770	− 647
−10	1330	−1443
− 9	362	374
− 8	1165	−1114
− 7	1380	1322
− 6	1750	1637
− 5	−1610	−1432
− 4	569	370
− 3	* 70	− 59
− 2	150	198
− 1	−1720	−1638
0	1010	− 804
1	396	367
2	1160	1064
3	1070	917
4	559	− 513
5	* 80	− 30
6	1160	1084
7	641	− 743
8	120	80
9	* 90	121
10	388	− 377
11	* 90	39
12	435	484
13	* 100	179
14	1040	1199
15	356	− 350
16	165	− 283
17	700	− 879
18	* 130	50
19	500	− 581
20	* 140	257
21	* 150	161
22	950	−1021
23	* 150	337
24	641	− 582
25	* 160	− 167
26	735	649
27	1090	1247
28	+1270	1299
29	390	− 546
30	* 180	50
31	* 170	360
32	510	492
33	* 150	17
34	826	808
35	286	− 245
36	746	590
	3 2 *l*	
−37	446	496
−36	794	− 749
−35	* 140	− 226
−34	675	653

	$10 \cdot F_o$	$10 \cdot F_c$
−33	* 160	− 40
−32	630	634
−31	* 160	− 211
−30	* 160	− 76
−29	− 901	− 917
−28	* 150	172
−27	580	− 514
−26	* 150	62
−25	* 140	40
−24	610	− 512
−23	520	− 673
−22	682	714
−21	* 120	− 186
−20	* 120	124
−19	935	−1192
−18	1081	− 982
−17	232	181
−16	450	437
−15	756	940
−14	* 90	− 16
−13	761	− 916
−12	* 80	− 68
−11	* 80	− 114
−10	505	− 612
− 9	486	− 392
− 8	1060	1057
− 7	516	516
− 6	224	− 275
− 5	622	749
− 4	615	771
− 3	426	421
− 2	603	729
− 1	426	− 442
0	1260	1171
1	485	− 641
2	382	520
3	* 70	35
4	* 70	36
5	739	− 857
6	* 80	− 31
7	705	996
8	480	− 337
9	700	− 843
10	229	204
11	420	− 633
12	* 100	− 125
13	522	455
14	328	− 386
15	757	1044
16	258	− 355
17	458	722
18	545	842
19	882	747
20	425	601
21	236	− 375
22	* 140	− 99
23	584	588
24	* 150	58

	$10 \cdot F_o$	$10 \cdot F_c$
25	258	534
26	740	706
27	460	— 351
28	* 160	109
29	* 160	250
30	855	— 648
31	* 150	— 393
32	* 140	255
33	* 120	32
34	540	— 604
35	717	— 656
	4 0 *l*	
—38	+ 485	— 641
—36	* 270	230
—34	+1070	927
—32	* 300	— 124
—30	* 300	— 536
—28	810	— 667
—26	* 280	339
—24	* 280	— 119
—22	1760	1801
—20	* 260	— 277
—18	+1390	1398
—16	+2470	2558
—14	642	— 636
—12	—1280	—1392
—10	— 986	— 998
— 8	970	—1127
— 6	346	— 351
— 4	—1230	— 990
— 2	* 250	— 338
0	+2110	2011
2	* 250	— 264
4	714	742
6	+1030	972
8	* 270	— 432
10	—2400	—2219
12	— 815	— 709
14	* 290	— 45
16	717	— 730
18	—1150	1269
20	—2220	—2355
22	* 290	372
24	+ 835	967
26	* 300	119
28	—1560	—1535
30	810	— 910
32	* 270	473
34	* 220	— 226
	4 1 *l*	
—38	385	454
—37	296	413
—36	202	372
—35	710	593
—34	* 160	— 2
—33	344	— 452

	$10 \cdot F_o$	$10 \cdot F_c$
—32	572	— 575
—31	840	754
—30	980	916
—29	329	— 442
—28	735	— 596
—27	+1260	1302
—26	* 150	133
—25	* 150	19
—24	* 150	101
—23	—1410	—1225
—22	* 140	— 26
—21	422	330
—20	635	— 586
—19	* 130	5
—18	1200	—1287
—17	523	379
—16	522	460
—15	247	— 201
—14	252	290
—13	660	— 525
—12	755	— 802
—11	* 90	— 109
—10	1100	—1104
— 9	1380	1430
— 8	630	— 521
— 7	196	185
— 6	840	— 769
— 5	* 80	— 81
— 4	460	408
— 3	265	— 255
— 2	262	261
— 1	118	88
0	1030	— 882
1	459	— 361
2	191	— 199
3	338	208
4	1160	1098
5	1120	— 988
6	716	— 588
7	794	— 722
8	137	202
9	615	651
10	439	400
11	885	— 916
12	—1670	—1744
13	635	584
14	925	—1029
15	* 130	— 217
16	656	669
17	424	403
18	531	493
19	* 150	— 6
20	* 150	— 327
21	350	— 405
22	* 150	— 97
23	* 160	— 210
24	* 160	274
25	* 160	— 301

	$10 \cdot F_o$	$10 \cdot F_c$
26	* 180	356
27	790	722
28	+1150	958
29	—1150	— 916
30	* 160	— 321
31	* 160	— 157
32	* 150	— 92
33	* 140	104
34	* 120	217
35	70	63
	4 2 *l*	
—36	* 120	105
—35	730	990
—34	440	— 467
—33	266	421
—32	270	240
—31	366	— 391
—30	* 160	103
—29	365	— 460
—28	635	— 622
—27	* 150	— 206
—26	670	678
—25	673	643
—24	* 140	179
—23	—1490	—1696
—22	825	— 716
—21	297	— 414
—20	984	—1056
—19	663	— 815
—18	* 120	183
—17	364	357
—16	437	— 518
—15	1069	1088
—14	227	— 395
—13	221	— 355
—12	433	566
—11	299	312
—10	* 90	42
— 9	* 90	— 52
— 8	469	411
— 7	522	— 602
— 6	576	783
— 5	442	— 581
— 4	226	240
— 3	176	— 210
— 2	358	— 410
— 1	1380	—1466
0	* 80	61
1	625	— 617
2	516	— 621
3	* 80	— 207
4	* 80	197
5	285	310
6	* 90	— 98
7	423	482
8	477	649
9	* 100	225

	$10 \cdot F_o$	$10 \cdot F_c$
10	* 100	66
11	440	— 561
12	* 110	66
13	* 110	301
14	* 120	242
15	* 120	123
16	675	874
17	663	— 904
18	* 130	— 160
19	805	888
20	869	— 777
21	336	— 536
22	580	704
23	* 150	301
24	* 160	238
25	* 160	— 194
26	* 160	76
27	* 160	283
28	614	635
29	470	636
30	* 150	— 201
31	* 130	63
32	* 120	72
33	730	— 805
34	648	662
	5 0 *l*	
−38	* 250	— 104
−36	* 270	448
−34	* 290	134
−32	* 300	538
−30	460	414
−28	+1110	1279
−26	+2170	1979
−24	* 290	— 159
−22	−1200	−1155
−20	* 280	160
−18	+ 991	939
−16	* 260	— 329
−14	* 260	56
−12	* 250	— 256
−10	+2170	2169
— 8	850	— 873
— 6	+1200	1238
— 4	* 300	— 267
— 2	522	— 445
0	582	— 436
2	438	— 247
4	+1700	1508
6	+ 853	843
8	970	934
10	777	— 697
12	* 280	91
14	576	509
16	430	— 447
18	−2110	−2158
20	931	— 954
22	374	418

	$10 \cdot F_o$	$10 \cdot F_c$
24	* 300	108
26	* 300	— 368
28	+1580	1638
30	485	628
32	611	— 831
	5 1 *l*	
−37	654	730
−36	418	590
−35	* 140	— 156
−34	+ 920	865
−33	885	— 863
−32	538	449
−31	* 180	219
−30	* 170	119
−29	* 180	136
−28	−1030	— 969
−27	730	566
−26	232	444
−25	* 160	7
−24	+1260	1208
−23	* 150	— 219
−22	660	— 704
−21	410	445
−20	* 140	— 68
−19	560	445
−18	* 130	— 83
−17	821	— 569
−16	1070	— 912
−15	654	561
−14	453	555
−13	161	— 272
−12	* 110	— 225
−11	348	387
−10	1330	−1178
— 9	250	327
— 8	332	231
— 7	160	— 202
— 6	762	684
— 5	+1190	1025
— 4	440	— 281
— 3	* 100	103
— 2	863	864
— 1	610	418
0	1570	1302
1	1100	−1050
2	−2120	−1935
3	* 110	34
4	818	— 745
5	* 110	— 119
6	* 110	— 24
7	* 110	122
8	675	— 771
9	* 110	61
10	731	— 742
11	803	— 891
12	855	— 954
13	296	343

	$10 \cdot F_o$	$10 \cdot F_c$
14	605	— 468
15	585	661
16	* 150	276
17	671	466
18	675	534
19	* 150	— 155
20	* 160	33
21	360	— 426
22	* 160	188
23	* 180	— 214
24	* 180	21
25	* 180	333
26	* 180	— 184
27	* 170	— 326
28	* 160	— 6
29	* 160	— 323
30	* 150	— 162
31	— 770	— 749
32	* 120	— 222
	5 2 *l*	
−36	926	1004
−35	* 120	386
−34	* 130	99
−33	540	— 529
−32	803	— 936
−31	842	— 903
−30	885	— 707
−29	* 160	100
−28	* 160	— 56
−27	635	838
−26	661	— 770
−25	470	679
−24	334	— 468
−23	262	144
−22	* 140	— 33
−21	747	826
−20	* 130	139
−19	* 130	30
−18	* 120	0
−17	346	— 508
−16	379	461
−15	* 110	22
−14	201	— 271
−13	222	— 219
−12	* 110	— 230
−11	767	— 653
−10	* 100	— 93
— 9	392	464
— 8	445	— 464
— 7	−1400	−1569
— 6	* 100	— 202
— 5	970	994
— 4	* 100	— 139
— 3	* 100	157
— 2	* 100	128
— 1	481	— 550
0	* 100	156

	$10 \cdot F_o$	$10 \cdot F_c$
1	* 100	— 310
2	622	— 716
3	546	— 670
4	* 100	198
5	324	— 475
6	* 100	— 102
7	* 110	— 197
8	358	— 539
9	517	730
10	855	— 632
11	667	— 477
12	666	800
13	350	427
14	* 130	118
15	430	— 410
16	* 130	94
17	* 140	— 133
18	673	856
19	580	635
20	* 150	201
21	810	— 761
22	* 160	129
23	−1620	−1503
24	350	453
25	* 160	— 242
26	496	— 666
27	* 160	— 20
28	1000	— 900
29	298	410
30	398	565
31	538	426
	6 0 *l*	
−36	368	512
−34	* 290	115
−32	−1400	−1321
−30	* 300	588
−28	+1500	1461
−26	800	— 689
−24	* 300	133
−22	* 290	— 225
−20	* 290	461
−18	— 924	— 978
−16	* 280	384
−14	* 280	— 71
−12	* 260	— 82
−10	* 251	211
— 8	541	— 392
— 6	+1960	1877
— 4	+1690	1750
— 2	* 250	226
0	* 250	— 82
2	* 250	105
4	460	317
6	+ 863	843
8	−2270	−2140
10	* 260	50
12	1020	912
14	* 270	— 317
16	* 270	428
18	+1300	1441
20	* 290	409
22	1140	−1262
24	+ 880	916
26	902	— 878
28	670	693
30	* 250	460
	6 1 *l*	
−36	+1110	1015
−35	496	— 572
−34	+1300	1206
−33	* 150	— 62
−32	907	696
−31	* 160	— 180
−30	554	428
−29	* 180	— 183
−28	* 170	298
−27	800	— 893
−26	705	— 643
−25	213	308
−24	369	335
−23	* 160	— 155
−22	960	— 835
−21	* 150	267
−20	955	— 670
−19	660	646
−18	1150	781
−17	* 140	— 174
−16	* 140	178
−15	+1410	1391
−14	940	761
−13	* 130	26
−12	+1530	1479
−11	492	— 413
−10	+1600	1505
— 9	462	— 501
— 8	372	— 172
— 7	* 110	— 244
— 6	−1120	−1052
— 5	* 110	7
— 4	445	319
— 3	163	166
— 2	890	— 753
— 1	* 110	69
0	580	— 395
1	* 110	— 85
2	745	— 802
3	720	801
4	* 120	176
5	706	656
6	* 130	16
7	* 130	241
8	835	782
9	* 130	— 147
10	* 140	189
11	* 140	5
12	* 150	— 24
13	747	— 613
14	583	— 578
15	894	785
16	* 150	— 75
17	640	— 588
18	822	— 835
19	* 160	317
20	* 160	161
21	* 180	174
22	* 180	224
23	* 170	— 113
24	* 170	— 341
25	* 160	226
26	717	— 553
27	* 160	— 257
28	* 140	99
29	722	520
30	+1120	888
	6 2 *l*	
−34	* 110	7
−33	560	512
−32	* 140	262
−31	* 150	— 45
−30	* 150	— 19
−29	* 160	194
−28	* 160	— 76
−27	* 160	239
−26	* 160	— 246
−25	* 160	— 255
−24	* 150	— 8
−23	1000	1300
−22	* 150	— 32
−21	* 150	231
−20	440	349
−19	307	429
−18	610	— 516
−17	430	— 508
−16	* 130	2
−15	840	964
−14	* 120	272
−13	* 120	269
−12	* 120	189
−11	381	— 438
−10	* 120	217
— 9	* 120	— 35
— 8	826	— 964
— 7	971	−1076
— 6	* 120	— 51
— 5	363	424
— 4	* 120	— 185
— 3	* 120	189
— 2	628	— 806
— 1	* 120	90
0	620	— 575
1	518	635

	$10 \cdot F_o$	$10 \cdot F_c$
2	370	334
3	203	171
4	264	— 375
5	338	— 381
6	* 120	— 37
7	546	636
8	529	597
9	* 120	7
10	* 130	0
11	530	— 394
12	* 140	— 129
13	862	— 859
14	* 140	236
15	636	— 527
16	472	— 547
17	* 150	— 21
18	876	— 779
19	* 160	217
20	810	672
21	* 160	— 14
22	* 170	— 332
23	— 920	— 722
24	340	— 347
25	672	609
26	* 140	19
27	908	— 638
28	540	590
29	* 100	— 49
	7 0 *l*	
—34	* 260	251
—32	980	—1008
—30	* 300	— 309
—28	* 300	— 335
—26	* 300	— 358
—24	750	505
—22	* 300	66
—20	—1410	—1470
—18	560	— 730
—16	555	702
—14	* 290	— 91
—12	* 280	— 41
—10	— 750	— 743
— 8	* 280	168
— 6	1440	1547
— 4	1280	1329
— 2	1860	—1859
0	1070	951
2	681	574
4	1570	—1680
6	571	724
8	* 270	115
10	* 270	— 165
12	* 270	7
14	* 300	200
16	* 300	452
18	+1260	1250
20	777	846

	$10 \cdot F_o$	$10 \cdot F_c$
22	1050	— 932
24	456	470
26	440	611
28	* 270	104
	7 1 *l*	
—34	610	— 789
—33	590	516
—32	* 140	— 146
—31	* 150	— 37
—30	1170	— 801
—29	* 160	— 254
—28	771	714
—27	* 180	— 187
—26	* 170	161
—25	970	893
—24	697	445
—23	515	— 587
—22	1040	926
—21	* 160	— 195
—20	+1280	1181
—19	* 160	— 369
—18	338	— 324
—17	477	— 438
—16	675	— 708
—15	336	385
—14	817	523
—13	210	361
—12	* 150	133
—11	309	— 405
—10	195	— 300
— 9	610	484
— 8	960	798
— 7	* 130	— 86
— 6	424	379
— 5	300	— 459
— 4	736	543
— 3	848	685
— 2	+1170	1011
— 1	948	— 725
0	522	— 430
1	* 130	0
2	* 130	— 113
3	614	— 357
4	535	— 460
5	695	489
6	210	— 200
7	334	341
8	751	— 550
9	+1060	879
10	755	626
11	* 150	209
12	+1480	1052
13	738	— 562
14	* 160	187
15	635	510
16	* 160	377
17	405	— 383

	$10 \cdot F_o$	$10 \cdot F_c$
18	* 180	92
19	* 180	282
20	924	700
21	* 180	— 284
22	970	— 797
23	866	— 722
24	1490	—1072
25	* 130	80
26	* 120	— 332
27	1220	929
	7 2 *l*	
—33	1070	1266
—32	* 120	206
—31	* 130	282
—30	* 140	450
—29	* 150	— 272
—28	* 150	— 5
—27	* 160	— 168
—26	* 160	— 77
—25	* 160	145
—24	700	534
—23	660	642
—22	* 160	144
—21	* 150	16
—20	* 150	78
—19	* 150	— 121
—18	* 150	— 10
—17	* 150	— 18
—16	618	498
—15	* 140	195
—14	* 140	35
—13	* 140	144
—12	304	— 392
—11	* 130	107
—10	* 130	— 253
— 9	380	496
— 8	400	442
— 7	* 130	135
— 6	281	— 368
— 5	281	— 447
— 4	281	— 380
— 3	+1088	1001
— 2	* 120	— 93
— 1	* 120	302
0	* 130	64
1	942	813
2	* 130	207
3	* 130	— 152
4	* 130	234
5	606	— 644
6	* 140	— 62
7	749	702
8	1060	— 931
9	* 140	— 24
10	1060	943
11	* 150	78
12	* 150	— 194

	$10 \cdot F_o$	$10 \cdot F_c$
13	333	— 408
14	575	— 532
15	* 160	— 215
16	* 160	— 223
17	* 160	— 202
18	* 160	86
19	* 160	177
20	613	— 666
21	677	606
22	* 150	26
23	* 140	— 156
24	* 130	170
25	* 120	123
26	481	— 430
27	717	— 571
	8 0 *l*	
−30	−1490	−1647
−28	−1200	−1406
−26	— 896	— 672
−24	* 280	— 422
−22	* 280	— 361
−20	−1070	— 878
−18	915	852
−16	1170	1219
−14	* 300	333
−12	595	— 486
−10	* 300	— 90
— 8	* 300	— 93
— 6	−2290	−2386
— 4	* 300	— 323
— 2	* 300	67
0	394	400
2	580	— 484
4	* 300	— 143
6	* 300	375
8	686	860
10	* 300	309
12	854	— 794
14	— 985	— 973
16	+1000	940
18	+ 650	735
20	583	— 587
22	850	869
24	* 280	— 252
	8 1 *l*	
−31	* 130	— 169
−30	445	477
−29	925	— 692
−28	−1740	−1276
−27	640	612
−26	376	— 472
−25	* 170	133
−24	* 180	417
−23	* 170	— 62
−22	* 180	95
−21	* 180	— 78

	$10 \cdot F_o$	$10 \cdot F_c$
−20	* 180	19
−19	* 160	— 274
−18	730	696
−17	231	— 346
−16	* 160	352
−15	369	— 334
−14	* 160	51
−13	370	269
−12	+1270	905
−11	−1070	— 891
−10	1360	−1260
— 9	213	269
— 8	* 150	— 6
— 7	675	— 598
— 6	* 150	— 266
— 5	338	331
— 4	675	— 608
— 3	1070	764
— 2	* 150	— 114
— 1	* 150	— 140
0	585	660
1	* 150	— 144
2	+1130	1056
3	* 150	— 188
4	550	565
5	* 150	— 43
6	* 160	203
7	* 160	23
8	* 160	391
9	* 160	14
10	+1160	784
11	590	— 565
12	* 160	— 310
13	* 180	— 4
14	946	— 717
15	* 180	199
16	* 180	142
17	557	545
18	* 170	— 25
19	* 160	— 153
20	* 160	— 302
21	* 150	231
22	+1210	1115
23	* 130	— 383
24	* 110	— 103
	8 2 *l*	
−31	549	590
−30	* 110	261
−29	585	— 492
−28	720	645
−27	* 140	308
−26	938	917
−25	450	— 246
−24	* 150	217
−23	614	— 785
−22	* 160	114
−21	* 160	74

	$10 \cdot F_o$	$10 \cdot F_c$
−20	* 160	— 155
−19	625	— 663
−18	727	772
−17	285	— 153
−16	872	— 830
−15	257	— 335
−14	471	— 533
−13	258	382
−12	* 150	— 21
−11	1085	1042
−10	* 150	296
— 9	775	658
— 8	367	511
— 7	* 150	57
— 6	535	521
— 5	756	— 735
— 4	* 140	— 19
— 3	1074	993
— 2	* 140	— 155
— 1	239	— 308
0	1260	1062
1	* 150	67
2	* 150	— 85
3	* 150	— 56
4	945	— 746
5	550	— 440
6	* 150	192
7	664	620
8	* 150	106
9	* 160	352
10	366	— 332
11	* 160	124
12	356	224
13	496	434
14	342	— 308
15	361	— 173
16	350	— 341
17	450	— 356
18	* 150	77
19	456	498
20	* 130	— 55
21	430	318
22	* 120	— 164
23	* 110	182
	9 0 *l*	
−30	579	— 605
−28	1070	950
−26	784	963
−24	* 300	— 181
−22	* 300	— 141
−20	* 300	— 30
−18	* 300	— 307
−16	1680	−1707
−14	* 300	49
−12	1000	942
−10	429	579
— 8	529	— 604

	$10 \cdot F_o$	$10 \cdot F_c$
— 6	* 300	— 401
— 4	* 300	— 264
— 2	* 300	35
0	* 280	— 419
2	—1610	—1682
4	710	— 753
6	—1060	841
8	800	1012
10	953	— 808
12	1630	1489
14	536	— 451
16	626	— 561
18	* 270	— 286
20	* 270	— 330
	9 1 *l*	
—29	* 110	— 376
—28	480	— 659
—27	595	362
—26	* 140	4
—25	* 150	— 245
—24	* 160	62
—23	* 160	280
—22	* 160	113
—21	* 170	— 168
—20	557	— 571
—19	* 180	36
—18	* 170	— 45
—17	— 800	— 588
—16	248	— 301
—15	* 180	7
—14	980	— 618
—13	* 180	190
—12	* 180	— 419
—11	363	— 302
—10	* 160	— 20
— 9	* 160	— 129
— 8	* 160	179
— 7	* 160	— 8
— 6	* 160	11
— 5	* 160	— 28
— 4	870	— 807
— 3	* 160	219
— 2	1160	803
— 1	* 160	79
0	635	612
1	364	— 399
2	* 160	— 356
3	* 160	254
4	* 180	— 10
5	570	— 519
6	* 180	48
7	* 180	— 22
8	* 180	21
9	* 170	— 182
10	* 170	37
11	* 180	— 93
12	550	403

	$10 \cdot F_o$	$10 \cdot F_c$
13	* 170	— 39
14	* 160	— 179
15	* 160	— 333
16	* 180	— 336
17	* 150	209
18	604	533
19	* 130	— 236
20	373	— 435
21	996	807
	9 2 *l*	
—27	* 110	10
—26	614	— 630
—25	* 130	— 330
—24	515	— 614
—23	243	— 270
—22	328	329
—21	1310	1125
—20	* 150	204
—19	* 160	— 282
—18	* 160	387
—17	* 160	— 351
—16	460	372
—15	695	— 578
—14	* 160	61
—13	* 160	— 287
—12	* 160	— 94
—11	* 160	45
—10	512	501
— 9	* 160	— 55
— 8	517	— 454
— 7	* 160	— 169
— 6	645	— 420
— 5	* 160	271
— 4	820	566
— 3	* 160	322
— 2	633	610
— 1	* 160	— 118
0	460	— 382
1	* 160	— 22
2	725	578
3	* 160	203
4	* 160	291
5	864	— 591
6	* 160	17
7	486	— 585
8	* 160	84
9	360	336
10	354	— 374
11	* 150	— 177
12	* 150	— 376
13	+1340	1291
14	* 140	72
15	307	— 241
16	409	521
17	* 120	218
18	* 110	15
19	421	388

	$10 \cdot F_o$	$10 \cdot F_c$
	10 0 *l*	
—26	745	— 853
—24	* 280	368
—22	+1570	1644
—20	725	806
—18	593	— 473
—16	440	473
—14	777	— 875
—12	* 300	240
—10	* 300	— 58
— 8	1640	—1733
— 6	* 300	115
— 4	675	801
— 2	* 300	127
0	* 300	— 191
2	+1440	1492
4	560	— 616
6	540	— 512
8	* 300	— 404
10	* 300	— 315
12	384	286
14	660	— 687
16	647	— 829
	10 1 *l*	
—25	* 110	292
—24	386	— 400
—23	* 130	— 223
—22	—1340	—1155
—21	* 140	200
—20	* 150	— 15
—19	* 160	121
—18	* 160	— 292
—17	* 160	— 184
—16	— 820	— 836
—15	530	622
—14	241	— 326
—13	386	322
—12	* 180	298
—11	* 180	— 18
—10	794	685
— 9	572	— 237
— 8	407	— 291
— 7	* 180	194
— 6	* 170	— 76
— 5	655	— 759
— 4	* 170	— 371
— 3	238	202
— 2	* 170	— 197
— 1	* 170	93
0	* 180	— 213
1	* 180	— 311
2	* 170	— 151
3	395	417
4	* 180	150
5	541	— 394
6	641	— 443
7	* 160	29

	$10 \cdot F_o$	$10 \cdot F_c$		$10 \cdot F_o$	$10 \cdot F_c$		$10 \cdot F_o$	$10 \cdot F_c$
				11 0 *l*				
8	* 160	239				— 6	* 300	373
9	* 160	185	—22	580	700	— 4	412	— 275
10	* 160	— 148	—20	* 280	105	— 2	* 300	143
11	* 150	16	—18	1150	—1057	0	937	852
12	* 140	— 275	—16	525	331	2	* 300	91
13	595	— 404	—14	* 290	94	4	583	— 625
14	630	588	—12	* 300	150	6	* 290	— 115
15	* 100	— 129	—10	* 300	— 182	8	* 280	— 36
16	804	— 551	— 8	712	967	10	* 280	— 371

As Fig. 1 shows, the H_2O molecules are to be found near the screw axis, so they form a screw line. Hydrogen bonds are not probable between the H_2O molecules as the distances are too large (3.19 Å), but they are possible between H_2O and oxygen atom (O_5, the distance is 2.87 Å) and between H_2O and sulphur atom ($S_3(1 - x, 1/2 + y, 1/2 - z)$, the distance is 3.43 Å). Similar hydrogen bonds were supposed in the structure of barium thiosulphate monohydrate.

The calculations were performed on a computer type Ural-2, in the University Computing Centre. The programs were composed in a machine language [14].

*

The author is very grateful to Dr. GY. MENCZEL for the preparation of the specimens and for his helpful advices, to the coworkers of the University Computing Centre for the aid at the computer, to Miss E. ZSOLDOS for her help during the work.

REFERENCES

1. TAYLOR, P. G., BEEVERS, C. A.: Acta Cryst. **5,** 341 (1952).
2. SÁNDOR E., CSORDÁS, L.: Acta Cryst. **14,**, 237 (1961).
3. NARDELLI, M., FAVA, G., GIRALDI, G.: Acta Cryst. **15,** 227 (1962).
4. NARDELLI, M., FAVA, G.: Acta Cryst. **15,** 477 (1962).
5. CSORDÁS, L., MENCZEL, GY.: Krist. Moscow, **3,** 372 (1958).
6. HAUPTMAN, H., KARLE, J.: Solution of the Phase Problem. I. A. C. A. Monograph No. 3. (1953).
7. SAYRE, D.: Acta Cryst. **5,** 60 (1952).
8. ZACHARIASEN, W. H.: Acta Cryst. **5,** 68 (1952).
9. KUTSCHABSKY, L., HŐHNE, E.: Acta Cryst. **19,** 747 (1965).
10. KUTSCHABSKY, L.: Monatsberichte D. A. W. **7,** 511 (1965).
11. CRUICKSHANK, D. W. J.: Acta Cryst. **5,** 511 (1952).
12. CRUICKSHANK, D. W. J.: Acta Cryst. **2,** 65 (1949).
13. DARLOW, S. F.: Acta Cryst. **13,** 683 (1960).
14. CSORDÁS, L.: Acta Chim. Acad. Sci. Hung. **57,** 147 (1968).

László CSORDÁS; Budapest VIII., Múzeum krt. 6—8.

Acta Chimica Academiae Scientiarum Hungaricae, Tomus 62 (4), pp. 395—399 (1969)

ON THE RESIDENCE TIME DISTRIBUTION IN COLUMN CHROMATOGRAPHY

(SHORT COMMUNICATION)

Á. PETHŐ and G. SCHAY

(Central Research Institute for Chemistry, Hungarian Academy of Sciences, Budapest)

Received November 23, 1968

1. In this paper we are concerned with packed columns of uniform cross section and finite length, when material transport in the mobile phase is taken into account in the axial direction only and the stationary phase is assumed to be uniformly distributed in each cross section of the column (capillary columns will be treated in a subsequent paper). Further, at the beginning of the process the quantity of the solute should be zero and that introduced in the time interval $0 \leq t \leq \infty$ should be finite. Now the continuity equation of the solute reads

$$\frac{\partial W}{\partial x} + \frac{\partial T}{\partial t} = 0\,, \tag{1}$$

with the notations:

$W(x, t)$ = the flux (*i.e.* the amount of solute transferred by convection and diffusion in the mobile phase in unit time), related to the *free* cross section of column [g s^{-1},]

$T(x, t)$ = the amount of solute in the column (both in the mobile and the stationary phase), related to unit length of column [g cm^{-1}],

x = the length coordinate [cm] and

t = the time [s].

The initial condition to Eq. (1) is $T(x, 0) = 0$, but as to the boundary condition for $x = 0$ we will consider the general case: $W(0, t) = W_0(t)$ with the only restriction that

$$\int_0^\infty W_0(t)\, dt = 1\,. \tag{2}$$

The integration of Eq. (1) with these conditions and assuming the sorption processes to be reversible:

$$\lim_{t \to \infty} T(x, t) = 0 \tag{3}$$

yields

$$\int_0^\infty W(x, t)\, dt = 1\,. \tag{4}$$

I.e., the amount of solute introduced to the column at $x = 0$ (see Eq. (2)) will completely leave the column section $[0, x]$ during the time interval $[0, \infty]$ again.

Now let us consider a particle of the solute and the time ϑ_x when this particle has just left the column section $[0, x]$. This time is a random variable and will be called the *residence time* (or passage time) of the particle with respect to x [1, 2]. Denoting the probability distribution function of ϑ_x by $\mathscr{P}(\vartheta_x \leqq t)$ we have for the *density function* of ϑ_x because of Eq. (4)

$$\frac{d}{dt}\,\mathscr{P}(\vartheta_x \leqq t) = W(x, t)\,. \tag{5}$$

In this equation no assumption about the form of $W(x, t)$ has yet been made. Presuming that the diffusion term in W can be described by FICK's law, we have

$$W = uY - D\frac{\partial Y}{\partial x} \tag{6}$$

with the notations:

u = the mean linear velocity of flow [cm s^{-1}],
D = the mean effective diffusivity in the mobile phase [cm^2 s^{-1}], and
$Y(x, t)$ = the amount of solute in the mobile phase, related to unit length of column [g cm^{-1}].

(At high concentrations the velocity u is not unaffected by the sorption and thus the constancy of u does not hold any more [3, 2], apart from the fact that, in the case of gas chromatography, the pressure drop along the column, unless negligible, also causes a variation of u.) If now a finite column of length L can be characterized by the assumption that at the end of the column diffusion may be neglected against convection [4, 5]:

$$\left.\frac{\partial Y}{\partial x}\right|_{x=L} = 0\,, \tag{7}$$

we have, in view of Eqs (5) and (6), for the density function of ϑ_L

$$\frac{d}{dt}\,\mathscr{P}(\vartheta_L \leqq t) = W(L, t) = uY(L, t)\,. \tag{8}$$

2. In order to describe a fairly general non-linear sorption kinetics to be discussed in this paper we first define $X(x, t)$ as the amount of solute in the stationary phase, related to unit length of column [g cm $^{-1}$], *i.e.*

$$X = T - Y \tag{9}$$

Let us now introduce the Laplace transforms of X and Y, defined generally by:

$$\mathscr{L}g(t) \equiv \mathbf{g}(s) = \int_0^\infty e^{-st} g(t)\, dt.$$

The non-linear kinetics mentioned should be defined as

$$\mathbf{X} = K\mathbf{f}\mathbf{Y}, \quad \mathbf{f}(0) = 1 \tag{10}$$

where:

K = the equilibrium constant (partition coefficient) of sorption and
$\mathbf{f}(s)$ = an arbitrary function (with the restriction $\mathbf{f}(0) = 1$), measuring the "distance" from equilibrium. From Eq. (10) there immediately follows that for any $\mathbf{f}$

$$\lim_{t \to \infty} \frac{X(x, t)}{Y(x, t)} = K. \tag{11}$$

(*Cf.* the "long-time approximation" or "near-equilibrium assumption" of GIDDINGS [6]).

Examples for actual forms of $\mathbf{f}$.

(1) If equilibrium is *a priori* established:

$$X = KY \tag{12}$$

then

$$\mathbf{f} = 1. \tag{13}$$

(2) If sorption kinetics is linear:

$$\frac{\partial X}{\partial t} = k(KY - X) \tag{14}$$

then

$$\mathbf{f} = \frac{k}{k + s} \tag{15}$$

where k = the sorption rate constant [s $^{-1}$].

(3) If the stationary phase is assumed to be a film of thickness d [cm], in which diffusion of the solute takes place vertically to the interface, then [7]

$$\mathbf{f} = \left[\frac{D_s}{kd^2}\varrho^2 + \frac{\varrho}{\tanh\varrho}\right]^{-1}, \quad \varrho = \sqrt{\frac{d^2 s}{D_s}} \tag{16}$$

where D_s = the diffusivity in the stationary phase [$cm^2\ s^{-1}$].

3. The density function of the residence time distribution at the end of the column being given by Eq. (8), the mean μ and variance σ^2 of ϑ_L will be defined as

$$\mu = u\int_0^\infty tY(L,t)\,dt \tag{17}$$

and

$$\sigma^2 = u\int_0^\infty (t-\mu)^2 Y(L,t)\,dt. \tag{18}$$

So from the Laplace transform solution of Eqs (1), (6) and (7) for $x = L$, say $\mathbf{Y}(s)$, we have [8]

$$\mu = -u\left.\frac{d\mathbf{Y}}{ds}\right|_{s=0} \tag{19}$$

and

$$\sigma^2 + \mu^2 = u\left.\frac{d^2\mathbf{Y}}{ds^2}\right|_{s=0}. \tag{20}$$

In the following table the values of μ and σ^2 are tabulated for $W_0(t) = \delta(t)$ (*i.e.* $\mathbf{W}_0 = 1$), $\delta(t)$ being the Dirac delta function (for details see [9]):

$\frac{\mu}{\beta}$	Generally P	Asymptotically if $L\to\infty$ P
$\frac{\sigma^2}{\beta^2}$	$2P\left[1-\frac{P}{\beta}\mathbf{f}'(0)\right] -2(1-e^{-P})$	$2P\left[1-\frac{P}{\beta}\mathbf{f}'(0)\right]$

with:

$$P = \frac{uL}{D}, \quad \beta = \frac{D}{u^2 q}, \quad p = \frac{K}{1+K}, \quad q = 1-p. \tag{21}$$

The values of $\mathbf{f}'(0) = [d\mathbf{f}/ds]_{s=0}$ can be obtained for the different cases of sorption kinetics (1), (2) and (3) mentioned in Section 2 as follows (see Eqs (13), (15) and (16)):

(1) $\quad \mathbf{f}'(0) = 0,$

(2) $\quad \mathbf{f}'(0) = -\dfrac{1}{k}.$

(3) $\quad \mathbf{f}'(0) = -\left(\dfrac{1}{k} + \dfrac{d^2}{3D_s}\right).$

Remark. After having defined an intermittent model of chromatography with continuous flow, one has for H [cm], the "height equivalent to one theoretical plate", according to the asymptotic value of σ^2[9, 10]

$$H = 2\left[\frac{D}{u} - up\,q\mathbf{f}'(0)\right]. \tag{22}$$

4. Considering the asymptotic case $L \to \infty$ again, it follows on the basis of a theorem about the "infinitely divisible distributions" [8] that the standardized random variable $(\vartheta_L - \mu)/\sigma$ will be *normally* distributed:

$$\lim_{L\to\infty} \mathscr{P}\left(\frac{\vartheta_L - \mu}{\sigma} \leq t\right) = \frac{1}{\sqrt{2\pi}} \int_{-\infty}^{t} e^{-\tau^2/2}\, d\tau \tag{23}$$

with

$$\mu = \frac{L}{uq}, \quad \sigma^2 = \frac{HL}{(uq)^2}. \tag{24}$$

This result has to be regarded as a generalisation of the theorem of VAN DER WAERDEN in the classical paper of VAN DEEMTER *et al.* [11].

REFERENCES

1. LEVENSPIEL, O., BISCHOFF, K. B.: Adv. Chem. Engng 4 (1963) 95.
2. KLINKENBERG, A.: Trans. Instn. Chem. Engrs **43** (1965) T141.
3. SCHAY, G.: Theoretische Grundlagen der Gaschromatographie. Berlin, 1960.
4. DANKWERTS, P. V.: Chem. Engng Sci. **2** (1953) 1.
5. PETHŐ, Á.: On the residence time distribution in continuous-flow system with sorption in a fixed bed. Chem. Engng Sci. (to be published).
6. GIDDINGS, J. C.: Dynamics of Chromatography, New York, 1965.
7. PETHŐ, Á.: in Leibnitz/Struppe: Handbuch der Gas-Chromatographie. Leipzig, 1966.
8. FELLER, W.: An Introduction to Probability Theory and its Applications II. New York, 1966.
9. PETHŐ, Á., SCHAY, G.: Über de Verweilzeitverteilung in gefüllten Säulen endlicher Länge. Chromatographia **2** (1969) 158.
10. PETHŐ, Á.: Chem. Engng Sci. **22** (1967) 1793.
11. VAN DEEMTER, L. I., ZUIDERWEG, F. J., KLINKENBERG, A.: Chem. Engng Sci. **5** (1956) 271.

Árpád PETHŐ
Géza SCHAY
Budapest II., Pusztaszeri út 57—69.

Acta Chimica Academiae Scientiarum Hungaricae, Tomus 62 (4), pp. 401—411 (1969)

INVESTIGATION OF THE ELECTRONIC STRUCTURE OF NUCLEOTIDE BASE ANTIMETABOLITE TYPE POSSIBLE ANTICARCINOGENS, I

MONOSUBSTITUTED PYRIMIDINES, URACILS, THYMINES AND CYTOSINES

J. LADIK and G. BICZÓ

(Central Research Institute for Chemistry of the Hungarian Academy of Sciences, Budapest)

Received November 26, 1968

The π electron densities in different monosubstituted (—F, —Cl, —Br, —I, —OH, —OCH_3, —SH, —NH_2, —CH_3, —COOH) pyrimidines, uracils, thymines and cytosines have been calculated by means of the semiempirical SCF LCAO MO method.

On the basis of the calculated charge distributions, in some cases correlations seem to exist between the electronic structure and anticarcinogenic activity of the compounds. For a better establishment of these correlations, calculations of further quantum chemical indices are necessary.

Introduction

To find correlations between the molecular structure of drugs and their pharmacological activity is an old ambition in pharmaceutical chemistry and pharmacology. Some correlations are known between the detailed chemical structure of some groups of compounds [1] and their activity, but only a few investigations have tried to establish correlations between pharmacological activity and electronic structure [2, 3].

The problem of connection between molecular structure and pharmacological activity is a rather complicated one. A supposed drug has to enter the cell, reach the site of its action within the cell, bind to given molecules (or macromolecules) within the cell and influence in a specific way the electronic structure of its receptor. At the same time it should bind to other molecules only in a low amount to avoid high toxicity. The ability of a molecule to get through the cell membrane and its diffusion properties depend first of all on its stereo structure, but they are influenced also by its electronic structure. The specific reactivity towards a given molecule (or macromolecule) and the ability to influence the electronic structure of the receptor molecule in a specific way are functions first of all of the electronic structure of the drug molecule, but, of course, also its stereo properties play a non-negligible role. Therefore it is evident that also in the case if the stereo structure of a molecule is known, it cannot be expected in the near future to predict *a priori* on the basis of its more or less well approximated electronic structure whether it possesses a given pharmacological activity or not.

There is, however, a possibility to find correlations between electronic structure and pharmacological activity in a more empirical way. Let us consider a series of similar molecules consisting of N members. A subseries of this series containing N_1 members is synthetized and tested for a given pharmacological activity, while the activity of the other N_2 members of the series is unknown ($N = N_1 + N_2$). Among the tested N_1 members of the series a small fraction consisting of N_{1a} members has been found active, while the remaining N_{1i} members of the subseries ($N_1 = N_{1a} + N_{1i}$) were inactive or had a too high toxicity. Our task is to find out from subseries N_2 its possibly small fraction containing N_{2a} members possessing the desired pharmacological activity ($N_2 = N_{2a} + N_{2i}$). If subseries N_2 is large, to synthetize all these molecules and to test them would be a rather hard and expensive work. If a suitable computer is available, it is more easy to calculate the electronic structure of all the N molecules belonging to the series under consideration. As first step we can compare the calculated charge distributions of molecules belonging to the subseries of tested molecules (N_1 members) with the charge distributions of the untested molecules (N_2 molecules). In a lucky case in this way we can predict at least a part of the N_{2a} molecules on the basis of the charge distributions of the N_{1a} active molecules of the tested subseries. In most cases, however, it should be expected that alone on the basis of charge distributions it will not be possible to make such predictions. Therefore we shall be obliged to look after more complicated quantum chemical indices to be able to establish a correlation between the electronic structure of the investigated molecules and the given pharmacological activity. These can be some reactivity indices (for instance free valence, some kind of localization energy, frontier electron density, etc.) or more probably some complex index constructed in a suitable way from different quantum chemical indices.

In the present paper we should like to report semiempirical SCF LCAO MO calculations done on a series of monosubstituted pyrimidines, uracils, thymines and cytosines, respectively, while in the subsequent paper the same type of calculations are described for monosubstituted purines, adenines and guanines, respectively. The substituents for which all these calculations have been performed were $-F$, $-Cl$, $-Br$, $-J$, $-OH$, $-O-CH_3$, $-SH$, $-NH_2$, $-COOH$ and $-CH_3$. These substituents were substituted on all such positions of the above mentioned 4 pyrimidine type and 3 purine type compounds, where the substitution does not interfere with the ability of these substances to build in DNA and to form there Watson—Crick-type base pairs. In Fig. 1 we show these positions for the pyrimidine type compounds, while for the purine type compounds this will be indicated in Fig. 1 of the subsequent paper. In this way we should obtain 140 compounds. Adding to this the 4 pyrimidine type and 3 purine type unsubstituted compounds the total number of calculated substances was 147.

Among the mentioned nearly 150 compounds about 50 are known to be synthetized and tested for anticarcinogenic activity ($N_1 \approx 50$) and about 15 have shown larger or smaller activity ($N_1 \approx 15$). Some of them, for instance 5-F-U, are used in the therapy as prominent anticarcinogens. Therefore it seemed worthwhile to perform the calculations for the not tested (at least published) $N_2 \approx 100$ compounds to find some correlations which can help to

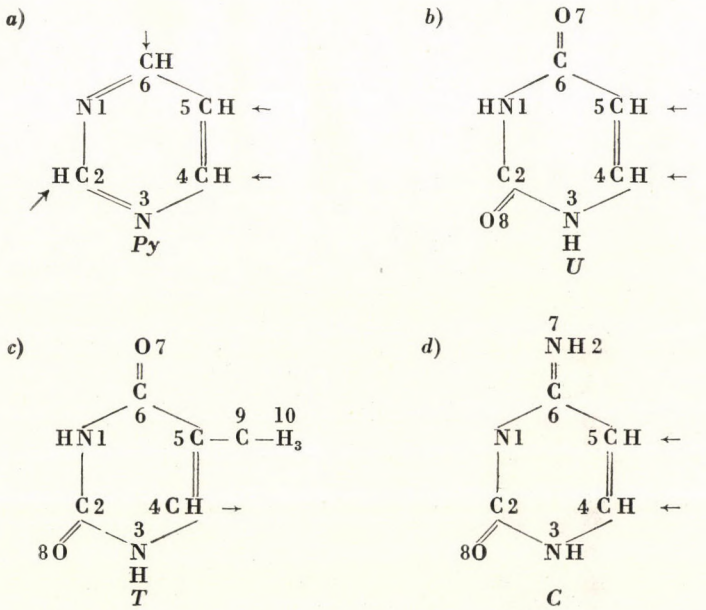

Fig. 1. The numbering of the considered pyrimidine type bases. The arrows indicate the positions, where the substitutions do not interfere with the ability to build in into DNA and for which the calculations have been performed. *a)* Py = pyrimidine, *b)* U = uracil, *c)* T = thymine and *d)* C = cytosine. It should be mentioned that pyrimidine probably cannot be built in into DNA, nevertheless calculations have been performed also for its derivatives. Further it should be remarked that by Py positions 4 and 6 are equivalent and therefore the calculation had to be done only once for these two positions

discover the active compounds (N_{2a}) among them without the necessity to synthetize and test all the ≈100 compounds.

At the present step of this research we have calculated only the charge distribution (see below) of the investigated compounds, but in the future we intend to form their different quantum chemical indices. We hope that in this way it will be possible to establish some useful correlations between the quantum chemical indices of these compounds and their anticarcinogenic activity.

Method

For the calculation of the delocalized π electrons of the monosubstituted derivatives of the mentioned pyrimidine type compounds the semiempirical SCF LCAO MO method (PARISER—PARR—POPLE method [4, 5]) has been used. In this method the eigenvalue equation

$$\mathbf{F}\mathbf{c}_i = \varepsilon_i \mathbf{c}_i \tag{1}$$

has to be solved, where

$$F_{r,r} = -I_r + \frac{1}{2} P_{r,r}(I_r - E_r) + \sum_{s \neq r} P_{s,s} - Z_s)\gamma_{r,s}, \tag{2}$$

$$F_{r,s} = \beta_{r,s} - \frac{1}{2} P_{r,s}\gamma_{r,s}. \tag{3}$$

Here I_r and E_r are the valence state ionization and electron affinity, respectively, which are given in the paper of HINZE and JAFFE [6]. Z_s is the number of π orbitals provided by atom s. The $\gamma_{r,s}$ Coulomb integrals were approximated by the expression given by MATAGA and NISHIMOTO [7].

$$\gamma_{r,s} = \frac{e^2}{R_{r,s} + a_{r,s}}, \quad \frac{e^2}{a_{r,s}} = \frac{1}{2}[I_r + I_s - E_r - E_s]. \tag{4}$$

Table I

Input data used for the unsubstituted compounds

X	a) I_X	a) E_X	Z_X	c) $\beta_{e,X}$
C	11.42	0.58	1	1.00
=N–	13.83	0.45	1	1.00
–N=	29.16	14.49	2	0.80
=O	17.28	2.70	1	1.30
–C (in methyl group)	10.69[b]	2.08[b]	1	0.70
$-H_3$ (in methyl group)	13.59	0.75	1	2.00

a) The I_i ionization potential and E_i electron affinity values are given in eV. We have taken them from the work of HINZE and JAFFE [6].

b) Values referring to an aliphatic carbon atom [6].

c) In $\beta = -2.39$ eV units. These values have been found previously to give a resonable charge distribution in these compounds [8].

Table II

Input data used for the substituents

Substituent	*a)* I_X	*a)* E_X	*b)* Z_X	*c)* $\beta_{C,X}$	*d)* $r_{C,X}$
—F	43.07	20.98	2	1.00	1.30
—Cl	28.67	15.09	2	0.75	1.69
—Br	24.60	13.72	2	0.65	1.86
—J	21.00	12.61	2	0.10	2.02
—OH	35.76	17.70	2	0.95	1.36
—O—C—H_3	O: 35.76 C: 10.69 H_3: 13.59	17.70 2.08 5.75	4 4 4	β C, O: 0.95 β O, C: 0.55 β C, H_3: 2.00	r C, O: 1.40 r O. C: 1.42 r C, H_3: 1.10
—SH	25.14	16.27	2	0.60	1.32
=S	12.70	2.76	1	0.80	1.27
—NH_2	29.16	14.49	2	0.80	1.34
—C—H_3	C: 10.69 H_3: 13.59	2.08 0.75	2	β C, C: 0.70 β C, H_3: 2.00	C, C: 1.54 C, H_3: 1.10
—C(=O)—O—N *e)*	C: 11.42 O: 26.52	0.58 10.20	4	β C, C: 1.00 β C, O: 1.35	r C, C: 1.48 r C, O: 1.30

a) In eV-s. Data taken from HINZE and JAFFE [6].
b) The total number of π electrons of the substituent.
c) In $\beta = -2.39$ eV units. These values have been determined on the basis of parameter variation.
d) In Å-s.
e) The two O atoms have been taken to be equivalent. The values

$$I_O = \frac{I_{=O} + I_{-O-}}{2}, \quad E_O = \frac{E_{=O} + E_{-O-}}{2}, \quad \beta_{C,O} = \frac{\beta_{C,O=} + \beta_{C,-O-}}{2} \text{ and } r_{C,O} = \frac{r_{C,O=} + r_{C,-O-}}{2}$$

have been used.

where $R_{r,s}$ is the distance between atomic nuclei r and s. Further the elements of the charge-bond order matrix **P** are defined by

$$P_{r,s} = 2 \sum_{i=1}^{n^*} c_{i,r}\, c_{i,s}\,, \tag{5}$$

where n^* indicates the highest filled MO.

$$\left(n^* = \frac{n_\pi}{2} = \sum_{s=1}^{n} \frac{Z_s}{2} \right);$$

Table III

*SCF π electron charge densities of the investigated monosubstituted pyrimidines**

Substituent position	1.	2.	3.	4.	5.	6.	7.	8.	9.
Py	1.114	0.901	1.114	0.928	1.014	0.928	—	—	—
2—F	1.139	0.875	1.139	0.927	1.027	0.927	1.967	—	—
2—Cl	1.127	0.892	1.127	0.928	1.021	0.928	1.978	—	—
2—Br	1.118	0.899	1.118	0.928	1.016	0.928	1.993	—	—
2—J	1.115	0.901	1.115	0.928	1.014	0.928	1.999	—	—
4—F	1.126	0.899	1.139	0.900	1.041	0.927	1.968	—	—
4—Cl	1.121	0.901	1.127	0.918	1.027	0.928	1.979	—	—
4—Br	1.116	0.901	1.118	0.926	1.018	0.928	1.993	—	—
4—J	1.115	0.901	1.115	0.928	1.014	0.928	1.999	—	—
5—F	1.111	0.915	1.111	0.955	0.983	0.955	1.972	—	—
5—Cl	1.113	0.908	1.113	0.941	1.002	0.941	1.982	—	—
5—Br	1.114	0.903	1.114	0.932	1.011	0.932	1.994	—	—
5—J	1.114	0.901	1.114	0.929	1.014	0.929	1.999	—	—
2—OH	1.138	0.880	1.138	0.927	1.028	0.927	1.963	—	—
2—O—C—H_3	1.137	0.885	1.138	0.926	1.026	0.925	1.950	0.923	1.091
2—SH	1.125	0.892	1.125	0.928	1.020	0.928	1.982	—	—
2—NH_2	1.138	0.887	1.138	0.927	1,028	0,927	1.954	—	—
2—C—H_3	1.113	0.909	1.113	0.927	1.011	0.927	0.925	1.075	—
2—C(=O)—O—H	1.077	0.944	1.077	0.924	0.984	0.924	0.563	1.753	1.753
4—OH	1.126	0.900	1.138	0.906	1.040	0.927	1.964	—	—
4—O—C—H_3	1.125	0.898	1.137	0.911	1,039	0.927	1.951	0.923	1.090
4—SH	1.120	0.900	1.125	0.918	1.026	0.928	1.983	—	—
4—NH_2	1.127	0.900	1.139	0.912	1.040	0.928	1.955	—	—
4—C—H_3	1.112	0.900	1.112	0.935	1.011	0.927	0.926	1.075	—
4—C(=O)—O—H	1.090	0.896	1.079	0.971	0.966	0.925	0.563	1.756	1.753
5—OH	1.111	0.915	1.111	0.954	0.988	0.954	1.968	—	—
5—O—C—H_3	1.111	0.912	1.110	0.952	0.993	0.953	1.955	0.923	1.091
5—SH	1.113	0.907	1.113	0.940	1.002	0.940	1.985	—	—
5—NH_2	1.111	0.915	1.111	0.954	0.994	0.954	1.961	—	—
5—C—H_3	1.114	0.898	1.114	0.924	1.020	0.924	0.926	1.080	—
5—C(=O)—O—H	1.118	0.866	1.118	0.877	1.054	0.877	0.569	1.760	1.760

* The numbering of atoms in the pyrimidine ring is the same as in Fig. 1. Position 7 means that atom of the substituent which is bound to the ring carbon atom. In the oxy-methyl substituent the numbering is —O—C—H_3 and in the case of the carboxyl group: —$C^7(=O^8)-O^9$ H

Table IV

*SCF π electron charge densities of the investigated monosubstituted uracils**

Substituent (Position)	1.	2.	3.	4.	5.	6.	7.	8.	9.	10.	11.
U	1.900	0.728	1.898	0.940	1.033	0.754	1.368	1.379	—	—	—
4—F	1.899	0.727	1.901	0.898	1.090	0.758	1.382	1.381	1.965	—	—
4—Cl	1.899	0.727	1.899	0.917	1.067	0.756	1.378	1.381	1.975	—	—
4—Br	1.899	0.728	1.899	0.925	0.049	0.755	1.374	1.381	1.992	—	—
4—J	1.899	0.728	1.898	0.927	1.043	0.755	1.372	1.381	1.999	—	—
5—F	1.898	0.728	1.900	0.977	1.014	0.757	1.373	1.382	1.971	—	—
5—Cl	1.898	0.728	1.899	0.953	1.032	0.755	1.373	1.382	1.980	—	—
5—Br	1.898	0.728	1.898	0.935	1.039	0.755	1.372	1.381	1.994	—	—
5—J	1.899	0.728	1.898	0.928	1.041	0.755	1.372	1.381	1.999	—	—
4—OH	1.899	0.727	1.901	0.904	1.089	0.758	1.383	1.381	1.959	—	—
4—O—CH_3	1.899	0.727	1.901	0.910	1.084	0.758	1.380	1.381	1.947	0.931	1.082
4—SH	1.899	0.727	1.899	0.917	1.364	0.756	1.377	1.381	1.979	—	—
4—NH_2	1.899	0.726	1.901	0.912	1.091	0.758	1.384	1.382	1.946	—	—
4—C—H_3	1.899	0.728	1.900	0.934	1.035	0.756	1.370	1.380	0.936	1.064	—
4—C(=O)—O—H	1.891	0.858	1.893	0.969	0.944	0.754	1.348	1.264	0.576	1.749	1.754
5—OH	1.898	0.728	1.900	0.976	1.020	0.757	1.374	1.382	1.966	—	—
5—O—C—H_3	1.898	0.728	1.900	0.970	1.025	0.756	1.374	1.384	1.953	0.923	1.092
5—SH	1.718	0.724	1.893	0.940	1.035	0.783	1.386	1.534	1.988	—	—
5—NH_2	1.898	0.728	1.900	0.979	1.026	0.755	1.374	1.383	1.957	—	—
5—C—H_3	1.898	0.728	1.897	0.921	1.046	0.755	1.370	1.380	0.929	1.076	—
5—C(=O)—O—H	1.899	0.730	1.892	0.840	1.070	0.758	1.356	1.375	0.571	1.745	1.764

* For the numbering of atoms in uracil see Fig. 1, the numbering of the substituent atoms is the same as in Table IV.

Table V

SCF π electron charge densities of the

Substituent (Position)	1	2	3	4	5	6
T	1.898	0,728	1,897	0.921	1.046	0.755
4—F	1.899	0.728	1.900	0.892	1.093	0.757
4—Cl	1.899	0,728	1.899	0.911	1.071	0.756
4—Br	1.899	0.728	1.898	0.919	1.054	0.755
4—J	1.899	0.728	1.897	0.921	1.047	0.755
4—OH	1.899	0.728	1.900	0.897	1.092	0.757
4—O—C—H_3	1.899	0.728	1.900	0.904	1.088	0.758
4—SH	1.899	0.728	1.899	0.911	1.067	0.756
4—NH_2	1.899	0.728	1.900	0.906	1.094	0.758
4—C—H_3	1.899	0.728	1.899	0.929	1.040	0.755
4—C(=O)—H	1.899	0.730	1.901	0.968	0.951	0.754

* For the numbering of atoms in thymine see Fig. 1, the numbering of substituent atoms

n is the number of atoms providing a π electron to the delocalized π electron system. For Py $n = n_\pi = 6$, for U $n = 8$ but $n_\pi = 10$, for T $n = 10$ and $n_\pi = 12$, for C $n = 8$ and $n_\pi = 10$. In the case of the four halogens and the —O—H, —NH_2, —SH substituents $n = 1$ and $n_\pi = 2$, for —COOH, —O—C—H_3 $n = 3$ and $n_\pi = 4$, and finally for —C—H_3 $n = n_\pi = 2$. Finally the $\beta_{r,s}$ resonance integrals are treated in this method as empirical parameters and are taken into account only for neighbouring atoms forming a π bond.

In the course of the calculation a starting matrix $\mathbf{P}^{(0)}$ was used. With the aid of it the matrix $\mathbf{F}$ could be formed. After solving its eigenvalue problem from the eigenvectors $\mathbf{c}_i$ obtained a new matrix $\mathbf{P}^{(1)}$ could be constructed with the aid of (5). Continuing this procedure the self consistent eigenvalues ε_i and eigenvectors $\mathbf{c}_i$ could be obtained. For criterium of self-consistency the inequality

$$|P_{r,s}^{(k+1)} - P_{r,s}^{(k)}| < 10^{-3} \text{ (for all } r \text{ and } s) \qquad (6)$$

has been used, where $P_{r,s}^{(k)}$ and $P_{r,s}^{(k+1)}$ mean the $P_{r,s}$ element of matrix $\mathbf{P}$ obtained in the k-th and $k + 1$-th iteration step, respectively.

To perform the calculations a program was written for the Gier computer. This program uses as input data the values I_r, E_r and Z_r for each atom possessing a π orbital, the starting charge-bond order matrix $\mathbf{P}^{(0)}$, the geometrical matrix $\mathbf{R}$ (which has as elements the distances $R_{r,s}$) and the matrix β, which has only off-diagonal elements (the $\beta_{r,s}$ parameters). As output the SCF eigenvalues $\varepsilon_i^{(SCF)}$ eigenvectors $\mathbf{c}_i^{(SCF)}$ and charge-bond order matrix $\mathbf{P}^{(SCF)}$ have been printed

*investigated monosubstituted thymines**

7	8	9	10	11	12	13
1.370	1.380	0.929	1.076	—	—	—
1.380	1.380	0.927	1.081	1.964	—	—
1.376	1.380	0.928	1.079	1.974	—	—
1.372	1.380	0.928	1.074	1.991	—	—
1.370	1.380	0.929	1.076	1.999	—	—
1.380	1.380	0.927	1.081	1.958	—	—
1.378	1.380	0.931	1.077	1.946	0.935	1.078
1.375	1.380	0.929	1.077	1.979	—	—
1.382	1.381	0.927	1.082	1.945	—	—
1.369	1.379	0.930	1.075	0.937	1.062	—
1.345	1,375	0.936	1.058	0.578	1.750	1.754

is the same as in Table III.

out. In the case of $n = 10$ the number of necessary iterations to reach self-consistency was usually 4—5 which has taken only 3—4 minutes for one compound on the Gier computer. In some instances the required computer time could be reduced by a factor 3 or 4 by constructing the starting matrix $\mathbf{P}^{(0)}$ from the matrix $\mathbf{P}^{(SCF)}$ of a similar compound. With this trick in some lucky cases just one iteration was needed for self-consistency.

In Table I we give the input data used for the unsubstituted compounds (Py, U, T, C), while in Table II they are summarized for the substituents. The geometries of the unsubstituted compounds which are not included in Table I, have been taken from the paper of SPENCER [9]. Using these geometries and the bond distances between the substituents and the ring carbon atoms given in Table II and further plausible valence angles for the substituents, the geometrical matrices **R** could be constructed for all the monosubstituted compounds.

Results and discussion

In Table III the SCF charge densities (the diagonal elements of matrix $\mathbf{P}^{(SCF)}$ are given for the investigated monosubstituted pyrimidines.

In Tables IV, V and VI the SCF charge densities of the monosubstituted uracils, thymines and cytosines, respectively, are given.

We can see from the Tables that in most cases the substituents change the charge densities of the parent molecules only at the place of substitution

Table VI

*SCF π electron charge densities of the investigated monosubstituted cytosines**

Substituent (Position)	1	2	3	4	5	6	7	8	9	10	11
C	1.170	0.760	1.881	0.916	1.051	0.857	1.946	1.418	—	—	—
4—F	1.186	0.761	1.884	0.881	1.096	0.855	1.947	1.425	1.964	—	—
4—Cl	1.179	0.760	1.882	0.902	1.075	0.857	1.946	1.423	1.975	—	—
4—Br	1.173	0.759	1.881	0.911	1.059	0.857	1.946	1.421	1.992	—	—
4—J	1.171	0.759	1.881	0.914	1.053	0.857	1.946	1.420	1.999	—	—
5—F	1.167	0.759	1.883	0.958	1.025	0.868	1.947	1.421	1.973	—	—
5—Cl	1.169	0.759	1.882	0.936	1.042	0.862	1.947	1.421	1.982	—	—
5—Br	1.170	0.759	1.881	0.921	1.050	0.858	1.946	1.421	1.994	—	—
5—J	1.170	0.759	1.881	0.915	1.052	0.857	1.946	1.420	1.999	—	—
4—OH	1.186	0.761	1.884	0.888	1.096	0.856	1.947	1.425	1.958	—	—
$4-O-C-H_3$	1.184	0.761	1.884	0.894	1.091	0.855	1.946	1.424	1.946	0.928	1.085
4—SH	1.178	0.760	1.882	0.902	1.073	0.857	1.946	1.423	1.979	—	—
$4-NH_2$	1.187	0.761	1.884	0.896	1.097	0.856	1.947	1.426	1.946	—	—
$4-C-H_3$	1.167	0.759	1.882	0.922	1.046	0.858	1.946	1.419	0.934	1.065	—
$4-C\langle^{O}_{O}\ H$	1.133	0.757	1.885	0.966	0.961	0.863	1.945	1.403	0.578	1.755	1.753
5—OH	1.167	0.759	1.882	0.957	1.029	0.867	1.947	1.421	1.969	—	—
$5-C-O-H_3$	1.166	0.760	1.882	0.952	1.035	0.868	1.947	1.420	1.956	0.926	1.089
5—SH	1.169	0.759	1.882	0.934	1.043	0.861	1.947	1.421	1.985	—	—
$5-NH_2$	1.168	0.759	1.883	0.958	1.035	0.866	1.947	1.421	1.962	—	—
$5-C-H_3$	1.169	0.759	1.880	0.907	1.056	0.857	1.946	1.419	0.930	1.078	—
$5-C\langle^{O}_{O}\ H$	1.190	0.943	1.928	0.843	1.086	0.893	1.950	1.063	0.577	1.764	1.764

* For the numbering of atoms in cytosine see Fig. 1, the numbering of the substituent atoms is the same as in Table III.

and in its immediate neighbourhood in a greater amount. Some substitutions (first of all the —COOH group) cause, however, larger changes in the overall charge distribution of the unsubstituted molecule.

Using the charge distributions of compounds which have been found experimentally to possess an anticarcinogenic activity [10] we have tried to find correlations between the anticarcinogenic activity and the π electron distributions of these compounds. Though in some cases such correlations seem to exist, it is very probable that to establish more general and better founded correlations between the electronic structure and anticarcinogenic activity, the calculation of the π electron distribution of these compounds alone is not sufficient. Using the obtained SCF eigenvalues and eingenvectors some other quantum chemical indices (free valence, different localization energies etc.) or some combined indices should be calculated to be able to find more characteristic correlations. Such calculations are in progress.

Finally it should be mentioned that already on the basis of the π electron charge distributions some suggestions have been made to synthetize some compounds belonging to the subseries with N_2 members (untested compounds). Among them so far only 4-Cl-U had been synthetized at the Organic Chemical Institute of the Technical University, Budapest. This compound has been tested at the Institute of Oncopathology, Budapest. It has not shown anticarcinogenic activity. From the experiments performed it is not possible to decide whether it was built in to DNA and was really inactive, or it was unable to build in. Therefore the failure of this first attempt does not mean — according to our opinion — that it is not worthwhile to continue this line of research.

We should like to express our gratitude to Dr. A. UDVARDY for collecting for us data from the literature concerning the experimentally found anticarcinogenic activity of the compounds calculated. We are further indebted to Professor K. LEMPERT, to Professor B. KELLNER, Corresponding Member of the Hungarian Academy of Sciences and to Dr. G. ELEK for synthetizing and testing 4-Cl-U. We should like to thank also to Miss A. JESZENÁK for tabulating the numerical results.

REFERENCES

1. See for instance: BOGDAN, R. E. in Experimental Chemotherapy, Vol II. p. 169. R. J. Ed. SCHNITZER, and E. HAWKING: Academic Press, New York—London, 1964.
2. PULLMAN, B., PULLMAN, A.: Rev. Mod. Phys. **32,** 428 (1960).
3. PULLMAN, B.: in Electronic Aspects of Biochemistry, p. 559. Ed. B. Pullman, Academic Press, New York—London, 1964.
4. PARISER, R., PARR, R. G.: J. Chem. Phys. **21,** 466, 767 (1953).
5. POPLE, J. A.: Trans. Far. Soc. **49,** 1375 (1953).
6. HINZE, T., JAFFE, J.: J. Am. Chem. Soc. **84,** 540 (1962).
7. MATAGA, N., NISHIMOTO, K.: Z. Physik. Chemie, **13,** 140 (1957).
8. LADIK, J., APPEL, K.: Theor. Chim. Acta **4,** 132 (1966).
9. SPENCER, M.: Acta Cryst. **12,** 59 (1959).
10. Cancer Chemotherapy Screening Data. V—VIII in Cancer Research **20** (1960); *ibid.* IX—XII in Cancer Research **21** (1961).

János LADIK
Géza BICZÓ
Budapest II., Pusztaszeri út 57—69.

Acta Chimica Academiae Scientiarum Hungaricae, Tomus 62 (4), pp. 413—423 (1969)

BERECHNUNG DER LADUNGSVERTEILUNG UND DES DIPOLMOMENTES GESÄTTIGTER, SAUERSTOFFHALTIGER HETEROCYCLISCHER VERBINDUNGEN

J. NAGY, J. RÉFFY und I. KÁDAS

(Anorganisch-chemisches Institut der Technischen Universität, Budapest)

Eingegangen am 2. Dezember 1968

Es wurden annähernde quantenchemische Berechnungen für das σ-Bindungssystem heterocyclischer, gesättigter, sauerstoffhaltiger Verbindungen nach der Methode von DEL RE durchgeführt. Bei den drei- und viergliedrigen stark gespannten Ringen wurde es notwendig, die Austausch-Integrale und die Coulomb-Parameter zu ändern. Ladungsverteilungen und Dipolmomente der geprüften Verbindungsreihe wurden berechnet. Die Ergebnisse stimmen mit den experimentellen Werten gut überein.

In einer früheren Arbeit [1] hat sich der eine von uns (I. K.) mit der Berechnung der Ladungsverteilung sauerstoffhaltiger aliphatischer Verbindungen beschäftigt. Es wurde untersucht, inwieweit die einfache quantenchemische Methode von G. DEL RE [2] zur Berechnung der Ladungsverteilung von solchen Verbindungen geeignet ist. In der Verbindungsreihe $(CH_3)_n-C-(OCH_3)_{4-n}$, wo n = 0, 1, 2, 3, 4 sein kann, wurde eine Korrelation zwischen den auf die einzelnen Atome berechneten partiellen Ladungsverteilungen und den NMR-Verschiebungen gefunden. Die Anwendbarkeit dieser Methode wurde auch noch durch eine Dipolmomentberechnung bewiesen die im Falle einer Verbindung mit der vektoriellen Addierung der Bindungspolaritätswerte bzw. der entsprechenden Bindungsmomente durchgeführt wurde. Das berechnete Dipolmoment stimmt mit dem experimentellen Wert innerhalb der Fehlergrenze überein.

Das Ziel der vorliegenden Arbeit ist die Untersuchung dessen, wie die Methode von DEL RE zur Berechnung der gespannten heterocyclischen Ringe anwendbar ist. Wir haben analog wie in der bereits zitierten Arbeit, Berechnungen für die ersten gesättigten cyclischen Äther: Äthylenoxyd, Trimethylenoxyd, Tetrahydrofuran und Tetrahydropyran durchgeführt. Die Deformation ist im Falle der fünf- und sechsgliedrigen cyclischen Äther so gering, daß diese Verbindungen den Charakter eines aliphatischen Äthers haben. Dementsprechend liefert die Methode von DEL RE mit den ursprünglichen Parametern die richtigen partiellen Ladungen und das experimentell gemessene Dipolmoment. In den dreigliedrigen und viergliedrigen Ringen existiert eine viel stärkere Deformation, die die Änderung der Hybridisation und sogar die Abnahme der Überlappung zur Folge hat. Die von DEL RE verwendeten ur-

sprünglichen Konstanten entsprechen aber im Falle des Kohlenstoffes der aliphatischen sp^3 Hybridisation und beim Sauerstoff der allgemeinsten Übergangshybridisation mit 18,9%-igem »s«-Charakter [3] sowie der vollkommenen Überlappung. Diese Tatsache wurde im Laufe der Berechnungen berücksichtigt, und so haben wir auch bei diesen gespannten Ringen richtige Ergebnisse erhalten.

Berechnung der Heteroringe vom aliphatischen Typ

Die Ladungsverteilung und die Bindungsdipolmomente der Moleküle wurden im Falle des Tetrahydrofurans und Tetrahydropyrans analog mit denen der aliphatischen Verbindungen berechnet. Durch die vektorielle Summation der Bindungsdipolmomente erhielten wir das resultierende Dipolmoment der Moleküle, welches mit den experimentellen Werten gut übereinstimmt (Tabelle II). Zu dieser Addition waren die experimentellen Bindungsabstände und Bindungswinkel dieser beiden Verbindungen nötig. Wir nahmen im Falle des Tetrahydrofurans ein regelmäßiges planares Fünfeck und beim Tetrahydropyran eine regelmäßige Sesselform an. Als Bindungsabstände wurden auf Grund der Elektronendiffraktionsmessungen [4] die aliphatischen Abstände als maßgebend betrachtet.

$$R_{CC} = 1{,}54 \text{ Å}$$
$$R_{CO} = 1{,}43 \text{ Å}$$
$$R_{CH} = 1{,}09 \text{ Å}$$

Das Gleichungsystem, das die Coulomb-Parameter des Tetrahydrofurans liefert, ist das folgende (die Kohlenstoff- und Wasserstoff-Atome wurden vom Sauerstoff-Atom ausgehend mit den Indexen 1 und 2 bezeichnet).

$$\delta_{H^1} = \delta_{H^0} + \gamma_{H(C)}\,\delta_{C^1}$$
$$\delta_{H^2} = \delta_{H^0} + \gamma_{H(C)}\,\delta_{C^2}$$
$$\delta_{C^1} = \delta_{C^0} + 2\,\gamma_{C(H)}\,\delta_{H^1} + \gamma_{C(C)}\,\delta_{C^2} + \gamma_{C(O)}\,\delta_O$$
$$\delta_{C^2} = \delta_{C^0} + 2\,\gamma_{C(H)}\,\delta_{H^2} + \gamma_{C(C)}\,\delta_{C^1} + \gamma_{C(C)}\,\delta_{C^2}$$
$$\delta_O = \delta_{O^0} + 2\,\gamma_{O(C)}\,\delta_{C^1}$$

Die Lösungen des Gleichungssystems sind:

$$\delta_{H^1} = 0{,}0666 \qquad \delta_{C^1} = 0{,}1664$$
$$\delta_{H^2} = 0{,}0525 \qquad \delta_{C^2} = 0{,}1313$$
$$\delta_O = 0{,}4333$$

Werte der Polaritätsgrade der einzelnen Bindungen:

$$Q_{C^1-H^1} = +0{,}0499$$
$$Q_{C^2-H^2} = +0{,}0394$$
$$Q_{C^1-C^2} = +0{,}0176$$
$$Q_{C^1-O} = -0{,}1405$$

Die partielle Ladungsverteilung des Moleküls ist in Abb. 1 dargestellt.

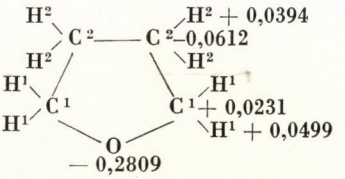

Abb. 1. Ladungsverteilung im Tetrahydrofuran

Die Berechnung des resultierenden Dipolmomentes bedeutete selbst in diesem einfachen Fall ein kompliziertes Vektorsummierungs-Problem.

Die Bindungsdipolmomentwerte sind:

$$m_{C^1-H^1} = 8{,}7 \cdot 10^{-3} \text{ Coulombmeter}$$
$$m_{C^2-H^2} = 6{,}85 \cdot 10^{-31} \text{ Cm}$$
$$m_{C^1-C^2} = 4{,}32 \cdot 10^{-31} \text{ Cm}$$
$$m_{O-C^1} = 32{,}1 \cdot 10^{-31} \text{ Cm}$$

Das berechnete resultierende Dipolmoment ist 1,60 D, das experimentell erhaltene 1,75 D.

Die Coulomb-Parameter des Tetrahydropyrans können aus dem folgenden Gleichungssystem erhalten werden. (Die Numerierung ist der beim Tetrahydrofuran angewendeten analog).

$$\delta_{H^1} = \delta_{H^0} + \gamma_{H(C)}\,\delta_{C^1}$$
$$\delta_{H^2} = \delta_{H^0} + \gamma_{H(C)}\,\delta_{C^2}$$
$$\delta_{H^3} = \delta_{H^0} + \gamma_{H(C)}\,\delta_{C^3}$$
$$\delta_{C^1} = \delta_{C^0} + 2\,\gamma_{C(H)}\,\delta_{H^1} + \gamma_{C(C)}\,\delta_{C^2} + \gamma_{C(O)}\,\delta_O$$
$$\delta_{C^2} = \delta_{C^0} + 2\,\gamma_{C(H)}\,\delta_{H^2} + \gamma_{C(C)}\,\delta_{C^1} + \gamma_{C(C)}\,\delta_{C^3}$$
$$\delta_{C^3} = \delta_{C^0} + 2\,\gamma_{C(H)}\,\delta_{H^3} + 2\,\gamma_{C(C)}\,\delta_{C^2}$$
$$\delta_O = \delta_{O^0} + 2\,\gamma_{O(C)}\,\delta_{C^1}\,.$$

Nach Substitution der Konstanten und Lösung des Gleichungssystems gelangen wir zu den folgenden Coulomb-Parametern:

$$\delta_{H^1} = 0{,}0665 \qquad \delta_{C^1} = 0{,}1663$$
$$\delta_{H^2} = 0{,}0522 \qquad \delta_{C^2} = 0{,}1306$$
$$\delta_{H^3} = 0{,}0506 \qquad \delta_{C^3} = 0{,}1265$$
$$\delta_{O} = 0{,}4333$$

Aus diesen wurden die Bindungspolaritäten berechnet. Die Werte sind die folgenden:

$$Q_{C^1-H^1} = +0{,}0499 \qquad Q_{C^1-C^2} = +0{,}0178$$
$$Q_{C^2-H^2} = +0{,}0392 \qquad Q_{C^2-C^3} = +0{,}0021$$
$$Q_{C^3-H^3} = +0{,}0379 \qquad Q_{C^1-O} = -0{,}1405$$

Die partielle Ladungsverteilung des Tetrahydropyrans ist in Abbildung 2 dargestellt.

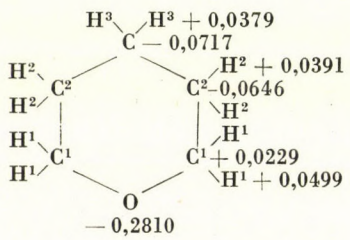

Abb. 2. Ladungsverteilung im Tetrahydropyran

Das berechnete resultierende Dipolmoment ist 1,44 D, der experimentelle Wert ist 1,55 D.

Berechnung der gespannten Heteroringe, Modifizierung der Parameter von Del Re

Es kann angenommen werden, daß die Sauerstoff- und Kohlenstoffatome in der aliphatischen Bindung in sp^3 bzw. in einem sehr ähnlichen Hybridzustand vorliegen. Der Valenzwinkel im Äthylenoxyd (60°) und im Trimethylenoxyd (90°) weicht jedoch stark von dem für die sp^3-Hybridisation charakteristischen Winkel (109° 9') ab. Diese Deformation des tetraederischen Valenzwinkels hat nach den quantenchemischen Berechnungen keine Realität. In diesen Fällen deformiert sich in erster Reihe nicht der Valenzwinkel, sondern es vermindert sich die Überlappung der sp^3 Molekülorbitale. D. h., ein Energieminimum kommt einerseits durch die geringere Modifizierung des Bindungswinkels, andererseits durch die stärkere Abnahme der Überlappung zustande.

Das Abnehmen der Überlappung der Atombahnen bzw. die proportionale Änderung des Austauschparameters kann mit dem folgenden Zusammenhang berücksichtigt werden:

$$\varepsilon' = \varepsilon(\cos \Theta) \tag{1}$$

wo Θ der Winkel zwischen zwei Molekülorbitalen ist.

Die Annäherung an das andere Problem, nämlich die Bestimmung des effektiven Hybridzustandes der einzelnen Atome, ist schon viel schwieriger. Wir haben hierzu die Angaben von PULLMANN u. Mitarb. [3] benutzt, die eine Korrelation zwischen der sogenannten Bahnelektronegativität und den konstanten Gliedern der Coulomb-Parameter der einzelnen Atome bzw. der durch diese

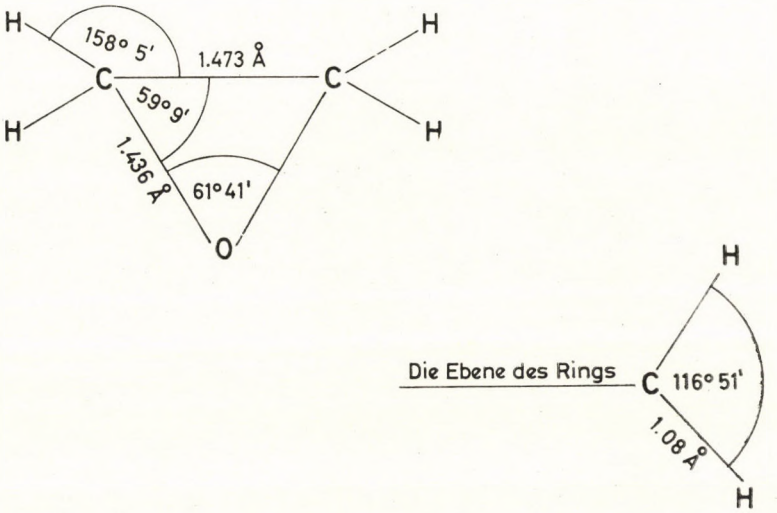

Abb. 3. Änderung des Coulomb-Parameters des Sauerstoffatoms als Funktion der Bahnelektronegativität

zustandegebrachten Bindungen angegeben haben. Die Bahnelektronegativitäten hängen vom Zustand der Hybridisation ab und können aus den Promotionsenergien nach der Methode von HINZE und JAFFE [5] berechnet werden. Es ist wichtig zu bemerken, daß im Gegensatz zum konstanten Glied der Coulomb-Parameter nach DEL RE, welches eine für das Atom charakteristische Größe ist, die Bahnelektronegativität für jede einzelne durch das betreffende Atom zustandegebrachte Bindung einen anderen Wert aufnehmen kann. Daher kann diese von PULLMANN gefundene Korrelation nur für solche Atome gültig sein, die gleichartige Bindungen eingehen, weil so alle Bindungen derselben Hybridisation, d. h. demselben »s« Charakter entsprechen der für das betreffende Atom charakteristisch ist. Diese Bedingung ist bei unseren Verbindungen

für Sauerstoff erfüllt, somit kann die PULLMANNsche Korrelation angewendet werden. Diese Korrelation wurde in Abbildung 3 dargestellt, wo die Änderung von δ_O^0, des konstanten Gliedes des Coulomb-Integrals des Sauerstoffatoms als Funktion der χ_p Bahnelektronegativität dargestellt ist.

In der Arbeit von HINZE und JAFFE [5] sind die Bahnelektronegativitätswerte für einige genau definierte Hybridzustände des Sauerstoffes angegeben. Wir stellten die Bahnelektronegativitäten als Funktion des entsprechenden »*s*« Charakters dieser Hybridzustände dar und erhielten so eine Gerade (Abb. 4).

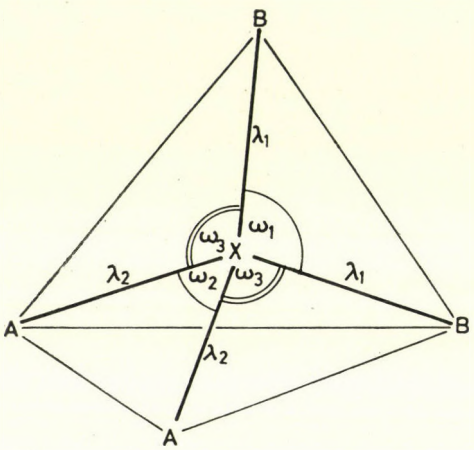

Abb. 4. Änderung der Bahnelektronegativität des Sauerstoffatoms als Funktion des »*s*«-Charakters der Bindungen

Die Bahnelektronegativität eines Übergangshybridzustandes zwischen den Grundhybridzuständen ist aus dieser Abbildung abzulesen, wenn es möglich ist den »*s*« Charakter der betreffenden Hybridisation zu berechnen. Für diesen ist der folgende Zusammenhang bekannt:

$$1 + \lambda^2 \cos \omega = 0, \tag{2}$$

wo ω der Winkel zwischen zwei gleichwertigen Bindungen eines Atomes und λ ein für den »*s*« Charakter kennzeichnender Parameter ist. In Kenntnis von λ ergibt die Gleichung (3) den »*s*« Charakter der Bindungen:

$$s_{\text{Char}}(\%) = \frac{1}{1 + \lambda^2} 100. \tag{3}$$

Handelt es sich um zwei Bindungen verschiedenen Charakters, so gilt Gleichung (4) statt (2), in diesem Falle ist nämlich für jede Bindung ein anderer Wert

charakteristisch

$$1 + \lambda_1\lambda_2 \cos\omega = 0 \tag{4}$$

$$s^1_{\text{Char}}(\%) = \frac{1}{1 + \lambda_1^2} \cdot 100 \tag{5}$$

$$s^2_{\text{Char}}(\%) = \frac{1}{1 + \lambda_2^2} \cdot 100. \tag{6}$$

Diese Verhältnisse wurden in Abbildung 5 dargestellt (für den Fall eines solchen X Atoms, welches eine Bindung mit zwei A Atomen und mit zwei B Atomen zustandebringt). Es ist auch bekannt, daß die Summe der »*s*« Charaktere aller Hybridorbitale eines Atoms gleich 1 ist.

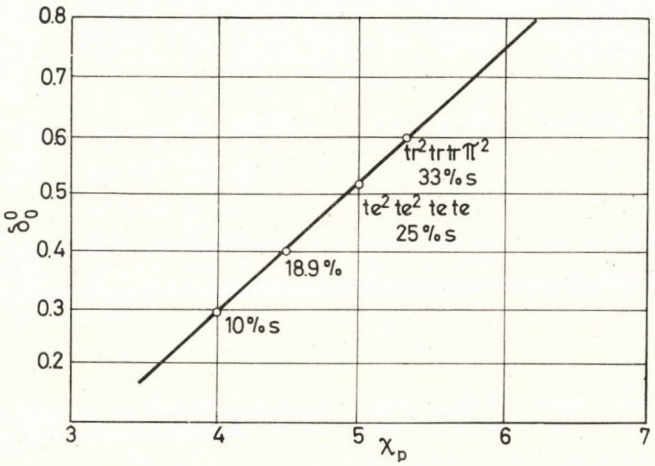

Abb. 5. Bindungen des Atoms X mit den Atomen A und B

Berechnung für das Äthylenoxyd-Molekül

Die Bindungsabstände und Bindungswinkel wurden aus den Mikrowellen-Rotationsspektren [6] sehr genau bestimmt (Abb. 6). Die genau bekannten Bindungswinkel gestatten es, die »*s*« Charaktere des Kohlenstoffes zu berechnen. Auf die Kohlenstoff-Wasserstoff-Bindungen in Äthylenoxyd entfallen nach den Berechnungen 31,05% »*s*« Charakter; für die anderen beiden Bindungen des Kohlenstoffatoms bleiben 18,9%, sofern diese als gleichwertig angenommen werden. In Kenntnis des »*s*«-Charakters konnte der tatsächliche ω_2 Bindungswinkel bestimmt werden, für den sich der Wert von 103° 25′ ergab.

Für den Sauerstoff ist diese Berechnung auf exakte Weise nicht durchzuführen, da die Bahnwinkel der beiden einsamen Elektronenpaare nicht bekannt sind, und man so lediglich auf Proben angewiesen ist. Wie man sieht,

ist der Wert des »*s*«-Charakters im Falle des Kohlenstoffes für die einzelnen Bindungen verschieden, und es ist daher nicht möglich, δ_C^0 den konstanten Teil der Coulomb-Integrale des Kohlenstoffes mit ihnen in Korrelation zu bringen, obwohl es sehr wahrscheinlich ist, daß die Änderung des kleinen Wertes 0,07 das Ergebnis nicht bedeutend beeinflussen würde.

Wir haben Ladungsverteilung- und Dipolmomentberechnungen für das Äthylenoxyd-Molekül mit mehreren δ_O^0-Werten durchgeführt, um zu unter-

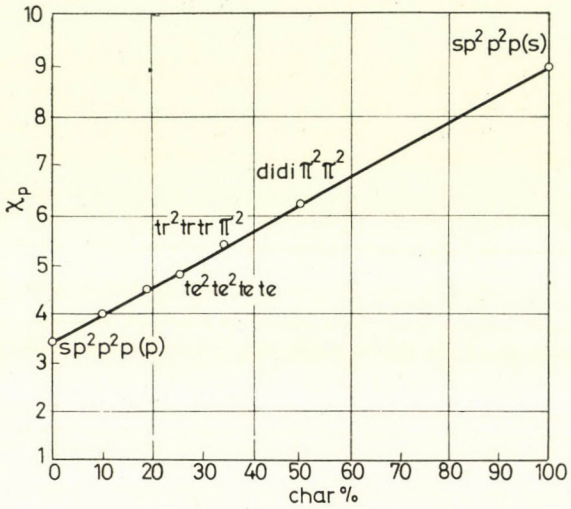

Abb. 6. Bindungsabstände und Bindungswinkel im Äthylenoxyd

suchen, welche Annäherung das beste Ergebnis liefert. Die wichtigeren Ergebnisse der Annäherungsberechnungen sind in Tabelle I zusammengestellt.

Die beste Annäherung für den Dipolmomentwert des Äthylenoxyds ist 1,85 D, d. h. dieser Wert stimmt mit dem experimentellen Wert gut überein (Tabelle II). Die Ladungsverteilung wurde in Abbildung 7 dargestellt.

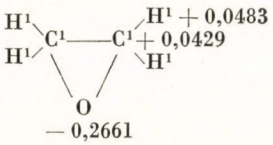

Abb. 7. Ladungsverteilung im Äthylenoxyd

Die Überlappung der Kohlenstoff-Sauerstoff-Bindung blieb während der Annäherungen selbstverständlich auch nicht konstant; dies wurde im Sinne von (1) berücksichtigt.

Tabelle I

Zusammenfassung der wichtigeren Ergebnisse der Annäherungsberechnungen für den Fall des Äthylenoxyd-Moleküls

Annäherung	»s« Char (Sauerstoff)	C—O—C effektiver Bindungswinkel	δ_O^0	μ
1.	11,5	97°08'	0,30	1,66
2.	12,0	97°32'	0,31	1,69
3.	12,5	98°3'	0.32	1,79
4.	13,0	98°36'	0,33	1,85
5.	18,9	103°25'	0,40	2,44

Berechnung für Trimethylenoxyd

Das Verfahren war im Falle des Trimethylenoxyds analog, aber eine Änderung von δ_O^0 war nicht nötig, da die Deformation von geringerem Maße war. Wenn wir annehmen, daß die Winkel im Trimethylenoxyd 90° sind und die Deformationen des tetraederischen Valenzwinkels nicht berücksichtigt werden, können wir mit $\Theta = 160°$ rechnen. In diesem Sinn wurden die Austauschparameter modifiziert ($\varepsilon_{CC} = 0{,}940$; $\varepsilon_{CO} = 0{,}893$) und die Rechnung

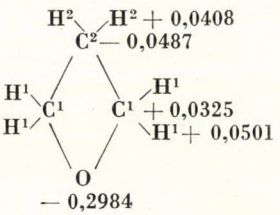

Abb. 8. Ladungsverteilung im Trimethylenoxyd

nach der Methode von Del Re durchgeführt. Für das Dipolmoment ergab sich so 1,925 D, was mit dem experimentellen Wert gut übereinstimmt (Tabelle II). Im Falle der völligen Überlappung hätten wir den Wert 1,765 D erhalten. Die Ladungsverteilung ist in Abbildung 8 dargestellt.

Tabelle II

Berechnete und gemessene Dipolmomente

Verbindung	Dipolmoment ber.	(D) gem.
Äthylenoxyd	1,85	1,83 [7]
Trymethylenoxyd	1,925	1,92 [8]
Tetrahydrofuran	1,60	1,75 [9]
Tetrahydropyran	1,44	1,55 [9]

Vergleich und Auswertung der Ergebnisse

Es lohnt sich nun, im weiteren die mit den Berechnungen erhaltenen Ladungsverteilungen zu untersuchen. Es ist bei jeder Verbindung deutlich zu erkennen, daß sich die partiellen Ladungen der vom Sauerstoff weiter entfernt liegenden Kohlenstoff- und Wasserstoffatome wegen der ständig abnehmenden elektronensaugenden Wirkung des Wasserstoffes schnell vermindern. (Der $-I$ Effekt wirkt in erster Reihe auf die unmittelbar benachbarten Atome).

Die NMR-Verschiebungen (τ-Signale) [10] des Wasserstoffs zeigen eine gute Korrelation mit den berechneten partiellen Ladungen. Einerseits nehmen die τ-Signale in einer Verbindung mit wachsender Entfernung vom Sauerstoff zu, da die Protonen negativer werden, andererseits finden wir wieder eine Korrelation beim Vergleich der partiellen Ladungen und der entsprechenden τ-Signale der Protonen in gleichen Stellungen in den vier Verbindungen. Interessanterweise zeigen die τ-Signale der Protonen in Position 1 zum Sauerstoff und die entsprechenden partiellen Ladungswerte beim Trimethylenoxyd einen Grenzwert. Gleichzeitig ist auch das Dipolmoment des Trimethylenoxyds das

Tabelle III

τ-Signale und partielle Ladungen (q) der entsprechenden Wasserstoffatome der ersten vier cyclischen Äther

Verbindung	H_1		H_2		H_3	
	τ-Signal (ppm)	q	τ-Signal (ppm)	q	τ-Signal (ppm)	q
Äthylenoxyd	7,42	0,0483	—	—	—	—
Trimethylenoxyd	5,27	0,0501	7,27	0,0408	—	—
Tetrahydrofuran	6,25	0,0499	8,15	0,0394	—	—
Tetrahydropyran	6,44	0,0499	8,42	0,0392	8,42	0,0379

Tabelle IV

Berechnete Bindungspolaritätsgrade

Bindung	Äthylenoxyd	Trimethylenoxyd	Tetrahydrofuran	Tetrahydropyran
C^1-H^1	0,0493	0,0502	0,0499	0,0499
C^2-H^2	—	0,0408	0,0394	0,0392
C^3-H^3	—	—	—	0,0379
C^1-C^2	—	0,0165	0,0176	0,0178
C^2-C^3	—	—	—	0,0021
$O-C^1$	0,1395	0,1492	0,1405	0,1405

größte in der Verbindungsserie. Auch diese gute Übereinstimmung ist ein Beweis für die Verläßlichkeit unserer Methode. Die τ-Signale und die entsprechenden partiellen Ladungswerte enthält Tabelle III.

Schließlich kann auch beobachtet werden, daß die Polarität der C—C Bindungen in den einzelnen Verbindungen mit der Distanz vom Sauerstoff stark abnimmt (Tabelle IV). Das gleiche gilt auch für die C—H Bindungen.

LITERATUR

1. KÁDAS, I.: Berechnung des σ-Bindungssystems einiger organischer Verbindungen mit der Methode van Del Re (ungarisch).
2. DEL RE, G.: Journal of the Chemical Society, **1958** 4031.
3. BERTOD, H., GIESSNER-PRETTE, Cl., PULLMAN, A.: Theoretica Chimica Acta (Berl.) **8**, 212 (1967).
4. BEACH, J. Y.: J. Chem. Phys. **9**, 54 (1941).
5. HINZE, J., JAFFE, H. H.: Journal of the American Chemical Society **84**, 540 (1962).
6. CUNNINGHAM: Journal of Chemical Physics **17**, 211 (1949).
7. ANGAL, BARCLAY, LEFEBVRE: Journal of the Chemical Society **1950**, 3370.
8. MILLER: Physical Review **89**, 341 (1953).
9. CUMPER, VOGEL, A.: Journal of the Chemical Society, **1959**, 3521.
10. SUHR, H.: Anwendungen der kernmagnetischen Resonanz in der organischen Chemie. Springer Verlag, Berlin, New York, Heidelberg.

József NAGY
József RÉFFY,
István KÁDAS
Budapest XI., Gellért tér 4.

Acta Chimica Academiae Scientiarum Hungaricae, Tomus 62 (4), pp. 425—428 (1969)

STOICHIOMETRIC HYDROGENATION OF OLEFINS WITH COBALT CARBONYL HYDRIDE

F. UNGVÁRY and L. MARKÓ

(University of Chemical Industries, Institute of Organic Chemistry and Research Group of Petrochemistry of the Hungarian Academy of Sciences, Veszprém)

Received October 24, 1968

Cobalt carbonyl hydride at low temperature hydrogenates heptene to neptane and conjugated diolefins to monoolefins, in stoichiometric reactions. In the latter case, the selectivity exceeds 90%.

Rather detailed studies have been reported concerning the reactions of monoolefins and diolefins with $HCo(CO)_4$. In the case of monoolefins, attention was focused on the formation of acylcobalt tetracarbonyls [1] and aldehydes [2], according the following stoichiometry:

$$RCH{=}CH_2 + HCo(CO)_4 \xrightarrow{CO} RCH_2CH_2COCo(CO)_4 \xrightarrow{HCo(CO)_4}$$
$$RCH_2CH_2CHO + Co_2(CO)_8.$$

With diolefins, the principal products were found to be π-allylcobalt-tricarbonyl complexes [3]:

$$RCH{=}CH{-}CH{=}CH_2 + HCo(CO)_4 \longrightarrow RCH_2 - \underset{\diagdown\ \diagup}{CH} \quad CH_2 + CO$$
$$Co(CO)_3$$

We have observed that hydrogenation reactions also take place to a considerable extent in these reaction mixtures.

In the reactions of *n*-heptene-1 and $HCo(CO)_4$ in pentane solution under an atmosphere of carbon monoxide or nitrogen at $+10°C$ and $0°C$, respectively, and striving to obtain as complete material balances as possible, the results shown in Figs 1 and 2 were obtained. As can be seen, the yield of heptane was highest at relatively low olefin : cobalt ratios, and sometimes exceeded 30% based on $HCo(CO)_4$. The products obtained at higher heptene : $HCo(CO)_4$ ratios also contained small amounts of acylcobalt tetracarbonyls, as evidenced by the infrared spectra.

In accordance with the generally accepted scheme [1] for reactions between olefins and $HCo(CO)_4$, the stoichiometric hydrogenation can be assumed

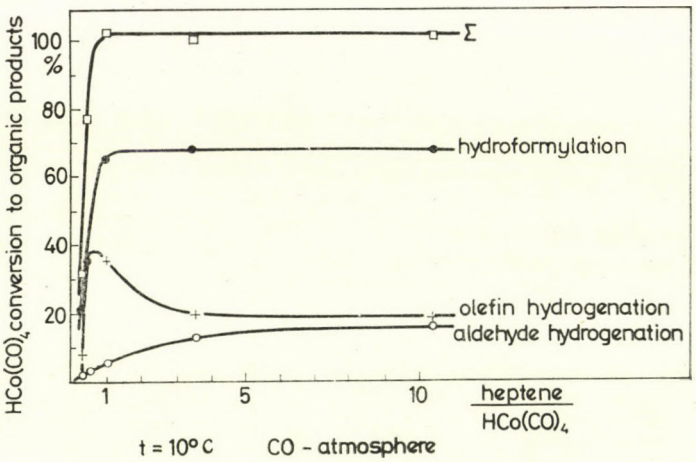

Fig. 1

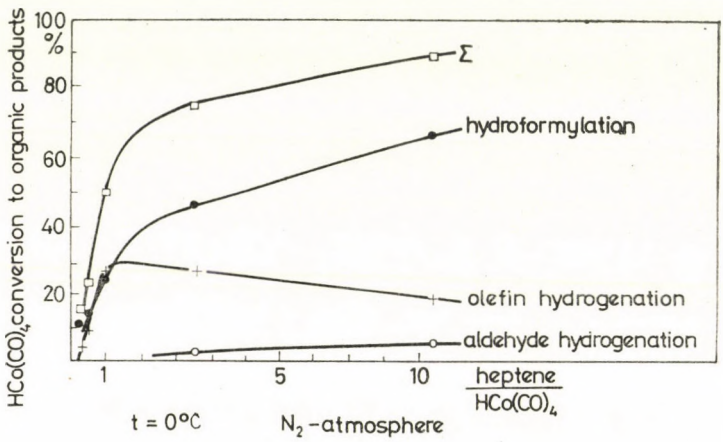

Fig. 2

to proceed by the reaction between an alkylcobalt carbonyl and cobalt carbonyl hydride before carbon monoxide insertion:

$$RCH{=}CH_2 + HCo(CO)_4 \longrightarrow RCH_2CH_2Co(CO)_4 \xrightarrow{HCo(CO)_4} RCH_2CH_3 + Co_2(CO)_8$$

$$\Downarrow\Uparrow$$

$$RCH_2CH_2COCo(CO)_3 \longrightarrow \text{hydroformylation products and acylcobalt tetracarbonyls}$$

This mechanism explains why the highest yields of heptane were observed at relatively low olefin : cobalt ratios, since obviously a large concentration of $HCo(CO)_4$ favours its reaction with the alkylcobalt carbonyl first formed.

Previous work [4] has shown that hydrogenation of olefins is a general side reaction under the conditions of oxo synthesis (150°C, 200 atm), though in the case of straight-chain olefins it takes place only to a relatively small extent. The higher selectivity in favour of hydroformylation in the catalytic synthesis, compared with the results obtained in this investigation, can be attributed to the high partial pressure of carbon monoxide prevailing under "oxo-conditions", a circumstance facilitating the insertion of carbon monoxide into the cobalt-carbon bond.

When conjugated diolefins were reacted with $HCo(CO)_4$ in pentane solution under carbon monoxide or nitrogen at 0°C, a highly selective and fast hydrogenation to the corresponding monoolefins was observed. In the case of butadiene and isoprene, the hydrogenated product was a mixture of isomeric butenes and methylbutenes (yield 94% and 83% respectively, based on $HCo(CO)_4$). Cyclohexadiene-1,3 yielded cyclohexene; with cyclopentadiene as the model substance, the results compiled in Table I were obtained.

Table I

Cyclopentadiene: $HCo(CO)_4$ ratio	$HCo(CO)_4$ used for hydrogenation of cyclopentadiene, % *	Atmosphere
0.45	78	N_2
0.58	97	CO
1.17	92	N_2
1.17	104	CO
2.94	99	N_2
2.94	97	CO
11.0	90	N_2
11.0	106	CO

* Based on $HCo(CO)_4$ introduced, and calculated from the amount of cyclopentene formed. The amount of $HCo(CO)_4$ used for hydroformylation (calculated from the amount of C_6-aldehydes formed) was always less than 1%.

According to the infrared spectra, the products obtained from different diolefins under such conditions contained only small amounts of π-allylcobalt--tricarbonyl type complexes. This rather unexpected result may be explained by the following sequence of reactions:

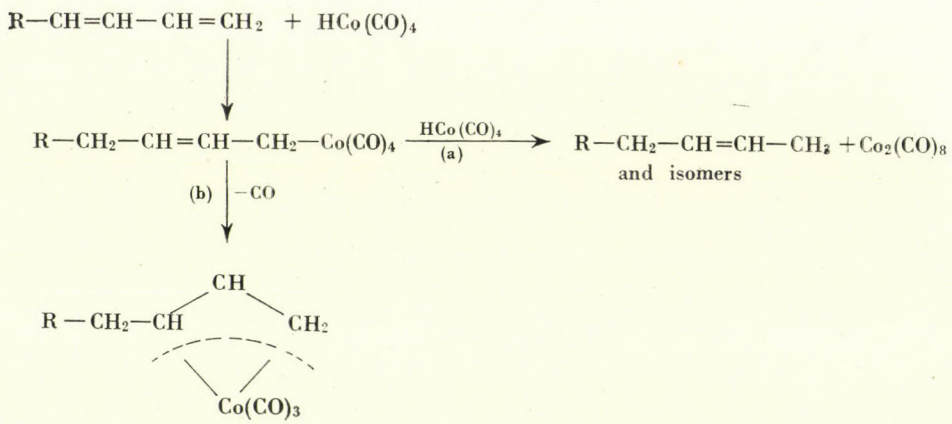

Accordingly, the product composition is determined by the relative rates of reactions (*a*) and (*b*). A relatively large concentration of $HCo(CO)_4$ should again favour the hydrogenation of the intermediate σ-allylcobalt carbonyl. If, however, low concentrations of $HCo(CO)_4$ are used, the σ-allyl complex can be transformed principally to the π-allyl derivative. This may explain the somewhat unusual conditions [3] employed in the preparation of the latter complexes.

Experimental

Reaction of $HCo(CO)_4$ with heptene-1

A solution of cobalt carbonyl hydride in pentane was prepared by the method of STERNBERG *et al.* [5]. This solution was cooled to —60°C and heptene-1 was added. When working under nitrogen, the reaction mixture was warmed to 0°C and allowed to stand at this temperature for 6 hrs. In the experiments under carbon monoxide, the reaction mixture was warmed to 10°C and stirred at this temperature for 6 hrs. After this time, samples were taken for infrared spectroscopy and gas chromatographic analysis. The yield of organic product was determined by the estimation of gas chromatographic peak areas, using known amounts of 2,3-dimethylpentane as the reference substance.

Reaction of $HCo(CO)_4$ with cyclopentadiene

The experimental procedure was essentially the same as that used for heptene-1 with the exception that the reaction time was 2 hrs. at 0°C. The reaction started even at —30°C as shown by the rapid crystallization of pure $Co_2(CO)_8$.

REFERENCES

1. HECK, R. F., BRESLOW, D. S.: J. Am. Chem. Soc. **83,** 4023 (1961).
2. KARAPINKA, G. L., ORCHIN, M.: J. Org. Chem. **26,** 4187 (1961); ROOS, L., ORCHIN, M.: J. Org. Chem. **31,** 3015 (1966).
3. JONASSEN, H. B., STEARNS, R. I., KENTTÄMAA, J., MOORE, D. W., WHITTAKER, A. G.: J. Am. Chem. Soc. **80,** 2586 (1958); HUSEBYE, S., JONASSEN, H. B.: Acta Chem. Scand. **18,** 1547 (1964).
4. MARKÓ, L.: Chem. Ind. (London), **1962,** 260.
5. STERNBERG, H. W., WENDER, I., FRIEDEL, R. A., ORCHIN, M.: J. Am. Chem. Soc. **75,** 2717 (1953).

László MARKÓ
Ferenc UNGVÁRY
Veszprém, Schönherz Z. u. 12. Hungary.

Acta Chimica Academiae Scientiarum Hungaricae, Tomus 62 (4), pp. 429—436 (1969)

NEW NITROCHALCONES, X*

CORRELATION OF THE CHOICE OF THE CONDENSING AGENT WITH THE STRUCTURE OF THE REACTANTS

T. SZÉLL and I. SOHÁR

(Department of Applied Chemistry, Attila József University of Szeged, Szeged)

Received November 21, 1968

The choice of condensing agent for the synthesis of chalcones from substituted benzaldehydes and acetophenones is clearly related to the Hammett substituent constants. In general, reactants having large Hammett's σ constants require sodium hydroxide, those having low values require hydrogen chloride, and the intermediate group can be condensed with either reagent. These generalization may, however, be offset by factors such as solubility, side reactions, etc. The Hammett equation has been found to hold for the base-catalyzed Claisen—Schmidt condensation, serving as a guide in correlating the structures of the reactants with their reactivity.

The effect of some side chain substituents has also been examined and three new chalcones have been synthesized.

Introduction

Chalcones are of considerable biological importance on account of their pharmacological activity and because they are isomeric with flavanones which are known to occupy a central position in flavonoid biosynthesis [1—3]. Nitrohydroxychalcones have proved to be suitable models for studying the formation of chalcones [4] from the appropriate acetophenone and aldehyde.

$$ArCOCH_3 + OHC-Ar' \rightarrow Ar-CO-CH=CH-Ar'$$

Previous communications in this series attempted to elucidate the correlation of the structure of the reactants with their reactivities and with the choice of the condensing agent. In the present work some of our relevant results of earlier works have been summarized, extended and final conclusions drawn.

Results and discussion

Substituents in the nucleus

Experiments carried out in the presence of sodium hydroxide or sodium alkoxides showed that the substituents increased the yield of chalcone formation in water, aqueous ethanol, or ethanol in the following way [5, 6, 10]:

* Part IX: SZÉLL, T., SOHÁR, I.: Canad. J. Chem. **47**, 1254 (1969).

(*a*) In the acetophenone component:

$$2\text{-}NO_2 > 4\text{-}NO_2 > 3\text{-}NO_2 \quad (1)$$

$$3\text{-}OH > 2\text{- and } 4\text{-}OH \quad (2)$$

$$6\text{-}NO_2\text{-}3\text{-}OH > 4\text{-}NO_2\text{-}2\text{-}OH > 5\text{-}NO_2\text{-}2\text{-}OH > 3\text{-}OH > 3\text{-}NO_2\text{-}4\text{-}OH \quad (3)$$

(*b*) In the aldehyde component:

$$4\text{-}NO_2 > 4\text{-}Cl > H \approx 3\text{-}OH > 4\text{-}OH \quad (4)$$

$$4\text{-CN} > H > 1\text{-naphthaldehyde} > 3,4\text{-methylenedioxy} > 4\text{-iPr} > 3,4\text{-diOMe} \approx 3,4\text{-diOEt} > 4\text{-OH-3-OMe} > 2\text{- and } 4\text{-OH} \quad (5)$$

$$H \gtrapprox 2\text{-OMe} \approx 2\text{-OEt} \quad (6)$$

$$2,3\text{-diOMe} \gtrapprox 2,5\text{-diOMe} > H > 2,4\text{-diOMe} \quad (7)$$

Results of experiments carried out in the presence of hydrogen chloride in ethanol showed the following order of effectiveness of the substituents [5, 6, 10];

(*a*) In the acetophenone component:

$$3\text{-}NO_2\text{-}4\text{-}OH > 4\text{-}NO_2\text{-}2\text{-}OH > 4\text{-}NO_2 \quad (8)$$

(*b*) In the benzaldehyde component:

$$4\text{-OH-3-OMe} > 3,4\text{-diOMe} > OH \approx 4\text{-OMe} > 4\text{-H} > \text{halogen} > 4\text{-}NO_2 \quad (9)$$

$$4\text{-OH} > 4\text{-}NO_2 \quad (10)$$

$$4\text{-OH} \gtrapprox 4\text{-OMe} \gtrapprox 4\text{-OH-3-OMe} > 3,4\text{-diOMe} \approx 3,4\text{-diOEt} \gtrapprox 4\text{-Me} > 4\text{-H} > 4\text{-Cl} > 4\text{-}NO_2 > 2,4\text{-di}NO_2 \quad (11)$$

$$2,4\text{-diOMe} \gtrapprox 2\text{-OMe} > H > 2,3\text{-diOMe} \approx 2,5\text{-diOMe} \quad (12)$$

In general, a definite parallelism can be observed between the effectiveness of a substituent in increasing the yield of the alkali-catalyzed condensation and in increasing the electrophilic character (pK_{BH+}) and the Hammett constants.* The order of substituents in the condensation carried out in the presence of hydrogen chloride is roughly the reverse to that found in alkaline solution. The more basic the aldehyde, *i.e.* the more negative the substituent constant, the higher the yield of chalcone formation. The choice of condensing

* *Cf.* the σ-values in Table I. While the *m* and *p*-substituent constants are simply additive (*e.g.*, in 3,4- or 3,5-disubstituted components), *ortho* constants are not. However, a comparison such as given in Series (8) and (13) is still possible, since the same *ortho* substituent is present in each compound. In some cases (*e.g.*, in Series (3) and (8)) no quantitative comparison is possible on the basis of the Hammett constants.

CORRECTION

In the paper by T. Széll and I. Sohár in Acta Chim. Acad. Sci. Hung. *62*, p. 430, an error was made in the order of the inequality series 11. Instead of 4-H > 4-Cl the correct order is 4-Cl > 4-H. In Fig. 3, the correct value of 4-Cl is 74%.

agent for the synthesis of chalcones is, therefore, related to the substituent constants.

Reactants with large Hammett's σ constants require bases (NaOH, NaOMe), those having low values require the use of hydrogen chloride, and the intermediate group can be condensed with either reagent. In other words, electron withdrawing substituents favour condensation by bases, whereas electron releasing groups favour the use of hydrogen chloride.

Table I

Hammett's σ constants of the substituents involved in this paper, taken from J. CLARK *and* D. D. PERRIN's *review* [7]

Substituent	Apparent *ortho* σ (in anilines)	*meta* σ	*para* σ
H	0.00	0.00	0.00
Me	0.10	−0.07	−0.17
Et	0.05	−0.07	−0.15
iPr	0.03	−0.07	−0.15
CN	—	0.56	0.66
			(1.00)
OH	−0.09	0.12	−0.37
O	—	−0.71	−0.52
OMe	0.00	0.12	−0.27
OEt	0.02	0.10	−0.24
Cl	0.67	0.37	0.23
Br	0.71	0.39	0.23
F	0.47	0.34	0.06
NO_2	1.72	0.71	0.78

These conditions are not surprising, since base-catalyzed condensation involves attack at the aldehyde carbon by a carbanion, formed by removal of a proton from the acetophenone. The acid-catalyzed condensation involves protonation of the carbonyl groups, thus the importance of the basicity of the reactants is evident (*cf.* with the references given under 15 in [5]).

The differences between the yields in the latter case, however, are sometimes not so marked as found in the base-catalyzed condensation. NOYCE [26] has suggested that the moderate difference between the effect of 4-OMe and 4-NO_2 substituents is due to two counterbalancing factors: a change in basicity of the aldehyde, and a change in the ease of bond formation between the reactants. Similarly, unsubstituted bi and tricyclic condensed aromatic aldehydes give chalcones in similar yields, in spite of definite differences in their basicities. Thus, for 9-anthraldehyde, 9-phenanthraldehyde and 1-naphthaldehyde, the

pK_{KB+} values are −4.81, −6.39 and −6.68, respectively [11]. The first aldehyde, being the most basic, should be the best for chalcone formation. Though actually all the three aldehydes readily give chalcones, the trend lies in the direction that the more basic* the aldehyde, the more complete the chalcone formation, but the differences are small [10]. Deviations from the pattern expounded above are also known, and some of them have been discussed previously [5]. In the base-catalyzed condensation, precipitation of the sodium salt of the chalcone may considerably improve the yield. On the other hand, condensation may go in the wrong direction in the presence of hydrogen chloride (*e.g.* with 2,4-dimethoxybenzaldehyde, *c.f.* [10]), resulting in decreased yields.

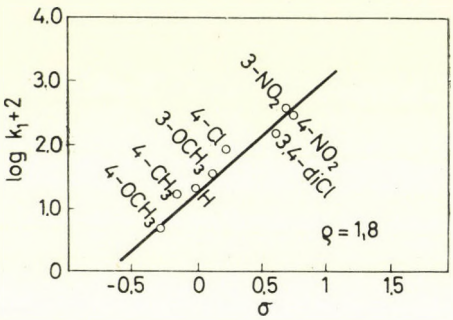

Fig. 1. Results of comparative experiments using substituted aldehydes and 5-nitro-2-hydroxyacetophenone in the presence of NaOH-EtOH-H_2O at 30°C. (k_1 = rate constant of chalcone formation)

The validity of the Hammett equation for chalcone formation was checked. As it can be seen in Figs 1 and 2, there is a linear correlation between the logarithm of the rate constants and Hammett's substitution constants, as expected on the basis of the Hammett function. Concerning this linear correlation, BROWN's σ^+ constants [12] did not give better results. An informative value for the reaction constant (ϱ) of the chalcone formation was graphically determined from Figs 1 and 2, the mean value being +1.9. The accuracy of this value is estimated to be 7.5%.

Owing to experimental difficulties, the Hammett treatment could not be carried out in the case of the HCl-catalyzed condensations as yet, however, it is obvious from Fig. 3 that in the latter case the reaction constant (ϱ) is negative, if the Hammet relation holds for the reaction.

Increase in the concentration of either condensing agent (NaOH or HCl) results in improving the yields of the chalcones.

* Basicity can be judged on the basis of BROWN's σ^+ constants [12], and also on that of $\Delta\nu$ of phenol, measured in the presence of the aldehyde examined in CCl_4 [13].

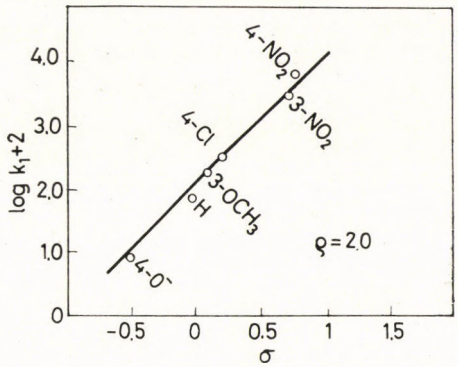

Fig. 2. Results of comparative experiments using unsubstituted benzaldehyde and substituted acetophenones in the presence of NaOH-EtOH-H_2O at 30°C (k_1 = rate constant of chalcone formation)

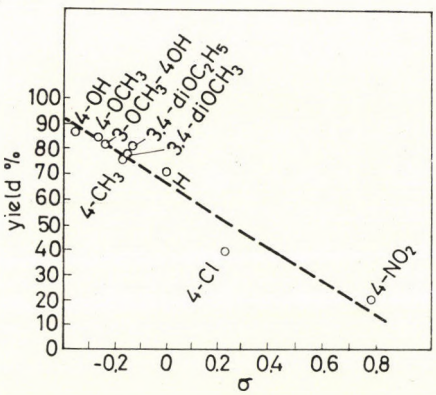

Fig. 3. The trend of correlation between the yield of chalcone formation and Hammett's σ constants, starting from 3-nitro-4-hydroxyacetophenone and different benzaldehydes, using HCl as the condensing agent. These results are taken from a previous work of the authors [10]

*ω-Substituents in the side chain of the acetophenone**

An *ω-nitro* substituent does not significantly increase the yield of chalcone formation. With this group the condensation cannot be performed in the presence of alkali, probably owing to enolization; the latter form has no active hydrogen available for the condensation, and the *trans* form of the enol may be stabilized by chelation (**I**).

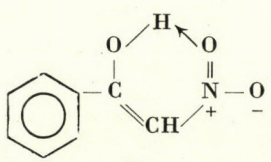

(I)

* In some papers named as α-substituents; cf. [14], [15].

Actually, the crystalline sodium salt of the enol form was isolated in these experiments. Furthermore, the lack of condensation is not the consequence of decomposition or of side-reactions (such as the Nef reaction), since ω-nitroacetophenone is surprisingly stable in alkali. The reaction could not be brought about in the presence of HCl either. In agreement with SORTER [14] and CAMPBELL [15], ω-nitroacetophenone can be successfully condensed with benzaldehyde Schiff bases under anhydrous conditions, *e.g.* in acetic anhydride, to give ω-nitrochalcones. However, the yields of 30—33% given by SORTER, could be increased up to 66% when hydrogen chloride was added to the reaction mixture containing the ketone and the Schiff base. Strangely enough, acetophenone and benzalbutylamine do not condense under the same conditions, and neither does ω-4-dinitroacetophenone. The latter compound is decomposed by acids. This starting ketone was directly obtained by a new synthetic route involving the nitration of 4-nitroacetophenone in the side chain.

The role of nitrogen bases in the preparation of ω-nitrochalcone is not clear, but they seem to be the only effective condensing agents. Thus, Russian authors [16] used ε-aminocapronic acid to prepare 2-benzyloxy- and 2-hydroxy-ω-nitrochalcone.

The *ω-methyl* group has only slight influence on base-catalyzed chalcone formation. In accordance with its electron releasing character, the yields are somewhat lower than with unsubstituted acetophenones, and in accordance with earlier observation [17] less yellow. 3'-Nitro-4'-hydroxy-ω-methylchalcone, a new compound, has been synthetized in this series.

Starting from 2,4,6-trihydroxypropiophenone and vanillin the base-catalyzed condensation gave a polymer, while the appropriate acetophenone reacted normally.

The *ω-benzoyl* group in acetophenone interfered with the synthesis of chalcone from benzaldehyde in the presence of sodium hydroxide, probably owing to enol formation. In acidic medium, flavone was formed, instead of chalcone, and benzaldehyde remained unchanged.

Experimental*

* All m. p.'s are uncorrected. The UV spectra were obtained with a Beckmann D. U. spectrophotometer.

Comparative experiments (Figs 1 and 2)

The experimental conditions of chalcone formation were the same as described previously [8]. The concentrations of the chalcones were determined in part by measuring the chalcones precipitated by acidification (Fig. 1), and partly spectrophotometrically. Rate constants were calculated following our earlier method [8]. The chalcones obtained during these measurements were in part identical with those mentioned in preceding papers of this series (5',4--diNO_2-2'-OH-, 5'-NO_2-2'-OH-4-Cl- and 5'-NO_2-2'-OH-chalcones) [8], (5'-NO_2-2'-OH-4-Me-

-chalcone) [10]. The rest of the chalcones did not give m.p. depression in admixture with samples prepared according to the literature: chalcone, m.p. 56—57°C [18], 4'-NO_2-chalcone, m.p. 148—150°C [19], 4'-OH-chalcone, m.p. 172—173°C [20], 4'-Cl-chalcone, m.p. 98—100°C [21], 3'-NO_2-chalcone, m.p. 130—131°C [22], 3'-OMe-chalcone, b.p. 4 mm 180—185°C [23], 5'NO_2--2'-OH-4-OMe-chalcone, m.p. 164—165°C [24]. 5',3-DiNO_2-2'-OH-chalcone melted, in contrast to one of our earlier communication [9], at (203)—206—207°C (EtOAc—AcOH).

5'-Nitro-2'hydroxy-3-methoxychalcone

This new chalcone was prepared in a yield of 33% in the same way as described previously [8], m.p. 128—129°C (EtOAc—EtOH). Calcd. N 4.7. Found N 4.6%.

5'-Nitro-2'-hydroxy-3,4-dichlorochalcone

This new chalcone was prepared in a yield of 80—83% from the appropriate ketone (1.81 g; 0.01 mole) and aldehyde (1.75 g; 0.01 mole) dissolved in ethanol (40 ml). After the addition of 20 ml of 5 *N* NaOH, the solution was kept at 60°C for 30 min. The chalcone was precipitated by acidifying the solution with acetic acid and it was recrystallized twice from ethyl acetate; m.p. 222°C.

Calcd. N 4.1 Found N 4.2%.

3'-Nitro-4'-hydroxy-ω-methylchalcone

0.2 g of 3-nitro-4-hydroxypropiophenone [25] was dissolved in 15 ml of 1 *N* NaOH and 0.4 ml of benzaldehyde was added. The alkaline solution was heated at 60°C for 3 hrs, and the new chalcone was precipitated by adding 5 *N* HCl. Yield: 60%. M.p.: 149—152°C. Recrystallization from ethanol raised the m.p. to 154—155°C. Calcd. N 4.9. Found N 4.8%.

Sodium salt of ω-nitroacetophenone

From the ethanolic solution of ω-nitrochalcone the sodium salt slowly crystallized on the addition of 2 *N* NaOH. The IR spectrum was consistent with the enol-salt structure.

*

It is a pleasure to express our gratitude to Prof. Dr. Á. Gerecs for suggestion to start this research, to Dr. A. M. Eastham (NRC, Ottawa) for reading the manuscript and to the N. R. C., Ottawa, for the gift of a number of aldehydes. The private communication from Professor R. D. Campbell (Iowa State University) is gratefully acknowledged. Thanks are due to Dr. A. Bajusz and Dr. Gy. Sipos for collaboration, to Mrs. K. Lakos-Láng and Mrs. G. Bartók (A. József University, Szeged, Hungary) for the microanalyses, to Miss Zs. Szegfű, Mr. T. Dudás and Mrs. I. Bartók for their assistance in this work. The authors are indebted to the Hungarian Ministry of Education for a grant.

REFERENCES

1. Moustafa, E., Wong, E.: Phytochemistry **6,** 625 (1967).
2. Patschke, L., Barz, W., Grisebach, H.: Z. Naturforsch. **19**b, 1110 (1964).
3. Grisebach, H., Kellner, S.: Z. Naturforsch. **20**b, 446 (1965).
4. Széll, T.: Ber. **91,** 2609 (1958).
5. Széll, T., Eastham, A. M., Sipos, Gy.: Can. J. Chem. **42,** 2417 (1964).
6. Sohár, I.: Theses submitted for Ph. D., Szeged (1968).
7. Clark, J., Perrin, D. D.: Quart. Rev. **18,** 294 (1964).
8. Sipos, Gy., Furka, Á., Széll, T.: Monatsh. **91,** 643 (1960).
9. Széll, T.: Ber. **92,** 1672 (1959).

10. SZÉLL, T., SOHÁR, I.: Can. J. Chem. **47,** 1254 (1969).
11. CULBERTSON, G., PETTIT, R.: J. Am. Chem. Soc. **85,** 741 (1963).
12. YATES, K., STEWART, R.: Can. J. Chem. **37,** 664 (1959).
13. TSUKERMAN, S. V., SUROV, U. M., LAVRUSHIN, V. F.: Zhur. Obshchei Khim. **37,** 364 (1967).
14. SORTER, P. F.: Theses submitted for Ph. D., Iowa State Univ., Iowa City, (1962).
15. CAMPBELL, R. D.: Private communication.
16. SAMOKHVALOV, G. I., SHAHOVA, M. K., BUDAGYANC, M. I., VEINBERG, A. Ya., LUCK'YANOVA L. V., PREOBRAZHENSKII, N. A.: Zhur. Obshchei Khim. **31,** 1147 (1961).
17. SZÉLL, T.: J. Prakt. Chem. **17,** 346 (1962).
18. VON KOSTANECKI, St.: Ber. **29,** 1492 (1896).
19. WEYGAND, C.: Annalen **459,** 99 (1927).
20. VON KOSTANECKI, St., TAMBOR, J.: Ber. **32,** 2260 (1899).
21. DILTHEY, W.: J. Prakt. Chem. **101,** 199 (1921).
22. SZÉLL, T., BAJUSZ, A.: Magyar Kém. Foly. **61,** 235 (1955).
23. C. A. **64,** 2031 d (1966). (Upjohn Co. Neth. Patent).
24. CHHAYA, G. S., TRIVEDI, P. L., JADHAV, G. V.: J. Univ. Bombay **25,** 8 (1957).
25. BROWN, F. C.: J. Am. Chem. Soc. **68,** 872 (1946).
26. NOYCE, D. S., PRYOR, W. A.: J. Am. Chem. Soc. **81,** 618 (1959).

Tamás SZÉLL
István SOHÁR } Szeged, Rerrich tér, Hungary.

Acta Chimica Academiae Scientiarum Hungaricae, Tomus 62 (4), pp. 437—443 (1969)

ÜBER DEN MECHANISMUS DER SULFILIMIN-BILDUNG, III*

KINETISCHE UNTERSUCHUNG DER REAKTION EINIGER METHYL-ARYL-SULFIDE MIT CHLORAMIN-T

(VORLÄUFIGE MITTEILUNG)

F. RUFF und Á. KUCSMAN

(Institut für Organische Chemie der L. Eötvös Universität, Budapest)

Eingegangen am 3 Oktober, 1969

Die von MANN und POPE entdeckte Reaktion der Thioäther mit Salzen der N-Chlor-Säureamide, z. B. Chloramin-T, führt zur Bildung von Sulfilminen (1). Enthält das Reaktionsmedium auch Wasser, so wird außer Sulfilmin auch mehr oder weniger Sulfoxyd gebildet (2):

$$\underset{\mathbf{I}}{RR'S} + \underset{\mathbf{II}}{TsNCl^{\ominus}Na^{\oplus}} \rightarrow \underset{\mathbf{III}}{RR'SNTs} + Na^{\oplus}Cl^{\ominus} \qquad (1)$$

$$RR'S + TsNCl^{\ominus}Na^{\oplus} + H_2O \rightarrow \underset{\mathbf{IV}}{RR'SO} + TsNH_2 + Na^{\oplus}Cl^{\ominus} \qquad (2)$$

Da die Angaben über den Mechanismus der MANN—POPE-Reaktion zumeist nur qualitativer Art [1, 2] und andererseits die bisher vorgezeigten, kinetischen, quantitativen Daten [3, 4] mangelhaft und somit die auf diesen beruhenden Folgerungen unseres Erachtens in vieler Hinsicht unzulässig sind, haben wir die eingehende kinetische Untersuchung dieser Reaktion in Angriff genommen. Über Ergebnisse unserer diesbezüglichen Untersuchung der Reaktion einiger Methyl-aryl-sulfide (**Ia:** R = Me, R′ = Ph; **Ib:** R = Me, R′ = *p*-C_6H_4OMe; **Ic:** R = Me, R′ = *o*-C_6H_4COOH; **Id:** R = Me, R′ = = *o*-C_6H_4COOMe) mit Chloramin-T wird untenstehend kurz berichtet.

Als Lösungsmittel wurde 50 Vol.%iger wäßriger Alkohol angewandt, der die entsprechenden Puffer (0,05—0,1*M* Phosphat, 0,2*M* Borat, 0,05*M* Succinat) enthielt. Die kinetischen Messungen wurden im pH Bereich 7—9 bei +20,00 ± ± 0,02 C° durchgeführt. Die Konzentration der Ausgangssubstanzen haben wir von $5 \cdot 10^3$ bis 10^{-4} mol/l variiert.

* Teil I und II: Tetrahedron **18**, 75, 79 (1962)

(A) Es waren vor allem zuverlässige Methoden auszuarbeiten, die die Analyse des Reaktionsgemisches zu ermöglichen hatten. Zur Unterbrechung der Reaktion ließ sich die äußerst schnelle Reaktion des Kaliumjodids mit Chloramin-T heranziehen, wobei das mit dem nicht verbrauchten Chloramin-T in äquivalenter Menge freigesetzte Jod bei 353 mμ spektrophotometrisch bestimmt werden konnte (Fehlergrenze: ±1%). Die Menge des während der Reaktion gebildeten Sulfilimins und Sulfoxyds ließ sich polarographisch bestimmen. Beide Reaktionsprodukte ergeben nämlich an der Quecksilber-Tropfelektrode ihrer Konzentration proportionale Diffusionsstufen, die bei entsprechender Wahl des pH-Wertes von einander gut getrennt werden können (so findet man für **IIIa** bei pH 4,5 $E_{1/2} = -600$ mV, für **IVa** bei pH 1 $E_{1/2} = -900$ mV). Die während eines Zeitintervalls umgesetzte Menge von Chloramin-T erwies sich der gebildeten Menge des Sulfilimins und Sulfoxyds äquivalent (Versuchsfehler ±3%); der Gleichung (1) und (2) eventuell nicht entsprechende Reaktionen können somit unberücksichtigt bleiben.

(B) Aus bisher mitgeteilten [3, 4] Versuchsergebnissen konnte man vermuten, daß die geschwindigkeitsbestimmende, langsamste Reaktionsstufe aus der Bildung von Zwischenprodukten besteht; sie setzt auf Einwirkung des Thioäthers (»S«) auf das aus dem Anion des Chloramin-T (»CT«) im Laufe einer schnellen Gleichgewichtsreaktion entstehende protonierte Produkt ein, worauf dann eine schnelle Umsetzung der Zwischenprodukte zu den Endprodukten erfolgt:

$$TsNCl^{\ominus} + H^{\oplus} \underset{K_a}{\overset{\text{schnell}}{\rightleftharpoons}} TsNHCl \qquad (3)$$

$$TsNHCl + RR'S \xrightarrow[\text{langsam}]{k_1'} \text{Zwischenprodukte}^{*} \xrightarrow{\text{schnell}} \text{Endprodukte} \qquad (4)$$

Unsere Versuchsergebnisse, die an Hand der Umsetzung von Methyl-phenyl-sulfid (**Ia**) mit Chloramin-T bei verschiedenen Konzentrationen in entsprechenden Pufferlösungen gewonnen wurden, haben erwiesen, daß sich die Reaktion mit der aus den Reaktionsgleichungen ableitbaren einfachen kinetischen Gleichung $v = k[CT]\,[S]$ nicht beschreiben läßt.

Analoge Versuche, bei welchen Dichloramin-T anstatt Chloramin-T eingesetzt wurde, haben ergeben, daß in diesem Falle die Reaktion zwar unmeßbar schnell verläuft, die quantitative Zusammensetzung des Endproduktes jedoch in beiden Fällen gleich ist. Diese Beobachtung macht darauf aufmerksam, daß bei der MANN—POPE-Reaktion die Umsetzung des Thioäthers nicht nur durch das protonierte Chloramin-T-Anion bewirkt wird, sondern dabei auch das Dichloramin-T (»DT«) eine Rolle spielen könnte; letzteres Produkt kann nämlich nach Gleichung (5) im Laufe einer langsamen, zu einem Gleich-

* Nach BENEŠ [3] bestünden die Zwischenprodukte aus $RR'SCl^{\oplus}$ und $TsNH^{\ominus}$.

gewicht führenden Reaktion des protonierten und unprotonierten Chloramin-T-Anions neben einem Toluolsulfonamid-Anion (»TSA«) entstehen [5]:

$$TsNHCl + TsNCl^{\ominus} \underset{k'_{-d}}{\overset{k'_d}{\rightleftharpoons}} TsNCl_2 + TsNH^{\ominus} \text{ (langsam)} \tag{5}$$

$$TsNCl_2 + RR'S \xrightarrow[\text{schnell}]{k_2} \text{Zwischenprodukte} \xrightarrow{\text{schnell}} \text{Endprodukte} \tag{6}$$

Da das Dichloramin-T im Sinne der Gleichung (6) mit dem Thioäther sehr schnell reagiert, kann als geschwindigkeitsbestimmende Reaktionsstufe dieser Reaktion die vorgeschaltete Gleichgewichtsreaktion (5) angesehen werden.

Auf Grund der Gleichungen (3)—(6) läßt sich für eine in Pufferlösung verlaufende Reaktion die Konzentrationsänderung des Chloramin-T mit Gleichung (7) beschreiben, wobei für die Konstanten k_1 und k_d die Gleichungen (7a) und (7b) gelten:

$$-\frac{d[CT]}{d\tau} = k_1[CT][S] + k_d[CT]^2 - k_{-d}[DT][TSA] \tag{7}$$

$$k_1 = \frac{[H^+]}{K_a + [H^+]} k'_1 \tag{7a}$$

$$k_d = \frac{K_a[H^+]}{(K_a + [H^+])^2} k'_d \tag{7b}$$

Wird aus der im Sinne der »steady state« Annäherung konstruierten Gleichung (8) die Konzentration [DT] ausgedrückt und dann in die Gleichung (7) substituiert, so erhält man Gleichung (9):

$$\frac{d[DT]}{d\tau} = k_d[CT]^2 - k_{-d}[DT][TSA] - k_2[DT][S] = 0 \tag{8}$$

$$-\frac{d[CT]}{d\tau} = k_1[CT][S] + \frac{k_d k_2[S][CT]^2}{k_{-d}[TSA] + k_2[S]} \tag{9}$$

Nimmt man an, daß $k_{-d}[TSA] \ll k_2[S]$ — was für die Anfangsphase der Reaktion sicher zutrifft, da hier die Konzentration des Toluolsulfonamids noch sehr gering ist — so läßt sich Gleichung (9) zur Gleichung (10) vereinfachen, deren bestimmtes Integral (11) darstellt.

$$-\frac{d[CT]}{d\tau} = k_1[CT][S] + k_d[CT]^2 \tag{10}$$

$$\frac{2{,}303}{k_1([S_0]-[CT_0])}\log\frac{k_d+k_1\dfrac{[S]}{[CT]}}{k_d+k_1\dfrac{[S_0]}{[CT_0]}}=\tau \tag{11}$$

$$\frac{-\dfrac{d[CT]}{d\tau}}{[CT]^2}=k_1\frac{[S]}{[CT]}+k_d \tag{12}$$

Die Gültigkeit der Gleichung (10) bzw. der aus dieser durch Dividieren durch $[CT]^2$ erhältlichen, einer Geraden entsprechenden Gleichung (12), ließ sich auf zweierlei Art überprüfen. Werden nämlich die aus der experimentell ermittelten Konzentration-Zeit Abhängigkeit durch graphische Differenzierung bestimmten $d[CT]/d\tau$ Werte durch $[CT]^2$ dividiert und die so erhaltenen Werte in Abhängigkeit von $[S]/[CT]$ graphisch dargestellt, so erhält man tatsächlich eine Gerade, deren Steilheit dem Wert k_1 entspricht, während ihr Schnittpunkt mit der Ordinate den k_d Wert ergibt. Die so erhaltenen, annähernden Werte der Geschwindigkeitskonstanten haben wir auf Grund der Gleichung (11) durch Anwendung der Methode der kleinsten Quadrate durch maschinelles Rechnen verfeinert. Mit den für die Umsetzung des Methylphenyl-sulfids (**Ia**) bei pH 8,50 $\pm$ 0,02 erhaltenen Werten $k_1 = 0{,}038$ und $k_d = 0{,}037$ l/mol.sec* geben die Gleichungen (10) und (11) die Reaktionsgeschwindigkeit nicht nur für die Anfangsperiode der Reaktion richtig an, sondern auch noch im Falle einer 70%igen Konversion; dies spricht dafür, daß die bei der Ableitung der Gleichungen angewandten Vereinfachungen zulässig sind. Gleichung (10) bewahrt in einem sehr breiten (0,3—30) Bereich des Konzentrationsverhältnisses $[S]/[CT]$ ihre Gültigkeit, somit ist der durch die Gleichungen (3)—(6) beschriebene Mechanismus als bewiesen zu betrachten.

(C) Nach unseren Messungen hängen die im pH Bereich 7—9 für die Reaktion **Ia** + **II** ermittelten Konstanten k_1 und k_d im Sinne der empirischen Gleichungen $\log k_1 = 6{,}89 - \text{pH}$ und $\log k_d = 6{,}93 - \text{pH}$ vom pH Wert ab. Beide Zusammenhänge lassen sich auf Grund der Gleichungen (7a) und (7b) gut deuten, wenn man in Betracht zieht, daß die bei den Versuchen obwaltenden $[H^+]$ Werte viel kleiner waren als die auf die Dissoziation des protonierten Chloramin-T-Anions sich beziehenden K_a Werte (vgl. [6]).

(D) Gleichung (10) beschreibt auch gut die Reaktion des Thioäthers **Ib** mit Chloramin-T (**II**); bei pH 8,50 $\pm$ 0,02 betragen die Konstanten $k_1 = 0{,}735$ und $k_d = 0{,}036$ l/mol. sec.* Daß die k_d Werte der Reaktion mit Chloramin-T beider Thioäther (**Ia** und **Ib**) praktisch übereinstimmen, entspricht vollkommen

* Die Summe der Konstanten k_1 und k_d stimmt erwartungsgemäß mit der von DELL'ERBA und SPINELLI [4] mitgeteilten Geschwindigkeitskonstante k innerhalb der Versuchsfehlergrenzen überein.

der Erwartung, während der verhältnismäßig große Wert von k_1 im Falle der Reaktion des Thioäthers **Ib** eine Folge seiner größeren Nukleophilität ist (vgl. [1, 4]).

(E) Ergebnisse orientierender Versuche, die mit den Thioäthern **Ic** und **Id** durchgeführt wurden, führten zur Erkenntnis, daß in diesen Fällen Gleichung (10) auf $v = k_1[\mathrm{CT}]\,[\mathrm{S}]$ bzw. $v = k_d[\mathrm{CT}]^2$ vereinfacht werden kann, da hier die Beziehung $k_1 \gg k_d$ bzw. $k_1 \ll k_d$ besteht. Bei der Reaktion der Thioäther **Ic** und **Id** kann somit als selektiv einwirkendes Reagens das protonierte Chloramin-T-Anion bzw. das im Reaktionsgeschehen entstehende Dichloramin-T betrachtet werden.

(F) Einige, untenstehend verzeichnete Versuchsergebnisse stehen in Einklang mit früheren Behauptungen qualitativer Art, daß nämlich im Laufe der MANN—POPE-Reaktion die beiden Endprodukte (d. h. Sulfilimin und Sulfoxyd) nicht nach einander, sondern neben einander, vermutlich sogar aus ein und demselben Zwischenprodukt in schnellen Reaktionsschritten gebildet werden (vgl. [1, 3]).

Tabelle I

	pH($\pm$0,02)	Sulfilimin %	Sulfoxyd %
0,1*M* Phosphat	8,00	18	82
0,05*M* Phosphat	8,05	23	77
0,05*M* Phosphat	7,48	23	77
0,05*M* Succinat	7,48	26	74
0,2*M* Borat	7,50	31	69

Das Mengenverhältnis des während einer bis zur 50—60%igen Konversion verlaufenden Reaktion gebildeten Sulfilimins und Sulfoxyds erwies sich — innerhalb der Versuchsfehlergrenze — als konstant. So enthielt z. B. das Endprodukt, das im Laufe der Reaktion **Ia** + **II** (wenn $[\mathrm{S}_0] = [\mathrm{CT}_0] = 1{,}17 \cdot 10^{-3}$ mol/l und der pH 8,05 $\pm$ 0,02 betrug) gebildet wurde, laut den Meßergebnissen bis zur 63%igen Konversion stets 23% Sulfilimin und 77% Sulfoxyd.

Verlief die Reaktion **Ia** + **II** in einer gegebenen Pufferlösung, dann waren die Geschwindigkeitskonstanten unabhängig von den Anfangskonzentrationen $[\mathrm{S}_0]$ und $[\mathrm{CT}_0]$, von denen aber die Zusammensetzung des Endproduktes abhing. Es wurden z. B. in 0,05*M* Phosphatpuffer im Falle der Anfangskonzentration $[\mathrm{S}_0] = [\mathrm{CT}_0] = 10^{-3}$ bzw. $5 \cdot 10^{-3}$ mol/l Endprodukte der Zusammensetzung 23 bzw. 29% Sulfilimin und 77 bzw. 71% Sulfoxyd gebildet.

Die in Pufferlösungen verschiedener Zusammensetzung aber gleicher pH-Werte verlaufende Reaktion **Ia** + **II** kennzeichnen immer dieselben k_1- und k_d-Konstanten, doch ist die Zusammensetzung der Endprodukte schon ungleich (s. Tabelle). Auf Grund dieser Beobachtung kann man vermuten, daß die Bildung des Sulfoxyds in der schnellen Reaktionsstufe von den nukleophilen Pufferanionen einigermaßen katalytisch beschleunigt wird (vgl. [7]). Diese Annahme steht in Einklang mit dem Befund, daß das Endprodukt einer in ungepufferter Lösung verlaufenden Reaktion bedeutend weniger Sulfoxyd enthält; so entstand z. B. im Falle der Anfangskonzentrationen $[S_0] = [CT_0] = 10^{-3}$ mol/l in Abwesenheit eines Puffers ein Endprodukt der Zusammensetzung 40% Sulfilimin und 60% Sulfoxyd.* Mit einer intramolekularen nukleophilen Katalyse läßt sich auch der Versuchsbefund deuten, daß im Laufe der Reaktion des Methyl-aryl-sulfids, der am aromatischen Ring eine zur CH_3S-Gruppe *o*-ständige Carboxylat- bzw. Carbomethoxygruppe enthält (**Ic** bzw. **Id**), ein Endprodukt gebildet wird, das sogar 100% bzw. 96% Sulfoxyd enthält (vgl. [2, 8, 9]).

Es ist bemerkenswert, daß das Mengenverhältnis Sulfilimin : Sulfoxyd bei einer gegebenen Konzentration des Puffers vom pH-Wert des Reaktionsgemisches praktisch unabhängig ist. So werden z. B. im 0,05*M* Phosphatpuffer zwischen pH 5,7—9,85 stets 23—26% Sulfilimin und 77—74% Sulfoxyd gebildet. Dieser Befund läßt darauf schließen, daß der von BENEŠ [3] vorgeschlagene Teilprozeß (13), laut welchem die in der Reaktionsstufe (4) etwa entstehenden Zwischenprodukte schnell unter Bildung des Sulfilimins mit einander reagieren, in unserem Falle nicht gültig sein kann.

$$RR'SCl^{\oplus} + TsNH^{\ominus} \xrightarrow{\text{schnell}} RR'SNTs + H^{\oplus}Cl^{\ominus} \qquad (13)$$

In dem bei unseren Versuchen angewandten pH-Bereich muß sich die Konzentration der $TsNH^{\ominus}$ Anionen um vier Größenordnungen verändern und dies hätte nach Gleichung (13) einen großen Einfluß auf die relative Menge des sich bildenden Sulfilimins.

Auf Grund unserer Versuchsbefunde läßt sich die etwaige Annahme, daß für die Bildung des einen bzw. anderen Endproduktes das als Zwischenprodukt auftretende protonierte Chloramin-T-Anion bzw. Dichloramin-T gesondert verantwortlich wäre, ausschließen. Dies bekräftigt außer dem mit Dichloramin-T ausgeführten Versuch (vgl. Punkt (B)) auch ein Vergleich der Reaktionen der Thioäther **Ic** und **Id**. In beiden Fällen wurde fast ausschließlich nur Sulfoxyd gebildet, obwohl die mit den Thioäthern reagierenden Zwischenprodukte

* Die Zusammensetzung des Endproduktes, das bei einer in ungepufferter Lösung verlaufenden Reaktion entsteht, hängt auch von der Zusammensetzung des Lösungsmittels ab. So ergibt z. B. die analoge, jedoch in 99,9%igem Alkohol verlaufende Reaktion ein Endprodukt, das 59% Sulfilimin und 41% Sulfoxyd enthält.

verschieden sind (vgl. mit Punkt (E)). Es sei dazu noch bemerkt, daß auch im Falle des Thioäthers **Ia** kein Zusammenhang zwischen dem Verhältnis $k_1 : k_d$ und dem Mengenverhältnis der gebildeten Endprodukte besteht.

Die Mitteilung der Ergebnisse noch im Gang befindlicher Untersuchungen nebst einer eingehenderen Diskussion wird später erfolgen.

*

Wir danken Herrn Prof. V. BRUCKNER für die Anregung dieser Arbeit.

LITERATUR

1. KUCSMAN, Á., KAPOVITS, I., BALLA, M.: Tetrahedron, **18,** 75 (1962)
2. KUCSMAN, Á., KAPOVITS, I., TANÁCS, B.: Tetrahedron, **18,** 79 (1962)
3. BENEŠ, J.: Collection Czech. Chem. Communs. **28,** 1171 (1963)
4. DELL'ERBA, C., SPINELLI, D.: Ric. Sci., Rend. Sez. A, **7,** 456 (1964)
5. HIGUCHI, T., IKEDA, K., HUSSAIN, A.: J. Chem. Soc. (B), **1967,** 546
6. MORRIS, J. C., SALAZAR, J. A., WINEMAN, M. A.: J. Am. Chem. Soc. **70,** 2036 (1948)
7. HIGUCHI, T., GENSCH, K. H.: J. Am. Chem. Soc. **88,** 5486 (1966)
8. GENSCH, K. H., PITMAN, I. H., HIGUCHI, T.: J. Am. Chem. Soc. **90,** 2096 (1968)
9. TAGAKI, W., OCHIAI, M., OAE, S.: Tetrahedron Letters, **1968,** 6131

Ferenc RUFF
Árpád KUCSMAN
Budapest VIII., Múzeum krt. 4/b

Computer Programs for Chemistry, Vol. 1. Ed. by DeLos F. DeTar. W. A. Benjamin Inc., New York, Amsterdam, 1968 pp. 208.

The introduction of computer techniques into chemical research is causing an unparalleled effect on the development of chemical sciences. Effective use of computers requires well-tested, easy-to-handle and powerful programs which, in most cases, are very expensive to produce. At the present stage of computerization when rather frequently considerable efforts are being made in many laboratories simultaneously to develop the same program, the publication of this research-directed open-end series is timely and welcome. "The purpose of Computer Programs for Chemistry", as pointed out by the Editor in his Preface, "is to make available in convenient form a wide range of programs of interest to chemists, and by providing a medium for publication, to encourage the discovery and application of quantitative mathematical models to problems in chemistry".

The first volume of the series contains seven programs. Four of them deal with analysis of high resolution NMR spectra.

LAOCN3 (the third revised version of earlier LAOCOONI and II), described in Chapter 3, can be used in two ways. (1) It calculates NMR line positions and intensities from an assumed set of chemical shifts and coupling constants for systems containing up to seven spin —1/2 nuclei ("direct calculation"). (2) If the theoretical spectrum thus calculated has a resemblance to the experimental spectrum the program can perform an iterative *l*east-squares *a*djustment *o*f *c*alculated *o*r *o*bserved *N*MR lines.

NMREN1 and NMREN2 used in conjunction with NMRIT (Chapter 4) perform the same type of calculations as does LAOCN3 but in a quite different way, and similarly, from an arbitrary set of parameters provide adjusted values of chemical shifts and coupling constants that give a best fit to an observed set of energy levels.

The programs LSG and LSKIN1 described in Chapter 5 and Chapter 6, respectively, treat first-order kinetic data. LSG provides a simple least-squares program that might be modified for use on small computers, and like the more sophisticated LSKIN1, accepts experimental rate data and calculates the best values of the first-order rate parameters.

PLOTLN (Chapter 7) is a general-purpose plotting subroutine package which uses the typewriter to form low resolution plots.

Chapter 1 gives instructions for the use of the programs, the preparation of correction and conversion decks, as well as informations for future authors about suggested content of the program chapters and recommended programming standards. Chapter 2 is a general introduction to the programs in the volume.

Each program chapter contains an explanation of theoretical basis and a brief description of the method of calculation. This is followed by input instructions, illustrative examples, description of the structure of the program, flow diagrams, indexed program listing and machine requirements. Each program has been tested under specified conditions.

As a companion to each volume, the Publisher makes available a magnetic tape containing all the programs described in the volume.

This ready source of reliable programs will undoubtedly prove invaluable to chemists who use, or who are potential users of computers.

L. RADICS

W. G. CREWTHER: *Symposium on Fibrous Proteins.* Butterworths, Australia, 1968. pp. 432

The Symposium on Fibrous Proteins held at the Academy of Sciences, Canberra, Australia, from August 14—18, 1957, was the third international conference to carry that title, the previous conferences having been held at Leeds in 1946 and in 1954.

A volume has been edited by W. G. CREWTHER and published by Butterworths (Australia) including the papers presented at the Symposium. These papers have been grouped under the headings: Relation between Amino Acid Composition and Conformation of Polypeptides and Proteins; Muscle and Bacterial Flagella; Collagen and Elastin; Keratin. The total number of the presented papers was as many as 39, comprising the following subjects:

The Structure and Activity of Lysozyme;
Variants of the Righthanded Alpha Helix;
Refinement of Molecular Structures in Crystalline Fibres;
The Structure of Beta Keratin;
Variety in Composition and Structure of Silk;
Fibroins: Some New Types of Silk from Hymenoptera;
Stability of Alpha Helices in Proteins and Polypeptides;
Nuclear Magnetic Resonance Study on the Conformation of Poly-gamma-benzyl-L-glutamate in Mixed Solvents;
Hydrogen Bonding and Conformation of Polypeptides;
C—H . . .O=C Hydrogen Bonding in Proteins;
Stereochemical Coding of a Polypeptide Chain;
Biosynthesis of Flagellin;
The Structure of Bacterial Flagella;
X-ray Diffraction Pattern of Paramyosin;
Subunits of Myosin by Enzymic Degradation;
The Structure and Denaturation of Topomyosin *B*;
Studies Designed to Locate the ATP Combining Site of Myosin;
Subunit Interactions of Myosin;
The Interaction of Actin and Myosin and its Modification by Other Protein Factors;
Ultraviolet Spectroscopic Studies on the Interaction of Nucleotides with Actin;
Experiments on the Action of Dinitrophenyl Amino Acids on Muscle Proteins;
Renaturation — An Aid in the Investigation of the Collagen Structure;
The Development of the Collagen Fold: The Role of Polar Regions and Interchain Cross-linkages;
The Chemistry and Biosynthesis of Interchain Crosslinks in Collagen;
The Nature of Some Aldehydes in Tropocollagen;
Thermal Transition in Some Invertebrate Collagens and their Relation to Amino Acid Content and Environmental Temperature;
Effect of Salts on the Denaturation of Collagen at Acid pH Values;
The Interaction between Acid Mucopolysaccharide-Protein Complexes and Tropocollagen;
Physico-Chemical Effects of Serotonin on Soluble Collagen;
Some Structural Aspects of Elastin Revealed by X-ray Diffraction and other Physical Methods;
Elastin Structure and Biosynthesis;
Electron Microscopy of Fibrous Keratins;
Substructure of the Alpha Keratin Microfibril;
Is Alpha Keratin a Coiled Coil?
Recent Work on the Chemical Structure of Wool Proteins;
Wool Proteins in Relation to Wool Structure;
Studies on the Chemical Structure of the Low-sulphur Proteins from Wool;
The Structure and Aggregation of Low-sulphur Proteins Derived from Alpha Keratins;
Distribution of Protein Fractions in Alpha Keratin Structure;
The Dietary Regulation of the Synthesis of Hair Keratin;
Cys-Cys Sequences in Keratins;
Properties of Reduced Wool Fibres;
Chemical Composition of the Histological Components of Wool;
The Acylation of Wool: The Side-chain Specificity of Active Esters and Amides;
Infrared Absorption Bands of Side Chains in Polypeptides and in Keratin and Other Proteins;
The Longitudinal Stability of Keratin Fibres;
Differential Thermal Analysis of Keratin and Related Protein Fibres;
Wool Structure Modified for Greater Durability: Some Considerations of Requirements.

Complete text of the presented papers, list of references and contributed items of discussion as well as answers by the authors have been recorded.

Due to the great number of papers a rather complete review of the latest achievements in the field of the fibrous protein research is available by studying this volume.

I. RUSZNÁK

T. W. GOODWIN: *The Metabolic Roles of Citrate*. Academic Press, London and New York, 1968. pp. 144

The book contains papers presented before the 27th Symposium of the English Biochemical Society (held in Oxford, July, 1967). The Citric acid cycle has been chosen as the central subject of the Symposium. Since Professor KREBS had an outstanding role in its discovery and in the elucidation of its key position in cell respiration, this Symposium was organized in honour of Professor Sir Hans KREBS and the papers were dedicated to him.

The following nine lectures are published in this book.

1. Opening remarks by F. DICKENS.

2. H. L. KORNBERG: "H. A. KREBS: A pathway in metabolism". This lecture describes the scientific carrier of Nobel prize winner Professor KREBS from the University of Freiburg to the professorship in Oxford; expresses appreciation of his most important scientific results (metabolism of amino acids: ornithine cycle, oxidative desamination, glutamine synthesis, oxidation of di- and tricarboxylic acids in the "KREBS cycle", etc.).

3. The paper by P. A. SRERE: "Studies on purified citrate-enzymes: metabolic interpretations" deals with the metabolic function of some of the purified enzymes of the citric acid cycle: citratase, citrate synthase and citrate cleavage enzyme.

4. D. E. ATKINSON: "Citrate and the citrate cycle in the regulation of energy metabolism". Some of the problems of regulation such as the hypothesis of adenilate control, regulation of the formation and consumption of citrate, and the energy accumulation are discussed.

5. P. B. GARLAND: "Control of citrate synthesis in mitochondria." Experiments were carried out on liver tissues and isolated mitochondria; the regulating role of palmitoyl-carnitine oxidation in the citrate cycle and related metabolic routes were studied.

6. J. M. LOWENSTEIN: "Citrate and the conversion of carbohydrate into fat". In this lecture the correlations between carbohydrates, fats and the citrate cycle are described with special attention to the role of extramitochondrial acetyl coenzyme *A* and the citrate cleavage enzyme in the synthesis of fat.

7. P. J. RANDLE *et al.*: "Citrate as a metabolic regulator in muscle and adipose tissue." In animal tissues (muscle of rat-hearts and adipose tissues) citrate affects the activity of two enzymes: phosphofructokinase is inhibited and acetyl CoA carboxylase activated. Physiological conditions influencing this regulating function of citrate were studied.

8. M. KLINGENBERG and E. PHAFF: "Metabolic control in mitochondria by adenine nucleotide translocation." The coordination of intra- and extramitochondrial metabolisms is especially well known in the hydrogen and energy transfer systems. The authors have studied the transfer of adenine nucleotide across a mitochondrial membrane with respect to the specific character, kinetics and regulation of the process.

9. J. B. CHAPPELL and B. H. ROBINSON: "Penetration of the mitochondrial membrane by tricarboxylic acid anions." In the absence of L-malate, the membrane of mitochondria is impermeable for tricarboxylic acids (citrate, *cis*-aconitate, isocitrate). L-malate activates systems transferring the tricarboxylic acids and α-ketoglutaric acid by active transport through the membrane. L-malate, owing to its regulating effect on permeability can be considered as a metabolic regulator.

All of the lectures express appreciation to the fruitful conceptions of Professor KREBS. Most of the papers concentrate on one of the central problems of the modern biochemistry: regulating mechanisms. At the end of each section detailed references and the discussion remarks and answers are given.

L. NYESTE

Progress in Medicinal Chemistry, Vol. 6. Ed. by G. P. ELLIS and G. B. WEST. Butterworth, London, 1969. pp. 372

Medicinal chemistry is a subject of increasing interest and importance and this new volume maintains the high standard set by the previous five. Perhaps the first chapter dealing with the work of the British Pharmacopoeia Commission cannot count on general interest but this is not the case with the other chapters.

The second chapter discusses the advances in our understanding of the coronary circulation which is of special importance today because of the widespread and serious effects of coronary diseases. Diseases involving the coronary arteries are a leading cause of death in industrialized countries. In the United States alone the incidence increased from 219.5 to 274.6 per 100,000 of the population between 1951 and 1961. In another study, up to 77 per cent of males under the age of 40 were found already to have arteriosclerotic changes in one or another of the coronary arteries. Over the past few years several new "coronary vasodilator" drugs have been introduced into therapeutics, with varying claims to effectiveness in treating coronary insufficiency. The purpose of the review is to give an account of the research in this field over the past 7 or 8 years, concentrating particularly on the mode of action of these compounds.

Of particular interest to the medicinal chemist is the third chapter in which the chemistry of some medicinally important pyrimidines is reviewed. The review tends to emphasize only those compounds in which the pyrimidine ring is the main constituent. Furthermore, with a few exceptions, thiamine (vitamin B_1), the regular constituents in nucleic acids and their derivatives, nucleosides, as well as many condensed pyrimidine systems such as purines, pteridines, quinazolines and pyrazolopyrimidines, are not covered in the present work. With the exception of pyrimidine antibiotics, pyrimidines in this review are classified on the basis of special structural features and functional groups. The following areas are included in the present review: 2,4-diaminopyrimidines, halogenated pyrimidines, sulfur-substituted pyrimidines, 2-substituted 4-amino-5-hydroxymethyl pyrimidines, pyrimidine sulfonamides and pyrimidine antibiotics. Pyrimidines of other areas will be presented in a forthcoming volume of this series.

The mode of action of antibacterial drugs is discussed in Chapter 4. Rapid advances are being made in this field and these are likely to have a significant effect on the development of new drugs designed to fight bacterial diseases.

The fifth chapter of the book is devoted to the biosynthesis and metabolism of the catecholamines. This chapter gives a comprehensive and detailed description of the synthesis and decomposition of catecholamines. It is clearly arranged, the most important results are emphasized, and in spite of the fact that 900 references are cited, the author does not become lost in details. Besides biochemical data, both pharmacological and clinical aspects are taken into consideration, so that the reader will obtain an overall picture of the whole domain of problems. This compilation is indispensable for everyone working with catecholamines.

The editors are to be congratulated on their decision to include a review dealing with the up-to-date literature of medicinal chemistry into the book. The explosive rate of growth of the scientific literature in recent years makes a heavy demand on the time of those who seek information on a particular topic. Those who are entering a new field or are attempting to keep up-to-date in several different subjects usually rely on reviews or monographs written by specialists. The last chapter of the book is a great help to every medicinal chemist — whether a postgraduate student or a more experienced researcher — in finding his way in the jungle of the dramatically growing scientific literature.

The articles, each of which is presented by a specialist in his field, are clear and informative. As in the earlier volumes, each chapter is well documented and the series is proving a valuable work of reference.

Gy. DEÁK

P. HEDVIG and Gy. ZENTAI: *Microwave Study of Chemical Structures and Reactions.* Akadémiai Kiadó, Budapest, 1969. pp. 445

Today's chemical and physical laboratories can hardly be distinguished from each other at first sight. Old characteristic equipment of a laboratory: flasks, test tubes are not the exclusive tools of a chemist any more. Naturally, real chemistry — today and long ago too — begins beyond the flask. Reactions occurring in flasks will seem reasonable and rationally related to other phenomena only by the help of human consideration.

Today, this "chemistry-creating" activity of the human sense seems to be easier in some respects, while in certain respects it has become more difficult. The "raw material" of modern chemistry — the basis for this activity of human intelligence — is produced not by test tubes and flasks only, but also by new instruments giving new information. This wider basis often makes the solution of problems easier. Today, in many cases, direct observation will provide data which in old times could be obtained only by long, indirect experimental and intellectual work. On the other hand, these new instruments lay a great charge on chemists. Data and curves obtained by the new techniques are useful in helping chemical thinking only for chemists thoroughly familiar with the complicated operating mechanism of these instruments and with the laws of nature applied when obtaining the actual information. Only such knowledge permits conclusions to be drawn from the "mirror image" referring to its "original", Nature.

So it is evident, that a great amount of information of non-chemical origin appears in chemistry now. However, these pieces of information require the knowledge of the "code" in which they are written and this can be mastered only by considerable efforts. The book "Microwave Study of Chemical Structures and Reactions" by P. HEDVIG and Gy. ZENTAI is an introduction to this "code", explaining the operating principles and operating mechanism of some new instruments and the right way of their use. It is a very useful source for all chemists using such equipment and the resulting data in their everyday work. It is of interest for physicists and engineers, too who are familiar with the "code". For them, the chemical importance of information given by these instruments will be instructive.

Of course, the authors could not deal with all new and widely used instruments of modern chemical laboratories. In the book instruments operating on the basis of interaction of substance with electromagnetic field are described. The underlying physical principles are those of modern quantum electrodynamics. The authors restrict themselves to instruments utilizing electromagnetic fields with frequencies in the ten gigahertz range. Thus the following sections are found in the book:

1. Microwave rotation-inversion spectroscopy
2. Electron spin resonance
3. Nuclear magnetic resonance
4. Quadrupole resonance
5. Dielectric spectroscopy

In all cases the authors introduce the physical laws which form the basis of the given method, keeping in mind the requirements of experimental research workers. The design of spectrometers is discussed and their most important parts are described. Attention is focussed on the correct application of various spectrometers providing easily interpreted results. Examples illustrating the problems arising from incorrect use are also given.

A great merit of the book is that it contains not only the description of different spectrometers as information-producing devices, but the chemical application of the resulting information is also emphasized. Namely, several examples based on recent work are used to show the performance of different spectrometers in the field of

1. free radicals
2. investigation of chemical structure
3. chemical reactions.

The authors give detailed description of the chemical results obtained by electron spin resonance (ESR) spectrometers. They describe the use of ESR spectrometers for the detection of different free radicals, together with methods for determining the concentration and structure of these radicals. About one quarter of the book deals with the results of ESR spectrometry in studying different chemical reactions. Radical reactions, chemical exchange processes, photolysis and radiolysis, polymerization and catalysis are branches of chemistry where the use of ESR spectrometers is especially fruitful. Also the recent biochemical ESR investigations are mentioned. Results obtained in connection with studies on photosynthesis and enzyme reactions by ESR spectrometers are the most interesting examples given in the book.

Another important tool in the investigation of chemical structures is nuclear magnetic resonance (NMR) spectroscopy the main results of which are also discussed.

Studies on resonance absorption of hydrogen, carbon^{-13}, fluorine, phosphorous, boron atoms and on its correlation with the arrangement of these atoms in molecules have given information useful in the determination of molecular structures by NMR spectroscopy. These very important relations are discussed and numerous examples of their application and performance in stereochemistry and polymer chemistry are given.

All five sections of the book contain numerous references for readers interested in the details.

This book was published by Akadémiai Kiadó and Iliffe Books Ltd in 1969. Akadémiai Kiadó can be proud of the beautiful representation and printing. It is a pity that the figures of this finely printed book are quite primitive in most cases, referring not to the artistical sense of this work.

B. Монов

INDEX

INORGANIC AND ANALYTICAL CHEMISTRY – ANORGANISCHE UND ANALYTISCHE CHEMIE – НЕОРГАНИЧЕСКАЯ И АНАЛИТИЧЕСКАЯА ХИМИЯ

PHYSICAL CHEMISTRY – PHYSIKALISCHE CHEMIE – ФИЗИЧЕСКАЯ ХИМИЯ

ORGANIC CHEMISTRY – ORGANISCHE CHEMIE – ОРГАНИЧЕСКАЯ ХИМИЯ

Printed in Hungary

A kiadásért felel az Akadémiai Kiadó igazgatója — Műszaki szerkesztő: Farkas Sándor

A kézirat nyomdába érkezett: 1969. IX. 4. — Terjedelem: 11,50 (A/5) ív, 34 ábra

69.68259 Akadémiai Nyomda Budapest, — Felelős vezető: Bernát György

ACTA CHIMICA

ТОМ 62 – ВЫП. 4

РЕЗЮМЕ

Изучение фосфоров на основе $LiF—CaF_2$, активированных марганцем

И. КАША, Е. ГЕРЕ-БУЗАГ и И. ТЁРЁК

При обсуждении роли активатора марганец(II)-фторид было установлено, что добавление его в количестве, доходящем до 1 весового процента, значительно увеличивает интенсивность пика, относящегося к 190—195°C, и постепенно уменьшает интенсивность пика, относящегося к 280°C.

При содержании активатора марганец(II)-фторид, превышающем 1 весовой процент, создается пик в области 252—255°C, характерный для CaF_2 : Мм, который по мере увеличения концентрации активатора начинает доминировать. Таким образом, открывается возможность с увеличением концентрации активатора получить такой фосфор, для которого на кривой нагрева находится лишь один пик около 255°C.

Для всех образцов справедливо то заключение, что активатор марганец(II)-фторид увеличивает чувствительность на целый порядок, а также тот факт, что кривые нагрева полностью совпадают в том случае, когда возбуждение проводится с помощью рентгеновского или β-излучения.

С точки зрения затухания, поведение образцов, содержащих 0,2—1,0% активатора, наиболее благоприятное, т. к. уменьшение суммарного светоиспускания после значительного падения в течение первых 4—6 часов становится затем низким. В случае образцов с содержанием активатора 2,5—5% уменьшение и в последующих периодах немного более значительно. Поэтому, с точки зрения практического использования, наилучшими оказались образцы с содержанием активатора 0,2—1%.

Энергетическая зависимость всех образцов отвечает ожидаемой на основе среднего порядкого номера.

Преимущество этих световых порошков, с точки зрения дозиметрического использования, заключается также и в том, что, ввиду вхождения в их состав Li^6, они могут быть использованы и в дозиметрии термических нейтронов.

Изучение зависимости между масс-спектрами молекул и их структурой в случае некоторых кремнеорганических соединений, содержащих два атома кремния

Й. ТАМАШ, К. УЙСАСИ, Т. СЕКЕЙ и Дь. БУЙТАШ

В работе приводятся 50 эв-ные масс-спектры гексаметил-дисилана, гексаметил-дисилилметилена, гексаметил-дисилоксана, гексаметил-дисилазана и N-метилгексаметил-дисилазана, а также те исследования, которые проводились для изучения фрагментации, происходящей вследствие бомбардировки этих соединений электронами.

Определение суммарной формулы наиболее важных наблюдаемых типов ионов, а также основных путей фрагментации базировались на исследованиях полученных полиизотопных спектров, на индикации с O^{18}, а также на подробных исследованиях метастабильных пиков.

Изучались корреляции между типами и количеством наиболее важных ионов, наблюдаемых в масс-спектрах перечисленных соединений и строением молекулы и выясненными путями разложения.

Изучались зависимости между рядом стабильности молекулярных ионов и строением молекулы, между относительным количеством ионов, содержащих скелет двух атомов

кремния, связанных атомами или группой атомов (Si—X—Si), и строением молекулы, и путями разложения, соответственно.

Среди большого числа реакций перегруппировки наблюдаются также и реакции, связанные с перегруппировкой в самом молекулярном скелете. В качестве одного из типов разложения скелета Si—X—Si полагался гетеролитический (связанный со смещением заряда) разрыв связи.

Приводится последовательная схема для образования двух зарядных ионов и их распада. Путем сравнения относительных количеств последних могут быть сделаны заключения о распределении положительных зарядов на ионы.

О свободном радикале ДФПГ в приближении МО—ЛКАО

М. М. ХЕДЬХАТИ

Получены распределения плотности неспаренного электрона в ДФПГ как функция значений кулоновского интеграла α_N для центральных азотных атомов методом молекулярных орбит (МО) в приближении Хюккеля и конфигурационного взаимодействия (КВ) типа Маклачлана в обоих случаях и с учетом перекрывания и без него. Предположено, что группы NO_2 пикрилового кольца не участвуют в образовании сопряженной системы П-электронов, при этом свободный радикал ДФПГ может быть произведен из трифенилэтилового основного скелета путем пятиэтапной «систематической пертурбации». Калькуляции МО с использованием наиболее вероятных величин параметров по литературным данным ($\alpha_N = 0{,}3—0{,}5$) дают отношение плотностей спинов неспаренных электронов на азотных атомах гидразина 0,77—0,86) в хорошем согласии с измеренным значением (0,77—0,84) [1,2] только в том случае, если спиновые плотности по Маклачлану принимаются пропорциональными к измеренным значениям, так как расщепления довольно критически зависят от знака плотностей неспаренных спинов [26].

Кристаллическое строение $K_2S_2O_3 \cdot 1/3H_2O$

Л. ЧОРДАШ

Определялось строение модификации тиосульфата калия, содержащего 1/3 молекулы кристаллической воды, $K_2S_2O_3$ $1/3H_2O$. Кристалл является моноклинным, с пространственной группой $P\,2_1/c$. Параметры элементарной ячейки:

$$a = 9{,}389 \pm 0{,}005,\ b = 6{,}006 \pm 0{,}006,\ c = 30{,}98 \pm 0{,}01\ Å\ ß = 98°22' \pm 3',\ z = 12$$

Проекция (010) структуры определялась прямым методом, а координаты y_j атомов — с помощью системы линейных уравнений структурных факторов и обобщенной проекции электронной плотности. Трехмерное уточнение проводилось с помощью синтеза типа Крюкшанка ($\varrho_0 - \varrho_c$) из 2500 независимых рефлексий. Рассчитывались анизотропические температурные коэффициенты. Конечный фактор $R = 0{,}13$ и, принимая в учет и ненаблюдаемые, $=0{,}15$. Длины связей в тетраэдре S_2O_3 и углы связей показывают хорошее согласие с наблюдаемыми в известной структуре тиосульфата. Молекулы H_2O представляют собой линию винта вокруг оси винта.

Расчет электронной структуры потенциальных антикарциногенов — нуклеотидных оснований антиметаболитного типа, I

Монозамещенные пиримидины, урацилы, тимины и цитозины

Я. ЛАДИК и Г. БИЦО

π-Электронная структура различных монозамещенных (—F, —Cl, —Br, —I, —OH, $—OCH_3$, —SH, $—NH_2$, $—CH_3$, —COOH) пиримидинов, урацилов, тиминов и цитозинов рассчитывалась с помощью полуэмпирического метода ССП ЛКАО МО.

Между плотностями заряда изученных веществ и их антикарциногенными свойствами в отдельных случаях наличие корреляции кажется вероятным. Для уточнения и обобщения корреляций необходимо определение дальнейших квантово-химических индексов.

Расчет распределения зарядов и дипольных моментов насыщенных, кислородосодержащих гетероциклических соединений

Й. НАДЬ, Й. РЕФФИ и И. КАДАШ

В качестве продолжения нашей предыдущей работы, с помощью метода Дель Ре проводились квантово-химические расчеты системы *д*-связей в насыщенных, кислородосодержащих гетероциклических соединениях. В случае трех- и четырехчленных сильно напряженных колец стало необходимым изменение интегралов обмена и кулоновских параметров. Рассчитывались распределение зарядов и дипольные моменты для членов данного ряда соединений. Результаты находятся в хорошем согласии с экспериментальными данными.

Стехиометрическое гидрирование олефинов с помощью кобальт-карбонил-гидрида

Ф. УНГВАРИ и Л. МАРКО

При низких температурах кобальт-карбонил-гидрид в стехиометрической реакции гидрирует гептен в гептан и сопряженные диолефины в моноолефины. Селективность последней реакции выше 90%.

Новые нитрохалконы, X

Выбор конденсирующего агента и зависимость между строением реагентов

Т. СЕЛЛ и И. ШОХАР

Соответствующий выбор конденсирующего агента при образовании халконов из замещенных бензальдегидов и ацетофенонов зависит от констант Гамметта для заместителей (*д*). В случае заместителей с высокими константами Гамметта используется гидроокись натрия, с низкими константами Гамметта — хлористый водород, а со средними значениями *д* — могут быть использованы оба агента. Однако, вследствие некоторых факторов (побочные реакции, условия растворимости) могут наблюдаться отклонения от этого общего правила. Уравнение Гамметта справедливо для реакции Клейзен-Шмидта, катализированной основаниями, и это одновременно может служить исходным пунктом для нахождения зависимости между строением реагирующих компонентов и их реакционной способностью.

The AALC collection, including approx. 5500 punched cards gives the individual the advantages of modern data processing, without the need for expensive machines.

The advantages of cards!

The AALC collection of cards offers many advantages to its user. First, because only a card-file can be kept complete and up-to-date at any time. Book-form bibliographies are difficult to handle and are not apt for cross-indexing. Secondly with a card-file you do not have to make personal notes. If you wish to retain items of information from a book-bound bibliography, you cannot avoid noting them down (if you don't want to tear out the relevant pages!); with the AALC-file, however, you can indulge in the luxury of picking out the cards you are looking for.

The advantages of p u n c h e d cards!

By having the AALC collection on *punched* cards, you never have to replace cards in any particular order. Through the selection operation the cards you are looking for fall unerringly from the whole pack, irrespective of the place they occupy in the card-file. Using simple methods, you can collect all the cards that are particularly important for the topical field you are engaged in at a given time. A punched card file allows any questions to be combined according to the nature of your problem: it allows cross-indexing as well.

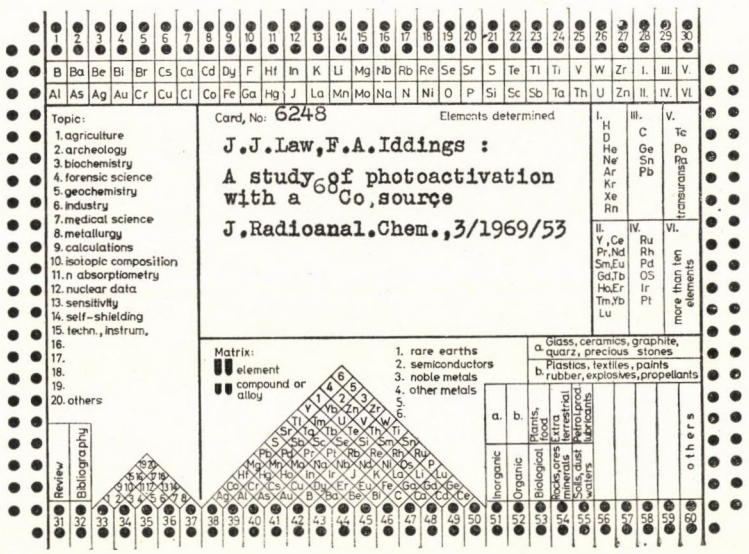

AALC—File
ACTIVATION
ANALYSIS
LITERATURE
CARDS
1935—1968

Unslotted:
US$ 0.05/card

Slotted:
US$ 0.06/card

IN PREPARATION

Ask for leaflets at the following address

AKADÉMIAI KIADÓ

Publicity Department, Budapest 502. P.O.B. 24

ACTIVATION ANALYSIS DOCUMENTATION CENTER

AKADÉMIAI KIADÓ

PUBLISHING HOUSE OF THE HUNGARIAN ACADEMY OF SCIENCES

The Acta Chimica publish papers on chemistry, in English, German, French and Russian.

The Acta Chimica appear in volumes consisting of four parts of varying size, 4 volumes being published a year.

Manuscripts should be addressed to

Acta Chimica
Budapest 112/91 Műegyetem

Correspondence with the editors should be sent to the same address.

The rate of subscription is 165 forints a volume. Orders may be placed with "*Kultúra*" Foreign Trade Company for Books and Newspapers (Budapest I., Fő utca 32. Account No. 43-790-057-181) or with representatives abroad.

Les Acta Chimica paraissent en français, allemand, anglais et russe et publient des mémoires du domaine des sciences chimiques.

Les Acta Chimica sont publiés sous forme de fascicules. Quatre fascicules seront réunis en un volume (4 volumes par an).

On est prié d'envoyer les manuscrits destinés à la rédaction à l'adresse suivante:

Acta Chimica
Budapest 112/91 Műegyetem

Toute correspondance doit être envoyée à cette même adresse.

Le prix de l'abonnement est de 165 forints par volume.

On peut s'abonner à l'Entreprise pour le Commerce Extérieur de Livres et Journaux «*Kultúra*» (Budapest I., Fő utca 32. Compte-courant No. 43-790-057-181) ou à l'étranger chez tous les représentants ou dépositaires.

«*Acta Chimica*» издают трактаты из области химической науки на русском, французском, английском и немецком языках.

«*Acta Chimica*» выходят отдельными выпусками разного объема. 4 выпуска составляют один том. 4 тома публикуются в год.

Предназначенные для публикации рукописи следует направлять по адресу:

Acta Chimica
Budapest 112/91 Műegyetem

По этому же адресу направлять всякую корреспонденцию для редакции.

Подписная цена «*Acta Chimica*» — 165 форинтов за том. Заказы принимает предприятие по внешней торговле книг и газет «*Kultúra*» (Budapest I., Fő utca 32. Текущий счет № 43-790-057-181) или его заграничные представительства и уполномоченные.

51,— Ft

Reviews of the Hungarian Academy of Sciences are obtainable at the following addresses:

ALBANIA

Ndermarja Shtetnore e Botimeve
Tirana

AUSTRALIA

A. Keesing
Box 4886, GPO
Sydney

AUSTRIA

Globus Buchvertrieb
Salzgries 16
Wien I

BELGIUM

Office International de Librairie
30, Avenue Marnix
Bruxelles 5
Du Monde Entier
5, Place St. Jean
Bruxelles

BULGARIA

Raznoiznos
1, Tzar Assen
Sofia

CANADA

Pannonia Books
2, Spadina Road
Toronto 4, Ont.

CHINA

Waiwen Shudian
Peking
P. O. B. 88

CZECHOSLOVAKIA

Artia
Ve Směčkách 30
Praha 2
Poštová novinová služba
Dovoz tisku
Vinohradská 46
Praha 2
Mad'arská Kultura
Václavské nám. 2
Praha I
Poštová novinová služba
Dovoz tlače
Leningradská 14
Bratislava

DENMARK

Ejnar Munksgaard
Nörregade 6
Copenhagen

FINLAND

Akateeminen Kirjakauppa
Keskuskatu 2
Helsinki

FRANCE

Office International de Documentation et Librairie
48, rue Gay Lussac
Paris 5

GERMAN DEMOCRATIC REPUBLIC

Deutscher Buch-Export und Import
Leninstraße 16
Leipzig 701
Zeitungsvertriebsamt
Fruchtstrasse 3—4
1004 Berlin

GERMAN FEDERAL REPUBLIC

Kunst und Wissen
Erich Bieber
Postfach 46
7 Stuttgart S.

GREAT BRITAIN

Collet's Holdings Ltd.
Dennington Estate
London Rd.
Wellingborough. Northants.
Robert Maxwell and Co. Ltd.
Waynflete Bldg. The Plain
Oxford

HOLLAND

Swetz & Zeitlinger
Keizersgracht 471—487
Amsterdam C.
Martinus Nijhof
Lange Voorhout 9
The Hague

INDIA

Current Technical Literature
Co. Private Ltd.
India House OPP
GPO Post Box 1374
Bombay I

ITALY

Santo Vanasia
Via M. Macchi 71
Milano
Libreria Commissionaria Sansoni
Via La Marmora 45
Firenze

JAPAN

Nauka Ltd.
92, Ikebukur O-Higashi 1-chome
Toshima-ku
Tokyo
Maruzen and Co. Ltd.
P. O. Box 605
Tokyo-Central
Far Eastern Booksellers
Kanda P. O. Box 72
Tokyo

KOREA

Chulpanmul
Phenjan

NORWAY

Johan Grundt Tanum
Karl Johansgatan 43
Oslo

POLAND

RUCH
ul. Wronia 23
Warszawa

ROUMANIA

Cartimex
Str. Aristide Briand 14—18
Bucureşti

SOVIET UNION

Mezhdunarodnaya Kniga
Moscow G—200

SWEDEN

Almquist & Wiksell
Gamla Brogatan 26
Stockholm

USA

Stechert Hafner Inc.
31, East 10th Street
New York, N. Y. 10003
Walter J. Johnson
111, Fifth Avenue
New York, N. Y. 10003

VIETNAM

Xunhasaba
19, Tran Quoc Toan
Hanoi

YUGOSLAVIA

Forum
Vojvode Mišića broj 1
Novi Sad
Jugoslovenska Knjiga
Terazije 27
Beograd

31. XII. 1969 **Index: 26.007**